Vol. 65 August, 1961 No. 8

THE JOURNAL OF PHYSICAL CHEMISTRY

(Registered in U. S. Patent Office)

CONTENTS

D. K. Anderson and A. L. Babb: Mutual Diffusion in Non-ideal Liquid Mixtures. II. Diethyl Ether-Chloroform 1281

G. M. Kramer and A. Schriesheim: Heptane Isomerization Mechanism 1283

Gilbert J. Mains, Amos S. Newton and Aldo F. Sciamanna: The Radiolysis of Biacetyl Vapor 1286

Robert D. Euler and Edgar F. Westrum, Jr.: Phase Behavior and Thermal Properties of the System NH_4F-HF 1291

R. J. Thorn and G. H. Winslow: Correction of the Potassium Vapor Pressure Equation by Use of the Second Virial Coefficient 1297

Doyle Britton and Roger M. Cole: Shock Waves in Chemical Kinetics: The Hydrogen–Bromine Reaction 1302

Robert Benz and Carl Wagner: Thermodynamics of the Solid System CaO–SiO_2 from Electromotive Force Data 1308

Martin Kilpatrick and Max W. Meyer: The Kinetics of the Reactions of Aromatic Hydrocarbons in Sulfuric Acid. IV. Durene, Isodurene, Prehnitene and Pentamethylbenzene 1312

H. M. Eiland and Milton Kahn: Some Observations on the Oxidation of Iodine at Low Concentrations 1317

D. W. Scott, J. F. Messerly, S. S. Todd, G. B. Guthrie, I. A. Hossenlopp, R. T. Moore, Ann Osborn, W. T. Berg and J. P. McCullough: Hexamethyldisiloxane: Chemical Thermodynamic Properties and Internal Rotation About the Siloxane Linkage 1320

W. N. Hubbard, F. R. Frow and Guy Waddington: The Heats of Combustion and Formation of Pyridine and Hippuric Acid 1326

E. W. Davies: Spectrophotometric Studies of *cis*- and *trans* - Dichloro - bis - (ethylenediamine) - cobalt (III) Chlorides in Water, Methanol and in Methanol/Water Mixtures 1328

C. Peterson and T. K. Kwei: The Kinetics of Polymer Adsorption onto Solid Surfaces 1330

W. J. Svirbely and August D. Kuchta: The Kinetics of the Alkaline Hydrolysis of Diethyl Malonate, Diethyl Succinate and Diethyl Sebacate in Water–Dioxane Mixtures 1333

Jack L. Settle, Harold M. Feder and Ward N. Hubbard: Fluorine Bomb Calorimetry. II. The Heat of Formation of Molybdenum Hexafluoride 1337

R. M. Skomoroski and A. Schriesheim: The Hydrogenation of Pyridine in Acid Media 1340

H. H. Podgurski and F. N. Davis: Thermal Transpiration at Low Pressure. The Vapor Pressure of Xenon below 90°K 1343

V. Stubican and Rustum Roy: Proton Retention in Heated 1:1 Clays Studied by Infrared Spectroscopy, Weight Loss and Deuterium Uptake 1348

Richard A. Holroyd: Radiation Chemistry of Neopentane 1352

W. J. McDowell and Kenneth A. Allen: Thorium Extraction by Di-*n*-decylamine Sulfate in Benzene 1358

G. H. Cartledge: The Comparative Roles of Oxygen and Inhibitors in the Passivation of Iron. IV. Osmium-(VIII) Oxide 1361

D. G. Walker: Molecular Species and Activity for Paraffin Isomerization Catalysis in the System Dimethyl Ether–Aluminum Bromide 1367

M. E. Nicholas, P. A. Joyner, B. M. Tessem and M. D. Olson: The Effect of Various Gases and Vapors on the Surface Tension of Mercury 1373

F. J. C. Rossotti and Hazel Rossotti: Graphical Methods of Determining Self-Association Constants. III. Refined Treatment of Molecular Weight Data 1376

Joseph Berkowitz, D. A. Bafus and Theodore L. Brown: The Mass Spectrum of Ethyllithium Vapor 1380

A. E. Woodward, A. Odajima and J. A. Sauer: Proton Magnetic Resonance of Some Poly-(α-olefins) and α-Olefin Monomers 1384

Ulrich P. Strauss and Bernard L. Williams: The Transition from Typical Polyelectrolyte to Polysoap. III. Light Scattering and Viscosity Studies of Poly-4-vinylpyridine Derivatives 1390

R. A. Laudise and A. A. Ballman: The Solubility of Quartz under Hydrothermal Conditions 1396

Harold W. Goldstein, Patrick N. Walsh and David White: Rare Earths. I. Vaporization of La_2O_3 and Nd_2O_3: Dissociation Energies of Gaseous LaO and NdO 1400

David White, Patrick N. Walsh, Harold W. Goldstein and David F. Dever: Rare Earths. II. A Mass Spectrometric Determination of the Heats of Sublimation (or Vaporization) of Neodymium, Praseodymium, Gadolinium, Terbium, Dysprosium, Holmium, Erbium and Lutetium 1404

Patrick N. Walsh, David F. Dever and David White: Rare Earths. III. A Mass-Spectrometric Investigation of the Isomolecular Oxygen-Exchange Reactions of Lanthanum, Cerium, Praseodymium and Neodymium with their Monoxides 1410

John E. Lind, Jr., and Raymond M. Fuoss: Conductance of the Alkali Halides. II. Cesium Iodide in Dioxane–Water Mixtures 1414

Max T. Rogers and James M. Canon: Electric Dipole Moments of Some Disubstituted Cyclohexane Derivatives in the Vapor State 1417

Meyer M. Markowitz and Daniel A. Boryta: The Decomposition Kinetics of Lithium Perchlorate 1419

W. T. Berg, D. W. Scott, W. N. Hubbard, S. S. Todd, J. F. Messerly, I. A. Hossenlopp, Ann Osborn, D. R. Douslin and J. P. McCullough: The Chemical Thermodynamic Properties of Cyclopentanethiol 1425

John P. McCullough and William D. Good: Correlation of Heat of Formation Data for Organic Sulfur Compounds 1430

S. J. Gill, J. Hutson, J. R. Clopton and M. Downing: Solubility of Diketopiperazine in Aqueous Solutions of Urea 1432

Lois Nash Kauder, W. Spindel and E. U. Monse: Fractionation of Oxygen Isotopes by the Distillation of Azeotropic Solutions 1435

Michael O'Keeffe and Walter J. Moore: Diffusion of Oxygen in Single Crystals of Nickel Oxide 1438

NOTES

Walter Rose, H. C. Tung and Claude Newman: Dead-End Pore Volume as Distributed Sources and Sinks 1440

Henry E. Wirth: Estimation of Dissociation Constants of Electrolytes 1441

Michael Ardon and Amos Linenberg: Cryoscopic Determination of Molecular Weights in Aqueous Perchloric Acid 1443

Robert W. Kiser and I. C. Hisatsune: Electron Impact Spectroscopy of Nitrogen Dioxide 1444

Russell S. Drago and Devon Meek: The Infrared Spectra of Some Dimethyl Sulfoxide Complexes 1446

Henry E. Wirth and Paul I. Slick: Solubility and Conductivity of Substituted Ammonium Iodides in Pentaborane 1447

THE JOURNAL OF PHYSICAL CHEMISTRY

(Registered in U. S. Patent Office)

Published monthly by the American Chemical Society at 20th and Northampton Sts., Easton, Pa.

Second-class mail privileges authorized at Easton, Pa. This publication is authorized to be mailed at the special rates of postage prescribed by Section 131.122.

The *Journal of Physical Chemistry* is devoted to the publication of selected symposia in the broad field of physical chemistry and to other contributed papers.

Manuscripts originating in the British Isles, Europe and Africa should be sent to F. C. Tompkins, The Faraday Society, 6 Gray's Inn Square, London W. C. 1, England.

Manuscripts originating elsewhere should be sent to W. Albert Noyes, Jr., Department of Chemistry, University of Rochester, Rochester 20, N. Y.

Correspondence regarding accepted copy, proofs and reprints should be directed to Assistant Editor, Allen D. Bliss, Department of Chemistry, Simmons College, 300 The Fenway, Boston 15, Mass.

Business Office: Alden H. Emery, Executive Secretary, American Chemical Society, 1155 Sixteenth St., N. W., Washington 6, D. C.

Advertising Office: Reinhold Publishing Corporation, 430 Park Avenue, New York 22, N. Y.

Articles must be submitted in duplicate, typed and double spaced. They should have at the beginning a brief Abstract, in no case exceeding 300 words. Original drawings should accompany the manuscript. Lettering at the sides of graphs (black on white or blue) may be pencilled in and will be typeset. Figures and tables should be held to a minimum consistent with adequate presentation of information. Photographs will not be printed on glossy paper except by special arrangement. All footnotes and references to the literature should be numbered consecutively and placed in the manuscript at the proper places. Initials of authors referred to in citations should be given. Nomenclature should conform to that used in *Chemical Abstracts*, mathematical characters be marked for italic, Greek letters carefully made or annotated, and subscripts and superscripts clearly shown. Articles should be written as briefly as possible consistent with clarity and should avoid historical background unnecessary for specialists.

Notes describe fragmentary or incomplete studies but do not otherwise differ fundamentally from articles and are subjected to the same editorial appraisal as are articles. In their preparation particular attention should be paid to brevity and conciseness. Material included in Notes must be definitive and may not be republished subsequently.

Remittances and orders for subscriptions and for single copies, notices of changes of address and new professional connections, and claims for missing numbers should be sent to the American Chemical Society, 1155 Sixteenth St., N. W., Washington 6, D. C. Changes of address for the *Journal of Physical Chemistry* must be received on or before the 30th of the preceding month.

Claims for missing numbers will not be allowed (1) if received more than sixty days from date of issue (because of delivery hazards, no claims can be honored from subscribers in Central Europe, Asia, or Pacific Islands other than Hawaii), (2) if loss was due to failure of notice of change of address to be received before the date specified in the preceding paragraph, or (3) if the reason for the claim is "missing from files."

Subscription rates (1961): members of American Chemical Society, $12.00 for 1 year; to non-members, $24.00 for 1 year. Postage to countries in the Pan-American Union $0.80; Canada, $0.40; all other countries, $1.20. Single copies, current volume, $2.50; foreign postage, $0.15; Canadian postage, $0.10; Pan-American Union, $0.10. Back volumes (Vol. 56–64) $30.00 per volume; foreign postage, per volume $1.20, Canadian, $0.40; Pan-American Union, $0.80. Single copies: back issues, $3.00; for current year, $2.50; postage, single copies: foreign, $0.15; Canadian, $0.10; Pan-American Union, $0.10.

The American Chemical Society and the Editors of the *Journal of Physical Chemistry* assume no responsibility for the statements and opinions advanced by contributors to This Journal.

The American Chemical Society also publishes *Journal of the American Chemical Society, Chemical Abstracts, Industrial and Engineering Chemistry*, International Edition of *Industrial and Engineering Chemistry, Chemical and Engineering News, Analytical Chemistry, Journal of Agricultural and Food Chemistry, Journal of Organic Chemistry, Journal of Chemical and Engineering Data, Chemical Reviews, Chemical Titles* and *Journal of Chemical Documentation*. Rates on request.

Paul Allen, Jr., and Leo Reich: Disproportionation of 1-Dodecanesulfinic Acid in Solution 1449

Albert T. Fellows and Robert H. Schuler: The Radiation-Induced Reaction between Benzene and Iodine. 1451

Walter C. Hamilton and Martha Petrie: Confirmation of Disorder in Solid Nitrous Oxide by Neutron Diffraction 1453

R. G. Cunninghame and G. N. Malcolm: The Heats of Mixing of Aqueous Solutions of Polypropylene Glycol 400 and Polyethylene Glycol 300 1454

M. V. Milnes and W. E. Wallace: The Residual Entropy of the Equimolal KCl–KBr Solid Solution in Relation to Wasastjerna's Theory of Alkali Halide Solid Solutions 1456

G. Blauer: *p*H-Dependent Spectral Shifts in the System Acridine Orange–Polymethacrylic Acid 1457

J. C. Rohrer, H. Hurwitz, and J. H. Sinfelt: Kinetics of the Catalytic Dehydrocyclization of *n*-Heptane 1458

Louis Watts Clark: The Behavior of Oxanilic Acid in Quinoline and in 8-Methylquinoline 1460

R. Benz and R. M. Douglass: Phase Equilibria in the Binary Systems $PuCl_3$–RbCl and $PuCl_3$–CsCl 1461

Riyad R. Irani: Metal Complexing by Phosphorus Compounds. V. Temperature Dependence of Acidity and Magnesium Complexing Constants 1463

W. R. Gilkerson and J. H. Stewart: Polarizabilities and Molar Volumes of a Number of Salts in Several Solvents at 25° 1465

W. R. Gilkerson and R. E. Stamm: The Conductance of Tetra-*n*-butylammonium Picrate in 50 mole % Benzene-*o*-Dichlorobenzene and Bromobenzene as a Function of Temperature 1466

Charles M. Cook, Jr., and Robert B. Hand: The Systems Tantalum Pentachloride–Ferric Chloride and Niobium Pentachloride–Ferric Chloride 1467

COMMUNICATIONS TO THE EDITOR

Rolf Buchdahl, Herbert A. Ende, and Leighton H. Peebles, Jr.: Detection of Structural Differences in Polymers in a Density Gradient Established by Ultracentrifugation 1468

Harris E. Kluksdahl and Robert J. Houston: The State of Platinum in Reforming Catalysts 1469

D. Clark, T. Dickinson and W. N. Mair: On the Oxidation of Gold 1470

Robert R. Hentz: Gamma-Irradiation of Isopropylbenzene Adsorbed on Microporous Silica-Alumina 1470

Lloyd H. Reyerson, Aage Solbakken and Richard W. Zuehlke: The Magnetic Susceptibility of Small Palladium Crystals 1471

THE JOURNAL OF
PHYSICAL CHEMISTRY

(Registered in U. S. Patent Office)

VOLUME 65 AUGUST 24, 1961 NUMBER 8

MUTUAL DIFFUSION IN NON-IDEAL LIQUID MIXTURES. II. DIETHYL ETHER–CHLOROFORM

BY D. K. ANDERSON AND A. L. BABB

Department of Chemical Engineering, University of Washington, Seattle, Washington

Received May 3, 1960

Mutual diffusivities and viscosities have been measured for diethyl ether–chloroform over the entire concentration range at 25.0°. The experimental data are discussed in terms of an equation similar in form to that of Hartley and Crank which was derived by assigning an intrinsic diffusivity to the one:one complex formed by ether:chloroform as well as to the monomeric species of ether and chloroform.

Introduction

The diffusion behavior of non-ideal binary liquid mixtures has been studied in this laboratory in the hope that progress could be made toward explaining the diffusion mechanism. As part of this continuing program, diffusivities and viscosities were measured for the system diethyl ether–chloroform at 25° over the entire concentration range.

Experimental

Diffusivities were measured with the use of a Mach–Zehnder diffusiometer described fully elsewhere[1] and viscosities were determined using an Ostwald viscometer. The reagent grade solvents were obtained from the Mallinckrodt Chemical Works and were used without further purification, except for removal of the ethanol stabilizer from chloroform with anhydrous calcium chloride.

Results and Discussion

Experimental Data.—The experimental diffusivities were obtained by measuring the inter-diffusion of two solutions of very nearly equal concentrations. The measured value was taken to be that of a solution with a concentration equal to the average of the two. The results are given in Table I and Fig. 1. Diffusion coefficients for the same system at 17° were reported by Lemonde[2] and are shown in Fig. 1 for comparison with this work. Lemonde's results appear to be in error since his values at 17° are higher than the authors' at 25° over most of the concentration range, whereas the opposite should be true. A similar disagreement with Lemonde's results was reported previously for the system acetone–chloroform.[3] Experimental viscosities are listed in Table II.

Comparison with Results from Hartley and Crank Equation.—Hartley and Crank[4] have shown that for non-ideal systems, the concentration dependence of mutual diffusivities could be predicted from an equation of the form

(1) C. S. Caldwell, J. R. Hall and A. L. Babb, *Rev. Sci. Instr.*, **28**, 816 (1957).

(2) H. Lemondè, *Ann. Phys.*, **9**, 399 (1938).

(3) D. K. Anderson, J. R. Hall and A. L. Babb, *J. Phys. Chem.*, **62**, 404 (1958).

(4) G. S. Hartley and K. Crank, *Trans. Faraday Soc.*, **45**, 801 (1949).

TABLE I

SUMMARY OF EXPERIMENTAL DIFFUSIVITIES FOR DIETHYL ETHER–CHLOROFORM

Mole fraction ether in lower layer of cell	0	0.2007	0.399	0.597	0.789	0.789	0.890	0.994
Mole fraction ether in upper layer of cell	0.00870	0.2082	0.409	0.605	0.798	0.798	0.901	1.000
Av. mole fraction ether	0.00435	0.2044	0.404	0.601	0.794	0.794	0.896	0.997
$D_{AB} \times 10^5$, cm.²/sec.	2.147	2.909	3.683	4.211	4.381	4.442	4.488	4.509

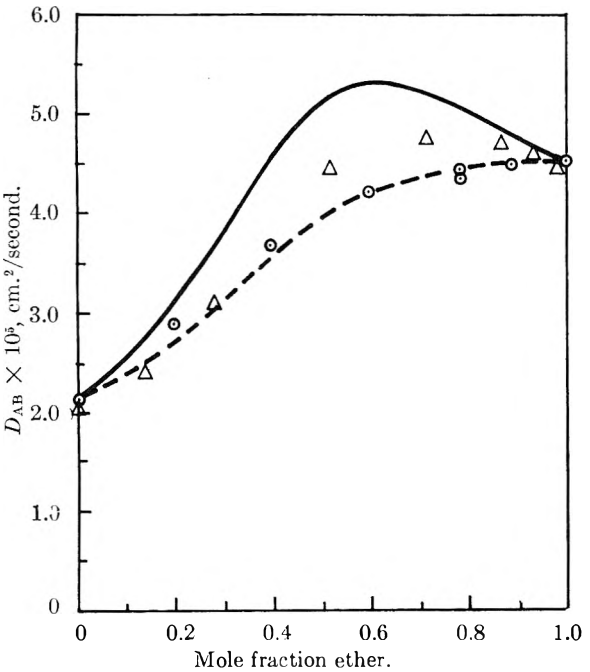

Fig. 1.—Mutual diffusion data for the diethyl ether–chloroform system: ⊙, experimental, 25° (the authors); △, experimental, 17° (Lemonde[2]); – – –, calculated from equation 4; ———, calculated from equation 3 (Hartley and Crank[4]).

TABLE II

SUMMARY OF EXPERIMENTAL VISCOSITIES FOR DIETHYL ETHER–CHLOROFORM

Mole fraction ether	0	0.274	0.528	0.672	0.863	1.000
Viscosity, cp.	0.535	0.472	0.397	0.340	0.268	0.225

TABLE III

EXPERIMENTAL VALUES OF THE EQUILIBRIUM CONSTANT K

Temp., °C.	20	33.25	60	80	100
Equilibrium constants:					
Ref. 5	2.96	2.36	1.0	0.80	0.71
Ref. 6	2.60				
Ref. 7	10 (room temp.)				

$$D_{AB} = \mathfrak{D}_A V_B C_B + \mathfrak{D}_B V_A C_A \qquad (1)$$

where D_{AB} is the mutual diffusivity, $\mathfrak{D}$ is the so-called intrinsic diffusivity, V is the molar volume, C is the molar concentration and the subscripts A and B refer to components A and B in the binary solution. They have also shown that if the driving force acting to cause a component to diffuse is the gradient of the chemical potential of that component, then the intrinsic diffusivity is given by

$$\mathfrak{D}_i = \frac{RT}{Nf_i\eta} \frac{\mathrm{d} \ln a_i}{\mathrm{d} \ln C_i} \qquad (2)$$

where a_i is the activity of the component, η is the solution viscosity and f_i is a friction coefficient dependent only on molecular size. These intrinsic diffusion coefficients are defined with respect to a reference frame through which no volume flow by bulk-motion occurs.

If equations 1 and 2 are combined, the well-known Hartley and Crank equation is obtained.

$$D_{AB} = \frac{RT}{N\eta}\left[\frac{X_A}{f_B} + \frac{X_B}{f_A}\right] \frac{\mathrm{d} \ln a}{\mathrm{d} \ln X} \qquad (3)$$

To compute values of D_{AB} from this equation, the friction factors f_A and f_B were determined and found to be 35.8 and 40.5 Å., respectively, from the intercepts of the experimental diffusivity-mole fraction (X) curve. These values were assumed to be constant over the entire concentration range and were used in equation 3 together with activities calculated from data available in the literature[5] to compute the diffusivity-mole fraction curve shown in Fig. 1. From Fig. 1, it is seen that the experimental results do not compare favorably with the results calculated from equation 3. This lack of agreement probably lies in the assumption inherent in equation 3 that the diffusing species are single molecules; whereas, it is well known that ether and chloroform molecules can combine in solution to form weakly bonded one:one complexes.[6,7] Consequently, as others also have suggested,[8,9] it is reasonable to assume that this complex diffuses as an entity so that intrinsic diffusivities should be assigned to each of three species in solution, rather than two species as in the Hartley and Crank treatment.

Modified Form of the Hartley and Crank Equation.—Dolezalek and Schulze[5] applied a one:one complex model for the prediction of vapor–liquid equilibria for the system ether–chloroform by assuming the true species in solution (*i.e.*, monomers and complexes) to behave as an ideal solution. They related the concentrations of the true species to an equilibrium constant given by[10]

$$K = \frac{X_{12}}{X_1 X_2}$$

Using the same model, the authors modified the Hartley and Crank equation to include the effect of molecules diffusing as one:one complexes, by assigning the intrinsic diffusivities given by equation 2 to each of the true species in solution. The details of the development are presented elsewhere[11] and will not be reproduced here. The final form of the equation is

$$D_{AB} = \frac{RT}{N\eta}\left[\frac{X_B X_1^0}{f_1 X_A} + \frac{X_A X_2^0}{f_2 X_B} + \frac{(X_B - X_A)^2 X_{12}^0}{f_{12} X_A X_B}\right] \frac{\mathrm{d} \ln a}{\mathrm{d} \ln X} \qquad (4)$$

where

$$X_1^0 = C_1/C_A + C_B = X_1/1 + X_{12}$$
$$X_2^0 = C_2/C_A + C_B = X_2/1 + X_{12}$$
$$X_{12}^0 = C_{12}/C_A + C_B = X_{12}/1 + X_{12}$$

Equation 4 reduces to the Hartley and Crank equation for the case when no association occurs (*i.e.*, when $X_1 = X_A$, $X_2 = X_B$ and $X_{12} = 0$). For associating systems the equation contains the ad-

(5) F. Dolezalek and A. Schulze, *Z. physik. Chem.*, **83**, 45 (1913).

(6) J. H. Van Santen, *Rec. trav. chim. Pay-Bas*, **62**, 222 (1943).

(7) R. C. Lord, B. Nolin and H. D. Stidham, *J. Am. Chem. Soc.*, **77**, 1365 (1955).

(8) B. R. Hammond and R. H. Stokes, *Trans. Faraday Soc.*, **52**, 781 (1956).

(9) P. C. Carman and L. Miller, *ibid.*, **55**, 1838 (1959).

(10) Numerical subscripts will be used to denote true species in solution and alphabetical subscripts to denote stoichiometric quantities in solution.

(11) D. K. Anderson, Ph.D. Thesis, University of Washington, 1960 (*Dissertation Abstracts*, *XXI*, No. 6, 1388 (1960)).

ditional friction coefficient, f_{12}, for the one:one complex.

Application of Modified Equation.—It is not possible to assign a definite value to f_{12} since not enough is known about the diffusion mechanism. However, a qualitative check of the validity of equation 4 may be obtained by determining a single value for f_{12} empirically from the data in Fig. 1, and then using equation 4 to see how well the entire diffusivity-mole fraction curve may be predicted.

To do this, values for x_1^0, X_2^0 and X_{12}^0 were calculated using an equilibrium constant of 2.71 at 25° interpolated from Dolezalek's vapor pressure results given in Table III. Values reported by Van Santen[6] based on dielectric constant measurements and by Lord, Nolin and Stidham[7] based on infrared measurements are also reported in Table III to show the range of equilibrium constants available. Using this value of K, the maximum value of X_{12} is about 0.3 at $X_A = 0.5$.

With these data, values of $f_1 = 22.2$ Å., $f_2 = 30.0$ Å. were obtained from the intercepts of the experimental diffusivity–mole fraction curve, and a value of $f_{12} = 45.9$ Å. was found to give the best agreement with the experimental curve over the entire concentration range. These values of f_1, f_2 and f_{12} correspond to Stokes–Einstein radii of 1.18, 1.59 and 2.43 Å., respectively. It should be noted that if a higher value of K had been used, a smaller and more reasonable value of f_{12} would be obtained.

Consequently, for this system forming a one:one complex the three parameter equation derived by the authors can give a better fit than the original Hartley and Crank equation if the proper value for f_{12} is used. Until more accurate association data and diffusivity measurements for similar systems become available, however, no generalizations can be made regarding the best value for f_{12} apart from an empirical fit of experimental data.

The authors have applied this same approach with encouraging results to systems in which one component dimerizes and to systems in which one component associates over a wide range of polymer sizes.

Acknowledgments.—This work was supported by the Office of Ordnance Research, U. S. Army.

HEPTANE ISOMERIZATION MECHANISM

BY G. M. KRAMER AND A. SCHRIESHEIM

Esso Research and Engineering Company, Linden, New Jersey

Received August 9, 1960

The acid-catalyzed isomerization of several heptane isomers has been studied over $AlBr_3$–H_3PO_4 catalysts. This research was carried out in order to extend our knowledge of acid-catalyzed reactions into higher molecular weight hydrocarbon regions. It was found that the isomerization reaction could be interpreted on a stepwise carbonium ion basis. The rates of isomerization of each isomer were proportional to the relative ease of forming the ion (tert. > sec.). These results fit in well with previously established theories of acid-catalyzed paraffin hydrocarbon reactions.

Introduction

As part of a general program in the area of acid catalysis, the reactions of certain pure heptane isomers have been studied over an activated Friedel-Crafts catalyst—$AlBr_3/H_3PO_4$. A previous paper has discussed the equilibrium isomer distribution[1] found with these heptane isomers over an aluminum halide catalyst system. This paper discusses the mechanism of the heptane isomerization reaction.

Experimental

Phillips research grade isomers, 2,3-dimethylpentane, 2,4-dimethylpentane, 3-methylhexane and *n*-heptane were used as starting compounds. 2,2-Dimethylpentane also was used, and it was supplied by Dr. M. R. Fenske of the Petroleum Refining Laboratory of the Pennsylvania State University. The isomers were passed over a zeolitic adsorbent to remove olefins before use. A heterogeneous catalyst system composed of 4.9 cc. of 84% phosphoric acid, 66 g. of aluminum bromide, 6 cc. of benzene and 60 cc. of the heptane isomer was used. Aluminum bromide was purified by repeated distillations and stored in a dry box before use. Benzene, a cracking inhibitor, was obtained from the Baker Company. Experiments were carried out at 36.8° in a three neck reaction flask fitted with a stirrer, and a reflux condenser connected to a gas bag. The flask was also fitted with a rubber diaphragm through which a hypodermic syringe could be inserted to remove samples from the hydrocarbon phase of the heterogeneous system. The composition of the product was determined by gas chromatographic analysis throughout a 24 hour reaction period. All samples were analyzed with a squalene on firebrick column at 0°. This column permitted separation and identification of each one of the nine isomers.

(1) G. M. Kramer and A. Schriesheim, *J. Phys. Chem.*, **64**, 849 (1960).

Results

A kinetic approach was adopted throughout the course of this investigation. Reactants were contacted with the catalysts as described in the Experimental section, and rates calculated from the change in product distribution with time. This approach was used mainly because of its obvious application to mechanism studies. The results of these experiments are summarized in tabular form (Table I). The relative rates of isomerization of the heptane isomers as determined by analysis of the C_7 fraction for the starting compound were found to vary by more than 100-fold. The precision of the data in the cases of 3-methylhexane, 2,3-dimethylpentane and 2,4-dimethylpentane is roughly estimated as ± 0.5 hr.$^{-1}$ in view of the lack of low conversion points, but of the similarity of the rates obtained with each of the dimethylpentanes. As explained below these rates refer not to isomerization of the starting isomer to initial products, but to the rate of conversion of ions which are assumed to be reaction intermediates, of a particular structural type to those of another structural type. Isomers which contain tertiary carbon atoms such as 3-methylhexane,

2,3-dimethylpentane and 2,4-dimethylpentane isomerize more rapidly than those isomers without tertiary carbon atoms (*n*-heptane and 2,4-dimethylpentane), and the isomerization reactions appear to follow first-order kinetics. The observed and relative rates for the "over-all" disappearance as obtained from log % isomer remaining *vs.* time plots are listed in Table I.

TABLE I

ISOMERIZATION OF HEPTANE ISOMERS

Isomer	Ion type	Obsd. rate, k_{iso}, hr.$^{-1}$	Rel. rate, k_{iso}, hr.$^{-1}$
2,2-Dimethylpentane	Secondary	0.037 ± 0.01	0.04
n-Heptane	Secondary	0.90 ± 0.1	1.0
2,3-Dimethylpentane	Tertiary	3.96 ± 0.5	4.4
2,4-Dimethylpentane	Tertiary	3.96 ± 0.5	4.4
3-Methylhexane	Tertiary	4.80 ± 0.5	5.3

It is however important to observe that isomerization between compounds with the same number of branches occurred too rapidly to be measured whenever a tertiary carbonium ion could be formed from the starting isomer. Thus, the data most likely measure the rate of disappearance of ion types (methylpentyl, dimethylpentyl, etc.) rather than the rate of isomerization of the starting compound to the initial product. In general, it was found that reactions involving a change in branching are slower than those involving a simple methyl shift. Thus, 2-methylhexane and 3-methylhexane equilibrate before they can convert to other isomers (Fig. 1). Rapid equilibration was

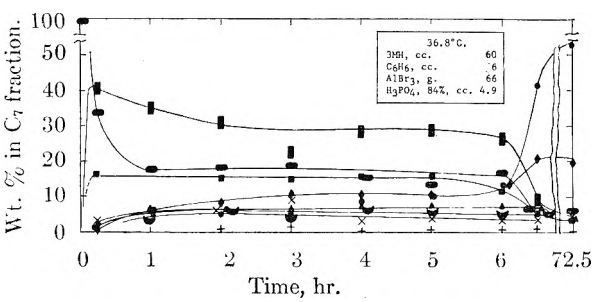

Fig 1.—3-Methylhexane and 2-methylhexane equilibrate before isomerizing to other isomers: ●, 2,2-DMP; ■, 2,4-DMP; ▲, 2,2,3-TMB; ◆, 3,3-DMP; ×, 2,3-DMP; ▮, 2-MH; ⬬, 3-MH; +, 3-EP; ◡, nC_7.

also found with 2,3-dimethylpentane and 2,4-dimethylpentane (Fig. 2). This reaction probably

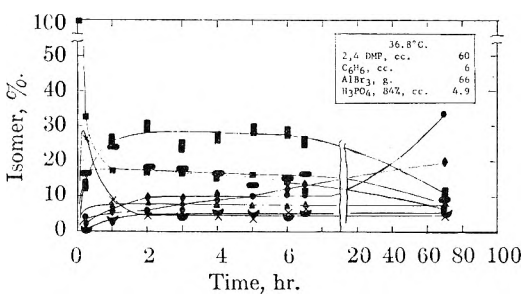

Fig. 2.—2,4-Dimethylpentane and 2,3-dimethylpentane equilibrate before isomerizing to other isomers: ●, 2,2-DMP; ■, 2,4-DMP; ▲, 2,2,3-TMB; ◆, 3,3-DMP; ×, 2,3-DMP; ▮, 2-MH; ⬬, 3-MH; ◡, nC_7.

takes place at about the same rate as the methylhexane interconversion. However, the precision of our data precludes the determination of differences in initial rates.

Normal heptane isomerized to methyhexanes, Fig. 3 and 5, which subsequently converted to

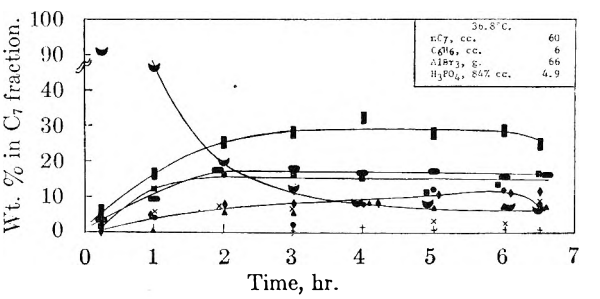

Fig. 3.—*n*-Heptane isomerization: ●, 2,2-DMP; ■, 2,4-DMP; ▲, 2,2,3-TMB; ◆, 3,3-DMP; ×, 2,3-DMP; ▮, 2-MH; ⬬, 3-MH; +, 3-EP; ◡, nC_7.

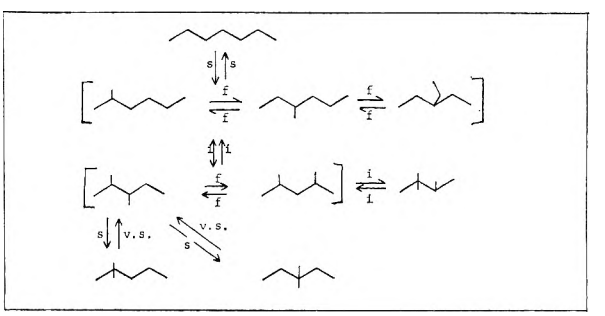

Fig. 4.—The isomerization of heptanes follows a stepwise path. Relative rates are indicated by the symbols: f = fast, s = slow, v.s. = very slow, i = intermediate.

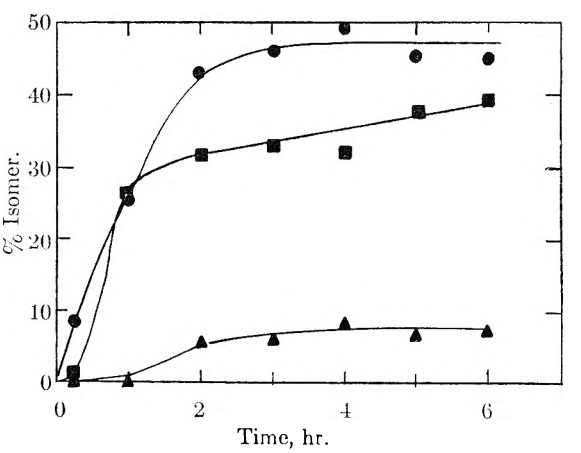

Fig. 5.—The appearance of isomers from *n*-heptane illustrates the stepwise isomerization process: ●, methylhexanes; ■, dimethylpentanes; ▲, triptane.

dimethylpentanes. It is likely that the methylhexanes are formed in their equilibrium ratios although the data are not sufficiently clear on this point.

During the course of the isomerization studies, work was carried out at relatively long contact times. At these contact times cracking occurred. The only light hydrocarbons found were butanes, pentanes and hexanes, and these were largely the

iso derivatives. Also, at these conditions, 2,2-dimethylpentane, 3,3-dimethylpentane and *n*-heptane were found to build up in the hydrocarbon fraction (Table II).

TABLE II

TERTIARY ISOMERS DEGRADE EASILY, 36.8°

Isomer, % of heptane fraction	Before degradation	After degradation
2,2-Dimethylpentane	6.4	33.7
3,3-Dimethylpentane	9.6	20.0
2,3-Dimethylpentane	8.8	4.5
2,4-Dimethylpentane	17.2	7.0
2,2,3-Trimethylbutane	9.1	8.2
2-Methylhexane	24.0	11.2
3-Methylhexane	18.6	8.2
3-Ethylpentane	1.7	0.5
n-Heptane	4.6	6.7
% C_6^- Formed	4	31

Discussion

The results of these experiments may be rationalized in terms of a stepwise ionic reaction. Such concepts have been reviewed recently by Condon,[2] and applied in detail to the mechanism of hexane isomerization by McCaulay,[3] and by Schriesheim and Khoobiar.[4] The conversion of *n*-heptane to branched isomers is assumed to require the formation of a secondary carbonium ion. Since the formation of a secondary ion requires more energy than the formation of a tertiary ion,[5] it is reasonable to expect *n*-heptane to isomerize more slowly than isomers with tertiary atoms.

From Table I it is seen that the isomerization of *n*-heptane is slow compared to the isomerization of structures involving tertiary C–H bonds such as 2-methylhexane, 3-methylhexane, 2,3-dimethylpentane or 2,4-dimethylpentane. The isomerization of 2,2-dimethylpentane is also assumed to require the formation of a secondary carbonium ion, but its rate of isomerization is only $^1/_{25}$ that of *n*-heptane. Since secondary ions are conceivably involved in both cases, these relative rates might be due to the difficulty in forming structures such as I, because of steric hindrance involving the methyl groups and the secondary carbonium ion.

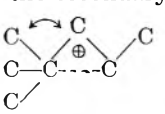

I

The over-all isomerization of the heptane fraction is depicted in Fig. 4. The isomerization reactions are shown here as occurring in a stepwise fashion.

(2) F. E. Condon, in "Catalysis," Vol. 6, Reinhold Publ. Corp., New York, N. Y., 1958, pp. 43–189.

(3) D. A. McCaulay, Symposium on Isomerization and Related Processes, presented before the Division of Petroleum Chemistry, Am. Chem. Soc., Boston Meeting, April 5–10, 1959.

(4) A. Schriesheim and S. Khoobiar, Proceedings, 2nd International Catalysis Congress, Division of Kinetics and Mechanisms, Paris, France, 1960.

(5) F. H. Field and J. Franklin, "Electron Impact Phenomena," Academic Press, Inc., New York, N. Y., 1957, p. 263. The heat of formation of a secondary butyl ion requires about (180–190) kcal./mole as compared with only 166 kcal./mole for the *t*-butyl ion. Assuming solvation energies to be equal in both cases, there is a difference of about (14–24) kcal./mole in favor of tertiary ion formation. It is assumed that differences of the same order of magnitude exist with the heptanes.

The proposed scheme is based upon the following observations and conjectures which fit all data concerning the heptanes.

n-Heptane isomerizes to methylhexanes first.

Methylhexanes equilibrate faster than they convert to *n*-heptane or the dimethylpentanes. It is likely that 3-ethylpentane also is found in equilibrium with the methylhexanes by rapid isomerization of the 3-methylhexyl ion but the data are not sufficiently reliable to prove this point.

2,3-Dimethylpentane and 2,4-dimethylpentane equilibrate before they isomerize to methylhexanes, trimethylbutane, or the other dimethylpentanes. Attempts have been made to decide whether the methylhexanes or triptane is formed as an initial product of the isomerization of 2,4- and 2,3-dimethylpentane, but it has not been possible to reach a firm conclusion. The fact that 2,3- and 2,4-dimethylpentane equilibrate and then convert to the methylhexanes and 2,2,3-trimethylbutane at "intermediate" rates is responsible for the production of a readily reached pseudo-equilibrium among these compounds. This pseudo-equilibrium is fairly well maintained, even under cracking conditions, as may be seen from the relative amounts of the isomers present before and after degradation (Table II).

The only reasonable path to 2,2-dimethylpentane and 3,3-dimethylpentane, invoking carbonium ion formation and single hydride and methide shifts is through 2,3-dimethylpentane. A possible alternate path to 2,2-dimethylpentane by isomerization of 2,2,3-trimethylbutane exists but does not seem probable, since, if this were true one should see a sizable increase in the triptane concentration under cracking conditions where the 2,2-dimethylpentane concentration rises fivefold (Table II). Actually, the triptane concentration remains about the same under these conditions.

A further illustration of the stepwise nature of the reaction is shown in Fig. 5, where the production of methylhexanes, dimethylpentanes and 2,2,3-trimethylbutane from *n*-heptane is shown. It is evident from the curves that methylhexanes are produced before dimethylpentanes and that 2,2,3-trimethylbutane is formed last. The latter isomer was produced before the occurrence of side reactions and is thus the result of isomerization.

As a consequence of the stepwise nature of this reaction and the variation in isomerization rates, it is possible to prepare mixtures of the heptanes confined to a small range of isomers which exist in an internal equilibrium between themselves. In Table III are listed the fractions which have been obtained over a variety of catalysts. From this table it is seen that it is possible to obtain selective mixtures of 2-methylhexane and 3-methylhexane as well as 2,3-dimethylpentane and 2,4-dimethylpentane over sulfuric acid, chlorosulfonic acid, aluminum chloride and aluminum bromide.

Side Reactions.—Side reactions are common to Friedel–Crafts isomerizations and lead to the production of saturated hydrocarbons containing more and less carbon atoms than the reactants as well as highly unsaturated cyclic compounds. The occurrence of these reactions during an isomerization must be controlled to obtain valid equilibrium

TABLE III

FRACTIONS IN EQUILIBRIUM IN THE LIQUID PHASE

Catalyst	Temp., °C.	3-MH ⇄ 2-MH Mole % 2-MH	2,3-DMP ⇄ 2,4-DMP Mole % 2,4-DMP
$ClSO_3H$	−33.4[6]	65.5	72.8
H_2SO_4:$ClSO_3H$	0[6]	62.8	70.6
$AlCl_3$	20[7]	62	60
H_2SO_4	25[8]	56–59	65–66
($AlBr_3$:H_3PO_4)	36.8[1]	58.5	65.4
H_2SO_4	60[6]	59.5	59.6

composition data. If degradation is not controlled, the product distribution is altered in favor of the isomers which best resist alkylation, cracking and isomerization.[4]

The most resistant isomers are those which cannot form tertiary carbonium ions and these are preferentially retained in the heptane fraction undergoing degradative reactions. This is illustrated by the data in Table II which compare the heptane isomerate at equilibrium and after extensive cracking. 2,2-Dimethylpentane, 3,3-dimethylpentane and *n*-heptane build up preferentially under these conditions. Degradation of the tertiary isomers formed from 2,2-dimethylpentane also occurred after 10–30% conversion of this isomer. Since the rate of disappearance of the heptane fraction was approximately equal to the rate of isomerization of 2,2-dimethylpentane at these conversion levels, equilibrium could not be reached with this isomer. As noted above, degradation reactions lead to the formation of hydrocarbons containing more and less carbon atoms than the starting molecule. The large molecules are usually highly unsaturated, the light compounds contain isomers with four or more carbons. Isobutane and isopentane generally predominate, indicating the tendency of paraffins to crack ionically to yield tertiary structures. Possible mechanisms of degradation have been postulated and discussed by several investigators.[4]

(6) C. P. Maury, R. L. Burwell, Jr., and R. H. Tuxworth, *J. Am. Chem. Soc.*, **76**, 5831 (1954).

(7) J. J. B. van Eijk van Voorthuijsen, *Rec. trav. chim.*, **66**, 323 (1947).

(8) A. K. Roebuck and B. L. Evering, *J. Am. Chem. Soc.*, **75**, 1631 (1953).

THE RADIOLYSIS OF BIACETYL VAPOR[1]

BY GILBERT J. MAINS, AMOS S. NEWTON[2] AND ALDO F. SCIAMANNA

Lawrence Radiation Laboratory, University of California, Berkeley, California

Received October 7, 1960

The radiolysis of biacetyl vapor was studied at 25, 120 and 200° with pulsed electrons from a 4.2 Mev. microwave linear accelerator. Effects of pressure, pulse rate and total dose were studied. At room temperature the relative yields of methane and ethane were only slightly dependent on experimental parameters, but at higher pressures the relative yields were pressure dependent. A free radical mechanism has been proposed to explain the formation of the major products and this is shown to account qualitatively for the experimental observations.

Introduction

Preliminary studies of the radiolysis of some simple ketones as liquids and vapors have been reported[3–5] but extensive investigations of these systems have not been carried out. Ausloos and Paulson[3] have indicated that 85% of the methane produced in the radiolysis of *liquid* acetone could be explained in terms of a normal abstraction reaction by a methyl radical. The relative yield of methane to ethane found in the vapor phase radiolysis appears to be too large compared to the ratio found in the photolysis of acetone[6–9] to be explained completely in terms of thermal radical reactions. A similar effect was found in the radiolysis of methyl ethyl ketone and diethyl ketone.[3] In view of the results cited, a thermal radical mechanism by itself might be insufficient to account for the product distribution obtained in the vapor-phase radiolysis of small aliphatic ketones.

In order to investigate this point further, the radiolysis of biacetyl vapor has been studied over the pressure range 5 to 30 mm. at 25, 120 and 200° by use of a pulsed electron beam current from a 4.2-Mev. microwave linear accelerator. In several experiments the pulse rate was varied, and in two experiments the current was varied. To determine microscopic dose-rate effects at 25° a few experiments were carried out with lower electron beam currents from a 2-Mev. Van de Graaff accelerator. Iodine scavenging experiments also have been run at each of these temperatures.

Experimental

Eastman Kodak White Label biacetyl was purified by a method similar to that of Groh.[10] It was dried by allowing the liquid to stand overnight under vacuum and in contact with pre-ignited anhydrous sodium sulfate. After it was dried, the biacetyl monomer was vacuum distilled from the polymer and degassed by trap-to-trap distillation *in vacuo*. It was finally distilled onto another sample of pre-ignited anhydrous sodium sulfate in the storage bulb to stand overnight. The biacetyl prepared in this manner was found to be free of impurities by both mass spectrographic and vapor chromatographic analysis. It was stored in an ampoule on the vacuum line at −80° until used. Aside from the formation of possible traces of photolysis products, it was

(1) This work was performed under the auspices of the U. S. Atomic Energy Commission.

(2) Author to whom requests for reprints are to be addressed.

(3) P. Ausloos and J. F. Paulson, *J. Am. Chem. Soc.*, **80**, 5117 (1958).

(4) J. D. Strong and J. G. Burr, *ibid.*, **81**, 775 (1959).

(5) J. C. McLennan and W. L. Patrick, *Can. J. Res.*, **5**, 470 (1931).

(6) P. Ausloos and E. W. R. Steacie, *ibid.*, **33**, 47 (1955).

(7) W. A. Noyes, Jr., G. B. Porter and J. E. Jolly, *Chem. Revs.*, **56**, 49 (1956).

(8) R. K. Brinton and E. W. R. Steacie, *Can. J. Chem.*, **33**, 1840 (1955).

(9) P. Ausloos, *ibid.*, **36**, 400 (1958).

(10) H. J. Groh, *J. Chem. Phys.*, **21**, 674 (1953).

found possible to store solid biacetyl at −80° for more than a month under these conditions without repurification.

The Pyrex bombardment cells were cylinders, 5.4 cm. in diameter and 60 cm. long. One end of the cell was a thin concave window through which the electron beam was directed; the other end was fitted with a glass break-seal to facilitate analysis. The clean dry cell was evacuated and flamed. When the cell was cool, the biacetyl vapor was admitted to the desired pressure as read on an oil multiplying manometer. The cell was isolated and a sample of the biacetyl vapor checked by mass spectrometric analysis for the absence of air, water and other contaminants. After this check, the biacetyl in the bombardment cell was condensed in a liquid nitrogen cooled finger at one end of the cell and the cell was sealed off.

Irradiations were made using a microwave linear electron accelerator (Linac) at the Lawrence Radiation Laboratory. This produces a pulsed beam of electrons with a pulse length of 5 microseconds and a pulse current variable from 10 to 100 milliamperes. The pulse repetition rate is variable. Most irradiations were made at 50 ma./pulse and 30 pulses per second. The electrons have a mean energy of about 4.2 Mev. and hence traverse the entire target cell in gas phase work. Because of scattering in the windows, the entire cell, except for a small region at the front, was covered by the beam, though variations in intensity undoubtedly occurred along the length of the cell. During this work it was found that the reproducibility of individual pulses from this accelerator probably was not better than ±20%, and variations in dose and dose rate were occurring within these limits. A regulating circuit later was added to the injector and deviations were reduced to about ±5%. Most of the work reported here was done without the additional regulation. The Van de Graaff accelerator used was a 2 Mev. High Voltage Engineering Company machine at the California Research Corporation. Owing to insensitivity of the current metering systems in both the Linac and Van de Graaff installations, measurements of the integrated beam current at the levels of operation used were only approximate.

In early bombardments at room temperature the cells, cooled only with an air blast warmed to about 35° during the irradiation. In Van de Graaff experiments the cells were immersed in a water tank to reduce the temperature rise to less than 1°, and in later microwave accelerator bombardments the cells were fitted with water jackets and the water temperature controlled to 25°. If the bombardment was to be carried out at elevated temperatures the cell was inserted into a thick wall brass tube, 70 mm. o.d. and 85 cm. long. This was wrapped with three 300 watt heating tapes connected in parallel, then with asbestos tape and, finally, with glass wool matting. The power to the heaters was controlled manually by means of a variable transformer. The temperature of the system was determined by a thermocouple inserted near the middle of the brass oven. The temperature variation along the length of the oven was less than 2 at 200°. After some experience, the temperature of the cell could be controlled to ±2° during bombardment.

In experiments where I_2 was added, the cell was equilibrated at 25° with I_2 vapor, this was then frozen out in a side-arm tube connected with a stopcock, the biacetyl added to the desired pressure, frozen out and the I_2 added from the sidearm. If more than 0.31 mm. I_2 pressure were added, it was achieved by making multiple equilibrations of the cell and respectively freezing each in the sidearm. Blank experiments in which the I_2 was titrated with sodium arsenite indicated that the system used achieved 88% saturation of I_2 at 25° in the two minute time allowed for equilibration. Blank experiments also showed the thermal reaction between iodine and biacetyl at 200° to be negligible in one hour of heating. Stopcocks through which I_2 was passed were greased with Fluorolube MG (Hooker Electrochemical Company). Some experiments at 25° were run with no stopcocks in the loading system. These gave the lowest yields.

After bombardment the cell was fitted with a stopcock and break-in device. The cell was then attached to the inlet of a Consolidated Electrodynamics Corporation Model 21-103A Mass Spectrometer, the connecting line evacuated, the break seal ruptured, and the mass spectrum of the total gas determined. The cell was then removed to a vacuum line where the gaseous products were separated into three fractions, volatile at −160°, volatile at −119°, and volatile at −80°. The PV of each fraction was measured and the mass spectrum of that fraction determined. The mass spectrum of the residual liquid also was run. Not all samples were subjected to all these measurements, but in all cases at least a −160° fraction was analyzed.

Most of the gaseous products were found to be in the −160° fraction, which consisted of H_2, C_2H_2, C_2H_4, CO, C_2H_6 and CO_2. The −119° fraction always constituted less than 10% of the total products (frequently less than 5%) and was found to contain mostly ketene (in the higher-temperature runs) and lesser amounts of C_2H_2, C_2H_4, C_2H_6, C_3H_4, C_3H_6, C_3H_8, CO_2 and possibly C_4H_{10}. Because this fraction was small it was analyzed only for the ketene and CO_2. Since acetylene forms a complex with ketones and appears partly in the incompletely analyzed −119° fraction,

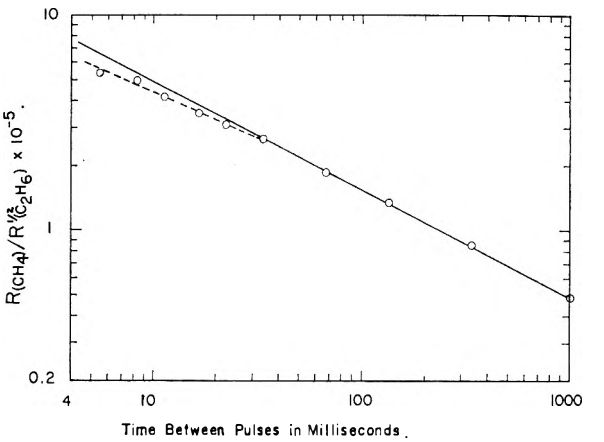

Fig. 1.—Plot of $R_{CH_4}/R^{1/2}_{C_2H_6}$ *vs.* time between pulses for the irradiation of biacetyl vapor at 25°, 20 mm. pressure, 50 ma. pulse current, and selected repetition rates. Points at high repetition rates have been corrected for falloff in pulse current by normalization to a constant CO yield/pulse. Points at 16.7 and 33.3 msec. are averages of several close points. Solid line is of slope $t^{-1/2}$.

the acetylene yields, although somewhat higher than the ethylene yields, are minimum yields. The −80° fraction consisted mainly of acetone and acetaldehyde in approximately equal amounts. The acetone was found to be incompletely removed from biacetyl at −80°, and therefore the acetone yield was estimated from the mass 58 peak in the mass spectrum of the total gas. It is possible that acetaldehyde was also incompletely removed and the acetaldehyde yields reported should be regarded as minimal. A small peak in the mass spectrum of the total gas at mass 100 was assumed to be all due to acetyl propionyl and a yield was estimated on this basis. Some very small peaks in the total mass spectrum at masses 101, 102 and 128 were not identified but probably arose from products of additions of H atoms, methyl radicals, or acetyl radicals to biacetyl during radiolysis. Acetone, acetyl propionyl and acetic acid were identified by gas chromatography and mass spectrometry in the residual liquid.

Results and Discussion

Products and Yields.—Approximate yields of products, expressed as molecules of product per 100 e.v. absorbed, have been calculated for the major radiolysis products and are listed in Table I. These values are normalized to a constant H_2 yield, as this product was found to be almost independent of variations in the radiation parameters. The dose calibration was done in a special target cell consisting of a 12-liter flask with a thin window blown in one side. The geometry of this cell was such that all electrons, except the few scattered at very wide angles, had approximately the same path length through the cell. Hence the energy absorbed was calculated from the mass of biacetyl in the path and the mass absorption coefficient of

4 Mev. electrons. Such runs were limited to 25°. As some product yields are dependent on pulse rate, total dose, pressure, or pulse current, these G-values should be used only as guides to the order of magnitude of yields under other conditions of irradiation.

TABLE I

YIELD[a] OF PRODUCTS FROM THE IRRADIATION OF BIACETYL VAPOR WITH ELECTRONS

Temperature	G (product) at temp. specified 25°	120°	200°
Product			
H_2[b]	0.55	0.55	0.55
CH_4[c]	.22	1.4	5.9
C_2H_2	.15	0.15	0.15
C_2H_4	.06	0.1	0.2
C_2H_6	2.0	2.2	1.8
CO	7.4	9.2	16
C_3H_6	0.03	..	...
C_3H_8	.06	..	...
CO_2	.1	0.4	0.6
CH_2CO[c,d]	.5	0.7	2.0
CH_3CHO	.3	0.4	0.3
CH_3COCH_3[c]	1.1	1.1	2.4
$CH_3CH_2COCOCH_3$	0.3	0.5	0.7

[a] Values listed are for irradiation with a pulsed beam, 5 μsec./pulse, 50 ma. pulse current, 30 pulses/sec., 90 min. irradiation, and 20 mm. biacetyl (measured at 25°), and cell geometry described in experimental section. [b] Values normalized on H_2 yield which apparently is dependent only on amount of radiation absorbed. Yields probably are accurate to ±20%. [c] Value depends on radiation parameters. [d] Not found in all irradiations at 25 and 120°; behavior is erratic.

A few other products are present in small yield and analyses for them were not feasible nor was the identification certain in all cases. These include methylacetylene, diacetylene, vinylacetylene, butadiene, vinyl methyl ketone, acetic acid (yield at 25° about equal to that of acetyl propionyl), and at least two unidentified products boiling higher than acetyl propionyl.

Effects of Experimental Parameters at Room Temperature.—The effect of pressure, total dose, and pulse repetition rate, and the effect of a continuous beam as compared to a pulsed beam were studied at 25°. Table II summarizes these data. The outstanding feature of these results is the small effect of these experimental parameters on the relative yields of the various products. Within experimental error the yield of C_2H_6/CO, H_2/CO and CO_2/CO are constant. The ratio of CH_4/C_2H_6 increases slightly with increasing pressure and with total dose. This latter ratio is lower in the Van de Graaff runs than in the Linac runs. On the other hand the ratio CH_4/C_2H_6 is higher in the 12-liter cell where dead space exists. This result is expected where diffusion of methyl radicals into areas of low radical density is possible. The apparent agreement in $R_{CH_4}/R_{C_2H_6}^{1/2}$(B) (hereafter designated as Z) between the Linac and the Van de Graaff runs at the same pressure probably is fortuitous. If a different pulse rate on the Linac had been chosen, the agreement would not have been as good.

The effect of pulse rate gives a measure of radical lifetime in the system. If one considers the disappearance of methyl radicals to form ethane, then a single 5 μsec. pulse at 50 ma. current will yield an initial methyl radical concentration of 0.7×10^{12} radicals per ml. (assumed equal to the CO yield). Using the rate constant for methyl radical recombination of $10^{13.6}$ mole^{-1} cc. sec.$^{-1}$,[11] the calculated time to reduce the methyl radical concentration to half its initial value is 22 milliseconds. Because methyl radicals also disappear by reaction with other radicals, *e.g.*, with acetyl, this probably represents a maximum value.

If $R_{CH_4}/R_{C_2H_6}^{1/2}$ for each pulse rate (at constant pressure) is plotted against the time between pulses, and if each pulse is an individual event, then the points should follow a line proportional to $t^{-1/2}$. On the other hand, if the pulses are overlapping, there should be a deviation from this line. In Fig. 1, this has been plotted and it is apparent that the deviations from the $t^{-1/2}$ law start at about 30 milliseconds between pulses. Therefore the mean radical life in this system must be less than 30 milliseconds. The agreement between the calculated value of 22 milliseconds and the curve is sufficient to conclude that the bulk of the methane and ethane must be formed by thermal radical reactions at room temperature. A small increase in the ratio $R_{CH_4}/R_{C_2H_4}$ with time between pulses was observed even to times of one second between pulses. This observation might be interpreted as indicating the existence of a few very long lived methyl radicals in the system, these disappearing mainly by abstracting hydrogen from biacetyl.

Experiments at Elevated Temperatures.—The results of ten experiments at 120° and four experiments at 200° are shown in Table III. Although the ratio of H_2, CO, C_2H_6 and CO_2 do not change with pressure, the relative yield of methane increases with pressure at both 120 and 200°. At 200° the relative yield of ketene increases directly with pressure. Hydrogen and ethane show no temperature coefficient. The No. 88 series of experiments shows a small effect of total dose on the products. Whereas the rate of H_2/CO is constant, the ratio C_2H_6/CO decreases with total dose and the ratios CH_4/CO and CO_2/CO increase with dose. This would lead one to infer that a reaction product is competing for the ethane precursors. At the lower and higher beam currents in expts. 87A and 87B, the ratios of CH_4/CO and C_2H_6/CO definitely indicate more methane to result at 10 ma. than at 80 ma. beam current.

Iodine Scavenger Experiments.—The results of adding I_2 vapor as a radical scavenger are shown in Table IV. These results have been converted to G-values for comparison with Table I. The yield of CO at 25° was used as a basis for the conversion from the yield of product per unit time of irradiation to G-values.

In all cases the yield of CH_3I is about equal to the yield of CO. While the CO does show a small temperature variation in the presence of I_2, this is not much beyond the variations in CO yield at 25°, and is much less than found in the absence of iodine. It is also curious that in several cases the I_2 uptake was measured and while the variations were fairly large (±20%), at 25 and 120° the I_2

(11) R. Gomer and G. B. Kistiakowsky, *ibid.*, 19, 85 (1951).

TABLE II

RADIOLYSIS OF BIACETYL VAPOR AT ROOM TEMPERATURE

Electron source	←Microwave linear accelerator→								Van de Graaff		
Variable	←Pressure→				←Total dose→			Geom.[a]			
Experiment no.	75A	75B	75C	75D	89A	89B	89C	85D	79B	82C	84B
Pressure (mm.)[c]	5	10	20	30	20	20	20	20	5	20	20
Beam current (ma.)	50	50	50	50	25	50	50	50	22.5 μa[b]	22.5[b]	50[b]
Bomb time (min.)	90	90	90	90	20	40	120	90	30	30	13.5
Temp., °C.	25–35	25–35	25–35	25–35	22.5	22.5	22.5	25–35	25–50	25	25
H_2	4.77	7.23	15.62	19.50	1.80	7.09	19.75	11.72	1.68	7.29	4.77
CH_4	1.73	2.73	6.22	8.73	0.63	2.85	7.34	5.08	0.77	2.20	1.61
Product C_2H_2[d]	...	...	...	...	0.41	1.49	3.64	1.92	0.26	0.24	0.49
yields C_2H_4	1.02	0.73	1.25	3.22	0.27	1.66	2.07	0.84	0.41	1.07	0.28
(μmoles) C_2H_6	15.8	25.3	53.4	69.2	6.59	27.21	65.35	38.77	7.32	22.4	15.96
CO	63.5	93.0	209.7	258.5	22.7	97.0	239.6	144.7	25.8	97.2	63.1
CO_2	0.89	1.61	3.07	4.64	0.33	2.43	6.6	1.29	...	..	0.54
$R_{CH_4}/R_{C_2H_6}$	.109	0.108	0.116	0.126	.096	0.105	0.112	0.131	0.105	0.098	.101
$R_{C_2H_6}/R_{CO}$	.249	.272	.255	.268	.290	.281	.272	.267	.284	.230	.253
R_{H_2}/R_{CO}	.075	.078	.074	.075	.079	.073	.082	.081	.065	.075	.076
$[R_{CH_4}/R_{C_2H_6}^{1/2}$ [B)] $\times 10^{13}$	8.58	5.25	4.18	3.34	2.55	4.03	3.86	...	9.70	3.95	5.11

[a] Irradiation cell was 12 liter spherical flask. [b] Continuous beam, beam current in μamp. [c] Volume of cells = 1100 ± 50 ml. [d] Minimum yield.

TABLE III

RADIOLYSIS OF BIACETYL VAPOR AT ELEVATED TEMPERATURE

Variable	←Pressure→			←Total dose→			←Dose rate→		←Pressure→			
Run no.	78B	78A	78C	88A	88B	88C	87A	87B	83A	83B	83C	83D
Temp., °C.	110–130	110–130	110–130	120	120	120	120	120	200	200	200	200
Pressure (mm.)[a]	5	20	30	20	20	20	20	20	5	10	20	30
Beam current (ma.)	50	50	50	50	50	50	10	80	50	50	50	50
Time bombardment (min.)	90	90	90	20	40	120	450	45	90	90	90	90
H_2	2.62	11.4	24.3	4.48	7.16	22.8	15.7	11.6	5.17	6.82	15.64	19.76
CH_4	5.92	42.6	113.8	9.11	17.35	59.3	45.5	29.0	28.7	62.1	167.7	279.6
C_2H_2[b]	0.5	1.4	4.6	0.8	1.5	4.3	...	2.3	1.1	1.7	3.3	9.8
Product C_2H_4	0.5	1.2	3.2	0.4	1.1	2.7	...	2.4	1.9	3.4	5.9	7.5
yields C_2H_6	10.4	46.3	93.1	20.6	32.7	89.7	53.8	52.6	17.25	24.1	45.7	79.4
(μmoles) CO	52.8	223	489.6	74.9	124.7	369.2	261.5	203.3	103.7	192.7	428.2	709.7
CO_2	...[c]	7.9	23.5	2.5	4.6	17.0	6.6	8.9	4.4	7.2	12.8	22.6
CH_3CHO	...	...	6.7	3.5	7.0	13.9	10.5	9.4	2.8	5.4	6.3	6.9
CH_2CO	...	11.0	39.8	...	...	...	...	...	0.3	11.6	55.7	131
$(CH_3)_2CO$	...	25	10	...	10	43	16	25	13	33	68	106
CH_3B[d]	...	9.8	6.6	...	8.8	14.0	4.4	11.0	4.9	11.5	18.5	22.7
CH_4/C_2H_6	0.57	0.92	1.22	0.44	0.53	0.66	0.85	0.55	1.66	2.57	3.67	3.52
C_2H_6/CO	.197	.208	0.190	.275	.262	.243	.206	.259	0.166	0.125	0.107	0.112
H_2/CO	.051	.051	0.050	.060	.057	.062	.060	.057	0.050	0.035	0.036	0.028
$[R_{CH_4}/R_{C_2H_6}^{1/2}$ (B)] $\times 10^{12}$	3.6	3.1	3.9	2.10	2.24	2.67	1.36	2.77	13.5	12.4	12.2	10.3

[a] Pressure measured at 25°. Vol. cells 1100 ± 50 cc. in each case. [b] Minimum yield. [c] Blanks refer to no determination of the product in these runs. [d] Acetyl propionyl.

used is approximately equal to the CH_3I found. At 200° the I_2 uptake was about twice the CH_3I found, but the results at 120 and 200° are single experiments.

At room temperature, iodine reduces the yields of H_2, CO, C_2H_2 and CO_2 by about 25-30%. Methane is reduced by 85% and ethane by 99%. The methane result was, however, extremely variable, and apparently trace impurities (unidentified) were able to greatly increase this figure. In one case a value of methane was found in the presence of I_2 which was 2.5 times as large as that found in the absence of I_2. Such large variations in the yield of methane were not observed in the absence of I_2, so the effect probably is specific for the presence of iodine. These observations cast a doubt on whether or not there would be any methane which would not be scavenged by I_2 in an ideal experiment.

At high temperatures the amount of methane not scavenged by I_2 increases slightly, but the temperature coefficient is small compared to that observed in the absence of iodine. One can thus conclude that most of the methane and essentially all the ethane is produced by a precursor which is scavenged by I_2. Presumably this precursor is the methyl radical. The results on iodine uptake indicate the acetyl radical either to be not scavenged (which we find difficult to believe), or the acetyl iodide undergoes a further reaction to regenerate iodine, either in the cell or in the titration of the excess iodine after separation.

Table IV

Yields of Products from the Irradiation of Biacetyl Vapor plus Iodine Vapor with Electrons

Temp., °C.	25[a]	120	200
I_2 pressure, mm.	0.3	0.9	0.9
Biacetyl pressure, mm.	20.0	20.0	20.0
Product[c]	——G for product——		
H_2	0.38	0.35	0.49
CH_4	.03[b]	.07	.22
C_2H_2	.1	.09	.14
C_2H_4	.03	.02	.05
C_2H_6	.02	.02	.01
CO	6.3	5.5	8.4
C_3H_6	0.013	...	...
C_3H_8	.006	...	...
CO_2	.07	0.07	0.16
CH_3I	5.9	5.2	7.7
I (atoms used)	6.4	5.3	14.8

[a] Represents average values from 7 experiments. Values at 120 and 200° are single experiments. 5 and 10 minute irradiations at 25°, 15 minute at 120 and 200°. Beam conditions 50 ma./pulse, 30 pulses/sec. [b] Result variable. Value listed represents lowest values found. [c] Acetone, ketene, acetaldehyde and acetyl propionyl were not studied.

Mechanism.—It is apparent from the studies at 25° that most of the products must arise from a mechanism which is essentially independent of dose rate, total dose and biacetyl pressure. Iodine scavenging shows the precursors of ethane and most of the methane to be scavenged at all temperatures, and presumably these precursors are thermal methyl radicals. Ion molecule reactions for the production of methane do not appear likely as only two peaks in the mass spectrum of biacetyl appear (from pressure dependence measurements) to have an ion molecule origin. One is at mass 129 and presumably arises from the reaction

$$CH_3CO^+ + (CH_3CO)_2 \longrightarrow (CH_3CO)_3^+ \quad (1)$$

whereas the other is a mass 59 and may arise from the reaction

$$CH_3^+ + (CH_3CO)_2 \longrightarrow CH_3(CH_3CO)_2^+ \longrightarrow CH_2CO + (CH_3)_2CHO^+ \quad (2)$$

It is difficult to see how these ion molecule reactions can contribute to methane, though reaction (2) might contribute to ketene and acetone. Similarly excited molecule reactions might contribute but little is known about reactions of this type. However, products such as acetylene, diacetylene, methyl vinyl ketone, and butadiene may arise from highly excited precursors. Except for hydrogen and a small fraction of the methane, the results are indicative of a thermal radical mechanism for the major products. Since such a mechanism has been suggested to account for photolysis and pyrolysis experiments[12-17] it appears reasonable to modify these mechanisms to account for the radiolysis results. Stief and Ausloos[18] have used thermal radical reaction in a proposed mechanism for the radiolysis of azomethane vapor. Such a mechanism must account for the following results. (1) The relative yields of radiolysis products are essentially dose, dose rate and pressure independent at 25°. (2) Iodine scavenger reduces methane by about 80%, H_2 by 20% and ethane by essentially 100%. (3) The rates of hydrogen and ethane production are essentially independent of temperature while the methane shows a temperature coefficient which increases with temperature.

The failure to completely scavenge the hydrogen may be caused by hot radical reactions, molecular detachment, or failure of I_2 as an H atom scavenger. It is not easy to formulate reactions in which molecular detachment can occur to leave stable products. Therefore most of the hydrogen is postulated to occur by a hot radical mechanism and it is possible that a small part of the methane is also formed by a hot radical mechanism. Since ion neutralization might be expected to yield highly excited species, it is not unreasonable that such reactions occur.

The following sequence represents the mechanism suggested

Radical Formation.—

$$(CH_3CO)_2 \longrightarrow CH_3 + CO + CH_3CO \quad (3)$$
$$\longrightarrow CH_3CO + CH_3CO^* \quad (4)$$
$$\longrightarrow H^* + CH_2COCOCH_3 \quad (5)$$
$$CH_3CO^* \longrightarrow CH_3 + CO \quad (6)$$
$$CH_3CO \longrightarrow CH_3 + CO \quad (7)$$
$$H^* + M \longrightarrow H + M \quad (8)$$

Reactions 3, 4 and 5 should not be regarded as elementary kinetic steps since the formation of these species may be the result of ion neutralization as well as direct energy absorption. There is no evidence of reaction 8 in this investigation and reaction 7 becomes of importance only at elevated temperatures. Sheats and Noyes[14] have shown their photolysis data to be generally consistent with an initial fragmentation according to reaction 3 rather than fragmentation into two acetyl radicals.

Product Formation. Hydrogen.—

$$H^* + (CH_3CO)_2 \longrightarrow H_2 + CH_2COCOCH_3 \quad (9)$$
$$H + H + M \longrightarrow H_2 + H \quad (10)$$

The bulk of the hydrogen must be formed by reaction 9 and its thermal analog or by a molecular process. Since the H atom concentration is low, the absence of a temperature coefficient for H_2 production is not necessarily an unequivocal criterion for the presence of hot H atoms. The direct combination of H atoms with a third body is probably of little importance as the yield of H_2 is independent of geometry and pressure. Furthermore, carbonyl compounds are known[4] to be scavengers for thermal H atoms so they should have a very short lifetime in this system. The ultimate products of a reaction such as reaction 11 are not known.

$$H + (CH_3CO)_2 \longrightarrow CH_3COCOHCH_3\ (?) \quad (11)$$

Methane.—

$$CH_3^* + (CH_3CO_2) \longrightarrow CH_4 + CH_2COCOCH_3 \quad (12)$$
$$CH_3 + (CH_3CO)_2 \longrightarrow CH_4 + CH_2COCOCH_3 \quad (13)$$
$$CH_3 + CH_3CO \longrightarrow CH_4 + CH_2CO \quad (14)$$

(12) P. Ausloos and E. W. R. Steacie, *Can. J. Chem.*, **33**, 39 (1955).
(13) F. E. Blacet and W. E. Bell, *Disc. Faraday Soc.*, **14**, 70 (1953).
(14) G. F Sheats and W. A. Noyes, Jr., *J. Am. Chem. Soc.*, **77**, 1421 (1955).
(15) G. F. Sheats and W. A. Noyes, Jr., *ibid.*, **77**, 4532 (1955).
(16) J. Heicklen and W. A. Noyes, Jr., *ibid.*, **81**, 3858 (1959).
(17) E. W. R. Steacie, "Atomic and Free Radical Reactions," Reinhold Publ. Corp., New York, N. Y., 1954, p. 354.
(18) L. J. Stief and P. Ausloos, Paper presented at the 138th meeting of the Amer. Chem. Soc., New York, September, 1960.

Ethane.—

$$CH_3 + CH_3 \longrightarrow C_2H_6 \quad (15)$$

Carbon Monoxide.—Reactions (3), (6) and (7).

Acetone.—

$$CH_3 + CH_3CO \longrightarrow CH_3COCH_3 \quad (16)$$
$$CH_3 + (CH_3CO)_2 \longrightarrow CH_3COCH_3 + CH_3CO \quad (17)$$

Ketene and Acetaldehyde.—

$$2CH_3CO \longrightarrow CH_2CO + CH_3CHO \quad (18)$$
$$CH_2COCOCH_3 \longrightarrow CH_2CO + CH_3CO \quad (19)$$

Acetyl Propionyl.—

$$CH_3 + CH_3COCOCH_3 \longrightarrow CH_3CH_2COCOCH_3 \quad (20)$$

Except for the formation of H_2 and the hot methyl reaction (12), all of these reactions have been proposed in photolysis studies.

At 25°, reaction 14 must account for the bulk of the methane, with reaction 12 accounting for less than 20% of it and reaction 13 another 20% or so if one assumes Ausloos and Steacie's value of 0.65×10^{-13} for the function Z to represent the limiting value of the methane formed by abstraction by thermal radicals. These reactions thus account for the observation of a low activation energy near room temperature and for the relative independence of the methane/ethane ratio with pressure, dose rate, etc. The ratio of CH_4/C_2H_6 was significantly higher in the 12-liter flask where the radical could escape to a region of low radical concentration where reaction 13 would become significant. Reaction 14 has been shown to be of importance in the room temperature photolysis of biacetyl[12] and acetone.[6]

At elevated temperatures, reaction 13 is expected to become the major methane source. The evidence indicates it to do so. The activation energy for methane formation was an average of 4.7 kcal. between 25 and 120°, and 7.0 kcal. between 120 and 200°. This latter figure agrees with the photolysis results of Blacet and Bell,[14] but is lower than those of Ausloos and Steacie. This, together with the high values of the function Z at 120 and 200° compared to those of Ausloos and Steacie[12] and Sheats and Noyes[15] indicate that under the high intensity conditions of our irradiations, reaction 14 may be a significant contributor to methane production even at 200°.

At all temperatures the material balance of $CH_4 + 2(C_2H_6)$ is about 55% of the CO yield. If acetone and acetyl propionyl are added, about 80% of the CO yield is accounted in terms of methyl radical utilization. The fate of the remaining 20% of methyl radicals is not known. The mechanism described does not account for the unsaturated hydrocarbons or for CO_2. The latter compound does not appear to be a secondary product as its formation is approximately a linear function of total dose and pressure.

In experiments 87A and 87B, the effect of dose rate was compared and relatively more CH_4 was found at the low dose rate than at the higher dose rate. This is expected from the mechanism and the contribution of reaction 13 to methane formation at 120°.

The effect of temperature and pressure on the yields of acetone and ketene can be ascribed to the increased importance of reaction 17 to the production of acetone and reaction 19 to the production of ketene at elevated temperatures.

It is clear that the basic free radical mechanism which has been postulated to explain the photolysis of biacetyl, can also be used to explain qualitatively the major products in the radiolysis of biacetyl. Small contributions to methane at room temperature and most of the hydrogen production may be ascribed to "hot" radicals, though other mechanisms have not been completely eliminated. No mechanism has been proposed for the formation of unsaturated hydrocarbons and carbon dioxide, which products are not reported in the photolysis of biacetyl.

Acknowledgments.—The authors wish to thank Mr. William Everette for aiding in the electron irradiations with the microwave linear accelerator, and to Dr. K. L. Hall and Mr. Norman Shields of the California Research Corporation for use of their Van de Graaff accelerator and for aid in the irradiations with it. The authors also wish to thank Dr. Peter Ausloos of the National Bureau of Standards for helpful suggestions and criticisms.

PHASE BEHAVIOR AND THERMAL PROPERTIES OF THE SYSTEM NH_4F–HF[1]

BY ROBERT D. EULER AND EDGAR F. WESTRUM, JR.

Department of Chemistry, University of Michigan, Ann Arbor, Michigan

Received October 12, 1960

The system NH_4F–HF was studied by thermal analysis between the limits NH_4HF_2 and HF. No indication of the composition $NH_4H_2F_3$ previously reported by Ruff and Staube was found. Low temperature heat capacity measurements on four compositions approximating $NH_4H_3F_4$ confirmed and extended the thermal analysis and revealed the existence of a solid solution at this composition. Several thermal anomalies were found between 180°K. and the melting point. The decomposition pressure of $NH_4H_3F_4$ was also determined.

Introduction

Ruff and Staube[2] investigated the NH_4F–HF system over a composition range from 50 to 85 mole % HF. Their data indicated the occurrence of the congruently melting compounds NH_4HF_2, $NH_4H_2F_3$, $NH_4H_3F_4$ and $NH_4H_5F_6$, as well as a solid phase invariance occurring at −3° extending over the entire composition range investigated.

(1) From the dissertation of R. D. Euler submitted in partial fulfillment of the requirements of the Doctor of Philosophy Degree at the University of Michigan.

(2) O. Ruff and L. Staube, *Z. anorg. allgem. Chem.*, **212**, 399 (1933).

Analysis of the NH_4F–HF system was undertaken to extend the solid–liquid equilibrium over the entire composition range, with the further intention of investigating the unusual solid–solid transition calorimetrically. A thermal analysis of the system over the composition range from NH_4F to NH_4HF_2 has been made recently in this Laboratory.[3] In extending the phase behavior study to higher relative HF concentrations, important deviations from the data of Ruff and Staube were found in many features of the system. Melting point maxima occur at compositions corresponding to $NH_4H_3F_4$ and $NH_4H_5F_6$, but at lower temperatures than those previously reported. Furthermore, neither the compound $NH_4H_2F_3$ nor the indicated (−3°) solid–solid transition were found. Since the transition of original interest was not observed, four samples near $NH_4H_3F_4$ in composition were prepared for equilibrium calorimetric study to verify the new findings.

Experimental

Preparation of Ammonium Monohydrogen Difluoride.—NH_4HF_2 was prepared by addition of 48% aqueous HF to analytical reagent $(NH_4)_2CO_3$ in a large silver beaker to obtain a mole ratio of HF to NH_3 of slightly less than two. The resulting solution then was boiled to expel CO_2 and allowed to cool to room temperature with the formation of large acicular crystals of NH_4HF_2. After decanting the supernatant liquid, the crystals were allowed to air-dry for an hour and then were placed in a polyethylene beaker and evacuated for 40 hours. Spectrographic analysis of NH_4HF_2 prepared by this method shows no silica or water and only a trace of silver.

The samples were analyzed by titration of the excess HF with standardized 0.1 *N* NaOH solution using brom thymol blue as indicator. Phenolphthalein also was used as an indicator and yielded more reproducible results if the solution being titrated was cooled to the ice point. As a check on the acidimetry, the fluoride was determined gravimetrically by the precipitation of PbClF and good agreement (±0.15% of theoretical) was obtained.

Preparation of Ammonium Trihydrogen Tetrafluoride.—The preparation of the four calorimetric samples approximating $NH_4H_3F_4$ was accomplished by addition of HF to the NH_4HF_2 prepared and analyzed as described above. The NH_4HF_2 was weighed into a small, Monel reactor, with a Teflon-gasketed port and a needle valve for addition of a weighed increment of vacuum-distilled high purity anhydrous HF. The samples of $NH_4H_3F_4$ thus prepared by weight were further analyzed by acidimetric titration of HF with standardized 0.1 *N* NaOH to the phenolphthalein end-point and by Kjeldahl nitrogen determination. Water was not detected with Karl Fischer reagent although the practical lower limit of sensitivity of the test on this substance was 0.1% by weight.

Thermal Analysis Method.—The thermal analysis of the NH_4F–HF system was achieved with a ten-junction, copper-constantan thermel with reference junctions at the ice point and a millivolt potentiometer. The thermel was calibrated at the ice point, the carbon dioxide sublimation point, the oxygen boiling point, and compared between 273 and 373°K. with a thermometer certified by the National Bureau of Standards. Deviations from a standard thermocouple table were then interpolated from these data. The 155-ml. sample container consisted of a copper cylinder 5 cm. dia. by 7.5 cm. length and 0.7 mm. wall. Two copper ends, 0.7 mm. thick, were force-fitted against shoulders and silver-alloy-brazed in place. An axial Monel filling tube 9 mm. dia. by 6 cm. length was provided with a Teflon-packed needle valve at the upper (free) end to facilitate the addition or removal of increments of HF gas. A thermocouple well of 2 mm. dia. thin-wall Monel entered off-center through the cover and was so inclined that the end was centered 1.3 cm. from the bottom. The interior was deoxidized by heating in hydrogen and the exterior was buffed to a high polish. Samples of NH_4HF_2 were introduced into the container and vacuum corrected using the crystallographic density. Changes in composition were effected by addition of 99.8% anhydrous HF, distilled under vacuum into the sample container cooled with liquid nitrogen. The composition change was calculated on the basis of the difference in weight of the sample container before and after addition of HF.

The container was packed into two coaxial glass tubes with glass wool. An electrical heater was wound on the inner tube and the system partially immersed in a Dewar containing an appropriate cooling bath and centering rings of Styrafoam. No shaking was found necessary during the cooling curves and supercooling was infrequent.

Cryostat and Calorimeter.—The Mark I cryostat used was similar to the one described by Westrum, Hatcher and Osborne.[4] The adiabatic determinations of heat capacity were made by measuring the temperature increment produced by a measured electrical energy input. Current and potential measurements were made on the electrical heater during the input of energy and on the capsule-type platinum resistance thermometer during drift periods. An autocalibrated White double potentiometer was used in conjunction with a galvanometer having a sensitivity of 0.01 μv./mm. as used. Energy exchange between the calorimeter and surroundings was virtually eliminated by maintaining an adiabatic shield at the calorimeter temperature. Durations of the inputs were given by a timer operated by a thermostated, vacuum-jacketed, tuning fork.

The International Temperature Scale region was established by measurements of the resistance of the platinum thermometer (laboratory designation A-3) at the boiling point of oxygen, the steam point, and the boiling point of sulfur performed by the National Bureau of Standards and evaluation of the constants in the Callender–Van Dusen equation. Below the oxygen point the thermometer was calibrated by comparison with the Bureau's scale.[5]

Because an electrolytic reaction between lead–tin solder fused to copper and the $NH_4H_3F_4$ takes place, a silver calorimeter with a Teflon closure was constructed with all seams silver-alloy-brazed. This calorimeter (laboratory designation W-8) was basically similar to one already described[6] and had a measured internal volume of 88.21 ml. Twenty-four stamped, perforated silver vanes 0.02 mm. thick were stacked so as to fit firmly against the heater well and the cylindrical calorimeter wall. A Monel screw cap closure with a Teflon gasket was provided for introduction of the sample. This closure could be operated from outside the vacuum system and was vacuum-tight near 300°K. To positively prevent leakage at low temperature the closure was further secured by 50–50% by weight Pb–Sn solder. Small corrections were made for slight differences in weight of the Teflon gaskets using data on the heat capacity of molded Teflon.[7] Apiezon-T grease was used in weighed amount to establish thermal contact between calorimeter, heater sleeve and thermometer. The heat capacity of the calorimeter (empty except for helium gas) was determined separately. It contributed from 1 to 25% of the total heat capacity measured.

Loading the sample consisted of admitting the liquid into the calorimeter and screwing the cap against the Teflon gasket. The calorimeter then was placed in a glass system, cooled to liquid nitrogen temperature, the cap partially opened, and the system evacuated. Opening and closing of the calorimeter inside the glass system were accomplished with a special socket wrench attached to a running standard taper joint. One atmosphere pressure of helium was admitted, the calorimeter then warmed to room temperature, and the cap reclosed. Excess helium pressure could escape through the threads during the warming period. The calorimeter then was removed from the glass system and the cap soldered to the calorimeter. The correction for solder was minimized by re-

(3) E. Benjamins, G. A. Burney and E. F. Westrum, Jr., unpublished data.

(4) E. F. Westrum, Jr., J. B. Hatcher and D. W. Osborne. *J. Chem. Phys.*, **21**, 419 (1953).

(5) H. J. Hoge and F. G. Brickwedde, *J. Research Natl. Bur. Standards*, **22**, 351 (1939).

(6) D. W. Osborne and E. F. Westrum, Jr., *J. Chem. Phys.*, **21**, 1884 (1953).

(7) G. T. Furukawa, R. E. McCoskey and G. J. King, *J. Research Natl. Bur. Standards*, **49**, 273 (1952).

producing closely the weight of solder used on the empty calorimeter. A small correction for differences in the amount of helium present was made using the value for the density of liquid $NH_4H_3F_4$ at 300°K. of 1.30 g./ml. obtained in a rough pycnometric determination.

Results and Discussion

Thermal Analysis Measurements.—Five separate series of determinations were made, each employing a new sample of NH_4HF_2. The results are summarized in Table I and Fig. 1. Over the composition range 50 to 83.3 mole % HF the measurements were made between 403 and 223°K.; from 83.3 to 100 mole % HF from the melting point to 163°K.

TABLE I

THERMAL ANALYSIS DATA

Mole % HF	M.p. T, °K.	Eutectic T, °K.	Mole % HF	M.p. T, °K.	Eutectic T, °K.
		Series I			
			78.34	285.10	259.52
			79.54	279.07	258.02
51.27	395.91		80.47	273.60	258.57
52.39	395 49		81.54	264.92	258.57
53.79	391.75		81.76	262.82	258.65
54.98	388.90		82.26	259.67	258.82
56.13	386.21		82.69	261.40	258.67
62.48	349.05		82.90	262.07	258.43
63.25	338.25	267.70	87.91	200.15	171.32
66.04	303.47		88.28	193.95	172.08
69.27		267.27	89.20	174.82	172.15
			90.14	172.82	167.55
	Series II				
				Series III	
51.27	395.79	266.40			
56.94	379.21		74.18	293.83	
62.48	346.10	267.07	75.42	295.40	
65.96	302.63	266.75			
66.36	298.83	265.80		Series IV	
67.46	285.63				
68.09	276 13	267.50	82.97	262.90	255.67
69.08	270.40		83.47	264.62	
70.20		266.25	84.23	258.02	
70.99	278.15	266.00	86.47	226.60	
71.59	281.98	270.15	91.73	175.35	
73.44	289.78	266.00			
76.54	292.25			Series V	
76.68	291.38				
77.02	290.55	255.42	75.02	295.90	
77.81	287.70	255.75	74.99	296.25	

Several differences are evident between the data of Ruff and Staube[2] (dotted lines in Fig. 1) and those of the present investigation. The previously reported compound $NH_4H_2F_3$ was not observed. Moreover the eutectic temperatures and the melting points of $NH_4H_3F_4$ and $NH_4H_5F_6$ occur at considerably lower temperatures than those previously reported. The reported solid invariance did not appear. A comparison of the data of Ruff and Staube with those of this investigation is presented in Table II.

A single explanation for the discrepancies could not be found. Several factors may have contributed to the difference in results. The supposed solid invariance found by Ruff and Staube may have been in part confusion with the eutectic temperature of 266.5°K. The existence of 270, 292 and 290°K. halts may possibly have been due to a thermal conduction fluid used in the thermocouple well, or an impurity in the sample itself. The NH_4HF_2 sample used by Ruff and Staube melted at 397.8°K., whereas 399.3°K. was the orthobaric melting point obtained by Benjamins, *et al.*,[3] and confirmed here. This evidence suggests that their NH_4HF_2 was impure. The description of the experimental procedure of Ruff and Staube indicates that the HF used to alter the composition was poured into the copper system through a copper funnel, apparently in the open air. This method certainly involves some contamination by water since hydrogen fluoride is highly hygroscopic. If appreciable water were present in the system,

TABLE II

COMPARISON OF EQUILIBRIUM TEMPERATURES FOR THE NH_4F–HF SYSTEM

	Ruff and Staube[2]	This work
NH_4F–NH_4HF_2 eutectic	...	382.2 ± 0.4°K.
NH_4HF_2 melting point	397.8°K.	399.3 ± 0.1[a]
NH_4HF_2–$NH_4H_3F_4$ eutectic	292	266.7 ± 0 9
$NH_4H_2F_3$ melting point	301	...
$NH_4H_3F_4$ melting point	303	296.4 ± 0.5
$NH_4H_3F_4$–$NH_4H_5F_6$ eutectic	290	258.8 ± 0.3
$NH_4H_5F_6$ melting point	303	265.2 ± 0.5
$NH_4H_5F_6$–HF eutectic	...	172.6 ± 0.5
Solid–solid transition (50–85 mole % HF) (−3°)	270	...

[a] Including data from other work in this Laboratory[3] as shown on Fig. 1.

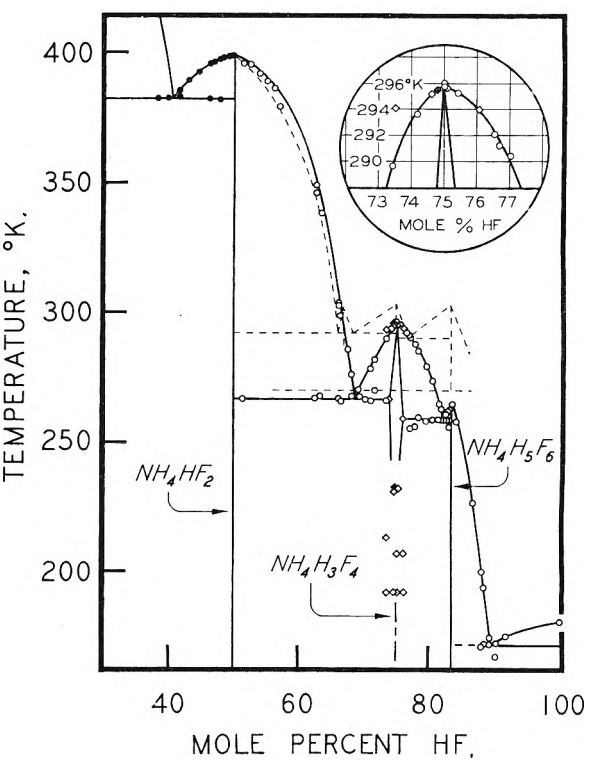

Fig. 1.—Partial phase diagram for the system NH_4F–HF. The open circles indicate thermal analysis data of this research, solid circles thermal analysis of Benjamins, *et al.*,[3] open squares calorimetric data from Samples A, B, C and D, and solid squares those from the preliminary sample. Dotted lines represent the diagram of Ruff and Staube.[2]

one would expect a break due to the NH_4HF_2–H_2O eutectic at 258.4°K.[8] There is, however, no evidence that Ruff and Staube studied the system to such low temperatures.

The existence of a hemi-hydrate of $NH_4H_2F_3$ was reported by Hassel and Kringstad in 1932.[9] The article, however, is very vague about experimental methods and the agreement between theoretical and analytically determined compositions is rather poor.

The discrepancy hardest to explain is that of the melting behavior over the composition range 65–86 mole % HF. As a further experimental check, compositions corresponding to the compounds $NH_4H_3F_4$ and $NH_4H_5F_6$ were prepared and allowed to stand in tightly sealed polyethylene bottles at 297–300°K. After more than six months, the material in both bottles remained in a completely liquid state.

Heat Capacity Data.—A sample of $NH_4H_3F_4$, upon which preliminary heat capacity measurements were made over the range 200 to 320°K., indicated an anomaly at 230°K. and a melting point of 295.85°K. with considerable premelting. It was suspected that since this sample had been transferred several times in the air it was quite impure. Consequently, another sample was prepared and analyzed. This sample was prepared by weight to be slightly richer in HF than the stoichiometric composition since it was considered that the preliminary sample might have been low in HF content. This sample, designated as Sample B, showed the same melting characteristics as found in the preliminary measurements but showed anomalous behavior below the melting point at 192 and 207°K. as well as a much smaller effect near the aforementioned 230°K.

In light of this unusually complex behavior, it was decided to prepare several samples, varying slightly from the stoichiometric composition, and to investigate their thermal properties. Samples A, C and D were prepared by appropriately altering the composition by weight of the previous sample with either NH_4HF_2 or anhydrous HF. Table III lists the four compositions investigated, together with a summary of the observed temperatures of melting and of heat capacity anomalies. The calorimetric samples varied in mass from 103 to 116 g.

TABLE III

SUMMARY OF CALORIMETRIC DATA ON $NH_4H_3F_4$

Sample	Mole % HF	M.p., °K.	Anomalies, °K.
A	76.08	294.2	192, 207, 254
B	75.05	295.9	192, 207, 232
C	74.62	295.4	192, 231
D	73.52	294.3	192, 213, 262

Experimental values of the heat capacities of Samples A, B, C and D are listed in Table IV as the "molal" values of heat capacity and energy but are arbitrarily calculated on the basis of 97.064 g., the mole weight of $NH_4H_3F_4$, although none of the samples had exactly stoichiometric composition. The results are expressed in terms of the defined thermochemical calorie equal to 4.1840 abs. j. and the ice point of 273.15°K. The data are listed in chronological sequence so the approximate temperature increments usually may be inferred from the adjacent mean temperatures. Curvature corrections were applied in regions where the heat capacity was normal. Values of the heat capacity are considered to have a probable error of 0.1%.

TABLE IV

HEAT CAPACITIES OF $NH_4H_3F_4$ SAMPLES ON ARBITRARY MOLE WEIGHT = 97.064 g.

Sample A—76.08 mole % HF: | T, °K.; C_P, cal./(deg. mole) | **Series I** | 196.95 41.90 | 201.82 39.69 | 205.00 43.22 | 207.55 63.89 | 210.19 39.93 | 216.23 41.62 | 225.06 43.92 | 233.86 48.11 | 242.37 56.43 | 249.43 75.22 | 254.36 87.01 | 257.55 63.56 | 263.32 62.37 | 271.26 74.17 | 277.82 94.80 | 284.95 167.5 | 290.96 396. | 296.52 184.6 | 303.10 55.20 | 308.51 55.29 | **SeriesII** | 154.27 32.30 | 163.02 34.36 | 171.80 35.93 | 180.38 37.71 | 188.24 41.22 | 192.61 45.66 | 194.05 43.83 | 195.30 61.22 | 196.40 57.60 | 197.79 38.42 | 249.30 73.29 | 251.80 84.52 | 253.13 88.60 | 254.03 92.05 | 255.14 85.08 | 256.40 69.70 | 257.89 60.39 | 259.53 58.42 | ΔHf Run No. 1 | **Series III** | 197.81 37.65 | 200.34 38.33 | 202.83 39.28 | 204.59 40.76 | 205.60 44.89 | 206.46 58.20 | 207.02 99.92 | 207.56 55.94 | 208.43 46.43 | 210.69 40.68 |

Sample B—75.05 mole % HF: Series I | 198.59 40.14 | 206.02 53.67 | 213.76 40.32 | 222.41 40.31 | 230.98 44.66 | 240.05 44.26 | 249.36 46.15 | 258.30 49.14 | 266.81 53.83 | 274.61 63.06 | 281.38 83.88 | 286.51 130.9 | 289.75 221.0 | 292.36 493. | 294.38 1000. | 295.33 1422. | 300.94 58.70 | 309.17 55.24 | 315.01 55.32 | **Series II** | 155.52 31.34 | 164.30 33.13 | 173.23 35.15 | 181.99 37.72 | 190.50 41.47 | 199.30 40.00 | 207.46 53.20 | 215.45 40.66 | 224.42 42.85 | 233.36 44.62 | 242.28 44.62 | 251.10 46.66 | 259.70 49.69 | ΔHf Run No. 1 | 307.89 55.27 | 313.70 55.34 | **Series III** | 65.51 15.04 | 70.08 16.08 | 75.98 17.13 | 82.68 18.45 | 89.90 19.80 | 97.32 21.09 | 105.12 22.44 | 113.59 23.91 | 122.38 25.42 | 128.95 26.31 | 132.75 27.20 | 138.85 28.30 | 147.62 29.82 | 156.29 31.58 | 164.82 33.30 | 173.47 35.31 | 182.09 37.63 | 187.57 39.84 | 189.86 41.32 | 192.52 42.81 | 195.61 41.93 | 199.07 36.89 | 202.57 37.84 | 205.65 50.40 | 207.09 140.6 | 207.39 187.0 | 208.69 39.95 | ΔHf Run No. 2 |

Sample C—74.62 mole % HF: Series I | 148.50 29.63 | 157.66 31.36 | 166.50 33.17 | 175.25 35.27 | 183.81 37.91 | 188.84 39.96 | 190.53 41.11 | 192.16 42.73 | 193.88 37.60 | 195.73 35.94 | 201.05 36.24 | 209.36 36.99 | 218.11 38.19 | 223.81 39.96 | 226.65 44.30 | 229.28 75.5 | 231.21 85.6 | 233.79 41.69 | 239.77 42.50 | 248.56 44.44 | 257.50 47.47 | 266.24 52.92 | 274.63 63.38 | 282.00 90.3 | 287.22 154.9 | 291.20 384. | 293.89 1029. | 299.06 171.0 | **SeriesII** | 62.61 14.38 | 69.94 16.03 | 76.31 17.14 | 82.25 18.30 | 88.91 19.55 | 96.90 20.93 | 105.17 22.33 | 113.31 23.64 | 122.00 25.14 | 131.03 26.58 | 140.02 28.11 | 149.12 29.77 | 158.14 31.46 | 167.00 33.31 | 175.69 35.44 | 184.30 38.13 | 189.40 40.34 | 190.65 41.14 | 191.47 41.90 | 192.28 42.82 | 193.09 41.95 | 197.40 36.04 | 206.18 36.67 | 215.40 37.73 | 223.24 39.80 | 227.27 44.52 | 228.70 53.51 | 229.79 82.9 | 230.41 217. | 231.12 84.3 | ΔHf Run No. 1 | 300.01 55.28 | 304.87 55.11 |

Sample D—73.52 mole % HF: Series I | 128.04 26.06 | 135.97 27.37 | 144.41 28.81 | 153.18 30.38 | 162.13 32.12 | 170.98 34.04 | 179.44 36.25 | 187.68 39.35 | 192.97 39.96 | 195.48 35.55 | 197.73 35.17 | 201.21 35.53 | 204.85 35.76 | 206.58 36.50 | 208.29 36.98 | 211.60 68.87 | 219.07 40.03 | 228.41 42.05 | 236.87 44.54 | 245.26 49.00 | 252.13 56.00 | 257.17 68.58 | 260.35 76.74 | 261.97 77.41 | 263.61 71.37 | 265.42 65.51 | 267.37 62.03 | 272.22 66.29 | 279.12 84.9 | 286.40 164.5 | 292.04 465. | 294.92 535. | 298.77 55.28 | 303.37 55.21 | **Series II** | 188.13 39.60 | 193.20 39.68 | 194.63 35.20 | 195.85 35.24 | 200.86 35.31 | 191.76 41.63 | 193.32 39.11 | 206.50 36.62 | 209.00 37.68 | 211.22 46.34 | 212.71 115.1 | 213.62 107.1 | 215.15 39.96 |

The Anomalies and Fusion Transition.—Since the heat capacities of the samples contain so many anomalies in a small temperature range, it is difficult to assign a curve for the normal or background heat capacity. Continuous "lattice" heat capacity curves, determined by extrapolating the heat capacity from above and below the anomaly to the temperature of transition were drawn for all maxima except those of fusion. Enthalpies were calculated by numerical quadrature of these continuous heat capacity *vs.* temperature curves and subtracted from the actual enthalpy inputs to de-

(8) V. S. Yatlov and E. M. Polyakova, *Zhur. Obshcheĭ Khim.*, **15**, 724 (1945).

(9) O. Hassel and H. Kringstad, *Z. anorg. allgem. Chem.*, **208**, 382 (1932).

termine the enthalpy associated with each maximum.

For heat of fusion calculations, a linear extrapolation of the solid heat capacity of Sample D to the melting point and a constant value of 55.25 cal./(deg. mole) for the liquid heat capacity were used. Enthalpies were calculated from these straight lines and subtracted from actual energy inputs to determine the enthalpy of fusion for all four samples. Since linear extrapolations of the solid heat capacity for Samples A, B, C and D were nearly the same, the extrapolation giving the lowest background enthalpy (that of Sample D) was used. A summary of the enthalpy increments associated with each anomaly is presented in Table V. Figure 2 presents heat capacity curves for the four samples

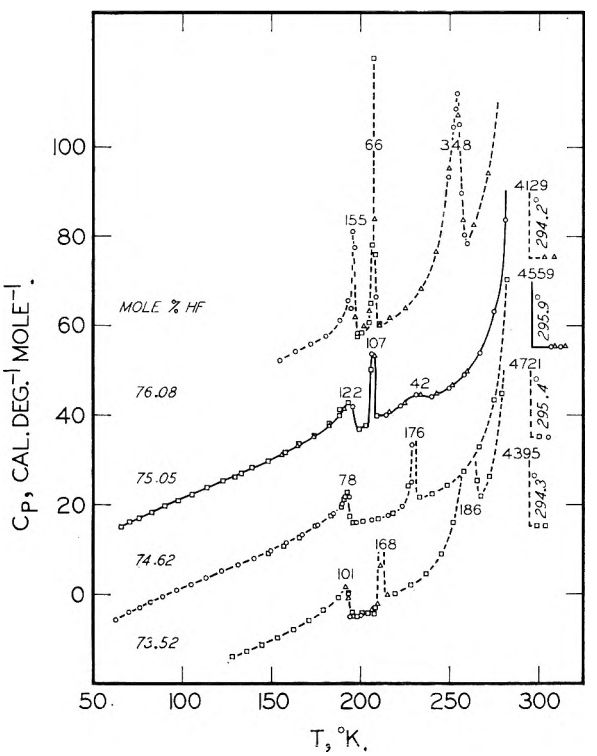

Fig. 2.—Heat capacity of four samples approximating $NH_4H_3F_4$ in composition. (Note that the lower curves are successively displaced by increments of 20 cal./(deg. mole) as a convenience in presenting the anomalies.

with the curves for Samples B, C and D displaced from that of the next higher HF composition by 20 cal./(deg. mole) to more conveniently display the anomalies. Hence, true heat capacities can be read directly from this graph for Sample B (75.05 % HF) only. Enthalpy increments beneath each anomaly and the observed melting temperatures are indicated in Fig. 2.

In order to obtain more accurate enthalpy of fusion data some enthalpy-type runs were made over the entire fusion region for the various samples. As a test of the heat capacity-type runs through these regions of relatively slow equilibrium, the enthalpy increments of these runs are compared in Table VI with the integrated heat capacity under the curve over the same temperature region. The heat capacity points and the enthalpy increments of the anomalies were determined as essentially equilibrium values and were completely reproducible for a given sample. This may be verified by noting the series of repeated determinations shown in Fig. 2.

TABLE V

ENTHALPY INCREMENTS FOR TRANSITIONS

Sample	Mole % HF	Temp. of anomaly (in °K.) 192	207	213	231	254	262	Fusion
A	76.08	155	66			348		4129
B	75.05	122	109		42			4558
C	74.62	78			177			4721
D	73.52	102		168			186	4378

TABLE VI

ENTHALPY TYPE RUNS THROUGH THE FUSION REGION

(In cal./mole; arbitrary mole weight = 97.064 g.)

Sample	T_1, °K.	T_2, °K.	$\Delta H_{obs.}$	$\int_{T_1}^{T_2} C_p dT$
A	260.22	298.87	5786	5789
B (No. 1)	263.96	304.98	6663	6663
(No. 2)	268.03	307.75	6599	6597
C	264.74	297.59	6401	6399
D	266.42	296.78	5688	5691

Samples A and D show heat capacity maxima at 254 and 262°K., but it will be noted that the curves begin to rise steeply at 258.7 and 266.2°K., which correspond closely to the eutectic temperatures determined from cooling curves.

Since Samples B and C show no eutectic peaks, one concludes that there is a narrow solid solution range about the stoichiometric composition. This phenomenon, involving only a small heat effect, was not detected in the thermal analysis studies, but with the much more sensitive methods employed in the equilibrium low temperature calorimetry it was readily observed.

The premelting observed in the preliminary sample persisted in Sample B and was accentuated in the other three. Since premelting is so marked, even in the most nearly stoichiometric sample, it is important that all analytical data in support of these compositions be given. Analysis of Sample B gave 75.00 mole % HF by titration to a phenolphthalein end-point with standardized 0.1 *N* NaOH. The method of immersing the flask in ice-water during the titration was used. Kjeldahl nitrogen determinations gave 17.47 and 17.54 wt. % NH_3 in comparison to the theoretical value of 17.54 wt. % NH_3. Samples A, C and D were prepared by weight from the previous sample. Analyses for water were made with Karl Fischer reagent on Samples A and B and indicated less than 0.1 mole % water. An analysis for water in the solid starting material (NH_4HF_2) also indicated less than 0.1% water. Analysis of the anhydrous HF used by titration with NaOH showed it to be 99.77 and 99.71 wt. % HF on the assumption that the only anion present was fluoride. About one mole % of impurity would be required to explain the premelting observed (in the absence of solid solutions) on this basis. The stoichiometry (for example of Sample B) is too well-defined to explain the premelting arising as a deviation from stoichiometric composition. Since water is excluded as a significant impurity, the presence of other impurity components must be considered. The only metals

in contact with the sample—copper, silver and nickel—can also be eliminated.

It therefore seems likely that this "premelting" behavior or abnormal increase of heat capacity below the melting point is due to some phenomenon other than the presence of an impurity. Ubbelohde[10] suggests that many substances including ammonium compounds show abnormal increase in heat capacity over a range of temperature below the melting point due to the presence of thermal flaws in the crystal structure. These flaws may be present in thermodynamic equilibrium because the increased entropy due to increased disorder in the crystal more than compensates for the increase in enthalpy, thereby lowering the free energy of the system. For substances with high entropies of fusion considerable disorder within the crystal is possible prior to melting and the consequent higher enthalpy gives rise to extensive "premelting" behavior. When solid solutions are present in the crystal structure, the presence of the minor constituent may leave isolated holes in the lattice or result in interstitial atoms being packed into the lattice. This effect results in the presence of thermal flaws; consequently, solid solutions would be expected to give the same type of "premelting" behavior. The formation of Schottky defects (or holes) in the crystalline lattice is a somewhat analogous phenomenological explanation.

The melting point of the compound $NH_4H_3F_4$ was interpolated as 296.4°K. from the calorimetric data and corresponds closely to the results of the phase studies. An entropy of fusion of nearly 16 e.u. was found. A narrow range of homogeneity is observed on both sides of 75 mole % HF, *i.e.*, for the compound $NH_4H_3F_4$. The two series of anomalies occurring below the melting point are as yet unexplained, but it is likely that they are related to a disordering of the crystal due to the presence of the ammonium ion. Further examinations of more compositions in the range 73.5 to 76.1 mole % HF are desiderata for clarification of the complex character of this system.

(10) A. R. Ubbelohde, *Sci. J. Roy. Coll. Sci.*, **15**, 40 (1945).

Decomposition Pressure and Enthalpy of Decomposition.—Static decomposition pressure measurements on $NH_4H_3F_4$ at five temperatures between 263°K. and the melting point (296.4°K.) yielded the equation $p(\text{mm.}) = -5288/T + 20.97$. The probable error in the pressure is estimated to be ±1.5 mm. and the enthalpy of decomposition corresponding to the reaction

$$NH_4H_3F_4(\text{c, soln. of mole \% HF} = 75) \longrightarrow 2HF(g) + NH_4HF_2(c)$$

is $10._5 \pm 1$ kcal. The change in solid composition at the highest temperatures due to reversible decomposition into the gas space in the calorimeter (*ca.* 10 ml.) would be less than 0.01 mole % and, moreover, no significant sublimation enthalpy correction is involved.

Concluding Remarks.—The utility of adiabatic low temperature calorimetric measurements in the elucidation of phase diagrams has been demonstrated in the detection and quantitative evaluation of anomalies not readily discernible on thermal analysis curves. The existence of a solid solution at the composition $NH_4H_3F_4$ was demonstrated. It is considered likely that the same situation might obtain at other of the congruently melting compounds in this system. A further discussion of the data obtained here and correlation with thermochemical data on this system are presented in a publication of the results of another investigation.[11]

Acknowledgment.—The partial financial support of the Division of Research of the United States Atomic Energy Commission is acknowledged. J. J. McBride and E. Greenberg assisted in the heat capacity measurements and Mrs. Emelia Martin did many of the calculations. One of us (R.D.E.) derived support during the 1953–1954 academic year from the du Pont Post-graduate Fellowship.

(11) T. L. Higgins and E. F. Westrum, Jr., *J. Phys. Chem.*, **65**, 830 (1961).

CORRECTION OF THE POTASSIUM VAPOR PRESSURE EQUATION BY USE OF THE SECOND VIRIAL COEFFICIENT[1]

BY R. J. THORN AND G. H. WINSLOW

Chemistry Division, Argonne National Laboratory, Argonne, Illinois

Received November 4, 1960

The available thermodynamic properties of saturated potassium vapor have been used to predict the dissociation energy of the dimer on the basis of a perfect gas treatment including the diatomic molecules, and on the basis of predictions from an imperfect gas treatment in which it was assumed that the inclusion of the second virial coefficient in the equation of state was adequate. Recognition of the necessary (although not sufficient) criterion that the measured entropy of vaporization must agree with that derived from absolute entropies establishes that the effusion experiments of Edmondson and Egerton can be accepted as a reliable starting point for the analysis. A statistically certain experimental distinction between the two treatments cannot be made because of a large discrepancy in the high temperature vapor pressure measurements, though sufficient precision can be obtained to make the distinction. The evidence supports the imperfect gas treatment and the spectroscopic value of the dissociation energy. The most consistent set of thermodynamic properties is: $\log p_1(\text{ideal}) = -4802.27/T - 1.97108 \log T + 4.9800 \times 10^{-4} T - 1.0659 \times 10^{-7} T^2 + 10.14506$. $\log p_2(\text{ideal}) = -6.98 \times 10^3/T - 4.44216 \log T + 1.04976 \times 10^{-3} T - 2.1317 \times 10^{-7} T^2 - 321.28/T^2 + 18.0093$. $\log p(\text{total}) = \log p_1(\text{ideal}) + (1946.9/T) \exp(-4351.0/T)$. $\Delta H^0_{01} = 21747.0 \pm 10.3$ cal./mole. $D_0 = 11.85 \pm 0.10$ kcal./mole. In the first three equations the pressures are in atmospheres.

Introduction

It should be possible to make sufficiently accurate vapor pressure measurements, over a sufficiently wide temperature range, that they provide a means of checking, by use of thermal data, those values for dissociation energies which are obtained by extrapolation of spectroscopically measured vibration bands. In particular the easiest application should be to the dissociation energy of metal dimers formed as the temperature of the *saturated* vapor and, hence, its density are increased.

Unfortunately, there are very few measurements which are sufficiently precise and extensive to justify such an analysis. An examination of the periodic table quickly suggests that of all the elements, the alkali metals are the optimum ones for the purpose. In fact there have been several attempts to study and correlate the vapor pressures and dissociation energies which have been published for them.[2,3] In no case, however, has the analysis been founded on any sort of explicitly stated, plausible basis which would allow the judicious selection of the best of the available measurements from a number of discordant values.

We support the necessity of looking for a basis for the *selection* of data by the following arguments. The mere fact that there is a small random error associated with the measuring equipment used in a particular experiment does not mean necessarily that the results are accurate. That is, the small random error does not testify to the absence of a fixed systematic error or to the absence of a systematic error that varies in a precise way with the recognized variables of an experiment. Thus, it is necessary, when there is discordance between experimental results which is greater than their precision, to try to select those which do not contain a systematic error (granting that there are such in the group). It is obvious that while the degree of precision might be a factor to be considered in choosing the basis to be used for the selection it is also obvious that there can be no *fundamental* relation between the precision and the basis chosen. Indeed, it could well turn out that the least precise results are the most accurate.

It should be emphasized next that if one has applied some rule for selection it is totally illogical to make any sort of combination of the rejected results and the accepted one by use of a weighting procedure based on the precision of the various results. On the other hand, after correction of the rejected results (supposing that this becomes possible *via* discovery of the source of the systematic error) such that the several sets now appear to be identical within the limits of precision, they can *then* be combined by appropriate (weighting) techniques.

With this in mind, we propose the following "rules" for the present case: 1. Of all the possible numbers that could be used in such an analysis, it will be assumed that the electronic levels of the atoms, the vibrational, rotational, and electronic levels of the molecules (all relative to the corresponding ground levels) and the heat capacities of the condensed phases are the most accurate and/or reliable. 2. Satisfaction of the following criterion, *or an equivalent*, is necessary for the acceptance of vapor pressure measurements: The measured entropy of vaporization must agree with that calculated from the measurements mentioned in the first rule. 2a. An equivalent which is pertinent to the present problem, is that vapor pressure data must extend over a sufficiently large range that the ratio of monomer to dimer changes significantly but that values of the dissociation energy calculated at various points in the range are identical within the experimental error.

One of the few substances to which the above rules can be applied successfully is potassium but, heretofore, its near uniqueness in this regard has not been recognized. For instance, Evans, *et al.*, attempted to average all the data together without realizing that of all the measurements at low temperatures (about 440°K.)[4] only those by Edmond-

(1) Based on work performed under the auspices of the U. S. Atomic Energy Commission and presented before the American Chemical Society, Division of Physical Chemistry, September, 1959.

(2) W. H. Evans, R. Jacobson, T. R. Munson and D. D. Wagman, *J. Research Natl. Bur. Standards*, **55**, 83 (1955).

(3) M. Sittig, "Sodium; Its Manufacture, Properties and Uses," Reinhold Publ. Corp., New York, N. Y., 1956. See Chapter by G. W. Thomson and E. Garelis.

(4) At these temperatures the concentration of the dimer is sufficiently small that it can be calculated accurately enough (with any reasonable dissociation energy) to be subtracted out.

son and Egerton[5] yield an entropy of vaporization to the monatomic form (20.50 ± 0.27 e.u.) which is in excellent agreement with that (20.63 ± 0.02 e.u.) calculated from the absolute entropies of the gaseous and condensed phases.[2] Admittedly this agreement may be fortuitous, but it certainly appears to be better to assume that it is not, than to assume that the others are equally reliable but unfortuitously disagree with the third law of thermodynamics and/or all the other results such as the specific heats of the condensed phases. Consequently we attempted to analyze the existing information[2,5-10] on potassium.

It immediately became apparent that the various results were not consistent, to the degree we believe possible[11] when treated within the framework of perfect gas theory, with the equilibrium concentration of diatomic molecules included. We therefore began to look into the application of imperfect gas theory to this problem as being a possible answer to part of the difficulty.

Theoretical Background.—The principal problem to be faced is that imperfect gas theory is usually applied to gases in S_0 states and, indeed, to these when above their critical points[12]; certainly there have been exceptions, particularly to the latter restriction. The present application is to a gaseous atom with a single unpaired electron. The process of dimerization, then, involves an attractive potential which gives rise to non-degenerate bound states. Interaction at positive energy will involve this potential plus a repulsive potential which gives rise to (unbound) triply degenerate states, as with hydrogen atoms.[13] Hence, we reached the same conclusion as subsequently published by Sinanoğlu and Pitzer,[14] *i.e.*, that the second virial coefficient should be

$$B = (1/4)B_A + (3/4)B_R \qquad (1)$$

Here B_A is calculated with the attractive potential function, and B_R is calculated with the repulsive potential function, according to

$$B_i = 2\pi N_0 \int_0^\infty \{1 - \exp[-\phi_i(r)/kT]\} r^2 dr \qquad (2)$$

The B's in eq. 1 and 2 are per mole of atoms; N_0 is Avogadro's number and $\phi_i(r)$ is the appropriate potential function.

It is found, of course, that it is B_A that makes the greatest contribution to B in the temperature range of interest here (900 to 1200°K.). This means that as good a function as possible, within reason, should be chosen for the attractive potential; the repulsive potential is much less critical. After due consideration of the discussion of potential functions given by Varshni[15] we chose the Rydberg function.[16]

$$\phi_A = -D_e(1 + b\rho)\exp(-b\rho) \qquad (3)$$

$$\rho = r - r_e \qquad (3a)$$

This is a three parameter function; r_e is the value of r at the minimum of depth D_e. The constant b enables independent adjustment of the force constant or, equivalently, the second derivative of the function at its minimum. In order to estimate B_R we used, in $\rho > 0$

$$\phi_R = D_e(1 + b\rho + b/\rho)\exp(-b\rho) \qquad (4)$$

as the repulsive potential function. The virial coefficients were calculated by Simpson rule integration on an IBM 650; the simple alteration of eq. 3 to give eq. 4 was easy to program and, we believe, gave a function sufficiently good for the purpose.

Virial coefficients were calculated at 900, 1200 and 1500°K. for various values of D_e. This was in agreement with the attitude that we are using thermal measurements to determine dissociation energies as an independent check of extrapolations of spectroscopic measurements. On the other hand, the second derivative of the potential function, at the minimum, can be determined very precisely from the spectroscopic observations. Thus, when D_e was altered the b of eq.3 and 4 was also altered so that this second derivative was held constant.

Derivation of the Vapor Pressure Equations.—In order to determine a free energy function for liquid potassium to use for interpolation between tabulated values,[2] where needed, we were guided by the work of Douglas, *et al.*[6] The function used was made to conform to the tabulated values. This was done by making slight changes (in the constant and in the term which is linear in the temperature) in the function we had worked out from Douglas' results. In units of cal./mole,[17] this function is

$$(F^0 - H_0^0)_l/T = -226.65/T - 20.4582 \log T + 41.3972 + 2.2787 \times 10^{-3}T - 4.877 \times 10^{-7}T^2 \qquad (5)$$

Two alternative equational descriptions of the total vapor are to be given. If the vapor is treated as a two component perfect gas, the free energy function (per mole) for the monatomic component is

$$(F^0 - H_0^0)_a/T = -R'\{(3/2)\log M + (5/2)\log T + \log[(2\pi k)^{3/2}/h^3 N_0^{5/2}] + \log R + \log 2\} \qquad (6)$$

(5) W. Edmondson and A. Egerton, *Proc. Roy. Soc. (London)*, **A113**, 520 (1927).

(6) T. B. Douglas, A. F. Ball, D. C. Ginnings and W. D. Davis, *J. Am. Chem. Soc.*, **74**, 2472 (1952).

(7) J. W. Johnson, H. R. Bronstein and M. A. Bredig, an unpublished manuscript privately communicated by M. A. Bredig. The data cited herein for these authors were taken entirely from this manuscript. After the preparation of our present paper, but before its submission for publication, Dr. Bredig informed us that additional measurements had turned out to be significantly different from those in the manuscript. This unsatisfactory experimental situation at the higher temperature (see ref. 8 and 11) is largely due to the difficulty of determining the true equilibrium temperature for a given pressure. It seems to make it even more certain that the equations deduced in our paper and collected, with the other desirable information, in the Summary are the best available description of the thermodynamic properties of potassium vapor.

(8) M. M. Makansi, M. Madsen, W. A. Selke and C. F. Bonilla, *J. Phys. Chem.*, **60**, 128 (1956).

(9) F. W. Loomis, *Phys. Rev.*, **38**, 2153 (1931).

(10) F. W. Loomis and R. E. Nusbaum, *ibid.*, **39**, 89 (1932).

(11) The most obvious inconsistency is the lack of agreement between the high temperature vapor pressure measurements.[7,8]

(12) Probably the most extensive discussion to be found in any one place is J. O. Hirschfelder, C. F. Curtiss and R. B. Bird, "Molecular Theory of Gases and Liquids," John Wiley and Sons, Inc., New York, N. Y., 1954.

(13) Ref. 12, p. 1054.

(14) O. Sinanoğlu and K. S. Pitzer, *J. Chem. Phys.*, **31**, 960 (1959).

(15) Y. P. Varshni, *Revs. Modern Phys.*, **29**, 664 (1957).

(16) R. Rydberg, *Z. Physik*, **73**, 376 (1931).

(17) Following Evans *et al.*,[2] the constants given by D. D. Wagman, J. E. Kilpatrick, W. J. Taylor, K. S. Pitzer and F. D. Rossini, *J. Research Natl. Bur. Standards*, **34**, 143 (1945) have been used, except for the calorie. Here as with Evans *et al.*, 1 cal = 4.1840 abs. j. This means that R = 1.98719 cal. and R' (R ln 10) = 4.57567.

and that for the diatomic component is

$$(F^0 - H_0^0)_m/T = -R'\{(3/2)\log(2M) + (5/2)\log T + \log[(2\pi k)^{3/2}/h^3 N_0^{5/2}] + \log R + \log Q_i\} \quad (7)$$

In eq. 6 the log 2 appears because of the doublet nature of the ground state of the atom; correspondingly the Q_i in eq. 7 is the internal partition function of the dimer. We take Q_i from Mayer and Mayer[18]; a factor of 2 is included because the molecule is homonuclear, and the terms in log Q_i, log $[1 - \exp(-u)]$, $[\exp(u) - 1]$, and $[\exp(u) - 1]^{-2}$ have been expanded. Thus

$$\log Q_i = -\log 2\sigma u + 0.434294[8\gamma^2/\sigma + \delta/u + 2x/u - \delta/2 - 2x + \sigma/3 + u/2 + u\delta/12 + 5ux/6 - u^2/24 - u^2x/6] \quad (8)$$

The terms in eq. 8 were evaluated by use of the accepted numbers[19] to give

$$\log Q_i = -1.3335 + 2\log T + 28.929/T - 321.28/T^2 + 5.375 \times 10^{-5}T \quad (9)$$

From eq. 5 through 9, then

$$\log p_1 = -[226.65 + \Delta H_0^0(1)]/R'T - 1.97108\log T + 4.9800 \times 10^{-4}T - 1.0659 \times 10^{-7}T^2 + 10.14506 \quad (10)$$

and

$$\log p_2 = -[320.93 + \Delta H_0^0(2)]/R'T - 4.44216\log T + 1.04976 \times 10^{-3}T - 2.1317 \times 10^{-7}T^2 - 321.28/T^2 + 18.0093 \quad (11)$$

The observed pressure is to be compared with log $(p_1 + p_2)$.

In the above treatment the only interactions recognized are those corresponding to the bound states of two particles. With the aid of the second virial coefficient one accounts for all the states corresponding to free particles and, to some degree of accuracy, for all states of interaction, bound and unbound, between pairs of particles. That is, it is not only recognized that some pairs will be bound as *bona fide* molecules, but that the behavior of the others will be altered because of their mutual potential energy.

If the second virial coefficient is used, the free energy function for the vapor is the same as eq. 6 except that $-R'\log(1 + B/V) + 2R'B/(V \ln 10)$ is to be added on the right.[20] If the right side of eq. 10 is called log $p_1^{(i)}$ then the vapor pressure equation, when the vapor is treated as an imperfect gas, is

$$\log p = \log p_1^{(i)} + \log(1 + B/V) - 0.86859B/V \quad (12)$$

The obviously unknown quantities in eq. 10 through 12 are the heat of vaporization to the monatomic vapor and the heat of vaporization to, or, alternatively, the heat of dissociation of the diatomic form. It is the investigation of the thermal determination of the latter that is the object of the present discussion. As for the former, it was mentioned earlier that we used the observations by Edmondson and Egerton.[5] This was done by first making small corrections to their individual observations for diatomic molecules. The corrections were calculated with eq. 11 and the heat given by Evans, *et al.*[2] A least squares line was put through the corrected and weighted observations with the result

$$\log p_1(\text{atm}) = 4.48 \pm 0.06 - (4513.4 \pm 0.4)/T \quad (13)$$

The weights for the individual values of log p_1 were determined according to the form of the actual observation equation. From the least squares results, it was determined that the value of log p_1 which was determined most accurately was

$$\log p_1(\text{atm}) = -5.7750 \pm 0.0026$$

at

$$T = 440.2_5\,^\circ\text{K.}$$

When this information is used in eq. 10 it is found that

$$\Delta H_0^0(1) = 21747.0 \pm 10.3 \text{ cal./mole}$$

The error given here includes that in the free energy functions[2,21] as well as that in the vapor pressure.

Predicted Values of Dissociation Energy.—The description of the calculations of the second virial coefficient was given previously. The results are given here in Table I where, for convenience, dissociation energies are given in e.v. and in cal./mole. The various determinations of D_0 *via* perfect and imperfect gas treatments are shown in Table II and the error[21] situation is shown in Table III. The information in the latter table is that on which the meaning of the information in the former is to be judged. A graphical picture of the content of these tables is shown in Fig. 1 in order to make it easier to grasp their meaning quickly.

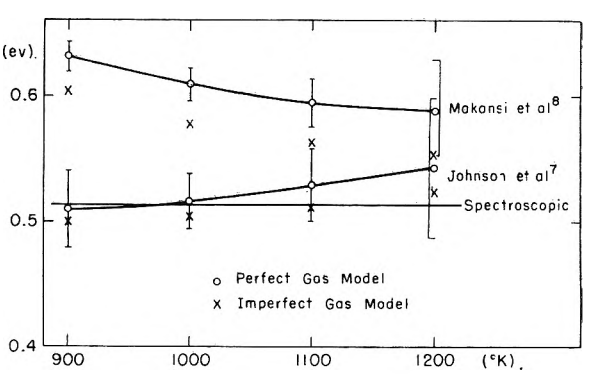

Fig. 1.—Dissociation energy as determined thermally. The errors shown with the perfect gas model also should be associated with the imperfect gas model.

In order to make these calculations we have recalculated least squares lines from the observations reported[7,8] for the high temperature vapor pressure measurements. In each case we weighted the values of log p by p^2. This corresponds to un-

(18) J. E. Mayer and M. G. Mayer, "Statistical Mechanics," John Wiley and Sons, New York, N. Y., 1940. See page 164 where corrections, also discussed by Evans, *et al.*,[2] for non-rigid rotation and anharmonicity are given. Note here that if the problem were merely one of determination of the dissociation energy and of the numerical differences between the perfect and imperfect gas treatments, it could be done *via* the tabulations in ref. 2, except for the determination of ΔH_0^0 (1) to be described later. On the other hand, we wish to summarize this work by proposing what appears to us to be the best vapor pressure equations; we approach that by giving all these introductory equations.

(19) See ref. 2 Table I and the accompanying text for definitions, values, reference and comment.

(20) See ref. 18, p. 292. Note that $B = -\beta_1/2$. For the Mayers' v under the ln in their eq. 13.49, $(RT/N_0P)(1 + B/V)$ has been substituted. Compare, for instance ref. 12, p. 230.

(21) See Appendix.

TABLE I

SECOND VIRIAL COEFFICIENTS FOR POTASSIUM VAPOR

D_0		$-B^a$ (cm.³/mole)			
e.v.	cal./mole	900°K.	1000°K.	1100°K.	1200°K.
0.477	11000.8	7598.0	4298.7	2626.1	1703.1
.494	11392.8	9519.6	5287.4	3192.8	2056.7
.514[b]	11854.1	12334.2	6702.0	3988.8	2545.9
.529	12200.0	14887.7	7957.8	4683.2	2966.8
.546	12592.1	18592.3	9742.4	5654.4	3547.8
.563	12984.1	23203.5	11914.6	6815.8	4232.7
.580	13376.2	28943.5	14558.4	8204.6	5040.1

[a] The values originally calculated on the IBM 650 were at 900, 1200 and 1500°K. The values listed here at 1000 and 1100°K. were interpolated *via* ln $|B| = \alpha + \beta/T + \gamma \ln T$. [b] This is the spectroscopic value. See ref. 9 and 10.

TABLE II

PREDICTED DISSOCIATION ENERGY (E.V.)

	Perfect gas		Imperfect gas	
T, °K.	Johnson, *et al.*[7]	Makansi, *et al.*[8]	Johnson, *et al.*[7]	Makansi, *et al.*[8]
900	0.510	0.631	0.500	0.604
1000	.517	.609	.504	.578
1100	.530	.595	.512	.563
1200	.543	.589	.523	.554
$\lvert\Delta D_0\rvert_{max}$	0.033	0.042	0.023	0.050
$\lvert D_0 - 0.514\rvert$	0.011	0.092	0.004	0.061

TABLE III

ERROR PICTURE (E.V.)

	Total error		Exptl. vapor pressure error		$\lvert\Delta D_e\rvert$ between models	
T, °K.	Johnson, *et al.*[7]	Makansi, *et al.*[8]	Johnson, *et al.*[7]	Makansi, *et al.*[8]	Johnson, *et al.*[7]	Makansi, *et al.*[8]
900	0.031	0.012	0.008	0.005	0.010	0.027
1000	.022	.013	.003	.004	.013	.031
1100	.029	.019	.001	.002	.018	.032
1200	.056	.040	.002	.001	.020	.035

weighted treatment of the pressure; it appears that each group of workers measured pressures directly. The results are: for Johnson, *et al.*[7]

$$\log p = 4.176 \pm 0.007 - (4332.3 \pm 7.6)\,(1/T)$$

and for Makansi, *et al.*[8]

$$\log p = 4.927 \pm 0.011 - (4243.4 \pm 13.8)(1/T)$$

From these equations and other necessary information which is developed during the calculations we also determined p for each set of observers at each of the temperatures shown in Tables II and III and the errors in those pressures.[21]

The perfect gas results in Table II were obtained by finding p_1, subtracting it from the experimentally observed p and calculating $\Delta H^\circ_0(2)$, and hence D_0 [$= 2\Delta H^\circ_0(1) - \Delta H^\circ_0(2)$], from eq. 11 or the corresponding tabulations in ref. 2. The imperfect gas results were obtained graphically, as follows. By a method of successive approximations on an IBM 610 simultaneous solutions of eq. 12 and

$$pV = RT(1 + B/V) \qquad (14)$$

for p and V were obtained at each of the several values of B. [That is, it is *via* B that D_0 (or D_e) enters the imperfect gas model.] The resulting pressures were plotted *vs.* the trial values of D_0 and the solution obtained by graphical interpolation at the experimentally observed pressures.

The errors given in Table III were all calculated on the basis of the perfect gas model. These are errors which arise from various sorts of experimentation and would be expected to propagate about the same in each model.

A systematic (theoretical) error which would arise from using a perfect gas model when an imperfect gas model is required is one of the items to be examined here *via* the tabulated differences. Such a difference would be expected to be larger for materials with larger values of dissociation energy; the larger D_0 would mean increased interaction (imperfection) even in unbound states. In addition, as here, the difference will also increase with temperature because a high T will correspond to a higher density (smaller molar volume) of the (saturated) vapor. On the other hand, the accuracy of either model as used here will be expected to go down for greater interaction, or at higher temperature, because of the restriction to only diatomic molecules or, alternatively, only the second virial coefficient. Mathematically, in the second case for instance, one can see that a complete factor such as the $(V - b)^{-1}$ of van der Waals' equation is needed to turn the calculated pressure back up at small values of the volume (condensed phase); the use of $V^{-1}(1 - B/V)$ leads to a maximum (corresponding to the one in van der Waals' equation) at $V = 2|B|$, but then to zero pressure at $V = |B|$. It should be noted, however, that in the present example, the molar volume, 1.58×10^4 cm.³, for the saturated vapor at 1200°K. and $D_0 = 0.580$ e.v., the last entry in the tables, is still greater than $2|B|$ ($= 1.01 \times 10^4$ cm.³).

Of principal interest here, then, is the effect of the experimental error situation on conclusions about the distinction between the present two models and about the value of the dissociation energy. The statements to be made can be verified by referring to Tables II and III and to Fig. 1.

The most obvious point is, as has been mentioned, the large difference between the results derived from the two sets of high temperature vapor pressure measurements. The difference is quite large compared to the standard deviation. We believe the principal difficulty to be temperature measurement (as do Makansi, *et al.*[8]) rather than pressure measurement. We[22] are in the process of making a third set of measurements of the vapor pressure in this region, and are obtaining results closer to those of Johnson, Bronstein and Bredig.[7]

The next point to note is that our criterion *2a* is not strictly satisfied in any case. Indeed, it is not satisfied within the error by the results from Makansi, *et al.*,[8,23] although it is by the results from Johnson, *et al.*[7]

Johnson's results are improved by the use of the imperfect gas model, whereas Makansi's are worsened, in the sense of criterion *2a*. Although, in both cases, the difference between models is greater than the error which arises only from the random error in the pressure measurement at high temperatures, the over-all error is such that one

(22) R. J. Thorn, R. R. Walters and G. H. Winslow, to be published.

(23) The propagation of errors to the error in D_0 involves, at many points, the presence of p_2 in the denominators of fractions or, more importantly, the presence of the ratio p_1/p_2. The higher the observed pressure the smaller will be the propagated error for a given p_1.

cannot conclude unequivocally that the imperfect gas model is required to treat the present data. An illustration of the contributions to this over-all error is shown in Table IV.[21]

The principal difficulty is that it is necessary to extrapolate the liquid free energy function outside the region in which it was measured in order to reach the region in which the distinction between the perfect and imperfect gas models becomes important. This problem cannot be dismissed unless one is satisfied merely with empirical tables of vapor pressures. As temperatures of interest become higher, the imperfect gas treatment and values of the liquid free energy function measured at those temperatures will become more important.

The final items to notice are the comparisons with the spectroscopically observed dissociation energy. The results which come closer to satisfying our criterion *2a* (regardless of model) also tend to confirm that value. Although it is an event which is well bounded by the size of the errors, the application of the imperfect gas model to the results by Johnson, *et al.*,[7] does improve their agreement, on the average, with the spectroscopic value. Our conclusion is that the vapor pressure of potassium is best described, at the present time, by use of the imperfect gas model with the spectroscopically observed dissociation energy used for evaluation of the second virial coefficient.

TABLE IV

CONTRIBUTIONS TO ERROR IN D_0 (E.V.) FOR THE PERFECT GAS MODEL, JOHNSON'S DATA, 1000°K.

Source	Error
Pressure measurement	0.0027
Monomer free energy function	.0016
Dimer free energy function	.0087
Liquid free energy function	.0179
$\Delta H^0_0(1)$[a]	.0092
Accumulated error	.022

[a] Because of the large difference in temperature between 1000°K. and the temperature (440.25°K.) at which $\Delta H_0^0(1)$ was determined, the contribution of the liquid free energy function error to the error in $\Delta H_0^0(1)$ was considered to be independent of that entered in the table.

Summary

If B/V is treated as a small number in eq. 12, the last two terms can be combined to give $BP/R'T$. In the range up to 1200°K. it is sufficient to represent B by a term of the form $\alpha \exp(\beta/T)$. Since p is also of this form, quite closely, the product BP can be combined into one term of that form. The constants can be evaluated *via* the values of log p determined by successive approximations at 900° K. and 1200°K. for $D_0 = 0.514$ e.v. We conclude, then, that the most consistent set of the thermodynamic properties is

$$\log p_1(\text{ideal}) = -4802.27/T - 1.97108 \log T + 4.9800 \times 10^{-4}T - 1.0659 \times 10^{-7}T^2 + 10.14506$$

$$\log p_2(\text{ideal}) = -6.98 \times 10^3/T - 4.44216 \log T + 1.04976 \times 10^{-3}T - 2.1317 \times 10^{-7}T^2 - 321.28/T^2 + 18.0093$$

$$\log p(\text{total}) = \log p_1(\text{ideal}) + (1915.4/T) \exp(-4338.9/T)$$

$$\Delta H^0_{01} = 21747.0 \pm 10.3 \text{ cal./mole}$$

$$D_0 = 11.85 \pm 0.10 \text{ kcal./mole}$$

Appendix

Since so much depends on experimental error when it comes to reaching conclusions in this paper, it is deemed desirable to describe the situation in some detail. Reference will be made to the compilation by Evans, *et al.*,[2] as a source of illustrative material. Any remarks that appear to be critical are not to be taken as pointed at these authors, however, but at a situation existing throughout this field.

The terms "uncertainty" and "over-all uncertainties" are used.[2] Statements are made which could be easily rephrased to use "maximum uncertainty." There is no clear statement, however, as to what is meant when these terms are applied to the tabulated values of the thermodynamic functions.

The "uncertainties" given in data tables are stated to be "probable errors of the mean"; on the other hand, one result is given in the text as being the "weighted average of the starred values" listed in one of the tables. Earlier in the text it is implied that this means "weighted inversely as the probable error." In the case cited, however, one of the starred values is the result of a single reading and has no probable error attached. Further, a comparison of the differences between starred values and the errors cited for these values strongly suggests that at least some of the differences are systematic. A systematic error is not compensated for by taking a large number of readings and the resulting small (random) error is not a proper basis for weighting.

Many of the tabulated values[2] arise as the result of drawing the "best" (these quotes are taken from the reference) curve presumably by eye, through points plotted on a large-scale graph. We have had experience with this procedure and have concluded that it is very subjective. The determination of an equational fit could be easily described and, then, reproduced by anyone.

The errors that we cite as a result of our own least squares treatment of data are the standard deviations. The formulas we use for two parameters, for instance, are eq. 33–38 and eq. 40 of Birge[24] except that we omit the coefficient 0.6745 (which converts standard deviation to probable error) in eq. 38.

We assume that all single observations of the same quantity have the same weight. Thus, if we know that p has been observed directly, but it is convenient to fit the observations to

$$\log p = a + b/T$$

each log p is weighted by p^2. This is on the basis that the weight of log p is inversely proportional to the square of the error in log p.[25]

In the present paper we have combined these standard deviations with "uncertainties" from ref. 2 as though the latter were also standard deviations.

For extrapolation of the liquid free energy function we were guided by the results of Douglas, *et*

(24) R. T. Birge, *Phys. Rev.*, **40**, 207 (1932).

(25) J. B. Scarborough, "Numerical Mathematical Analysis," The Johns Hopkins Press, Baltimore, Md., 1958, p. 474.

al.[6,26] We computed the standard deviation in the heat content, from their published data, with the use of Birge's eq. 40. This was done in the range of the observations (up to ~1000°K.) and also at 1100 and 1200°K. It was found that the error in the function was nearly constant in the range of observation and that it went up, from that constant value, by a factor of two at 1100°K. and a factor of five at 1200°K. We applied these factors to the uncertainties given by Evans, *et al.*,[2] in the liquid free energy function in the extrapolated region.

(26) Douglas, *et al.*, use the average deviation, a measure of spread which is frowned on by statisticians. See W. J. Youden, "Statistical Methods for Chemists," John Wiley and Sons, Inc., New York, N. Y., 1951, p. 8.

SHOCK WAVES IN CHEMICAL KINETICS: THE HYDROGEN–BROMINE REACTION

BY DOYLE BRITTON AND ROGER M. COLE

School of Chemistry, University of Minnesota, Minneapolis, Minnesota

Received December 5, 1960

The reaction between H_2 and Br_2 to form HBr has been studied between 1300 and 1700°K. in a shock tube. The rate of the reaction Br + H_2 → HBr + H has been directly determined for H_2 and D_2. The rate of the reaction Br + HBr → Br_2 + H has been directly determined. The relative rates of the reactions H + HBr → H_2 + Br and H + Br_2 → HBr + Br have been determined independently from the forward and reverse reaction data. All of these results are in general agreement with the predictions which could be made from the low temperature results of earlier workers. As a necessary preliminary to the preceding the efficiency of HBr as a third body for the recombination of Br atoms was determined, and found to be slightly greater than the efficiency of argon.

Introduction

The reaction between H_2 and Br_2 is the classic example of a chain reaction. It has been studied here by shock wave techniques both to extend the temperature range over which the rate constants have been determined experimentally and to further test the shock tube method. This reaction has been well reviewed, for example by Pease[1] and by Campbell and Fristrom,[2] and only those pieces of earlier work which are of specific interest will be mentioned below.

The simple reactions which occur in the hydrogen–bromine system, and which are of importance, are[3]

$$Br_2 + M = 2Br + M \quad (1)$$
$$Br + H_2 = HBr + H \quad (2)$$
$$H + Br_2 = HBr + Br \quad (3)$$

Reactions 2 and 3 are the propagation reactions, and if it is assumed that the steady-state approximation can be applied to the H atom concentration then

$$\frac{d(HBr)}{dt} = (Br)\left[\frac{2k_{2f}k_{3f}(H_2)(Br_2) - 2k_{2r}k_{3r}(HBr)^2}{k_{3f}(Br_2) + k_{2r}(HBr)}\right] \quad (4)$$

Reaction 1 is the source of the bromine atoms. At low temperatures or at large relative H_2 and Br_2 concentrations the reverse reaction can be ignored and equation 4 can be rearranged to

$$\frac{d(HBr)}{dt} = \frac{2k_{2f}(Br)(H_2)}{1 + k_{2r}(HBr)/k_{3f}(Br_2)} \quad (5)$$

At low temperatures the Br atoms maintain equilibrium with the molecules and

$$(Br) = [K_1(Br_2)]^{1/2}$$

If the correct assumptions are made that reaction 1 can be either ignored or studied independently and that all of the equilibrium constants for the various reactions are known, then two kinetic constants need to be determined to characterize the entire reaction. These two constants have generally been k_{2f}(or $k_{2f}K_1^{1/2}$) and the ratio k_{3f}/k_{2r}.

We have re-examined the data of Bodenstein and Lind,[4] who report[5] $k_{3f}/k_{2r} = 10$ without giving any error estimate nor any clear indication how the value was determined, and we find a temperature independent value of 10.2 ± 2.4. If their experiments with excess H_2, which yield a ratio 12.3 ± 1.5, are compared with their experiments with excess Br_2, which yield a ratio 6.9 ± 0.8, it is clear that some unknown systematic error is present. The value of Bodenstein and Jung[6] of 8.4 ± 0.6 seems therefore to be the better value, although the error estimate is optimistic. Fortunately an uncertainty of 20% in the value of this ratio only leads to a 3% uncertainty in the value of k_{2f}.[7] The data of Bodenstein and Lind were calculated using 8.4 and more modern values of K_1[8] to obtain the parameters given later in Table IV.

The other results at low temperatures were ob-

(1) R. N. Pease, "Equilibrium and Kinetics of Gas Reactions," Princeton University Press, Princeton, N. J., 1942, pp. 112–121.

(2) E. S. Campbell and R. M. Fristrom, *Chem. Revs.*, **58**, 173 (1958).

(3) The following notation will be used: K_i is the equilibrium constant for reaction (i) as written; k_{if} is the rate constant for the forward reaction in equation (i); k_{ir} is the rate constant for the reverse reaction. All concentrations will be expressed in moles/liter and all times in seconds unless otherwise noted. The units of the equilibrium and rate constants will be the appropriate combinations of moles/liter and seconds.

(4) M. Bodenstein and S. C. Lind, *Z. physik. Chem.*, **57**, 68 (1906).

(5) The units used in this paper are not the same as those used by Bodenstein and Lind. In all cases where comparisons are made their values have been converted to the present units. Similarly, some of the rate constants differ by factors of two from those given here since they were differently defined.

(6) M. Bodenstein and G. Jung, *Z. physik. Chem.*, **121**, 127 (1926).

(7) Campbell and Fristrom[2] make a mistake on this point in their review paper. Both Bodenstein and Lind, and Bach, Bonhoeffer and Moelwyn-Hughes calculate values of $k_{3f}K_1^{1/2}K_2$ from their experimental data assuming that $k_{3f}/k_{2r} = 10$. This value of 10 should therefore be used to convert their results to values of k_{2f}. Campbell and Fristrom used the value of 8.4 to make this conversion, with the result that their Table 9 has values for k_{2f} (k_2^f in their notation) which are too large by about 15%.

(8) National Bureau of Standards, "Selected Values of Chemical Thermodynamic Properties," Series III, Washington, 1948, 1954.

tained by Bach, Bonhoeffer and Moelwyn-Hughes[9] who also studied the D_2–Br_2 reaction. They assumed that the ratio k_{3f}/k_{2r} was 10 for both H_2 and D_2. Their results also have been recalculated using modern values of K_1. Table IV gives the parameters for the smooth curves through the new values.

As Pease[3] noted, the internal agreement among either set of low temperature results is better than the agreement between the two sets.[10]

There have been three studies of this reaction at high temperatures. Britton and Davidson,[11] in shock tube experiments around 1500°K. found that the values of k_{2f} extrapolated from the low temperature values seemed to be low by a factor of about two. They did only a few experiments of a preliminary nature. Plooster and Garvin[12] compressed mixtures of H_2 and Br_2 in a shock tube and measured the induction times for the onset of explosions. The dependence of these times on temperature was explained reasonably on the basis of values of k_{2f} extrapolated from low temperature values, and the assumption that the Br atom concentration increased with time at the high temperatures behind the shock waves, that is, that the steady-state approximation did not apply to Br atoms. Levy[13] studied this reaction in a flow system in which the H_2 and Br_2 were preheated before being mixed together. The steady-state approximation was a reasonable one in view of this preheating and the results could be explained in terms of the low temperature mechanism. Values of k_{2f} were measured between 600 and 1500°K. The scatter in these values at high temperature was quite large, but in general the agreement with the low temperature results was good. In the experiments reported here it was hoped to improve the accuracy of the high temperature measurements and to extend the range to higher temperatures.

Experimental

Apparatus.—The shock tube, the associated vacuum line, and the observation arrangements have all been described previously.[14] In all of the experiments reported here the Br_2 concentration was followed spectrophotometrically at 5000 Å. Under the experimental conditions emission at this wave length was negligible. Duplicate observations were routinely made at two stations 40 cm. apart.

Chemicals.—The Br_2 was Mallinckrodt Analytical Reagent. A bulb-to-bulb distillation was performed in the vacuum line and the middle fraction taken. The H_2 was obtained from the National Cylinder Gas Company and was stated to be 99.6% pure. It was further purified by passing it over platinum in a heated quartz tube to induce any oxygen which might be present to react, and by collecting any water in a liquid nitrogen trap. The D_2 was supplied by the Bio-Rad Laboratories and was stated to be 99.5% pure. It was used without further purification. The HBr[15] was obtained from the Matheson Co., Inc., and was stated to be 99.8% pure; it was distilled into a trap on the line where it was frozen and any non-condensable gas pumped off.[16] It then was distilled into a storage bulb, the first and last fractions being discarded. The infrared spectrum of a gas sample showed a peak attributable to a small amount of HCl as well as three other small unidentified peaks. In the later experiments the HBr was prepared by bubbling H_2 through liquid Br_2, passing the mixture through a heated quartz tube, collecting the HBr in a trap, and pumping off the excess H_2. The infrared spectrum for this HBr showed no impurity peaks. Matheson argon stated to be 99.9% pure was used without further purification.

Reaction mixtures were prepared by adding Br_2, H_2, HBr and argon to a storage bulb and noting the total pressure after each addition. The gases were allowed to stand in the bulbs at least 48 hours before being used, to allow complete mixing.

Calculations

Calculation of an Apparent Rate Constant in the Reaction between H_2 and Br_2.—A shock wave was run in a mixture of Ar, Br_2, H_2 and perhaps HBr, and a trace similar to Fig. 1 obtained. The bromine

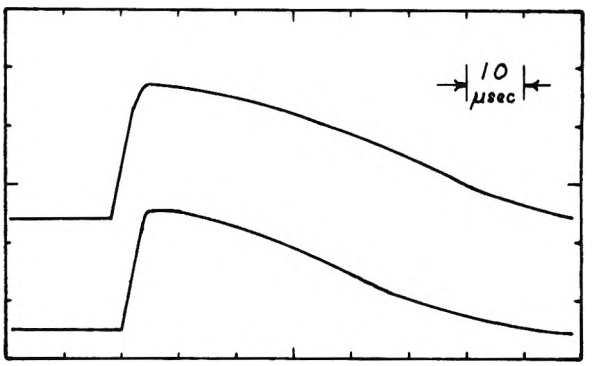

Fig. 1.—Oscillogram of typical shock used for kinetic studies. This shock was run in a 1% H_2–1% Br_2–98% Ar mixture, and reached a temperature of 1448°K. at the shock front. Note the acceleration in the rate of disappearance of Br_2 as more Br atoms are produced. (In all of the oscillograms the lower trace records the Br_2 concentration at the first observation station as a function of time, and the upper trace records at the second observation station, 40 cm. from the first.)

disappearance after the shock front is the sum of two effects, first the dissociation of Br_2 according to reaction 1, and second the formation of HBr according to reactions 2 and 3. These two effects were separated in the following way. All of the concentrations were determined as a function of time. The Br_2 concentration could be determined directly from the oscilloscope trace. The compression ratio generally could be assumed to be constant after the shock since the endothermic dissociation of Br_2 which tends to increase this ratio was more or less balanced by the exothermic formation of HBr which tends to decrease this ratio. This also meant that the temperature was much more nearly constant than in a shock involving only the dis-

(9) F. Bach, K. F. Bonhoeffer and E. A. Moelwyn-Hughes, *Z. physik. Chem.*, **27B**, 71 (1935).

(10) Pease also noted, correctly, that Bach, Bonhoeffer and Moelwyn-Hughes misstate the conversion factor between their units and those of Bodenstein and Lind. He did not note that they used a conversion factor which was neither the one they stated nor the correct one but was lower than the correct one by about 3%. Since Bach, *et al.*, made their original calculations in moles/liter their figures presumably are correct and have been used here. The 3% correction increases the discrepancy between the two sets of data.

(11) D. Britton and N. Davidson, *J. Chem. Phys.*, **23**, 2461 (1955).

(12) M. N. Plooster and D. Garvin, *J. Am. Chem. Soc.*, **78**, 6003 (1956).

(13) A. Levy, *J. Phys. Chem.*, **62**, 570 (1958).

(14) D. Britton, *ibid.*, **64**, 742 (1960).

(15) In the experiments with Br_2 Dow Corning silicone vacuum grease and Kel-F 90 fluorocarbon grease had been about equally satisfactory in the vacuum line. With HBr present the Kel-F was the more satisfactory of the two.

(16) A sample of the tank gas was collected in a 62 ml. gas buret that was subsequently opened under water. About 2 ml. of the collected gas would not dissolve. This would imply a 3% impurity. A larger sample of this impurity gas was collected and found to be inflammable so presumably it was hydrogen.

sociation reaction.[17] The Br atom concentrations could be obtained by graphical integration of the Br_2 concentration since[18]

$$\frac{d(Br)}{dt} = 2k_{1f}(Br_2)(M) - 2k_{1r}(Br)^2(M) \qquad (6)$$

and in the reactions between H_2 and Br_2 the last term could be ignored.[19] The HBr concentration follows from a mass balance of the bromine

$$(HBr) = 2[(Br_2)_0 - (Br_2)] - (Br) + (HBr)_0 \qquad (7)$$

The H atom concentration can always be assumed to be negligibly small so that the hydrogen molecule concentration also follows from mass balance

$$(H_2) = (H_2)_0 - 1/2[(HBr) - (HBr)_0] \qquad (8)$$

From the concentrations as a function of time $d(HBr)/dt$ and therefore $k^* = 2k_{2f}/[1 + k_{2r}(HBr)/k_{3f}(Br_2)]$ could be calculated at any time. In the early stages of the reaction, when the Br atom concentration is small, the rate of formation of HBr is small and the uncertainty in k^* is quite large. In the later stages the back reaction is beginning to be important and the errors in estimating the changes in the temperature and density are becoming large. Therefore it was decided to use the value of k^* at 25% disappearance of the Br_2 in each shock as the best value for that shock.

Calculation of the Rate Constant in the Back Reaction, Br + HBr.—The calculations in this case are very similar to those for the forward reaction described in the preceding section. A shock wave was passed through a mixture of HBr and Br_2, and a trace similar to Fig. 2 obtained. The change in

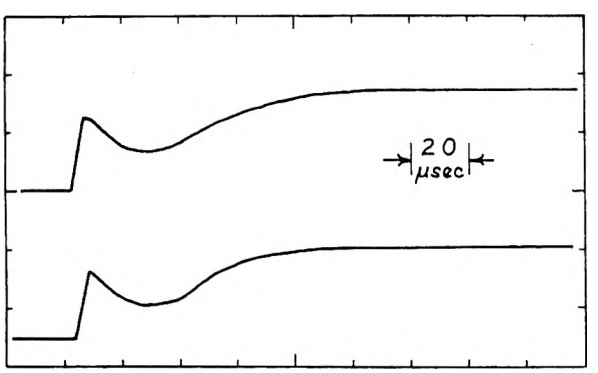

Fig. 2.—Oscillogram of shock showing the reverse reaction. This shock was run in a 0.5% Br_2–99.5% HBr mixture and reached a temperature of 1635°K. at the shock front. Note the production of molecular Br_2 when the Br atom concentration becomes sufficiently large.

the Br_2 concentration is again the sum of two effects, the dissociation of Br_2, and the formation of Br_2 from the reaction between HBr and Br. Since both of these reactions are endothermic it is necessary here to correct for the temperature decrease and the density increase that take place as the reaction proceeds. These changes were approximated as being linear with time, which is not correct, but which does not introduce a large error. The Br_2 concentration could be calculated at all times directly from the oscilloscope trace. The Br atom concentration could be calculated from equation 6, this time including the recombination reaction since the reaction between HBr and Br is slower than the dissociation and recombination of Br_2. A numerical, point by point, integration was performed to give (Br) as a function of time. The H_2 molecule concentration could be calculated from mass balance

$$(H_2) = 1/2(Br) - [(Br_2)_0 - (Br_2)] \qquad (9)$$

The HBr concentration also could be calculated from mass balance

$$(HBr) = (HBr)_0 - 1/2(H_2) \qquad (10)$$

The H_2 concentration was plotted as a function of time and $d(H_2)/dt$ could be determined from the plot.

The rate constant for the back reaction, k_{3r}, could be calculated from the following rearranged form of equation (4)

$$\frac{d(H_2)}{dt} = \frac{d(H_2)}{\Delta d\tau} = \frac{k_{3r}(Br)[(HBr) - K(Br_2)(H_2)/(HBr)]}{1 + 1_{3f}(Br_2)/k_{2r}(HBr)} \qquad (11)$$

The first term in the numerator represents the reaction in question. The second term represents the reverse of this reaction, that is, the reaction which has previously been called the forward reaction. K is the equilibrium constant for the reaction $H_2 + Br_2 = 2HBr$. Since at equilibrium only a small fraction of the HBr has disproportionated this second term must be included. The denominator can be estimated from the known value of the ratio k_{3f}/k_{2r} and is not much greater than 1. The rate constant k_{3r} was generally calculated at a point corresponding to about 25% reaction for reasons similar to those given for the forward reaction.

Estimation of the Rate Constant for the Dissociation of Br_2.—The value of the rate constant for the recombination of Br atoms in the presence of argon was taken to be given by $\log k_{1r} = 8.222 + 403/T$. This was found by combining the results of flash photolysis experiments at and just above room temperature[20] with the results of shock tube experiments at high temperatures.[14] This combined result was used rather than the shock tube results alone since these experiments generally were at lower temperatures than the experiments on the dissociation of Br_2, and interpolation surely gives a more reliable value than extrapolation. The dissociation rate constant, k_{1f}, which was usually desired was found from the value of k_{1r} given above and the value of K_1 from the N. B. S. Tables.[8]

The dissociation rate constants, strictly speaking, should be corrected to allow for the 1 or 2% H_2 and Br_2 which are present. However, these corrections are quite uncertain and would be small in any case so they have been omitted. Similarly in the shocks with added HBr, although the HBr is 10% of the

(17) In a few cases this temperature change was as large as 50° and had to be corrected for. Corrections generally were made assuming that rate constants and compression ratios were linear functions of the amount of Br_2 reacted.

(18) It must always be remembered in observations on a moving shock wave that the time on the oscilloscope trace, τ, and the time that the gas has been heated, t, are related by $dt = \Delta d\tau$ where Δ is the compression ratio in the shock.

(19) Strictly speaking equation 10 gives the rate of formation of atoms of either Br or H since the Br originally formed could be converted to H through the operation of reactions 2 or 3. Since the H atom concentration is a small fraction of the Br atom concentration this has been ignored.

(20) R. Strong, J. Chien, P. Graf and J. Willard, *J. Chem. Phys.*, **26**, 1287 (1957).

total the change in composition can be ignored since the HBr has about the same efficiency as a third body as the argon. In the section of the results, "*The Forward Reaction, $H_2 + Br_2$*," the changes that would result from changing the value of k_{1r} used here are discussed.

In the experiments where HBr was the third body the dissociation rate constants were measured in the same experiments in which the Br + HBr reaction was studied. Nevertheless it was decided to use a smoothed set of values in making calculations about the second reaction. This was chosen in the following way. HBr was a 30% more efficient third body than argon at 1400°K. and 20% more efficient at 1600. Using these two observations to correct the equation given in the first paragraph of this section the rate constant for the recombination of Br_2 in the presence of HBr is given by $\log k_{1r} = 8.056 + 795/T$. As before the dissociation rate constants then were calculated from a knowledge of the equilibrium constants.

Equilibrium in the HBr System.—In order to determine the equilibrium conditions in the various shock waves it was found very convenient to have a set of graphs of equilibrium conditions at constant volume as a function of temperature for a variety of initial conditions. These were calculated from the necessary equilibrium equations plus the mass balance equations for H and Br. This was originally done by hand by successive approximations, but finally by using a Minimatic program on the Univac Scientific 1103 computer.

The necessary equilibrium constants were obtained from the N. B. S. tables.[8] For reactions involving HBr above 1500°K. the necessary constants were not available, and were computed from spectroscopic data in the usual way assuming the HBr molecule to be an anharmonic oscillator with centrifugal stretching.[21] The spectroscopic data were taken from Herzberg.[22] The values of the constants obtained in this way were about 2% larger than the N. B. S. values at 1300 and 1500. It was assumed that this was due to slight differences in the natural constants used and was not looked into further, since this accuracy was sufficient unto the experiment at hand.

Results

HBr as a Third Body for the Recombination of Br Atoms.—Five series of shocks were run to determine the efficiency of HBr as a third body for the recombination of Br atoms. In the first series shocks were run in a 2% Br_2–20% HBr–78% Ar mixture. Seven shocks at temperatures from 1250–1850°K. gave $\log k_{1r} = 7.265 + 2048\ (\pm 194)/T$. If these results are compared with the results in 2% Br_2–98% Ar[14] of $\log k_{1r} = 7.608 + 1368/T$ it would appear that the HBr is slightly more efficient than Ar. However there is the question of the vibrational relaxation of HBr (it was assumed to be relaxed), and the large spread of the experimental points makes the difference in efficiency rather uncertain. Therefore four more series of shocks were run in Br_2–HBr mixtures with no argon diluent.

From the initial rise in concentration in the shock waves in essentially pure HBr it was possible to decide that the HBr was vibrationally relaxed at the shock front and that the apparent dissociation rate constants were not complicated by the simultaneous relaxation of the inert gas. Hydrogen bromide is not truly an inert gas since it can and does disproportionate to H_2 and Br_2, but it does not do this until a reasonable number of Br atoms are present, so that the initial slope of the oscilloscope trace does give the desired dissociation rate constant for Br_2. Figure 2 shows the initial dissociation of Br_2 as well as the subsequent decomposition of HBr in a typical shock in an HBr–Br_2 mixture. The point of the inertness of the HBr will be covered more fully in the section "Direct Observation of the Back Reaction." The results of these experiments are summarized in Table I. The temperature range in the experiments generally ran from about 1400° to about 1700°K., and the final total concentrations were 10^{-3}–10^{-2} mole/l. The 1500° point more or less represents the center of the range.

TABLE I

RECOMBINATION RATE CONSTANTS FOR HBr AS THIRD BODY FROM SHOCKS IN Br_2–HBr MIXTURES

% Br_2	No. of exptl. points[a]	$\log k_{1r} = A + B/T$ A[b]	B[b]	k_{1r} at 1500°K. mole^{-2} l. sec.$^{-1}$)
0.48	12	6.694	2317	3.2×10^3
1.00	11	6.123	3705	3.9
2.00	24	6.760	2821	4.4
4.41	8	7.024	2399	4.2

[a] In general this is about twice the number of shock waves since usually two observations were made on each shock. [b] The probable errors in A at the mean value are about 0.02, in B about 300°.

There are two ways of looking at these data. The first is to take the average k from all the mixtures as the best value. The other is to regard the trend with mole fraction of Br_2 as real and extrapolate to the limits, one limit for HBr as third body, and the other for Br_2 as third body. In Table II this has been done at 1500 and 1600°K. for HBr, and also for Ar[14] for comparison.

TABLE II

RECOMBINATION RATE CONSTANTS[a] FROM Br_2–HBr AND Br_2–Ar MIXTURES

Inert gas	Temp., °K.	Mean k[b]	Extrapolated values of k_{1r}[c] k_{HBr} or k_{Ar}	k_{Br_2}
HBr	1500	4.0×10^8	3.6×10^8	24×10^8
	1600	3.1	2.8	21
Ar	1500	3.7	2.6	37
	1600	3.2	2.3	30

[a] Moles^{-2} liter^2 sec^{-1}. [b] This is the mean value from mixtures of all compositions; 0.48, 1.00, 2.00 and 4.41% Br_2 in HBr, and 2.00 and 5.00% Br_2 in Ar. [c] It is difficult to estimate the probable errors in these constants but $\pm 0.4 \times 10^8$ for k_{HBr} and k_{Ar} and $\pm 10 \times 10^8$ for k_{Br_2} are surely conservative.

Two conclusions may be drawn from Table II. First, HBr is only slightly more efficient than Ar as a third body for the recombination of Br atoms, perhaps 10–30% more. Second, there is further support for the suggestion that at these temperatures Br_2 is closer to 10 times more efficient than Ar rather

(21) J. Mayer and M. Mayer, "Statistical Mechanics," John Wiley and Sons, Inc., New York, N. Y., 1940, pp. 440–453.

(22) G. Herzberg, "Spectra of Diatomic Molecules," 2nd ed., D. Van Nostrand Co., New York, N. Y., 1950.

than 3 times as has been suggested.[23] This support is not very strong, but it is consistent with the Ar results within experimental error.

The Forward Reaction, $H_2 + Br_2$.—About one hundred shocks were run in various mixtures of Br_2, H_2, HBr and Ar. The argon was the principal constituent, and was added in every mixture to serve as a heat capacity buffer, and also in order to provide a third body with known efficiency for the dissociation of Br_2. An apparent rate constant $k^* = k_{2f}/[1 + k_{2r}(HBr)/k_{3f}(Br_2)]$ was calculated at the point of 25% reaction as described previously. For any particular mixture the values of k^* were compared as a function of temperature. For one sample mixture, 1% Br_2–1% H_2–98% Ar, the experimental points are displayed in Fig. 3 as log k^* *vs.* $1/T$. A straight line has been fitted through these points by the method of least squares. The best straight lines, but not the experimental points, for three other mixtures also are shown in the same figure.

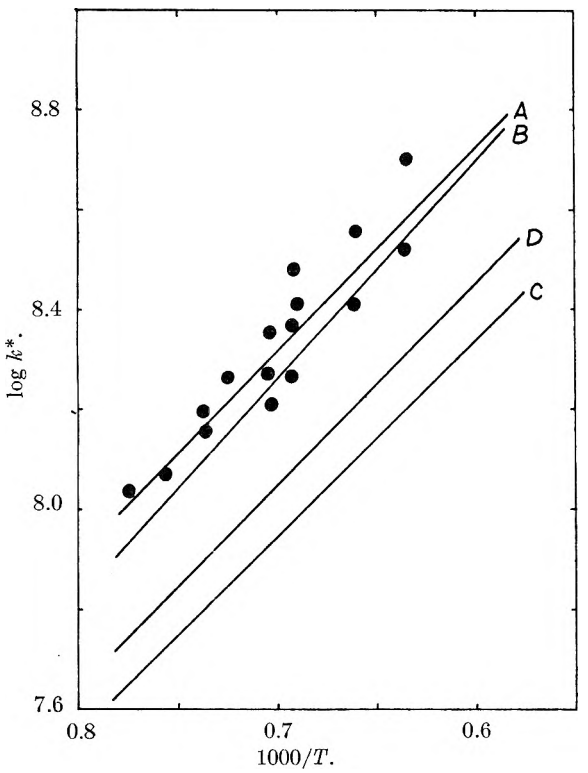

Fig. 3.—Apparent rate constants for the reaction between Br and H_2 at 25% reaction. The points are the experimental points for line A: A, 1% Br_2–1% H_2; B, 2% Br_2–2% H_2; C, 1% Br_2–1% H_2–10% HBr; D, 2% Br_2–2% H_2–10% HBr.

The actual values of k_{2f} and the ratio k_{3f}/k_{3r} were calculated at several temperatures from points taken from the smoothed curves of Fig. 3. Two independent estimations were made, one by comparing the results of the 1% Br_2–1% H_2 shocks with the results of the 1% Br_2–1% H_2–10% HBr shocks, and the other by comparing the 2% Br_2–2% H_2 with the 2% Br_2 H_2–10% HBr. The values obtained are shown in Table III.

Some experiments also were done using higher percentages of bromine and some using excess hydrogen. It was found that when more than 5% of the mixture was reacting the flow behind the shock (or at least the Br_2 concentration) was not smooth even at a distance of forty tube diameters from the membrane.[24] The trace for an extreme case of this type of a shock is shown in Fig. 4. The results with high concentrations of reactants seemed to be consistent with the rate constants determined in the low concentration mixtures, but the shocks were sufficiently unsteady that no meaningful numerical results could be obtained.

TABLE III

RATE CONSTANTS DERIVED FROM THE APPARENT RATE CONSTANTS SHOWN IN FIG. 3

Temp., °K.	$k_{2f} \times 10^{-8}$ (moles^{-1} l. sec.$^{-1}$) from 1% Br_2	2%	avg.	k_{3f}/k_{2r} 1%	2%	avg.
1300	1.16	0.98	1.07	9.5	12.7	11.1
1500	3.07	2.76	2.92	8.8	12.8	10.8
1700	6.34	5.88	6.11	8.5	8.2	8.4

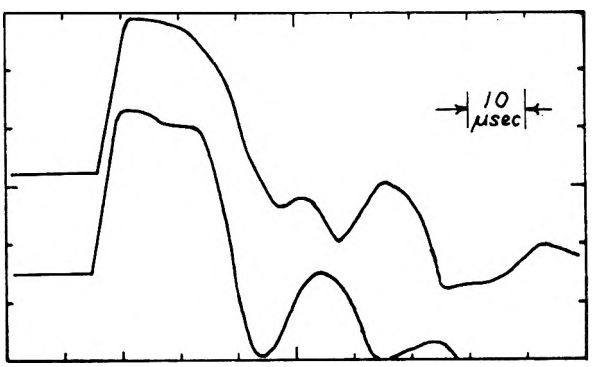

Fig. 4.—Oscillogram of shock in highly exothermic reaction mixture. This shock was run in a 5% Br_2–20% H_2–75% Ar mixture and reached a temperature of 1424°K. at the shock front. It is apparent that no useful kinetic data could be obtained in the shocks in concentrated mixtures.

In many of the experiments observations were made at two observation stations 40 cm. apart, and both oscilloscope traces were analyzed for the value of the rate constant. In these cases it always appeared as if the rate of the reaction were slightly higher (about 10%) at the first station. Both rate constants were used in each case in determining the straight lines of Fig. 3. This effect may be related to the fact that the shock was not steady in more concentrated mixtures since it was not noticed in the earlier work on the dissociation of Br_2.[14]

As can be seen from the experimental points in Fig. 3 the spread of the points from the line is about ± 0.1 in log k^*. This is due in part to the difference between the two traces mentioned in the preceding paragraph, and in part to the unavoidable scatter of the points which must be attributed to the

(23) H. B. Palmer and D. F. Hornig, *J. Chem. Phys.*, **26**, 98 (1957).

(24) Ten shocks were run in a 2% Br_2–10% H_2 mixture, of which only two traces were smooth enough to be measured; the values of k^* were in fair agreement with the 2%–2% values, but not enough data were available to make an accurate comparison. In twelve shocks in 2% Br_2–10% H_2–10% HBr only four traces could be measured; the values of k^* were in fair agreement with the 2%–2%–10% values. The twelve shocks in the 5%–20% mixture showed the greatest amount of turbulence and none were measurable. It would be of considerable interest to have a record of density or pressure as a function of time behind these turbulent shocks, but these measurements are not possible in our apparatus.

TABLE IV

THE RATE CONSTANT, k_{2f}, FOR THE REACTION BETWEEN Br AND H_2

Temp. range, °K.	Ref.	$\log k_{2f} = A - B/T$		$k_{2f} = CT^{1/2}e^{-H/RT}$	
		A	B, °K.	C, l. mole^{-1} sec.$^{-1}$	H, kcal./mole
500–575	5	11.357	4235 ± 46	5.92×10^9	18.8 ± 0.2
550–600	10	10.927	4053 ± 141	2.15	18.0 ± 0.7
1300–1700	This work	11.254	4195 ± 400	3.54	18.3 ± 1.8
500–1700	All	11.238	4190 ± 21	3.35	18.3 ± 0.1
Br + D_2					
550–650	10	10.889	4440 ± 56	1.93×10^9	19.7 ± 0.3
1300–1700	This work	11.082	4461 ± 209	1.91	19.8 ± 0.9
550–1700	All	10.985	4497 ± 9	1.84	19.7 ± 0.1

limited accuracy of the shock wave technique. There is further uncertainty introduced by the uncertainty in the value to use for the rate constant for Br_2 recombination. If the value of k_{1r} which was used in the calculations is increased by 5% (this would be the case if Br_2 is five times as efficient as Ar as a third body or if HBr is 50% more efficient) the calculated values of k^* and k_{2f} would be decreased by about 10% and the value of the ratio k_{3f}/k_{2r} would be decreased by about 15%. A conservative estimate of the uncertainty in the constants reported in Table III is that they are all uncertain by at least 25% and that they are more likely to be too large than too small.

The Forward Reaction, D_2–Br_2.—Twenty-one shocks were run in mixtures of Br_2, D_2 and Ar. These mixtures were either 1% Br_2–1% D_2–98% Ar or 2%–2%–96% since it was felt that high concentrations would not yield any useful information in the light of the H_2–Br_2 results. No shocks were run in mixtures containing DBr so it was not possible to make an estimate of k_{3f}/k_{2r} for this system. Rather it was assumed that the value 8.6 from the H_2–Br_2 system also was correct for the D_2–Br_2 system.[25] Since this ratio was taken as known it was possible to calculate k_{2f} directly for each shock. The 1% and 2% mixtures gave essentially the same results which can be combined to yield $k_{2f} = 1.91 \times 10^9\ T^{1/2} \exp(-19800/RT)$. As was the case with the H_2–Br_2 shocks the rate constant determined from the oscilloscope trace at the second observation station was lower than that determined at the first station. Both traces were available more consistently here than in the case of H_2–Br_2 and it would appear that the effect is slightly greater at high temperatures than at low and is about a 30–40% discrepancy. As with the H_2–Br_2 data both sets here have been averaged in the results.

Direct Observation of the Back Reaction.—In many of the shocks in the HBr–Br_2 mixtures it was apparent from the oscilloscope traces that equilibrium had been reached at much higher concentrations of Br_2 than would be expected if the only reaction were the dissociation of Br_2. In four of the shocks in the 0.482% Br_2–99.5% HBr mixtures the Br_2 concentration clearly went through a minimum. The most striking example of this was shown in Fig. 2. In these four shocks the rate constant, k_{2r}, for the reaction between HBr and Br was calculated as outlined in the section on calculations. The points show an average scatter of about 10% from $k_{3r} = 8.1 \times 10^9\ T^{1/2}e^{-4450/RT}$ which was fit to them by the method of least squares. These values of k_{3r} can be combined with the previous values of k_{2f} to obtain an independent estimate of the ratio $k_{3f}/k_{2r} = (k_{3r}/k_{2f})/K$. When the actual values of k_{3r} are combined with the smoothed values of k_{2f} from Table IV the resulting values of the ratio show no variation with temperature and have an average value of 8.3 ± 0.7, which can be compared with the value 10.1 ± 1.7 obtained from the measurements of the forward reaction with and without added HBr.

Discussion

The results of the various studies of the value of k_{2f} are collected in Table IV where they are given in two forms, first as $\log k_{2f} = A - B/T$ for convenience in calculation, and second as $k_{2f} = CT^{1/2}e^{-\Delta H/RT}$ since this form has some theoretical justification for a bimolecular reaction. The probable errors would indicate that neither of these two forms is to be preferred over the other on the basis of the experimental data. The agreement between the low temperature results and the high temperature shock wave results is quite good. The difference between D_2 and H_2 which was found at low temperature is confirmed in the shock wave results; k_{2f} for reaction with D_2 has a smaller preexponential factor and a larger activation energy than for reaction with H_2.

The ratio k_{3f}/k_{2r} which was known to be temperature invariant at low temperatures within experimental error has now been shown to be temperature invariant over the temperature range 300–1700° K. within experimental error. The best low temperature value, 8.4 ± 0.6, is almost exactly the same as the weighted average of the two independent measurements of the ratio at high temperature, 8.3 ± 0.7 and 10.1 ± 1.7.

The activation energy associated with k_{2f} is 18.3 kcal./mole (Table IV). The heat of the reaction at 0°K. is 16.2 kcal./mole. This means that k_{3f} and k_{2r} must have an identical activation energy of about 2 kcal./mole. If the value of the ratio at high temperature differs from that at low temperatures by 10% the activation energies would differ by

(25) It is worthy of note that this ratio never has been measured for D_2–Br_2 at any temperature. In their work at lower temperatures Bach, Bonhoeffer and Moelwyn-Hughes made the same assumptions we have. The value of k_{2f} is not greatly affected by an error in this ratio; in the work here changing k_{3f}/k_{2r} by 10% would change k_{2f} by slightly less than 1%.

about 0.1 kcal./mole. This pair of activation energies is an embarrassing case for any rule which tries to predict the activation energy from the bond energy of the bond being broken since D_{Br_2} (=45 kcal./mole) and D_{HBr} (=87 kcal./mole) differ by a factor of 2. It would be very interesting to determine this ratio and its temperature dependence in the D_2–Br_2 system.

Acknowledgments.—We wish to thank the Research Corporation, the Office of Ordnance Research, U. S. Army, and the Graduate School of the University of Minnesota for their support of this work.

THERMODYNAMICS OF THE SOLID SYSTEM CaO–SiO_2 FROM ELECTROMOTIVE FORCE DATA

BY ROBERT BENZ[1] AND CARL WAGNER

Max-Planck-Institut für physikalische Chemie, Göttingen, Germany

Received December 13, 1960

The chemical potentials and the relative integral molar free energy of mixing for the binary system CaO–SiO_2 at 700° are deduced from e.m.f. measurements on galvanic cells of type Pt, O_2(g)/CaO(s)/CaF_2(s)/CaO–SiO_2(s)/Pt, O_2(g) where CaO–SiO_2(s) denotes one of the solid two-phase mixtures Ca_2SiO_4–$Ca_3Si_2O_7$, $Ca_3Si_2O_7$–$CaSiO_3$ or $CaSiO_3$–SiO_2.

Introduction

For a rational treatment of metal–slag equilibria, it is imperative to know activities in both the alloy and the slag. Since, in steel-making, the liquid ternary slag CaO–Al_2O_3–SiO_2 plays an important role, the thermodynamics of this system[2–5] and of the liquid binary system CaO–SiO_2[6–12] has been investigated at several laboratories. In conjunction herewith, data for the solid binary system CaO–SiO_2 are needed. The heats of formation of the compounds $CaSiO_3$,[13] Ca_2SiO_4 and Ca_3SiO_5[14] from CaO and SiO_2 have been determined as the differences of the heats of solution in aqueous hydrofluoric acid. The heat capacities of $CaSiO_3$,[15–17] Ca_2SiO_4, $Ca_3Si_2O_7$ and Ca_3SiO_5[18–20] have been determined and the corresponding standard entropies have been computed.[17,18] From these data and the heats of formation and heat capacities of CaO and SiO_2,[21,22] the free energies of formation of the solid silicates (excepting $Ca_3Si_2O_7$ for which ΔH^0 is lacking) can be calculated. To supplement present information, direct measurements of the free energies of formation of the solid calcium silicates at elevated temperatures seem desirable.

The free energy of formation of $CaSiO_3$ from CaO and SiO_2 may be calculated from the e.m.f. of a galvanic cell in which the virtual cell reaction on passing current is

$$CaO + SiO_2 = CaSiO_3 \qquad (1)$$

To this end, one may use the cell

$$Pt,\ O_2(g)\ |CaO(s)\ |CaF_2(s)\ |CaSiO_3(s),\ SiO_2(s)\ |Pt,\ O_2(g) \qquad (Ia)$$

in which CaF_2 is an ionic conductor with fluorine ions migrating mostly as interstitials.[23] Thus, on passing two faradays (= 2$\mathfrak{F}$) across cell Ia, the reaction on the left-hand side is

$$CaO(s) + 2F^- (\longleftarrow) = CaF_2(s) + {}^1/_2O_2(g) + 2e^- (\longleftarrow) \qquad (2)$$

and the reaction on the right-hand side is

$$CaF_2(s) + SiO_2(s) + {}^1/_2O_2(g) + 2e^- (\longleftarrow) = CaSiO_3(s) + 2F^- (\longleftarrow) \qquad (3)$$

Upon adding equations 2 and 3, one sees that, when two faradays are passed across cell Ia, there results reaction 1. Thus, the free energy change ΔF of the cell reaction 1 is related to the e.m.f. E of cell Ia by

$$\Delta F = -2E\mathfrak{F} \qquad (4)$$

The cell reaction on passing two faradays may also be formulated as the transfer of one mole CaO from the pure state at the left-hand to the bound state at the right-hand electrode of cell Ia. Thus

$$(\mu_{CaO} - \mu^0_{CaO}) = -2E\mathfrak{F} \qquad (5)$$

where μ^0_{CaO} and μ_{CaO}, respectively, are the chemical potentials of CaO in the pure state and in the two-phase mixture at the right-hand side of cell Ia.

(1) Los Alamos Scientific Laboratory, Los Alamos, New Mexico.

(2) C. Fulton and J. Chipman, *Trans. AIME*, **200**, 1136 (1954).

(3) F. C. Langenberg, H. Kaplan and J. Chipman, "The Physical Chemistry of Steelmaking," J. Chipman (ed.), The Technology Press of M.I.T. and John Wiley and Sons, Inc., New York, N. Y., 1958, p. 65.

(4) F. D. Richardson, "The Physical Chemistry of Steelmaking," J. F. Elliott (ed.), The Technology Press of M.I.T. and John Wiley and Sons, Inc., New York, N. Y., 1958, p. 68.

(5) F. C. Langenberg and J. Chipman, *Trans. AIME*, **215**, 958 (1959).

(6) L. Chang and G. Derge, *ibid.*, **172**, 90 (1947).

(7) L. S. Darken, "Thermodynamics and Physical Metallurgy," Am. Soc. for Metals, Cleveland, O., 1950, p. 340.

(8) F. D. Richardson, "The Physical Chemistry of Melts," Inst. of Min. and Met., London, 1953, p. 75.

(9) P. T. Carter and J. G. MacFarlane, *J. Iron and Steel Inst.*, **185**, 62 (1957).

(10) J. P. Baird and J. Taylor, *Trans. Faraday Soc.*, **54**, 526 (1958).

(11) C. J. B. Fincham and F. D. Richardson, *Proc. Roy. Soc. (London)*, **A223**, 40 (1954).

(12) L. Yang, C. L. McCabe and R. Miller, "The Physical Chemistry of Steelmaking," J. F. Elliott (ed.), The Technology Press of M.I.T. and John Wiley and Sons, Inc., New York, N. Y., 1958, p. 63.

(13) D. R. Torgeson and Th. G. Sahama, *J. Am. Chem. Soc.*, **70**, 2156 (1948).

(14) E. G. King, *ibid.*, **73**, 656 (1951).

(15) G. S. Parks and K. K. Kelley, *J. Phys. Chem.*, **30**, 1175 (1926).

(16) J. C. Southard, *J. Am. Chem. Soc.*, **63**, 3142 (1941).

(17) K. K. Kelley, *U. S. Bur. Mines Bulletin*, 477 (1950).

(18) S. S. Todd, *J. Am. Chem. Soc.*, **73**, 3277 (1951).

(19) E. G. King, *ibid.*, **79**, 5437 (1957).

(20) J. P. Coughlin and C. J. O'Brien, *J. Phys. Chem.*, **61**, 767 (1957).

(21) O. Kubaschewski and E. L. Evans, "Metallurgical Thermochemistry," Pergamon Press, New York, N. Y., 1958.

(22) Circular of the National Bureau of Standards 500, p. 629, U. S. Printing Office, Washington, D. C., 1952.

(23) R. W. Ure, Jr., *J. Chem. Phys.*, **26**, 1363 (1957).

Using the two-phase mixture $Ca_3Si_2O_7$ + $CaSiO_3$ or Ca_2SiO_4 + $Ca_3Si_2O_7$ instead of $CaSiO_3$ + SiO_2 at the right-hand side of cell Ia, one may, therefore, obtain the relative chemical potential of CaO in these mixtures. Therefrom the corresponding values for SiO_2 ($\mu_{SiO_2} - \mu^0_{SiO_2}$) and the standard free energies of formation of the various compounds of the system CaO–SiO_2 from CaO and SiO_2 may be calculated with the help of the Gibbs-Duhem equation.

For practical reasons, the cells may be modified in various ways.

(1) Inasmuch as CaO, $CaSiO_3$ and SiO_2 are known to exhibit very low conductivities even at 1000°, one may add CaF_2 to the left-hand and to the right-hand side of cell Ia in order to decrease the internal resistance of the cell. An addition of CaF_2 does not change the half-cell reactions formulated in eq. 2 and 3.

(2) Because the transformation of unstable to stable phases of the system CaO–SiO_2 may be sluggish and, moreover, equilibrium among the stable solid phases at each side of the cell may be attained rather slowly, one may add a solvent in which the solid phases dissolve to some extent. Then one may expect a performance similar to electrodes of second kind in aqueous solutions with sparingly soluble salts, *e.g.*, Ag(s)/AgCl(s), KCl(aq). As a suitable solvent, one may take a mixture of NaF and KF with the eutectic temperature of 710° for the ternary system NaF–KF–CaF_2. In contrast to cells with aqueous solutions, however, only small amounts of the liquid phase at each side are recommendable in order to retain the advantages of solid CaF_2 serving as a diaphragm which separates the various substances present on the left-hand and the right-hand side of the cell, and as an intermediate electrolyte involving conduction exclusively by virtue of migration of fluorine ions.

(3) Since electrochemical equilibrium with oxygen electrodes is not attained readily at lower temperatures, one may use a catalyst for the electrochemical reaction between oxygen molecules, electrons and oxygen ions. Irman[24] has shown that a definite ratio of hexavalent to trivalent chromium in a borate melt is reached by equilibrating the melt with a gas phase involving a definite oxygen partial pressure. Thus, adding either Cr_2O_3 or $K_2Cr_2O_7$ to an auxiliary liquid electrolyte next to the electrodes in cell Ia, one may try to ensure a more rapid attainment of equilibrium potentials. Similarly, one may use compounds of other elements occurring in different valence states, *e.g.*, PbO, Mn_2O_3 or V_2O_5 which are referred to as catalysts in what follows. Use of catalysts has been found to be profitable even without the presence of an auxiliary liquid electrolyte. The mechanism of the attainment of equilibrium at the electrodes, however, has not yet been clarified.

For a significant thermodynamic evaluation, e.m.f. values must be reproducible. It is expedient to check the reproducibility of the half cells by investigating symmetrical cells involving either CaO or one of the two-phase mixtures, *viz.*

Pt, O_2(g) |CaO(s) |CaF_2(s) |CaO(s) |Pt, O_2(g) (II)

In particular, one may set up cells with different additions of catalysts at the right-hand and the left-hand side in order to check whether the e.m.f. is sufficiently close to zero as expected from a thermodynamic point of view.

Experimental

Materials.—As the solid electrolyte in the middle of the cells, single crystals of calcium fluoride obtained from Fa. E. Leitz, Wetzlar, Germany, were used. Crystals were in part nearly clear and in part milky owing to the presence of imperfections. CaF_2 used as an additive was prepared by digesting calcium carbonate in hydrofluoric acid.[25]

Calcium oxide was prepared by thermal decomposition of $CaCO_3$, p.a.; silica, p.a., was available in granular form. A two-phase mixture $CaSiO_3$+SiO_2 was prepared in a platinum crucible by melting together SiO_2 and CaO at a weight ratio of 0.692:1 nearly corresponding to the composition of the eutectic melt coexisting with solid $CaSiO_3$+SiO_2 at 1436°. The two-phase mixture $Ca_3Si_2O_7$+$CaSiO_3$ was prepared by sintering for 24 hours at 1250° equimolar quantities of the compounds which in turn were prepared by sintering stoichiometric quantities of CaO and SiO_2 at 1400° for 40 hours with intermittent grindings. The two-phase mixture Ca_2SiO_4+$Ca_3Si_2O_7$ was prepared by sintering a quantity of CaO and SiO_2 with the weight ratio 1.70:1 at 1380° for 18 hours with intermittent grindings. The attainment of equilibrium in two-phase mixtures is an essential aspect of these preparations. Equilibrium was verified by sintering the mixtures until the e.m.f. values of the cells were independent of the sintering time.

CaO and the two-phase mixtures of the system CaO–SiO_2 were ground to a fine powder in an agate mortar, mixed with additions and pressed to tablets in a die.

Apparatus.—Cells involving only solids were assembled by pressing together platinum discs with leads, tablets of the mixtures next to the electrodes, and a single CaF_2 crystal (*ca.* 6 mm. thick) in a holder designed by Schmalzried.[26]

For cells involving a melt of NaF–KF as an auxiliary electrolyte, CaF_2 crystals about 5 × 5 × 15 mm. were used with small depressions accommodating the liquid electrolyte and platinum wires as leads.

Cells were placed in a quartz tube in a wire-wound electrical furnace. Pick-up of stray currents was avoided by surrounding the quartz tube by a grounded stainless steel tube separated from the quartz tube by an air gap. A slow stream of oxygen purified over heated CuO and thoroughly dried was passed in order to provide oxygen of atmospheric pressure. Presence of moisture was avoided in order to eliminate the possible side reaction CaF_2+H_2O = CaO+ 2HF.

Results

First, cell Ia was investigated without any of the modifications mentioned above. E.m.f. readings were found to be erratic, ranging from 0.05 to 0.15 v. at 900 to 1100°.

Second, cell Ia was investigated with additions of 10 weight % of CaF_2 on both sides in order to lower the internal resistance. Readings were again erratic ranging from 0.25 to 0.45 v. at 800 to 1000°.

Third, cell Ia was investigated with liquid NaF–KF present at the electrode and PbO, Cr_2O_3 or $K_2Cr_2O_7$ as catalysts. E.m.f. values were found to be somewhat lower and to decrease in the course of time. Initial values were between 0.43 and 0.40 v. at 750°. It is possible that a drift of e.m.f. values was due to creep of the liquid electrolyte along the surface of the CaF_2 crystals resulting in bypass.

Fourth, cell Ia was investigated with additions

(24) F. Irman, *J. Am. Chem. Soc.*, **74**, 4767 (1952).

(25) G. Brauer, "Präparative anorganische Chemie," Ferdinand Enke Verlag, Stuttgart, 1954, p. 184.

(26) H. Schmalzried, *Z. physik. Chem. N.F.*, **25**, 178 (1960).

of 10 weight % solid CaF_2 and PbO, Cr_2O_3 or $K_2Cr_2O_7$ as catalysts. Steady e.m.f. values were observed for several hours. Typical results along with extreme limits of fluctuations during the time of observations are listed in Table I. In essence, the same e.m.f. values were obtained with different catalysts.

TABLE I

E.M.F. VALUES OF CELLS OF TYPE

$$\text{Pt}, O_2 \mid \text{CaO} \mid CaF_2 \mid CaSiO_3, SiO_2 \mid \text{Pt}, O_2$$

WITH VARIOUS ADDITIONS

Temp., °C.	Catalyst, mole per mole CaO	Time, hr.	E.m.f., mv.
785	0.03 Cr_2O_3	7	462 ± 2
625	.03 $K_2Cr_2O_7$	24	463 ± 2
665	.03 $K_2Cr_2O_7$	5	465 ± 2
670	.03 $K_2Cr_2O_7$	3	463 ± 2
750	.03 $K_2Cr_2O_7$	5	463 ± 1
875	.03 $K_2Cr_2O_7$	1	463 ± 2
662	.05 PbO	24	460 ± 1
700	.05 PbO	6	460 ± 1
730	.05 PbO	2	460 ± 1
763	.05 PbO	2	461 ± 1
810	.05 PbO	5	460 ± 2
830	.05 PbO	3	458 ± 1
		Mean value	461 ± 4

Next cells of type

$$\text{Pt}, O_2(g) \mid CaO(s) \mid CaF_2(s) \mid Ca_3Si_2O_7(s), CaSiO_3(s) \mid \text{Pt}, O_2(g) \quad \text{(Ib)}$$

were investigated with additions of 10% CaF_2. In the absence of catalysts, e.m.f. values decreased continually from the initial value of approximately 0.4 v. More consistent results were obtained with cells containing catalysts and are listed in Table II.

TABLE II

E.M.F. VALUES OF CELLS

$$\text{Pt}, O_2 \mid \text{CaO} \mid CaF_2 \mid Ca_3Si_2O_7, CaSiO_3 \mid \text{Pt}, O_2$$

WITH VARIOUS ADDITIONS

Temp., °C.	Catalyst, mole per mole CaO	Time, hr.	E.m.f., mv.
670	0.03 Cr_2O_3	6	421 ± 1
670	.03 Cr_2O_3	12	419 ± 4
680	.03 Cr_2O_3	5	418 ± 1
700	.03 Cr_2O_3	2	417 ± 1
700	.03 Cr_2O_3	6	415 ± 2
680	.03 $K_2Cr_2O_7$	12	416 ± 4
700	.03 $K_2Cr_2O_7$	6	417 ± 2
700	.03 $K_2Cr_2O_7$	6	420 ± 2
710	.03 $K_2Cr_2O_7$	6	421 ± 1
730	.03 $K_2Cr_2O_7$	4	418 ± 1
		Mean value	418 ± 6

Next, cells of type

$$\text{Pt}, O_2(g) \mid CaO(s) \mid CaF_2(s) \mid Ca_2SiO_4(s), Ca_3Si_2O_7(s) \mid \text{Pt}, O_2(g) \quad \text{(Ic)}$$

were investigated with additions of 10% CaF_2 and catalysts. Results are listed in Table III. The e.m.f. values are essentially independent of the presence or absence of additives although equilibrium generally was attained more rapidly with the additives.

TABLE III

E.M.F. VALUES OF CELLS

$$\text{Pt}, O_2 \mid \text{CaO} \mid CaF_2 \mid Ca_2SiO_4, Ca_3Si_2O_7 \mid \text{Pt}, O_2$$

WITH VARIOUS ADDITIONS

Temp., °C.	Catalyst, mole per mole CaO	Time, hr.	E.m.f., mv.
760	None	4	61 ± 1
760	None	3	60 ± 2
810	None	4	63 ± 1
870	None	4	62 ± 1
670	0.03 Cr_2O_3	21	57 ± 1
698	.03 Cr_2O_3	5	58 ± 1
727	.03 Cr_2O_3	15	63 ± 1
735	.03 Cr_2O_3	5	66 ± 1
690	.03 $K_2Cr_2O_7$	5	60 ± 1
735	.03 $K_2Cr_2O_7$	10	63 ± 1
690	.05 PbO	25	58 ± 1
725	.05 PbO	5	61 ± 2
730	.05 PbO	15	60 ± 1
		Mean value	60 ± 4

The temperature dependence of the e.m.f. of each cell was found to be small as is usually the case for cells involving reactions between solids as the change in entropy is low. The reproducibility of the half cells was tested by investigating cells of type II, see Table IV. The e.m.f. of the cells was very close to zero if different amounts of catalysts were present and, also, if the initial stage of oxidation of chromium was different at the two sides of the cell.

TABLE IV

E.M.F. VALUES OF CELLS OF TYPE II WHICH ARE SYMMETRICAL EXCEPT FOR THE PRESENCE OF CATALYSTS IN VARIOUS AMOUNTS

Phases of system CaO–SiO_2	Catalyst, mole per mole CaO Left	Right	Temp., °C.	Time, hr.	E.m.f., mv.
CaO	0.03 Cr_2O_3	None	660	2	2 ± 0.5
	.03 $K_2Cr_2O_7$	0.03 Cr_2O_3	850	8	1.8 ± 0.5
	.05 PbO	None	770	2	0 ± 0.5
Ca_2SiO_4 + $Ca_3Si_2O_7$	.03 Cr_2O_3	0.001 Cr_2O_3	800	9	0 ± 1
	.03 $K_2Cr_2O_7$	.001 $K_2Cr_2O_7$	710	10	1 ± 1
	.03 $K_2Cr_2O_7$	.03 Cr_2O_3	710	14	2 ± 1
	.05 PbO	.001 PbO	700	11	1 ± 1
$Ca_3Si_2O_7$ + $CaSiO_3$	.03 Cr_2O_3	.005 Cr_2O_3	740	9	5 ± 1
	.03 $K_2Cr_2O_7$	.005 $K_2Cr_2O_7$	700	3	1 ± 1
	.03 $K_2Cr_2O_7$	.05 Cr_2O_3	710	8	1 ± 2
$CaSiO_3$ + SiO_2	.03 Cr_2O_3	.005 Cr_2O_3	730	13	2 ± 1
	.03 $K_2Cr_2O_7$	.005 $K_2Cr_2O_7$	730	2	1.5 ± 0.2
	.03 Cr_2O_3	.03 $K_2Cr_2O_7$	730	12	2 ± 1.5
	.01 PbO	.05 PbO	720	11	1 ± 1

Discussion

Values of the partial molar free energies of mixing for CaO as component 1, $F_1^M \equiv \mu_{CaO} - \mu^0_{CaO} = -2E\mathfrak{F}$, in the various two-phase regions of the system CaO–SiO_2 are listed in Table V where Roman numerals are used to denote the phases of the system CaO–SiO_2 which are stable between 600 and 1000°, *viz.*

I = CaO, $X_2 = 0$
II = Ca_2SiO_4, $X_2 = 0.333$
III = $Ca_3Si_2O_7$, $X_2 = 0.40$
IV = $CaSiO_3$, $X_2 = 0.50$
V = SiO_2, $X_2 = 1.00$

where X_2 is the mole fraction of SiO_2.

TABLE V

PARTIAL MOLAR FREE ENERGIES OF MIXING OF CaO AND SiO_2 IN THE SYSTEM CaO–SiO_2 AT 700°

Phases	X_2	F_1^M, kcal.	F_2^M, kcal.
I + II	0 to 0.333	0.0	-32.3 ± 0.5
II + III	0.333 to .400	-2.8 ± 0.2	$-26.7 \pm .8$
III + IV	.400 to .500	$-19.3 \pm .3$	$-2.0 \pm .5$
IV + V	.500 to 1.000	$-21.3 \pm .2$	0.0

Values of the partial molar free energy of mixing for SiO_2 as component 2 have been calculated with the help of the Gibbs–Duhem equation. Since values of F_1^M and F_2^M are constant in each two-phase region, integration of the Gibbs-Duhem equation yields these algebraic formulas

$$F_2^M(\text{III} + \text{IV}) = -[F_1^M(\text{III} + \text{IV}) - F_1^M(\text{IV} + \text{V})] \quad (6a)$$

$$F_2^M(\text{II} + \text{III}) = -\tfrac{3}{2}F_1^M(\text{II} + \text{III}) + \tfrac{1}{2}F_1^M(\text{III} + \text{IV}) + F_1^M(\text{IV} + \text{V}) \quad (6b)$$

$$F_2^M(\text{I} + \text{II}) = +\tfrac{1}{2}F_1^M(\text{II} + \text{III}) + \tfrac{1}{2}F_1^M(\text{III} + \text{IV}) + F_1^M(\text{IV} + \text{V}) \quad (6c)$$

Numerical values also are listed in Table V.

TABLE VI

INTEGRAL MOLAR FREE ENERGIES OF MIXING FOR THE SYSTEM CaO–SiO_2 AT 700°

Phases	X_2	F^M, kcal. E.m.f.	Calorimetry
II (Ca_2SiO_4)	0.333	-10.8 ± 0.1	-10.5 ± 0.1
III ($Ca_3Si_2O_7$)	.40	$-12.4 \pm .15$	
IV ($CaSiO_3$)	.50	$-10.6 \pm .15$	-10.6 ± 0.1

Moreover, integral molar free energies of mixing corresponding to the formation of silicates involving X_1 mole CaO and X_2 mole SiO_2 have been calculated. From the general formula

$$F^M = X_2 \int_{X_2}^{1} (F_1^M/X_2^2)\, dX_2 \quad (7)$$

one obtains, in view of the constancy of F_1^M in each two-phase field

$$F^M(X_2 = 0.5) = 0.5F_1^M(\text{IV} + \text{V}) \quad (8a)$$

$$F^M(X_2 = 0.4) = 0.4F_1^M(\text{IV} + \text{V}) + 0.2F_1^M(\text{III} + \text{IV}) \quad (8b)$$

$$F^M(X_2 = 0.333) = 0.333F_1^M(\text{IV} + \text{V}) + 0.167F_1^M(\text{III} + \text{IV}) + 0.167F_1^M(\text{II} + \text{III}) \quad (8c)$$

Numerical values and their uncertainties are listed in Table VI.

For comparison, Table VI contains data based on calorimetric data. For 298°K., one has

$2CaO(s) + SiO_2(quartz) = Ca_2SiO_4(s)$;
$\Delta H^0 = -30.19 \pm 0.23$ kcal.[14]
$\Delta S^0 = +1.5$ e.u.[22] (9a)

$CaO(s) + SiO_2(quartz) = CaSiO_3(wollastonite)$;
$\Delta H^0 = -21.25 \pm 0.13$ kcal.[13]
$\Delta S^0 = +0.1$ e.u.[22] (9b)

Upon adding enthalpy and entropy increments as listed by Kelley,[27] one may calculate values for 700°C. = 973°K. and therefrom values of F^M for $X_2 = 0.33$ and 0.50 shown in the last column of Table VI. Values deduced from e.m.f. values and values based on calorimetric measurements are in close agreement.

Acknowledgments.—The authors wish to thank Dr. H. Schmalzried who has constantly placed himself at their disposal for stimulating discussions of the experimental work, and the firm E. Leitz for the gift of calcium fluoride crystals. The first author wishes to thank the U. S. Atomic Energy Commission for leave from the Los Alamos Scientific Laboratory during the course of this investigation.

(27) K. K. Kelley, U. S. Bureau of Mines Bulletin 584 (U. S. Government Printing Office, Washington, D. C., 1959).

THE KINETICS OF THE REACTIONS OF AROMATIC HYDROCARBONS IN SULFURIC ACID. IV. DURENE, ISODURENE, PREHNITENE AND PENTAMETHYLBENZENE

BY MARTIN KILPATRICK AND MAX W. MEYER

Department of Chemistry, Illinois Institute of Technology, Chicago 16, Ill.

Received January 3, 1961

The tetramethylbenzenes isomerize in hydrofluoric acid yielding isodurene, but the end product in sulfuric acid is the stable prehnitenesulfonic acid. This product results from disproportionation rather than isomerization. The monosulfonic acids of durene, isodurene and pentamethylbenzene desulfonate at conveniently measurable rates in sulfuric acid, but at higher concentrations durene isomerizes to isodurene and isodurene slowly disproportionates. Prehnitenesulfonic acid does not show desulfonation, isomerization or disproportionation over the range 8–18 *M* sulfuric acid. The results are interpreted in terms of isomerization and disproportionation of the hydrocarbon rather than the sulfonic acid.

Introduction

Interest in the behavior of polymethylbenzenes arose from the fact that the conductance of prehnitene and durene in anhydrous hydrofluoric acid at 20° changed with time.[1] This was interpreted as an isomerization to isodurene.

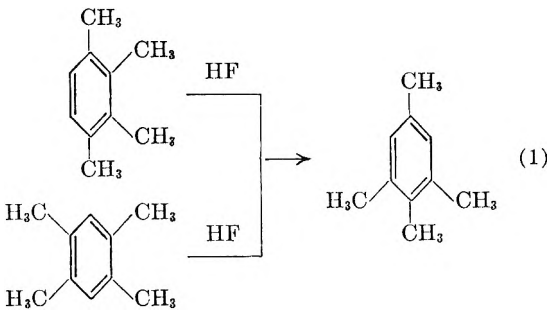

(1)

However, when the solvent is concentrated sulfuric acid at room temperature, the product is prehnitene, as the sulfonic acid, rather than isodurene. This called our attention to the Jacobsen reaction,[2] which deals with the migration of alkyl groups in polyalkylbenzenes, and of halogens in halobenzenes, under the influence of sulfuric acid. Jacobsen found that when a heterogeneous mixture of durene and concentrated sulfuric acid was allowed to stand at room temperature with frequent shaking, the mixture turned brown and large amounts of SO_2 were given off.[3] The products isolated were hexamethylbenzene, prehnitenesulfonic acid, and two isomers of pseudocumenesulfonic acid. The reaction was presumed to go through two consecutive disproportionations

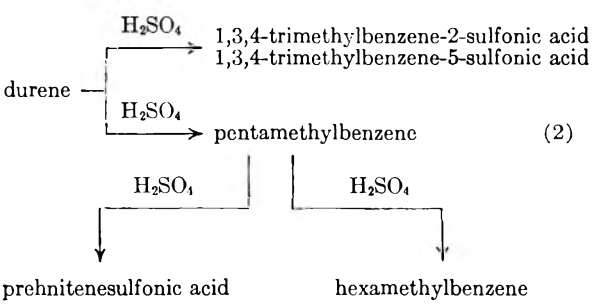

(2)

Smith and Cass[4] showed that in the polymethylbenzene series only durene, isodurene and pentamethylbenzene undergo the Jacobsen reaction. All the other methylbenzenes are stable in concentrated sulfuric acid over an extended period of time. Both Jacobsen and Smith contended that it is the sulfonic acid and not the hydrocarbon that rearranges. In view of the fact that prehnitene is the end product in sulfuric acid and isodurene in anhydrous hydrofluoric acid, and the fact that no kinetic study of isomerization or disproportionation in a single liquid phase without co-catalyst had been made, a study of the kinetics of the Jacobsen reaction in sulfuric acid was undertaken. The present paper reports the results on sulfonation, desulfonation, resulfonation, isomerization and disproportionation of the tetra- and pentamethylbenzenes in sulfuric acid.

Experimental

Materials.—All hydrocarbons were standard A.P.I. samples unless otherwise stated.

The sodium salt of pentamethylbenzenesulfonic acid was prepared in accordance with the procedure given by Jacobsen.[5] Powdered pentamethylbenzene was treated with chlorosulfonic acid to form a mixture of sulfone and sulfochloride. The reaction products were treated with sodium hydroxide in 95% alcohol to form the sodium salt of pentamethylbenzenesulfonic acid and the sulfone removed by ether extraction. Purification was effected by repeated crystallization from water.

The sodium salt of durenesulfonic acid was prepared and purified in a similar manner.[6] Isodurenesulfonic acid was prepared according to the method given by Smith and Cass.[4] Isodurene was sulfonated in concentrated sulfuric acid at room temperature, the mixture poured onto ice, the sulfonic acid filtered off and dried on a porous plate. It was purified by dissolving in water and reprecipitating with hydrochloric acid at low temperature. This process was repeated to a constant melting point of 82°; Smith and Cass give 79°. Prehnitenesulfonic acid was prepared in a manner similar to that for isodurenesulfonic acid and purified as the sodium salt after the procedure for durenesulfonic.

Experimental Procedure.—Pentamethylbenzene and the tetramethylbenzenes are sparingly soluble in aqueous sulfuric acid and care must be taken to have a homogeneous solution throughout the experiment. The procedure followed to bring just the right amount of sulfonic acid into solution was to weigh out 2 mg. of the sodium salt or the acid, shake for three minutes with 100 ml. of cold (5°) sulfuric acid of the required concentration, filter through a fritted glass filter to remove undissolved salt, and fill a 10 cm. absorption cell. The cell was placed in the thermostated compartment of the Cary spectrophotometer and the disappearance of the sulfonic acid with time followed by

(1) M. Kilpatrick and F. Luborsky, *J. Am. Chem. Soc.*, **78**, 577 (1953).

(2) L. I. Smith, "Organic Reactions," John Wiley and Sons Inc., New York, N. Y., Vol. I, p. 370.

(3) O. Jacobsen, *Ber.*, **19**, 1209 (1886).

(4) L. I. Smith and D. W. Cass, *J. Am. Chem. Soc.*, **54**, 1614 (1932).

(5) O. Jacobsen, *Ber.*, **20**, 896 (1887).

(6) O. Jacobsen and E. Schnappauf, *ibid.*, **18**, 284 (1885).

recording the change in optical density for a particular wave length. For durene, isodurene, prehnitene and pentamethylbenzene the wave lengths followed were 291, 286, 283 and 291 mμ, respectively. The spectrum between 270 and 300 mμ was often periodically recorded during the run.

When the starting material was the solid hydrocarbon durene or pentamethylbenzene, the solution was prepared in an analogous fashion. For the liquid hydrocarbons, prehnitene and isodurene, one drop of the liquid (3–4 mg.) was dissolved in 300–400 ml. of sulfuric acid and the rate of appearance of the sulfonic acid followed as above. The tetramethylbenzenes are quite insoluble in sulfuric acid in the range 13–17 *M* and care must be taken to have a homogeneous solution for the kinetic measurements.

Experiments starting with the sulfonic acids showed that complete desulfonation could be measured conveniently in sulfuric acid over these concentration ranges: 14.9 to 13.1 *M* for durenesulfonic acid, 13.5 to 11.5 *M* for isodurenesulfonic acid, and 10.2 to 8.7 *M* for pentamethylbenzenesulfonic acid. The experimental results are presented in Table I; all first-order velocity coefficients were computed using decadic logarithms and are 0.4343 times the true constant. Figure 1 shows that log k_D increases linearly

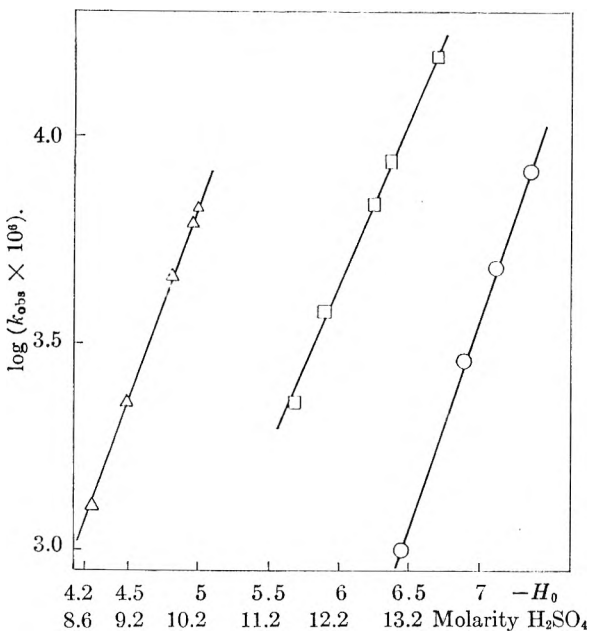

Fig. 1.—Desulfonation of sulfonic acids in sulfuric acid at 12.3°; log (k_{obs} × 10⁶) *vs.* H_0 and *vs.* molarity H_2SO_4.

	vs. H_0	Slopes *vs.* molarity H_2SO_4
△ pentamethylbenzenesulfonic acid	0.95	0.48
□ isodurenesulfonic acid	.85	.42
○ durenesulfonic acid	.99	.51

with the molarity of the sulfuric acid, and with $-H_0$, the Hammett acidity function.

Prehnitenesulfonic acid dissolved in sulfuric acid 8–18 *M* is completely stable at 12.3°. This is in accord with the general rule[7] that where the sulfonic acid group is vicinal to two methyl groups, the sulfonic acid is less stable; prehnitene (1,2,3,4-methyl) forms the only tetra-alkylsulfonic acid without two vicinal methyl groups. Prehnitene gives convenient rates of monosulfonation in sulfuric acid of concentration 13–14 molar. The equation obtained by the method of least squares is

$$\log (k_S \times 10^6) = -9.088 + 0.9087[H_2SO_4]_{st} \quad (3)$$

Before proceeding to the other hydrocarbons, a general picture of the spectra of the sulfonic acids is presented in Figs. 2–7. The spectra of pseudocumenesulfonic acid and hexamethylbenzene are added as these would be included in the products of the Jacobsen reaction. Comparing the spectra in 18 *M* sulfuric acid with the spectra in water, it is to be noted that there is a shift to longer wave lengths at

(7) J. M. Crafts, *Ber.*, **34**, 1350 (1901).

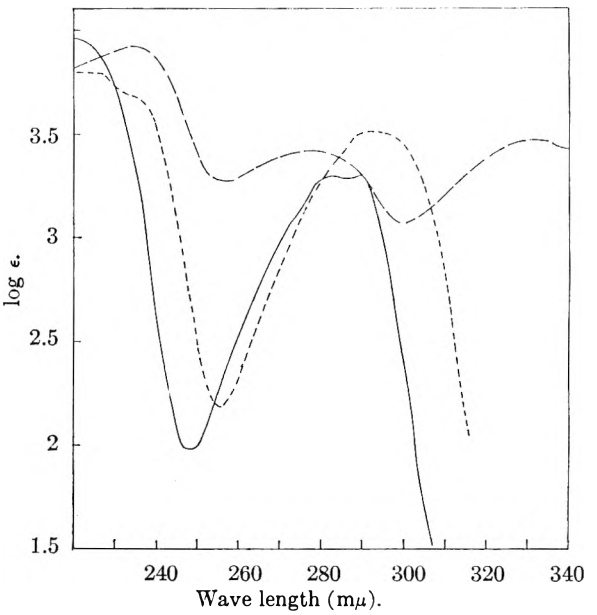

Fig. 2.—Ultraviolet spectra of durenesulfonic acid (1,2,4,5-tetramethylbenzene-3-sulfonic acid): ———, in water; - - - -, in concd. sulfuric acid; — —, in concd. sulfuric acid after 30 min. at 100°.

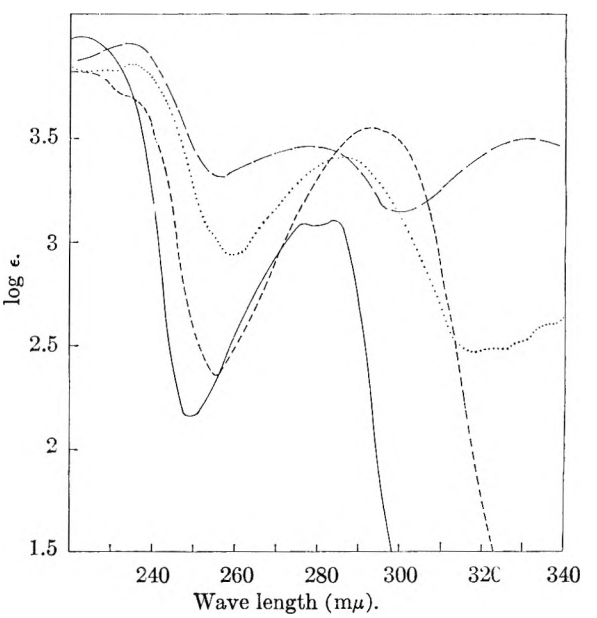

Fig. 3.—Ultraviolet spectra of isodurenesulfonic acid (1,2,3,5-tetramethylbenzene-4-sulfonic acid): ———, in water; - - - -, in concd. sulfuric acid; . . . . . , in concd. sulfuric acid after 24 hours; — —, in concd. sulfuric acid after 30 min. at 100°.

the maximum with an increase in the molar absorption coefficient. There is no absorption in water between 300 and 340 mμ. Inspection of the changes in spectra with time and temperature show no change for pseudocumenesulfonic acid and very little change for prehnitenesulfonic acid except in the 300–340 mμ range at high temperature. The spectra of durenesulfonic acid, isodurenesulfonic acid and pentamethylbenzenesulfonic acid on heat treatment are strikingly similar with peaks between 300 and 340 mμ and peaks in the 270–290 range at 10–20 mμ lower wave lengths. Hexamethylbenzene dissolves readily in concentrated sulfuric acid with the formation of a yellow solution, due to the protonation, with maxima at 281 and 395 mμ and molar absorptions of 12,800 and 18,000, respectively, but the spectra are

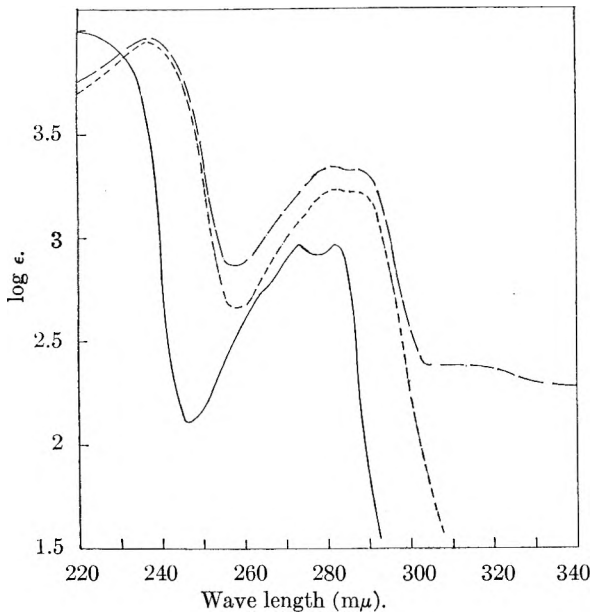

Fig. 4.—Ultraviolet spectra of prehnitenesulfonic acid (1,2,3,4-tetramethylbenzene-5-sulfonic acid): ———, in water; – – – –, in concd. sulfuric acid; — —, in concd. sulfuric acid after 30 min. at 100°.

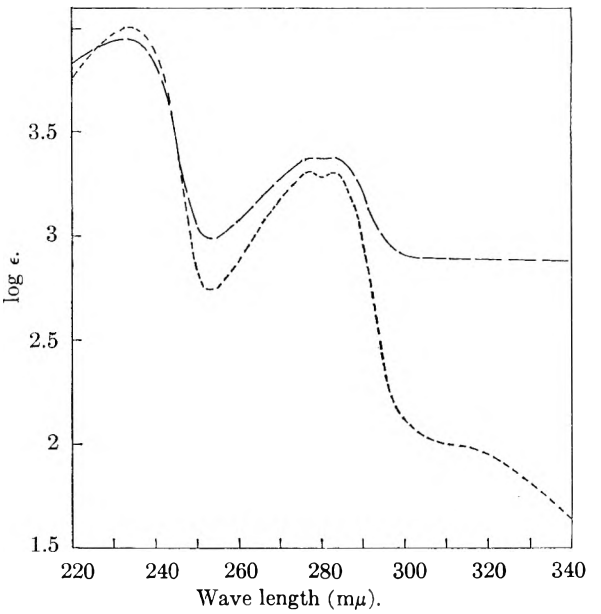

Fig. 6.—Ultraviolet spectra of pseudocumenesulfonic acid (1,3,4-trimethylbenzene-6-sulfonic acid): – – – –, in concd. sulfuric acid; — —, in concd. sulfuric acid after 30 min. at 100°.

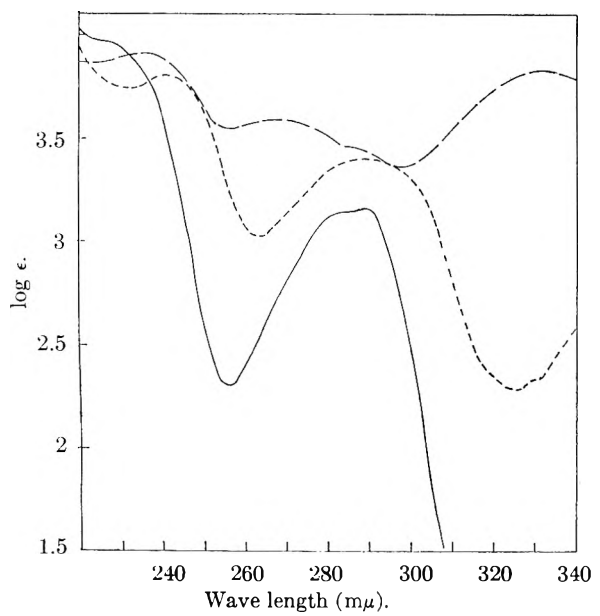

Fig. 5.—Ultraviolet spectra of pentamethylbenzenesulfonic acid: ———, in water; – – – –, in concd. sulfuric acid; — —, in concd. sulfuric acid after 30 min. at 100°.

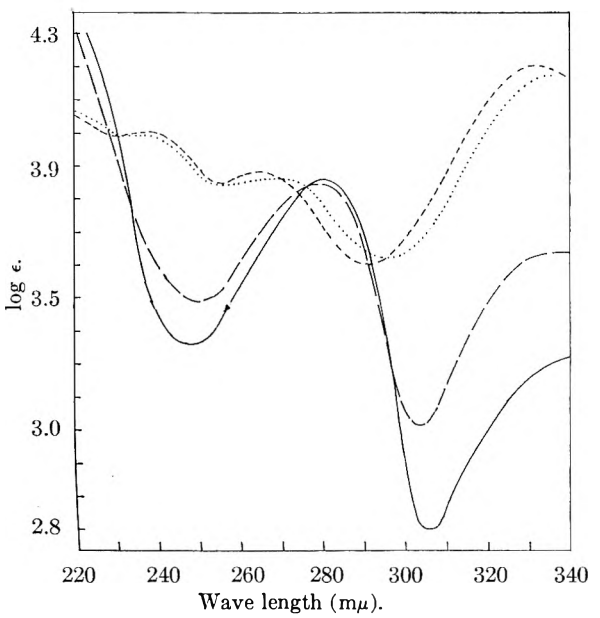

Fig. 7.—Ultraviolet spectra of hexamethylbenzene in concd. H_2SO_4: ———, initial spectrum; — —, after 7 hours; – – – –, after 30 min. at 100°; . . . . . , after 13 hours at room temp.

unstable, the solution turning deep red within an hour.[8] Deno[9] and his co-workers have also reported that hexamethylbenzene disappears irreversibly in 97% sulfuric acid by a first-order process.

We followed the protonation peak of hexamethylbenzene at 393 mμ in 18.44 *M* sulfuric acid and measured the decrease with time at 12.5°. The reaction was first order in hexamethylbenzene with a velocity constant $0.434k = 1.0 \times 10^{-3}$ min.$^{-1}$, corresponding to a half-time of 300 minutes. In 18.83 *M* sulfuric and in oleum up to 20% SO_3 the reaction is no longer first order in the hydrocarbon.

Figure 7 shows the change in the spectrum of hexamethylbenzene in 18.1 *M* H_2SO_4 after 7 hours at room temperature, then 30 minutes at 100°, and the subsequent change on standing 13 hours at room temperature. The ultraviolet protonation peak is at 281 mμ. We have not identified the products of this irreversible decomposition.

The results of all the kinetic experiments are summarized in Table II. The experiments were carried out starting with the hydrocarbon or the corresponding sulfonic acid, and the rate of appearance or disappearance of the sulfonic acid with time was obtained from the recorded spectrum at suitable time intervals over the wave length range 260–300 mμ. All rates were first order in the hydrocarbon or the sulfonic acid unless otherwise stated and the half-time at 12.3° varied from 10 to 500 minutes.

(8) M. Kilpatrick and H. H. Hyman, *J. Am. Chem. Soc.*, **80**, 77 (1958).

(9) N. C. Deno, Paul T. Groves and G. Saines, *ibid.*, **81**, 5790 (1958).

TABLE I

DESULFONATION OF DURENE, ISODURENE AND PENTAMETHYLBENZENE SULFONIC ACIDS AT 12.3

H_2SO_4, moles/l.	$-H_0$	$k_D \times 10^4$, min.$^{-1}$
	Durenesulfonic acid	
14.86	7.37	82.3
14.40	7.13	48.0
13.95	6.90	28.6
13.08	6.45	10.0
	Isodurenesulfonic acid	
13.50	6.67	155
12.90	6.37	86.7
12.65	6.24	68.5
11.99	5.91	37.4
11.55	5.68	22.6
	Pentamethylbenzenesulfonic acid	
10.22	5.00	68.0
10.13	4.96	62.2
9.86	4.82	46.4
8.73	4.24	12.9

As shown in column four, prehnitene, as already reported, gives conveniently measurable rates of sulfonation in 13–14 *M* acid, is quite stable as the sulfonic acid in sulfuric acid, and even on heating the solution in 18 *M* sulfuric acid shows little change in spectrum except in the 300–340 mμ range. Pseudocumene (1,2,4-trimethylbenzene), which sulfonates in the 13.5–14.5 *M* range to form the sulfonic acid in position 6, yields a sulfonic acid which is at least as stable as prehnitenesulfonic acid.

Durene, the sulfonic acid of which desulfonates at conveniently measurable rates in the 13–15 *M* range, gave first-order kinetics for sulfonation or desulfonation at 15.5 with the ratio (*R*) of sulfonic acid to hydrocarbon equal to 0.6. The half-time was 10 minutes, but above 16 *M* sulfuric acid the rate was much slower, was no longer first order in the sulfonic acid, and the time for half reaction was approximately 400 minutes. The initial maximum in the spectrum was at 292 and the final peak was at 286 mμ for an experiment in 16.12 *M* sulfuric acid, 287 for 16.54, 287 for 16.76 and 283 for 16.90 *M*. The product could be isodurenesulfonic acid or prehnitenesulfonic acid, or both. In the first case the process would be isomerization and in the second case disproportionation (*cf.* 2). When durenesulfonic acid was dissolved in 17.42 *M* sulfuric acid, the peak remained unchanged over a 1200 minute interval, while in 18.1 molar the peak remained unchanged over a corresponding period. This could mean that durenesulfonic acid is formed and does not isomerize or disproportionate or that the durene has isomerized to isodurene which sulfonates to isodurenesulfonic acid.

In sulfuric acid of concentration 16–17 *M* durene and durenesulfonic acid come to equilibrium rapidly with the equilibrium favoring the sulfonic acid. The decrease in optical density with time can be explained by the disproportionation of durene or durenesulfonic acid or the isomerization to isodurene. That disproportionation takes place is made evident after two or three days by the darkening of the solution and the appearance of a peak at 279 mμ. However, the decrease of optical density at 292 mμ with time becomes slower as the sulfuric acid concentration is increased. This fact favors the interpretation that the predominant reaction is the isomerization of durene to isodurene which is rapidly sulfonated. Above 17 *M* there is very little durene in the solution and this is isomerized to isodurene which rapidly sulfonates. At this acid concentration the peaks for the sulfonic acids of durene and isodurene are both at 293 mμ so that no change in wave length is observed. The shift to wave lengths below 287 is not observed indicating that the more stable isodurenesulfonic acid has been formed.

Pentamethylbenzene, the sulfonic acid of which completely desulfonates in 8–11 *M* sulfuric acid, showed no sign of sulfonation in 15.30 *M* acid, but showed a little sulfonation at 15.51 and 15.84 *M*. However, a series of experiments at 16.12, 16.32, 16.37 and 16.54 yielded rates first order in the hydrocarbon with half-time between 46 and 35 minutes, the final maximum peak being at 283 mμ. Since no isomerization can be involved here the process must be disproportioning of the hydrocarbon and sulfonation of the product, or else disproportionation of the sulfonic acid. The fact that the solution is largely pentamethylbenzene indicates that it is the hydrocarbon which disproportionates rather than the sulfonic acid. At higher concentrations disproportionation is indicated by the spectrum and the odor of sulfur dioxide. Figure 5 shows that when pentamethylbenzenesulfonic acid is dissolved in 18 *M* sulfuric acid disproportionation takes place.

In oleum the disulfonic acids are formed and these are, in general, more stable than the corresponding monosulfonic acids. It already has been shown that mesitylenesulfonic acid sulfonates in 18.5 *M* acid[10] but that other sulfonic acids,

(10) M. Kilpatrick and M. W. Meyer, *J. Phys. Chem.*, **65**, 530 (1961).

TABLE II

ACID RANGES FOR OBSERVABLE REACTIONS OF TETRA- AND PENTAMETHYL BENZENES AT 12.3°

Hm = hexamethylbenzene; S = sulfonic acid; disp. = disproportionation

H_2SO_4, moles/l.	Durene (D)	Isodurene (iD)	Prehnitene (Pr)	Pentamethylbenzene (Pm)
8–11	DS stable	iDS stable	PrS stable	PmS → Pm
11–13	DS stable	iDS → iD	PrS stable	PmS → Pm
13–15	DS → D	iD ⇄ iDS	Pr → PrS	PmS → Pm
15–16	D ⇄ DS; R < 1[a]	iD → iDS	PrS stable	
16–17	DS ⇄ D D → iD iD → iDS Slow disp. of D	iDS stable	PrS stable	Pm → Pr + Hm Pr → PrS
17–18	DS ⇄ D R ≫ 10[a] D → iD iD → iDS		PrS stable	Pm ⇄ PmS Pm → Pr + Hm Pr → PrS
18.1	Slow disp. See Fig. 2	Slow disp. See Fig. 3	See Fig. 4	See Fig. 5
Oleum	D → DS fast DS → DS_2	iD → iDS fast iDS → iDS_2	Pr → PrS fast PrS → PrS_2	

[a] R = [$ArSO_3H$]/[ArH] at equilibrium.

with the possible exception of isodurenesulfonic, require oleum. The kinetics of disulfonation will be the subject of another paper.

Discussion

In another solvent of high proton availability, $HF-BF_3$,[11] isomerization has been found to predominate at low temperatures and disproportionation at higher temperatures. In anhydrous hydrofluoric acid there is no problem of reaction with the solvent and a detailed kinetic study in a homogeneous system is underway.[12]

One should distinguish between the thermodynamic equilibrium, where the reaction is allowed to go to completion, and the initial products of a kinetic study. For example, in the disproportioning of methylbenzenes in $HF-BF_3$ the final thermodynamic equilibrium mixture would contain all of the methylbenzenes as well as benzene. When this equilibrium is reached, the isomer distribution of the tetramethylbenzenes would be the equilibrium distribution and not the distribution reached at the completion of a kinetic run in the isomerization of durene to isodurene, the strongest base. The picture in sulfuric acid is complicated by the complete or partial sulfonation of the tetramethylbenzenes, the desulfonation of certain sulfonic acids, and resulfonation of the products of isomerization or disproportionation. In the solvent sulfuric acid one fact stands out, namely, that whenever isomerization or disproportionation takes place there is hydrocarbon present. In the solvent anhydrous hydrofluoric acid both durene and prehnitene give largely the more basic isodurene, while in the solvent sulfuric acid the main product is the stable prehnitenesulfonic acid. The difference between the processes in the two solvents is that prehnitene forms a stable sulfonic acid while the other hydrocarbons, durene and isodurene, only partially form sulfonic acids, and if one starts with the sulfonic acid, the cycle of desulfonation, isomerization or disproportionation, and resulfonation favors the formation of the stable prehnitenesulfonic acid.

The general mechanism of disproportionation is not unlike the mechanism of transalkylation, except that one molecule protonated by the solvent of high proton availability reacts with another like but unprotonated molecule to transfer an alkyl group to that molecule. The proton may be attached to any carbon in the ring but for transfer to take place the proton must be attached to the ring carbon with the alkyl group to be donated. This protonated molecule reacts with an unprotonated molecule to give a product with one alkyl group less than the original hydrocarbon and a product with one alkyl group more. If the fraction of the protonated molecules is small, the concentration of the unprotonated molecules is practically the same as the over-all stoichiometric concentration and the simple first-order equation applies. If this is not so, the kinetic equation is more complicated and when the concentrations are equal the bimolecular process will require an equation second order in the hydrocarbon. Since the introduction of a sulfonic acid group into the molecule will reduce the basicity of the metnylbenzene the fraction of protonated methylbenzenesulfonic acid will be small and may even be kinetically negligible. Of course, the sulfonic acid is a fairly strong acid itself, but the proton is attached to oxygen or to solvent molecules. For these reasons it appears that disproportionation involves the hydrocarbon rather than the sulfonic acid. Jacobsen's[3] argument that 1,3,4-trimethylbenzene-2-sulfonic acid can only come from disproportionation of the 1,2,4,5-tetramethylbenzene-3-sulfonic acid is difficult to refute, but we are surprised that a sulfonic acid group with two methyls in the vicinal position would be more stable than 1,3,4-trimethylbenzene-6-sulfonic acid. However, one should remember that Jacobsen worked with a mush of durene and sulfuric acid and not with one homogeneous phase containing a small amount of substrate. The arguments of Smith are unconvincing.[2] Spryskov, in a study of the isomerization of benzenedisulfonic acids in sulfuric acid at higher temperatures, expresses the view that the isomerization is the result of their partial hydrolysis and resulfonation.[13]

Acknowledgment.—This research was supported in part by a grant from the Petroleum Research Fund administered by the American Chemical Society. Grateful acknowledgment is hereby made to the donors. Thanks are also due to the Simoniz Company for yearly grants to the department.

(11) D. A. McCaulay and A. F. Lien, *J. Am. Chem. Soc.*, **74**, 6246 (1952).

(12) M. Kilpatrick and J. A. S. Bett, unpublished results.

(13) A. A. Spryskov and S. P. Starkov, *J. Gen. Chem., U.S.S.R.*, **27**, 2816, 3097 (1957).

SOME OBSERVATIONS ON THE OXIDATION OF IODINE AT LOW CONCENTRATIONS[1]

BY H. M. EILAND AND MILTON KAHN

Department of Chemistry, University of New Mexico, Albuquerque, New Mexico

Received January 6, 1961

Mild oxidation of "carrier-free" iodine-131 in aqueous solutions produced, among other uncharacterized species, one which was about equally soluble in benzene and 0.5 *M* nitric acid. This species was not radiocolloidal in nature and comprised as much as 25% of the total activity in a reaction mixture. Some of the chemical and physical properties of this species are reported. Optimum conditions for the formation of this species were investigated.

Introduction

The chemical forms assumed by iodine-131 on oxidation of iodide at concentrations of the order of 10^{-7} *M* were investigated by Kahn and Wahl.[2] Oxidation at room temperature in 1 *M* sulfuric acid by chromium(VI) or cerium(IV) resulted in the formation of molecular iodine and three unidentified fractions. One of the fractions, designated as the Z fraction, was found to be composed of iodate and at least one unidentified species of iodine and was not readily extracted from aqueous acid-oxidizing solutions by benzene. The purpose of this study was to further characterize the non-iodate component of the Z fraction.

Formation of the Z fraction *via* oxidation by nitric acid and acid solutions of chromium(VI) and cerium(IV) was investigated in order to establish conditions which would lead to a maximum amount of Z fraction composed chiefly of the non-iodate constituent.

Results of successive extractions of 0.5 *M* nitric acid solutions of the Z fraction with benzene suggest that the non-iodate component consists of at least two fractions. Some chemical and physical properties of the predominant fraction, which we designate as the R species, are reported here.

Experimental

Chemicals.—All chemicals were of Reagent Grade, and, except for the specific instances mentioned below, were used without further purification. Reagents were prepared by solution of sodium or potassium salts of desired anions and sulfates of desired cations. Benzene was purified according to the method of Fieser.[3] Potassium iodate was crystallized twice from water. Concentrated nitric acid was decolorized by passing dry, oxygen-free nitrogen through the solution for two hours. The water used was obtained by distillation of ordinary distilled water from an alkaline permanganate solution.

Radioactivity.—The "carrier-free" 8.0-day iodine-131, obtained from the Oak Ridge National Laboratory, was purified according to the method of Kahn, Freedman and Shultz[4]; the final solution was 0.005 *M* in sodium sulfite.

Procedures.—The extraction techniques used are described elsewhere.[2] Except where specifically noted, all experiments were carried out under ordinary laboratory lighting conditions.

The Z fraction was isolated from an aqueous oxidizing solution by successive extraction of 1 ml. of the solution with 5 ml. of benzene, 4 ml. of 0.007 *M* iodine in benzene and two 4-ml. portions of benzene. The activity remaining in the aqueous phase was designated as the Z fraction. The iodate content of the Z fraction was determined as described elsewhere.[2]

Stock solutions of the R species in benzene were prepared from activity that had been oxidized by 0.5 *M* nitric acid at 125°, in the dark, for 18 to 24 hours. A 10-ml. portion of the solution of oxidized iodine-131 was treated with 1 ml. of a solution, 0.25 *M* in nitric acid and 0.007 *M* in iodine. Subsequently, this solution was extracted with four successive 1-ml. portions of benzene which were discarded and then with four successive 4-ml. portions of benzene. The combined 4-ml. portions of benzene extract were back-extracted with two 1-ml. portions of 0.5 *M* nitric acid; the extracted benzene solution constituted a stock solution of the R species. This stock solution proved to be stable at room temperature over a period of at least 85 hours. Solutions of the R species in 0.5 *M* nitric acid or 0.25 *M* sulfuric acid were prepared just prior to use by extracting the R species from the benzene stock solution into the desired acid.

Detection of Radioactivity.—The γ-radiation associated with the decay of iodine-131 was detected with a scintillation counter employing a no. 5819 RCA photomultiplier tube and a thallium-activated sodium iodide crystal. Liquid samples were prepared according to the procedure of Keneshea and Kahn.[5]

Results and Discussion

Formation of the Z Fraction.—Typical results of studies of the formation of the components of the Z fraction by oxidation of "carrier-free" iodide solutions with cerium(IV) and chromium(VI) at 29.2° and with chromium(VI) at 74° are given in Tables I and II, respectively. It is seen that whereas the amount of iodate produced at 29.2° increased with the acid concentration, oxidizing power of reagent, and time, the formation of the non-iodate component was relatively independent of these factors. Raising the temperature of the chromium(VI) oxidation in 1 *M* sulfuric acid produced more iodate and caused the non-iodate component to be consumed slowly; there was no significant change in the amount of each component formed in 0.25 *M* sulfuric acid at the higher temperature. These results suggest that a Z fraction of satisfactory yield with a minimum amount of iodate can be prepared by oxidation with chromium (VI) in 0.25 *M* sulfuric acid at 29.2 or 74°. However, because it was thought desirable to work with solutions of the non-iodate component which contained a minimum number of electrolytes, the possibility of oxidation by nitric acid was explored. The most satisfactory method for the preparation of the Z fraction proved to be oxidation by 0.5 *M* nitric acid at 125° in the dark for eighteen to 24

(1) This communication is based on work done under the auspices of the Los Alamos Scientific Laboratory and the Atomic Energy Commission and submitted in partial fulfillment of the requirements for the degree of Doctor of Philosophy in the Graduate School of the University of New Mexico, June, 1957, by H. M. Eiland. Presented before the Physical and Inorganic Division of the American Chemical Society in San Francisco, April, 1958.

(2) M. Kahn and A. C. Wahl, *J. Chem. Phys.*, **21**, 1185 (1953).

(3) L. F. Fieser, "Experiments in Organic Chemistry," D. C. Heath and Company, New York, N. Y., 1941, p. 363.

(4) M. Kahn, A. J. Freedman and C. G. Shultz, *Nucleonics*, **12**, 72 (1954).

(5) F. J. Keneshea, Jr., and M. Kahn, *J. Am. Chem. Soc.* **74**, 5254 (1952).

hours. Under these conditions, the ratio of the non-iodate component to iodate was a maximum (~8 to 1), the absolute yield of the non-iodate component was sufficient (~16%), and no electrolyte other than nitric acid was present.

TABLE I

FORMATION OF COMPONENTS OF THE Z FRACTION AT 29.2°

Oxidizing soln.	Time, hr.	Iodate, %[a]	Non-iodate, %[a]
0.25 *M* H_2SO_4, 0.015 *M* Ce(IV), 0.015 M Ce(III)	0.5	20	14
	19.0	35	16
	52.5	44	16
0.25 *M* H_2SO_4, 0.01 *M* Cr(VI), 0.005 *M* Cr(III)	1.0	2	10
	16.5	2	16
	37.5	3	19
	154	6	26
1.0 *M* H_2SO_4, 0.01 *M* Cr(VI), 0.005 *M* Cr(III)	2.5	22	19
	16.0	24	26
	62.0	31	24
	93.5	34	23

[a] Per cent. of total activity present in reaction mixture.

TABLE II

FORMATION OF COMPONENTS OF THE Z FRACTION IN CHROMIUM(VI) SOLUTIONS AT 74°[a]

Sulfuric acid concn., *M*	Time, hr.	Iodate, %[b]	Non-iodate, %[b]
0.25	0.5	2	12
	24.75	3	19
	49.0	3	20
1.0	1.5	31	18
	10.0	44	17
	21.0	58	13
	47.0	75	6
	96.0	90	3
3.0	1.0	43	19
	19.0	71	12
	45.0	81	7

[a] Chromium(VI) concentration = 0.01 *M*; chromium(III) concentration = 0.005 *M*. [b] Per cent. of total activity present in reaction mixture.

The effects of light and iodide concentration on the production of the components of the Z fraction by oxidation with chromium(VI) are summarized in Table III. The appearance of significant quantities of the non-iodate component in the iodide concentration range 10^{-5} to 10^{-6} *M* is in accord with the observations reported by Kahn and Wahl.[2] The production of the non-iodate component is essentially independent of lighting conditions; the formation of iodate is enhanced by light and an increase in iodide concentration.

Search for Radiocolloids in the Z Fraction.—The results of centrifugation and filtration experiments suggest that the Z fraction did not contain radiocolloids with a radius greater than 5 mμ. No stratification of activity was detected in a centrifugal field of about 60,000 *g* over a period of one hour; centrifugation, under the same conditions, of a hydrous ferric oxide sol[6] containing colloidal particles of a mean radius equal to 5 mμ resulted in considerable intensification of the color and in some

(6) H. N. Holmes, "Laboratory Manual of Colloid Chemistry," John Wiley and Sons, Inc., New York, N. Y., 1934, pp. 22, 34.

TABLE III

EFFECT OF LIGHT AND IODIDE CONCENTRATION ON THE FORMATION OF COMPONENTS OF THE Z FRACTION IN CHROMIUM(VI) SOLUTIONS AT 29.2°[a]

Iodide concn., *M*	Oxidation in the light: Iodate, %[b]	Oxidation in the light: Non-iodate, %[b]	Oxidation in the dark: Iodate, %[b]	Oxidation in the dark: Non-iodate, %[b]
C. F.[c]	3	29	3	24
10^{-7}	4	27	2	23
10^{-6}	19	17	1	15
10^{-5}	55	4	0.5	4
10^{-4}	68	3	2	2
10^{-3}	74	2	0.6	0.9

[a] Composition of reaction mixtures: 0.25 *M* H_2SO_4, 0.005 *M* Cr(VI). Reaction time: 48 hours. [b] Per cent. of total activity present in reaction mixtures. [c] Carrier-free.

deposition of the solid. Also, less than 2% of the activity was retained by a type VF Millipore Filter[7] (pore diameter = 10 ± 2 mμ).

Resolution of the Z Fraction.—The non-iodate portion of the Z fraction was resolved into two components by exhaustive extraction of the Z fraction with benzene. The experimental results are summarized in Table IV. In experiments 1 and 2 a 1-ml. aliquot of the Z fraction was extracted with successive portions of benzene; in experiment 3 the first benzene extract of experiment 2 was back-extracted with successive portions of 0.5 *M* nitric acid.

TABLE IV

DISTRIBUTION OF ACTIVITY IN THE Z FRACTION BETWEEN BENZENE AND 0.5 *M* NITRIC ACID

Extraction no.	Experiment 1: D_1[a,b]	Experiment 1: Benzene extract, ml.	Experiment 2: D_2[a,b]	Experiment 2: Benzene extract, ml.	Experiment 3 (0.5 *M* HNO_3 extract): D_3[a,b]	Experiment 3 (0.5 *M* HNO_3 extract), ml.
1	1.0	4	0.92	4	1.3	2
2	0.45	4	.47	2	1.4	2
3	.18	4	.20	2	1.5	2
4	.082	4	.090	2	1.5	2
5	.060	4	.044	4	1.6	4
6	.048	4	.029	4	1.7	4
7	.049	4	.026	4	1.7	4
8	.047	4	.023	4	1.7	8
9			.028	5	1.8	8
10			.029	5	1.9	8
11			.024	10	1.4	8
12			.024	10		

[a] The partition coefficient D is defined as C_b/C_w where C_b represents the concentration of activity in the benzene phase and C_w represents the corresponding concentration in the aqueous phase. [b] The values of D_1 and D_2 have been corrected for the small amount of activity which did not extract into benzene; the values of D_3 have been corrected for the small amount of activity which was not removed by repeated extraction with 0.5 *M* nitric acid.

It is interesting to note that the values of D_1 and D_2 are in good agreement for the first three extractions even though a separate preparation of the Z fraction was used in each experiment. In this connection it is noteworthy that neither substitution of a 6-minute shaking interval for the usual 3-minute shaking interval for extraction nor substitution of 0.007 *M* iodine in benzene for pure

(7) Millipore Filter Corporation, Watertown, Massachusetts.

benzene had significant effect on the extraction results. Analysis of the variation of D_1 and D_2 with successive extractions suggests the presence of two iodine species. The predominant component, designated as the R species, was about equally distributed between the two phases; the minor component had a much greater affinity for 0.5 M nitric acid than for benzene. The average values of the partition coefficient D_R, of the R species, calculated from the first three extractions of experiments 1 and 2 are 1.1 ± 0.1 and 1.2 ± 0.1, respectively. These results compare favorably with the average value of 1.4 ± 0.1 obtained from the first three extractions of experiment 3. Because these values of D_R were reproducible and essentially independent of the direction of approach to equilibrium it is believed that the R component is a molecularly dispersed substance.

Of the total activity present in the oxidized solutions used for experiments 1 and 2, 29 and 18%, respectively, were in the R form; in each instance, only about 1% of the total activity was in the form of the extractable minor component.

Isotopic Exchange.—The isotopic exchange between the R species and molecular iodine (2.5×10^{-4} M) in benzene at 29.2° was followed by extraction of aliquots of the benzene solution with two successive portions of 0.25 M sulfuric acid. The fraction exchange was calculated using the experimentally determined value of 1.5 for the partition coefficient of the R species between benzene and 0.25 M sulfuric acid and assuming all the activity in the second sulfuric acid extract was R species. That the R species was not radiocolloidal is further evidenced by the plot of ln (1 − fraction exchange) *versus* time which yielded a straight line in accordance with the first-order isotopic exchange law[8]; the half-time was 41 hours.

Migration in an Electric Field.—An apparatus similar to that employed by Johnson, Leininger and Segre[9] was used to investigate the direction of migration of the R species in an electric field. Electrolysis was carried out with a potential of 150 volts applied across platinum electrodes separated by a migration path of 14 cm. Because no significant migration of activity was detected on electrolysis of two 0.5 M nitric acid solutions of R species for 45 and 85 minutes, respectively, it is believed that the R species was uncharged.

Coprecipitation and Adsorption.—The silver chloride and silver iodate used in these experiments were precipitated in two ways: (1) with an excess of silver ion, and (2) with an excess of the appropriate anion. In the coprecipitation experiments the R species was present during the precipitation, whereas in the adsorption experiments the preformed precipitates were added to the R solutions. The amount of R species removed from 0.5 M nitric acid solution by these precipitates varied from 1–7%.

Reactivity of the R Species.—The results of extractions of 5-ml. aliquots of the benzene stock solution of the R species with 2-ml. aliquots of various reagents are summarized in Table V. Large fractions of the R species reacted with hydriodic acid, sulfurous acid or sodium bicarbonate to yield water-soluble iodine species; no significant reaction was observed with iron(II). The reaction with sodium bicarbonate was irreversible, leading to iodine species rapidly exchangeable with molecular iodine at room temperature. Thus only 3% of the activity was extracted into benzene from the acidified sodium bicarbonate solution, whereas 95% was extracted into benzene containing carrier iodine. No iodate was detected in the acidified sodium hydroxide extract which was allowed to stand at room temperature for 12 hours and then heated for one hour in a steam-bath.

TABLE V

EXTRACTION OF R SPECIES FROM BENZENE BY VARIOUS REAGENTS

Extracting reagent	Activity in aqueous phase,[a] %	Activity in benzene phase,[a] %
0.25 M H_2SO_4	26	76
0.05 M $FeSO_4$ 0.25 M H_2SO_4	29	70
0.10 M KI 0.25 M H_2SO_4	88	13
0.05 M Na_2SO_3 0.25 M H_2SO_4	85	15
0.1 M $NaHCO_3$	95	7
6 M NaOH	96	4

[a] Volume of aqueous phase = 2 ml.; volume of benzene phase = 5 ml.

Conclusions

The R species may be an inorganic compound of iodine or an organic compound formed by reaction between organic impurities in the reaction mixtures and some oxidized form of iodine. We tend to favor the first possibility because of the chemical behavior and reproducibility of formation of the R species.[10] The irreversible decomposition of an uncharged inorganic R species in alkaline solution to species which on acidification undergo rapid isotopic exchange with molecular iodine may be explained as follows:

1. Iodine, in an oxidation state of +2 or +3, disproportionates in alkaline solution to produce oxidation states stable at these concentrations and rapidly exchangeable with molecular iodine in acid solution. The +1 and +4 oxidation states were eliminated because the former, initially, would exchange rapidly with molecular iodine[11] and the latter should certainly yield iodate on disproportionation.

2. An oxidation state intermediate between +1 and +5 is reduced in alkaline solution to the +1, zero, or −1 state by an organic impurity. The hypothetical oxide IO_2 is a reasonable possibility in

(8) G. Friedlander and J. W. Kennedy, "Nuclear and Radiochemistry," John Wiley and Sons, Inc., New York, N. Y., 1955, p. 316.

(9) G. L. Johnson, R. F. Leininger and E. Segre, *J. Chem. Phys.*, **17**, 1 (1948).

(10) Experiments involving the production and properties of the R fraction recently repeated by one of us (M.K.) at the Lawrence Radiation Laboratory in Livermore, California, yielded essentially the same results reported here.

(11) H. Hellaver and H. Spitzy, *Biochem. Z.*, **325**, 40 (1953).

light of the known properties of the compound ClO_2.[12]

(12) (a) J. F. White, M. C. Taylor and G. P. Vincent, *Ind. Eng. Chem.*, **34**, 782 (1942); (b) M. I. Sherman and J. D. H. Strickland, *Anal. Chem.*, **27**, 1778 (1955); (c) H. Dodgen and H. Taube, *J. Am. Chem. Soc.*, **71**, 2501 (1949).

Acknowledgments.—One of the authors (M.K.) wishes to express his appreciation to Dr. R. H. Goeckermann and N. A. Bonner of the Radiochemistry Group of the Lawrence Radiation Laboratory, Livermore, California, for the opportunity to investigate this problem further during the Summer of 1960.

HEXAMETHYLDISILOXANE: CHEMICAL THERMODYNAMIC PROPERTIES AND INTERNAL ROTATION ABOUT THE SILOXANE LINKAGE[1]

BY D. W. SCOTT, J. F. MESSERLY, S. S. TODD, G. B. GUTHRIE, I. A. HOSSENLOPP, R. T. MOORE, ANN OSBORN, W. T. BERG AND J. P. MCCULLOUGH

Contribution No. 106 from the Thermodynamics Laboratory, Bartlesville Petroleum Research Center, Bureau of Mines, U. S. Department of the Interior, Bartlesville, Oklahoma

Received January 10, 1961

Thermodynamic, spectroscopic, and molecular structure information was used to show that internal rotation about an Si—O bond in hexamethyldisiloxane is free or nearly so. Thermodynamic functions for hexamethyldisiloxane in the ideal gas state (0 to 1500°K.) were calculated by methods of statistical mechanics. Experimental studies provided the following information: values of heat capacity for the solid (11°K. to the triple point), the liquid (triple point to 375°K.) and the vapor (363 to 500°K.); the triple point temperature; the heat of fusion; thermodynamic functions for the solid and liquid (0 to 375°K.); heat of vaporization (332 to 374°K.); parameters of the equation of state; and vapor pressure (309 to 412° K.). Thermodynamic functions also were calculated for the related substance tetramethylsilane.

Studies of hexamethyldisiloxane, $(CH_3)_3SiOSi(CH_3)_3$, were made as part of thermodynamic research on organic derivatives of the lighter elements. In these studies, the height of the barrier restricting internal rotation about a siloxane bond was determined for the first time. The experimental work consisted of low temperature calorimetry, vapor flow calorimetry and comparative ebulliometry; detailed results are given in the Experimental section. For convenience, the results needed for discussing the barriers to internal rotation and the thermodynamic functions are collected in Table I.

TABLE I

OBSERVED AND CALCULATED THERMODYNAMIC PROPERTIES OF HEXAMETHYLDISILOXANE

	Entropy, $S°$, cal. deg.$^{-1}$ mole^{-1}			Heat capacity, $C_p°$, cal. deg.$^{-1}$ mole^{-1}	
T, °K.	Obsd.	Calcd.	T, °K.	Obsd.	Calcd.
332.31	134.25	134.25	363.20	64.45	64.44
351.50	137.73	137.73	393.20	67.68	67.67
373.67	141.66	141.67	429.20	71.40	71.41
			465.20	74.95	74.93
			500.20	78.16	78.17

Molecular Structure, Vibrational Assignment and Barriers to Internal Rotation

Certain differences in physical properties between methyl silicones and hydrocarbons have been attributed to freer internal rotation about the Si–O bond than about the C–C bond. These differences include the lower temperature coefficient of viscosity of silicone oils and the wider temperature range of elasticity of silicone rubbers. However, the height of the barrier restricting internal rotation about an Si–O bond never had been determined before the present study of hexamethyldisiloxane was undertaken.

Determining the barrier height required accounting for all degrees of freedom of the molecule. To that end, moments and reduced moments of inertia were calculated from molecular structure data, the fundamental vibrational frequencies were obtained from the molecular spectra or estimated by normal coördinate calculations, and the barrier height for the methyl rotations was transferred from the related substance tetramethylsilane.

Moments of Inertia.—The product of principal moments of inertia and the reduced moments of inertia for internal rotation were calculated by the general methods of Kilpatrick and Pitzer.[2] The values used for bond distances and angles, based in part on electron diffraction results,[3] are Si–O, 1.63 Å.; Si–C, 1.88 Å., C–H, 1.09 Å.; Si–O–Si, 135°; all other angles tetrahedral. For this structure, the product of principal moments of inertia is 7.126×10^{-112} g.^{3} cm.^{6}; the average "effective" reduced moments of inertia (taken so their product over all internal rotations equals $[D]$, the determinant of the internal rotational kinetic energy matrix) are 5.252×10^{-40} g. cm.^{2} for methyl rotations and 86.12×10^{-40} g. cm.^{2} for rotations about the Si–O bonds. The symmetry number is 2 for over-all rotation and 3 for each of the internal rotations.

Spectra and Normal Coördinate Treatment.—The molecular spectra of hexamethyldisiloxane

(1) This research was supported by the United States Air Force and the Advanced Research Projects Agency of the U. S. Department of Defense through the Air Force Office of Scientific Research of the Air Research and Development Command under Contract No. CSO 59-9. ARPA Order No. 24–59, Task 3. Reproduction in whole or in part is permitted for any purpose of the United States Government.

(2) J. E. Kilpatrick and K. S. Pitzer, *J. Chem. Phys.*, **17**, 1064 (1949).

(3) K. Yamasaki, A. Kotera, M. Yokoi and Y. Ueda, *ibid.*, **18**, 1414 (1950).

have been studied repeatedly.[4] Raman and infrared frequencies that appear well established are summarized in Table II.

TABLE II

VIBRATIONAL SPECTRA OF HEXAMETHYLDISILOXANE, CM.$^{-1}$

Raman, liquid[a]	Infrared, liquid	Interpretation
69–86		?
179 d		Skeletal bending, b_1 & a_2
190 p		Skeletal bending, a_1
219 d		Skeletal bending, b_2 & a_1
253 d		Skeletal bending, b_1
329 d	331	Skeletal bending, b_2
520 p	524	Si—O stretching, a_1
610	619	Si—C stretching, b_1
662 p		Si—C stretching, a_1
685 d	687	Si—C stretching, b_1, a_2 & b_2
751 d	756	Si—C stretching, a_1
835 p ?	832	CH_3 rocking, b_1
848 d	850	CH_3 rocking, a_1, b_1, a_2 & b_2
890 d		CH_3 rocking, a_1
1044 p		$2 \times 520 = 1040$ A_1
	1060	Si—O stretching, b_1
1254 p	1256	Sym. CH_3 bending, a_1, b_1, a_2 & b_2
1405 d	1410	Unsym. CH_3 bending,
	1438	a_1, b_1, a_2 & b_2
Region from 1450 to 2800 cm.$^{-1}$ omitted		
2900	2900	C—H stretching
2960	2960	a_1, b_1, a_2 & b_2
Region above 3000 cm.$^{-1}$ omitted		

[a] p, polarized; d, depolarized.

Normal coördinate calculations were made as an aid in interpreting the observed spectra and in estimating unobserved frequencies. The Wilson GF matrix method[5] was used, and the higher C–H stretching and CH_3 bending frequencies were factored out. The degrees of the secular equations were reduced thereby from 20, 19, 14 and 14 to 10, 9, 6 and 6. An approximate potential function was assumed, and force constants were transferred from tetramethylsilane for the CH_3 rocking, Si–C stretching and C–Si–C bending coördinates and estimated for the other coördinates. The secular equations were solved first for a trial set of force constants by Southwestern Computing Service, Inc., Tulsa, Okla., and later, after the set of force constants had been revised on the basis of the first results, at the Los Alamos Scientific Laboratory, courtesy of Dr. F. H. Kruse.

For the final calculations, the bond stretching force constants were: Si–C stretching, 2.723; Si–O stretching, 4.288; interaction between a pair of Si–C or Si–O stretching coördinates with a silicon atom in common, 0.131; and interaction between the two Si–O stretching coördinates, −0.423; all $\times 10^5$ dynes cm.$^{-1}$. The angle bending force constants were: Si–C–H bending, 0.442; C–Si–C and C–Si–O bending, 0.625; Si–O–Si bending, 0.500; and interaction between a pair of C–Si–C or C–Si–O bending coördinates with a Si–C or Si–O bond in common, 0.076; all $\times 10^{-11}$ ergs radian^{-2}. All other interactions were neglected.

Calculated and observed frequencies are compared in Table III. The assignment of observed skeletal stretching and bending frequencies is straightforward. The interpretation of the observed CH_3 rocking frequencies is reasonable but ignores the polarization results for the 835 and 890 cm.$^{-1}$ Raman bands. Apparently, the six lowest CH_3 rocking frequencies, calculated 809–812 cm.$^{-1}$, have not been observed. The low intensity of these last frequencies is understandable if the vibrational modes are related to the CH_3 rocking modes of tetramethylsilane of species f (inactive) and e (permitted but not observed in the Raman effect). Further discussion of the fundamental vibrations is deferred until the barriers to internal rotation have been considered.

Barrier Heights.—The barrier height for the methyl rotations was taken to be 1600 cal. mole^{-1} as in tetramethylsilane. This value for tetramethylsilane was obtained from a re-examination of the calorimetric and spectral data for that compound as discussed in the Appendix. Values from microwave spectroscopy for methylsilane (1700 ± 100 cal. mole^{-1})[6] and dimethylsilane (1665 ± 10 cal. mole^{-1})[7] are in satisfactory agreement with the

TABLE III

CALCULATED AND OBSERVED FREQUENCIES OF HEXAMETHYLDISILOXANE, CM.$^{-1}$

	a_1		b_1		a_2		b_2	
	Calcd.	Obsd.	Calcd.	Obsd.	Calcd.	Obsd.	Calcd.	Obsd.
CH_3 rocking	868	890	846	(850)	846	(850)	847	(850)
	859	850	824	834	812	...	812	...
	812	...	812	...	809	...	809	...
Si–C stretching	748	754	704	686	704	(686)	706	(686)
	679	662	617	619				
Si–O stretching	563	520	1089	1060				
C–Si–C bending	341	...	259	253	235	...	315	330
	220	(219)	233	...				
C–Si–O bending	169	190	165	179	164	(179)	214	219
Si–O–Si bending	82	...						

(4) N. Wright and M. J. Hunter, *J. Am. Chem. Soc.*, **69**, 803 (1947); I. Simon and H. O. McMahon, *J. Chem. Phys.*, **20**, 905 (1952); H. Murata and M. Kumada, *ibid.*, **21**, 945 (1953); R. Sh. Malkovich and V. A. Kolesova, *Zhur. Fiz. Khim.*, **28**, 926 (1954); R. Ulbrich, *Z. Naturforsch.*, **9b**, 380 (1954); C. C. Cerato, J. L. Lauer and H. C. Beachell, *J. Chem. Phys.*, **22**, 1 (1954); Ya. M. Slobodin, Ya. E. Shmulyakovskiĭ and K. A. Rzhedzinskaya, *Doklady Akad. Nauk S.S.S.R.*, **105**, 958 (1955); A. P. Kreshkov, Yu. Ya. Mikhailenko and G. F. Yakimovich, *Zhur. Fiz. Khim.*, **28**, 537 (1954); C. A. Frenzel, E. W. Scott, and J. P. McCullough, Bureau of Mines Report of Investigations No. 5658 (1960).

(5) E. Bright Wilson, Jr., J. C. Decius and P. C. Cross, "Molecular Vibrations," McGraw-Hill Book Co., Inc., New York, N. Y., 1955.

(6) R. W. Kilb and L. Pierce, *J. Chem. Phys.*, **27**, 108 (1957).

(7) L. Pierce, *ibid.*, **31**, 547 (1959).

thermodynamic value for tetramethylsilane. This observation shows that the barrier for a methyl group attached to silicon is relatively independent of the molecular environment, as was assumed when the barrier height for tetramethylsilane was transferred to hexamethyldisiloxane.

Comparisons with the calorimetric data were made to investigate internal rotation about the Si–O bonds. When calculated values were used for all unobserved vibrational frequencies, and internal rotation about the Si–O bonds was assumed to be free, both the entropy and the heat capacity were calculated to be greater than the observed values. Agreement between calculated and observed entropy could be obtained by selection of a suitable barrier height for the siloxane rotation, but only at the expense of a greater discrepancy between the calculated and observed heat capacity. On the other hand, agreement for both entropy and heat capacity could be obtained by suitable adjustment of unobserved vibrational frequencies if the siloxane rotation was assumed to be free. These observations are evidence for relatively free siloxane rotation. For calculating thermodynamic functions, the siloxane rotations were taken to be completely free, although the thermodynamic evidence does not rule out a modest barrier height of a few hundred cal. mole^{-1}.

The explanation of the unusual physical properties of methylsilicones as arising from relatively free internal rotation about Si–O bonds is confirmed by the thermodynamic results. Another explanation that has been advanced, weaker intermolecular forces between methylsilicone molecules, can be rejected because the gas imperfection data for hexamethyldisiloxane reported in the Experimental section indicate normal intermolecular forces.

Fundamental Vibrational Frequencies.—The unobserved skeletal bending frequencies of species a_1, calculated 82 and 341 cm.$^{-1}$, depend upon the Si—O—Si bending force constant, for which only an order-of-magnitude estimate was used in the normal coördinate treatment. Therefore these frequencies may be adjusted to conform with the thermodynamic data. Also, the average value for the six unobserved CH_3 rocking frequencies, calculated 809–812 cm.$^{-1}$, may be adjusted within reason. The values actually taken for these eight unobserved frequencies, selected to fit the thermodynamic data, are 102, 360 and 820(6) cm.$^{-1}$.

The complete set of fundamental vibrational frequencies used for calculating thermodynamic functions is listed in Table IV. Average or conventional values were taken for the C–H stretching and CH_3 bending frequencies, which are not all resolved in the observed spectra and make unimportant contributions to the thermodynamic functions except at high temperatures.

Thermodynamic Functions

The molecular structure parameters described in the preceding paragraphs were used to compute the values of thermodynamic functions listed in Table V. Empirical anharmonicity contributions,[8] with $\nu = 1130$ cm.$^{-1}$ and $Z = 0.52$ cal. deg.$^{-1}$ mole^{-1}, were included to give better agreement with the experimental values of heat capacity at the higher temperatures.[9] The contributions of anharmonicity are only 0.001 and 0.005 cal. deg.$^{-1}$ mole^{-1} in S° and C_p° at 298.15°K. but increase to 0.48 and 0.88 cal. deg.$^{-1}$ mole^{-1} at 1500°K. Calculated values of S° and C_p° are compared with the observed values in Table I. Agreement well within the accuracy uncertainty of the experimental data was obtained over the entire temperature range of the experiments.

(8) J. P. McCullough, H. L. Finke, W. N. Hubbard, W. D. Good, R. E. Pennington, J. F. Messerly and G. Waddington, *J. Am. Chem. Soc.*, **76**, 2661 (1954).

TABLE IV

FUNDAMENTAL VIBRATIONAL FREQUENCIES OF HEXAMETHYLDISILOXANE,[a] CM.$^{-1}$

	a_1	b_1	a_2	b_2
C–H stretching	2950 (5)	2950 (5)	2950 (4)	2950 (4)
CH_3 unsym. bending	1420 (3)	1420 (3)	1420 (3)	1420 (3)
CH_3 sym. bending	1255 (2)	1255 (2)	1255	1255
CH_3 rocking	890	(850)	(850)	(850)
	850	834	{820}	{820}
	{820}	{820}	{820}	{820}
Si–C stretching	754	686	(686)	(686)
	662	619		
Si–O stretching	520	1060		
C–Si–C bending	{360}	253	[235]	330
	(219)	[235]		
C–Si–O bending	190	179	(179)	219
Si–O–Si bending	{102}			

[a] ( ), observed frequency used more than once; [ ], from normal coördinate calculations; { }, selected to fit calorimetric data.

TABLE V

THE MOLAL THERMODYNAMIC FUNCTIONS OF HEXAMETHYLDISILOXANE IN THE IDEAL GAS STATE[a]

T, °K.	$(F^\circ - H^\circ_0)/T$, cal. deg.$^{-1}$	$(H^\circ - H^\circ_0)/T$, cal. deg.$^{-1}$	$H^\circ - H^\circ_0$, kcal.	S°, cal. deg.$^{-1}$	C_p°, cal. deg.$^{-1}$
0	0	0	0	0	0
273.15	−89.61	33.40	9.122	123.00	54.02
298.15	−92.61	35.24	10.51	127.85	57.00
300	−92.83	35.38	10.61	128.20	57.22
400	−103.98	42.26	16.90	146.23	68.40
500	−114.10	48.49	24.24	162.58	78.16
600	−123.44	54.14	32.48	177.58	86.48
700	−132.18	59.29	41.50	191.47	93.67
800	−140.41	63.99	51.19	204.40	99.95
900	−148.19	68.31	61.48	216.49	105.48
1000	−155.58	72.28	72.28	227.86	110.33
1100	−162.64	75.94	83.54	238.58	114.59
1200	−169.39	79.33	95.19	248.72	118.33
1300	−175.86	82.46	107.20	258.32	121.60
1400	−182.07	85.37	119.52	267.44	124.47
1500	−188.05	88.06	132.10	276.12	126.99

[a] To retain internal consistency, some of the values are given to one more decimal place than is justified by the absolute accuracy.

Experimental

The basic experimental techniques are described in published accounts of apparatus and methods for low tem-

(9) The contributions of vibration and anharmonicity were computed by the Bureau of Mines Electronic Computer Service, Pittsburgh, Pa. The contributions of restricted internal rotation were computed by Denver Electronic Computing Service, Inc., by two-way curvilinear interpolation in the tables of K. S. Pitzer and W. D. Gwinn, *J. Chem. Phys.*, **10**, 428 (1942).

perature calc... apor flow ...y,[11] and com- parative ebul... The re... s are based on a molecular w... 384 g. ... 1 International Atomic Weight... 1 val... mental physical constants[14] and ... : 0 ... K.[15] and 1 cal. = 4.184 joules (exa... st... temperature were made with platin... ters calibrated in terms of the Int... e Scale,[16] between 90 and 500°K., an... le[17] of the National Bureau of Standard... 0°K. All electrical and mass measurem... to standard devices calibrated at the Nat... tandards.

Material.—Dow C... purified grade (99%) hexamethyldisiloxane... starting material for highly efficient fraction... a and silica gel percolation, which was done by C. J. Thompson and H. J. Coleman of this Center. The combined best fractions used for low temperature calorimetry and comparative ebulliometry had a purity of 99.996 mole %, determined by calorimetric studies of melting point as a function of fraction melted. Combined second-best fractions were used for vapor flow calorimetry.

Heat Capacity in the Solid and Liquid States.—The observed values of heat capacity, C_{satd}, are listed in Table VI. Above 30°K., the accuracy uncertainty is estimated to be no greater than 0.2%. The heat capacity curves (C_{satd} *vs.* T) are normal for both crystals and liquid. The observed values for the liquid may be represented within 0.05% between the triple point and 375°K. by the empirical equation

$$C_{satd}(liq) = 65.834 - 8.2399 \times 10^{-2}T + 5.1874 \times 10^{-4}T^2 - 4.8933 \times 10^{-7}T^3, \text{ cal. deg.}^{-1} \text{ mole}^{-1} \quad (1)$$

Heat of Fusion, Triple Point Temperature, Cryoscopic Constants and Purity of Sample.—Values of the heat of fusion, ΔHm, from three determinations were 2848.4, 2848.9 and 2850.7 cal. mole^{-1}. The accepted value is 2849.4 ± 1.5 cal. mole^{-1}. The results of a study of the melting temperature, T_{obsd}, as a function of the fraction of total sample melted, F are listed in Table VII. Also listed in Table VII are the values obtained for the triple point temperature, $T_{T.P.}$, the mole fraction of impurity in the sample, N^*, and the cryoscopic constants[18] A = $\Delta Hm/RT_{T.P.}^2$ and B = $1/T_{T.P.} - \Delta Cm/2\Delta m$, calculated from the observed values of $T_{T.P.}$, ΔHm, and ΔCm (the heat capacity of the liquid less that of the solid, 6.42 cal. deg.$^{-1}$ mole^{-1}).

Thermodynamic Properties in the Solid and Liquid States.—Values of thermodynamic functions for the condensed phases were computed from the calorimetric data for selected temperatures between 10 and 375°K. The results are given in Table VIII. The values at 10°K. were computed from a Debye function for 7.5 degrees of freedom with $\theta = 101.73°$; these parameters were evaluated from the heat capacity data between 12 and 21°K. Corrections for the effects of premelting have been applied to the "smoothed" data recorded in Table VIII.

(10) H. M. Huffman, *Chem. Rev.*, **40**, 1 (1947); H. M. Huffman, S. S. Todd and G. D. Oliver, *J. Am. Chem. Soc.*, **71**, 584 (1949); D. W. Scott, D. R. Douslin, M. E. Gross, G. D. Oliver and H. M. Huffman, *ibid.*, **74**, 883 (1952).

(11) G. Waddington, S. S. Todd and H. M. Huffman, *ibid.*, **69**, 22 (1947); J. P. McCullough, D. W. Scott, R. E. Pennington, I. A. Hossenlopp and G. Waddington, *ibid.*, **76**, 4791 (1954).

(12) G. Waddington, J. W. Knowlton, D. W. Scott, G. D. Oliver, S. S. Todd, W. N. Hubbard, J. C. Smith and H. M. Huffman, *ibid.*, **71**, 797 (1949).

(13) E. Wichers, *ibid.*, **74**, 2447 (1952).

(14) F. D. Rossini, F. T. Gucker, Jr., H. L. Johnston, L. Pauling and G. W. Vinal, *ibid.*, **74**, 2699 (1952).

(15) Some of the results originally were computed with constants and temperatures in terms of the relation 0° = 273.16°K. Only results affected significantly by the new definition of the absolute temperature scale [H. F. Stimson, *Am. J. Phys.*, **23**, 614 (1955)] were recalculated. Therefore, numerical inconsistencies, much smaller than the accuracy uncertainty, may be noted in some of the reported data.

(16) H. F. Stimson, *J. Research Natl. Bur. Standards*, **42**, 209 (1949).

(17) H. J. Hoge and F. G. Brickwedde, *ibid.*, **22**, 351 (1939).

(18) A. R. Glasgow, A. J. Streiff and F. D. Rossini, *ibid.*, **35**, 355 (1945).

TABLE VI

THE MOLAL HEAT CAPACITY OF HEXAMETHYLDISILOXANE IN CAL. DEG.$^{-1}$

T, °K.[a]	C_{satd}[b]	T, °K.[a]	C_{satd}[b]
Crystals[c]		133.15	43.804
11.57	1.641	139.00	45.206
12.77	2.087	140.52	45.540
14.35	2.757	147.36	47.175
15.78	3.402	154.52	48.824
16.64	3.795	161.96	50.494
17.64	4.256	169.68	52.206
18.62	4.709	175.62	53.495
19.68	5.195	177.18	53.867
20.47	5.566	182.47	55.040
21.48	6.029	183.22	55.230
22.42	6.457	184.49	55.476
23.40	6.913	189.83	56.704
24.68	7.493	190.63	56.866
25.86	8.008	197.86	58.351
27.03	8.518	Liquid	
28.90	9.291	208.94	66.776
29.76	9.632	216.95	67.398
32.21	10.643	222.34	67.766
35.98	12.159	226.86	68.133
39.85	13.665	231.28	68.465
43.67	15.117	236.66	68.910
47.91	16.773	246.83	69.769
50.22	17.694	257.35	70.651
52.65	18.649	267.76	71.601
56.17	20.028	278.04	72.504
62.45	22.501	288.19	73.475
68.74	24.832	298.23	74.430
75.51	27.241	299.85	74.568
82.26	29.610	309.61	75.526
88.97	31.840	320.33	76 597
92.22	32.812	330.90	77 641
95.71	33.847	341.35	78.684
100.54	35.237	351.66	79.736
108.39	37.433	361.84	80.771
115.86	39.436	370.89	81.667
122.99	41.277		

[a] T is the mean temperature of each heat capacity measurement. [b] C_{satd} is the heat capacity of the condensed phase at saturation pressure. [c] Values of C_{satd} for crystals are not corrected for the effect of premelting.

TABLE VII

HEXAMETHYLDISILOXANE: MELTING POINT SUMMARY
$T_{T.P.}$ = 204.93 ± 0.05°K.; N_2^* = AF($T_{T.P.} - T_{obsd}$) = 0.00004; A = 0.03414 deg.$^{-1}$; B = 0.00375 deg.$^{-1}$

Melted, %	1/F	T_{obsd}, °K.	T_{graph}, °K.[a]
11.36	8.805	204.9165	204.9165
26.01	3.845	.9217	.9217
50.34	1.986	.9236	.9236
69.83	1.432	.9241	9242
89.28	1.120	.9245	9245
100.00	1.000		9246
Pure	0		204.9257

[a] Temperatures read from a straight line through a plot of T_{obsd} *vs.* 1/F.

Vapor Pressure.—Observed values of vapor pressure are listed in Table IX. The condensation temperature of the sample was 0.004° lower than the ebullition temperature at 1 atm. pressure. The Antoine and Cox equations selected to represent the results are

$$\log p = 6.77651 - 1203.556/(t + 208.427) \quad (2)$$

TABLE VIII

THE MOLAL THERMODYNAMIC PROPERTIES OF HEXAMETHYLDISILOXANE IN SOLID AND LIQUID STATES[a]

T, °K.	$-(F_{satd.} - H°_0)/T$, cal. deg.$^{-1}$	$(H_{satd.} - H°_0)/T$, cal. deg.$^{-1}$	$H_{satd.} - H°_0$, cal.	$S_{satd.}$, cal. deg.$^{-1}$	$C_{satd.}$, cal. deg.$^{-1}$
		Crystals			
10	0.091	0.274	2.74	0.365	1.125
12	.156	.470	5.64	.626	1.792
14	.246	.716	10.02	.962	2.603
16	.359	1.008	16.12	1.367	3.499
18	.496	1.336	24.04	1.832	4.421
20	.655	1.690	33.80	2.345	5.342
25	1.133	2.651	66.27	3.784	7.632
30	1.705	3.659	109.77	5.364	9.726
35	2.345	4.672	163.53	7.017	11.768
40	3.034	5.682	227.27	8.716	13.717
45	3.762	6.680	300.6	10.442	15.631
50	4.517	7.674	383.7	12.191	17.602
60	6.091	9.657	579.4	15.748	21.540
70	7.728	11.626	813.8	19.354	25.283
80	9.407	13.555	1084.4	22.962	28.825
90	11.113	15.441	1389.7	26.554	32.15
100	12.834	17.260	1726.0	30.09	35.08
110	14.563	19.007	2090.8	33.57	33.87
120	16.288	20.691	2482.9	36.98	40.51
130	18.009	22.313	2900.7	40.32	43.03
140	19.721	23.879	3343	43.60	45.43
150	21.421	25.393	3809	46.81	47.79
160	23.108	26.863	4298	49.97	50.06
170	24.779	28.294	4810	53.07	52.26
180	26.433	29.689	5344	56.12	54.47
190	28.077	31.05	5900	59.13	56.72
200	29.702	32.39	6478	62.09	58.96
204.93	30.50	33 04	6771	63.54	60.03
		Liquid			
204.93	30.50	46.94	9620	77.44	66.45
210	31.65	47.42	9958	79.07	66.89
220	33.88	48.32	10631	82.20	67.60
230	36.04	49.18	11311	85.22	68.37
240	38.16	49.99	11998	88.15	69.19
250	40.21	50.78	12694	90.99	70.03
260	42.23	51.53	13399	93.76	70.89
270	44.18	52.27	14112	96.45	71.79
273.15	44.79	52.49	14339	97.28	72.07
280	46.09	52.98	14835	99.07	72.69
290	47.96	53.68	15567	101.64	73.66
298.15	49.46	54.23	16170	103.69	74.42
300	49.80	54.36	16308	104.16	74.58
310	51.59	55.03	17058	106.62	75.57
320	53.35	55.68	17819	109.03	76.56
330	55.07	56.33	18590	111.40	77.55
340	56.76	56.97	19370	113.73	78.55
350	58.42	57.60	20161	116.02	79.57
360	60.05	58.23	20961	118 28	80.59
370	61.66	58.84	21772	120.50	81.58
375	62.45	59.15	22181	121.60	82.06

[a] The values tabulated are the free energy function, heat content function, heat content, entropy and heat capacity of the condensed phases at saturation pressure.

and

$$\log (p/760) = A(1 - 373.669/T)$$

$$\log A = 0.891266 - 9.2338 \times 10^{-4}T + 9.0805 \times 10^{-7}T^2 \quad (3)$$

In these equations, p is in mm., t is in °C., and T is in °K. The observed and calculated vapor pressure for both the Antoine and Cox equations are compared in Table IX. The normal boiling point is 100.52° (373.67°K.).

TABLE IX

VAPOR PRESSURE OF HEXAMETHYLDISILOXANE

Boiling point, °C. Ref. compd.[a]	Hexamethyldisiloxane	p(obsd.),[b] mm.	p(obsd.) − p(calcd.) Antoine eq. 2	Cox eq. 3
19.061	36.206	71.87	−0.02	−0.02
21.720	38.984	81.64	.00	+ .01
24.388	41.777	92.52	+ .01	.02
27.068	44.585	104.63	.01	.04
29.757	47.407	118.06	.01	.04
32.460	50.241	132.95	.02	.05
(35.174) 60.000	53.099	149.41	− .03	.00
65	58.837	187.57	− .04	− .02
70	64.625	233.72	− .01	.00
75	70.469	289.13	+ .01	.00
80	76.363	355.22	.09	+ .06
85	82.320	433.56	.07	.03
90	88.330	525.86	.06	.02
95	94.399	633.99	− .01	− .04
100	100.520	760.00	− .05	− .02
105	106.696	906.06	− .07	+ .02
110	112.932	1074.6	− .1	.0
115	119.222	1268.0	− .2	.0
120	125.567	1489.1	− .2	.0
125	131.971	1740.8	− .1	− .2
130	138.417	2026.0	+ .7	+ .1

[a] The reference compound from 71.87 to 149.41 mm. was pure benzene; that from 149.41 to 2026.0 mm. was pure water. [b] From vapor pressure data for benzene [F. D. Rossini, K. S. Pitzer, R. L. Arnett, R. M. Braun and G. C. Pimentel, "Selected Values of Physical and Thermodynamic Properties of Hydrocarbons and Related Compounds," Carnegie Press, Pittsburgh, Pa., 1953, Table 21k] and for water [N. S. Osborne, H. F. Stimson and D. C. Ginnings, *J. Research Natl. Bureau Standards*, **23**, 261 (1939)].

Heat of Vaporization, Vapor Heat Capacity and Effects of Gas Imperfection.—The experimental values of heat of vaporization and vapor heat capacity are given in Tables X and XI. The estimated accuracy uncertainty of the values of ΔHv and $C_p°$ are 0.1 and 0.2%, respectively. The heat of vaporization may be represented by the empirical equation

$$\Delta Hv = 11794 - 2.5429T - 2.4172 \times 10^{-2}T^2, \text{ cal. mole}^{-1} \quad (332 - 374°\text{K.}) \quad (4)$$

The effects of gas imperfection were correlated by the procedure described in an earlier paper.[19] The empirical equation for B, the second virial coefficient in the equation of state, $PV = RT(1 + B/V)$, is

$$B = 560 - 282.1 \exp(800/T) \text{ cc. mole}^{-1} \quad (332 - 500°\text{K.}) \quad (5)$$

"Observed" values of B and $-T(d^2B/dT^2) = \lim_{P\to 0}(\partial C_p/\partial P)_T$ and those calculated from eq. 5 are compared in Tables X and XI. The observed gas imperfection is

TABLE X

THE MOLAL HEAT OF VAPORIZATION AND SECOND VIRIAL COEFFICIENT OF HEXAMETHYLDISILOXANE

T, °K.	P, atm.	ΔHv, cal.	B(obsd.), cc.	B(calcd.), cc.[b]
332.31	0.250	8280 ± 4[a]	−2493	−2572
351.50	0.500	7914 ± 2[a]	−2191	−2187
373.67	1.000	7469 ± 2[a]	−1856	−1840

[a] Maximum deviation from the mean of three or more determinations. [b] Calculated from eq. 5.

(19) J. P. McCullough, H. L. Finke, J. F. Messerly, R. E. Pennington, I. A. Hossenlopp and G. Waddington, *J. Am. Chem. Soc.*, **77**, 6119 (1955).

TABLE XI

THE MOLAL VAPOR HEAT CAPACITY OF HEXAMETHYLDISILOXANE IN CAL. DEG.$^{-1}$

T, °K.	363.20	393.20	429.20	465.20	500.20
C_p (1.000 atm.)		68.942	72.215	75.467	78.556
C_p (0.500 atm.)	65.273	68.288	71.793	75.202	78.354
C_p (0.333 atm.)		68.074			
C_p (0.250 atm.)	64.846				
$C_p°$	64.45	67.68	71.40	74.95	78.16
$-T(d^2B/dT^2)$[a]					
obsd.	1.53	1.14	0.76	0.48	0.38
calcd.[b]	1.58	1.09	.74	.52	.39

[a] Units: cal. deg.$^{-1}$ mole^{-1} atm.$^{-1}$ [b] Calculated from eq. 5.

roughly that expected for a substance of the molecular size and shape of hexamethyldisiloxane and with normal intermolecular forces.

The heat of vaporization at 298.15°K. was calculated by extrapolation with eq. 4 (8.89 kcal. mole^{-1}), by use of the Clapeyron equation with eq. 3 and 5 (8.87 kcal. mole^{-1}) and by use of a thermodynamic network with the thermodynamic functions of Table V (8.90 kcal. mole^{-1}). From the last value, selected as the most reliable, and eq. 5, the standard heat of vaporization was calculated, $\Delta Hv^{\circ}_{298.15}$ = 8.92 kcal. mole^{-1}.

Entropy in the Ideal Gaseous State.—The entropy in the ideal gaseous state at 1 atm. pressure was calculated as shown in Table XII.

TABLE XII

THE MOLAL ENTROPY OF HEXAMETHYLDISILOXANE IN THE IDEAL GASEOUS STATE IN CAL. DEG.$^{-1}$

T, °K.	332.31	351.50	373.67
S_{satd} (liq)[a]	111.95	116.37	121.31
$\Delta Hv/T$	24.92	22.51	19.99
S(ideal) − S(real)[b]	0.14	0.23	0.36
$R \ln P$[c]	−2.76	−1.38	0.00
$S°$(obsd.) ± 0.25[d]	134.25	137.73	141.66

[a] By interpolation in Table VIII. [b] The entropy in the ideal gas state less that in the real gas state, calculated from eq. 5. [c] Entropy of compression, calculated from eq. 3. [d] Estimated accuracy uncertainty.

Appendix

Barrier to Internal Rotation and Thermodynamic Functions of Tetramethylsilane.—Calorimetric[20] and spectral[21] data for tetramethylsilane were reexamined to determine the height of the barrier restricting the methyl rotations. The set of fundamental vibrational frequencies taken for thermodynamic calculations is in Table XIII. The two unobserved CH_3 rocking frequencies were calculated in the course of normal coördinate calculations to obtain force constants for transfer to hexamethyldisiloxane. The values obtained (813 and 809 cm.$^{-1}$) do not differ grossly from the values calculated by Kovalev[22] (855 and 829 cm.$^{-1}$) and by Shimizu and Murata[23] (830 and 825 cm.$^{-1}$). For Si–C distance 1.888 Å., C–H distance 1.10 Å.[24] and all angles tetrahedral, the product of principal moments of inertia is 2.012×10^{-113} g.^{3} cm.^{6}, and the reduced moment of inertia for internal rotation is 5.292×10^{-40} g. cm.^{2}

(20) J. G. Aston, R. M. Kennedy and G. H. Messerly, *J. Am. Chem. Soc.*, **63**, 2343 (1941).

(21) D. H. Rank, B. D. Saksena and E. R. Shull, *Disc. Faraday Soc.*, **9**, 187 (1950).

(22) I. F. Kovalev, *Optika i Spectroskopia*, **6**, 387 (Eng. ed.) (1959).

(23) K. Shimizu and H. Murata, *J. Molecular Spectroscopy*, **5**, 44 (1960).

(24) W. F. Sheehan, Jr., and V. Schomaker, *J. Am. Chem. Soc.*, **74**, 3956 (1952).

TABLE XIII

FUNDAMENTAL VIBRATIONAL FREQUENCIES OF TETRAMETHYLSILANE,[a] Cm.$^{-1}$

	a_1	e	f_1	f_2
C–H stretching		(2967)	(2967)	2967
C–H stretching	2900			(2900)
CH_3 unsym. bending		1418	(1418)	1430
CH_3 sym. bending	1263			1250
CH_3 rocking		[813]	[809]	862
Si–C stretching	593			694
Skeletal bending		199		245

[a] (), observed frequency used more than once; [], from normal coördinate calculations.

A Cox vapor pressure equation was fitted to the data of Aston and co-workers because it is more reliable for obtaining derivatives than the type of four-constant equation originally used by those workers. With this Cox equation

$$\log (p/760) = A(1 - 299.80/T)$$

$$\log A = 0.819737 - 9.1552 \times 10^{-4}T + 1.2078 \times 10^{-6}T^2$$

and an estimated value for the second virial coefficient (−2.7 l.), the heat of vaporization at 227°K., calculated by use of the Clapeyron equation, is 6750 cal. mole^{-1}. This value is 2.5% lower than the one originally reported by Aston, *et al.*

TABLE XIV

THE MOLAL THERMODYNAMIC FUNCTIONS OF TETRAMETHYLSILANE IN THE IDEAL GAS STATE; RIGID ROTATOR, HARMONIC OSCILLATOR, INDEPENDENT INTERNAL ROTATOR APPROXIMATION[a]

T, °K.	$-(F° - H°_0)/T$, cal. deg.$^{-1}$	$(H° - H°_0)/T$, cal. deg.$^{-1}$	$H° - H°_0$, kcal.	$S°$, cal. deg.$^{-1}$	$C_p°$, cal. deg.$^{-1}$
273.15	−62.00	20.87	5.701	82.87	32.61
298.15	−63.87	21.92	6.537	85.79	34.39
300	−64.00	22.00	6.600	86.00	34.52
400	−70.89	25.99	10.40	96.88	41.30
500	−77.10	29.67	14.83	106.76	47.32
600	−82.81	33.05	19.83	115.86	52.53
700	−88.15	36.16	25.32	124.31	57.06
800	−93.16	39.03	31.23	132.19	61.04
900	−97.91	41.69	37.52	139.59	64.57
1000	−102.42	44.14	44.14	146.56	67.67
1100	−106.73	46.41	51.05	153.14	70.40
1200	−110.86	48.51	58.21	159.37	72.79
1300	−114.82	50.46	65.60	165.28	74.88
1400	−118.62	52.28	73.19	170.90	76.71
1500	−122.28	53.96	80.95	176.24	78.32

[a] To retain internal consistency, some of the values in this table are given to one more decimal place than is justified by the absolute accuracy.

Addition of the revised value of entropy of vaporization to the calorimetric value of entropy for the liquid gives for the gas, $S°_{227}$ = 77.00 cal. deg.$^{-1}$ mole^{-1}. This value of $S°_{227}$ and the original value of $S°_{298.16}$, based on a calorimetric determination of the heat of vaporization, were used in calculating the barrier height. At both temperatures, a value close to 1600 cal. mole^{-1} is obtained; this is the value transferred to hexamethyldisiloxane, as already discussed.

T, °K.	227	298.16
$S°$(free int. rot.), cal. deg.$^{-1}$ mole^{-1}	80.73	88.31
$S°$(obsd.), cal. deg.$^{-1}$ mole^{-1}	77.00	85.79
$S_f - S$, cal. deg.$^{-1}$ mole^{-1}	3.73	2.52
Barrier height, cal. mole^{-1}	1651	1598

ous molecular structure para
lsilane were used in compu
thermodynamic functions in Tal
ulated values of entropy, $S°_{227}$ =
$_{8.16}$ = 85.79 cal. deg.$^{-1}$ mole^{-1}, n
d with the experimental values given
s paragraph. As effects of anharmo
were not taken into account and no vapor
capacity data were available for checking,
thermodynamic functions for tetramethylsil
in Table XIV are less reliable than those for hex
methyldisiloxane in Table V. The values
Table XIV differ from those published by Shimizu and Murata[23] mainly in the use of a value of barrier height based on a reinterpretation of Aston and co-workers' data.

THE HEATS OF COMBUSTION AND FORMATION OF PYRIDINE AND HIPPURIC ACID[1]

BY W. N. HUBBARD, F. R. FROW AND GUY WADDINGTON[2]

Contribution No. 101 from the Thermodynamics Laboratory, Petroleum Research Center, Bureau of Mines, U. S. Department of the Interior, Bartlesville, Oklahoma

Received January 10, 1961

The heats of combustion of pyridine and hippuric acid were determined by precision oxygen-bomb calorimetry, and these values, in kcal. mole^{-1}, are reported for the standard heat of formation, $\Delta Hf°_{298.15}$, from graphite, and gaseous hydrogen, oxygen and nitrogen: pyridine(liq.), 23.89; hippuric acid(c), −145.54. Recommendations are made for methods of determining the amount of reaction in combustion calorimetry. The suitability of hippuric acid as a reference substance for the combustion calorimetry of organic nitrogen compounds is discussed.

Heat of combustion measurements are part of a continuing study by the Bureau of Mines of the thermodynamic properties of organic nitrogen compounds important in petroleum technology. This paper gives the results of heat of combustion measurements on pyridine and presents related thermochemical data that were used in an earlier comprehensive report on the chemical thermodynamic properties of this substance.[3] Also given are the results of measurements on hippuric acid, which has been proposed as a reference substance

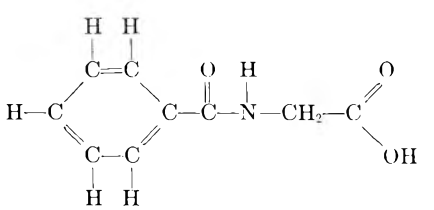

for combustion calorimetry of organic nitrogen compounds.[4]

Experimental

Materials.—The sample of pyridine used for this study has been described[5]; it was dried in the liquid phase by calcium hydride and handled in a vacuum distillation system at all times. The sample of hippuric acid was prepared by recrystallizing commercial material three times from distilled water. Part of the recrystallized material was dried in a vacuum oven at 80°, and part was dried in air at 105 to 110°. An attempt to purify part of the recrystallized material further by zone refining failed because the sample decomposed at a temperature only slightly higher than the melting point. Pellets of dried hippuric acid were stored over P_2O_5.

Units of Measurements and Auxiliary Quantities.—All data reported are based on the 1951 International Atomic Weights[6a] and fundamental constants[6b] and the definitions: 0°C. = 273.15° K.; 1 cal. = 4.184 (exactly) joules. The laboratory standard weights had been calibrated at the National Bureau of Standards.

For use in reducing weights in air to *in vacuo*, in converting the energy of the actual bomb process to the isothermal process, and in reducing to standard states,[7] the values tabulated below, all for 25°, were used for density, ρ, specific heat, c_p, and $(\partial E/\partial P)_T$ of the substances.

	ρ, g. ml.$^{-1}$	c_p, cal. deg.$^{-1}$ g.$^{-1}$	$(\partial E/\partial P)_T$, cal. atm.$^{-1}$ g.$^{-1}$
Pyridine	0.978	0.401	−0.0076
Hippuric acid	1.371	.286	− .0027

Calorimetry.—The bomb, Ta-1,[8] and rotating-bomb

(1) This investigation was performed as part of American Petroleum Institute Research Project 52 on "Nitrogen Constituents of Petroleum," which is conducted at the University of Kansas in Lawrence, Kansas, and at the Bureau of Mines Petroleum Research Centers in Laramie, Wyoming, and Bartlesville, Oklahoma.

(2) Requests for reprints should be addressed to the Thermodynamics Laboratory, Bartlesville Petroleum Research Center, Bureau of Mines, U. S. Department of the Interior, Bartlesville, Oklahoma.

(3) J. P. McCullough, D. R. Douslin, J. F. Messerly, I. A. Hossenlopp, T. C. Kincheloe and Guy Waddington, *J. Am. Chem. Soc.*, **79**, 4289 (1957).

(4) H. M. Huffman, *ibid.*, **60**, 1171 (1938).

(5) R. V. Helm, W. J. Lanum, G. L. Cook and J. S. Ball, *J. Phys. Chem.*, **62**, 858 (1958).

(6) (a) E. Wichers, *J. Am. Chem. Soc.*, **74**, 2447 (1952). (b) F. D. Rossini, F. T. Gucker, Jr., H. L. Johnston, L. Pauling and G. W. Vinal, *ibid.*, **74**, 2699 (1952).

(7) W. N. Hubbard, D. W. Scott and G. Waddington, "Experimental Thermochemistry," F. D. Rossini, Editor, Interscience Publishers, Inc., New York, N. Y., 1956, Chapter 5, pp. 75–128.

(8) W. N. Hubbard, J. W. Knowlton and H. M. Huffman, *J. Phys. Chem.*, **58**, 396 (1954).

calorimeter system, BMR-1,[9] have been described. Rotation of the bomb is not required in the combustion calorimetry of nitrogen compounds, so the apparatus was used as a static-bomb calorimetric system. The samples of pyridine were sealed in Pyrex ampoules of a kind previously described.[10] The samples of hippuric acid were in the form of pellets. One gram of water was added to the bomb. The bomb was purged with oxygen to remove air originally present and charged to 30 atmospheres with pure oxygen. The energy equivalent of the calorimetric system, $\mathcal{E}$(calor.), was determined by combustion of benzoic acid (National Bureau of Standards Sample 39g). Each combustion experiment was initiated at 23° and the quantities of pyridine plus auxiliary oil (Sample USBM-P3a, empirical formula $CH_{1.891}$) and of hippuric acid were chosen to produce a temperature increment of 2°. The amount of reaction was checked by determining the amount of carbon dioxide in the combustion products; an absorption train similar to that described by Prosen and Rossini[11] was used for this purpose. Carbon dioxide recovery in the combustion experiments with pyridine was 99.99 ± 0.01$_2$% of that predicted from the mass of sample. Carbon dioxide recovery in the combustion experiments with hippuric acid was only 99.93$_5$ ± 0.03% of that predicted from the mass of sample.

Results.—It is impractical to report all experiments in detail, but data for single experiments selected as typical for each compound are summarized in Table I. The amount of reaction was based on mass of sample for pyridine. However, as the low recovery of CO_2 for hippuric acid shows the sample contained significant impurity (probably water), the amount of reaction for this compound was computed from the mass of CO_2 produced. The results of all the combustion experiments are summarized in Table II. The experimental values of $\Delta Ec°/M$ for pyridine apply to the idealized combustion reaction (1). For this

$$C_5H_5N(liq) + 6.25\ O_2(g) = 5\ CO_2(g) + 2.5\ H_2O(liq) + 0.5\ N_2(g) \quad (1)$$

reaction the standard change in internal energy, $\Delta Ec°_{298.15}$, is −664.50 ± 0.10[12] kcal. mole^{-1} and the standard heat of combustion, $\Delta Hc°_{298.15}$, is −664.95 ± 0.10 kcal. mole^{-1}. This value of $\Delta Hc°_{298.15}$ is in good agreement with the value of Cox, Challoner and Meetham,[13] −665.00 ± 0.36 kcal. mole^{-1}. The value of $\Delta Hc°_{298.15}$ for pyridine and values of the heat of formation of water[14] and carbon dioxide[15] were used to compute the heat of formation in the liquid state according to reaction (2). Addition of the standard heat of

$$5C(c, graphite) + 5/2H_2(g) + 1/2N_2(g) = C_5H_5N(liq) \quad (2)$$

$$\Delta Hf°_{298.15} = 23.89 \pm 0.12 \text{ kcal. mole}^{-1}$$

vaporization from ref. 3 gives $\Delta Hf°_{298.15}$ for pyridine in the ideal gas state, 33.50 kcal. mole^{-1}.

The value of $\Delta Ec°/M$ for hippuric acid applies to the idealized combustion reaction (3). For

$$C_9H_9O_3N(c) + 9.75O_2(g) = 9CO_2(g) + 4.5H_2O(liq) + 0.5N_2(g) \quad (3)$$

this reaction $\Delta Ec°_{298.15}$ is −1008.20 ± 0.39[12] kcal. mole^{-1} and $\Delta Hc°_{298.15}$ is −1008.35 ± 0.39 kcal. mole^{-1}. This value of $\Delta Hc°_{298.15}$ may be compared with those of Huffman,[4] −1008.2 ± 0.3 kcal. mole^{-1}, and Cole and Gilbert,[16] −1008.3 ± 0.9 kcal. mole^{-1}. (The original value of Huffman[4] has been made consistent with the revised value of the heat of combustion of benzoic acid.[17]) The value of $\Delta Hc°_{298.15}$ for hippuric acid was used with values of the heat of formation of water[14] and carbon dioxide[15] to compute the heat of formation of solid hippuric acid according to reaction (4).

$$9C(c, graphite) + 9/2H_2(g) + 3/2O_2(g) + 1/2N_2(g) = C_9H_9O_3N(c) \quad (4)$$

$$\Delta Hf°_{298.15} = -145.54 \pm 0.40 \text{ kcal. mole}^{-1}$$

TABLE I

SUMMARY OF TYPICAL COMBUSTION EXPERIMENTS[a,b]

Compound	Pyridine	Hippuric acid
m' (compound), g.	0.80342[c]	1.37985[d]
$\Delta t_c = t_f - t_i - \Delta t_{cor.}$, deg.	2.00032	2.00004
$\mathcal{E}$(Calor.)$(-\Delta t_c)$, cal.	−7786.47	−7785.38
$\mathcal{E}$(Cont.)$(-\Delta t_c)$,[e] cal.	−9.84	−9.74
$\Delta E_{ign.}$, cal.	1.35	1.35
$\Delta E^f_{deo.}$ (HNO_3 + HNO_2), cal.	13.78	10.63
ΔE, cor. to st. states,[f] cal.	3.90	6.29
$-m''\Delta Ec°/M$ (auxiliary oil), cal.	1012.27	.....
$-m'''\Delta Ec°/M$ (fuse), cal.	15.42	15.50
$m'\Delta Ec°/M$ (compound), cal.	−6749.59	−7761.35
$\Delta Ec°/M$ (compound), cal. g.$^{-1}$	−8401.07	−5624.78

[a] The symbols and abbreviations in this table are those of ref. 7, except as noted. The values of $\Delta Ec°/M$ for the auxiliary oil and fuse are −10,984.8 and −3923 cal. g.$^{-1}$, respectively. [b] Auxiliary data: $\mathcal{E}$(calor.) = 3892.61 ± 0.15 cal. deg.$^{-1}$ (mean and standard deviation); V(bomb) = 0.344 l. [c] Actual mass of sample. [d] Mass of hippuric acid calculated from mass of CO_2 recovered. [e] $\mathcal{E}^i$ (Cont.)$(t_i - 25°) + \mathcal{E}^f$(Cont.)$(25° - t_f + \Delta t_{cor.})$. [f] Items 81–85, incl., 87–90, incl., 93 and 94 of the computation form of ref. 7.

TABLE II

SUMMARY OF CALORIMETRIC RESULTS

Compound	Pyridine	Hippuric acid
$\Delta Ec°/M$, cal. g.$^{-1}$	−8402.62	−5632.18[a]
	8399.23	5634.11[a]
	8400.84	5621.65[a]
	8400.01	5627.54[a]
	8401.71	5625.75[a]
	8401.27	5627.15[b]
	8401.17	5626.38[c]
	8401.07	5624.64[a]
		5626.79[d]
		5626.65[d]
		5624.78[d]
Mean and std. dev.	−8400.99 ± 0.36	−5627.06 ± 1.04

[a] Material recrystallized three times and vacuum dried. [b] Material recrystallized twice and vacuum dried. [c] Material recrystallized once and vacuum dried. [d] Material recrystallized three times and air dried.

(9) W. N. Hubbard, C. Katz and Guy Waddington, *ibid.*, **58**, 142 (1954).

(10) G. B. Guthrie, Jr., D. W. Scott, W. N. Hubbard, C. Katz, J. P. McCullough, M. E. Gross, K. D. Williamson and Guy Waddington, *J. Am. Chem. Soc.*, **74**, 4662 (1952).

(11) E. J. R. Prosen and F. D. Rossini, *J. Research Natl. Bur. Standards*, **27**, 289 (1941).

(12) "Uncertainty interval" equal to twice the final "over-all" standard deviation. See F. D. Rossini and W. E. Deming, *J. Wash. Acad. Sci.*, **29**, 416 (1939).

(13) J. D. Cox, A. R. Challoner and A. R. Meetham, *J. Chem. Soc.*, 265 (1954).

(14) E. J. Prosen, R. S. Jessup and F. D. Rossini, *J. Research Natl. Bur. Standards*, **33**, 447 (1944).

(15) D. D. Wagman, J. E. Kilpatrick, W. J. Taylor, K. S. Pitzer and F. D. Rossini, *ibid.*, **34**, 143 (1945).

(16) L. G. Cole and E. C. Gilbert, *J. Am. Chem. Soc.*, **73**, 5423 (1951).

(17) R. S. Jessup, *J. Research Natl. Bur. Standards*, **29** 247 (1942).

Discussion

The amount of reaction in combustion calorimetry may be determined either from the mass of the sample or the mass of some combustion product such as CO_2, the latter method having been used by Cox, *et al.*,[13] for example. Basing heat of combustion values on the amount of CO_2 produced has obvious advantages when the sample used may contain unknown amounts of non-isomeric impurity, usually water. However, this investigation has shown that, even with hygroscopic materials such as pyridine, the use of mass of sample as the basis of computation is equally reliable if the sample is pure enough and is handled by techniques that ensure its dryness. Because the amount of reaction can be determined with higher precision, and perhaps better accuracy, from the mass of sample, the method described herein is preferred. With this method, determination of the amount of CO_2 produced serves as a useful check on the purity and dryness of the samples used.

However, if the amount of CO_2 produced differs from that corresponding to the mass of sample and there is no reason to suspect incomplete combustion, it is clear that the sample is impure and that more accurate, though less precise, results will be obtained by using the amount of CO_2 in computing the amount of reaction. This was true in the study of hippuric acid. Although the procedures of previous workers[4,16] were followed carefully in preparing and drying the sample of hippuric acid, some water (about 0.06%) must have remained. The earlier workers did not determine the amount of CO_2 produced in their experiments, so the almost exact agreement with their results may be fortuitous. The apparent difficulty in preparing pure, dry samples of hippuric acid is an undesirable characteristic for a proposed reference substance. Nevertheless, hippuric acid is satisfactory in other important respects, and the purity problem could be solved if an appropriate organization prepared a suitable large sample for distribution to qualified investigators.

SPECTROPHOTOMETRIC STUDIES OF *cis*- AND *trans*-DICHLORO-BIS-(ETHYLENEDIAMINE)-COBALT(III) CHLORIDES IN WATER, METHANOL AND IN METHANOL–WATER MIXTURES

BY E. W. DAVIES

Chemistry Department, Llandaff Technical College, South Wales, Great Britain

Received January 11, 1961

A rate constant of $1.3_9 \times 10^{-4}$ sec.$^{-1}$ ($\pm 2\%$) has been obtained by spectrophotometry for the acid hydrolysis of *cis*-[Co en$_2$ Cl$_2$]Cl in water at 25°. This value is compared with previously cited values obtained by various methods. The corresponding rate obtained for the *trans* isomer is $2.7_0 \times 10^{-5}$ sec.$^{-1}$ ($\pm 1.5\%$). *cis*-[Co en$_2$ Cl$_2$]Cl is completely converted into the thermodynamically more stable *trans* isomer in methanol, following a first-order rate law throughout (rate constant = $2.2_0 \times 10^{-5}$ sec.$^{-1}$ ($\pm 2\%$)) at 25°. The hydrolysis rates of the *cis* isomer in methanol–water mixtures are also reported.

Introduction

A number of values for the acid hydrolysis rate constants of *cis*- and *trans*-[Co en$_2$ Cl$_2$]Cl at 25° have been reported. These (listed below) show considerable variations which are partly attributed to a number of misconceptions. The present work aims to clarify the situation.

Experimental

A Hilger Uvispek spectrophotometer was fitted with a water-jacketed cell holder which could be kept at 25 ± 0.1°. Some of the measurements were made with the aid of a photomultiplier-recorder unit. *trans*-Dichloro-bis-(ethylenediamine)-cobalt(III) chloride was prepared by a published method.[1] A small amount of tris-(ethylenediamine)-cobalt(III) chloride was present and this, being less soluble, was removed by filtering a saturated aqueous solution, then precipitating the pure *trans*-dichloro compound with ethanol and recrystallising it from methanol in which it was shown to be stable over a considerable period of time. Some of this *trans*-compound was converted into the *cis*-isomer by evaporating an aqueous solution to dryness on a water-bath. Any unchanged *trans*-compound was removed by adding a little water during filtration under suction when it dissolved preferentially. The sample was dried over phosphoric oxide. The *cis*-aquochloro compound was prepared as described by Werner.[2] Methanol was purified by the method of Maryott.[3] Stoppered quartz cells were tried for the kinetic studies but they were not completely successful owing to some evaporation losses. Such errors were, however, eliminated by keeping the reaction solution in a stoppered flask in the thermostat and pipetting portions into the cells (emptied by suction jet) at timed intervals for each reading. The cells were not handled once they had been placed in the cell holder.

(1) "Inorganic Syntheses," Vol. II, McGraw-Hill Book Co., Inc., New York, N. Y., 1946, p. 222.

(2) A. Werner, *Lieb. Ann.*, **386**, 17 (1911).

Results and Discussion

(i). *cis*-[Co en$_2$ Cl$_2$]Cl.—The several values which have been published for the hydrolysis rate constant of *cis*-[Co en$_2$ Cl$_2$]Cl in water are

1.22×10^{-4} sec.$^{-1}$ (Mathieu,[4] conductance)

2.5×10^{-4} sec.$^{-1}$ (Pearson, Boston and Basolo,[5] spectrophotometry)

1.76×10^{-4} sec.$^{-1}$ (Selbin and Bailar,[6] chloride-concentration cell)

Mathieu[4] reported that the rate of loss of optical activity of *l-cis*-[Co en$_2$Cl$_2$]Cl is one-tenth as fast as its rate of acid hydrolysis and attributed this to the formation of either the *trans*-aquochloro product

(3) A. A. Maryott, *J. Am. Chem. Soc.*, **63**, 3079 (1941).

(4) J. P. Mathieu, *Bull. soc. chim.*, **3**, 2121 (1936).

(5) R. G. Pearson, C. R. Boston and F. Basolo, *J. Phys. Chem.*, **59**, 304 (1955).

(6) J. Selbin and J. C. Bailar, Jr., *J. Am. Chem. Soc.*, **79**, 4285 (1957).

or its racemic *cis*-isomer. This means that the maximum rate of formation of the *trans*-aquochloro compound is only one-tenth of the rate of acid hydrolysis. Pearson, Meeker and Basolo[7] showed that the loss of optical activity was in fact due to the formation of the *trans*-aquochloro compound and, using the rates determined by Mathieu,[4] calculated that the maximum concentration of this *trans*-aquochloro isomer is 20%. The value[5] of 2.5×10^{-4} sec.$^{-1}$ for the acid hydrolysis of *cis*-[Co en$_2$ Cl$_2$]Cl depended on an ϵ_∞ value obtained by "levelling off" ϵ, the molecular extinction coefficient to a minimum, but this minimum value would be influenced by the 20% formation of *trans*-[Co en$_2$ (H$_2$O) Cl]$^{++}$ so would not therefore give a true indication of the acid hydrolysis

$$cis\text{-}[\text{Co en}_2\ \text{Cl}_2]^{+} \longrightarrow cis\text{-}[\text{Co en}_2\ (\text{H}_2\text{O})\ \text{Cl}]^{++}$$

The effect which the 20% *trans*-aquochloro compound has on ϵ_∞ was determined in the present work where an aqueous solution of *cis*-[Co en$_2$ (H$_2$O) Cl]$^{++}$ was made up and its absorptions extrapolated to zero time, the average value of ϵ being 55 at 540 mμ whereas the acid hydrolysis of *cis*-[Co en$_2$ Cl$_2$]$^{+}$ experimentally gave an average value of $\epsilon = 45$. In addition, the value of ϵ_0 obtained by these workers[5,8] for *cis*-[Co en$_2$ Cl$_2$]$^{+}$ is 75.8 at 530 mμ. Their absorption curve and the present work showed 530 mμ to be an absorption maximum so that their value is very low compared with 98 (Mathieu[4]), 92 (Uspensky and Tschibisoff[9]) and 93 (Brown and Ingold[10], in methanol), all these values are for 540 mμ.

For the present studies, various concentrations of the *cis*-salt were made up into aqueous and 0.1 *M* nitric acid solutions at 25 ± 0.1°. Optical densities were then extrapolated to zero time and Beer's law was found to hold within experimental error giving $\epsilon_0 = 94$ at 540 mμ. Changes in the optical absorptions of a 0.00465 *M* solution of the *cis*-salt in 0.10 *M* nitric acid were followed continuously for 7 hours and then periodically over 7 days. The results were treated by the method of Guggenheim[11] plotting log $(\epsilon_t - \epsilon_t')$ against time (t), where $\epsilon_t' = \epsilon_{t+s}$ and s is a suitable constant interval of time. $k/2.303$ was obtained from the slope (least mean square) of the graph giving a rate constant k of $1.4_0 \times 10^{-4}$ sec.$^{-1}$. Since ϵ_0 and ϵ_∞ need not be known, this method of calculation is useful in cases such as this where subsequent reactions made the determination of ϵ_∞ uncertain. Substituting $\epsilon_0 = 94$ and $\epsilon_\infty = 55$ into

$$k = \frac{2.303}{t} \log \frac{(\epsilon_0 - \epsilon_\infty)}{(\epsilon_t - \epsilon_\infty)} \qquad (1)$$

gave the rate constant of $1.3_9 \times 10^{-4}$ sec.$^{-1}$ (± 2%) for the first 75 minutes of the hydrolysis. After 75 minutes, the rate was found to decrease appreciably due to the effect of the formation of the *trans*-aquochloro compound on the above extinction coefficient figures.

(ii). *trans*-[Co en$_2$ Cl$_2$]Cl.—Previous values for the acid hydrolysis of this compound are

1.6×10^{-5} sec.$^{-1}$ (Werner and Herty,[12] conductance and f.p. depressions)

3.2×10^{-6} sec.$^{-1}$ (Pearson, Boston and Basolo,[13] spectrophotometry)

2.75×10^{-6} sec.$^{-1}$ (Mathieu,[4] conductance)

1.8×10^{-6} sec.$^{-1}$ (Haworth, Neuzil and Kittsley,[14] spectrophotometry)

The most recent work is that of Haworth, Neuzil and Kittsley.[14] A value of $k = 1.8 \times 10^{-5}$ sec.$^{-1}$ at 25° was obtained by extrapolating their values quoted at 26, 35.3, 40 and 50° from the least mean squares slope of log k against $1/T$°K. The reason why this figure is so different from the other spectrophotometric values is that these workers assumed the reaction to be *trans* → *cis* isomerism rather than hydrolysis, so they used extinction coefficients which are not relevant. The differences between the values quoted by Mathieu[4] and Pearson, Boston and Basolo[13] are greater at other temperatures, *e.g.* at 35° they are[4] 9.6×10^{-5} sec.$^{-1}$ and [13] 1.6×10^{-4} sec.$^{-1}$; these figures lead to a large uncertainty in activation energies.

Various concentrations of this isomer were found to obey Beer's law and the average ϵ_0 extrapolated to zero time was 8.5. The mechanism of acid hydrolysis has been described by Mathieu[4] as

$$trans\text{-}[\text{Co en}_2\ \text{Cl}_2]^{+} \xrightarrow{\text{H}_2\text{O}} trans\text{-}[\text{Co en}_2(\text{H}_2\text{O})\text{Cl}]^{++} \longrightarrow cis\text{-}[\text{Co en}_2(\text{H}_2\text{O})\text{Cl}]^{++} \quad (a)$$

$$[\text{Co en}_2(\text{H}_2\text{O})\text{Cl}]^{++} \xrightarrow{\text{H}_2\text{O}} [\text{Co en}_2(\text{H}_2\text{O})_2]^{+++} \quad (b)$$

$$\uparrow\downarrow \qquad\qquad \uparrow\downarrow$$

$$[\text{Co en}_2(\text{OH})\text{Cl}]^{+} \longrightarrow [\text{Co en}_2(\text{H}_2\text{O})\ \text{OH}]^{++} \quad (c)$$

The rate of acid hydrolysis of the second chlorine from the aquo complex as in (b) is very slow whereas the hydroxo complex (c) aquates fairly rapidly. The effect of carrying out this hydrolysis in acid solution is to suppress reactions (b) and (c) without affecting reaction (a). The first hydrolysis was carried out with 0.00963 *M* *trans*-[Co en$_2$ Cl$_2$]Cl in 0.0105 *M* nitric acid. Applying the Guggenheim[11] method of calculation gave a rate constant of 2.7×10^{-5} sec.$^{-1}$ consistent with $\epsilon_\infty = 51.0$. ϵ_{max} experimentally was found to be 51.6 after 3 days decreasing to a final ϵ_∞ of 49.6 after one week so that ϵ_∞ obtained by "levelling off" again does not agree with that obtained above. A larger difference in the "levelling off" and extrapolated values are obtained for this *trans*-isomer since Mathieu[4] claims 100% conversion of the *trans*-aquochloro into the *cis*-aquochloro compound. Substituting $\epsilon_0 = 8.5$ and $\epsilon_\infty = 51.0$ in equation 1 showed the rate to be $2.7_0 \times 10^{-5}$ sec.$^{-1}$ (± 1.5%) for 180 minutes increasing slightly to 3.05×10^{-5} sec.$^{-1}$ after 7 hours. Similar treatment of the absorption values obtained with a 0.00956 *M* aqueous solution in the absence of acid gave a rate constant of $2.8_7 \times 10^{-5}$ sec.$^{-1}$ for one hour when the equation of the hydroxo com-

(7) R. G. Pearson, R. E. Meeker and F. Basolo, *ibid.*, **78**, 2673 (1956).

(8) F. Basolo, *J. Am. Chem. Soc.*, **72**, 4394 (1950).

(9) A. Uspensky and K. Tschibisoff, *Z. anorg. allgem. Chem.*, **164**, 326 (1927).

(10) D. D. Brown and C. K. Ingold, *J. Chem. Soc.*, 2686 (1953).

(11) E. A. Guggenheim, *Phil. Mag.*, **2**, 538 (1926).

(12) A. Werner and A. Herty, *Z. physik. Chem.*, **38**, 331 (1901).

(13) R. G. Pearson, C. R. Boston and F. Basolo, *J. Am. Chem. Soc.*, **75**, 3089 (1953).

(14) D. T. Haworth, E. F. Neuzil and S. L. Kittsley, *ibid.*, **77**, 6198 (1955).

pound (c) became apparent, the rate constant increased rapidly.

(iii). **Mixed Solvents.**—Brown and Nyholm[15] have studied the rate of isomerization of *cis*-[Co en$_2$ Cl$_2$]Cl in methanol where there are no complications due to the formation of stable methanol complexes nor due to solubilities. At equilibrium, the *cis*-isomer is almost quantitatively transformed into the *trans*-form. Basolo and Pearson[16] explain the racemization in methanol as being due to the formation of unstable *trans*-[Co en$_2$(CH$_3$OH)Cl]$^{++}$. Absorptions consistent with Beer's law again were obtained in methanol, the average ϵ_0 extrapolated to zero time being 93.9 which decreased to 11.3 after 3 days in agreement with the extinction coefficient of *trans*-[Co en$_2$ Cl$_2$]$^+$ at this wave length in methanol. The absorptions were taken every 30 minutes for 10 hours and were analyzed by both Guggenheim's method[11] and by substitution into equation 1, both methods giving a first-order rate of $2.2_0 \times 10^{-5}$ sec.$^{-1}$ ($\pm 2\%$). Brown and Nyholm did not obtain data at 25° but their values at higher temperatures extrapolate to 2.1×10^{-5} sec.$^{-1}$ at this temperature. Basolo[8] has stated that *cis*-[Co en$_2$ Cl$_2$]Cl remains virtually unchanged for several weeks in methanol–water (99%). This solvent was used in the present study but was found to give the same rate of isomerization as in pure methanol. Pearson, Boston and Basolo[13] have also studied the aquation of *trans*-[Co en$_2$ Cl$_2$]Cl in 50% methanol–water and obtained a rate of 1.3×10^{-5} sec.$^{-1}$ in water. Corresponding isomerization/aquation rates obtained for *cis*-[Co en$_2$ Cl$_2$]Cl in methanol–water in the present work are shown here

Methanol	Rate $\times 10^4$ (sec.$^{-1}$)	Time for which this rate was constant
0	1.4 ($\pm 2\%$)	1.25 hours
20%	1.2	2 hours
40%	0.86	3 hours
60%	0.64	4 hours
80%	0.39	6 hours
100%	0.22 ($\pm 2\%$)	To completion

(15) D. D. Brown and R. S. Nyholm, *J. Chem. Soc.*, 2696 (1953).

(16) F. Basolo and R. G. Pearson, "Mechanisms of Inorganic Reactions," John Wiley and Sons, Inc., New York, N. Y., 1958, p. 266.

The author is indebted to Dr. C. B. Monk (University College of Wales, Aberystwyth) and to Mr. A. H. Henson (Welsh College of Advanced Technology, Cardiff) for the use of their spectrophotometers.

THE KINETICS OF POLYMER ADSORPTION ONTO SOLID SURFACES

BY C. PETERSON AND T. K. KWEI

Interchemical Corporation, Central Research Laboratories, 432 West 45th Street, New York 36, New York

Received February 1, 1961

The kinetics of adsorption of polyvinyl acetate from dilute benzene solution (10^{-4} to 10^{-6} g./ml.) onto the surface of chrome-plate was studied by a radioactive tracer method using C^{14}-labelled polymer. The initial rate of adsorption was found to be rapid. This early stage of the adsorption from very dilute solutions can be represented by a kinetic equation of the Langmuir type. It is concluded that the initial adsorption of polyvinyl acetate from very dilute solutions is two-dimensional rather than three-dimensional, with little or no interaction between adsorbed molecules up to fairly high surface coverages. The adsorption from more concentrated solutions, however, seems to be predominantly three-dimensional.

Introduction

Recently the equilibrium sorption of polymer molecules from solution onto solid surfaces has been studied by many authors.[1,2] Few data on the rate of adsorption, however, are available in the literature, owing partly to the experimental difficulties encountered in the measurement of the rate of this fast process. We wish to report some preliminary results on the kinetics of adsorption of C^{14}-labelled PVAC from dilute benzene solution (10^{-4} to 10^{-6} g./ml.) onto the surface of chrome-plate.

Experimental

The adsorbent surfaces used were squares of chrome-plate about one centimeter on a side. Surfaces were cleaned preparatory to the adsorption by a procedure similar to that used by Gottlieb.[3] After a gentle flaming to remove any organic surface contamination, each plate was cooled in air for 20 seconds and immediately immersed in the solution of the radioactive adsorbate. Plates were immersed for various periods of time. On removal from the solution, each plate was immediately given a quick dip in solvent in order to remove clinging excess solution. The plate was then drained, dried and counted. The adsorption of polymer in base moles/cm.^{2} then was calculated from the measured radioactivity on the plate and the apparent area of the plate. Plates cooled in air and plates cooled in benzene[3] before adsorption gave essentially the same results. Radioactive polyvinyl acetate having a specific activity of 1.1 mc./g. was obtained from Tracerlab, Inc. The radioactive polymer had been prepared by irradiation–polymerization of vinyl acetate labelled with C^{14} at the two-vinyl position. Molecular weight has been estimated as 140,000 from intrinsic viscosity measurements. The chrome-plate used was commercial ferrotype plate. Samples were obtained from Apollo Metal Works, Chicago, Illinois. C.P. benzene was purified by distillation from sodium.

Results

Typical experimental results are plotted in Figs. 1 and 2. Values were reproduced readily when plate-to-plate variations were taken into consideration. It is noteworthy that curve C (solution concentration equals 2.30×10^{-6} mole/l.) appears to reach a plateau at about 1×10^{-9} mole/cm.^{2} adsorbed within a few minutes and remains near that value for a rather prolonged period. It is seen that the curve ultimately attains a maximum ordinate value of about 1.6×10^{-9} mole/cm.^{2} at several hundred hours duration. This final value we shall call the "maximum adsorption" as

(1) J. Koral, R. Ullman and F. R. Eirich, *J. Phys. Chem.*, **62**, 541 (1958).

(2) E. R. Gilliland and E. B. Gutoff, *J. Appl. Polymer Sci.*, **3**, 26 (1960).

(3) M. Gottlieb, *J. Phys. Chem.*, **64**, 427 (1960).

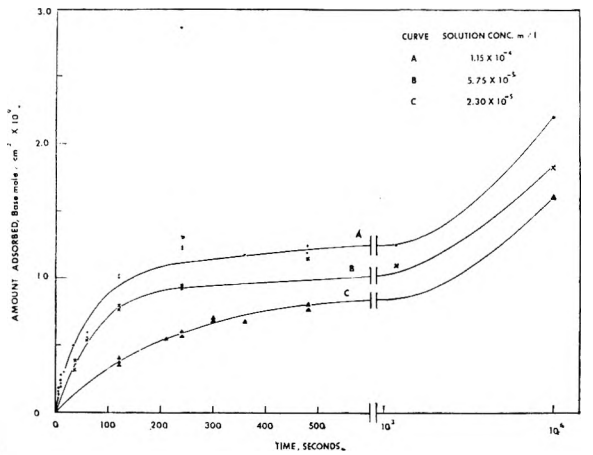

Fig. 1.—Rate of adsorption of PVAc.

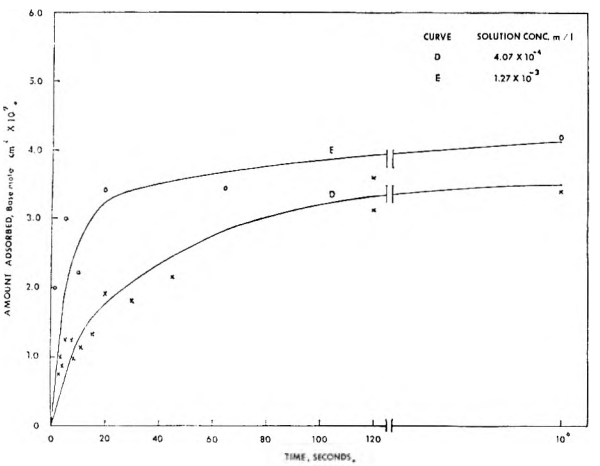

Fig. 2.—Rate of adsorption of PVAc.

distinguished from the plateau value for reasons which will be explained in the discussion. The curves for concn. = 5.75×10^{-5} and concn. = 1.15×10^{-4} mole/l. are similar to curve C, their plateau values being slightly higher. At solution concentrations below 5×10^{-6} mole/l. the adsorption of polymer becomes highly dependent on the rate of stirring and is probably diffusion-controlled. At high solution concentration (concn. = 4.07×10^{-4} mole/l. in Fig. 2) the amount adsorbed reaches 1×10^{-9} mole/cm.^{2} in less than ten seconds, increasing with time continually to a maximum value of about 3.8×10^{-9} mole/cm.^{2}.

Discussion

Since macromolecules in "dilute" solution can be considered as discrete entities,[4] it seems not unreasonable to expect that the adsorption of polymer molecules from dilute solutions onto a solid surface might be amenable to simple kinetic treatment, at least at low surface coverages. The adsorption of PVAc from benzene onto the surface of chrome-plate is especially suitable for such an analysis. Work in this Laboratory has indicated that under the experimental conditions benzene does not tend to displace adsorbed PVAc molecules from the chrome-plate surface at any appreciable rate.[5] Serious complications which might otherwise result from competitive adsorption of the solvent are therefore avoided. In our treatment of the data we have assumed that adsorption of polymer from our very dilute solutions, up to the plateau region, can be expressed by the common kinetic formula

$$\frac{d\theta}{dt} = k_1(1 - \theta)c - k_{-1}\theta \qquad (1)$$

where θ is the fraction of total surface coverage and c is the concentration of the polymer solution. k_1 and k_{-1} are the rate constants for adsorption and the reverse process, respectively. If we assume the absence of interaction between adsorbed polymer molecules in this case (such that for a monodisperse polymeric system each adsorbed molecule would occupy the same fraction of the total adsorbent surface) the value of θ can be considered as directly proportional to n, the amount of PVAc adsorbed. θ's relationship to n then can be expressed as

$$\theta = n/N \qquad (2)$$

where N is the value of n at total single layer surface coverage. The value of N cannot be determined experimentally, *a priori*. It may be reasonable to assume that the relationship between the adsorption at the plateau and single layer coverage by polymer molecules is analogous to that which is found between saturation adsorption and monolayer coverage in the case of small molecules. Curve B was obtained at the highest solution concentration where a long, horizontal section in the adsorption curve can be discerned. The plateau value of adsorption from this curve is 0.96×10^{-9} base mole/cm.^{2}. In the following discussion we have given N the value 1×10^{-9} base mole/cm.^{2} with solution concentrations of 1.15×10^{-4} mole/l. and less. This is approximately the amount adsorbed at the plateau of our kinetics curves in Fig. 1. Comparable values for adsorption of octadecyl acetate and polyvinyl acetate on the same surface at monolayer coverage have been estimated from surface potential measurements.[3] These values are 1×10^{-9} base mole/cm.^{2} and $0.9 \pm 0.1 \times 10^{-9}$ base mole/cm.,^{2} respectively.

If $d\theta/dt$ can be considered as zero from the onset of the plateau region, the "steady state" fractional surface coverage at this phase of the adsorption can be expressed for each case as

$$\theta_s = \frac{n_{\text{plateau}}}{N} \qquad (3)$$

θ_s can now be calculated for several concentrations from the adsorption data and N's assigned value. Table I summarizes calculated θ_s data for three different solution concentrations.

TABLE I

"EQUILIBRIUM" ADSORPTION DATA

c (moles/l.)	θ_s	C/θ_s (moles/l.)
1.15×10^{-5}	0.80[a]	1.44×10^{-5}
2.30×10^{-5}	.84	2.74×10^{-5}
5.75×10^{-5}	.96	6.1×10^{-5}

[a] Obtained with vigorous stirring (not shown in Fig. 1).

(4) P. J. Flory "Principles of Polymer Chemistry," Cornell University Press, Ithaca, N. Y., 1953, Chapter 12.

(5) C. Peterson, unpublished results.

From equation 1, when $d\theta/dt$ is equal to zero, it follows that

$$\frac{c}{\theta_s} = c + \frac{k_{-1}}{k_1} \qquad (4)$$

A plot of values for c/θ_s, taken from Table I, against c yields a straight line with a slope of about unity and an intercept k_{-1}/k_1 of 2.01×10^{-6} mole/l. Integration of equation 1 results in the expression below.

$$-\ln\left[1 - \left(1 + \frac{k_{-1}}{k_1 c}\right)\theta\right] = k_1 ct \qquad (5)$$

A plot of $-\log[1 - (1 + k_{-1}/k_1 c)\theta/]$ *vs.* t should therefore yield a straight line with a slope of $k_1 c/2.303$. Figure 3 shows the kinetic data plotted

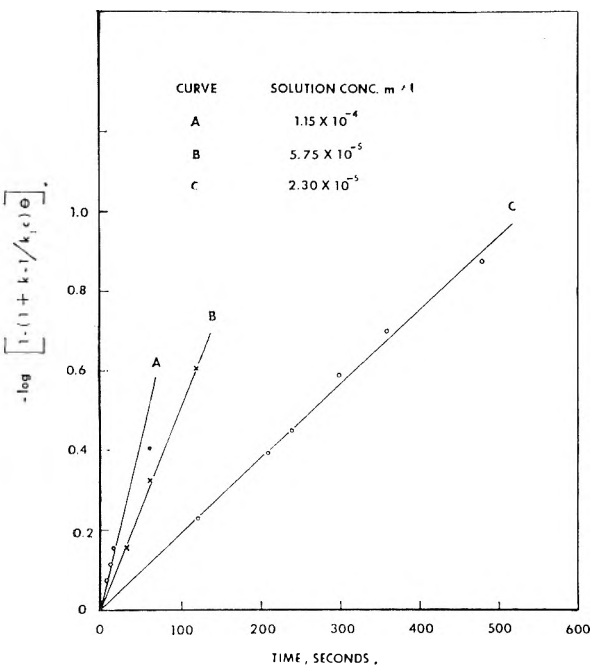

Fig. 3.—Plot of the kinetic data according to equation 5.

according to equation 5. The slopes of the straight lines obtained are listed in Table II and are proportional to the concentration of the polymer solution. This proportionality lends further credence to the applicability of our kinetic treatment. The average value of k_1 obtained from these curves is 191 sec.$^{-1}$ mole^{-1} l. The value of k_{-1} then is calculated to be 3.84×10^{-4} sec.$^{-1}$, from the ratio k_{-1}/k_1.

TABLE II

RATE CONSTANTS k_1 AND k_{-1}

c (moles/l.)	Slope (sec.$^{-1}$)	k_1 (sec.$^{-1}$ mole^{-1})	k_{-1} (sec.$^{-1}$)
2.30×10^{-5}	1.9×10^{-3}	190	
5.75×10^{-5}	4.95×10^{-3}	198	
1.15×10^{-4}	9.3×10^{-3}	186	
		Av. 191	3.84×10^{-4}

As an additional test of our assumptions various other values for N were selected and calculations made. If a value of 1.1 or 1.2×10^{-9} base mole/cm.^{2} is used for N, the resulting plots show more scatter. When the "maximum" adsorption values, 1.6 and 2.2×10^{-9} base mole/cm.^{2} are used for N, the experimental data can no longer be represented by equation 5.

Equation 1, from which equation 5 is derived, does not take into account possible interactions between adsorbed molecules. The fact that plots of the data according to equation 5 do not deviate from a straight line even at calculated coverages of 50% for $c = 1.15 \times 10^{-4}$ mole/l. and 75% for the two lower concentrations studied therefore seems to justify our neglect of such interactions.

Moreover, the applicability of equation 2 to a polydisperse system, as is the case in our experiment, seems to imply that the adsorbed polymer molecules occupy areas in proportion to their individual degree of polymerization. This can be understood if all, or nearly all, of the polymer segments are in contact with the surface. Thus it appears that the adsorption of PVAc onto chrome-plate can be described as essentially two-dimensional rather than three-dimensional even at fairly high surface coverages, if the concentration of polymer solution is sufficiently low. The fact that a value of 1×10^{-9} base moles per cm.^{2} for N, which is close to the monolayer coverage of octadecyl acetate on the same surface, can be used to represent the experimental data also strongly supports the argument. The same conclusion has been reached by Gottlieb from surface potential measurements. The slight dependence of adsorption of polymethyl methacrylate on molecular weight also has been interpreted by Ellerstein and Ullman as an indication of marked flattening of the polymer coil on the surface.[6] It appears that polymer molecules can undergo re-orientation from a coil-like configuration in solution to a two-dimensional layer on the solid surface. This re-orientation process is likely to be a kinetically fast step which follows the successful collision of the polymer molecule with the solid surface. The over-all process can be schematically depicted as

Polymer coil in solution	⟷	Polymer coil on the solid surface with only a few segment-surface contacts	→	Adsorbed polymer with nearly all the segments in contact with the surface
(A)		(B)		(C)

The rate of removal of adsorbed polymer (C) from the surface of the chrome-plate by pure benzene is negligible. This is to be distinguished from the rate of the relatively fast process (B) → (A) which involves the breakage of only a limited number of bonds to the surface. It is with the rate of this latter process that our experiments are concerned.

The "maximum" adsorptions of PVAc, even from the more dilute solutions, were often as much as several times greater than the value 1×10^{-9} mole/cm.^{2}. It is evident that at this point in the adsorption not all the segments are lying flat on the surface.

It is possible that the additional polymer adsorbed in excess of 1.0×10^{-9} base mole/cm.^{2} constitutes an overfilm with a random structure. It is likely, however, that these polymer molecules have at least some segments in contact with the

(6) S. Ellerstein and R. Ullman, Technical Report, Office of Naval Research—Project Nonr-83919.

surface since they are not easily removed by immersion of the plate in pure solvent. It is therefore conceivable that a point is eventually reached in the progress of our postulated initial two-dimensional adsorption where the subsequently adsorbed polymer molecules may retain a three-dimensional configuration. These molecules may also "crowd" the two-dimensionally adsorbed polymer molecules already on the surface into the three-dimensional configuration. Considerable rearrangement of the polymer segments on the surface is likely to take place during this crowding stage and maximum adsorption may be reached only slowly. This may account for the adsorption in the plateau region and the subsequent slow rise to the measured "maximum" adsorptions.

As the solution concentration was increased beyond 1.15×10^{-4} mole/l. the plateau region became less well defined. At the concentration 1.27×10^{-3} mole/l. a maximum adsorption of about 3.8×10^{-9} mole/cm.^{2} is reached within a few seconds (Fig. 2). The initial rates of adsorption at these concentrations, compared with that at 1.15×10^{-4} mole/l., are about 100% higher than that which would be accounted for by the concentration effect alone. It appears that three-dimensional adsorption, now being energetically more favorable, may have set in at an earlier stage so that a detailed kinetic analysis is no longer feasible.

The existing theories of polymer adsorption[7-11] predict isotherms other than the Langmuir type even for the two-dimensional case. Many experimental results can be represented by Langmuir type isotherms[12] rather than Simha–Frisch–Eirich isotherms although Frisch pointed out that a clear cut differentiation of the theoretical and the Langmuir type isotherms was often obscured by the scarcity of experimental data for very low concentrations. The present work indicates that the initial stage of the adsorption process can be represented kinetically by an equation of the Langmuir type, when the concentration of the polymer solution is sufficiently low. If our interpretation of the experimental data is correct, the parameter p in the previous theories, defined as the probability that any segment of an adsorbed molecule is in contact with the surface, may very well be a function of the maximum amount adsorbed. This will cause additional complication in comparing experimental data with SFE and GG theories.

Acknowledgements.—We wish to express our appreciation to the Directors of Interchemical Corporation for permission to publish this work. We also wish to thank Mr. C. A. Kumins for his constant encouragement and helpful suggestions.

(7) R. Simha, H. L. Frisch and F. R. Eirich, *J. Phys. Chem.*, **57**, 584 (1953); also *J. Chem. Phys.*, **21**, 365 (1953).

(8) H. L. Frisch and R. Simha, *J. Phys. Chem.*, **58**, 507 (1954); also *J. Chem. Phys.*, **27**, 702 (1957).

(9) H. L. Frisch, *J. Phys. Chem.*, **59**, 633 (1955).

(10) R. Simha, *J. Polymer Sci.*, **29**, 3 (1958).

(11) E. R. Gilliland and E. B. Gutoff, *J. Phys. Chem.*, **64**, 407 (1960).

(12) See for example, E. Treiber, G. Porod, W. Gierlinger and J. Schurz, *Makromol. Chem.*, **9**, 241 (1953); R. Perkel, Thesis, Polytechnic Institute of Brooklyn, Brooklyn, New York, 1959.

THE KINETICS OF THE ALKALINE HYDROLYSIS OF DIETHYL MALONATE, DIETHYL SUCCINATE AND DIETHYL SEBACATE IN WATER–DIOXANE MIXTURES[1]

BY W. J. SVIRBELY AND AUGUST D. KUCHTA

Chemistry Department, University of Maryland, College Park, Md.

Received February 3, 1961

The kinetics of the alkaline hydrolysis of diethyl malonate, diethyl succinate and diethyl sebacate were studied at 25° in dioxane–water mixtures varying in dielectric constant from 60 to 9. The alkaline hydrolysis of diethyl succinate was also studied over a temperature range from 35 to 6° in various dioxane–water mixtures. The effect of an added inert electrolyte was investigated. It was observed that the k_1/k_2 ratio varied from 165 to 1.46 for diethyl malonate, from 7.18 to 1.02 for diethyl succinate and from 2.97 to 1.36 for diethyl sebacate in the range of solvent mixtures used. Thermodynamic activation values have been calculated for both steps of the reaction. It is concluded that in the low dielectric media both steps of each reaction are proceeding by essentially the same mechanism. The experimental observations can be explained on the basis of the formation of ion-pairs or aggregates.

Introduction

A recent study[2] of the alkaline hydrolysis of 1,3,5-tri-(4-carbomethoxyphenyl)-benzene showed that there was a negative primary salt effect on the second and third steps of that reaction. That observation is not only at variance with theory for a reaction between ions of like charge sign but is also at variance with other observations involving the alkaline hydrolysis of an ester ion.[3,4] Since the study was made in low dielectric constant media (*i.e.*, $D \sim 9$) the existence of ion pairs is quite likely and it was concluded that we may not be dealing with the usual alkaline hydrolysis of an ester ion involving ions of like charge sign. Solubility limitations in dioxane–water media prevented studies being made in solutions of high dielectric constant.

To investigate more thoroughly the effect of the medium on the mechanism and the rate constant

(1) (a) Abstracted from a thesis by August D. Kuchta to the Graduate School of the University of Maryland in partial fulfillment of the requirements for the degree of Doctor of Philosophy; (b) presented in part at the New York City Meeting of the American Chemical Society, September, 1960.

(2) W. J. Svirbely and H. E. Weisberg, *J. Am. Chem. Soc.*, **81**, 257 (1959).

(3) L. Pekkarinen, *Ann. Acad. Sci. Fenn.*, **A11**, 62 (1954).

(4) W. J. Svirbely and I. Mador, *J. Am. Chem. Soc.*, **72**, 5699 (1950).

ratios of ester hydrolysis, it was decided to study the alkaline hydrolysis of several diesters differing markedly in length. Consequently, the alkaline hydrolysis of diethyl malonate, diethyl succinate and diethyl sebacate were studied at 25° in dioxane–water mixtures varying in dielectric constant from 60 to 9. The alkaline hydrolysis of diethyl succinate also was studied over a temperature range.

Materials and Apparatus

Dioxane, water, sodium hydroxide solutions and hydrochloric acid solutions were prepared or purified as before.[2]

The diesters were Eastman best grade. They were distilled under vacuum and a middle cut was taken in each case. The saponification equivalent of each ester indicated 99.9 ± 0.1% purity. The refractive indices were in excellent agreement with those previously reported.[5]

The potassium chloride used for salt studies was of analytical reagent grade and was used without further purification.

Apparatus.—The apparatus used in this research has been described.[2]

Procedure.—The procedure has been described.[2] However, the starting concentrations of the diester and the sodium hydroxide were adjusted so that equivalent amounts were used (*i.e.*, $A_0 = 2B_0$, where A_0 and B_0 were the initial concentrations in moles/liter of hydroxide and diester, respectively). At the completion of each run, the density of the solution was determined. This datum was used to transform weight data to volume data. Duplicate runs were made for each environmental condition.

Calculations and Discussion

Evaluation of Rate Constants.—The alkaline hydrolysis of the diesters used in this research may be represented by the chemical equations

$$A + B \xrightarrow{k_1} C + E$$

$$A + C \xrightarrow{k_2} D + E$$

where A, B, C and D represent hydroxyl ion, diester, monovalent ion of the ester and divalent ion of the ester, respectively. Frost and Schwemer[6] have integrated this kinetic system for the special case of stoichiometrically equivalent amounts of the reactants A and B (*i.e.*, $A_0 = 2B_0$) and have prepared tables that enable the evaluation of the rate constants. Table I shows a typical time–concentration set of data for run #31. In this study, the procedure of Frost and Schwemer[6] was used the most frequently in the calculation of rate constants. Values of α (defined as A/A_0) for duplicate runs were plotted against time on a large sheet of graph paper. From the resulting smooth curve, the times for fixed percentages of completion were determined. Time ratios were then calculated from these times for the various percentages of reaction. With the use of the Frost and Schwemer tables and these time ratios, values of 1/K (defined as k_1/k_2) were obtained for the reaction. The average 1/K value was calculated and used to obtain τ values at the various selected values of α. From the definition of τ, (*i.e.*, $\tau = B_0k_1t$), values of k_1 were then calculated. The average values of k_1 and 1/K next were used to determine k_2. Table II summarizes the calculations just described for run #31. The τ and time ratio tables of Frost and Schwemer do not go below a value of 1/K = 2, and so Tables III and IV were developed[7] for values of 1/K from 0 to 2.0.

(5) C. P. Smyth and W. S. Walls, *ibid.*, **53**, 527 (1931).
(6) A. A. Frost and W. C. Schwemer, *ibid.*, **74**, 1268 (1952).
(7) B. E. Fry, M.S. Thesis, University of Maryland, 1959.

TABLE I

DATA FOR THE DIETHYL SUCCINATE REACTION IN DIOXANE-WATER AT 24.93°

D = 13.10; A_0 = 12.417 × 10^{-3} mole/l.; B_0 = 6.209 × 10^{-3} mole/l.; run #31

Time, min.	$A \times 10^3$ mole/l.	$\alpha = A/A_0$	Time, min.	$A \times 10^3$ mole/l.	$\alpha = A/A_0$
6.00	10.244	0.8250	30.00	5.7972	0.4669
8.00	9.6263	.7753	32.00	5.5913	.4503
10.00	9.0910	.7321	34.00	5.3854	.4337
12.00	8.6381	.6957	48.00	4.3355	.3492
14.00	8.2264	.6625	50.00	4.2325	.3409
16.00	7.8352	.6310	52.00	4.1296	.3326
20.00	7.1764	.5779	60.00	3.7385	.3011
22.00	6.8265	.5498	70.00	3.3061	.2663
24.00	6.5795	.5299			

TABLE II

CALCULATIONS OF RATE CONSTANTS FOR RUN #31 ON DIETHYL SUCCINATE

% Reaction	t, min.	% Compared	t ratio	1/K	τ	k_1, l. mole^{-1} sec.$^{-1}$
20	6.95	60/20	5.597	1.536	0.2423	5.615
30	11.72	60/30	3.319	1.540	.4087	5.616
40	18.01	60/40	2.160	1.500	.6255	5.594
50	26.50	60/50	1.468	1.500	.9217	5.602
60	28.90	50/20	3.813	1.552	1.355	5.561
		50/30	2.261	1.567		
				Av. = 1.533		5.598± ADM 0.014

$$k_2 = \frac{5.598}{1.533} = 3.653 \text{ l. mole}^{-1} \text{ sec.}^{-1}$$

TABLE III

τ AS A FUNCTION OF K AND α_1

1/K	α = 0.8	0.7	0.6	0.5	0.4
0.0	0.1250	0.2143	0.3333	0.5000	0.7500
.2	.1710	.2701	.3958	.5670	.8199
.4	.1954	.3103	.4529	.6422	.9151
.6	.2103	.3384	.4974	.7074	1.008
.8	.2208	.3598	.5334	.7638	1.093
1.0	.2286	.3767	.5637	.8132	1.171
1.2	.2346	.3902	.5891	.8568	1.243
1.4	.2395	.4022	.6122	.8973	1.311
1.6	.2437	.4121	.6323	.9343	1.378
1.8	.2471	.4209	.6503	.9684	1.441

TABLE IV

TIME RATIOS AS A FUNCTION OF K

1/K	t_{60}/t_{20}	t_{50}/t_{30}	t_{60}/t_{40}	t_{60}/t_{50}	t_{50}/t_{20}	t_{50}/t_{30}
0.0	6.000	3.500	2.250	1.500	4.000	2.333
.2	4.795	3.036	2.072	1.446	3.316	2.099
.4	4.683	2.949	2.021	1.425	3.287	2.070
.6	4.793	2.979	2.027	1.425	3.364	2.090
.8	4.950	3.038	2.049	1.431	3.459	2.123
1.0	5.122	3.109	2.077	1.440	3.557	2.159
1.2	5.298	3.186	2.110	1.451	3.652	2.196
1.4	5.474	3.260	2.141	1.461	3.747	2.231
1.6	5.654	3.344	2.179	1.475	3.834	2.267
1.8	5.832	3.424	2.216	1.488	3.919	2.301

Table V summarizes the data at 24.93°. A_0 varied from 12.10 × 10^{-3} to 12.64 × 10^{-3} mole/l. in the various runs. Thus the data in Table V were obtained essentially under the same stoichiometric ionic strength conditions as far as the reactants are concerned.

TABLE V

RATE CONSTANTS FOR THE HYDROLYSIS OF THE ESTERS IN DIOXANE-WATER MEDIA AT 24.93°

Ester	D	Wt. % dioxane	Without salt k_1	Without salt k_2	Without salt k_1/k_2	KCl added[d] k_1	KCl added[d] k_2	KCl added[d] k_1/k_2
Diethyl sebacate	42.98	40.00	1.96	0.660	2.97			
	34.26	50.00	1.50	.533	2.82			
	17.69	70.00	0.843	.444	1.92			
	13.10	76.30	.736	.542	1.36	0.396	0.401	0.985
	10.71	80.00	.783[a]	.578[a]	1.36			
Diethyl succinate	60.79	20.00	10.5	1.46	7.18	10.3	2.09	4.91
	51.90	30.00	9.06	1.34	6.75			
	49.18	33.18	8.77	1.31	6.68			
	34.26	50.00	7.18	1.24	5.77			
	17.69	70.00	5.71	2.19	2.61	4.76	2.89	1.65
	13.10	76.30	5.60	3.65	1.53	3.99	3.62	1.10
	10.71	80.00	5.58	3.98	1.40			
	9.10	82.75	5.80	5.69	1.02			
Diethyl malonate	60.79	20.00	110[b]	0.666	165[b]			
	34.26	50.00	55.7[b]	.473	118[b]			
	13.10	76.30	27.7	2.90	9.56	24.5	4.35	5.63
	10.71	80.00	23.2	4.83	4.80			
	9.70	81.72	19.3	6.88	2.81			
	9.10	82.75	16.1	11.0	1.46			

[a] Computer calculations. [b] Estimated values. [c] Rate constant units are liter mole^{-1} minute^{-1}. [d] Reading down the column KCl added was = 0.1454, 0.1464, 0.1472, 0.1463 and 0.1463 mole/l., respectively.

Table VI summarizes the data over a temperature range in the absence of an inert electrolyte for the diethyl succinate reaction.

TABLE VI

RATE CONSTANTS FOR THE DIETHYL SUCCINATE REACTION AT DIFFERENT TEMPERATURES

t, °C.	D	Wt. % dioxane	k_1	k_2	k_1/k_2
34.88	60.79	16.42	19.1	2.83	6.75
	34.26	46.48	13.9	2.31	6.00
	13.10	75.22	11.8	6.00	1.97
	10.71	79.02	12.2	7.38	1.66
24.93	60.79	20.00	10.5	1.46	7.18
	34.26	50.00	7.18	1.24	5.77
	13.10	76.30	5.60	3.65	1.53
	10.71	80.00	5.58	3.98	1.40
14.94	60.79	23.45	5.03	0.717	7.02
	34.26	52.27	3.58	0.633	5.65
	13.10	77.38	2.66	2.03	1.31
	10.71	80.92	2.78	2.13	1.31
10.27	10.71	81.34	1.83	1.54	1.19
6.31	60.79	26.49	2.82	0.401	7.03
	34.26	54.08	1.84	0.340	5.40
	13.10	78.14	1.32	1.22	1.08

The above scheme of calculation of rate constants could not be employed in the case of the diethyl malonate reaction carried out in solvents whose dielectric constant values were 60.79 and 34.26 because the reactions occurred so rapidly that we could not obtain values of the hydroxyl ion concentrations until 40% of the original hydroxide was consumed. As a result we were unable to determine those time ratios which were defined previously in terms of t_{20} and t_{30}. Therefore, we plotted the $1/K$ values against the corresponding t_{60}/t_{50} values as listed in the Frost and Schwemer tables. The resulting straight line was extrapolated to include the experimental t_{60}/t_{50} ratio for the particular run and the value of $1/K$ corresponding to this particular time ratio was obtained. The k_2 value for each of these particular runs was obtained from the slope of the straight line produced on making a $1/A$ *vs.* t plot. The values of $1/A$ used in this latter plot included only those values existing in the last 45% of the reaction. Through the use of equation 1[6]

$$\alpha = \frac{\beta^K}{2(1-K)} + \frac{(1-2K)\beta}{2(1-K)} \qquad (1)$$

it can be shown that the diester remaining is less than 0.1% when $\alpha = 0.45$ and $K = 1/120$. Thus, it is evident that only the second step of the reaction is significant under such conditions. From the experimental value of k_2 and the estimated k_1/k_2 ratio for that run, a value of k_1 was determined.

In the case of the diethyl sebacate reaction carried out in a medium of dielectric constant 10.71, the rate constants were determined using a computer technique.[8] This was done because the di-ion product precipitated out before t_{60} could be experimentally determined. Thus only t_{50}/t_{20} and t_{50}/t_{30} time ratios were available for use with the Frost and Schwemer procedure and in our opinion, two ratios were not enough.

Salt Effects.—The stoichiometric ionic strength of this reaction in terms of the reacting species can be expressed by

$$\mu = A_0 + D \qquad (2)$$

Equation 2 indicates that as the reaction proceeds, the ionic strength of the solution increases. One would expect this increase in ionic strength to alter the second rate constant significantly during the course of the reaction since the second step of the reaction is supposedly between ions. Such changes in k_2 should be detectable in using the procedure of Frost and Schwemer. As this was not

(8) Discussion of this procedure will be the subject of a later paper. We gratefully acknowledge the assistance of Jay Blauer and Michael Rowan on this subject.

the case, it was concluded that changes in ionic strength during the course of the reaction did not cause a significant variation in k_2. Similar observations have been made in the past[2,4] for reactions between ions of like charge sign. It raises the question of the necessity of swamping the "ionic strength effect" in such reactions of changing ionic strength through the use of inert electrolyte. In light of the above, it is not necessary. It is actually undesirable since it may lead to other complications. To demonstrate this latter point, salt studies using KCl as an inert electrolyte were made under a number of environmental conditions. The mean stoichiometric ionic strength of each of the reaction mixtures was about 0.16 with the added salt and 0.013 without any added salt. Table V includes these results on which we shall comment shortly.

Thermodynamic Activation Terms.—Activation energies and the Arrhenius frequency factors (log A) for the succinate reaction in isodielectric media were calculated through use of the least squares method applied to the linear form of the Arrhenius equation, namely

$$\log k = \log A - \frac{E}{2.303RT} \qquad (3)$$

The results are listed in Table VII. The free

TABLE VII

ACTIVATION ENERGIES AND RELATED QUANTITIES (AT 24.93°) FOR THE DIETHYL SUCCINATE REACTION

D	60.79	34.26	13.10	10.71
E_1 (cal./mole)	11,580	12,070	13,110	13,140
E_2 (cal./mole)	11,750	11,470	9,590	10,950
ΔF_1^* (cal./mole)	18,490	18,710	18,860	18,860
ΔF_2^* (cal./mole)	19,660	19,750	19,110	19,060
ΔS_1^* e.u.	−25.22	−24.25	−21.24	−21.08
ΔS_2^* e.u.	−28.49	−29.77	−33.95	−29.17
log A_1	9.4860	9.7062	10.3639	10.4001
log A_2	8.7804	8.5015	7.5869	8.6314

energy and the entropy of activation at 24.93° were calculated by means of the equations[9]

$$\Delta F^* = 2.3RT\left(\log \frac{RT}{Nh} - \log k\right) \qquad (4)$$

$$\Delta S^* = 2.3R\left(\log A - \log \frac{eRT}{Nh}\right) \qquad (5)$$

Some of the results are summarized in Table VII.

Discussion.—The variation of log k_1 and log k_2 with decrease in the dielectric constant is strikingly shown in Fig. 1 and Fig. 2. While in high dielectric media there is a marked difference between the values of k_1 and k_2 for each diester reaction, this difference disappears in low dielectric media. It is apparent that the k_1/k_2 ratio is approaching unity. One concludes that the mechanisms of both steps of the reaction are becoming more nearly alike as the dioxane content of the medium is increased. If one plots log k against D, one will observe that with the exception of the first step of the malonate reaction, there is evidence of linearity over two distinct dielectric ranges, with a change in slope occurring at a dielectric value of about

(9) S. Glasstone, K. J. Laidler and H. Eyring, "The Theory of Rate Processes," McGraw-Hill Book Co., Inc., New York, N. Y., 1941, p. 195.

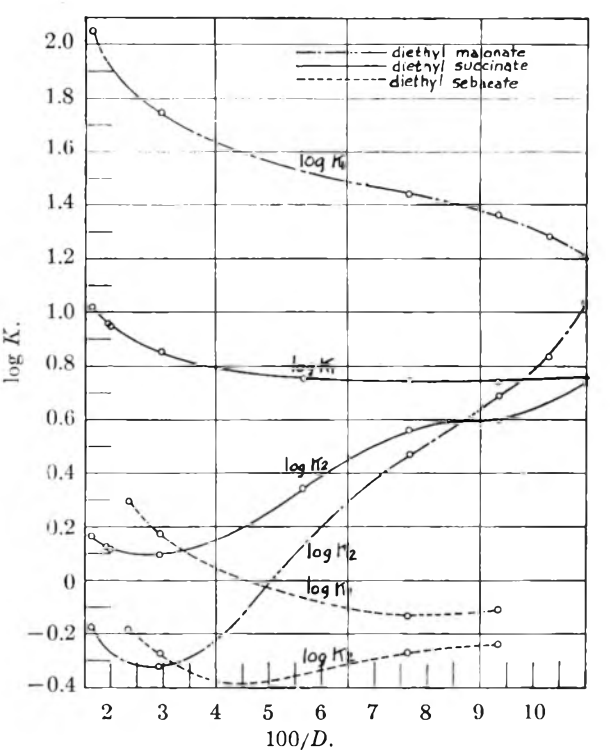

Fig. 1.—log K *vs.* $100/D$ at 24.93°.

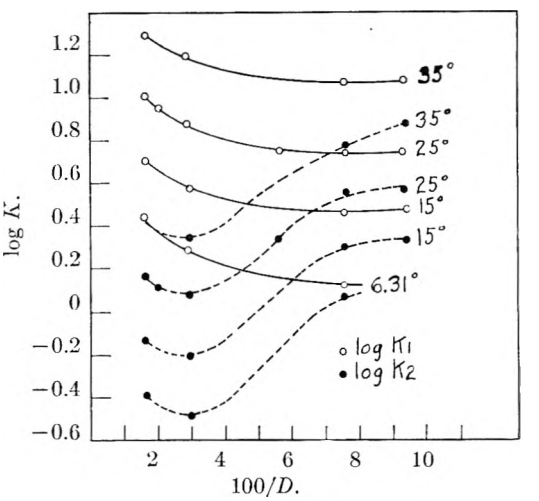

Fig. 2.—log K *vs.* $100/D$ at various temperatures for the alkaline hydrolysis of diethyl succinate.

25. Based on conductance measurements,[10] evidence has been presented that ion-pairing occurs in media where the dielectric constant is equal to or lower than 30. This value of 30 would correspond to a value of $100/D$ equal to 3.33. Reference to Fig. 1 shows that at a $100/D$ value of 3 to 4, each of the log k_2 curves is going through a minimum. This could be the point at which ion-pair formation becomes important and the second step of each reaction is changing from an ion–ion reaction in media of high dielectric constant to one involving ion-pairs in media of lower dielectric constant. On going to still lower dielectric media, the formation of ion pairs or large ion clusters for both steps of

(10) A. L. Jacobson and J. B. Hyne, *J. Am. Chem. Soc.*, **82**, 2418 (1960).

the reaction would be accentuated. Thus both steps of each diester reaction would be to a large extent between more similar aggregates, leading to values of the rate constants approaching each other. It should also be noted that while at high dielectrics the values of k_2 decrease with a decrease in dielectric constant in accordance to theory for a reaction between ions of like sign yet at values of dielectric constant lower than 25, values of k_2 increase with further decrease in dielectric constant. In terms of the theory this latter observation implies that we are no longer dealing with a reaction between ions of like sign.

Reference to Table V shows that on the addition of the same stoichiometric amount of an inert electrolyte, the k_1/k_2 ratios decreased in all cases from the values obtained in the absence of the inert electrolyte. However, the magnitude and the direction of the salt effect depend on the medium, the reaction step and the diester or monoester ion involved. In the same medium of $D = 13.1$ for all three diester reactions, there was a negative salt effect on the first step of the reaction, its magnitude being proportionately larger, the larger the diester. However, in the same medium, the salt effect on the second step of the reaction was negative, zero and positive for the sebacate monoester, succinate monoester and malonate monoester reactions, respectively. Considering the fact that the basic difference in the three diesters is size, thus leading to various distances between the attached ester groups, we believe that this structural difference makes a difference in the extent and nature of the ion-pairs or aggregates formed with the ions of the added electrolyte and is reflected in the nature of the observed salt effect. In the high dielectric media, $D = 60.79$, the second step of the succinate reaction showed a positive salt effect, an observation in accordance with theory for a reaction between ions of like charge sign.

A comparison of calculated free energies of activation shows that the free energies of activation of the two steps in each of the diester reactions approach each other as the dielectric constant of the medium is lowered. If one accepts the argument that the free energy of activation is a measure of the coulombic interaction in the formation of the activated complex, again one must conclude that the two steps of the reaction become more nearly alike as the dielectric constant is lowered.

Thus it is evident that our results can be explained by ion-association. The extent and the nature of the ion aggregates formed would depend on the reactants and the dielectric constant of the medium. It would also be affected by the presence of an added inert electrolyte.

It is not expected that the activation energies would be nearly the same for both steps of the reaction at any one dielectric constant unless we are dealing with the same kind of aggregates in both steps. Having obtained constancy in the activation energy for any step in two different media implies that we are now dealing with the same kind of aggregates in the two media.

Several of the k_1/k_2 ratios were used to calculate "r" by means of Ingold's equation,[11] namely

$$\frac{k_1}{k_2} = 2e^{\epsilon^2/DrkT}$$

While acceptable values of "r" are obtained in high dielectric media ($D = 60.79$) the results are meaningless in low dielectric media. The effect of the media on the k_1/k_2 ratios clearly demonstrates the inadequacy of Ingold's equation as a general equation.

Acknowledgment.—We wish to express our appreciation to E. I. du Pont de Nemours and Company for the du Pont Fellowship held by A. Kuchta from 1959–1960.

(11) C. K. Ingold, *J. Chem. Soc.*, 1375 (1930).

FLUORINE BOMB CALORIMETRY. II. THE HEAT OF FORMATION OF MOLYBDENUM HEXAFLUORIDE[1]

By Jack L. Settle, Harold M. Feder and Ward N. Hubbard

Chemical Engineering Division, Argonne National Laboratory, Argonne, Illinois

Received February 6, 1961

The heat of formation of molybdenum hexafluoride was measured by direct combination of its elements in a bomb calorimeter. $\Delta Hf°$ at 25° of molybdenum hexafluoride gas was found to be $-372.3_5 \pm 0.2_2$ kcal. mole^{-1}.

Introduction

This Laboratory has undertaken to obtain precise thermochemical data for refractory substances such as the borides, carbides, nitrides and silicides of the transition metals, the rare earth metals, uranium and thorium. Typical of the substances to be studied are the borides and silicides of molybdenum which have recently achieved technological importance. Because of the difficulty of obtaining well-defined products by combustion of these substances in oxygen, or by solution or synthesis reactions, an alternative technique, namely, combustion in fluorine has been proposed[2] for calorimetry. To determine the desired heats of formation by fluorine combustion calorimetry, however, it is necessary to have available the heats of formation of MoF_6, BF_3 and SiF_4. The heat of formation of BF_3 has recently been determined[3] with an estimated over-all uncertainty

(1) This work was performed under the auspices of the U. S. Atomic Energy Commission.

(2) E. Greenberg, J. L. Settle, H. M. Feder and W. N. Hubbard, *J. Phys. Chem.*, **65**, 1168 (1961).

(3) S. Wise, W. N. Hubbard, H. M. Feder and J. L. Margrave, "Fluorine Bomb Calorimetry: III. The Heat of Formation of Boron Trifluoride," to be published.

interval of 0.1%, and the heat of formation of SiF_4[4] has been measured recently with the same uncertainty. The estimated uncertainty interval of the heat of formation of MoF_6[5] is, unfortunately, greater than 1%. It was evident that a more precise determination of the heat of formation of MoF_6 was a desirable step in the proposed program. Accordingly, this determination was undertaken by means of the direct synthesis of the compound from its elements in a bomb calorimeter.

Experimental

Calorimeter and Bomb.—The calorimeter, laboratory designation ANL-R1, was similar in design and construction to that described by Hubbard, Katz and Waddington[6] with a direct gear drive modification[7] for rotation of the bomb. The operational procedure was conventional[6] except that the bomb was not rotated in the combustion experiments. The nickel combustion bomb, laboratory designation Ni-1, was similar to one already described,[2] except that the gasket which sealed the cap to the body of the bomb was made of soft aluminum instead of gold.

Calibration.—The energy equivalent of the calorimetric system, ε(calor.), was determined by combustion in oxygen of National Bureau of Standards Sample 39g benzoic acid under prescribed conditions. A series of six combustions yielded a value of 3575.67 cal. deg.$^{-1}$ for ε(calor.) with a standard deviation of 0.32 cal. deg.$^{-1}$.

Materials.—Molybdenum was obtained from the Fansteel Metallurgical Corp. in the form of 0.005-inch thick sheet and 0.005-inch diameter wire. Spectrochemical examination of the samples revealed no metallic impurities present in concentrations above the limits of detection. Specific elemental analyses showed that the sheet molybdenum contained 0.011% carbon, 0.002% silicon, 0.0042% oxygen, 0.006% nitrogen, 0.0001% hydrogen, and less than 0.005% sulfur.

Purified fluorine was obtained by distilling commercial fluorine in a low temperature still.[2] The distilled fluorine was 99.94% pure, as indicated by a mercury titration analysis by the method of Armstrong and Jessup.[8] Mass spectrometric analysis of the impurity fraction indicated that the fluorine contained 0.04% oxygen, 0.01% nitrogen, and traces of helium and argon.

Combustion Technique.—A method of sample support was devised to minimize the amount of extraneous material near the burning sample. A piece of the sheet molybdenum in the form of a rectangle was suspended by a short length of the wire from a relatively massive nickel rod. A separate length of the wire, used for ignition, was threaded through three holes drilled near the bottom edge of the sample and attached to the electrodes by nickel nuts. In a glass trial bomb[9] combustion was observed to start at the bottom edge of the sheet and proceed upward, so that virtually all of the molybdenum was consumed as the flame front progressed.

Auxiliary Observations.—Auxiliary experiments were made to define (a) the fore period reaction, (b) the main reaction, and (c,d) the side reactions.

(a) The possibility of a fore period reaction between a typical molybdenum sample and fluorine gas at pressures up to 20 atm. was studied. Weight losses of less than 0.01 mg. of molybdenum per hour were observed, *provided* that moisture was rigorously excluded from the bomb by pumping on it overnight with a diffusion pump before filling it with fluorine. It was concluded that the amount of fore period reaction in the calorimetric experiments could be safely neglected.

(b) The main product of the reaction was shown to be molybdenum hexafluoride by chemical and infrared absorption analyses of the combustion gases. The amount of product formed was always less than that calculated to saturate the volume of the bomb at room temperature, hence no liquid molybdenum hexafluoride was present at the end of the calorimetric experiments. In the infrared spectrum of the combustion gases CF_4, SiF_4, SF_6 and traces of HF could also be detected in about the concentrations expected from the known impurities. Fluorides of oxygen and nitrogen were not detected. Some of the molybdenum sample survived the combustion. This consisted of portions of wire that had been gripped by the nickel nuts and a few small, flattened spheres of molybdenum that were found on a nickel catch plate at the bottom of the bomb. It was evident that some of the molybdenum had melted, dropped onto the catch plate, and had been quenched without having reacted with nickel. The molybdenum metal residues were washed, dried and weighed after each calorimetric combustion.

(c) Significant amounts of yellowish, lower molybdenum fluoride(s) were deposited on the walls and fittings of the bomb when the initial fluorine pressure, though in excess of stoichiometric requirements, was less than 10 atm. Attempts to define the nature of the deposit by X-ray diffraction analysis were unsuccessful. At higher pressures of fluorine (14–21 atm.), the formation of such deposits was completely suppressed, except that a thin yellow film appeared on the surface of the unreacted molybdenum metal. Peacock[10] has described molybdenum pentafluoride as a yellow solid at room temperature which dissolves to form a colored solution that subsequently fades. This description accorded with observations made on the behavior of the yellow film and it was therefore assumed to be MoF_5. The amount of material undergoing this side reaction was estimated by analysis of the bomb washings for molybdenum content. In a typical experiment 0.10 ± 0.05% of the molybdenum burned was found in the washings; in one experiment, in which more than the usual amount of film was observed, 0.20 ± 0.05% was found.

(d) The bomb and its fittings (nickel electrodes, nuts, screws and catch plate) were prefluorinated to form a very thin, protective nickel fluoride film. However, these parts, especially the fittings near the combustion zone, may undergo further fluorination. Nickel fluoride was, in fact, identified by X-ray diffraction in scrapings from the fittings. The bomb proper was periodically washed and weighed and was observed to have undergone a weight loss of less than one milligram during the series of eight calorimetric experiments. The fittings were washed and weighed after each combustion and the weight losses were determined to vary from 0.1 to 2.1 mg. per combustion. It was assumed that the weight losses were due to removal of nickel fluoride formed during the combustion.

Experimental Results

Table I is a summary of the results of eight successful combustion experiments, expressed in terms of the defined calorie equal to (exactly) 4.184 absolute joules. The corrections to standard states were applied in the usual manner[11] with suitable modification for fluorine bomb calorimetry.[12] The numbered entries in Table I are: (1) the mass *in vacuo* of the molybdenum reacted, which was determined by subtracting the mass of molybdenum metal recovered from the mass of molybdenum sheet and wire introduced into the bomb; (2) the initial pressure of fluorine; (3) the observed increase in the calorimeter temperature, corrected for heat exchanged between the calorimeter and its surroundings; (4) the energy equivalent of the calorimetric system, multiplied by the corrected temperature increase; (5) the energy

(4) A. F. Vorobiev, V. P. Kolesov and S. M. Skuratov, reported in the *Bull. Chem. Thermodynamics*, 3 (1960).

(5) O. E. Myers and A. P. Brady, *J. Phys. Chem.*, **64**, 591 (1960).

(6) W. N. Hubbard, C. Katz and G. Waddington, *ibid.*, **58**, 142 (1954).

(7) W. D. Good, D. W. Scott and G. Waddington, *ibid.*, **60**, 1080 (1956).

(8) G. T. Armstrong and R. S. Jessup, *J. Research Natl. Bur. Standards*, **64A**, 49 (1960).

(9) R. L. Nuttall, M. A. Frisch and W. N. Hubbard, *Rev. Sci. Instr.*, **31**, 461 (1960).

(10) R. D. Peacock, *Proc. Chem. Soc.*, 59 (1957).

(11) W. N. Hubbard, D. W. Scott and G. Waddington, Chapter 5, "Experimental Thermochemistry," F. D. Rossini, Editor, Interscience Publishers, Inc., New York, N. Y., 1956, pp. 75–128.

(12) W. N. Hubbard, Chapter 5, Vol. II, "Experimental Thermochemistry," H. A. Skinner, Editor, Interscience Publishers, Inc., New York, N. Y., to be published.

TABLE I

RESULTS OF COMBUSTION EXPERIMENTS[a]

V_i = 0.341 l., t_i = 24.235°

Molybdenum sheet and wire, g.	0.65633	0.60386	0.50147	0.52597	0.51355	0.52430	0.55991	0.53988
Molybdenum recovered, g.	.01337	.08950	.00461	.00287	.00715	.00332	.02086	.00670
Molybdenum in washings, g.	.0006	.0006	.0006	.0006	0006	.0006	.0013	.0016
Nickel reacted, g.	.0001	.0005	.0016	.0006	0006	.0006	.0021	.0008
1. m', molybdenum reacted, g.	.64296	.51436	.49686	.52310	50640	.52098	.53905	.53318
2. $P^i(F_2)$, atm.	13.9	15 0	15 0	15.0	15 0	15.0	20 0	21.0
3. Δt_c, deg.	0.69493	0.55612	0.53805	0.56562	0.54736	0.56276	0.58479	0.57724
4. ε (calor.)$(-\Delta t_c)$, cal.	−2484.84	−1988.50	−1923.89	−2022.47	−1957.18	−2012.24	−2091.02	−2064.02
5. $\Delta E_{contents}$, cal.[b]	−5.08	−4.12	−3.98	−4.18	−4.04	−4.15	−4.75	−4.74
6. $\Delta E_{ignition}$, cal.	1.09	0.57	1.07	1.12	0 95	1.10	4.25	1.95
7. $\Delta E_{impurities}$, cal.	0.72	.58	0.56	0.59	.57	0.58	0.60	0.60
8. $\Delta E_{MoF_6\ formation}$, cal.	− .10	− .10	− .10	− .10	− .10	− .10	−.22	− .10
9. $\Delta E_{NiF_2\ formation}$, cal.	.27	1.35	4.33	1.62	1.62	1.62	5.68	2.17
10. ΔE_{gas}, cal.[c]	− .03	−0.03	−0.03	−0.03	−0 02	−0 03	−0.05	−0.05
11. $\Delta E_c^\circ/M$, cal. g.$^{-1}$	−3869.56	−3869.37	−3868.37	−3868.19	−3866.90	−3864.29	−3868.85	−3871.47

Av. $\Delta E_c^\circ/M$ = −3868.4 cal. g.$^{-1}$ Std. dev. of mean = ±0.75 cal. g.$^{-1}$

[a] The symbols employed are explained in ref. 11. [b] $\Delta E_{contents} = \varepsilon^i(\text{cont.})(t_i - 25) + \varepsilon^f(\text{cont.})(25 - t_f + \Delta t_{corr.})$. [c] $\Delta E_{gas} = \Delta E^i(\text{gas})]_0^{P^i(gas)} + \Delta E^f(\text{gas.})]^{0}_{Pt(gas.)}$.

absorbed by the contents of the bomb during the hypothetical isothermal process at 25°; (6) the electrical energy input (measured with a current integrating circuit[13]) for the ignition of the fuse; (7) the net correction for impurities in the molybdenum sample; (8) and (9) the corrections for molybdenum pentafluoride and nickel fluoride formation; (10) the net correction due to the hypothetical compression and decompression of the bomb gases; and (11) the energy change per gram of molybdenum for the reaction

$$Mo(c) + 3F_2(g) \longrightarrow MoF_6(g) \qquad (1)$$

with the reactants and product in their respective standard states at 25°.

For calculation of item 5 the following values were assumed: Heat capacities at constant pressure of 0.105_8 and 0.058_5 cal. deg.$^{-1}$ g.$^{-1}$ for Ni[14] and Mo,[14] respectively; heat capacities at constant volume of 5.50 and 26.3 cal. deg.$^{-1}$ mole^{-1} for F_2[15] and MoF_6,[16] respectively.

Carbon, silicon, oxygen, nitrogen and sulfur were assumed to be present in the sample as Mo_2C, Mo_3Si, MoO_2, Mo_2N and MoS_2, respectively. The infrared spectrum of the bomb gases was interpreted as indicating that the minor combustion products were CF_4, SiF_4, O_2, N_2 and SF_6, respectively. The appropriate heats of formation for the impurity correction were taken from ref. 14 except for CF_4,[7] SiF_4,[4] SF_6,[17] Mo_2N[18] and Mo_3Si.[19]

No correction was applied for the traces of hydrogen and sulfur present in the sample. The net impurity correction (item 7) was 1.11 ± 0.60 cal./g. of sample reacted. The large uncertainty attached to this correction arises partly from analytical uncertainties and partly from a generous allowance for the possibility that the impurity elements existed in other states of combination.

The correction for the reaction to form molybdenum pentafluoride is given in item 8. To make the correction, the heat of formation of the solid pentafluoride was estimated by assuming that its fluorination has about the same exothermicity as the fluorination of solid uranium pentafluoride to gaseous uranium hexafluoride.[14] This estimate, −355 ± 15 kcal. mole^{-1}, could have been substantially different without affecting the final results. The correction for the reaction to form nickel fluoride on the fittings, given in item 9, was computed using −159.5 kcal. mole^{-1} [14] as the heat of formation.

The data required for the evaluation of item 10 were calculated as follows. The coefficients $(\partial E/\partial P)_T$ and μ (in the equation $PV = nRT(1 - \mu P)$) were estimated from the intermolecular force constants by the method outlined by Hirschfelder, *et al.*[20]

Fluorine was the only gas in the bomb in the initial state. Force constants for fluorine have been determined by White, *et al.*[21] The estimated coefficients at 25° were

$$\mu = 0.000801 \text{ atm.}^{-1} \qquad (2)$$

$$(\partial E/\partial P)_T = -1.780 \text{ cal. atm.}^{-1} \text{ mole}^{-1} \qquad (3)$$

The structural similarity of MoF_6 to SF_6 and UF_6 was used as a guide for the estimation of its force constants. From these estimates, the required coefficients were calculated for mixtures of F_2

(13) G. Pilcher and L. E. Sutton, *Phil. Trans. Roy. Soc. London*, **A248**, 23 (1955).

(14) "Selected Values of Chemical Thermodynamic Properties," National Bureau of Standards Circular 500, U. S. Government Printing Office, Washington, D. C., 1952.

(15) W. H. Evans, T. R. Munson and D. D. Wagman, *J. Research Natl. Bur. Standards*, **55**, 147 (1955).

(16) J. Gaunt, *Trans. Faraday Soc.*, **49**, 1122 (1953).

(17) P. Gross, C. Hayman and D. L. Levi, *XVIIth Int. Cong.-Pure and Applied Chem. Abstracts*, **1**, 90 (1959).

(18) A. D. Mah, U. S. Bureau of Mines Report RI5529 (1960).

(19) (a) L. Brewer and O. H. Krikorian, *J. Electrochem. Soc.*, **103**, 38 (1956); (b) L. Brewer and O. Krikorian, U. S. Atomic Energy Comm., UCRL-3352 (March 1956); (c) A. W. Searcy and A. G. Tharp, *J. Phys. Chem.*, **64**, 1539 (1960).

(20) J. O. Hirschfelder, C. F. Curtiss and R. B. Bird, "Molecular Theory of Gases and Liquids," John Wiley and Sons, New York, N. Y., 1954.

(21) D. White, J. H. Hu and H. L. Johnston, *J. Chem. Phys.*, **21**, 1149 (1953).

and MoF_6 in the final state. The coefficients, as functions of composition, at 25° were

$$\mu = 0.000801\ (1 + 6.99x + 6.07x^2)\ \text{atm.}^{-1} \quad (4)$$

$$(\partial E/\partial P)_T = -1.780\ (1 + 3.905x + 2.585x^2)\ \text{cal. atm.}^{-1}\ \text{mole}^{-1} \quad (5)$$

where x represents the mole fraction of MoF_6 in the gaseous mixture.

All other corrections to standard states were negligible. $\Delta E_c^\circ/M$ is just the sum of items 4 through 10 divided by the mass of molybdenum reacted.

Derived Data.—The following data were derived for the formation of molybdenum hexafluoride gas at 25°

Energy of formation

$$\Delta Ef^\circ = \Delta Ec^\circ = -371.1_7 \pm 0.2_2\ \text{kcal. mole}^{-1}$$

Heat of formation

$$\Delta Hf^\circ = -372.3_5 \pm 0.2_2\ \text{kcal. mole}^{-1}$$

Entropy of formation

$$\Delta Sf^\circ = -72.13\ \text{cal. deg.}^{-1}\ \text{mole}^{-1}$$

(Gibbs) free energy of formation

$$\Delta Ff^\circ = -350.8_3 \pm 0.2_2\ \text{kcal. mole}^{-1}$$

The atomic weight of molybdenum[22] was taken as 95.95 g. (g.-atom)$^{-1}$. The entropies, S°, at 25°, of Mo(c),[14] F_2(g)[15] and MoF_6(g)[16] were taken as 6.83, 48.45 and 80.01 cal. deg.$^{-1}$ mole^{-1}, respectively. The uncertainties given in these estimates are uncertainty intervals[23] equal to twice the overall standard deviation arising from known sources.

Conclusion

The standard heat of formation of molybdenum hexafluoride gas has been determined to be $-372.3_5 \pm 0.2_2$ kcal. mole^{-1} by direct combination of the elements in a bomb calorimeter. No significant trend in the final results was observed although the initial fluorine pressure in the bomb and the extent of certain (minor) side reactions varied in the course of the experiments. The value derived by the direct reaction is believed to be more reliable than a value of -382 ± 4 kcal. mole^{-1} obtained by Myers and Brady[5] from the heats of hydrolysis and solution of MoF_6(l), MoO_3 and NaF in dilute sodium hydroxide. Further work is required to shed light on the source of the discrepancy.

Acknowledgments.—The assistance of Messrs. R. W. Bane, J. F. Goleb, B. D. Holt and R. P. Larsen, who provided the special analyses required, is gratefully acknowledged.

(22) E. Wichers, *J. Am. Chem. Soc.*, **80**, 4121 (1958).

(23) F. D. Rossini, Chapter 14, "Experimental Thermochemistry," F. D. Rossini, Editor, Interscience Publishers, Inc., New York, N. Y., 1956, pp. 297–320.

THE HYDROGENATION OF PYRIDINE IN ACID MEDIA

BY R. M. SKOMOROSKI AND A. SCHRIESHEIM

Esso Research & Engineering Company, Linden, New Jersey

Received February 6, 1961

Pyridine hydrogenation was studied in aqueous solutions of acetic and sulfuric acids using platinum dioxide catalyst at 25 ± 2° and 21 atm. hydrogen pressure. The purpose of this research was to investigate the role of the medium in hydrogenation reactions involving nitrogen compounds. It was found that the acid medium profoundly influenced the course of the reaction. With both acids the rate of reaction was found to vary as a function of the acid to pyridine mole ratio. Maxima in the rate were discovered at acid to pyridine mole ratios of 0.5–1.5 and at higher ratios the rates decreased. The data may be interpreted on the basis of a reduction of pyridinium ions rather than pyridine.

Introduction

The hydrogenation of basic compounds, such as pyridine and its alkyl substituted derivatives, is known to occur readily in acid media over platinum oxide catalyst.[1–3] However, the choice of solvent can influence the hydrogenation rate markedly. For example, pyridine alone in most solvents poisons platinum oxide catalyst and no reduction takes place at 25° and 2–3 atmospheres pressure, but in glacial acetic acid it is reduced to piperidine easily at these conditions. Also pyridine hydrochloride and pyridinium salts are reduced more readily than pyridine in absolute alcohol.[1] However, no extensive work appears to have been done on pyridine hydrogenation in media of different acidity.

The purpose of this research was to investigate in some detail the mechanism of pyridine hydrogenation in acid media. Accordingly, pyridine hydrogenation was studied in aqueous solutions of acetic and sulfuric acids using platinum dioxide catalyst. Also, experiments have been made in other solvents using pyridine or benzene for comparison purposes.

(1) T. S. Hamilton and R. Adams, *J. Am. Chem. Soc.*, **50**, 2260 (1928).

(2) P. H. Emmett, "Catalysis," Chap. 4, Reinhold Publ. Corp., New York, N. Y., 1957.

(3) H. Gilman, "Organic Chemistry," Chap. 9, 2nd Ed., John Wiley and Sons, Inc., New York, N. Y., 1948.

Experimental

Materials.—The platinum dioxide catalyst (84.12% Pt) used in this study was obtained from the Baker Catalysts Co., Inc., and used as received without further treatment. Standard BET measurements using nitrogen adsorption gave 54 m.^{2}/g. for catalyst surface area, 0.15 cc. average pore volume and 58 Å. average pore radius. The catalyst particle size distribution (in microns) as determined by standard size screen sieves was: (8%) > 250, (19%) 250–177, (49%) 177–149, (24%) <149. Samples of catalyst from the same batch were used for all the experiments reported here.

Pyridine, benzene, ethyl acetate, sulfuric acid and acetic acid were Reagent Grade chemicals obtained from the J. T. Baker Co. Pyridine was dried using silica gel and stored under nitrogen; the other chemicals were used as received without further purification. Trifluoroacetic acid, b.p. 70–72° at 760 mm., was Practical Grade material and contained approximately 10 vol. % acetic acid. Research Grade hydrogen (99.9%) and oil pumped nitrogen (99.7%) were used.

Apparatus.—The reactor used in this research was a stainless steel autoclave, Model ABE-300, obtained from Autoclave Engineers, Inc. The autoclave was equipped with an electric heater and stirrer, and coils were provided for circulating a coolant. Temperature measurements were made with an iron–constantan thermocouple using a Leeds and Northrup potentiometer. Pressure was measured with Heise Co. pressure gauge, Model H-18755, which was graduated from 0–750 p.s.i.g. in 1 p.s.i.g. intervals (diameter of gauge, 45 cm.).

Procedure.—In all the hydrogenation experiments, 6 ± 0.1 cc. of pyridine (or 6 ± 0.1 cc. benzene) was used with 0.3 g. of platinum dioxide catalyst and 50 cc. of solvent. After the pyridine, solvent and catalyst were placed in the reactor, it was purged three times with hydrogen and the pressure was adjusted to an average initial value of 21 atm. The extent of reaction was followed by recording the hydrogen pressure every minute during the initial 10–15 minutes and then every 5 or 10 minutes; pressure measurements were made for at least one hour and often for two hours. The reaction products at the conclusion of an experiment were analyzed by gas liquid partition chromatography and infrared spectral methods. Briefly, the infrared method consisted of neutralizing a product sample with excess aqueous caustic, then extracting the neutralized sample with carbon tetrachloride. The CCl_4 phase now was analyzed in the infrared for pyridine (at 14.29 μ), piperidine (at 11.72 μ, 7.59 μ) and qualitatively scanned for other reaction products. These infrared and chromatographic methods will be described in greater detail elsewhere.

Results

First-order rate constants were calculated using the equation[4,5]

$$\log \frac{P_0}{P} = \frac{k_a t}{2.30 V}$$

where the symbol P_0 indicates the initial pressure, P represents the pressure at time t (minutes), V is the reactor volume (0.30 liter) and k_a (l./min./g.) is the rate constant. The actual volume, V, used to calculate k_a was corrected for the volume of the stirrer and solution present in the reactor. The values of k_a have been referred to one gram of platinum dioxide by dividing by the catalyst weight. Values of log P_0/P were plotted *versus* t and the slope of the straight line was used to calculate k_a. The pyridine to piperidine conversions varied from 0–95% depending on the stirring rate and the acid concentration used. However, the log P_0/P *versus* t curves were linear even for conversions as high as 80–90%.

The reproducibility of the experiments is shown in Table I for pyridine hydrogenation in acetic and trifluoroacetic acids. The average deviation of the first-order rate constants is ±10%. Similar precision was obtained for pyridine hydrogenation in sulfuric acid. Comparable runs in ethyl acetate and acetic acid (Table I) show that pyridine and benzene are hydrogenated more easily in acidic than non-acidic media.

The effect of stirring speed (600–4100 r.p.m.) on hydrogenation rate was explored in several experiments using pyridine dissolved in sulfuric acid. The hydrogenation rates increased with stirring speed up to about 2760 r.p.m., but at higher stirring speeds the rate was approximately constant. Because of the precautions taken to ensure efficient mixing, it is believed that chemical reaction on the catalyst surface is the rate-controlling step at high stirring speeds (2700 r.p.m.).

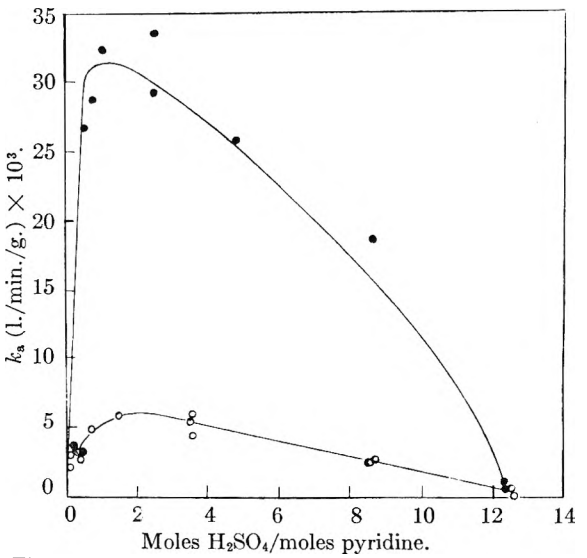

Fig. 1.—Hydrogenation rate of pyridine at 600 and 2760 r.p.m., as a function of H_2SO_4/pyridine mole ratio; 0.3 g. PtO_2, 6 cc. C_5H_5N, 50 cc. solvent: ○ 600 r.p.m.; ●, 2760 r.p.m.

The effect of acid concentration on pyridine hydrogenation rate is shown in Fig. 1. At constant stirring speed, the rate first increases with H_2SO_4/pyridine mole ratio, and then it decreases. When chemical reaction is rate-controlling (2760 r.p.m.), the maximum hydrogenation rate occurs at H_2SO_4/pyridine mole ratios of 0.5–1.5 approximately.

Excellent correlation was obtained between hydrogen consumption data and pyridine disappearance and piperidine formation as determined by chemical analysis of the liquid products. For example, the mole ratio of hydrogen to pyridine reacted had an average value of 3.1 and an average deviation of ±0.2 for six experiments. No products other than piperidine and unreacted pyridine were detected in our experiments.

Some typical first-order plots for pyridine hydrogenation in sulfuric acid solutions are shown in Fig. 2. These were obtained by using the correlation between hydrogen pressure and reacted pyridine to calculate the pyridine conversion (X), although similar plots may be obtained by using the pressure data directly. At high acid concentrations (H_2SO_4/C_5H_5N, mole ratio >0.5) the curves are linear up to 80 or 90% pyridine conversion, but at lower acid concentrations, the hydrogenation rate decreases and becomes very slow. For example, in the case shown in Fig. 2, the initial first-order rate constant decreases from 2.9×10^{-3} to approximately 1.6×10^{-3} l./min./g. after one hour.

Discussion

Pyridine hydrogenation in acid solution is first order with respect to hydrogen pressure (Fig. 2); however, the first-order rate constants in glacial acetic acid (Tables I and II) are smaller than those measured by Smith and Stanfield (0.142–0.178 l./min./g., 30°)[6]. This difference probably is partly

(4) J. F. Fuzek and H. A. Smith, *J. Am. Chem. Soc.*, **70**, 3743 (1948).

(5) R. D. Schuetz, L. R. Caswell and J. C. Sternberg, *J. Org. Chem.*, **24**, 1080 (1959).

(6) P. H. Emmett, "Catalysis," Reinhold Publ. Corp., New York, N. Y., 1957, Vol. 5, p. 237.

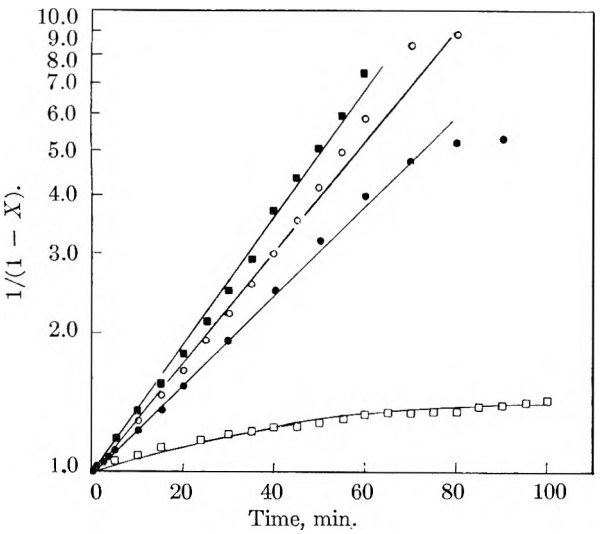

Fig. 2.—First-order plots of pyridine hydrogenation in sulfuric acid solutions (0.3 g. PtO_2, 6 cc. C_5H_5N, 50 cc. solvent, 25 ± 2°, 2760 r.p.m.): Acid/Pyridine mole ratio □ 0.25, ○ 0.50, ■ 2.48, ● 8.54.

due to different methods of catalyst preparation. More important, however, is the higher initial hydrogen pressure used in the present work.[5]

TABLE I

HYDROGENATION RATES IN VARIOUS SOLVENTS[a]

Solvent	R.p.m.	First-order rate constant k_a (l./min./g.) × 10^3
CH_3COOH	600 (4 expts.)	13.7 ± 0.8[d]
CF_3COOH	600 (3 expts.)	10.9 ± 1.2[d]
$CH_3COOC_2H_5$	600	0.47
H_2O	600	0.79
CH_3COOH in EtOAc[b]	2760	1.8
CH_3COOH[c]	2760	48.1
$CH_3COOC_2H_5$[c]	2760	1.7

[a] 50 cc. solvent, 0.3 g. PtO_2, 25 ± 2°, 6 cc. pyridine. [b] 8.6 vol. % acetic acid in ethyl acetate. [c] 6 cc. benzene. [d] Average value and average deviation.

TABLE II

HYDROGENATION RATE OF PYRIDINE IN CH_3COOH–H_2O SOLUTIONS[a]

CH_3COOH/C_5H_5N, mole ratio	First-order rate constants, k_a (l./min./g.) × 10^3
0.26	6.9[b]
0.50	5.8[b]
0.73	6.3
1.00	10.6
1.50	10.6
6.66	17.4
9.99	21.2
11.6	13.7

[a] 6 cc. pyridine, 50 cc. solvent, 0.3 g. PtO_2, 2760 r.p.m., 25 ± 2°. [b] Reaction rate becomes very slow after ~90 minutes.

The rate equation used to represent the data is based on the assumptions that pyridine (or pyridinium ion) is strongly adsorbed and hydrogen is weakly adsorbed on the catalyst surface. Then, the data obtained in sulfuric acid solutions (Fig. 1) can be explained on the basis of the following mechanism. Pyridine in sulfuric acid solutions is rapidly protonated, and the concentration of free pyridine is low in solutions containing excess acid (mole ratio $H_2SO_4/C_5H_5N > 0.5$). In the presence of acid, pyridinium ion is adsorbed on the catalyst surface and reduced to piperidine. In the absence of acid, any piperidine formed is probably adsorbed on the catalyst more strongly than pyridine and inhibits the hydrogenation rate. Experiments in ethyl acetate and acetic acid (Table I) support the hypothesis that pyridine must be protonated for reduction to occur at these conditions. This mechanism implies that the hydrogenation rate should increase with acid concentration as more pyridine is protonated and becomes available for reduction; the maximum hydrogenation rate should occur at a H_2SO_4/C_5H_5N mole ratio of 0.5 and CH_3COOH/C_5H_5N mole ratio of 1. In sulfuric acid the maximum rate does occur at approximately the predicted acid concentration, but in acetic acid the rate slowly increases at higher acid concentrations (Table II). However, more complete agreement with theory is not expected because other solvent physical properties besides acidity are changing with acid concentration.

Complete reduction of pyridine does not occur at low acid concentrations (mole ratio $H_2SO_4/C_5H_5N < 0.5$), the rate decreasing rapidly from its initial value and becoming very slow (Fig. 2). The pyridine conversion at this point is in most cases less than the amount calculated assuming that only the protonated form is reduced (Table III). Piperidine[7] ($K_b = 2 \times 10^{-3}$) is a stronger base than pyridine ($K_b = 2.3 \times 10^{-9}$) and it apparently decreases effectively the amount of acid available for pyridine protonation.

TABLE III

PYRIDINE CONVERSION AT LOW ACID CONCENTRATIONS[c]

Acid, C_5H_5N, mole ratio	$\frac{C_5H_5N \text{ reacted}}{\text{Acid present}}$ mole ratio, Obsd.	Calcd.
0.25[a]	1.3	2
.42[a]	0.84	2
.50[a]	2.0	2
.50[b]	1.0	1
.73[b]	0.78	1

[a] Sulfuric acid. [b] Acetic acid. [c] 6 cc. pyridine, 50 cc. solvent, 0.3 g. PtO_2, 2760 r.p.m., 25 ± 2°.

The proposed mechanism accounts for the initial rate dependence on acid concentration, but it does not predict the subsequent rate decrease at higher acid concentrations (Fig. 1). Inhibition by piperidine does not appear to be a plausible explanation of this rate decrease because a constant amount of pyridine was used at all acid concentrations. The decreased rates at high acid concentrations are explained best as the result of solvent effects. Adsorption of sulfuric acid may be important at higher concentrations which could result in decreased hydrogenation rates. Such pronounced solvent effects have been observed in liquid phase benzene hydrogenation.[8]

Although other mechanisms can be postulated to account for pyridine hydrogenation in acid media, it is felt that the one suggested above is the simplest.

(7) R. T. Morrison and R. N. Boyd, "Organic Chemistry," Allyn and Bacon, Inc., Boston, Mass., 1959, p. 850.

(8) E. De Ruiter and J. C. Jungers, *Bull. soc. chim. Belg.*, **58**, 210 (1949).

The general result that pyridine is hydrogenated more easily in acidic than non-acidic media is an interesting one theoretically. It is usually assumed that during hydrogenation an aromatic molecule is adsorbed flat against the catalytic surface.[2] Pyridine has an unshared pair of electrons on the nitrogen atom which it may use to coördinate with other molecules or catalyst surface atoms.[9] It is reasonable to postulate, therefore, that pyridine may adsorb edgewise on the catalyst surface, and this could account for the low hydrogenation rate. However, pyridine is readily protonated in acid media and the lone pair of electrons on the nitrogen atom then is unavailable for direct interaction with the catalyst surface. Hence, the pyridinium ion may be more susceptible to a flatwise adsorption on the catalyst surface than pyridine, which should result in relatively rapid hydrogenation rates. Whether this mechanism is generally true is not known. Further research is planned to determine the hydrogenation mechanism of nitrogen compounds.

Acknowledgment.—The authors wish to thank Esso Research and Engineering Co., Linden, New Jersey, for permission to publish this work. Stimulating discussions with Mr. D. L. Baeder and Drs. P. J. Lucceshi, G. M. Kramer and H. Pobiner are gratefully acknowledged. Also, we wish to thank Professor M. Boudart for reading the manuscript and suggesting improvements.

(9) C. A. Coulson, "Valence," Oxford Univ. Press, London, 1952, p. 240.

THERMAL TRANSPIRATION AT LOW PRESSURE. THE VAPOR PRESSURE OF XENON BELOW 90°K.

BY H. H. PODGURSKI AND F. N. DAVIS

Edgar C. Bain Laboratory For Fundamental Research, United States Steel Corporation Research Center, Monroeville, Pennsylvania

Received February 11, 1961

Thermal transpiration measurements were made with hydrogen, neon, argon and xenon. The pressure ratios for both hydrogen and neon measured through 2 mm. (i.d.) glass tubing at 5×10^{-4} mm. were 8% higher than the limit set by the Knudsen equation $[P_1/P_2 = \sqrt{T_1/T_2}]$. The empirical equation first proposed by Liang,[1-4] and which has been used recently by many investigators, also failed to describe the behavior of neon and hydrogen at low pressures. However, our data for xenon and argon, within the limits of experimental error, could be fitted to curves described by this equation. Thermal transpiration values for xenon were determined by vapor pressure measurements. The vapor pressure was measured through glass tubes ranging from 2.00 to 36.3 mm. (i.d.): at $T_1 = 77°K.$ and $T_2 = 299°K.$ neither the limit $P_1/P_2 = \sqrt{T_1/T_2} = 0.51$ nor $P_1/P_2 = 1.00$ was realized for xenon vapor in equilibrium with solid xenon for this range of tube diameters; at 90°K. the vapor pressure of xenon measured through a 21.7 mm. (i.d.) tube needed no transpiration correction, *i.e.*, $P_1/P_2 = 1.00$. In the temperature range 85 to 90°K. our measured xenon vapor pressure values are described by the equation $\log P(\text{mm.}) = -833.33/T + 8.044$. The streaming of mercury vapor from the McLeod gages to the refrigerated traps (195°K.) developed pressure gradients in our apparatus which interfered with the measurement of thermal transpiration. With xenon at 10^{-3} mm. this mercury drag effected a differential in pressure of 6%. This source of error in such measurements appears to have remained unnoticed by many investigators.

Introduction

When gas is held at low pressures in a system consisting of two vessels connected by a narrow tube, one vessel at temperature T_1 and the other at T_2, a pressure difference develops between the two vessels. The ratio of the pressures (P_1/P_2) at steady state in the two vessels in such a closed system will be called the thermal transpiration value. A knowledge of these values is necessary when the pressure in only one of the vessels is measurable but the pressures must be known in both—a situation frequently encountered in low-pressure adsorption measurements. The ratio of pressures will range between two extremes: a value of unity at high pressures and the Knudsen value, $\sqrt{T_1/T_2}$, at low pressures.

Several years ago the authors undertook adsorption studies employing xenon as an adsorbate at 77°K. At that time it was assumed that the Knudsen equation would accurately describe the transpiration effect at pressures up to the vapor pressure of xenon at 77°K. because the mean free path of the xenon in the system was greater than "ten times" the diameter (d = 2 mm.) of the connecting tube passing through the temperature gradient. The factor of ten appears to have found its way into the literature[5] without evaluation of the errors involved. Actually, the xenon vapor pressure value predicted by the Knudsen equation was in error by 15%.

Liang[1-3] proposed an empirical equation to describe thermal transpiration at all pressures. Its principal appeal stemmed from the use of only a single parameter in the equation for any one gas. Recently the equation was examined by Bennett and Tompkins[4] who imposed certain limitations upon its use. However, the accuracy of their data in the low-pressure region did not allow a critical test of the equation. Recent improvements at our Laboratory in the construction of McLeod gages and in techniques for measuring low pressures motivated this investigation. Specifically, it was intended to test at low pressures the basic working assumption in Liang's empirical equation: "For a certain temperature difference, *e.g.*, 77.3 *vs.* 298°K.,

(1) J. Liang, *J. Appl. Phys.*, **22**, 148 (1951).
(2) J. Liang, *J. Phys. Chem.*, **56**, 660 (1952).
(3) J. Liang, *ibid.*, **57**, 910 (1953).
(4) M. J. Bennett and F. C. Tompkins, *Trans. Faraday Soc.*, **57**, 185 (1957).
(5) S. Dushman, "Vacuum Techniques," J. Wiley and Sons, Inc., New York, N. Y., 1949, p. 67.

when R [thermal transpiration value, P_1/P_2] is plotted against the product of pressure and tube diameter, *i.e.*, P_2d, each gas will give only one curve, regardless of the absolute value of d."[1] The analysis of Bennett and Tompkins restricts the validity of this assumption to a limited range of tube diameters.

Experimental

The spectroscopically pure gases, hydrogen, neon, argon and xenon, were obtained from Linde Air Products Company. Our isotope analysis of the xenon is included in Table I. Attempts at purification of xenon were made by vacuum distillation. Neon and hydrogen were passed through charcoal refrigerated at 78°K.

Specially designed McLeod gages[6] were employed in this investigation. The maximum error in our pressure measurements down to 10^{-4} mm. was estimated at $\pm 2\%$. This may be compared with the accuracy of $\pm 0.1 \times 10^{-3}$ mm. claimed by Bennett and Tompkins for the pressure range 10^{-1} to 10^{-3} mm.

Initially it was intended that thermal transpiration measurements would also be made with helium. However, the discovery of an unexpected source of error in the helium transpiration values led to its exclusion. When the dead space of an isothermal system was measured by expanding helium from a McLeod gage, the resulting apparent volume was greater than the true volume. (The true volume was determined volumetrically with water.) Dead space measurements with the other gases gave no discrepancies. We concluded,[6] contrary to expectation based on available diffusion data, that, during a single pressure measurement, enough of the helium dissolves in the ground Pyrex capillary of the gage to account for an error $\geq 3\%$.

Thermal transpiration was measured by the two methods commonly referred to in the literature as "absolute" and "relative." "Absolute" implies that no assumption relating to thermal transpiration itself need be made in order to evaluate it by experiment. When either adsorption or condensation of the gas occurs in the system at the temperature of concern, only the "relative" method can be used; when neither occurs, both methods may be used. During this investigation a new "absolute" method was found useful for gases whose condensation pressures are near the pressure of interest for a specified temperature. Such was the case for xenon between 77 and 90°K.

TABLE I

MASS SPECTROMETRIC ANALYSIS OF XENON FOR ISOTOPE DISTRIBUTION

Isotope mass	Atom per cent. This investigation	Clusius[3]
124	0.09	0.08
126	0.09	0.08
128	2.3	2.3
129	27.4	27.13
130	4.7	4.18
131	20.4	20.67
132	26.8	26.45
134	9.9	10 31
136	8.3	8.79
	100.0	99.99

The experimental arrangements as used in our measurements are illustrated in Figs. 1a, 1b and 1c. "B" in Fig. 1a labels the unsymmetrical U-tube used in the relative method. When using this method P_1 is assumed to be related in a known manner to either measured pressure, P_2 or P_2^*. (The asterisk is used to identify the pressure in the larger arm of the U-tube). For example, at very low pressure, P_1/P_2 for the small arm may be assumed to equal $\sqrt{T_1/T_2}$, or at high pressure P_1 may be assumed equal to P_2^* for the large arm. In either case P_1/P_2 and P_1/P_2^* are established for P_2d and $P^*_2d^*$, respectively.

(6) H. H. Podgurski and F. N. Davis, *Vacuum*, **10**, 377 (1960).

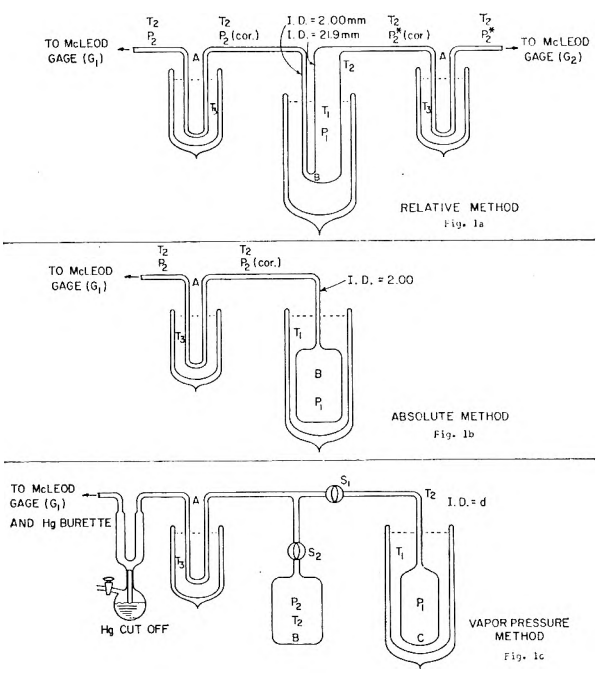

Fig. 1a.—Relative method
Fig. 1b.—Absolute method
Fig. 1c.—Vapor pressure method

} Experimental arrangements for thermal transpiration measurements.

In all the arrangements used for our experiments, refrigerated symmetrical U-traps were included to prevent the mercury vapor escaping the gages from condensing on the walls of the tubes along which transpiration was being measured. It usually has been assumed by most investigators that no pressure differences are generated across symmetrical U-traps. However, in our study with xenon gas a large pressure difference was measured. Because this difference varied considerably, but was always such that the pressure at the gage side of the trap was lower than that at the side free of mercury vapor, the effect has been attributed to a dragging action by the mercury vapor as it streams along the transfer lines from the gages to the traps. The mercury-drag effect was measured by employing the arrangement illustrated in Fig. 1b with the temperature T_1 of "B" set equal to T_2. In turn, this fixed P_1 equal to $P_{2(cor)}$.[7] With a known quantity of gas metered into the system, the extent to which the gas distributed itself at steady state between the calibrated volume elements on each side of trap "A" was established, and $P_{2(cor)}$ thereby calculated, P_2 being measured directly. The symmetrical trap labeled "A" was held at 195°K. (T_3). A negligible amount of xenon was adsorbed in this trap. At these pressures and temperatures the ideal gas law may be justifiably used. The following values were obtained for $P_{2(cor)}$

xenon	$P_{2(cor)} = 1.055\ (\pm\ 0.02)P_2$
argon	$P_{2(cor)} = 1.02\ \ (\pm 0.01)P_2$
neon and hydrogen	$P_{2(cor)} = P_2$

They appear reasonable in light of estimates made with equation 6 given on page 178 in "Vacuum Techniques" by S. Dushman. In all the graphs the P_2 values plotted actually correspond to the $P_{2(cor)}$ values.

In principle, the same sort of experiments described above were involved when employing the "absolute" method for thermal transpiration measurements with the exception that attention was focussed on the partitioning of a gas sample between the parts of the system fixed at temperatures T_1 and T_2 ($T_1 \neq T_2$). In actual operation of the system illustrated in Fig. 1b, the amount of gas contained in the small volume of trap "A" at 195°K. was estimated sufficiently well so as not to introduce significant error into the determinations.

(7) P_2(cor) would be equal to P_2, the measured pressure, if there were no mercury-drag effect.

The effect of tube diameter on the apparent vapor pressure was first studied in a system similar to that illustrated in Fig. 1b with the exception that the 2.00 mm. (i.d.) tube attached to vessel "B" was replaced with successively larger tubes for each vapor pressure measurement (2.00 to 36.3 mm.). The uncertainty in the mercury drag correction, however, led to the adoption of the following procedure for vapor pressure measurements. (Refer to Fig. 1c.) After a steady state was established between the condensed xenon phase in vessel "C" at T_1 (77–90°K.) and the vapor phase in vessel "B" at T_2 (gage temperature), S_1 and S_2 were closed. The gas was pumped out of the remaining part of the system, namely, the McLeod gage, cutoff, trap "A," and transfer lines up to S_1 and S_2. S_2 was then opened and the gas collected in the gage side of the cutoff for measurements. The exact number of moles of xenon, m_{Xe}, transferred from "B" then was determined. With the volume of "B" known at T_2 and with m_{Xe}, the value of P_2 was calculated. Thus, additional vapor pressure measurements were made from 77 to 90°K. through tube diameters, d, ranging from 2.00 to 21.7 mm. (i.d.). The squares in Fig. 9 were data obtained by this method as measured through a 21.7 mm. (i.d.) tube.

Results and Discussion

With our thermal transpiration data on neon and hydrogen the Liang equation became amenable to testing in the low-pressure region. Bennett and Tompkins[4] recommended the following version of the Liang equation

$$\frac{P_1}{P_2} = \frac{\alpha[f\phi_g P_2 d]^2 + \beta[f\phi_g P_2 d] + (T_1/T_2)^{1/2}}{\alpha[f\phi_g P_2 d]^2 + \beta[f\phi_g P_2 d] + 1.00}$$

where $f = 1$ for tubing i.d. < 10 mm. and $f = 1.22$ for i.d. > 10 mm. (P_2, mm.; d, mm; T, °K.); and

$$\alpha = 3.7\,[1.70 - 2.6 \times 10^{-3}(T_2 - T_1)]^{-2}$$
$$\beta = 7.88\,[1 - (T_1/T_2)^{1/2}] \text{ for } (T_1/T_2)^{1/2} < 1$$

ϕ_g is the only parameter that relates to a specific gas. As Liang had presented this equation, α was not a function of temperature and the factor f was assumed to be equal to one for all values of d. For either case we can rewrite the equation as

$$\frac{P_1}{P_2} = \frac{A\phi_g^2(P_2d)^2 + B\phi_g[1 - (T_1/T_2)^{1/2}](P_2d) + (T_1/T_2)^{1/2}}{A\phi_g^2(P_2d)^2 + B\phi_g[1 - (T_1/T_2)^{1/2}](P_2d) + 1.00}$$

where

$$A = \alpha f^2 \text{ and } B = \frac{\beta f}{[1 - (T_1/T_2)^{1/2}]} = 7.88f.$$

Rearranging terms

$$\frac{[(T_1/T_2)^{1/2} - P_1/P_2]}{(P_2d)^2(P_1/P_2 - 1)} = A\phi_g^2 + B\phi_g \frac{[1 - (T_1/T_2)^{1/2}]}{P_2d}$$

According to Liang, A and B would be invariant with temperature and tube diameter, d. For any one value of d, a plot of

$$\frac{[(T_1/T_2)^{1/2} - P_1/P_2]}{(P_2d)^2(P_1/P_2 - 1)} \text{ vs. } \frac{[1 - (T_1/T_2)^{1/2}]}{P_2d}$$

should give a straight line whose slope equals $B\phi_g$ and which intercepts the ordinate at $A\phi_g^2$. Actually, the large range in magnitude for the term on the left makes such a plot impractical. However, the same terms plotted on log-log scaled graph paper should yield a linear curve of unit slope for the low range of P_2d values, *i.e.*, where $B\phi_g\,[1 - (T_1/T_2)^{1/2}]P_2d >> A\phi_g^2$. This range is labeled R in Fig. 2. It is apparent from Figs. 2 to 5 that our data for hydrogen and neon do not satisfy Liang's equation.

In Figs. 3, 4, 5, 6 and 7 are graphed (P_2d *vs.* P_1/P_2) all of the transpiration data for hydrogen, neon, argon and xenon. T_2 in all cases was fixed at 299 ± 1°K. The numbered points on these curves correspond to the usual pairs of values obtained by the relative method. Because we were interested

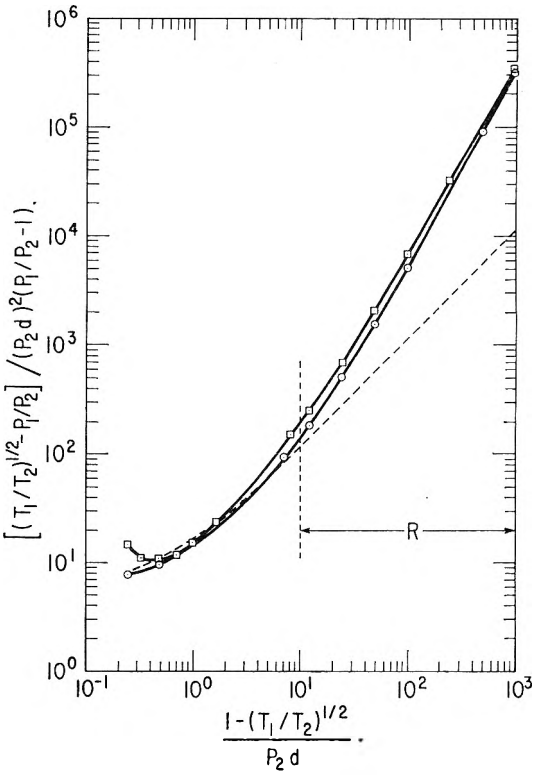

Fig. 2.—Test of conformity to Liang equation: ⊡, neon; T_1 = 77°K., T_2 = 299°K.; ⊙, hydrogen; T_1 = 77°K., T_2 = 299°K. For a perfect fit to the Liang equation the experimental points would have fallen on the dotted straight line of unit slope in the region R.

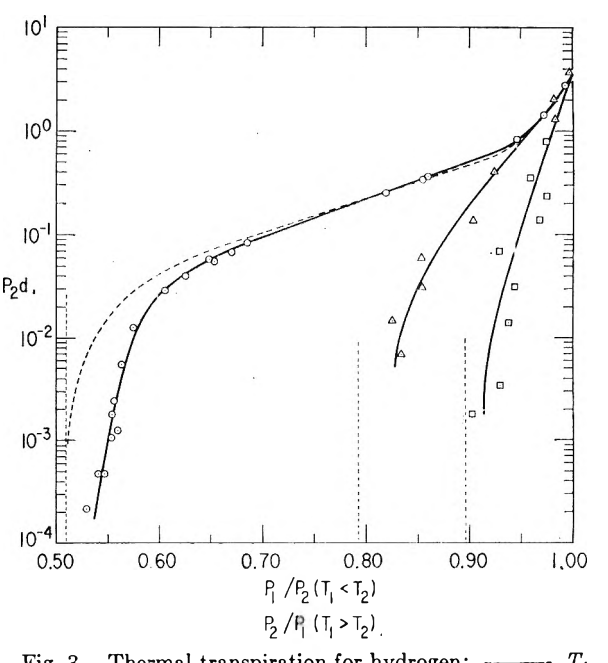

Fig. 3.—Thermal transpiration for hydrogen: ———, T_1 = 77°K., Bennett and Tompkins; △, T_1 = 478°K., absolute method; ⊙, T_1 = 77°K., absolute method; ⊡, T_1 = 372°K., absolute method. T_2 = 299 ± 1°K. in all instances; units of P_2d = mm. × mm.; the dotted vertical lines correspond to the Knudsen limits, *i.e.*, $P_1/P_2 = \sqrt{T_1/T_2}$.

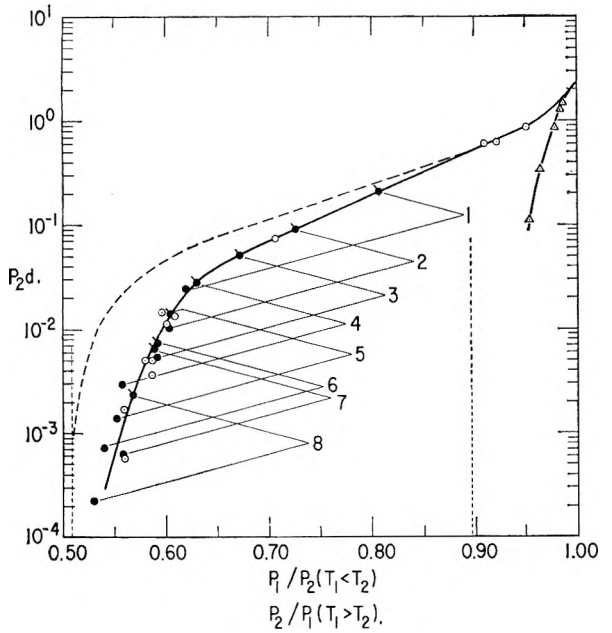

Fig. 4.—Thermal transpiration for neon: ---------, T_1 = 77°K., Bennett and Tompkins; ⊙, T_1 = 77°K., absolute method; ● & ●, T_1 = 77°K., relative method; △, T_1 = 372°K., absolute method. T_2 = 299 ± 1°K. in all instances; units of P_2d = mm. × mm.; the dotted vertical lines correspond to the Knudsen limits, *i.e.*, $P_1/P_2 = \sqrt{T_1/T_2}$. The numbered points correspond to the usual pairs of values obtained by the relative method.

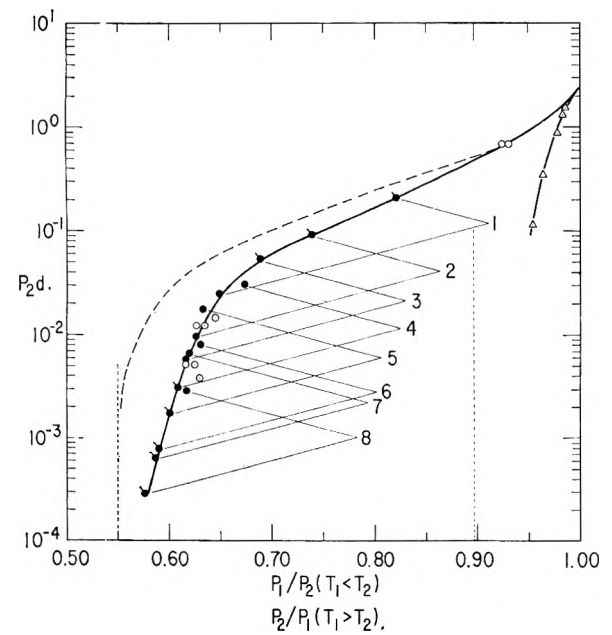

Fig. 5.—Thermal transpiration for neon: ---------, T_1 = 90°K., Bennett and Tompkins; ⊙, T_1 = 90°K., absolute method; ● & ●, T_1 = 90°K., relative method; △, T_1 = 372°K., absolute method. T_2 = 299 ± 1°K. in all instances; units of P_2d = mm. × mm.; the dotted vertical lines correspond to the Knudsen limits, *i.e.*, $P_1/P_2 = \sqrt{T_1/T_2}$. The numbered points correspond to the usual pairs of values obtained by the relative method.

in low-temperature corrections, most of the data were obtained with T_1 at either 77 or 90°K. However, some measurements were made at 372 and 478°K. in order to establish an independent fix by an "absolute" method for the part of the xenon

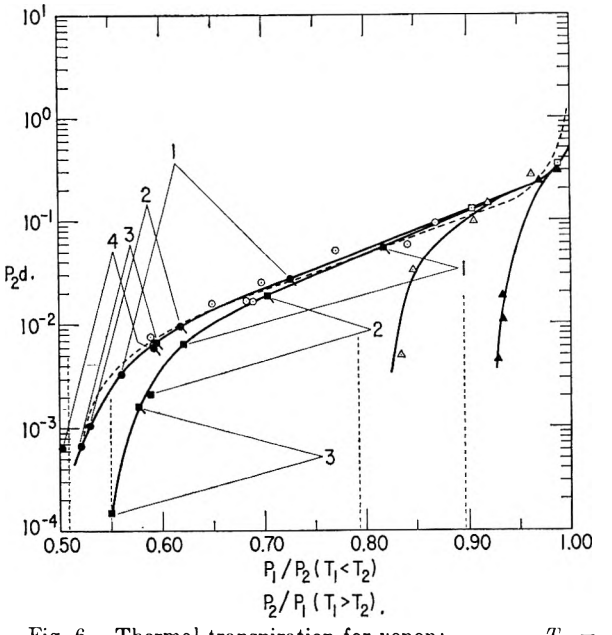

Fig. 6.—Thermal transpiration for xenon: ---------, T_1 = 77°K., Bennett and Tompkins; ■ & ■, T_1 = 90°K., relative method; ⊙, T_1 = 77°K., vapor pressure method; △, T_1 = 478°K., absolute method; ● & ●, T_1 = 77°K., relative method; ▲, T_1 = 372°K., absolute method; ⊡, T_1 = 90°K., vapor pressure method. T_2 = 299 ± 1°K. in all instances; units of P_2d = mm. × mm.; the dotted vertical lines correspond to the Knudsen limits, *i.e.*, $P_1/P_2 = \sqrt{T_1/T_2}$. The numbered points correspond to the usual pairs of values obtained by the relative method.

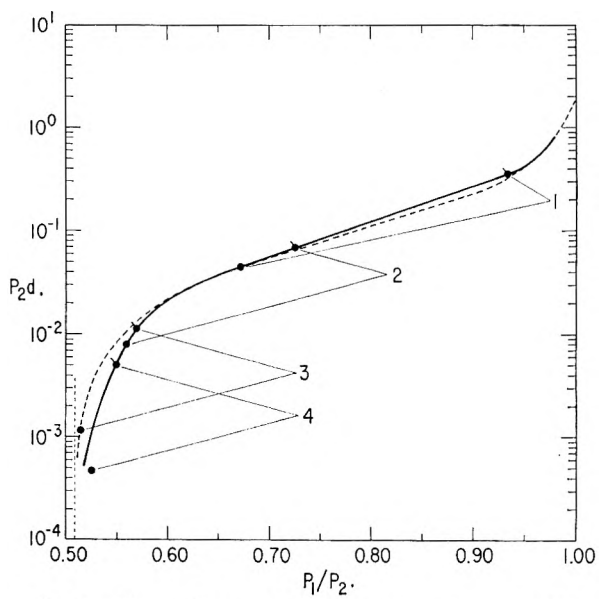

Fig. 7.—Thermal transpiration for argon: ---------, T_1 = 77°K., Bennett and Tompkins; ● & ●, T_1 = 77°K., relative method. T_2 = 299 ± 1°K.; P_2d = mm. × mm. The numbered points correspond to the usual pairs of values obtained by the relative method.

curve near $P_1/P_2 = 1$ in the P_2d *vs.* P_1/P_2 plot. This was tried because of the apparently insensitive nature of such curves to temperature in this region. In order to include both the high-($T_2 < T_1$) and the low ($T_2 > T_1$) temperature transpiration data on the same graphs, P_2/P_1 and P_1/P_2 values were graphed for the high- and low-temperature data, respectively, along the abscissa. Because P_1d and P_2d

are identical at $P_1/P_2 = 1$, P_2d was graphed along the ordinate for both cases. No traps were included in the arrangement for the high-temperature transpiration studies; presumably no corrections had to be made for mercury drag. However, the large scatter ($\pm 1.5\%$) of the points about the drawn curves cannot be explained in the light of the accuracy of our pressure measurements. In spite of this, the transpiration curves fixed by xenon vapor pressure data extrapolated quite well into the high-temperature curves.

The neon data obtained by the "relative" method, although not overlapping any of the limiting transpiration values, were fitted with moderate success to the curves established by the "absolute" method; see Fig. 4 and 5. Assuming that P_2d was a single valued function of P_1/P_2 as originally proposed by Liang, the fitting was conducted by placing a P_2d value on the curve or that part of a curve fixed by the "absolute" method and calculating P_1 from the corresponding P_1/P_2 read along the abscissa. In turn, this P_1 value fixed the $P_1/P_2{}^*$ corresponding to $P_2{}^*d^*$ (see Fig. 1a; $d = 2.00$, $d^* = 21.9$ mm.). These $P_1/P_2{}^*$ values and those read off the existing curves agreed within the limits set by experimental error, thus supporting the hypothesis first proposed by Liang for range $\sqrt{T_1/T_2} < P_1/P_2$ and $P_1/P_2{}^* < 1$. The transpiration curves for argon at $T_1 = 77°$K. and xenon at $T_1 = 90°$K. were fixed essentially by data from the "relative" method and by assuming that P_2d was a single valued function of P_1/P_2. It should be pointed out that no corrections for mercury drag were made on the measured pressures of hydrogen and neon; pressure values for argon and xenon were corrected upward by 2 and 5.5%, respectively, before the curve fitting was attempted.

Xenon Vapor Pressure.—The effect of tube diameter, d, on the apparent vapor pressure of xenon near 77°K. is demonstrated in Fig. 8. The

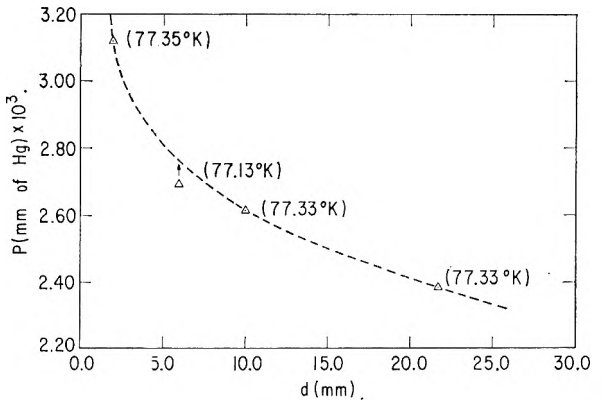

Fig. 8.—Variation of apparent vapor pressure of xenon with tube diameter (d) $T_2 = 299 \pm 1$°K.).

absence of a plateau near either end of the curve indicates that neither of the transpiration limits mentioned earlier had been reached, and it should be apparent that each of the values on the curve, if corrected for the mercury-drag effect and then divided into the true vapor pressure, yields a P_1/P_2 value greater than $\sqrt{T_1/T_2}$, but less than unity. Our xenon transpiration curve was fixed by such measurements. In the temperature ranges 87 to 90°K. for $d = 21.9$ mm., and 85 to 90°K. for $d \geqq 36.3$ mm., the measured vapor pressure of xenon required no corrections for thermal transpiration. The data are shown in Fig. 9. The two methods

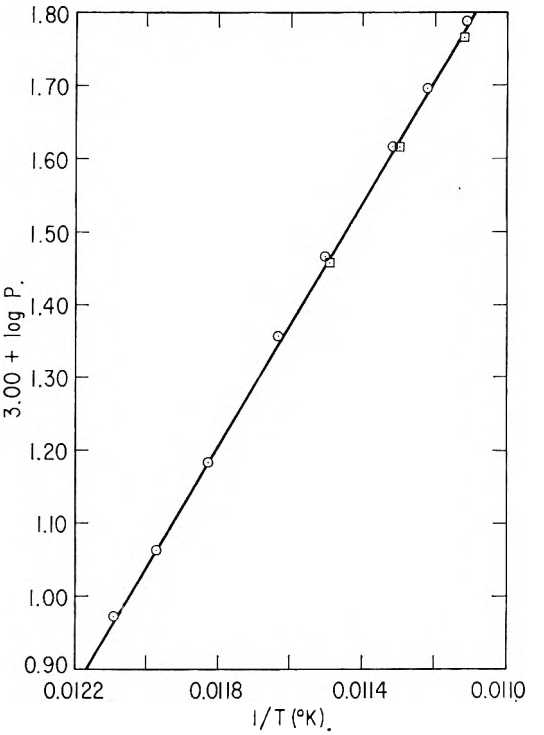

Fig. 9.—Xenon vapor pressure: ⊙, $d = 36.3$ mm. (required + 5.5% correction for mercury drag); ⊡, $d = 21.7$ mm. (no correction required); units of P = mm.

employed in these vapor pressure measurements gave slightly different results; the best straight line through the points (± 2%) includes most of the data. These vapor pressure data and the heat capacity data of Clusius and Riccoboni[8] were used to establish the equation

$$\log P_{Xe}\,(\text{mm.}) = 4.464 - \frac{3795}{4.576T} + 2.50 \log T - \frac{\int_0^T \frac{C_p dT}{T}}{4.576} + \frac{\int_0^T C_p dT}{4.576T}$$

where 3795 cal./mole corresponds to the heat of sublimation of xenon at 0°K. and 4.464 is the constant of integration. This equation cannot be used to predict accurately the vapor pressure of xenon at a temperature where the vapor phase is not behaving as an ideal gas; between 77 and 90° K. we have assumed ideal gas behavior. A linear extrapolation to 77°K. ($1/T = 0.0128$) of the straight line through the experimental points above 85°K. is predicted by the above equation. Hence, the vapor pressure of xenon in this temperature region may be described by the simpler equation

$$\log P_{Xe}\,(\text{mm.}) = -\frac{833.33}{T} + 8.044$$

To the best of our knowledge the only vapor pressure data in the literature for xenon in this temperature range were given by Liang.[1] He reported 1.93

(8) Clusius and Riccoboni, *Z. physik. Chem.*, **38B**, 81 (1937).

$\pm$ 0.01 $\times$ 10^{-3} mm. at 77.3 $\pm$ 0.05°K.; our vapor pressure equation yields 1.81 to 1.86 $\times$ 10^{-3} mm. for the temperature range 77.25 to 77.35°K. It should be noted that Liang assumed his measured value to be related by the Knudsen equation to the true vapor pressure, as he had measured the pressure through a capillary (1.6 mm. i.d.), *i.e.*, he assumed $P_1/P_2 = \sqrt{T_1/T_2} = 0.51$; however, the present investigation sets $P_1/P_2 = 0.59 \neq \sqrt{T_1/T_2}$ for Liang's measurement ($P_2d = 6 \times 10^{-3}$ mm.).

TABLE II

SMOOTHED TRANSPIRATION VALUES FROM THIS INVESTIGATION

	P_2d					
	T_1 = 77°, T_2 = 299 $\pm$ 1°K.				T_1 = 90°, T_2 = 299 $\pm$ 1°K.	
P_1/P_2	H_2	Ne	A	Xe	Ne	Xe
1.000	3.5	2.5	...	0.5	2.5	0.4
0.950	0.920	0.880	0.440	0.181	0.870	.190
.900	.500	.520	.275	.117	.505	.118
.800	.216	.190	.124	.0495	.177	.0465
.700	.0930	.0690	.0555	.0210	.0600	.0179
.650	.0590	.0395	.0370	.0136	.0236	.0103
.625	.0420	.0250	.0295	.0103	.00830	.00690
.600	.0250	.0117	.0204	.00740	.00157	.00375
.575	.00950	.00335	.0117	.00450	.00021	.00130
.550	.00095	.00064	.00480	.00215	...	~10^{-4}
.525	...	...	.00086	.00070	...	
.508	...	...	...	~10^{-4}	...	

Summary

Our smoothed transpiration values for hydrogen, neon, argon and xenon are presented in Table II for T_1 at 77 and 90°K. and for T_2 at 299 $\pm$ 1°K.

Using the ϕ_s values given by Bennett and Tompkins,[4] it is likely that the Liang equation predicts moderately well the behavior of gases with collision diameters greater than that of argon. However, no justification has been found for introducing the new constant $f = 1.22$ into the Liang equation as has been suggested by Bennett and Tompkins for $d >$ 10 mm.

Our work with xenon demonstrates that vapor pressure measurements afford a new method for studying thermal transpiration. High-temperature absolute transpiration measurements have also been found useful for fixing low-temperature transpiration curves over a small range near $P_1/P_2 = 1$.

For the temperature range 70 to 90°K. the following vapor pressure equation for xenon is recommended on the basis of this research

$$\log P(\text{mm.}) = -833.33/T + 8.044$$

Acknowledgment.—The authors are grateful to Drs. J. C. M. Li, R. A. Oriani and O. D. Gonzalez for their informative discussions and advice in the preparation of this paper.

PROTON RETENTION IN HEATED 1:1 CLAYS STUDIED BY INFRARED SPECTROSCOPY, WEIGHT LOSS AND DEUTERIUM UPTAKE

BY V. STUBIČAN[1] AND RUSTUM ROY

Contribution No. 60-66, College of Mineral Industries, Pennsylvania State University, University Park, Pennsylvania

Received February 15, 1961

Clearcut differences between the weight loss curves automatically recorded by a thermobalance have been correlated with the extent of stacking disorder in the kaolin family. The amount of H^+ retained above the initial loss (*i.e.*, from 700–1000°) decreases from the most disordered phase halloysite through the "fire-clay-type" synthetic kaolinite to "large" crystals of well-ordered kaolinite. The amount of H^+ retention could be determined quantitatively from infrared spectra after resynthesizing the kaolinite with pure D_2O, but not by direct infrared examination. The absorption spectra of specimens of heated kaolinite and pyrophyllite were recorded from 11–25 μ. The 538 cm.$^{-1}$ band in kaolinite, previously assigned by us to some mode of Si–O–Al^{VI}, disappears in the samples heated between 600–950° and reappears at higher temperatures. The same band does not disappear in heated pyrophyllite but shifts progressively from 545 to 565 cm.$^{-1}$. These data are compared with present theories concerning coördination changes in heated clays.

Introduction

The kinetics of the loss of water from kaolinite upon heating has been studied many times and various mechanisms for the dehydroxylation process have been proposed on the basis of the data obtained.[2–4] However, recent developments in infrared spectroscopy make it possible to obtain additional data concerning the dehydroxylation process in solids by studying the changes of absorption in the OH-spectral regions, where absorption bands appear which are the result of the presence of hydroxyl groups in the structure.

Two such regions can be detected with certainty with the layer structure silicates which contain mainly aluminum ions in the octahedral sites. The first absorption region is between 3300 and 3800 cm.$^{-1}$ and the second between 900 and 960 cm.$^{-1}$. With a well crystallized and dry kaolinite in the first hydroxyl region, three distinct bands appear if a prism of high resolving power (CaF_2 or LiF prism) is used.[5–7] There is at present no generally accepted theoretical explanation for the multiplicity of the absorption bands in the hydroxyl region with solids such as gibbsite, brucite or clay minerals. Some authors[6,8–11] hence tried to correlate the

(1) Visiting Associate Professor, Department of Geophysics and Geochemistry, The Pennsylvania State University (1960–1961).

(2) P. Murray and F. White, *Trans. Brit. Cer. Soc.*, **54**, 137, 151, 189 (1955).

(3) G. W. Brindley and M. Nakahira, *J. Am. Cer. Soc.*, **40**, 346 (1957).

(4) J. B. Holt, I. B. Cutler and M. E. Wadsworth, *Am. Ceram. Soc. Bull.*, **39**, 187 (1960).

(5) H. Beutelspacher, *Landwirtsch. Forsch.*, **7**, 74 (1956).

(6) L. A. Romo, *J. Phys. Chem.*, **60**, 987 (1956).

(7) D. M. Roy and R. Roy, *Geochim. et Cosmochim. Acta*, **11**, 72 (1957).

(8) A. Auskern, M. S. Thesis, Pennsylvania State University, 1955.

(9) M. E. Wadsworth, T. L. Mackay and I. B. Cutler, *Bull. Amer. Cer. Soc.*, **33**, 15 (1955).

spectra in this region with the different degree of hydrogen bonding in clay minerals. Others[7] on the basis of deuterium exchange came to the conclusion that there is no simple correlation between OH-absorption frequencies in clays and types of hydroxyls or extent of hydrogen bonding. However, in spite of the fact that the "fine structure" of the absorption bands in the first hydroxyl region is poorly understood, there is no doubt that absorption in this region is due to the stretching vibrations of proton against oxygen. The location of the second hydroxyl region recently was experimentally established by the substitution of D^+ for H^+ under hydrothermal conditions.[12]

Stubičan[13] previously has studied the changes of infrared spectra in the first hydroxyl region with kaolin minerals and was able to show that the specimens obtained by relatively fast heating retain some of the protons even at high temperatures (600–800°). At the same time Kulbicki and Grim[14] have also adduced evidence for the retention of "water" in metakaolinite. However, to understand the mechanism of the proton retention at such high temperatures, more quantitative data are necessary which can be obtained using deuterium uptake, hydrothermal synthesis and infrared spectroscopy.

Furthermore, due to our extensive study[12,15] of the infrared spectra of synthetic layer structure silicates, it was possible to assign the absorption bands in the region 400–5000 cm.$^{-1}$ to the proper bonds and show the extreme sensitivity of the infrared spectra to the changes of the Metal—(O-Si) distances in such structures. It was interesting to study the extent to which infrared spectroscopy can reveal changes which occur on heating of clays and how the results obtained can be correlated with the present theories concerning the structure of high temperature phases.

Experimental

Materials.—The kaolinite used in this study was highly purified well crystallized Georgia kaolinite. The purification was done by sedimentation and the purity of material was checked carefully by X-rays. The specimen of halloysite from Eureka, which was used in its native form, was also highly pure and no other mineral such as gibbsite or micas could be detected by X-rays. For the resynthesis of the heated specimens of kaolinite and halloysite under hydrothermal conditions, D_2O was used the purity of which was claimed to be 99.5%.

Apparatus and Procedure.—Dehydration studies were carried out with a fully automatic thermobalance equipped with a Mauer magnetic recording analytical balance. The investigated specimens, usually 0.5 g., were heated in two flat Pt dishes (diameter = 27 mm.) which were suspended on a Pt wire in a Pt-wound furnace. The material to be heated was loosely spread in *thin layers* in order to minimize the possible influence of thickness and compaction on the obtained results. The rate of heating was 3°/min.

The synthesis of kaolinite-OD for the infrared investigation was done using specimens of kaolinite and halloysite heated in the thermobalance up to the desired temperature (650, 800, 900, 1000°). When the desired temperature was reached, the specimens were taken out of the furnace and immediately quenched into D_2O. The obtained suspension was transferred to a gold tube, and hermetically sealed. The hydrothermal synthesis of the kaolinite-OD was carried out in a "cold seal" or "test-tube" bomb previously described by Tuttle[16] and Roy and Osborn.[17] The condition of the synthesis was always kept constant at 305° and 30,000 p.s.i. for 20 days. In such a way a well crystallized kaolinite was obtained on which quantitative measurements of the residual OH-content with infrared spectroscopy was possible.

Infrared measurements were made with a Perkin–Elmer model 21 double beam spectrometer using an NaCl prism. The calibration curve for the quantitative estimation of OH-groups was obtained by mixing intimately 15.0, 7.5, 6, 4.5, 1.5 and 0.75 mg. of well-crystallized kaolinite with KBr to obtain 3 g. of mixture. Three hundred mg. of each mixture was pressed in a vacuum die under 70,000 p.s.i. for 3 min. into a window with the area of 1.2 cm.^{2}. With the specimens of kaolinite prepared hydrothermally in the presence of D_2O, always 30 mg. was mixed with KBr so that a 3 g. mixture was obtained. Three hundred mg. of each mixture was pressed under the same conditions as mentioned before.

Infrared spectra were obtained with the scanning speed 3, the gain 5–6, and for the quantitative measurements scale factor 4 cm./μ was used. The spectra of the heated specimens of kaolinite and pyrophyllite were obtained using a KBr prism, and the scale factor 1 cm./μ.

Results and Discussion

In Fig. 1 is shown the quantitative weight loss as a function of temperature (obtained on a recording thermobalance) for three specimens which differ in degree of crystallinity and particle size. These included halloysite (meta) and poorly crystallized kaolinite (obtained hydrothermally from metakaolinite at 300°, 1200 p.s.i. for two days) which represent disordered phase with small particle size, and well crystallized kaolinite from Georgia. The

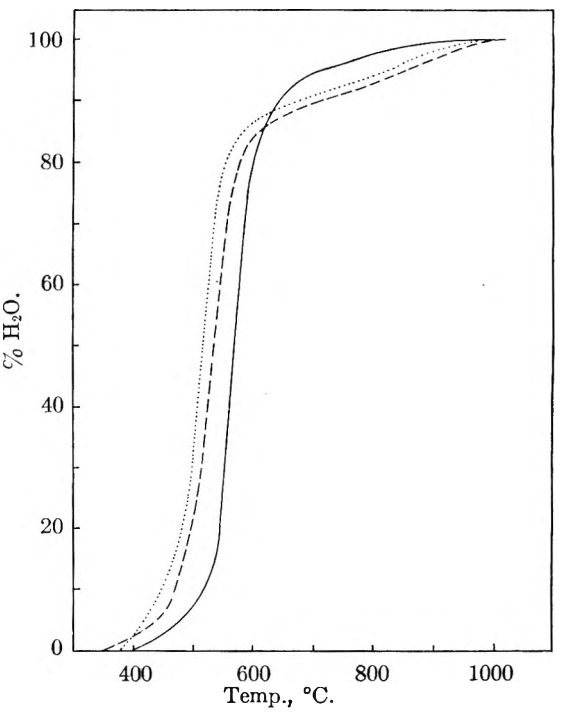

Fig. 1.—Typical weight loss *vs.* temperature curves obtained on a recording thermobalance for kaolinite, Georgia (full line), a disordered synthetic kaolinite (dotted line), and halloysite (meta), Eureka, Ind. (dashed line). The theoretical amount of "water" in kaolinite (13.9%) is expressed as 100%.

(10) H. Scholze and A. Dietzel, *Naturwiss.*, **42**, 342 (1955).
(11) H. W. van der Marel and J. H. L. Zwiers, *Silic. Ind.*, **24**, 349 (1959).
(12) V. Stubičan and Rustum Roy, *Z. Kristallogr.* (in press).
(13) V. Stubičan, *Min. Mag.*, **32**, 38 (1959).
(14) G. Kulbicki and R. E. Grim, *ibid.*, **32**, 53 (1959).
(15) V. Stubičan and Rustum Roy, *Am. Miner.*, **46**, 32 (1961).
(16) O. F. Tuttle, *Bull. Geol. Soc. Amer.*, **60**, 1727 (1949).
(17) R. Roy and E. F. Osborn, *Econ. Geol.*, **47**, 717 (1952).

early stage of dehydroxylation of disordered phases occurs about 50° below the ordered phase. Above 600°, however, the hydroxyls are released only very slowly as a function of temperature, so that these phases contain more hydroxyls than well ordered kaolinite heated above 600°. Due to the influence of stacking order and particle size it is difficult to expect that the absolute values for the energy of activation for such reactions will have much significance.

Quantitative infrared absorption measurements in the first hydroxyl region of the almost dehydrated samples yield values for the hydroxyl content which differ greatly from the thermobalance data (see Table I). These values were obtained by applying the calibration curve using well crystallized kaolinite as described earlier. The thermobalance indicated (under the conditions of our experiment), *e.g.*, that with Georgia kaolinite heated to 650°, 21% of the water is still present, while in the infrared pattern there is no indication at all of any absorption in the hydroxyl region with the same specimen. The remarkable difference in the amount of hydroxyl revealed in the infrared pattern brought out by re-constituting under pressure a long range order phase is illustrated in Fig. 2. Moreover, fair

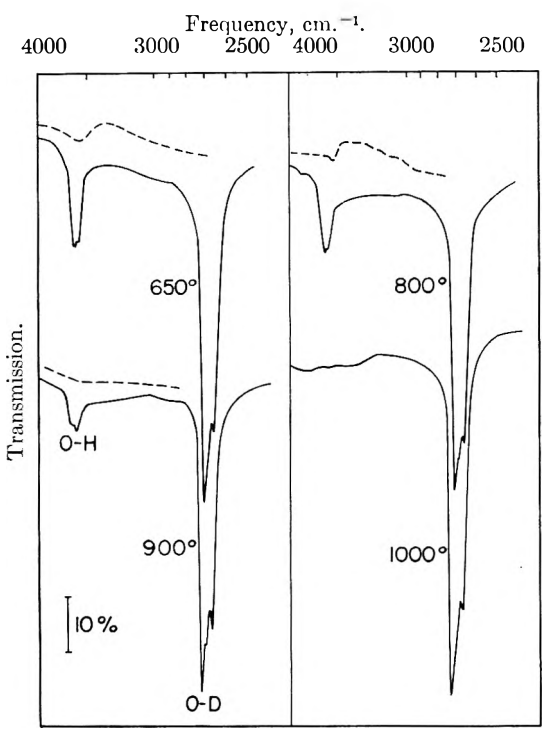

Fig. 2.—Influence of reconstitution of long order phase shown in the absorption in the OH-region with specimens of halloysite heated at various temperatures (dashed lines), and the same specimens after resynthesis with D_2O (full lines).

quantitative agreement can be obtained between the amount of hydroxyl groups obtained from the thermogravimetric and infrared measurements after *resynthesis* of kaolinite with D_2O from the heated specimens (Table I).

The experimental results reported above may be explained if one considers the possible influence of the surroundings in the crystals on the vibration

TABLE I

AMOUNT OF "WATER" LEFT AT DIFFERENT TEMPERATURES AS FOUND BY (A) THERMOBALANCE, (B) DIRECT INFRARED EXAMINATION, (C) AFTER RESYNTHESIS OF KAOLINITE WITH D_2O

The total of 13.9% "water" in kaolinite is expressed as 100%.

	A %	B %	C %
	Kaolinite, Georgia		
650°	21.0	0	[a]
800	2.5	0	2.3
900	0.4	0	0.5
1000	0.0	0	0.0
	Halloysite, Eureka		
650°	12.0	1.2	10.5
800	6.8	0.5	7.0
900	3.1	0.0	2.8
1000	0.0	0.0	0.0

[a] Quantitative determination was not possible due to the appearance of the absorption band at *ca.* 3 μ (Fig. 5).

modes involving stretching vibrations of the O–H bond. In a crystalline kaolinite the Al–OH distances as well as OH–O bonds are determined by the structure and fall within narrow limits, consequently the vibrations of proton against oxygen give rise to the well defined bands. In the almost dehydroxylated products it is clear that there is a wide spread of oxygen–proton distances in spite of the preservation of two dimensional order as shown by Roy, Roy and Francis.[18]

Recently Dachille and Roy[19] were able to show the relation between infrared spectra and the coordination of metal ions in simple compounds. Recorded spectra (in the region 11–25 μ) of the heated specimens of kaolinite show considerable differences compared with the spectrum of the original kaolinite (Fig. 3). To evaluate the obtained results it is convenient to compare these spectra with the spectra of the heated specimens of pyrophyllite (Fig. 4).

If mainly trivalent ions are present in the structure of a layer lattice silicate, a strong absorption band in the region 500–600 cm.$^{-1}$ appears. The frequency of this band depends on the Me^{3+}-(O-Si) distance and bond strength as was previously shown by Stubičan and Roy[12,15] who have described this band as Si–O–Al^{VI} for the case when aluminum ions are involved in the octahedral sites of a layer silicate.

With pyrophyllite heated at 650° (15 min.) or 750° (4 hours), one can observe the gradual displacement of the Si–O–Al^{VI} band from 545 to 565 cm.$^{-1}$, which indicates a small decrease in the Al–(O–Si) distance. The present understanding of the infrared spectra of such complex structures does not allow a more quantitative approach. However, as with all anhydrous aluminosilicates containing aluminum ions in sixfold coördination (*e.g.*, mullite, sillimanite), the frequency of the corresponding band is 560–565 cm.$^{-1}$, consequently the infrared spectra do not indicate the change of the coördination of aluminum in the dehydroxylated product of pyrophyllite. On the basis of X-ray data, Grim

(18) R. Roy, D. M. Roy and E. E. Francis, *J. Am. Ceram. Soc.*, **38**, 198 (1955).

(19) F. Dachille and R. Roy, *Z. Kristallogr.*, **111**, 462 (1959).

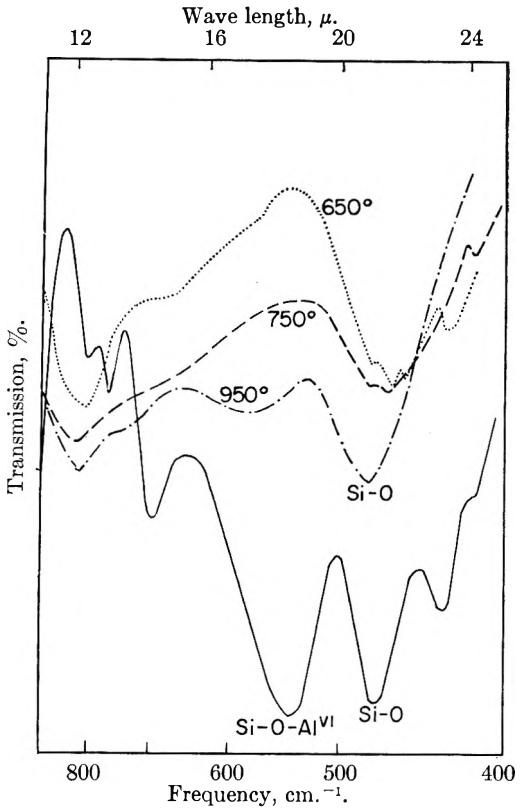

Fig. 3.—Infrared spectra of kaolinite, Georgia (full line) and of the same specimen heated at different temperatures, showing the influence of the change of coördination of Al.

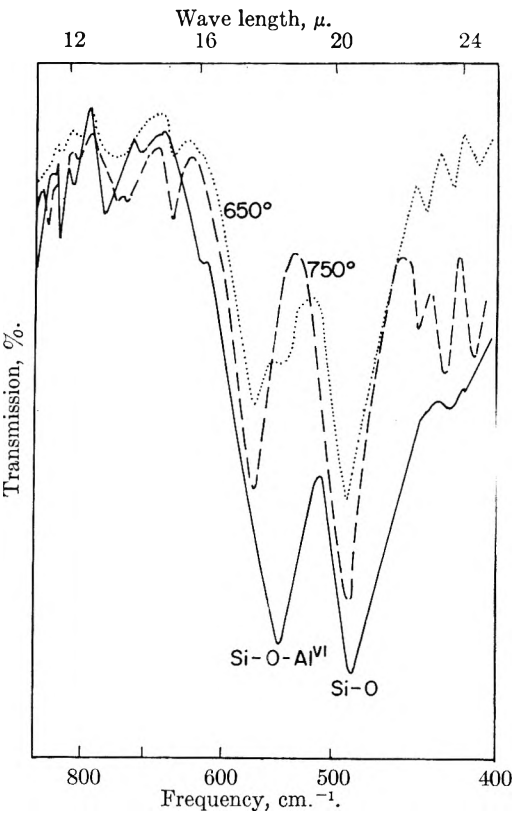

Fig. 4.—Infrared spectra of a synthetic pyrophyllite (full line) and of the same specimen heated at different temperatures, illustrating absence of a major coördination change for Al.

and Bradley[20] and Bradley and Grim[21] have proposed structures of dehydrated montmorillonite or muscovite with aluminum in sixfold coördination, which agree with our observations.

With heated specimens of kaolinite (Fig. 3) this same vibration mode completely disappears although it is in no way connected with OH ions, and the Si–O bending frequency moves slightly toward a lower value. The infrared spectrum of metakaolinite is, in fact, almost identical with the spectrum of analcite and an Al_2O_3–SiO_2 glass. There is this clearcut evidence for a major coördination change of the Al^{3+} and almost certainly a change to tetrahedral sites as in the glass and analcite, since the Al^{VI}–O–Si band is completely lost and certainly there is no major change in the coördination of the Si^{4+}. Unfortunately no new band corresponding to Al^{IV}–O–Si appears, but this is attributed to the overlapping with main Si–O stretching frequency at 800–1100 cm.$^{-1}$. The shift from the 560 cm.$^{-1}$ for Al^{VI}–O–Si is in the right direction and of the right magnitude for such a change. Thus the infrared spectra provide direct experimental proof of the change of the coördination in metakaolinite proposed by Buessem, *et al.*,[22] and also used in their dehydration scheme by Brindley and Nakahira.[23] It should be noted that a specimen of kaolinite heated at 950° shows a broad absorption band at 565 cm.$^{-1}$ which indicates the persistence of aluminum ions in sixfold coördination under these conditions.

Acknowledgment.—Work done on this study was sponsored by the American Petroleum Institute, Project 55.

(20) R. E. Grim and W. F. Bradley, *J. Am. Ceram. Soc.*, **23**, 242 (1940).

(21) W. F. Bradley and R. E. Grim, *Am. Miner.*, **36**, 182 (1951).

(22) L. Tscheischwili, W. R. T. Buessem and W. Weyl, *Ber. deut. ker. Ges.*, **20**, 249 (1939).

(23) G. W. Brindley and M. Nakahira, *J. Am. Cer. Soc.*, **42**, 314 (1959).

RADIATION CHEMISTRY OF NEOPENTANE[1]

BY RICHARD A. HOLROYD

Radiation Research Laboratories, Mellon Institute, Pittsburgh, Pa.

Received February 20, 1961

The products of the radiolysis of liquid neopentane have been examined in detail at several different dose rates and as a function of the concentration of isobutene. The major products from pure neopentane are those expected from reactions of hydrogen atoms and methyl, *t*-butyl and neopentyl radicals. The major unsaturate formed is isobutene. In addition there are unexpected products in the C_8 and C_9 region which result from the reaction of hydrogen atoms with isobutene. When large amounts of isobutene are present, radicals are also scavenged. A dose rate effect is observed in pure neopentane and is attributed mainly to the competition between methyl radicals abstracting hydrogen from neopentane and radical combination reactions, the latter being favored at high dose rates.

One of the difficulties encountered in detailed studies of the radiation chemistry of liquid hydrocarbons has been the large variety of products formed. This diversity of products precludes in many cases complete analysis of the system after irradiation and makes difficult any real understanding of the mechanisms which underlie the overall effects. For example, Dewhurst[2] has reported that in the radiolysis of *n*-hexane six different isomers of $C_{12}H_{26}$ are formed. Such a range of products seems to be largely the result of the formation of a number of different radical intermediates which are produced initially by the radiation. This present study was undertaken to examine the details of the radiation chemistry of neopentane, a molecule with only two types of chemical bonds. Since only hydrogen atoms and methyl, *t*-butyl and neopentyl radicals are expected to result from simple bond rupture one might expect the products to predominantly consist of ethane, neohexane, 2,2,3,3-tetramethylbutane, 2,2,4,4-tetramethylpentane and 2,2,-5,5-tetramethylhexane formed from radical combination reactions[3,4] and hydrogen and methane produced as a result of radical abstraction reactions. Abstraction of hydrogen atoms from neopentane by *t*-butyl radicals is expected to be unimportant[5] at room temperature. However, *t*-butyl radicals will disproportionate to isobutane and isobutene. Methyl and neopentyl radicals are not known to disproportionate in reactions between themselves because of the absence of β-hydrogens.

The only previous work reported on the radiolysis of liquid neopentane is that of Burton and coworkers[6,7] who have shown that under the conditions of their irradiations the yields of most products are temperature dependent over the range -196 to 50°. Major products reported were hydrogen, methane, ethane, isobutane, isobutene, isopentane, neohexane, octanes, nonanes and 2,2,5,5-tetramethylhexane. From this study it was concluded that both free radical and excited molecule reactions are involved and that part of the methane is formed by a primary rearrangement decomposition.

The present study was undertaken to identify as many as possible of the individual products formed in the radiolysis and to measure radiation yields at various dose rates and at different total absorbed doses.

Experimental

The neopentane used in most experiments was Phillips research grade (99.92% pure), which was purified further by passage through a trap containing degassed silica gel. This effectively removed all unsaturates detectable by gas chromatography. The main impurity, *n*-butane, was removed by degassing at -110°. In a few experiments the neopentane used was a standard sample from the American Petroleum Institute certified as being 99.978% pure. No difference was observed in the yields of products when this sample was used. Phillips research grade (99.51%) isobutene was used without further purification. Other hydrocarbons necessary for product identification were obtained from Phillips except 2,2,4,4-tetramethylpentane which was an API standard sample and 2,2,3,3-tetramethylbutane and 2,2,5,5-tetramethylhexane which were API uncertified samples (at least 98% pure).

For irradiation with Co-60 γ-rays, samples of from 1 to 20 ml. were sealed in Pyrex cells. The temperature of the irradiations was 22 ± 2° at which the vapor pressure of neopentane is approximately 1.5 atm. The volume of the vapor phase was minimized so that only from 2 to 5% of the absorbed energy was dissipated in the vapor phase. Absolute yields were calculated relative to the yield of the Fricke dosimeter [$G(Fe^{+++}) = 15.5$].

For Van de Graaff electron irradiations at 2.5 and 3.0 mev., 20-ml. samples of neopentane were sealed in thin window ($\sim$ 33 mg./cm.^{2}) Pyrex cells. In spite of the large vapor pressure of the neopentane, the thin windows did not rupture. The absorbed dose was determined in an absolute manner using the power input method.[8] A correction of 4% was made for attenuation of the electron energy in the windows assuming an energy loss of 1.73 mev. g.$^{-1}$ cm.$^{-2}$. By varying the current from 2×10^{-9} amp. to 10^{-6} amp. the dose rate in the irradiation zone was varied from 3×10^{16} to 15×10^{19} e.v. ml.$^{-1}$ sec.$^{-1}$ (3×10^6 to 15×10^9 rad./hr.).

After irradiation, samples were transferred to a vacuum line and the H_2 and CH_4 collected. These gases were measured in a microgas buret and analyzed mass spectrometrically. In most cases methane was also determined chromatographically. All other products were determined by gas chromatography. Samples were transferred from the vacuum line to the chromatograph in a U-tube equipped with 3-way stopcocks. In some runs the liquid neopentane was cooled to 0° and transferred to the chromatograph with a syringe also cooled to 0°. The two methods gave comparable results. For most analyses a 5-meter column packed with 25% Dow–Corning silicone grease on Celite was used. Isobutene was analyzed separately on a 2.5 m. column packed with a specially prepared silica gel which delayed the isobutene so that it was well separated from the large neopentane peak. Activated silica gel was used for determining all other gaseous hydrocarbons. For identification of unsaturated hydrocarbons in the C_5, C_8 and C_9 regions a column packed with 25% Carbowax-600 on Celite was used. Identifications of products were made by comparison of the retention times of the products with those of

(1) This work was supported, in part, by the U. S. Atomic Energy Commission.

(2) H. A. Dewhurst, *J. Phys. Chem.*, **62**, 15 (1958).

(3) A. E. de Vries and A. O. Allen, *ibid.*, **63**, 879 (1959).

(4) C. D. Wagner, *ibid.*, **64**, 231 (1960).

(5) P. J. Boddy and E. W. R. Steacie, *Can. J. Chem.*, **38**, 1576 (1960).

(6) M. Hamashima, M. P. Reddy and M. Burton, *J. Phys. Chem.*, **62**, 246 (1958).

(7) W. H. Taylor, M. Burton, and S. Mori, *J. Am. Chem. Soc.*, **82**, 5817 (1960).

(8) R. H. Schuler and A. O. Allen, *J. Chem. Phys.*, **24**, 56 (1956).

authentic samples on various columns. As confirmation, the various products in the C_8, C_9 and C_{10} region were collected separately and the mass spectrometric patterns were compared with authentic samples.

Results and Discussion

Products.—The major products of the radiolysis of neopentane found in this study are those suggested in the Introduction. In addition, however, there are several unexpected products. Three major peaks were observed in the C_8 region where only one, 2,2,3,3-tetramethylbutane, was expected (see Table I). By combined chromatographic and mass spectrometric techniques the additional components were shown to be 2,2,4-trimethylpentane and 2,4,4-trimethyl-1-pentene. The octene was usually formed in greater yield than the other two. In the C_9 region 2,2,5-trimethylhexane was found in addition to the expected nonane. There was also a nonene formed in small yield. Complete identification of this product was not made. In the C_5 region isopentane was observed as well as small amounts of 2-methyl-1-pentene and 2-methyl-2-pentene.

TABLE I

PRODUCTS IN THE C_8 AND C_9 REGION

Product	Mole % in C_8 fraction[a]	G[b]
2,2,4-Trimethylpentane	22	0.09
2,4,4-Trimethyl-1-pentene	43	.18
2,2,3,3-Tetramethylbutane	24	.08
Other C_8[c]	11	
	Mole % in C_9 fraction[a]	
2,2,4,4-Tetramethylpentane	64	0.24
2,2,5-Trimethylhexane	29	.09
Other C_9	7	...

[a] Percentages are based on mass spectrometric analyses of isolated fractions after samples were irradiated to ~ 40 megarads. [b] Yields are based on chromatographic analysis of a sample given a dose of ~ 9 megarads. The units for G are molecules/100 e.v. [c] A small peak at mass 110 indicated some octadiene or octyne must be present. The yield of 2,5-dimethylhexane was < 3%. A small amount (< 2%) of 2,4,4-trimethyl-2-pentene may be present.

Since the formation of several of the products in the C_8–C_9 region cannot be explained in terms of random combination of radicals formed by bond cleavage in neopentane, other processes must be invoked. Inspection of the structure of the three C_8 products reveals that they all could be formed by combination reactions of *t*-butyl radicals and isobutyl and methyl propenyl-1 radicals. Similarly the major C_9 products can be considered to result from the combination of neopentyl radicals with either isobutyl or *t*-butyl radicals. These sets of products suggest very strongly that in addition to the four radicals expected from simple bond cleavage, isobutyl and methyl propenyl-1 radicals are important intermediates in the radiolysis of neopentane. Their origin is discussed below.

Effect of Total Dose.—The yields of both H_2 and 2,2,5,5-tetramethylhexane decrease rapidly in the region where the absorbed dose is less than one megarad (Table II). A similar effect of dose on the hydrogen yield was reported by Hardwick[9] in the radiolysis of cyclohexane at doses greater than one megarad. The yield of isobutene is initially 2.4 but decreases to zero with prolonged irradiation. Isobutene actually reaches a very low steady state concentration of 0.007 *M*. Initially the radiation yields of isopentane, 2,2,4-trimethylpentane and 2,2,5-trimethylhexane are small but increase with dose to values of 0.21, 0.10 and 0.10, respectively.

The differences in the yields of H_2 and isobutene as reported in Table II and by Burton[7] can be explained, at least partially, as an effect of total dose. For example, Burton found $G_{H_2} = 1.57$ after total doses in the range 2 to 8 × 10^{19} e.v./ml. In Table II the yield of H_2 is reduced from its initial value of 2.4 to 1.68 after a total dose of 3.4 × 10^{19} e.v./ml.

Effect of Iodine.—Iodine was added to determine the methyl radical yield in irradiated neopentane. It was found that significant yields of several gaseous products are obtained even in the presence of

TABLE II

RADIATION YIELDS[a] USING Co^{60} γ-RAYS. SOURCE STRENGTH ≅ 50,000 RADS/HR.

Hr. of irradiation	1.2	3.0	7.2	17.0	50.0	69.0	124.	161.
Dose, e.v./ml. × 10^{-19}	0.23	.596	1.44	3.39	9.80	14.8	26.9	35.2
CH_4	...	...	3.76	3.51	3.86	3.8	4.1	3.6
H_2	2.57	2.2	2.02	1.68	1.57	1.33	...	...
C_2H_6	...	.42	.43	.50	...	.45	.48	.46
C_3H_6	...	.22	.20	.19	...	.17	.16	.14
i-C_4H_{10}	...	.56	.71	...	...	.42	.46	.33
i-C_4H_8	2.41	2.34	1.84	1.75	...	1.44	1.37	1.19
i-C_5H_{12}	...	.04	.06	.06	.11	...	.18	.21
2-Methyl-1-butene	...	.12	...	...	.05	...	.06	.11
2-Methyl-2-butene	...	.07	.07	.07	.06	...	.05	.10
2,2-Dimethylbutane	...	.28	.35	.45	.50	...	.57	.53
2,2,4-Trimethylpentane	...	.03	.05	.05	.07	.11	.11	.09
2,4,4-Trimethyl-1-pentene	...	.14	.16	.15	.16	.12	.18	.18
2,2,3,3-Tetramethylbutane	...	.05	.05	.08	.10	.07	.08	.08
2,2,4,4-Tetramethylpentane	...	.40	.48	.45	.32	.35	.31	.24
2,2,5-Trimethylhexane	...	0	~0	...	.10	.10	.10	.09
Nonene	...	0	...	...	...	.04	.06	.05
2,2,5,5-Tetramethylhexane	1.53	1.46	1.22	.96	.69	.63	.54	.43

[a] Yields are given in units of molecules/100 e.v.

(9) W. S. Guentner, T. J. Hardwick and R. P. Nejak, *J. Chem. Phys.*, **30**, 601 (1959).

iodine. The yields found for neopentane–iodine solutions ($\sim$ 0.03 M) using Co-60 γ-radiation are: CH_3I = 2.3, CH_4 = 1.66, H_2 = 1.05, i-C_4H_8 = 1.2, i-C_4H_{10} = 0.12, C_3H_6 = 0.14, and C_2H_6 = 0.35. Burton[7] has reported yields of 1.65, 1.1 and 0.82 for methane, hydrogen and isobutene, respectively. The agreement is good in each case except isobutene. It was found that the determination of isobutene was complicated by the presence of t-butyl iodide which decomposed on the silica gel column normally used for analysis. To avoid this difficulty isobutene was separated on a silicone grease column at room temperature in the iodine runs. This large yield of isobutene (1.2) with iodine present suggests there is a molecular process forming methane and isobutene simultaneously

$$\text{neo-}C_5H_{12} \longrightarrow CH_4 + i\text{-}C_4H_8$$

The persistence of small yields of ethane, propylene, and isobutane in the presence of iodine indicates that non-radical processes are involved here.

Effect of Dose Rate.—The yields of products from electron irradiation at various beam currents are shown in Table III. At very high dose rates

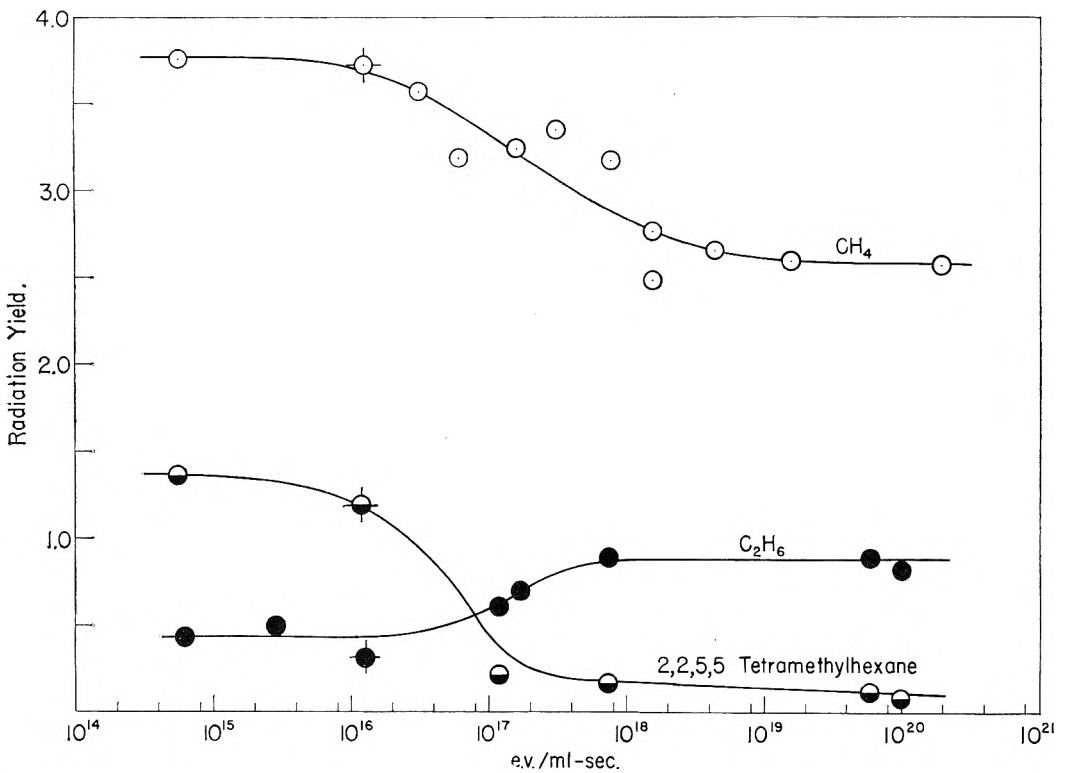

Fig. 1.—Dose rate dependence of radiation yields (molecules/100 e.v.). Flagged circles are the results of Burton, *et al.*, ref. 7.

TABLE III

RADIATION YIELDS[a] WITH 2.5 MV. ELECTRONS FROM A VAN DE GRAAFF

T = 23°

Beam current $\times 10^6$, amp.	0.1	0.3	1.0	10.	10.	10.	100
Dose rate, e.v. ml.$^{-1}$-sec.$^{-1}$[b]	1×10^{17}	2×10^{17}	7×10^{17}	6×10^{19}	6×10^{19}	6×10^{19}	$\sim 10^{20}$
(CH_4)[c]	(3.2)	(3.1)	(2.9)	(2.6)	(2.6)	(2.6)	(2.6)
H_2	1.25	1.3	...	1.2	...	...	1.2
C_2H_6	.61	.71	.90	.85	.91	1.22	.83
C_3H_6	.20	...	.26	.20	.20	.17	.19
i-C_4H_{10}	.61	...	.73	.26	.35	...	...
i-C_4H_8	1.66	...	1.94	1.21	1.30	...	...
i-C_6H_{12}	.13	.17	.26	...	.27	...	...
2,2-Dimethylbutane	.72	.71	.96	.69	.81	.78	.65
2,2,4-Trimethylpentane	.10	.08	.09	.09	.08	.08	.07
2,4,4-Trimethyl-1-pentene	.10	.09	.21	.09	.14	.13	.16
2,2,3,3-Tetramethylbutane	.08	.07	.09	.06	.11	.11	.09
2,2,4,4-Tetramethylpentane	.19	.16	.21	.15	.17	.17	.11
2,2,5-Trimethylhexane	.06	.06	.05	.05	.06	.06	.05
2,2,5,5-Tetramethylhexane	.21	.18	.13	.11	.15	.13	.09

[a] Samples received a dose of $\sim$2 to 8 megarads. Yields in units of molecules/100 e.v. [b] The absorbed dose in these experiments was estimated from the rate of CH_4 formation. [c] Methane yields in these runs were interpolated from the curve of G_{CH_4} *vs.* dose rate in Fig. 1.

the yields appear to be independent of dose rate and to not change greatly with total dose in the range from 2 to 8 megarads. However, the results contrast greatly with the results of Co-60 γ-irradiation. Figure 1 shows the results at different dose rates. The yields of CH_4, H_2 and 2,2,5,5-tetramethylhexane are lower at the higher dose rates, whereas C_2H_6 and neohexane increase as the rate of energy absorption increases. Only slight changes are observed in the yields of other products.

Part of the dose rate effect can be understood as a competition between methyl radical abstraction (1)

$$CH_3 + \text{neo-}C_5H_{12} \longrightarrow CH_4 + \text{neo-}C_5H_{11} \quad (1)$$

which is important at low dose rates, *versus* combination with radicals, which is important at high dose rates. The major radical species present, besides methyl, are *t*-butyl and neopentyl. Thus methyls can be removed at high dose rates by (2), (3) and (4a).

$$CH_3 + CH_3 \longrightarrow C_2H_6 \quad (2)$$

$$CH_3 + \text{neo-}C_5H_{11} \longrightarrow \text{neo-}C_6H_{14} \quad (3)$$

$$CH_3 + t\text{-}C_4H_9 \longrightarrow \text{neo-}C_5H_{12} \quad (4a)$$

The yield of ethane using Co-60 γ-radiation is 0.45 most of which is a molecular yield since $G_{C_2H_6}$ = 0.35 with I_2 present. The increase in yield to 0.9 (Fig. 1) at high dose rates represents the contribution of reaction 2. At high dose rates reaction 1 is suppressed by the competing reactions and the yields of products formed from neopentyl, such as 2,2,5,5-tetramethylhexane, are lowered. In this case the yield is lowered more than expected from suppression of (1) because of secondary reactions (see below) occurring at the relatively large ($\sim$ 5 megarads) doses used in these experiments.

At high dose rates the methane yield is 2.6 while the iodine scavenging experiments indicate that the molecular yield is 1.66. It is suggested that the following reaction accounts for the excess methane at high dose rates

$$CH_3 + t\text{-}C_4H_9 \longrightarrow CH_4 + i\text{-}C_4H_8 \quad (4b)$$

The ratio $k_{4b}/\!/k_{4a}$ is known to be 0.9 in the gas phase.[10] From the present results the value of this ratio is about 2.0, assuming that reaction 4a accounts for all methyls not reacting in (2), (3), and (4b).

From inspection of Fig. 1 it can be seen that the methane and ethane yields are changing most rapidly at an intermediate dose rate of approximately 10^{17} e.v. ml.$^{-1}$ sec.$^{-1}$. The dose rate at which the yields are expected to change as a result of competition of reaction 1 with 2, 3 and 4 can be calculated from the known values of rate constants. Taking $k_1 = 2 \times 10^{-20}$ ml. molecule^{-1} sec.$^{-1}$,[5] and $k_2 = k_3k_4 = 7 \times 10^{-12}$ ml. molecule^{-1} sec.$^{-1}$,[11] the calculated value is 10^{17} e.v. ml.$^{-1}$ sec.$^{-1}$. The observed dose rate dependence is seen, therefore, to be in complete accord with other kinetic information.

Effect of Isobutene.—Although pentenes are not formed in large yield in the radiolysis of neopentane, isobutene is formed initially in high yield ($G \sim 2.4$). As the radiolysis progresses the yield of isobutene decreases rapidly with dose and a steady state is reached at 0.007 *M* isobutene. Other investigators already have shown that unsaturates are important intermediates in the radiolysis of hydrocarbons.[12–14] Burton and co-workers[7] also have suggested that the H_2 yield in the radiolysis of solid neopentane at $-78°$ is low because of the addition of H-atoms to isobutene.

With the above in mind a study of the effect of added isobutene was initiated in hopes that the role of isobutene in the radiolysis would be thereby elucidated. In the first few runs with 1 mole % added initially an unusually large increase was observed in the yields of 2,2,4-trimethylpentane and 2,4,4-trimethyl-1-pentene. Isobutene was consumed in these experiments. A thorough study was then made in which the average isobutene concentration was varied over the range from 6×10^{-4} to 0.2 *M*. The results are shown in Figs. 2a and 2b.

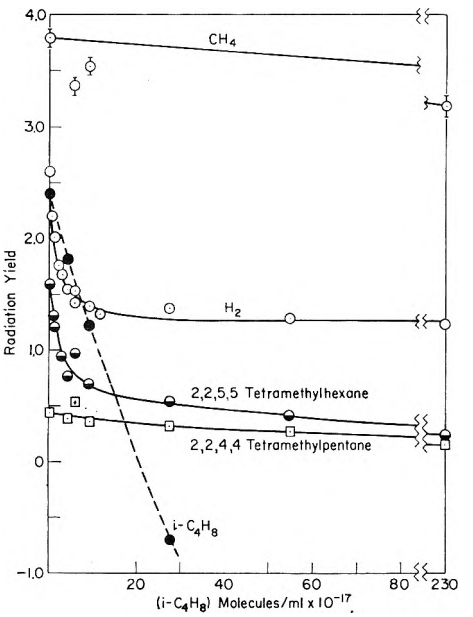

Fig. 2a.—Yields as a function of isobutene concentration.

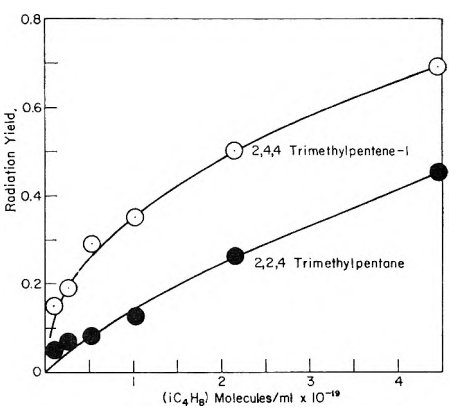

Fig. 2b.—Yields as a function of isobutene concentration.

(10) G. R. McMillan, *J. Am. Chem. Soc.*, **82**, 2422 (1960).

(11) The rate constant for combination of ethyl radicals in liquid ethane: R. W. Fessenden and R. H. Schuler, *J. Chem. Phys.*, **33**, 935 (1960).

(12) T. J. Hardwick, *J. Phys. Chem.*, **64**, 1623 (1960).

(13) P. J. Dyne and J. W. Fletcher, *Can. J. Chem.*, **38**, 851 (1960).

(14) R. A. Back, *J. Phys. Chem.*, **64**, 124 (1960).

In the region where the isobutene concentration is between 0 and 20×10^{17} molecules/ml. the yields of H_2, 2,2,5,5-tetramethylhexane and isobutene formation decrease rapidly (Fig. 2a). At the same time the yield of methane drops only slightly. For isobutene concentrations above 20×10^{17} molecules/ml., G_{H_2} is constant at an average value of 1.28, but the radiation yields of 2,2,4,4-tetramethylpentane and 2,2,5,5-tetramethylhexane are further reduced to minimum values of 0.05 and 0.25, respectively and $G_{i\text{-}C_4H_8}$ is negative and large. The 2,2,4-trimethylpentane and 2,4,4-trimethyl-1-pentene yields are greatly enhanced by isobutene (see Fig. 2b). The yields of the pentenes, 2,2,5-trimethylhexane, isopentane and the nonene also increase with increasing isobutene concentration. Both ethane and neohexane appear to have constant yields independent of isobutene concentration: $G_{C_2H_6} = 0.48$, $G_{C_6H_{14}} = 0.36$. For concentrations of isobutene above 2 mole % all yields decrease and higher molecular weight products (above C_{10}) are formed in substantial quantities.

It appears from the foregoing results that the radiation chemistry of neopentane is complicated by reactions of intermediates with a product, isobutene. The yield of hydrogen from a sample of pure neopentane is 2.6 after a dose of 50,000 rad., but after a dose of only 300,000 rad. the hydrogen yield is reduced by 25%. The isobutene yield is similarly reduced by larger and larger doses. The results are best explained by assuming that isobutene is an efficient scavenger for thermal H-atoms; thus

$$H + \text{iso-}C_4H_8 = t\text{-butyl} \qquad (5a)$$

$$= \textit{iso}\text{-butyl} \qquad (5b)$$

$$= H_2 + CH_2{=}C(CH_3){-}CH_2 \qquad (5c)$$

$$H + \text{neo-}C_5H_{12} = H_2 + \text{neo-}C_5H_{11} \qquad (6)$$

As isobutene depresses the yield of H_2 from reaction 6 the yield of products from neopentyl (C_9 and C_{10}) should also decrease simultaneously. The reaction of H-atoms with isobutene would be expected to produce mainly *t*-butyl radicals. Isobutyl radicals are expected, also, and in addition methyl propenyl radicals would result from hydrogen abstraction. These are the radicals postulated earlier as responsible for the formation of unexpected products in the C_8 and C_9 regions. These products are formed in reactions of the resultant radicals.

With reactions 5 and 6 the following kinetic expression is obtained for the ratio of yields, $G_H/[G_{H_2}(o)-G_{H_2}(s)]$, at a given isobutene concentration[12]

$$\frac{G_H}{G_{H_2}(o) - G_{H_2}(s)} = \frac{k_6(\text{neo-}C_5H_{12})}{(k_{5a} + k_{5b})(i\text{-}C_4H_8)} + \frac{k_{5c}}{k_{5a} + k_{5b}} + 1$$

where $G_{H_2}(o) = 2.6$, the initial yield of hydrogen from neopentane; $G_H = 1.5$, the yield of thermal hydrogen atoms; and $G_{H_2}(s)$ is the yield of hydrogen in the presence of isobutene. A plot of the left-hand side of the above equation *vs.* $(\text{neo-}C_5H_{12})/(i\text{-}C_4H_8)$ for the present results is shown in Fig. 3. The value of $(k_{5a} + k_{5b})/k_6$ as determined by a least squares calculation is 3.3×10^4; that is, hydrogen atom addition to isobutene is 33,000 times faster

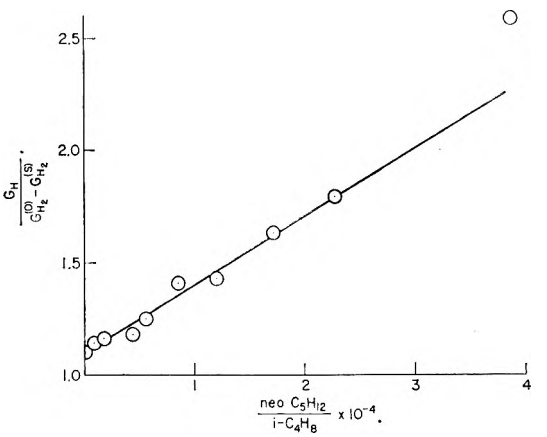

Fig. 3.—Kinetic plot of $G_H/[G_{H_2}(o) - G_{H_2}(s)]$ *vs.* neo-C_5H_{12}/i-C_4H_8.

than hydrogen atom abstraction from neopentane. From gas phase studies it is known that at room temperature reactions 5 and 6 have collision efficiencies of 6×10^{-4} [15] and 2×10^{-8}, [16] respectively. The fact that the present result is in excellent agreement with the ratio of these two collision efficiencies *i.e.*, 3×10^4, gives considerable weight to the importance of hydrogen atoms as intermediates in this radiolysis. The value of the intercept gives $(k_{5a} + k_{5b})/k_{5c} = 10.6$. For comparison Hardwick[12] found that the value of this ratio was 2.0 for hexene-1.

It is difficult from the present data to estimate the relative importance of reactions 5a and 5b because of limited data on the extent of disproportionation of these radicals in liquid hydrocarbons. However from the ratio of yields of 2,4,4-trimethyl-1-pentene and 2,2,4-trimethylpentane with added isobutene it is estimated that k_{5c} is approximately equal to k_{5b}. Combining this with the value of $(k_{5a} + k_{5b})/k_{5c}$ above leads to the value $k_{5a}/k_{5b} \cong 10$. That is, *t*-butyl radicals are the major product of reaction 5.[17] However, the yield of 2,2,3,3-tetramethylbutane is only 0.05 initially and increases only slightly with added isobutene. This is at first rather surprising but is in accord with previous kinetic information since it is known that *t*-butyl radicals disproportionate at a rate 4.6 times their rate of combination in the gas phase.[18] The present results can be used to estimate the ratio of disproportionation to combination. The largest source of isobutane is reaction 7; only a small yield ($G = 0.12$) is

$$2\ t\text{-}C_4H_9 \longrightarrow i\text{-}C_4H_8 + i\text{-}C_4H_{10} \qquad (7)$$

$$\longrightarrow 2,2,3,3\text{-tetramethylbutane} \qquad (8)$$

produced in a non-radical process. The ratio $(G_{i\text{-}C_4H_{10}} - 0.12)/G_{C_8H_{18}} = k_7/k_8$ is approximately 7 for the few runs in which isobutane was determined.

Although millimolar quantities of isobutene are sufficient to reduce the hydrogen yield, greater concentrations are necessary to suppress the methane

(15) P. E. M. Allen, H. W. Melville and J. C. Robb, *Proc. Roy. Soc.* (*London*), **A218**, 311 (1953).

(16) W. R. Trost and E. W. R. Steacie, *J. Chem. Phys.*, **16**, 361 (1948).

(17) R. W. Fessenden and R. H. Schuler (private communication) using EPR techniques have observed that *t*-butyl radicals are the major radical species present in liquid neopentane at 0° during irradiation with an electron beam from a Van de Graaff accelerator.

(18) J. W. Kraus and J. G. Calvert, *J. Am. Chem. Soc.*, **79**, 5921 (1957).

yield. A yield of methane of $\cong$ 2.2 is reached at 0.2 M isobutene. This indicates that methyl radicals are reacting according to

$$CH_3 + i\text{-}C_4H_8 = C_5H_{11} \qquad (9)$$

instead of reaction 1 when the isobutene concentration is great enough. The pentenes and isopentane which are found as products would be formed by disproportionation reactions of the pentyl radical formed in (9).

Since reactions 2, 3 and 4 are radical–radical reactions and can be neglected at the low intensity used, the methane yields should be represented by the kinetic equation

$$\frac{G_r}{G_{CH_4}(o) - G_{CH_4}(s)} = \frac{k_1}{k_9}\frac{(C_5H_{12})}{(i\text{-}C_4H_8)} + 1$$

where G_r is the yield of methyl radicals, equal to be 2.3. Evaluation of the constants from Fig. 4 gives

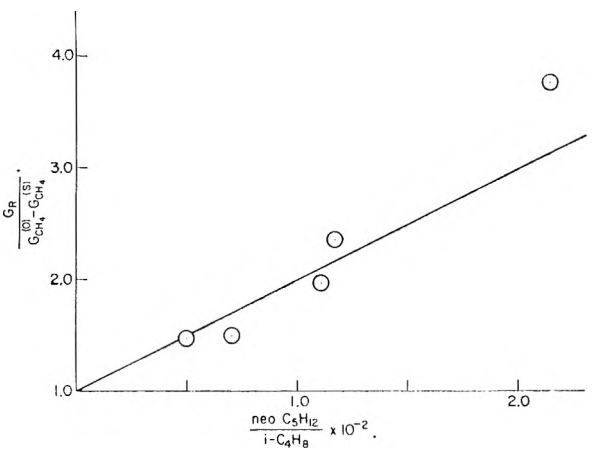

Fig. 4.—Kinetic plot of $G_r/[G_{CH_4}(o) - G_{CH_4}(s)]$ *vs.* neo-$C_5H_{12}/i\text{-}C_4H_8$.

$k_9/k_1 = 100$. For comparison, Szwarc[19] has found $k_9/k_{10} = 54$ in liquid octane at 22°.

$$CH_3 + \text{2,2,4-trimethylpentane} \longrightarrow CH_4 + C_8H_{17} \qquad (10)$$

It is expected that *t*-butyl radicals also add to isobutene.

$$t\text{-}C_4H_9 + i\text{-}C_4H_8 \longrightarrow CH_3\text{—}\underset{\displaystyle CH_3}{\overset{\displaystyle CH_3}{\underset{|}{\overset{|}{C}}}}\text{—}CH_2\text{—}\underset{\displaystyle CH_3}{\overset{\displaystyle CH_3}{\underset{|}{\overset{|}{C}}}}\text{—}CH_3 \qquad (11)$$

The C_8 radical thus formed would be expected to disproportionate with other radicals. This process would contribute to the yield of unexpected C_8 products at intermediate isobutene concentrations. Above one mole % isobutene, the yields of all products are reduced and higher molecular weight products are formed as a result of the addition of the product radicals to the unsaturated materials present.

Results at High Dose Rates.—The yields reported in Table III for electron beam irradiations at high dose rates are for total doses of approximately 5×10^6 rad. Therefore enough isobutene was present as a product of the irradiation to affect the results. For example, G_{H_2} is seen to have an average value of 1.24, the same as the yield of hydrogen with isobutene added initially (Fig. 2a). This suggests that all thermal hydrogen atoms have been effectively scavenged. The production of neopentyl radicals is thereby reduced from suppression of reaction 6. Reaction 1 is unimportant at high intensities thus eliminating another source of neopentyl radicals. It is not surprising therefore that the yield of 2,2,5,5-tetramethylhexane is low, *i.e.*, 0.14. This low value at high dose rates indicates that a major fraction of the neopentyl radicals are formed in the radiolysis as a result of abstraction reactions, *i.e.*, (1) and (6).

Ion–molecule Reactions.—It has been shown that hydride-ion transfer reactions occur in the ionization chamber of a mass spectrometer using neopentane vapor.[20] The largest peak in the mass spectrum is 57, that of the *t*-butyl ion, but this ion is not believed to undergo a hydride ion transfer reaction with neopentane. The next largest peak is mass 41, therefore reaction 12

$$C_3H_5^+ + \text{neo}C_5H_{12} \longrightarrow C_5H_{11}^+ + C_3H_6 \qquad (12)$$

would be the important ion molecule reaction. However, little propylene (G = 0.21) is formed in the radiolysis and from a consideration of the energetics of reaction 12 the pentyl ion formed will have the tertiary structure.[20] On neutralization these ions would form *t*-pentyl radicals. However, the major products of the radiolysis are not characteristic of *t*-pentyl radicals; *i.e.*, the C_{10} product is 2,2,5,5-tetramethylhexane, indicating the pentyl radical intermediates have the neo-structure. If it is assumed that *t*-pentyl radicals disproportionate, then larger yields of isopentane and 2-methylbutene would have been formed. From the above it must be concluded that hydride ion transfer reactions are at most of minor importance in the radiolysis of liquid neopentane.

It appears instead that known radical reactions will account for a major fraction of the products of the radiolysis. Although considerable amounts of hydrogen, methane and isobutene as well as smaller amounts of ethane and propylene are formed in molecular processes, a satisfactory and consistent interpretation of the results is possible in terms of radical abstraction, combination and disproportionation steps.

(19) M. Feld and M. Szwarc, *J. Am. Chem. Soc.*, **82**, 3791 (1960).

(20) F. H. Field and F. W. Lampe, *J. Am. Chem. Soc.*, **80**, 5587 (1958).

THORIUM EXTRACTION BY DI-*n*-DECYLAMINE SULFATE IN BENZENE

By W. J. McDowell and Kenneth A. Allen

Chemical Technology Division, Oak Ridge National Laboratory,[1] *Oak Ridge, Tennessee*

Received February 22, 1961

The extraction of thorium from acidic sulfate aqueous systems by di-*n*-decylamine sulfate in benzene is inversely dependent on sulfuric acid activity and sulfate ion concentration. At low thorium levels, thorium distribution coefficients are independent of the total thorium concentration, and at high thorium levels the organic thorium molarity levels off at a value corresponding to $n = 6 \pm 1$ equivalents of amine sulfate per thorium sulfate. This approximate complex composition was confirmed by measurements of the acid transfers accompanying thorium extraction, according to the equilibrium $nx\overline{RH_2SO_4} + (n/2)(1 - x)\overline{R_2H_2SO_4} + Th(SO_4)_2 = \overline{R_nH_nTh(SO_4)_{2+n/2}} + nx/2H_2SO_4$, where $R = (C_{10}H_{21})_2NH$ and $x = [\overline{RH_2SO_4}]/([\overline{RH_2SO_4}] + 2[\overline{R_2H_2SO_4}])$. Measurements of the thorium distributions as a function of aqueous sulfuric acid activity, at constant sulfate ion molarity, permitted computation of an equilibrium constant for this reaction, and in addition provided a simultaneous, independent evaluation of n which was in good agreement with the results from extraction isotherm analysis and acid transfer. At low aqueous ionic strength, the thorium extraction coefficient variation with amine sulfate concentration was anomalously dependent on the mode of equilibration. As was the case with uranium, the coefficients observed with slow stirring were significantly higher than with vigorous agitation.

Introduction

Amine extraction processes for obtaining thorium and uranium from its ores have been demonstrated,[2] and the associated chemistry has been investigated in both the sulfate and nitrate systems.[3,4] While amines of different classes and structures exhibit important differences in extracting thorium and uranium[5] it has been shown that with a given amine many aspects of the behavior of thorium sulfate are similar to those observed in the case of uranyl sulfate. For example, loading numbers, which are obtained by saturating the organic phases with thorium, are in the range of from three to four amine sulfates per thorium, and the extraction coefficients ($E = [Th]_{org}/[TH]_{aq}$) are inversely dependent on the aqueous sulfate ion concentration. Also, the coefficients increase with sulfuric acid molarity up to the point corresponding to formation of the normal amine sulfate, and then decrease markedly at higher acid activities.[3] The present investigation was undertaken with a view toward further understanding of these phenomena. As in previous studies with both uranium and sulfuric acid,[4,6] the extractant was di-*n*-decylamine in benzene. In addition to the advantages accruing from long familiarity with this amine–solvent system, its thorium extraction coefficients *vs.* the acidic sulfate aqueous phases of interest were in a range suitable for the use of classical analytical methods.

Experimental

Materials.—Di-*n*-decylamine (DDA) was obtained from Eastman as technical grade material (*ca.* 90% DDA) and purified by precipitating its bisulfate from benzene on equilibration with 4 *M* H_2SO_4. The precipitate was washed with benzene three times, the solid bisulfate being separated by centrifugation. The bisulfate then was reconverted to the free amine with aqueous NaOH. The equivalent weight of the resulting amine was 298 (theor. 297.6), and its amine assay was <0.5% primary, >99% secondary, and <0.5% tertiary.

The thorium sulfate was prepared by adding sulfuric acid to a 1 *M* solution of $Th(NO_3)_4$. The resulting $Th(SO_4)_2$ was recrystallized three times from 0.03 *M* H_2SO_4. Analyses indicated this material to have a $Th:SO_4$ ratio of 1:1.99. The nitrate content was <0.005% and chloride was <0.002%. Other chemicals used were standard reagent grade.

Procedures.—The majority of the equilibrations were done by contacting the two liquids in a completely enclosed apparatus in which paddles rotated at 60 r.p.m. stirred both phases without breaking the interface. Some equilibrations were done by the more usual procedure of vigorous agitation in separatory funnels, a mechanical shaker operating at *ca.* 200 strokes per minute being used. Temperatures were maintained at 25 ± 0.05°. Further mechanical details of these two methods of equilibration have been described elsewhere.[7] The amine sulfate (DDAS) solutions were prepared by pre-equilibrating DDA in benzene with an appropriate sodium sulfate–sulfuric acid aqueous phase before the thorium distributions were measured. The aqueous thorium analyses were done colorimetrically, using thoron.[8] For aqueous phases which contained less than 2 p.p.m., or which contained sodium sulfate, the thorium was concentrated by re-extraction into a secondary amine in chloroform. Aliquots of the organic phase were then evaporated, and the amine was destroyed with nitric and perchloric acids. The residue thus contained only the thorium with a small amount of sulfuric acid (that equivalent to the amine used). Since the reliability of the thorium separation by this method was greater than that of the colorimetric determinations, the analytical uncertainty depended on the total amount of thorium available, being ±5% for aliquots containing over 50 μg. and ±10% from 20 to 50 μg. Other pertinent analytical methods have been described elsewhere.[4,6]

Results and Discussion

Extraction Isotherms.—Typical isotherms, illustrating the dependence of the organic thorium concentration on the equilibrium aqueous thorium concentration, with all other parameters held constant, are shown in Fig. 1. The approximately unit slope at low thorium levels indicates equal numbers of thorium atoms per particle in the two phases. Since it has been reasonably well established that in these acidity and ionic strength regions the aqueous thorium is monomeric,[9] it follows that the organic thorium species is monomeric with respect to thorium also. The plateau

(1) Operated for the U. S. Atomic Energy Commission by Union Carbide Nuclear Company.

(2) K. B. Brown, C. F. Coleman, D. J. Crouse, C. A. Blake and A. D. Ryon, Paper 509, Internatl. Conf. on Peaceful Uses of Atomic Energy, Geneva, 1958; D. J. Crouse and K. B. Brown, *Ind. Eng. Chem.*, **51**, 1461 (1959).

(3) C. Boirie, Doctoral Dissertation, University of Paris, May 20, 1959, pp. 37–42; D. J. Carswell and J. J Lawrance, *J. Inorg. and Nuclear Chem.*, **11**, 69 (1959).

(4) K. A. Allen, *J. Am. Chem. Soc.*, **80**, 4133 (1958); W. J. McDowell and C. F. Baes, *J. Phys. Chem.*, **62**, 777 (1958).

(5) C. F. Coleman, K. B. Brown, J. G. Moore and K. A. Allen, Paper 510, Internatl. Conf. on Peaceful Uses of Atomic Energy, Geneva, 1958.

(6) K. A. Allen, *J. Phys. Chem.*, **60**, 943 (1956).

(7) K. A. Allen and W. J. McDowell, *ibid.*, **64**, 977 (1960).

(8) We are indebted to the Analytical Division, Oak Ridge National Laboratory, for numerous carefully performed aqueous thorium determinations.

(9) K. A. Kraus and R. W. Holmberg, *J. Phys. Chem.*, **58**, 325 (1954); E. L. Zebroski, H. W. Alter and F. K. Heumann, *J. Am. Chem. Soc.*, **73**, 5646 (1951).

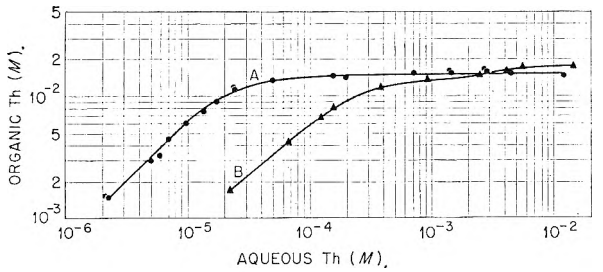

Fig. 1.—Thorium extraction from (A) 0.995 *M* Na_2SO_4–0.005 *M* H_2SO_4 and from (B) 0.75 *M* Na_2SO_4–0.25 *M* H_2SO_4 by 0.1 *N* DDAS in benzene.

heights indicate an average of 6 ± 1 equivalents of amine sulfate per thorium in the organic complex.

Complex Composition.—The number of equivalents of amine associated with each mole of thorium has been obtained by three independent methods. The first of these, which depends on saturating the organic phase with thorium, was mentioned in the preceding section. The other two methods yield results at low thorium–amine ratios as well as at high ones. The second method depends on the amount of acid transferred to the aqueous from the organic phase on the extraction of a known quantity of thorium. It is assumed that the thorium complexes only with the amine sulfate and not with the bisulfate, and that the fraction of the uncomplexed amine which is in the bisulfate form is not affected by the presence of organic phase thorium. These considerations lead to the following equilibrium expression (where R = $(C_{10}H_{21})_2NH$, and $x = [RH_2SO_4]/([RH_2SO_4] + 2[R_2H_2SO_4])$

$$nxRH_2SO_4 + (n/2)(1-x)R_2H_2SO_4 + Th(SO_4)_2 \rightleftharpoons R_nH_nTh(SO_4)_{(n/2)+2} + (nx/2)H_2SO_4 \quad (A)$$

from which it follows that for each mole of thorium extracted, $nx/2$ moles of sulfuric acid are transferred to the aqueous phase. The results of actual acid transfer measurements and subsequent computations based on equation (A) are presented in Table I. The values obtained by the two methods of equilibration are in good agreement and the amine–thorium association numbers obtained by acid transfer agree reasonably well with those obtained from plateaus in the equilibrium curves.

TABLE I

AMINE–THORIUM COÖRDINATION NUMBER BY ACID TRANSFER ON EXTRACTION OF THORIUM

Amine concentration 0.1039 *N*, equilibrium organic thorium concentration 0.0100 *N*, in all cases.

Aqueous acid, *N* Initial	Final	*x*	*n*
	By vigorous agitation		
0.1457	0.1550	0.187	5.0
.1916	.2037	.229	5.3
.2937	.3105	.309	5.4
.3601	.3796	.348	5.6
.4176	.4387	.384	5.5
	By limited interface equilibration		
0.1400	0.1496	0.180	5.3
.1800	.1917	.228	5.1
.2802	.2959	.311	5.1
.3393	.3591	.350	5.7
.3998	.4208	382	5.5

The third method of determining *n* is based on the use of extraction data at constant aqueous $[SO_4^=]$ and varying sulfuric acid activity. These data and the method of obtaining them are discussed in the following section. The value determined by this method, $n = 7$, probably is less accurate than either of the other two; however, it lends support, from an independent source, to the general range of values already established.

Process development studies with similar amines at this laboratory and elsewhere[10] also have generally indicated loading numbers in the range 6 to 8. This range of reported numbers suggests that there may be more than one thorium–amine sulfate compound in the organic phase. Coördination numbers of both 6 and 8 have been attributed to thorium.[11] If coördination to the thorium ion is through the sulfate oxygens then the number of amines associated with each thorium ion could vary between 2 and 16 since sulfate can act either as a monodentate or bidentate coördinating group.[12] The data, however, appear to eliminate the lower and most of the higher numbers in this range.

Acid Activity Dependence.—Examination of thorium extraction as a function of sulfuric acid activity was done at constant sulfate ion concentration. Solutions of 0.3 *M* sulfate ion but varying acid activity were prepared according to sulfuric acid activity relationships compiled by Baes.[13] Titrations of the acid contents of 0.10 *N* amine sulfate solutions equilibrated with these aqueous Na_2SO_4–H_2SO_4 solutions showed that the organic sulfate levels were in good agreement with the results of earlier work.[4,6] These organic phases then were contacted with an equal volume of a solution of the same Na_2SO_4–H_2SO_4 composition as that with which they had been pre-equilibrated but containing 0.005 *M* $Th(SO_4)_2$. The thorium concentration in the organic phase was thus sufficiently low to avoid loading complications. The resulting thorium extraction coefficients are listed in Table II. The decreasing thorium extraction with increasing sulfuric acid activity probably is due to competition for the amine sulfate between thorium and sulfuric acid according to equation (A).

TABLE II

AQUEOUS AND ORGANIC PHASE COMPOSITIONS FOR THORIUM EXTRACTIONS AT CONSTANT SULFATE ION MOLARITY

(Amine constant at 0.1039 *N*)

$[H_2SO_4]_{aq}$	$[Na_2SO_4]_{aq}$	$a_{H_2SO_4}$	$[H_2SO_4]_{org}$	$E = \frac{[Th]_{org}}{[Th]_{aq}}$
0.016	0.304	0.88×10^{-6}	0.0539	416
.035	.315	4.25×10^{-6}	.0570	326
.057	.323	1.14×10^{-5}	.0600	240
.082	.328	2.31×10^{-5}	.0629	144
.110	.330	5.44×10^{-5}	.0656	95
.147	.343	1.02×10^{-4}	.0684	67
.189	.351	1.66×10^{-4}	.0703	47

(10) R. Simard, Dept. of Mines and Technical Surveys, Ottawa, Canada, Reports IR-58-4 and TR-145/57. Similarly, in a study of thorium extraction by di-alkyl phosphoric acids, Peppard, *et al.*, concluded that the organic thorium was hexacoördinated: D. F. Peppard, G. W. Mason and S. McCarty, *J. Inorg. Nucl. Chem.*, **13**, 138 (1960).

(11) N. V. Sidgwick, "The Chemical Elements and Their Compounds," Vol. I, University Press, Oxford, 1951, p. 644.

(12) J. C. Bailar, Jr., Ed., "The Chemistry of the Coördination Compounds," Reinhold Publ. Corp., New York, N. Y., 1956, p. 29.

(13) C. F. Baes, Jr., *J. Am. Chem. Soc.*, **79**, 5611 (1957).

Since the present data were taken at constant aqueous sulfate ion molarity, the variation in extraction of thorium observed is due entirely to the variation in acid activity; *i.e.*, the relative aqueous concentrations of the thorium–sulfate complexes were held constant.[14] These considerations lead to the following derivation of an alternative independent estimate of n, based on the simultaneous estimation of a constant for reaction (A). The equilibrium constant for this reaction may be written

$$K = \frac{a_{R_nH_nTh(SO_4)_{2+n/2}}\, a_{H_2SO_4}^{nx/2}}{a_{Th(SO_4)_2}\, a_{R_2H_2SO_4}^{(1-x)n/2}\, a_{RH_2SO_4}^{nx}}$$

Rearranging, we obtain

$$K = \frac{a_{R_nH_nTh(SO_4)_{2+n/2}}}{a_{Th(SO_4)_2}\, a_{R_2H_2SO_4}^{n/2}} \left[\frac{a_{H_2SO_4}\, a_{R_2H_2SO_4}}{a^2_{RH_2SO_4}}\right]^{nx/2}$$

now the expression in brackets is simply the equilibrium constant, K_s, for the amine sulfate–bisulfate reaction in the absence of thorium. It has been demonstrated experimentally in previous work[6] that use of equivalent fractions in place of activities for the amine salts ($x = [RH_2SO_4]/([RH_2SO_4] + 2[R_2H_2SO_4])$ and $y = 2[R_2H_2SO_4]/([RH_2SO_4] + 2[R_2H_2SO_4])$) and the usual activity coefficient expression for $a_{H_2SO_4}$ leads to a constant value of K_s. Also, since the organic thorium was constant in a medium for which there is no reason for believing that its activity coefficients are markedly affected by changes in the amine sulfate–bisulfate ratio, and the aqueous thorium concentration was very low, in a medium of almost constant ionic strength, the approximation $E = a_{R_nH_nTh(SO_4)_{2+n/2}}/a_{Th(SO_4)_2}$ becomes acceptable. On making these substitutions we obtain

$$Ky^{n/2} = E(\gamma K_s)^{nx/2} \qquad \text{(B)}$$

from which[15]

$$\log K + n \log y^{1/2} = \log E + x \log (\gamma K_s)^{n/2} \qquad \text{(C)}$$

In equation (C) the quantities $\log y^{1/2}$, $\log E$ and x were computed from the data in Table II. Log K, n and $\log (\gamma K_s)^{n/2}$ then were obtained from a least squares analysis of the resulting polydimensional linear field. The values were

$$\log K = 2.0$$
$$\log (\gamma K_s)^{n/2} = 1.3$$
$$\text{and } n = 7.0$$

Of these three numbers, the only one subject to comparison with independent evaluations is n (*cf.* preceding section); the agreement here is considered remarkable, in view of the admittedly somewhat involved series of deductions necessary in getting from reaction (A) to equation (C).

Reagent Dependence.—Experiments to investigate the dependence of the extraction coefficients on the concentration of DDAS were arranged so that the fraction of amine sulfate complexed with the thorium was small (0.3) and constant. Thus, no correction for the complexed reagent was necessary. Two sets of experiments were performed. In one set the aqueous medium was 0.005 M H_2SO_4 and in the other it was 0.005 M H_2SO_4 + 0.995 M Na_2SO_4. In both sets comparisons between vigorous agitation and quiet interface equilibration were obtained.

The results (Fig. 2) were qualitatively similar to

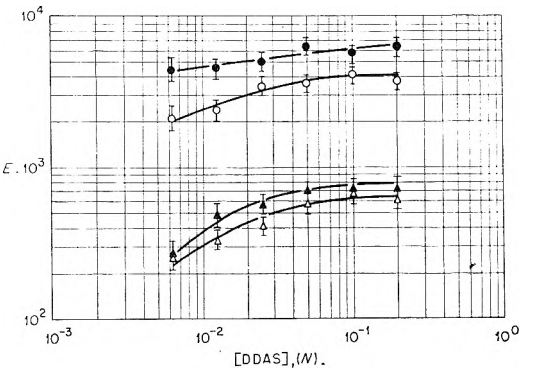

Fig. 2.—Thorium extraction as a function of DDAS concentration. The aqueous phases were 0.005 M H_2SO_4 (circles) and 0.005 M H_2SO_4–0.995 M Na_2SO_4 (triangles). Open points were by vigorous agitation, filled points by gentle equilibration (*cf.* ref. 7).

these obtained on extracting uranium from the same aqueous systems with DDAS.[4] In case of the low ionic strength aqueous system (sulfuric acid only), the slopes of the two curves were about the same, and of the expected magnitude.[16] The absolute values of the extraction coefficients, on the other hand, showed definite indications of the same kind of anomalous behavior as had been observed with uranium.[7] At high aqueous ionic strength the differences were much less apparent.

Sulfate Ion Dependence.—The dependences of the thorium extraction coefficients on aqueous sulfate ion molarity at two sulfuric acid activities are shown in Fig. 3. Following Kraus

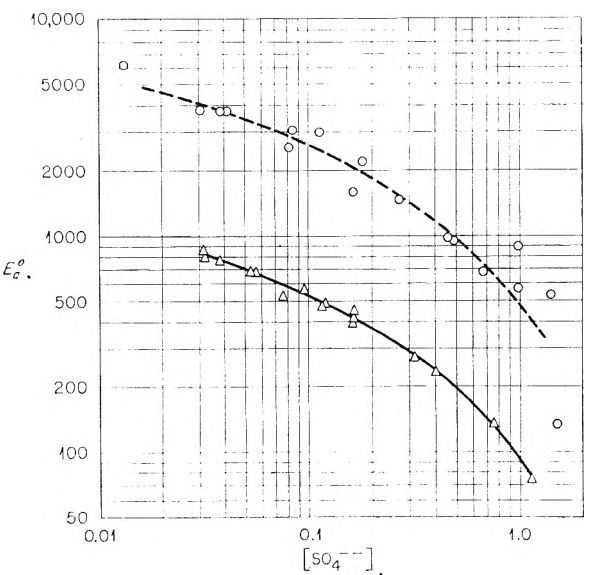

Fig. 3.—Thorium extraction as a function of aqueous sulfate ion concentration at constant sulfuric acid activities: $a_{H_2SO_4} = 1 \times 10^{-5}$ (circles) and $a_{H_2SO_4} = 6.4 \times 10^{-5}$ (triangles).

(14) Computations showed that the effects of the unavoidable small changes in ionic strength were negligible.[20]

(15) Since there is no way of relating the standard states of the substances represented in reaction (A), it is not permissible to insert the numerical value of K_s obtained in reference 6. K_s appears in (B), therefore, with an undetermined (but constant) multiplier, γ, which could be evaluated subsequently from K_s and the quantity $(\gamma K_s)^{n/2}$.

and Nelson[17] the slopes of the curves at the various sulfate levels are interpreted as reflecting the average charges on the aqueous thorium species. Since the slopes become negative, it is apparent that the corresponding thorium sulfate ionic species must contain more than two sulfates.[18] While stability constants for the mono and disulfate complexes have been reported,[9,19] a reasonably thorough search of the literature has failed to reveal any prior mention of species containing three or more sulfates per thorium. The results of computations aimed at evaluating formation constants for these species will be reported in a subsequent paper.

Acknowledgment.—The authors are indebted to G. N. Case for invaluable technical assistance throughout the work.

(16) K. A. Allen, *J. Phys. Chem.*, **62**, 1119 (1958); since DDAS is highly aggregated (*ca.* 40 monomers per micelle) and since by analogy with the uranium system it was expected that the thorium sulfate–DDAS complex would be monomeric, we have

$$Th(SO_4)_2 + (n/2m)(R_2S)_m = (R_2S)_{n/2}\cdot Th(SO_4)_2$$

The predicted reagent dependence is, therefore, $n/2m = (6 \pm 1)/80 \sim 0.1$.

(17) K. A. Kraus and F. Nelson, in "The Structure of Electrolytic Solutions," W. J. Hamer, Editor, John Wiley and Sons, Inc., New York, N. Y., 1959, Chapter 23.

(18) Similar behavior has been observed by K. A. Kraus and F. Nelson of this Laboratory during studies of thorium sulfate sorption on an anion exchange resin.

(19) A. J. Zielen, *J. Am. Chem. Soc.*, **81**, 5022 (1959).

THE COMPARATIVE ROLES OF OXYGEN AND INHIBITORS IN THE PASSIVATION OF IRON. IV. OSMIUM(VIII) OXIDE

BY G. H. CARTLEDGE

Chemistry Division, Oak Ridge National Laboratory, Operated by Union Carbide Corporation for the U. S. Atomic Energy Commission, Oak Ridge, Tennessee

Received February 23, 1961

Cathodic polarization of iron electrodes after passivation in osmium(VIII) oxide has been used as a means of determining the relative contributions of oxygen and the passivating inhibitor to the total cathodic process. It was found that the rate of reduction of osmium(VIII) oxide greatly exceeds that of oxygen. The reduction product, $Os(OH)_4$, was shown to accelerate the reduction processes, as was found previously with reduction of the pertechnetate ion. A possible mechanism for this action is suggested. The results of the four papers in this series are summarized and discussed in their relation to theories of passivation.

In previous papers[1-3] it was shown that oxygen at atmospheric pressure is able to passivate iron in the presence of a suitable non-oxidizing inhibitor, and that even though a reducible inhibitor is used, oxygen may still be the chief contributor to the total cathodic process. This was shown to be the case with the pertechnetate and chromate ions as inhibitors. In the present study, similar polarization measurements have been made with osmium(VIII) oxide as the effective passivating agent.

The behavior of this compound as a passivator was described earlier,[4] where it was demonstrated that passivation was sufficiently thorough for the iron electrode to indicate the thermodynamically reversible potential of the OsO_4–$Os(OH)_4$ couple, exactly as given by a platinum wire coated with $Os(OH)_4$. Even a dilute solution (0.039 *f*) of OsO_4 produced passivation almost instantaneously, recalling the action of concentrated nitric acid in this respect. A specimen of low-carbon steel has been preserved in a sealed tube in 0.039 *f* OsO_4 solution containing 10^{-3} *f* $CuSO_4$ since early 1956. No deposition of copper has occurred, and only a dull grayish film is visible on the metal.

Experimental

The electrolytic iron and procedures used were the same as those of the earlier work.[1-3]. To provide a non-activating electrolyte, a 1.00×10^{-2} *f* phthalate buffer was used in the *p*H range of 5.5–6.0. "Osmic Acid" C.P. was added from a stock solution to make the OsO_4 concentration 2.0×10^{-3} *f*. Preliminary experiments showed that the reduction of osmium(VIII) oxide under these conditions was so very much faster than reduction of oxygen that it was unnecessary to exclude oxygen completely, as was essential in the measurements with pertechnetate and chromate ions. In the experiments designated as Series VI and X, stirring was provided by a slow stream of oxygen, while in Series VII, VIII and IX, a slow stream of helium was used. Under these conditions there was a slight loss of OsO_4 by vaporization, but the effect was subordinate to other effects to be described. Preelectrolyzed phthalate was chosen as a buffered supporting electrolyte in spite of the fact that it is slowly oxidized at high potentials,[1] and prevents the electrodes from coming quite up to the reversible OsO_4–$Os(OH)_4$ potential.[5] In the present measurements, the passivated iron electrode and a platinum electrode coated with $Os(OH)_4$ quickly came to essentially identical potentials in the phthalate–osmium system, but the values were 15–30 mv. less noble than the calculated reversible value.

Results

Figure 1 shows the results of several galvanostatic cathodic polarizations. In Series VI, the electrode was first passivated in oxygenated 1.00×10^{-2} *f* phthalate at *p*H 6.07. Curve VI-1,2 represents duplicate polarizations in fresh electrolyte and is typical of the data obtained for this system.[1] Osmium(VIII) oxide then was added to make the solution 2.0×10^{-3} *f*. The potential immediately rose by about 340 mv. to a stable value 25 mv. below the calculated reversible potential for the OsO_4–$Os(OH)_4$ couple. Curve VI-3 shows the results of cathodic polarization in the mixed electrolyte, the measurements having the sequence indicated by the numerals adjacent to the data points. Stable potentials on an apparent Tafel line were established quickly until a current density of about 10^{-5} amp./cm.^{2} was reached, when

(1) G. H. Cartledge, *J. Phys. Chem.*, **64**, 1877 (1960).
(2) G. H. Cartledge, *ibid.*, **64**, 1882 (1960).
(3) G. H. Cartledge, *ibid.*, **65**, 1009 (1961).
(4) G. H. Cartledge, *ibid.*, **60**, 1571 (1956).
(5) G. H. Cartledge, *ibid.*, **60**, 1468 (1956).

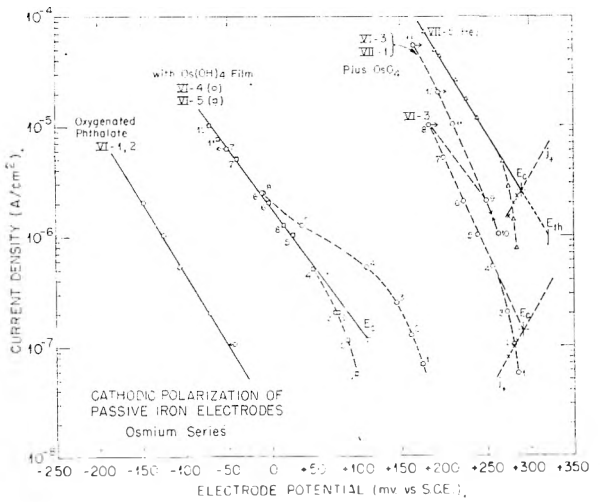

Fig. 1.—Cathodic polarizations to show relative reduction rates of OsO_4 and O_2 on passive iron, and the acceleration of reduction of O_2 by $Os(OH)_4$ on the electrode. Current density is in amp./cm.² of projected surface area.

the potential spontaneously ennobled by 21 mv. in 7 min. Points 9–13 represent potentials read 1 min. after a change of current density, before the autocatalytic ennobling process could proceed very far. It is seen that the data for the lower current densities may not be corrected to fall on the apparent Tafel line by assumption of an anodic process that is independent of potential, as is the case when the only anodic process is dissolution of the passive iron. In the present case, oxidation of both the phthalate ions and $Os(OH)_4$ may contribute to anodic current.

After the above measurements, the solution was removed, the system was thoroughly flushed and the cell again was filled with phthalate alone. Curve VI-4 shows the results of polarizing the electrode in the oxygenated solution, the measurements having been started 1 hr. after completion of VI-3. It is seen that an excess nobility was present during the first measurements (points 1–5), during which a total cathodic charge of *ca.* 1 mc./cm.² was passed. Thereafter, the points fell closely on the Tafel line established by another polarization (VI-5) in fresh electrolyte after the cell had been on open circuit with oxygen passing for 3 days. An essentially constant anodic current density of 1×10^{-7} amp./cm.² sufficed to bring the points for low current densities onto the line. From the previous polarizations in OsO_4 the electrode had acquired a deposit of $Os(OH)_4$, which obviously accelerated the reduction of oxygen nearly a hundredfold. (Reduction of $Os(OH)_4$ apparently was not a factor, since other experiments showed that substitution of helium for oxygen caused a very rapid debasing of more than 450 mv. when a platinum electrode heavily coated with $Os(OH)_4$ was polarized in the phthalate solution.)

Upon completion of the measurements of Series VI, sensitivity of the passive potential to added sulfate ions was confirmed.[4] At a current density of 1.1×10^{-7} amp./cm.², while the potential was still rising at +80 mv. S.C.E. the phthalate electrolyte was made 5×10^{-3} *f* in potassium sulfate. The potential became unsteady at once and oscillated downward to −160 mv. in 2 hr. Subsequently, severe corrosion set in on open circuit with oxygen still passing. Although the presence of $Os(OH)_4$ greatly accelerated the reduction of oxygen and, hence, favored passivation, the action was not sufficient to overcome the activating effect of competing anions.

In Series VII-1 a freshly etched electrode was passivated in 1.00×10^{-2} *f* phthalate containing 2.0×10^{-3} *f* OsO_4 at *p*H 6.02 in a helium atmosphere. The polarization data coincided closely with those obtained in oxygen in VI-3, points 9–12. It should be noted that the electrode in VII-1 was etched in 1 *N* H_2SO_4 just before passivation in a helium atmosphere, so that it already had some film of $Os(OH)_4$ before the polarization was begun. Two additional polarizations were made in a renewed OsO_4 solution under helium, as shown by curve VII-5 in Fig. 1. (The data for VII-3 fell on the same curve.) The slight shift to more noble potentials between VII-1 and VII-3,5 presumably was due to the accumulation of additional reduction product. The point E_{th} denotes the calculated reversible potential for the osmium couple.[5] This indicates that the exchange current is *ca.* 1×10^{-6} amp./cm.² for the prevailing conditions, the current density being referred necessarily to the projected area of the iron electrode on which the $Os(OH)_4$ was deposited. This current density, however, is clearly dependent upon the amount and activity of the surface film, as in the case of the pertechnetate system.[2]

The excess nobility observed in the first five points of curve VI-4 in Fig. 1, in spite of the careful removal of OsO_4, suggested that appreciable amounts of a reducible intermediate formed on the electrode during the 15 min. the system was on open circuit before the cell solution was changed. In taking these five points a total charge of 1.0 mc./cm.² was passed, and this apparently removed the active constituent. In another experiment, the same effect was observed in a still greater degree. Upon completion of Series VII-5, the OsO_4 solution was left in contact with the electrode for three days. A black deposit of $Os(OH)_4$ had been formed by the polarization in helium. The cell solution was removed and the cell thoroughly flushed with 1.00×10^{-2} *f* phthalate at *p*H 6.02. With oxygen passing, the potential came to the very noble value of 280 mv. S.C.E. and fell only to 230 mv. even after the polarizing current had been carried to 1.08×10^{-6} amp./cm.² and a charge of 3.4 mc./cm.² had been passed. The cell and electrode were flushed twice with 1.00×10^{-2} *f* K_2SO_4 on the suspicion of a possibility that adsorbed OsO_4 was responsible for the effect. Upon replacing the phthalate solution in the cell and resuming the measurements in a stream of oxygen, the initial polarizations gave potentials that were still over 150 mv. more noble than points 2–4 in curve VI-4 (Fig. 1), with very slow drifts to less noble values. The behavior resembled that observed in the chromate system,[3] to the extent that the presence of a reducible species on the electrode other than oxygen or passive film seemed to be

indicated. The treatment with K_2SO_4 makes it unlikely that adsorbed OsO_4 itself was still present.

Light *vs.* Heavy Deposits of $Os(OH)_4$.—The results of Series VI and VII were confirmed and somewhat extended by the measurements of Series IX and X. These series were designed to give a comparison between electrodes prepared, first, with the least possible deposition of $Os(OH)_4$ and then with a considerably greater amount. In IX-1-7, polarizations were made in the same sequence of conditions as that followed in Series VI (Fig. 1). The results were entirely similar and are not shown. After the polarization IX-7, the iron electrode was freed of the deposit of $Os(OH)_4$ by anodic polarization in 1 *N* H_2SO_4 for 5 min. at 45 ma./cm.^{2}. This produced evolution of oxygen, and at the end of the treatment the electrode was again bright. After equilibration in oxygenated phthalate, the electrode was successively polarized in the sequence shown in Fig. 2, curves IX-8-12.

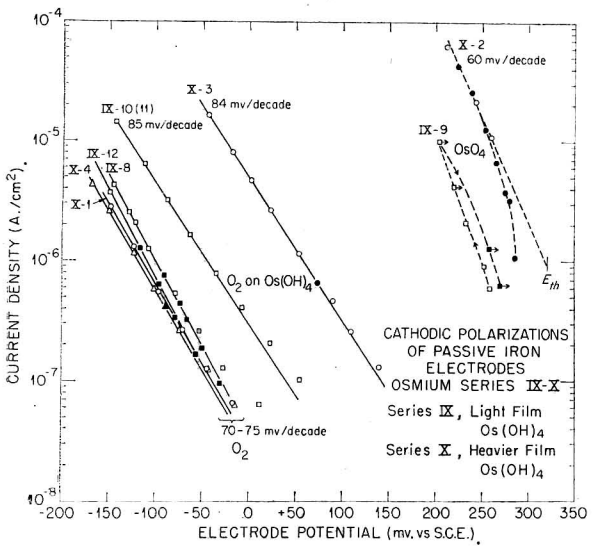

Fig. 2.—Cathodic polarizations to show the elimination of the catalytic effect by removal of $Os(OH)_4$ from the film, and also the effect of varying the amount of $Os(OH)_4$. Series IX, 1.7 mc./cm.^{2} film, Series X, 46 mc./cm.^{2}. Points marked by filled symbols were taken with decreasing current density.

For the light deposit of $Os(OH)_4$, the measurements with OsO_4 present were made within 1 to 2 min. after changing the current density, the lowest current densities being used first. The electrode already was passivated when the OsO_4 was added, hence for both these reasons the amount of $Os(OH)_4$ on the surface was kept to a minimum. The potential shifted so quickly after a change of current density, however, that the observed values served to locate curve IX-9 with sufficient accuracy. During this polarization in helium, a total charge of only *ca.* 1.7 mc./cm.^{2} was passed. Curves IX-10,11 (duplicates) and IX-12 show the results for reduction of oxygen in the phthalate solution, first, with $Os(OH)_4$ on the electrode and, second, after removing it by anodic treatment in dilute NaOH. It is seen that the final curve essentially duplicates the original one, IX-8.

For series X, the same electrode was again polarized in oxygenated phthalate (X-1, Fig. 2). Then a moderately heavy deposit of $Os(OH)_4$ was formed by polarization in OsO_4-phthalate solution, a charge of *ca.* 30.2 mc./cm.^{2} being passed during 33 min. before beginning the measurements. The polarization increased this to a total of 46 mc./cm.^{2} and this charge produced a dark gray color on the previously bright electrode. Curves X-2-4 (Fig. 2) show the results of the polarizations, and the greater acceleration of the cathodic processes by the heavier film is clearly shown by comparison of Series IX and X. The negative shift with the lighter film in OsO_4 corresponds to a decrease in the indicated exchange current for the Os(VIII–IV) couple by about one order of magnitude. As was found in Series VI, it is again shown that the reduction of OsO_4 at a given potential is nearly four orders faster than that of oxygen on the same electrode for either film weight. With the lighter film, reduction of oxygen in the simple phthalate solution is accelerated about 10-fold, whereas with the heavier film the acceleration is 100-fold. In both cases, removal of the $Os(OH)_4$ from the film by anodic polarization restored the electrode to essentially its original state, with respect to reduction of oxygen (curves IX-8, 12 and X-1, 4). All four of these curves are normal for the oxygenated phthalate system.[1] In Series X, no polarization corresponding to VI-4 was made; rather, the polarizations IX-10 and X-3 were made only after an overnight stabilization of the electrode in oxygenated phthalate and, in X-3, with a brief prepolarization before the overnight stabilization.

Discussion

The general purpose of this series of studies was to shed light on the question whether oxidizing inhibitors, such as the chromate ion, lead to passivation of iron solely by virtue of their own reduction or, alternatively, have some other function related to adsorption of the unreduced species. The relation of the electrochemical properties of passivating agents to the production of mixed potentials in the passive region on a metal capable of being passivated has been clearly treated schematically by a number of authors, most recently and fully by Stern.[6] These treatments proceed from the assumption that the corrosion rate is uniquely fixed by the existing potential, which, in turn, is determined by the sum total of anodic and cathodic processes available in the system, according to the theory of mixed potentials. From this point of view, the sole function of a reducible inhibitor is to contribute to cathodic current, whereby the anodic current of metal oxidation is raised to some value sufficient for passivation, as disclosed by a potentiostatically determined potential–current density diagram. In this treatment of the passivation process, there is no consideration of chemical effects related to the composition or structure of the passive film itself, nor of an alteration of the kinetics of any electrode reaction by intervention of some component of the system by

(6) Milton Stern, *J. Electrochem. Soc.*, **105**, 638 (1958). *Cf.* also N. Ya. Bune and Ya. M. Kolotyrkin, *Doklady Akad. Nauk*, **111**, 1050 (1956).

adsorption or otherwise, although Stern recognizes this as a possibility. Such effects, if present, would be expected to be specific for different solution species in a way not directly related to their own oxidation–reduction properties, if any.

Types of Inhibition.—From the point of view of passivation theory, at least three types of inhibitor action have to be distinguished. Firstly, there are the commercially important organic inhibitors which reduce corrosion rates in acidic media without producing much change in the corrosion potential. Such substances are known, in many instances, to be adsorbed on the bare metal surface, and some relationships between structure and effectiveness as inhibitors have been pointed out.[7] These inhibitors do not lead to passivity even when used in the presence of air, but, in certain instances, have been shown[8] to diminish the limiting cathodic current density for evolution of hydrogen, by which the corrosion rate is controlled. The iodide ion and carbon monoxide also are adsorbed and reduce the corrosion rate in sulfuric acid by modifying the kinetics, chiefly of the anodic process.[9] In all these cases the corrosion product dissolves in the acidic medium and no passivating film is formed. The inhibitors enter into no oxidation–reduction reactions of their own.

With other inhibitors, not only is the corrosion rate greatly reduced, but the corrosion potential rises by perhaps a volt above (noble to) the potential of the freely corroding system. These inhibitors are oxidizing agents. Ideally, if the anodic dissolution process is sufficiently slow in comparison with the exchange current density of the inhibitor under the prevailing conditions, the potential comes to the reversible potential of the oxidation–reduction couple. This rather uncommon behavior was demonstrated for passivation of iron by osmium(VIII) oxide.[4] In concentrated nitric acid, however, the corrosion rate remains sufficiently high to polarize the iron electrode by about 0.3 v. below the potential of a platinum wire in the same solution.[10] It is generally agreed that, in such cases, the formation and integrity of a film of reaction products (or of chemisorbed oxygen, according to Uhlig[11]) are essential. It is necessary, however, that the metal be capable of acquiring the unique surface state characteristic of passivation, since not all metals and not all active oxidants exhibit the phenomena. With nitric acid, the film and its electrochemical behavior are clearly the same as those obtained by application of anodic polarization in sulfuric acid. It is therefore doubtless correct to interpret the action of nitric acid entirely in terms of its own reduction process, without having recourse to any adsorption phenomena. Whether this is strictly true of osmium(VIII) oxide also will be considered below. Conceivably, as contended by Kolotyrkin and Bune,[12] the passivating action of such inhibitors as the chromate ion also involves no specific action of the passivator beyond its favorable oxidizing power. If so, we should then have to include it along with nitric acid in a class of passivating agents that are completely self sufficient.

In the present series of studies, however, it has been questioned whether the criteria for passivation by mere reduction of the inhibitor are uniquely sufficient when applied generally to the XO_4^{n-} inhibitors. It has been suggested previously[13,14] that, quite apart from formation of a film, an inhibitor may interact with the surface in such a way that the kinetics of one or more of the partial processes in corrosion is changed. This is certainly true of inhibition by iodide ions.[9] Hence, it was first demonstrated[1] that certain inhibitors which have no oxidizing properties of their own coöperate with oxygen in such a way that passivation is achieved by its reduction under conditions that lead to corrosion in the absence of the inhibitor. Such action is exhibited by the benzoate, phthalate and phosphate ions, as well as by molybdate and tungstate ions. Further, the present experiments have shown that oxygen at atmospheric pressure or less is reduced on the passive iron surface at a considerably faster rate than are the chromate and pertechnetate ions,[2,3] at potentials near or somewhat negative to the Flade potential. Oxygen is then primarily responsible for the production and maintenance of the passive potential in these instances, thus suggesting the possibility that these particular inhibitors also act on the kinetics by virtue of their adsorption, rather than by necessarily contributing to the total cathodic process. This possibility is made more likely by the further demonstration of the activating effect of low concentrations of sulfate and other ions which have no evident means of participating directly in the reduction of the passivating inhibitor. Whether the explicit mode of interaction of these inhibitors is understood or not, they must be recognized as a third class which permit passivation by oxygen without being able of themselves to contribute significantly to the cathodic current at the relatively noble potentials at which passivation is maintained. The experiments thus indicate that all the XO_4^{n-} ions mentioned belong in this class, along with the non-oxidizing benzoate and phthalate ions.

The action of osmium(VIII) oxide is different from that of the chromate and pertechnetate ions in certain important respects, although the sensitivity to sulfate ions suggests that even here adsorption plays a part. As pointed out previously,[2,3] diffusion control limits the contribution of oxygen to the oxidation process when an active iron surface is exposed to an aerated solution of $CrO_4^{=}$ or TcO_4^{-}. Some reduction product of the inhibitor consequently goes into the film, and to some extent

(7) See, for examples, N. Hackerman and J. D. Sudbury, *J. Electrochem. Soc.*, **97**, 109 (1950); N. Hackerman and A. H. Roebuck, *Ind. Eng. Chem.*, **46**, 1481 (1954); H. Kaesche and N. Hackerman, *J. Electrochem. Soc.*, **105**, 191 (1958).

(8) H. Fischer, M. Knaack and O. Volk, *Z. Elektrochem.*, **61**, 123 (1957); H. Fischer and G. Thoresen, *ibid.*, **62**, 235 (1958).

(9) K. E. Heusler and G. H. Cartledge, *J. Electrochem. Soc.*, **108**, 732 (1961).

(10) K. J. Vetter, *Z. Elektrochem.*, **55**, 274 (1951).

(11) H. H. Uhlig, *ibid.*, **62**, 626 (1958).

(12) Ya. M. Kolotyrkin and N. Ya. Bune, *Z. physik. Chem.*, **214**, 264 (1960).

(13) G. H. Cartledge, *Z. Elektrochem.*, **62**, 684 (1958), and earlier papers cited.

(14) Ya. M. Kolotyrkin, *ibid.*, **62**, 664 (1958); B. N. Kabanow and D. I. Leikis, *ibid.*, **62**, 660 (1958).

modifies the surface properties. As the potential becomes more noble, however, reduction of oxygen becomes increasingly important, and, as the very prolonged pertechnetate experiments showed,[2] finally is entirely responsible for maintenance of passivity. On the contrary, reduction of osmium(VIII) oxide is so very rapid that it is chiefly responsible for passivation even when oxygen is present. Passivation is almost instantaneous and is not immediately destroyed by transferring the specimen to a sufficiently dilute copper(II) sulfate solution. In these respects the phenomena exactly duplicate those observed in concentrated nitric acid.[4] Thus, in most respects, osmium(VIII) oxide behaves like nitric acid in being a self-sufficient passivator, but the destruction of passivity by sulfate ions indicates that adsorption is still involved kinetically in the total process.

Specific Effects of Ions.—In previous studies it was demonstrated that the noble electrode potential attained by an iron electrode in an aerated pertechnetate solution is quickly debased by addition of a sufficient (low) concentration of sulfate ions.[15] It was shown, further,[16] that other XO_4^{n-} inhibitors are similarly affected, and that the concentration of added ion required for disturbance of the passivation with a given inhibitor varies considerably when Cl^-, ReO_4^-, SCN^- and $SO_4^=$ are compared. The effect was interpreted in terms of competitive adsorption, since there is no apparent reason why the ordinary oxidation–reduction reactions should be modified unless the kinetics was altered by adsorption. The sulfate ion was originally chosen as the agent for demonstrating foreign-ion effects in order to avoid the various complications attending the presence of chloride ions so much used in corrosion work. By means of the sulfate additions it has been shown that the activating effect occurs with all the inhibitors used in these studies, and that the sensitivity to sulfate ions varies from one inhibitor to another.

Adsorption of sulfate ions on iron or its surface oxide was definitely established by Hackerman and Stephens,[17] who made use of radioactive sulfate. It was shown also that the ion is displaced in competition with other ions, especially the chromate ion. Similar specific effects have been observed in this Laboratory,[18] in that addition of benzoate to a certain perchloric acid solution led to inhibition of the corrosion of iron, whereas no inhibition by benzoate resulted when the system consisted of a sulfate medium of the same normality and *p*H value.

That a reducible inhibitor has a role other than the possession of a sufficient oxidation–reduction potential and exchange current is shown by another observation. In a solution of OsO_4 containing considerable sulfate, a platinum wire coated with $Os(OH)_4$ indicated a very noble potential, whereas an iron electrode in the same solution corroded badly at a potential 750 mv. less noble than that of the platinum electrode.[19] The experiments make it clear that the inhibitor must do something at the corroding interface before the passive potential can be attained by reduction of any available oxidizing agent. The evidence seems to justify the conclusion that this "something" is counteracted by rather low concentrations of adsorbable anions, and hence that a dual role must be ascribed to inhibitors that are reducible.

With respect to specific effects of the various inhibitors at the corroding interface, it may be noted that all the oxidizing inhibitors may react with active iron to form a mixture of hydrated oxides, though such films are not necessarily passivating. The chromate ion can also convert iron(II) ions to an insoluble product, which the pertechnetate ion cannot do under conditions which nevertheless permit effective inhibition.[2] Inhibition is sensitive to addition of foreign ions in both cases, and on the passive electrode both ions are reduced much less rapidly than oxygen. Both must be maintained above some minimum concentration in aerated solutions for maintenance of passivation, chiefly, if not totally, by reduction of oxygen. Buffering of the environment can be excluded as an explanation of inhibitory properties since the pertechnetate system has no buffering action.

The considerations which led to the discovery of the inhibitory properties of the pertechnetate ion derived from the observation that neither precipitation, buffering, oxidation nor electrical effects of the ionic charge seemed adequate for the specific differentiation between inhibiting and non-inhibiting ions. This conclusion was strengthened by the subsequent discovery of the profound difference between the externally very similar pertechnetate and perrhenate ions with respect to inhibition.[20] It was then proposed to seek the kinetic effect of the XO_4^{n-} inhibitors, in particular, in short-range electrostatic interactions at the surface on which the unreduced ion is adsorbed.[13]

Such an assumption finds close parallels in connection with other phenomena that depend upon changes in the electrical state of a surface as a consequence of adsorption. Thus, Boudart[21] has interpreted the variation of the heat of adsorption with coverage in terms of a shift in the Fermi level of the adsorbent as a consequence of adsorption. Likewise, shifts in the infrared absorption spectrum of CO on a metal due to addition of oxygen may be correlated with corresponding changes in surface conductivity and work function by the assumption of alterations of the electrical state of the surface. Such changes have been demonstrated in certain cases in the effect of the ambient atmosphere or surface films upon the surface conduction of semiconductors.[22] It is therefore not unreasonable to assume that similar actions on the part of adsorbed inhibiting species are the specific source of their effectiveness in diminishing corrosion rates. At

(15) G. H. Cartledge, *J. Phys. Chem.*, **60**, 28 (1956).
(16) R. F. Sympson and G. H. Cartledge, *ibid.*, **60**, 1037 (1956).
(17) N. Hackerman and S. J. Stephens, *ibid.*, **58**, 904 (1954).
(18) E. J. Kelley, unpublished results.
(19) The solution was 0.25 *f* K_2SO_4 plus 0.050 *f* OsO_4 at *p*H 4.40. At the same OsO_4 concentration and *p*H value iron would have shown the reversible couple potential, had the sulfate ion concentration not exceeded *ca.* 2×10^{-3} *f*.[4]
(20) G. H. Cartledge, *J. Phys. Chem.*, **60**, 32 (1956).
(21) M. Boudart, *J. Am. Chem. Soc.*, **74**, 1531, 3556 (1952).
(22) *Cf.*, for examples, A. R. Moore and Robert Nelson, *R. C. A. Rev.*, **17**, 5 (1956), and T. M. Buck and F. S. McKim, *J. Electrochem. Soc.*, **105**, 709 (1958).

least in the case of adsorbed iodide ions and carbon monoxide, effects on the kinetics of corrosion have been demonstrated.[9] Unfortunately, direct electrochemical verification of the electrostatic hypothesis as a generalization is rendered difficult because of the ambiguities attending the determination of the kinetics of reactions at an iron electrode even when inhibitors are absent.

In two recent papers the attempt has been made to demonstrate that oxidizing agents have no specific function in passivation other than the production of a mixed potential in the passive region for the metal in question. Thus, Kolotyrkin and Bune[12] measured the corrosion rate and potential of nickel in 1 N H_2SO_4 containing different oxidizing agents. It was observed that the corrosion rate and potential in the presence of the oxidizing agents fell on the polarization curve established by potentiostatic anodic polarization in the absence of the oxidants. It should be noted, however, that this correspondence occurred only at concentrations of oxidant that were small in comparison with the concentration of sulfuric acid. The potentials produced were in the active region and were determined, as the authors suggest, by diffusion-controlled reduction of the oxidant. At higher concentrations of the oxidant certain specific differences are apparent in the data. Makrides and Stern[23] measured the effect of iron(III) ions on the passivation of a type-410 stainless steel in 1 N H_2SO_4. Their results were similar to those of Kolotyrkin and Bune for nickel, in that the effects due to the low concentrations of Fe(III) used could be accounted for quantitatively by the diffusion-controlled cathodic process. Although the interpretation of the data is certainly correct electrochemically, neither experiment furnishes a valid argument against the view that there are specific effects upon the kinetics arising from adsorption. The measurements in this Laboratory have been made deliberately under conditions of concentration, acidity, etc., that were marginal for passivation, in order that any specific actions of the inhibiting species might not be masked by an excess of foreign ions, such as the sulfate ion.

Autocatalytic Effects.—The polarization measurements showed marked acceleration of the reduction of both oxygen and the inhibitors by $Tc(OH)_4$ or $Os(OH)_4$ formed on the electrode, but none by the reduction product of the chromate ion. It is possible to suggest a mechanistic interpretation of these observations based on the existence of valence states intermediate between 8+ and 4+ for osmium and between 7+ and 4+ for technetium, whereas Cr^{3+} is not oxidizable readily unless it is converted to Cr^{6+}. Thus, the Tafel slope for reduction of the pertechnetate ion in helium suggests that a one-electron process may be rate determining. Technetium is reported[24] to form no isolable oxide TcO_3, and estimates of its free energy suggest that it is slightly unstable with respect to disproportionation into Tc(IV) and Tc(VII) in contact with water. There is no evidence of its formation as an intermediate in the polarographic reduction of the pertechnetate ion.[25] A Tc(V) state may be formed under conditions where stabilization is effected by complex formation.[26] The hexavalent state of rhenium is fairly stable. It is not unreasonable then to postulate that reduction of the pertechnetate ion at the passive iron electrode is initiated by the reaction $TcO_4^- + e^- \xrightarrow{k_{-1}} TcO_4^=$, for which

$$j_{-1} = k_{-1} a_{TcO_4^-} \exp\left(\frac{-\alpha F E}{RT}\right) \qquad (1)$$

The technetate ion, $TcO_4^=$, would be expected to be reduced rapidly in one or two steps to $Tc(OH)_4$. The initial cathodic current density would then be three times that indicated by eq. 1. The accumulation of $Tc(OH)_4$ on the electrode could affect the kinetics either by providing a new path of low activation energy for electron transfer to the reducible species, or, possibly, by direct chemical reaction with TcO_4^- to form one of the intermediate valence states that is rapidly reducible. Either of these processes would account for the autocatalytic effects observed.

Oxygen and its peroxide reduction product also oxidize $Tc(OH)_4$, particularly when it is freshly formed, hence the observed acceleration of the reduction of oxygen (ref. 2) may also be accounted for by the same mechanism. Likewise, the marked acceleration of the reduction of oxygen represented by curves VI-5 in Fig. 1 and X-3 in Fig. 2 may be interpreted in a similar manner, perhaps by fast processes going through Os(VI) or labile intermediate complexes of Os(VIII) and Os(IV). It is significant that no such effects were observed in the reduction of $CrO_4^=$, in agreement with the difficulty of oxidizing Cr(III) in acidic solutions.

Summary of Polarization Data.—It is obvious that polarization measurements on the systems studied are limited to a range of 2.5 to 3.5 decades of current density because of the approach to the corrosion current density at the low values and to the region of concentration polarization at high values. The data thus cover current densities extending from about 1×10^{-8} to 5×10^{-6} amp./cm.^{2}, or somewhat higher in particular instances. Extrapolations to the reversible potentials are reasonably reliable for the pertechnetate and osmium couples, because of their relatively high exchange currents, though the extrapolations to the oxygen and chromate potentials are subject to considerable error. Nevertheless, the curves shown in Fig. 3 may be seen to represent correctly the facts observed with respect to passivation in the various situations considered.

Curve 1 is taken from the polarization of the electrode in 1.00×10^{-2} f chromate at pH 6 in helium (ref. 3, Series IV-B). The reversible potential is calculated for the reaction: $CrO_4^= + 5H^+ + 3e^- \rightarrow Cr(OH)_3$ (hydrous) $+ H_2O$, using the free energies given by Latimer.[27] As was pointed out previously,[3] four such polarizations extrapolated

(23) A. C. Makrides and M. Stern, *J. Electrochem. Soc.*, **107**, 877 (1960).

(24) J. W. Cobble, Thesis, University of Tennessee, 1952, p. 17.

(25) H. H. Miller, M. T. Kelley and O. F. Thomason, "Advances in Polarography," Vol. II, I. S. Longmuir, Ed., Pergamon Press, Oxford, England, 1960, p. 716.

(26) C. E. Crouthamel, *Anal. Chem.*, **29**, 1756 (1957).

(27) W. M. Latimer, "Oxidation Potentials," 2nd Ed., Prentice–Hall Inc., New York, N. Y., 1952.

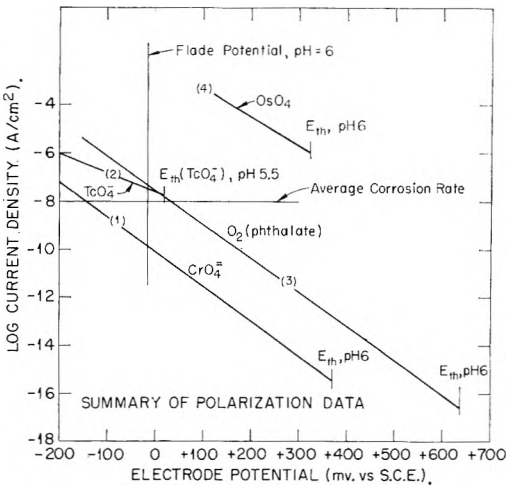

Fig. 3.—Summary of polarization data, showing relation to the calculated Flade potential and passive corrosion current density of iron.

to log j_0 values between −15 and −16, the other two being −14 and −17, respectively. If the free energy for $Cr(OH)_3(c)$ were used in the calculation, j_0 would become about 2 orders less.

The reversible potential for the pertechnetate couple is calculated for the reaction: $TcO_4^- + 4H^+ + 3e^- \rightarrow Tc(OH)_4(ppt.)$; $E_H^0 = 0.738$ v.,[28] and curve 2 is taken from ref. 2, Fig. 3, for a concentration of $1.00 \times 10^{-2} f$ at *p*H 5.5 and in helium. Another polarization under similar conditions indicated an exchange current only slightly lower. Curve 3 is based on many polarizations in oxygenated phthalate solutions $1.00 \times 10^{-2} f$ at *p*H values approximately 6.0. The curve is drawn for the average current density at −75 mv. S.C.E. and the average value of the Tafel slope. The reversible potential is calculated from the reaction: $O_2 + 4H^+ + 4e^- \rightarrow 2H_2O$; $E_H^0 = 1.229$ v. Curve 4 is for Fig. 1, curve VII-5 of the present paper, the reversible potential being found for the reaction: $OsO_4 + 4H^+ + 4e^- \rightarrow Os(OH)_4(ppt.)$; $E_H^0 = 0.964$ v.[5] The vertical line indicates the Flade potential calculated for *p*H 6, and the horizontal line shows the corrosion current density approximated for the different systems.[29]

Figure 3 shows the comparative cathodic current densities contributed by the different electrode processes. It is clear that, at potentials negative to the Flade potential, reduction of oxygen is the chief process, in comparison with reduction of the pertechnetate and, more particularly, the chromate ions. The reverse is true with osmium(VIII) oxide as passivator. In this case, the passive corrosion current density of iron is so much less than the indicated exchange current that it is understandable how iron is able to serve as an indicator electrode for this couple potential. With the pertechnetate ion in helium, the corrosion rate is of the same order as the exchange current density for the oxidation–reduction couple, and is usually sufficiently large to polarize the potential slightly negative to the calculated couple potential.

By comparing curve 4 with ref. 1, Fig. 2, it is seen that the curve for reduction of OsO_4 on passive iron falls in the same region as that for reduction of oxygen on platinum in a phthalate solution.

(28) G. H. Cartledge and Wm. T. Smith, Jr., *J. Phys. Chem.*, **59**, 1111 (1955).

(29) As pointed out in ref. 1 and 2, the indicated corrosion rates shown in the present measurements are values for passivation times of at least 16 hr. The values apparently decrease very slowly. In the phthalate system, the corrosion rate is often about 10^{-7} amp./cm.^{2}, after brief passivation at *p*H 6, provided the solution is replaced to prevent accumulation of iron ions formed while the electrode is still active. It may be 1–1.5 orders of magnitude lower if passivation is continued without renewal of the electrolyte.

MOLECULAR SPECIES AND ACTIVITY FOR PARAFFIN ISOMERIZATION CATALYSIS IN THE SYSTEM DIMETHYL ETHER–ALUMINUM BROMIDE

BY D. G. WALKER

Humble Oil and Refining Company, Manufacturing Division, Research and Development Division, Baytown, Texas

Received February 24, 1961

Experimental phase diagrams for the Me_2O–AlX_3 system for X = Br and Cl are reported. Thermodynamic considerations on the phase diagrams show that a previously unknown addition molecule, $Me_2O:2AlX_3$, is an important species which exists only in the liquid phase in equilibrium with $Me_2O:AlX_3$ and $1/2\ Al_2X_6$. Experimental determination of catalytic activity for paraffin isomerization as a function of phase composition for Me_2O–$AlBr_3$ liquid phases is also reported. $Me_2O:2AlBr_3$ appears to be the catalytically active species in the Me_2O–AlX_3 system.

Introduction

Aluminum halides have been used extensively as catalysts for the isomerization of paraffin hydrocarbons. The need for co-catalysts or promoters in order to obtain high catalytic activity at low temperatures has been widely recognized. A number of substances which act as co-catalysts with aluminum have been described in patents.[1] Francis[2] found that solutions of aluminum chloride in ethyl and isopropyl ethers, ethyl and isopropyl acetates, acetone, benzophenone, nitrobenzene and SO_2 all were vigorous catalysts for the isomerization of paraffins provided that the aluminum halide was present in molar excess. The necessity for using a molar excess of aluminum halide over co-catalytic molecules containing oxygen atoms in order to get good catalytic activity has not been explained.

The experimental work of this paper shows that

(1) A. W. Francis, U. S. 2,389,250, November 20, 1945.

(2) A. W. Francis, *Ind. Eng. Chem.*, **42**, 342 (1950).

the observed catalytic activity of liquid methyl ether–aluminum bromide phases for paraffin isomerization is related to the concentration of the molecular species $Me_2O:2AlBr_3$ and that the species $2Me_2O:AlBr_3$, $Me_2O:AlBr_3$ and Al_2Br_6 are inactive catalytically at ambient temperature.

Results and Discussion

A. Catalytic Activity–Composition of Liquid Dimethyl Ether–Aluminum Bromide Mixtures.—Aluminum bromide was synthesized and purified within a standard chemical high vacuum system with the rigid exclusion of moisture and air (see Experimental section). The data shown in Table I were obtained by combining the materials in the vacuum system and sealing them off under vacuum into ampules. An extremely low order of catalytic activity was found for pure Al_2Br_6 and an undetectable activity for the molecular species $Me_2O:AlBr_3$. Combining these two molecular compounds, however, under identical conditions and impurity levels yielded a highly active catalytic medium.

TABLE I

CATALYTIC ACTIVITY FOR *n*-PENTANE CONVERSION AT 25° OF Me_2O–$AlBr_3$ MIXTURES

1–1 volume ratio of catalytic material *n*-pentane

Test	1	2	3
Material	Al_2Br_6(s) (m.p. 97.5°)	$Me_2O:AlBr_3$ (m.p. 39.4°)	Al_2Br_6 + $Me_2O:AlBr_3$ 2.4 to 1 mole ratio
Reaction time	30 days	7 days	3 hr.
Hydrocarbon product analysis volume %, GPC			
Isobutane	0.0	0.0	8.1
n-Butane	0.0	0.0	0.1
i-Pentane	12.7	0.0	32.0
n-Pentane	86.6	100.0	51.8
$C_6 + C_7$ paraffin	0.0	0.0	8.0
isomers	99.3	100.0	100.0
First-order rate *n*-C_5 disappearance in $(hr.)^{-1}$	2×10^{-4}	1×10^{-5}	0.2

A large amount of $Me_2O:AlBr_3$ (m.p. 39.3°) was then synthesized and the following experiments were made. $Me_2O:AlBr_3$ and Al_2Br_6 were mixed in varying proportions with a constant amount of *n*-hexane and stirred vigorously for 1 hour at room temperature. The amount of isomerization of *n*-hexane which had occurred then was determined by GPC analysis of the hydrocarbon phase. The amount of dissolved $[AlBr_3]$ in the hydrocarbon phase was determined by chemical analysis for Al and Br content of the water used to wash the hydrocarbon phase. Three series of runs were performed: (ratios shown are in moles)

$$\frac{n\text{-hexane}}{\left(\frac{Al_2Br_6}{2} + Me_2O:AlBr_3\right)} = 7.5 \qquad (1)$$

$$\frac{n\text{-hexane}}{Al_2Br_6} = 13.7 \qquad (2)$$

$$\frac{n\text{-hexane}}{Me_2O:AlBr_3} = 9.6 \qquad (3)$$

The experimental results for the first series of runs are shown in Fig. 1. The other two series yielded similar data. Upon completion of the three

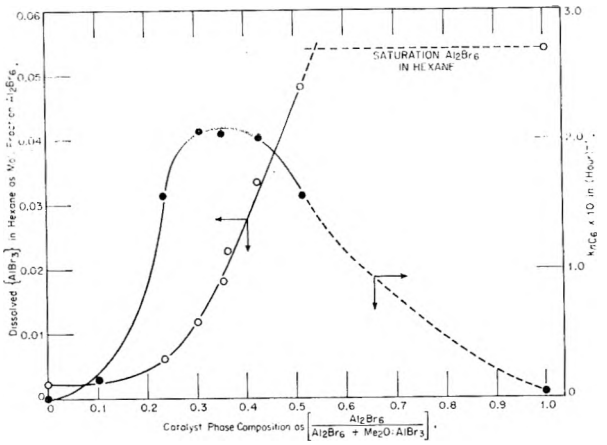

Fig. 1.—Phase composition and catalytic activity of series *n*-Hexane/(Al_2Br_6/2 + $Me_2O:AlBr_3$) = 7.5.

series it was realized that all of the data could be combined when the catalytic activity was based on a weight *n*-hexane per weight catalytic phase basis. The combined experimental data for all three series and the $[AlBr_3]$ solubility function in the paraffin phase are shown in Fig. 2. This solu-

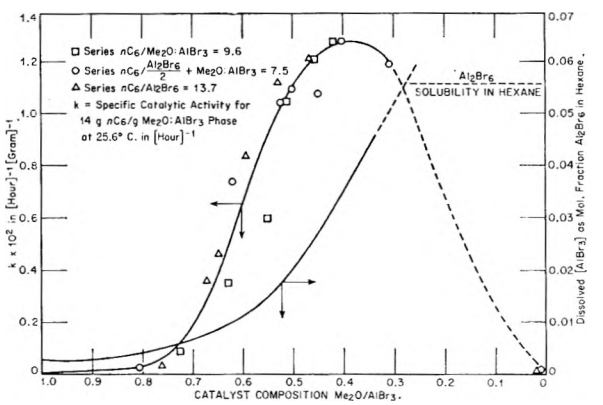

Fig. 2.—Phase composition–catalytic activity for *n*-hexane isomerization.

bility function is, in itself, indicative of the fact that Al_2Br_6 and $Me_2O:AlBr_3$ complex upon mixing and form other molecular species because of the high change in slope found in the composition region $Me_2O/AlBr_3$ = 0.6 to 0.4. Simple non-ideal behavior of Al_2Br_6 and $Me_2O:AlBr_3$ should give an $[AlBr_3]$ solubility function which would be concave downward instead of upward as is found.

The catalytic activity of liquid Me_2O–$AlBr_3$ mixtures is highly dependent upon the composition. It is undetectable when the liquid is pure $Me_2O:AlBr_3$, very low when the phase is solid Al_2Br_6 and rises to a high activity maximum in the region of composition $Me_2O/AlBr_3$ about 0.4.

B. The Phase Diagram of $Me_2O:AlBr_3$ and Al_2Br_6.—The experimental data are shown graphically in Fig. 3. No solid compound other than $Me_2O:AlBr_3$ and Al_2Br_6 is evident. However, as is well known, molecular species may be present in the liquid phase in high concentration and yet not exist as a solid. The existence or non-existence of other molecular species in the liquid phase is best inferred by the comparison of the experimental phase dia-

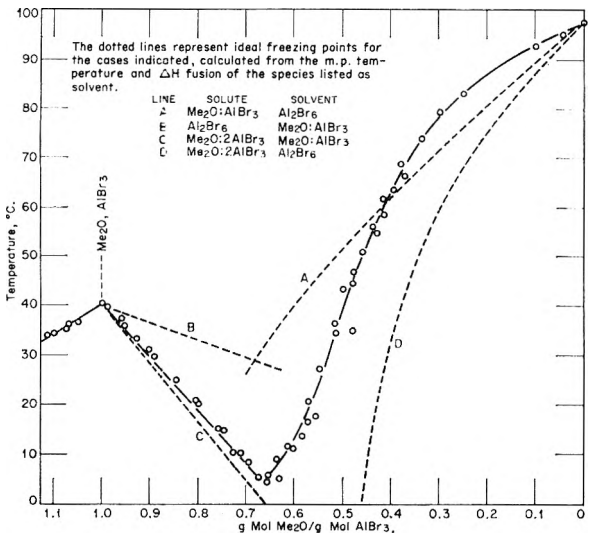

Fig. 3.—Phase diagram methyl ether–aluminum bromide.

gram lines, which are experimental solubility curves of $Me_2O:AlBr_3$ and of Al_2Br_6, with various ideal solubility curves computible from the ideal solubility equation shown in Table II. The heat of fusion and melting point temperature of Al_2Br_6 are known already.

TABLE II

CRYOSCOPIC DETERMINATION OF THE LATENT HEAT OF FUSION OF $Me_2O:AlBr_3$

Computed from:

$$H_f = \frac{RT_1T_0 \ln X_1}{\Delta T}$$

H_f = heat of fusion, $Me_2O:AlBr_3$
T_0 = m.p. of $Me_2O:AlBr_3$
T_1 = solution freezing point
$\Delta T = T_0 - T_1$
X_1 = mole fraction $Me_2O:AlBr_3$

Solute	X_1	ΔT, °C.	H_f
n-Pentane	0.9904	0.70	2,670
	.9804	1.48	2,580
	.9733	1.91	2,730
	.9577	2.90	2,870
Methyl bromide	0.9746	1.58	3,150
	.9542	3.42	2,630
	.9337	4.73	2,770
	.9050	6.78	2,800
Cyclopentane	0.9814	1.36	2,660
	.9443	3.80	2,880
	.9058	6.17	3,050
	.8787	7.94	3,080

$H_f = 2{,}820 \pm 120$ cal./g. mole

Experimental data for the lowering of the freezing point of $Me_2O:AlBr_3$ with solute concentration are shown in Table II. Three different solutes are seen to give a concordant value for the heat of fusion of $Me_2O:AlBr_3$. By the use of this heat of fusion and the melting point of $Me_2O:AlBr_3$, two ideal solubility lines for $Me_2O:AlBr_3$ have been computed and are lines C and B, Fig. 3. Two additional lines were computed using the heat of fusion of Al_2Br_6 and its melting point in the ideal solubility equation. These lines are A and D, Fig. 3.

By a comparison of lines A and B with the experimental phase diagram, it is clear that extensive complexing must exist between $Me_2O:AlBr_3$ and Al_2Br_6. If these two molecules simply mixed with each other, the experimental phase diagram should lie entirely on lines A and B (ideal behavior) or else lie entirely above lines A and B (normal non-ideal behavior). Instead the experimental phase diagram dips far below lines A and B, indicating a far greater than ideal solubility of Al_2Br_6 in $Me_2O:AlBr_3$ and a greater than ideal solubility of $Me_2O:AlBr_3$ in Al_2Br_6.

Line C, Fig. 3 is seen to conform quite closely to the experimental phase diagram all of the way from pure $Me_2O:AlBr_3$ to the eutectic point of the diagram. This conformation is so close that a detailed consideration of the possible reasons why they do not conform exactly is fruitful. The small but significant deviation of the experimental phase diagram from line C may be due to any or all of the following reasons: (a) the heat of fusion of $Me_2O:AlBr_3$ changes significantly between 39.4 and 6°; (b) the species $Me_2O:AlBr_3$ and $Me_2O:2AlBr_3$ do not form ideal mixtures; (c) the reaction between $Me_2O:AlBr_3$ and $^1/_2Al_2Br_6$ to form $Me_2O:2AlBr_3$ is not complete but the three species exist in an equilibrium.

Reason (a) is not thought to be important because of the small temperature interval in question. Reason (b) might be of some importance. The deviation of the experimental phase diagram from line C is in the direction to be expected for non-ideal behavior. However, the observed deviation is so small that even modest non-ideal behavior (such as between a paraffin and benzene) would result in a far greater deviation of line C from the experimental line than is found. Thus it can be argued that $Me_2O:AlBr_3$ and $Me_2O:2AlBr_3$ must mix nearly ideally.

Reason (c) probably is the major cause of the deviation of line C from the experimental phase diagram. That the reaction $Me_2O:AlBr_3 + {}^1/_2 Al_2Br_6$ to form $Me_2O:2AlBr_3$ is not complete is evident from the experimental phase diagram. If this reaction were complete, $Me_2O:2AlBr_3$ would exist in the solid phase and a melting point maximum would have been observed at $Me_2O/AlBr_3 = 0.5$. Also if this reaction were complete Al_2Br_6 could not begin to precipitate out of the liquid phase at $Me_2O/AlBr_3 = 0.66$ because no Al_2Br_6 could be in the liquid phase until a composition $Me_2/AlBr_3 = 0.5$ were reached.

At the experimental eutectic point (5.9° at $Me_2O/AlBr_3 = 0.667$) the liquid phase is simultaneously saturated with $Me_2O:AlBr_3$ and Al_2Br_6. An estimation of the equilibrium constant at the eutectic point may be done by attributing all deviation of line C from the experimental line to (c). When this is done, equilibrium (I) is computed

$$K_{\text{equil. at } 5.9°} = \frac{(Al_2Br_6)^{1/2}(Me_2O:AlBr_3)}{(Me_2O:2\ AlBr_3)} = \frac{(0.044)^{1/2}(0.573)}{(0.38)} = 0.32 \quad (I)$$

(ideal solubility of Al_2Br_6 at 5.9° = 0.104).

Alternatively, the solubility of Al_2Br_6 at this temperature in $Me_2O:AlBr_3$ and $Me_2O:2AlBr_3$ can

be estimated by the regular solution equation of Hildebrand and Scott[3] from the experimental data given in Table IV (see Section D). Thus, assume that $Me_2O:AlBr_3$ and $Me_2O:2AlBr_3$ behave ideally and have the same solubility parameter as that determined for $Me_2O:AlBr_3$ experimentally (see Table IV). The solubility of Al_2Br_6 ($\delta = 9.3$) in mixtures of $Me_2O:AlBr_3$ and $Me_2O:2AlBr_3$ should be then

$$\ln \frac{1}{X_{Al_2Br_6}} = 1.180 \left(\frac{1}{T} - 2.7012\right) + \frac{178\,(11.5 - 9.3)^2}{RT} \quad (1)$$

At 5.9°, the calculated solubility of Al_2Br_6 is 0.02 ($K_{equil.}$ for $I = 0.17$) mole fraction. This is regarded as in reasonable agreement with the value ($X_{Al2Br6} = 0.044$ and $K_{equil.}$ for $(I) = 0.32$) previously estimated by the deviation of line C from the experimental phase diagram. This latter estimate is probably a more accurate estimate of the true Al_2Br_6 concentration in the liquid phase at the eutectic point. The first estimate could well be high because any small non-ideal behavior of mixing of $Me_2O:AlBr_3$ and $Me_2O:2AlBr_3$ would cause a high estimate of the Al_2Br_6 present by the method used.

In Fig. 3, the experimental phase diagram from the eutectic point to pure Al_2Br_6 rises above both lines A and D in the higher temperature region. In the lower temperature region, the experimental line is seen to drop below line A and approach somewhat line D. The same three reasons for this behavior might be operative as was previously discussed for the deviation of line C from the experimental line. One additional reason is undoubtedly important here. The equilibrium constant (I) is undoubtedly temperature dependent. In Fig. 4 the experimental line is compared with two non-ideal solubility lines computed from the Hildebrand δ's and the other physical properties of $Me_2O:AlBr_3$, $Me_2O:2AlBr_3$ and Al_2Br_6 given in Table IV, Section D, by the Hildebrand–Scott method.[3]

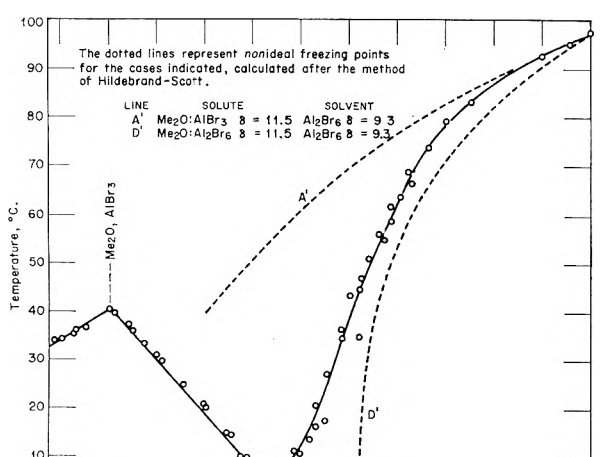

Fig. 4.—Phase diagram methyl ether–aluminum bromide.

(3) J. H. Hildebrand and R. L. Scott, "The Solubility of Non-Electrolytes," Reinhold Publ. Corp., New York, N. Y., Chapter XVII.

The behavior of the experimental line when compared with lines A and D, Fig. 4, is interpreted as showing that the equilibrium

$$Me_2O:2AlCl_3 \rightleftharpoons 1/2\ Al_2Cl_6 + Me_2O:AlCl_3. \quad (II)$$

has a temperature dependence of the equilibrium constant such that at 100° the equilibrium lies mostly to the left, while at lower temperatures considerable concentrations of $Me_2O:2AlBr_3$ exist in the liquid phase.

Raman spectra also have been obtained on Me_2O–$AlBr_3$ solutions.[4] In addition to other interesting results, this spectrum confirms the existence of the species $Me_2O:2AlBr_3$ in the liquid phase and yields an estimate of the equilibrium constant of (I) similar to that deduced here from the phase diagram.

C. Molecular Species and Catalytic Activity of a Liquid Me_2O–$AlBr_3$ Phase for Paraffin Isomerization.—In Fig. 5 are plotted the catalytic activity data of Fig. 2 with the estimated concentration of the species present in that phase if $K_{equil.}$ at 25° = 0.2. If the equilibrium constant were larger or smaller than 0.2, the concentration of the species $Me_2O:2AlBr_3$ would vary but the form of its concentration curve would be the same. It is clear that the catalytic activity found is closely associated with the concentration of the molecular species $Me_2O:2AlBr_3$. A definite sag in the catalytic activity curve occurs which does not appear in the $Me_2O:2AlBr_3$ concentration curve at low concentrations of $Me_2O:2AlBr_3$. This could be due to the fact that n-hexane is more soluble in the $Me_2O:AlBr_3 + Al_2Br_6$ than it is in $Me_2O:AlBr_3$ and that a higher concentration of n-hexane is dissolved in the catalytic phase when it is rich in $Me_2O:2AlBr_3 + Al_2Br_6$. This sag in the catalytic activity curve at low $Me_2O:2AlBr_3$ concentrations might also be due to a mild inhibition of the catalysis by $Me_2O:AlBr_3$. This might occur by a preferential ordering in the liquid of $Me_2O:AlBr_3$ around $Me_2O:2AlBr_3$ over n-hexane molecules which would effectively "crowd" the n-hexane away from the catalytically active species.

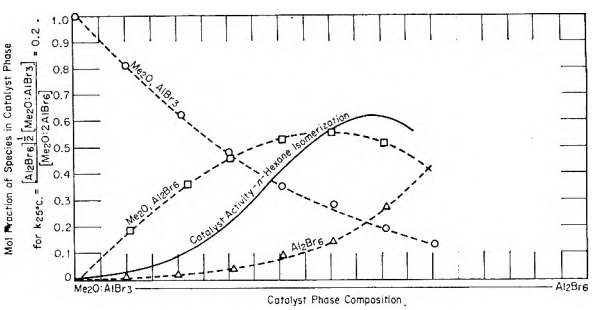

Fig. 5.—Estimated concentration of molecular species in liquid phase of $Me_2O:AlBr_3$–Al_2Br_6 mixtures compared with catalytic activity.

D. Some Molecular Properties of $Me_2O:AlBr_3$ and $Me_2O:AlCl_3$.—In section B, the existence and approximate concentration of $Me_2O:2AlBr_3$ was inferred from the experimental phase diagram of $Me_2O:AlBr_3 = 1.0$ to 0. In making this sort of inference it is vitally important to estimate cor-

(4) D. G. Walker and D. E. Nicholson, unpublished data.

rectly the deviations from ideal behavior of the system. A number of experimental determinations of the solubility of $Me_2O:AlBr_3$ and $Me_2O:AlCl_3$ in paraffins have been made and are shown in Table III. From these data the Hildebrand δ's for these two molecules have been computed and are shown in Table IV along with other molecular properties necessary to calculate non-ideal solubilities of these species.

One other question which remains to be answered is: molecules like $Me_2O:AlBr_3$ are highly polar species which contain most of their polarity in only one bond (Al–O). Are molecules like this self-associated in their liquid state and thus have highly non-ideal liquid entropies?

The data of $Me_2O:AlCl_3$'s solubility in *n*-heptane as function of temperature (Table V) is taken to show that $Me_2O:AlCl_3$ has an ideal solution entropy in *n*-heptane and, therefore, the pure $Me_2O:AlCl_3$ does not have an abnormal liquid entropy. The experimental entropy of solution measured from the change of solubility with temperature is in reasonably close agreement with the ideal entropy of dilution. While pure liquid $Me_2O:AlCl_3$ is not associated, it, very likely, is associated by dipole–dipole interaction in dilute solution of a paraffin. Ulrich[5] measured the cryoscopic molecular weight of $Et_2O:AlCl_3$ and $Et_2O:AlBr_3$ in benzene. He found these molecules to be monomeric in dilute solution but to have an association factor of about 1.5 in 0.025 mole fraction solution.

TABLE III

SOLUBILITY DATA OF LIQUID $Me_2O:AlX_3$–PARAFFIN PHASES

Temp., °C.	$X_{Me_2O:AlCl_3}$	$X_{Me_2O:AlBr_3}$	Hydrocarbon
25.5	0.0036	..	0.9964 *n*-Hexane
25.5	..	0.0045	.9955 *n*-Hexane
34.0	.981	..	.019 *n*-Heptane
42.6	.970	..	.030 *n*-Heptane
52.0	.957	..	.043 *n*-Heptane
35.2	.984	..	.016 2,3-Dimethylbutane
43	..	.978	.022 *n*-Hexane
52	..	.963	.037 *n*-Hexane

TABLE V

SOLUBILITY OF $Me_2O:AlCl_3$ IN *n*-HEPTANE

Temp., °C.	Exptl.	Calcd.[a]	% Dev.
25.6	0.00443	0.00398	−10.4
26.1	.00446	.00405	− 9.2
38.3	.00584	.00588	0.7
49.4	.00810	.00803	− 0.9
61.1	.0106	.01095	3.2
71.1	.0137	.0140	2.3
82.8	.0179	.0184	2.9
92.8	.0219	.0229	4.5

[a] Log $X_{Me_2O:AlCl_3} = -1.234(1/T) + 1.732$. Experimental ΔH_{soln} of liquid $Me_2O:AlCl_3$ into *n*-heptane = + 5,720 cal./g. mole. Experimental ΔS_{soln} of liquid $Me_2O:AlCl_3$ into *n*-heptane = 7.9 e.u. Ideal ΔS of diln. = R ln 0.01 = 9.1 e.u. for 1.0% solution.

It was not possible to obtain the full phase diagram ($Me_2O/AlCl_3$ = 1.0 to 0) experimentally because of the thermal breakdown of $Me_2O:AlCl_3$ into AlOCl and 2 MeCl. This occurs at a significant rate at temperatures above 150°. In Fig. 6 are shown the experimental points which were obtained without significant thermal breakdown of the species present. The heat of fusion of $Me_2O:AlCl_3$ was also determined cryoscopically (Table VI).

Using this heat of fusion for $Me_2O:AlCl_3$ and the known heat of fusion of Al_2Cl_6 (17.0 kcal./g. mole), two ideal freezing point lines were calculated and are shown on Fig. 6. Here, as in the analogous case of dimethyl ether–aluminum bromide, complexing between $Me_2O:AlCl_3$ and Al_2Cl_6 is clearly present. If these two species simply mixed, the experimental freezing temperature line should lie entirely on or above line A. Instead, the experimental line lies far below line A.

If one assumes that $Me_2O:AlCl_3$ and Al_2Cl_6 react quantitatively upon mixing to yield $Me_2O:2AlCl_3$ and that $Me_2O:AlCl_3$ and $Me_2O:2AlCl_3$ behave ideally, a freezing point line B should be observed. As is seen, the experimental line from $Me_2O/AlCl_3$ = 1.0 to 0.86 is identical with line B. Therefore, the assumptions used in the calculation of line B must be substantially correct.

TABLE IV

MOLECULAR PROPERTIES OF $Me_2O:AlX_3$

Compound	M.p., °C.	ΔH fusion (cal./g. mole)	Ideal solubility eq.	Molar volume at 40° (ml.)	Solubility parameter (26–40°).
$Me_2O:AlCl_3$	29.3	3515	$\log \frac{1}{X} = 0.768\left(\frac{10^3}{T} - 3.307\right)$	139	12.2[a] 11.6[b]
$Me_2O:AlBr_3$	39.4	2820	$\log \frac{1}{X} = 0.616\left(\frac{10^3}{T} - 3.200\right)$	151	12.0[a] 11.5[b]

[a] Based on solubility of $Me_2O:AlX_3$ in paraffin. [b] Based on solubility of paraffin in $Me_2O:AlX_3$.

E. The Phase Diagram of $Me_2O:AlCl_3$ and Al_2Cl_6. —Extensive catalytic activity–composition data have not been obtained on this phase as was the case with the $Me_2O:AlBr_3$ and Al_2Br_6 (section B). However, it has been established that $Me_2O:AlCl_3$ is not active for paraffin isomerization while saturated Me_2O–$AlCl_3$ solutions at 40–50° are highly active. From this it is assumed that this system is entirely analogous to the corresponding one of section B.

An estimation of equilibrium constant, entropy and enthalpy of reaction for

$$Me_2O:2AlCl_3 \rightleftarrows {}^1/_2Al_2Cl_6 + Me_2O:AlCl_3 \qquad (II)$$

can be made from the phase diagram. In a manner similar to that used in the ether–aluminum bromide system, the equilibrium constant at any experimental point can be estimated. Here, the concentration of Al_2Cl_6 must be very small and the major part of the solution always consists of $Me_2O:AlCl_3$ and $Me_2O:2AlCl_3$. Assuming that these two species behave ideally and that the Al_2Cl_6 activity

(5) H. Ulrich, *Z. physik. Chem.*, **B15**, 431 (sup. 1931).

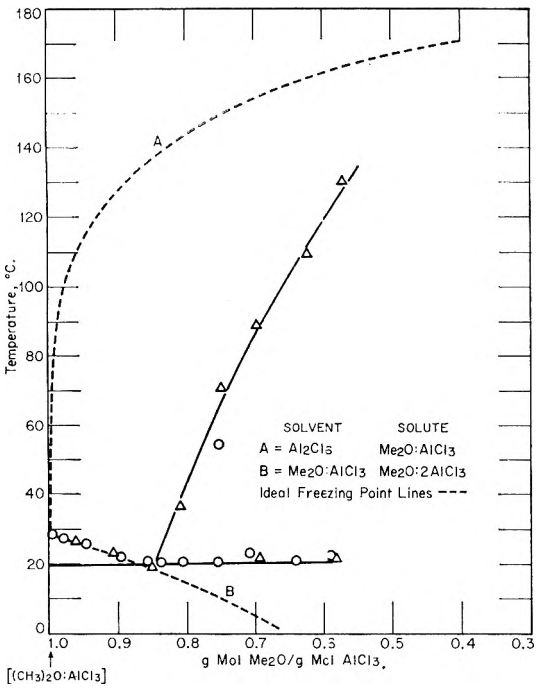

Fig. 6.—Phase diagram dimethyl ether–aluminum chloride.

TABLE VI

CRYOSCOPIC DETERMINATION OF THE HEAT OF FUSION OF $Me_2O:AlCl_3$

Solvent, $Me_2O:AlCl_3$ (m.p. 29.32°)[a]; Solute, *n*-pentane

$X_{Me_2O:AlCl_3}$	ΔT, °C.	Calcd. ΔH_f
0.9930	0.37	3430
.9899	.57	3220
.9870	.63	3760
.9834	.87	3470
.9788	1.07	3640
.9745	1.22	3800
.9690	1.62	3530
		3550 ± av. H_f

Cyclopentane

$X_{Me_2O:AlCl_3}$	ΔT, °C.	Calcd. ΔH_f
0.9918	0.40	3750
.9793	1.05	3610
.9580	2.30	3390
.9441	3.15	3310
.9297	3.99	3310
		3470 ± av. ΔH_f

[a] Computed in the same manner as in Table II.

is equal to that calculated from the theoretical equation, the equilibrium constant may be estimated from this computed value for the Al_2Cl_6 concentration and the experimental phase diagram. In Table VII are listed the mole fractions of the three species calculated by such a procedure as well as the estimated equilibrium constant. A least squares calculation of these data yields a value of $\Delta S = 5.9$ e.u. and a $\Delta H = 3.9$ kcal. for the forward reaction of (II). The entropy change seems too low to be plausible for such a reaction. The various assumptions involved in calculating the equilibrium constant by these methods are probably not of adequate accuracy for the accurate determination of ΔS and ΔH. However, reasonable estimates of the equilibrium constants are obtained by this method.

Experimental

Activity–Composition Studies.—The paraffin isomerization activity measurements were carried out employing: (1) *n*-Hexane (Phillips' technical containing 2.8% methylcyclopentane); (2) $Me_2O:AlBr_3$ (synthesized m.p. 39.3°); (3) Al_2Br_6. It was established in previous work that the disappearance of *n*-hexane during isomerization, under the conditions used, was first order in *n*-hexane and that the *n*-hexane could be isomerized to an equilibrium distribution of the hexane isomers (5% *n*-hexane) with only traces of any side reactions (0.3% of non-C_6 paraffin product).

Various quantities of $Me_2O:AlBr_3$ and Al_2Br_6 were weighed out and mixed with 20 ml. of the *n*-hexane. They were then stirred vigorously for 1 hour at 25.6° in a baffled flask which was protected from the atmosphere with a drying tube vent. Two homogeneous liquid phases resulted in all cases except where pure Al_2Br_6 was used alone.

At the end of the reaction period, an aliquot of the hydrocarbon phase was water-washed and analyzed by a calibrated gas-partition chromatograph apparatus to determine the extent of *n*-hexane isomerization. The catalytic activity constant k_{nC_6} = (hr.$^{-1}$) was computed from $k = 2.3/T(\text{hr.}) \log C_{nC_6} - 5/95$ where C_{nC_6} = mole % *n*-C_6 in the reaction product.

The aluminum and bromide dissolved in the hydrocarbon phase was determined by analysis of the water used for washing the hydrocarbon sample.

Phase Diagram.—Cooling curves were recorded on a Leeds and Northrup high precision recorder. The cell had a built-in thermowell with an NBS certified platinum resistance thermometer. Stirring of the cell was accomplished by a coiled chrome wire which was vibrated at 120 strokes per minute by an external mechanically driven magnet. Synthesized-aluminum bromide (aluminum strips + HBr) was distilled directly into the cell under a blanket of P_2O_5 dried nitrogen. Methyl ether (Matheson Chemical Company cylinder) was added in increments from a standard chemical vacuum system. The amount of the increment was measured by the use of a calibrated volumetric bulb and a mercury manometer.

Cyclopentane (Phillips' Chemical 99.9%), methyl bromide (Matheson Chemical Company), and *n*-pentane (Phillips'

TABLE VII

ESTIMATION OF $K_{equilibrium}$ FOR $K = \dfrac{(Al_2Cl_6)\ 1/2\ (Me_2O:AlCl_3)}{(Me_2O:Al_2Cl_6}$ AT VARIOUS TEMPERATURES

$Me_2O/AlCl_3$	Saturation temp., °K. for Al_2Cl_6	Solubility (theor.) $X_{Al_2Cl_6}$	$X_{Me_2O:AlCl_3}$	$X_{Me_2O:Al_2Cl_6}$	*est.* $K_{equil.}$	*calcd.* $K_{equil.}$[b]
0.57	405	0.062	0.355	0.583	0.152	0.161
.625	383	.018	.428	.554	.104	.122
.692	362	.0053	.561	.432	.095	.091
.750	345	.0016	.666	.329	.081	.070
.810	310	.00010	.764	.235	.032	.037
.850	295	.000023	.824	.177	.022	.029

[a] Calculated from $\log 1/X_{Al_2Cl_6} = 3.71\ (1/T - 2.7012)$. [b] Calculated from $K = e^{5.949/R} e^{-3882/RT}$ (obtained from a least squares analysis) of the estimated $K_{equil.}$ data from whence $Me_2O:Al_2Cl_6 \rightarrow Me_2O:AlCl_3 + 1/2\ Al_2Cl_6$, $\Delta H = +3.0$ kcal., $\Delta S = +5.9$ e.u.

Chemical 99.9%) were measured and added to the cryoscopic cell from the standard chemical vacuum apparatus.

The experimental phase diagrams were made while attached to the chemical vacuum system. Thus any volatile compound formed by decomposition of the Me_2O–AlX_3 phase during the experimental work could be detected and measured accurately. No H_2, CH_4 or HX ever were detected during the experimental work. When the solutions were heated above 100° a decomposition reaction yielding methyl halide as the only volatile product was noted. This is undoubtedly the reaction

$$Me_2O:AlX_3 \xrightarrow[\Delta]{} 2MeX + AlOX$$

Me_2O–AlX_3 phases in the absence of air or moisture are quite stable at room temperature and can be kept without detectible decomposition for months.

Solubility Data.—The solubility of $M_2O:AlX_3$ in paraffins was measured by stirring the two components vigorously for 1–2 hours together in a controlled temperature bath. The concentration of $Me_2O:AlX_3$ in the paraffin phase was determined by chemical analysis for Al and halogen.

The solubility of paraffins in $Me_2O:AlX_3$ was measured by adding the paraffin in measured increments to $Me_2O:AlX_3$ from the chemical vacuum system and observing the vapor pressure. Since $Me_2O:AlX_3$ has a negligible vapor pressure, the composition at which the vapor pressure first became independent of liquid composition was taken to be the saturation point of the paraffin in $Me_2O:AlX_3$.

Acknowledgment.—The author wishes to express his appreciation to Mr. B. L. Clark for his assistance in a number of the experimental measurements.

THE EFFECT OF VARIOUS GASES AND VAPORS ON THE SURFACE TENSION OF MERCURY[1]

BY M. E. NICHOLAS, P. A. JOYNER, B. M. TESSEM AND M. D. OLSON

Honeywell Research Center, Hopkins, Minnesota

Received February 25, 1961

The effects of He, H_2, N_2, O_2, CO_2, H_2O, CH_4, C_3H_8, and pump oil on the surface tension of highly purified Hg have been determined, utilizing a large sessile drop and Worthington's equation. Kemball's value of 484 dynes/cm. for the surface tension of Hg *in vacuo* at 25° was confirmed prior to the study of gases and vapors. Contrary to previously published results, it is found that He, H_2, N_2, O_2 and CO_2 do not adsorb on highly purified mercury at 25°. Previous results are due to inadequate purification of mercury and bases, or to presence of stopcock grease, pump oil or other contaminants. Details of the experimental method and purification techniques are given. The effects of H_2O, C_3H_8 and pump oil on the surface tension of mercury are discussed.

Introduction

A literature review of the adsorption of gases and vapors upon mercury surfaces, as measured by changes in the surface tension, revealed a wide range of reported effects. Indeed, the reported values for the surface tension of mercury *in vacuo* (in the presence of its own vapor only) range from 400 to 516 dynes/cm. at 25°. Table I contains some reported values for the surface tension of mercury *in vacuo*.

TABLE I

REPORTED VALUES FOR THE SURFACE TENSION OF MERCURY

Investigator	Date	Dynes/cm.[a]	Method
Harkins and Ewing[2]	1920	476	Drop weight
Hogness[3]	1921	476	Drop pressure
Iredale[4]	1922	472	Drop weight
Iredale[5]	1924	464	Sessile drop
Cook[6]	1929	516	Sessile drop
Kernaghan[7]	1931	435	Sessile drop
Burdon[8]	1932	488	Sessile drop
Bradley[9]	1933	498	Sessile drop
Kernaghan[10]	1936	476	Sessile drop
Kemball[11]	1946	484	Sessile drop

[a] Corrected to 25°.

Our objective in this study was to establish whether or not certain gases and vapors adsorb on the surface of highly purified mercury and the consequent effects on the surface tension.

Experimental Procedure

The apparatus utilized by this Laboratory was patterned after the studies of Bradley[9] and Kemball.[11] The surface tension values were obtained by measuring the dimensions of a large drop of mercury resting on a cup or flat plate. The corrected Worthington equation[12] was used to calculate the surface tension. It is

$$\gamma = \frac{\rho g h^2}{2} \frac{(1.641R)}{(1.641R + h)}$$

where

γ = surface tension
ρ = density of mercury
g = gravitational acceleration
h = max. height of the drop above the max. diameter
R = radius of the drop at max. horizontal

Burdon[8] reported that this equation is consistent and accurate only when a drop with a radius greater than 2 cm. is utilized. This was confirmed experimentally by this Laboratory.

The dimensions of the mercury drop were initially measured while it rested on a Pyrex cup within a Pyrex tee specially fabricated from 60 mm. Pyrex tubing. The two upper ends of the tee, for holding the optically polished Pyrex windows were optically ground perpendicular to the center line of the tube. The lip of the cup which had been optically polished was 46 mm. in diameter; it was aligned parallel to the same center line. A Gaertner cathetometer, specially fitted with an Abbe–Lamont eyepiece and fine crosshairs, was aligned with a damped plumb line, so as to

(1) Presented in part under the auspices of the Division of Colloid Chemistry, American Chemical Society, at the meeting in Cleveland, Ohio, April 11–14, 1960.

(2) W. D. Harkins and W. W. Ewing, *J. Am. Chem. Soc.*, **42**, 2539 (1920).

(3) T. R. Hogness, *ibid.*, **43**, 1621 (1921).

(4) T. Iredale, *Phil. Mag.*, **45**, 1088 (1923).

(5) (a) T. Iredale, *ibid.*, **48**, 177 (1924); (b) **49**, 603 (1925).

(6) S. G. Cook, *Phys. Rev.*, **34**, 513 (1929).

(7) M. Kernaghan, *ibid.*, **37**, 990 (1931).

(8) R. S. Burdon, *Trans. Faraday Soc.*, **38**, 866 (1932).

(9) S. Bradley, *J. Phys. Chem.*, **38**, 231 (1934).

(10) M. Kernaghan, *Phys. Rev.*, **49**, 414 (1936).

(11) C. Kemball, *Trans. Faraday Soc.*, **42**, 526 (1946).

(12) A. M. Worthington, *Phil. Mag.*, **20**, 51 (1885).

traverse in vertical and horizontal directions. The Pyrex window was aligned perpendicular to the cathetometer, and thus perpendicular to the plane of the lip of the cup. Next, the Pyrex cup was leveled by horizontal movement of the cathetometer, parallel to the window. This alignment procedure was necessary before each determination.

The height of the mercury drop, and thus the size, was controlled by using a U-tube. Mercury was spilled gently into the U-tube from a reservoir by means of a Pyrex bulb containing an iron ring. Thus, mercury was displaced into the U-tube as the bulb was lowered into the mercury with an electromagnet.

Mercury of the highest purity was utilized for this study. Information pertaining to the actual purity of commercial grade mercury is quite limited. Oxidation and chemical treatment, followed by distillation, seemed the best method of purification. Table II illustrates the relative efficiencies of some processes in the removal of metals.

TABLE II

REMOVAL OF METALS FROM MERCURY IN DESCENDING ORDER OF EASE OF REMOVAL[13]

Absorption of oxygen by amalgams	Metals removed by KOH	Metals removed by HNO_3	Metals removed by vacuum distn.
Na	Sn	Mg	Au
Mg	Zn	Al	Pt
Zn	Pb	Cr	Ag
Cd		Mn	Cu
Pb		Cd	Sn
Sn		Ni	Pb
Tl		Sn	Zn
		Pb	Cd
		Cu	

Oxidation will form insoluble oxides of the alkali and less noble metals. Treatment with sodium hydroxide and nitric acid will remove a large group of base metals. Distillation is the most effective method for reducing the concentration of noble metals. Consequently, the following procedure was used to purify the mercury. A series of solutions were placed over the mercury and pure air was bubbled through the mercury and the solution. The solutions were: (a) 3 *M* sodium hydroxide, (b) 3 *M* nitric, and (c) 0.001 *M* nitric acid. The air oxidizes some of the impurities and stirs the mercury. Thus, it continually renews the interface between the mercury and the solution. The progress of purification was followed by observing the clarity of the solution above the mercury. The solution picked up impurities rapidly and had to be changed frequently during the first few days. The entire solution was replaced with the next in the series when the solution appeared optically clear after 48 hours of bubbling. Solutions were removed from the mercury with a suction hose. The mercury was washed several times with distilled water before introducing the next solution. Deionized water was used for the final washing before distillation. The mercury received a double filtration through a pin hole in filter paper as it was poured into the reservoir of the still.

(13) *Ann. N. Y. Acad. Sci.*, **65**, 379 (1957).

The inverted U-tube still was fabricated from Pyrex glass. This system is greaseless since no valves are required. The still was protected from back diffusion of vacuum pump oil by a liquid nitrogen cold trap and carbon pellets. The distillate was gravitationally drained into a clean receiver. The flasks used for the chemical purification, being well rinsed with mercury, made good storage containers. Pure oxygen was bubbled gently through the hot mercury during distillation. The oxygen was purified by passing it through silica gel and carbon to remove water and organic vapors, respectively. There was no buildup of oxide films on the surface of the mercury in the pot, on the sides of the pot, or in the receiver during the long periods of usage, indicating that oxide forming metals were efficiently removed by the chemical treatment. Therefore, the use of oxygen during distillation may not be necessary. All mercury was distilled a minimum of three times. The easiest method of keeping the still clean and the glassware rinsed was by continual usage. Therefore, the mercury was cycled from the receiver back to the pot during those periods when mercury was not needed.

There are unresolved questions as to the best container for storing high purity mercury. Soft glass and pure iron are commonly used. Plastic containers, polyethylene specifically, will transfer vapors to the vacuum system. These vapors cannot be removed by pumping. Pyrex suction flasks were used exclusively for the storage of mercury in this research because it would contact Pyrex during experimentation. The containers were cleaned with hot concentrated nitric acid and rinsed with deionized water. However, all Pyrex surfaces do not react the same with mercury and only selected Pyrex containers were satisfactory; others readily interact with mercury to form an amalgam film. The glass surface was completely wetted by mercury in some cases.

All gases except water vapor were meticulously purified by the purification train utilizing the stages shown in Table III. The gas was gently purged through the train to the atmosphere for several hours before being admitted to the measuring system.

A further precaution was the use of a second U-tube cold trap. This was next to the entrance valve but on the measuring system manifold. This trap was heated at the conclusion of several experiments, and in no case caused a change in the surface energy of the mercury, demonstrating the adequacy of the purification train.

Water was purified by a different procedure. A liter beaker was cleaned and thoroughly rinsed with distilled water. A volume of approximately 500 ml. of distilled water was degassed by placing it in the beaker and boiling it to 200 ml.

The water container, to be attached to the valve of the measuring system, was cleaned with nitric acid and liberally rinsed with distilled water. This container, having a side arm U-tube trap, was fabricated from Pyrex. Copper tubing and a Pyrex-Kovar graded seal were used to facilitate the connection to the measuring system valve. The container was then liberally rinsed with the degassed water. The final 50 ml. of this water was added to the container and vigorously boiled to obtain steam for a second degassing of the water and added cleansing of the container surfaces. The final volume of water was 20 ml.

The hot container was immediately connected to the

TABLE III

Impurities removed	Agent	Container material	Gas or vapor: H_2	N_2	O_2	CO_2	He	CH_4	C_3H_8
Water rust	Silica gel	Copper	X	X	X	X	X	X	X
Carbon dioxide	Ascarite	Pyrex	X	X	X	..	X	..	..
Water	Silica gel	Pyrex	X	X	X	X	X	..	..
Organic vapors	Carbon granules	Pyrex	X	X	X	X	X	X	X
Hydrogen or oxygen	Deoxo Unit 125°	Iron	X	X	X	X	X	..	..
Water	Silica gel	Copper	X	...	...	..	X	..	..
Water	$CaSO_4$ and $Mg(ClO_4)_2$	Copper	...	X	X	X	...	..	..
Nitrogen	Mg 350°	Iron	X	...	X	X	X	..	..
Hydrogen	Ca 425°	Iron	...	X	X	X	X	..	..
Any residual vapors	Cold trap 0°	Copper	−192	−192	−192	−79	−192	−79	−35

measuring system valve. The U-tube was immersed in liquid nitrogen to eliminate any accumulation of atmospheric contaminants during cooling. The water was further degassed a total of three times by evacuation while cooling. It was then carefully frozen with liquid nitrogen with continued evacuation. The liquid nitrogen level was altered and all exposed parts of the container were flamed carefully and evacuated. The condensation line at each new level was observed for optical effects that would indicate the presence of vapor impurities. A total of three hours was spent flaming, lowering the liquid nitrogen level, and evacuating. The ice was melted and degassed one final time. The section of Pyrex tubing between the container and U-tube trap was torched and sealed leaving the pure water sealed to the system. A slightly modified method was also used to purify water. The results, within experimental error, were identical and substantiated the purity of the water.

Results

The value repeatedly obtained in this Laboratory for the surface tension of mercury *in vacuo* at 25° was 483.5 ± 1 dyne/cm. The value was obtained within experimental error in two completely separate systems both capable of maintaining pressures less than 1×10^{-7} mm. Hg (prior to introduction of Hg). The first system used a cup, the second a flat plate, to support the drop. After having established a value for the surface tension of mercury, the effects of various carefully purified gases and vapors were studied. A number of these gases caused no decrease in the surface tension of mercury (within experimental error) even at pressures up to one atmosphere and for periods of contact in excess of 24 hours. In some cases, this is contrary to previously reported results.[6,7,9,10,14-17] Since the surface tension of mercury has been shown to be susceptible to a great variety of impurities, particularly stopcock grease, we can only assume that previously, investigators did not take adequate precautions against such contamination. Table IV shows the values of surface tension of mercury for those gases where no effect was observed.

TABLE IV

SURFACE TENSION OF MERCURY UNDER ONE ATMOSPHERE OF PRESSURE GAS AT 25°

Gas	Dynes/cm. ±1.0
Helium	482.2
Hydrogen	483.4
Nitrogen	483.1
Oxygen	483.1
Carbon dioxide	484.2
Methane	484.3

Those vapors which affected the surface energy of mercury were water, propane and vacuum pump oil; methane did not noticeably affect the surface energy of mercury. The dependence of surface tension of mercury on pressure of water vapor and propane are shown in Fig. 1 and 2.

(14) R. C. L. Bosworth, *Trans. Faraday Soc.*, **34**, 1501 (1938).
(15) R. C. L. Bosworth, *ibid.*, **35**, 1353 (1939).
(16) J. Foryst, *Prace Glownego Inst. Met.*, 307 (1951).
(17) C. Kemball, *Proc. Roy. Soc. (London)*, **190**, 117 (1947).

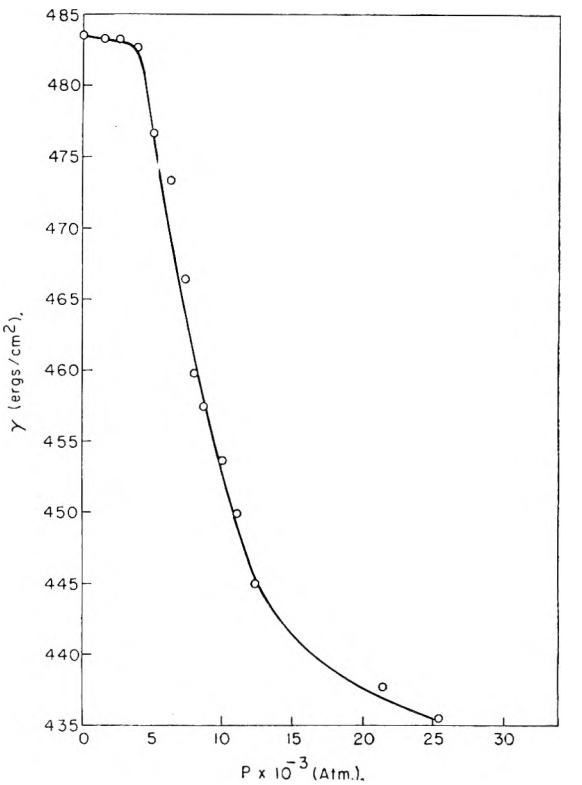

Fig. 1.—Dependence of surface tension of mercury on pressure of water vapor.

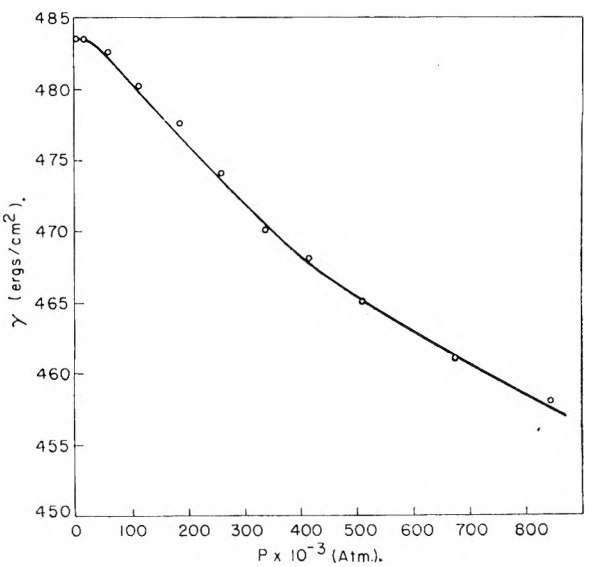

Fig. 2.—Dependence of surface tension of mercury on pressure of propane.

Vacuum and diffusion pump oils have reduced the surface energy of mercury to values ranging from 450 to 250 dynes/cm.² in extreme cases. The effect of atmospheric contaminants in our laboratory reduces the surface energy to values ranging from 400 to 380 dynes/cm.².

GRAPHICAL METHODS OF DETERMINING SELF-ASSOCIATION CONSTANTS. III. REFINED TREATMENT OF MOLECULAR WEIGHT DATA

BY F. J. C. ROSSOTTI* AND HAZEL ROSSOTTI

Department of Chemistry, The University of Edinburgh, Scotland

Received February 27, 1961

New graphical methods are proposed for evaluating self-association constants from the variation of the number average molecular weight with total concentration. They are applicable to systems containing one, two or three oligomers, or an extended series of multimers, and are particularly useful if appreciable association occurs at the lowest concentration studied. The methods are illustrated with reference to hydrogen fluoride and sulfur in the vapor phase; to N,N′-diphenylformamide in benzene; and to imidazole in carbon tetrachloride.

Methods[1-3] for computing equilibrium constants, β_q, for the self-association reactions

$$qB \rightleftharpoons B_q \quad 1 < q \leq Q$$

usually require a knowledge of one or both of the quantities

$$B = \sum_1^Q q[B_q] = \sum_1^Q q\beta_q b^q \qquad (1)$$

and

$$S = \sum_1^Q [B_q] = \sum_1^Q \beta_q b^q = \frac{BM_1}{M_n} \qquad (2)$$

as a function of the concentration, b, of free monomer. Here $\bar{M}_n$ is the number average molecular weight, and M_1 is the molecular weight of the monomer. The value of b may either be measured directly, or calculated from the relationship

$$\log b = \log b_0 + \log I \qquad (3)$$

where the Bjerrum integral[4] I is defined by

$$\log I = 0.4343 \int_{S_0}^{S} \frac{1}{\bar{B}}\, dS = \int_{S_0}^{S} \frac{S}{\bar{B}}\, d \log S \qquad (4)$$

and b_0, S_0 are the values of b and S at the lowest concentration studied. It is often difficult to obtain reliable values of b_0, especially if appreciable association occurs over the whole concentration range studied,[1] and any consequent error in b will result in errors in values of β_q obtained from the functions $B(b)$ or $S(b)$. In the absence of a knowledge of b, the function $B(S)$ has only been used to give values of β_q for systems which contain either a unique oligomer[1,5] or certain extended series of multimers.[5,6] The present paper describes more general methods for obtaining association in constants from the variation of B and S with the integral I, by treating b_0 as an extra unknown parameter.

Once the required parameters β_q and b_0 have been determined, they may be checked by (i) calculating b, and analyzing the functions $B(b)$ and $S(b)$ as described previously,[1-3] and (ii) recalculating the primary data $B(S)$ by substitution into equations 1 and 2. The latter procedure is the more sensitive to errors in the association constants, and always should be carried out.

A Single Oligomer

For a system containing only B and B_Q, combination of equations 1, 2 and 3 gives

$$L = BI^{-1} = b_0 + Q\beta_Q b_0^Q I^{Q-1} \qquad (5)$$

$$\text{and } \Lambda = SI^{-1} = b_0 + \beta_Q b_0^Q I^{Q-1} \qquad (6)$$

Normalization of L, Λ and I gives

$$\log \mathbf{L} = \log L - \log b_0 \qquad (7)$$

$$\log \mathbf{\Lambda} = \log \Lambda - \log b_0 \qquad (8)$$

$$\text{and } \log \mathbf{I} = \log I + \log b_0 + \frac{1}{Q-1} \log \beta_Q \qquad (9)$$

Thus for a given value of Q the experimental functions $\log L$ ($\log I$) and $\log \Lambda$ ($\log I$) have the same shape and separation as the pair of normalized curves $\log \mathbf{L}$ ($\log \mathbf{I}$) and $\log \mathbf{\Lambda}$ ($\log \mathbf{I}$) calculated by means of the relationships

$$\mathbf{L} = 1 + Q\mathbf{I}^{Q-1} \qquad (10)$$

$$\text{and } \mathbf{\Lambda} = 1 + \mathbf{I}^{Q-1} \qquad (11)$$

(*cf.* equations[7] I-21 and I-22). The correct value of Q is that used to calculate the normalized curves of the same shape as the experimental functions. The values of β_Q and b_0 and the appropriate limits of error may be obtained conveniently from equations 7, 8 and 9 by curve-fitting methods analogous to those described previously.[1-3]

N,N′-Diphenylformamide.—White and Kilpatrick's values[8] of $B(S)$ for N,N′-diphenylformamide in benzene at 5.5° have been analyzed by the method described above. A very good fit (see Fig. 1) was obtained for $Q = 2$, $\log \beta_2 = 1.83 \pm 0.04$ and $\log b_0 = -2.31_5 \pm 0.02_5$ (on the molal scale). The value of β_2 is in excellent agreement with that obtained from Dunken's formula[5] by the original authors, and gives a good description of the primary data $B(S)$.

A Pair of Oligomers

If a system contains two oligomers, B_C and B_Q, the three unknown parameters β_C, β_Q and b_0 may be obtained by separate graphical analysis of the variation of $(B - S)$ and of B/S with I.

* Inorganic Chemistry Laboratory, University of Oxford, England.

(1) F. J. C. Rossotti and H. Rossotti, *J. Phys. Chem.*, **65**, 926 (1961) (Part I).

(2) F. J. C. Rossotti and H. Rossotti, *ibid.*, **65**, 930 (1961) (Part II).

(3) F. J. C. Rossotti and H. Rossotti, "The Determination of Stability Constants," McGraw-Hill Book Co., Inc., New York, N. Y., 1961, Chap. 16.

(4) J. Bjerrum, *Kem. Maanedsblad*, **24**, 21 (1943).

(5) H. Dunken, *Z. physik. Chem.*, **45B**, 201 (1940); K. L. Wolf, H. Dunken and K. Merkel, *ibid.*, **46B**, 287 (1940).

(6) E. N. Lassettre, *J. Am. Chem. Soc.*, **59**, 1383 (1937); *Chem. Revs.*, **20**, 259 (1937).

(7) Equation and figure numbers preceded by I- and II- are given in Parts I and II (ref. 1 and 2).

(8) N. E. White and M. Kilpatrick, *J. Phys. Chem.*, **59**, 1044 (1955).

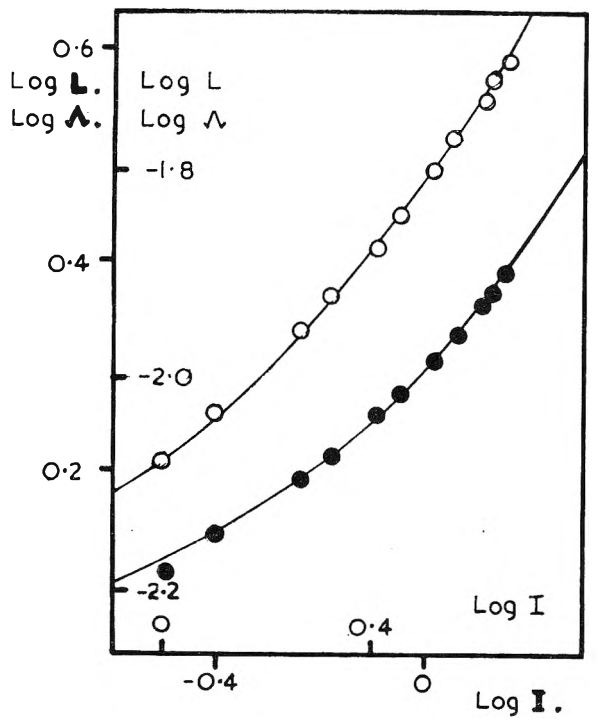

Fig. 1.—N,N'-Diphenylformamide in benzene at 5.5°. Normalized curves log **L** (log **I**) and log **Λ** (log **I**) for $Q = 2$ superimposed on the experimental data log L (log I) (○) and log Λ (log I) (●) in the position corresponding to lo $\beta_2 = 1.83$ and log $b_0 = -2.315$.

For a system containing B, B_C and B_Q, combination of equations 1, 2 and 3 gives

$$B - S = (C - 1)\beta_C (b_0 I)^C + (Q - 1)\beta_Q (b_0 I)^Q \quad (12)$$

The value of C may therefore be obtained from the limiting slope.

$$\lim_{I \to 0} \frac{\mathrm{d} \log (B - S)}{\mathrm{d} \log I} = C \quad (13)$$

and used to calculate the function

$$\Gamma = \frac{B - S}{I^C} = (C - 1)\beta_C b_0{}^C + (Q - 1)\beta_Q b_0{}^Q I^{Q-C} \quad (14)$$

Normalization of Γ and I gives

$$\log \mathbf{\Gamma} = \log \Gamma - \log (C - 1)\beta_C - C \log b_0 = \log \left\{1 + \frac{(Q - 1)\beta_Q}{(C - 1)\beta_C} (b_0 I)^{Q-C}\right\} \quad (15)$$

and

$$\log \mathbf{I} = \log I + \log b_0 + \frac{1}{Q - C} \log (Q - 1)\beta_Q - \frac{1}{Q - C} \log (C - 1)\beta_C \quad (16)$$

whence

$$\log \Gamma = \log (1 + \mathbf{I}^{Q-C}) \quad (17)$$

The family of normalized curves log Γ (log **I**)$_{C,Q}$ is calculated for the appropriate value of C and different values of Q. Values of Q, (log Γ − log Γ) and (log **I** − log I) are obtained by comparison of the experimental function log Γ (log I) with this family of normalised curves, *cf.* Fig. 2.

Alternative combination of equations 1, 2 and 3 gives

$$\bar{q} = \frac{B}{S} = \frac{1 + C\beta_C (b_0 I)^{C-1} + Q\beta_Q (b_0 I)^{Q-1}}{1 + \beta_C (b_0 I)^{C-1} + \beta_Q (b_0 I)^{Q-1}} \quad (18)$$

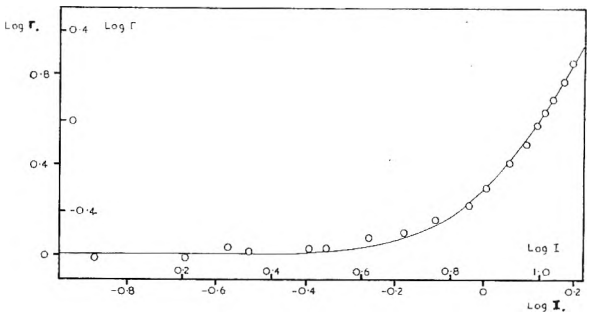

Fig. 2.—Hydrogen fluoride vapor at 38°. The normalized curve log **Γ** (log **I**) for $C = 2$ and $Q = 6$ superimposed on the experimental data log Γ (log I) in the position corresponding to (log **Γ** − log Γ) = 0.595 and (log **I** − log I) = −0.875.

$$= \frac{1 + R\,\mathcal{I}^{C-1} + Q\mathcal{I}^{Q-1}}{1 + R\,\mathcal{I}^{C-1} + \mathcal{I}^{Q-1}} \quad (19)$$

where

$$\log \mathcal{I} = \log I + \log b_0 + \frac{1}{Q - 1} \log \beta_Q \quad (20)$$

and

$$\log R = \log \beta_C - \frac{C - 1}{Q - 1} \log \beta_Q \quad (21)$$

Thus R determines the shape of the curve $\bar{q}$ (log I), and (log $\mathcal{I}$ − log I) its position on the log I axis.

The value of R is obtained either by trial and error or by the projection strip method.[9,10] The latter procedure is particularly convenient if the values of C and Q, and the approximate range of $\bar{q}$, are the same for a number of systems studied, *e.g.*, in investigations of related compounds or of the same substance at different temperatures, or in different solvents. From equation 19

$$R = \frac{1 - \bar{q}}{\bar{q} - C} \mathcal{I}^{1-C} + \frac{Q - \bar{q}}{\bar{q} - C} \mathcal{I}^{Q-C} \quad (22)$$

whence the family of normalized curves log R (log $\mathcal{I}$)$_{\bar{q}}$ may be calculated for a number of values of $\bar{q}$ within the experimental range. For these values of $\bar{q}$, the experimental projection strip (log I)$_{\bar{q}}$ is obtained by marking off the corresponding values of log I, together with the appropriate limits of error on the abscissa of the experimental plot. The projection strip is superimposed on the family of normalized curves log R (log $\mathcal{I}$)$_{\bar{q}}$ parallel to the log I axis and in the position which gives the best fit for all values of $\bar{q}$. The value of R can then be obtained from the ordinate of the family of curves, and the value of (log $\mathcal{I}$ − log I) from the difference between the abscissa of the normalised curves and that of the projection strip (see Fig. 3). The limits of error may be obtained from the maximum permissible vertical and horizontal movement of the strip on the family of normalized curves.

The values of β_C, β_Q and b_0 may be obtained from equations 15, 16, 20 and 21; since there are four equations and only three unknowns, it should be checked that consistent values of the parameters are obtained.

(9) F. J. C. Rossotti, H. Rossotti and L. G. Sillén, *Acta Chem. Scand.*, **10**, 203 (1956).

(10) F. J. C. Rossotti and H. Rossotti, *J. Phys. Chem.*, **63**, 1041 (1959).

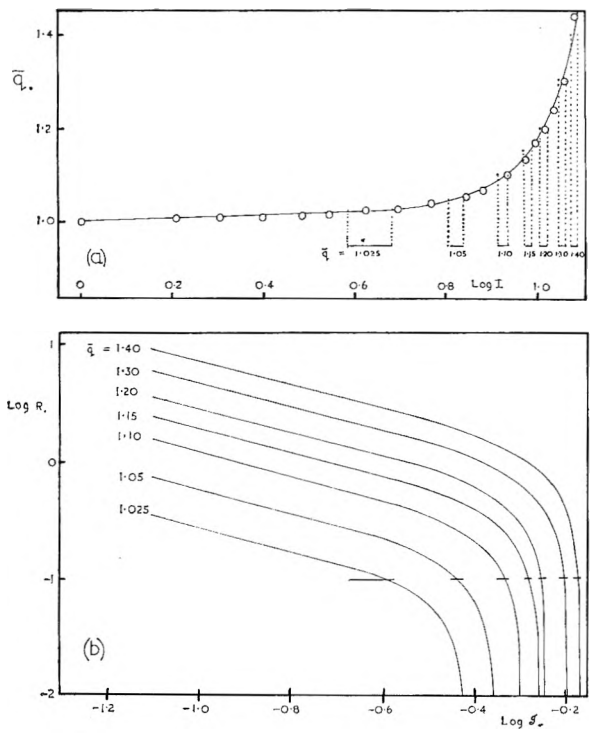

Fig. 3.—Hydrogen fluoride vapor at 38°. (a) Experimental data $\bar{q}$ (log I) and projection strip (log I)$_{\bar{q}}$. The full curve is calculated for log $\beta_2 = -4.005$, log $\beta_6 = -15.025$ and log $b_0 = 1.705$. (b) Normalized curves log R (log $\mathcal{G}$)$_{\bar{q}}$ for $C = 2$ and $Q = 6$, with projection strip superimposed in the position corresponding to log $R = -1.00$ and (log $\mathcal{G}$ − log I) = −1.30.

Hydrogen Fluoride.—Strohmeier and Briegleb's measurements[11] of the vapor density of hydrogen fluoride at 38° may be described in terms of the formation either of the dimer and hexamer[12] or of an extended series of multimers.[12,13] Analysis of the data by the method described above gives $C = 2$, $Q = 6$, log $\beta_2 = -4.00_6$, log $\beta_6 = -15.02_6$ and log $b_0 = 1.70_5$ (see Figs. 2 and 3). The values of β_2 and β_6 are in excellent agreement with those obtained[12] from the functions $B(b)$ and $S(b)$, and give a very good description of the primary data $\bar{q}(S)$.

Three Oligomers

Association constants for systems containing three oligomers may be obtained by applying curve-fitting methods separately to the functions log Γ (log I) and $\bar{q}$(log I). The method is described for the system containing B, B_2, B_3 and B_4, but may be modified readily for systems containing any other three oligomers of known formulas. For a system in which $Q = 4$, combination of equations 1, 2 and 3 gives

$$\Gamma = \frac{B - S}{I^2} = \beta_2 b_0^2 + 2\beta_3 b_0^3 I + 3\beta_4 b_0^4 I^2 \quad (23)$$

The variables Γ and I can be normalized to give

$$\log \mathbf{\Gamma} = \log \Gamma - \log \beta_2 - 2 \log b_0 \quad (24)$$

and

$$\log \mathbf{I} = \log I + \log b_0 + {}^1/_2 \log \beta_4 - {}^1/_2 \log \beta_2 \quad (25)$$

whence

$$\log \mathbf{\Gamma} = \log (1 + 2R\mathbf{I} + 3\mathbf{I}^2) \quad (26)$$

where

$$\log R = \log \beta_3 - {}^1/_2 \log \beta_2 - {}^1/_2 \log \beta_4 \quad (27)$$

The experimental plot log Γ (log I) is compared with the family of normalized curves log Γ (log $\mathbf{I}$)$_R$ calculated for a number of values of R by means of equation 26, *cf.* Fig. I-4. Values of R, and of (log Γ − log Γ) and (log $\mathbf{I}$ − log I) are obtained from the shape of the experimental curve, and from the difference between the experimental and normalized coördinates in the position of best fit.

Alternative combination of equations 1, 2 and 3 gives

$$\bar{q} = \frac{B}{S} = \frac{1 + 2\beta_2 b_0 I + 3\beta_3 (b_0 I)^2 + 4\beta_4 (b_0 I)^3}{1 + \beta_2 b_0 I + \beta_3 (b_0 I)^2 + \beta_4 (b_0 I)^3} = \frac{1 + 2\beta_2 \beta_4^{-1/3} \mathcal{G} + 3\beta_3 \beta_4^{-2/3} \mathcal{G}^2 + 4\mathcal{G}^3}{1 + \beta_2 \beta_4^{-1/3} \mathcal{G} + \beta_3 \beta_4^{-2/3} \mathcal{G}^2 + \mathcal{G}^3} \quad (28)$$

where

$$\log \mathcal{G} = \log I + \log b_0 + {}^1/_3 \log \beta_4 \quad (29)$$

From equations 27 and 28

$$\bar{q} = \frac{1 + 2P^{-1/2} \beta_4^{1/6} \mathcal{G} + 3RP^{-1/4} \beta_4^{1/12} \mathcal{G}^2 + 4\mathcal{G}^3}{1 + P^{-1/2} \beta_4^{1/6} \mathbf{I} + RP^{-1/4} \beta_4^{1/12} \mathcal{G}^2 + \mathcal{G}^3} \quad (30)$$

where

$$P = \frac{\beta_4}{\beta_2^2} = \text{antilog } \{\log \mathbf{\Gamma} - \log \Gamma + 2(\log \mathbf{I} - \log I)\} \quad (31)$$

Since P and R can be obtained from the plot of log Γ against log I, equation 30 contains the single unknown parameter β_4.

The value of β_4 may best be obtained by trial and error as that which, when combined with the appropriate values of P and R, gives a normalized curve $\bar{q}$ (log $\mathcal{G}$) of the same shape as the experimental plot $\bar{q}$ (log I). The range of possible values of β_4 may be obtained by substituting the experimental values of (log Γ − log Γ) and (log $\mathbf{I}$ − log I), together with the extreme possible values of b_0, into equations 24 and 25. The range of possible values of b_0 is given by

$$(2S_0 - B_0) \lesssim b_0 \lesssim S_0 \quad (32)$$

where the subscripts $_0$ refer to the lowest concentration studied.

Normalized curves $\bar{q}$ (log $\mathcal{G}$)$_{P,R,\beta_4}$ are calculated for each acceptable pair of values of P and R using different possible values of β_4 until a curve of the same shape as the experimental plot $\bar{q}$ (log I) is obtained. Equations 24, 25 and 29 are then solved for β_2, β_4, and b_0. The values of the parameters are only acceptable if the value of β_4 obtained in this way is identical with that used for calculating the normalized curve $\bar{q}$ (log $\mathcal{G}$)$_{P,R,\beta_4}$. When a consistent set of parameters β_2, β_4 and b_0 has been obtained, the value of β_3 may be calculated from equation 27.

Sulfur.—The method described above was used to analyze Preuner and Schupp's[14] measurements of the vapor pressure of sulfur at 450°. Since S_2 is undissociated at this temperature, the data may be

(11) W. Strohmeier and G. Briegleb, *Z. Elektrochem.*, **57**, 662 (1953).
(12) J. Maclean, F. J. C. Rossotti and H. Rossotti, to be published.
(13) G. Briegleb and W. Strohmeier, *Z. Elektrochem.*, **57**, 668 (1953).
(14) G. Preuner and W. Schupp, *Z. physik. Chem.*, **68**, 129 (1909).

described in terms of the self-association equilibria

$$qS_2 \rightleftharpoons S_{2q}\beta_q$$

of this species. The experimental functions log Γ (log I) and $\bar{q}$ (log I) are consistent with the formation of B_2, B_3 and B_4 with association constants given in Table I. The functions $B(b)$, $S(b)$ were calculated using the resultant value of log b_0 = 0.75. Analysis by methods described previously[1] gave concordant values of the association constants.

An attempt also was made to describe the data in terms of only trimer and tetramer using the method described on p. 1376. However the plot of log $(B - S)/I^3$ against log I was very scattered, and only approximate values of the parameters could be obtained (see Table I). Thus Preuner and Schupp's data give no definite evidence either for or against the presence of S_4 at 450°.

TABLE I

EQUILIBRIUM CONSTANTS, β_q, IN (mm. Hg)$^{1-q}$ FOR THE REACTIONS $qS_2(g) \rightleftarrows S_{2q}(g)$ AT 450°

	log β_2	log β_3	log β_4
This work[a] (S_2 + S_4 + S_6 + S_8)	−1.31 ± 0.05	−1.78 ± 0.05	−3.21 ± 0.08
This work[a] (S_2 + S_6 + S_8)	− ∞	∼ −1.8	∼ −3.4
Preuner and Schupp[14,a]	− ∞	−1.85	−3.46
Bjerrum[4,a]	− ∞	−2.09	−3.64
Braune, Peter and Neveling[15,b]	−1.26	−1.69	−2.86

[a] Preuner and Schupp's data. [b] Braune, Peter and Neveling's data.

Both the present sets of association constants give a satisfactory description of the primary data $\bar{q}(S)$, and the approximate values obtained by assuming the formation of only S_6 and S_8 are in excellent agreement with those obtained by the original authors.[14] However, they differ markedly from Bjerrum's values,[4] which were obtained using an erroneous value of log b_0 = 0.884 and which give a much less satisfactory description of the data. This discrepancy emphasizes the advantage of the proposed method in giving a reliable value of b_0, especially if appreciable association occurs at the lowest concentration studied. (For the present measurements, $\bar{q}_0$ = 1.8.) The values of β_2 and β_3 obtained assuming the formation of S_4, S_6 and S_8 are in fairly good agreement with those reported by Braune, Peter and Neveling,[15] who analyzed some recent measurements obtained over a narrower range of pressures.

Extended Series of Multimers

The formation of an extended series of multimers often can be described in terms of only one or two independent parameters.[2,3] In such cases, the data (B,S,I) can be analyzed by curve-fitting methods analogous to those described above for systems containing a few oligomers.

One Parameter Series.—If the stepwise association constants

$$K_q = \frac{\beta_q}{\beta_{q-1}} = K \qquad (33)$$

are identical for all values of $q \geq 2$ then

$$L = \frac{B}{I} = b_0 \sum_1^\infty q(b_0KI)^{q-1} = b_0(1 - b_0KI)^{-2} \qquad (34)$$

and

$$\Lambda = \frac{S}{I} = b_0 \sum_1^\infty (b_0KI)^{q-1} = b_0(1 - b_0KI)^{-1} \qquad (35)$$

for $b_0KI < 1$, *cf.* equations II-4 and II-5. Normalization of L, Λ and I gives the unique functions

$$\mathbf{L} = (1 - \mathbf{I})^{-2} \qquad (36)$$

and

$$\mathbf{\Lambda} = (1 - \mathbf{I})^{-1} \qquad (37)$$

where L and $\mathbf{\Lambda}$ are defined by equations 7 and 8, and

$$\log \mathbf{I} = \log I + \log b_0 + \log K \qquad (38)$$

Here $\mathbf{I}$ is identical with the normalized variable $\mathbf{b}$ used throughout Part II[2] (*cf.* equations 3, 39 and II-3). The values of b_0 and K may be obtained from the pair of experimental plots log L (log I) and log Λ (log I) by means of curve-fitting methods exactly analogous to those proposed above for treating a unique oligomer B_Q. Similar procedures may be used for one parameter series in which K_q is a function of both K and q.

Two-Parameter Series.—The formation of an extended series of multimers may more often be described in terms of two independent parameters, β_2 and K, such that $K_q = f(K,q)$. Various models have been suggested[2] for the relationship between K_q and K (see Table II). The parameters β_2, K

TABLE II

NORMALIZED VARIABLES $\mathbf{\Omega}$ FOR TWO PARAMETER HYPOTHESES

Hypothesis	K_q $(q \geq 3)$	$\mathbf{\Omega}$
I	K	$\frac{\mathbf{I}}{(1 - \mathbf{I})^2}$ $(\mathbf{I} \leq 1)$
II	$\frac{q-2}{q-1} K$	$\frac{\mathbf{I}}{1 - \mathbf{I}}$ $(\mathbf{I} \leq 1)$
III	$\frac{K}{q-1}$	$\mathbf{I}\, e^{\mathbf{I}}$
IV	$\frac{q-1}{q-2} K$	$\frac{\mathbf{I}(1 + \mathbf{I})}{(1 - \mathbf{I})^3}$ $(\mathbf{I} \leq 1)$

and b_0 may be obtained by using curve-fitting methods to analyze the variation of $(B - S)$ and of $\bar{q}$ with I.

The experimental plot of log Ω = log $(B - S)/I$ against log I is compared with the unique normalized curves log Ω (log $\mathbf{I}$), calculated for four different models (*cf.* Fig. II-1) by means of the relationships given in Table II. Once the best hypothesis has been selected, the values of

$$\log \Omega - \log \Omega = \log K - \log \beta_2 - \log b_0 \qquad (40)$$

and

$$\log \mathbf{I} - \log I = \log K + \log b_0 \qquad (41)$$

may be obtained from the coördinates in the position of best fit.

For each of the hypotheses, the value of $\bar{q}$ is given by

(15) H. Braune, S. Peter and V. Neveling, *Z. Naturforsch.*, **6a**, 32 (1957).

$$\bar{q} = \frac{1 + R\mathbf{T}}{1 + R\theta} = f(\mathbf{I}) = f(\mathbf{b}) \qquad (42)$$

where **T** and θ are defined by equations II-8 and II-12, and

$$R = \beta_2/K \qquad (43)$$

The relationships **T**(b) and θ(b) for the different hypotheses are given in Part II.[2] The value of R may be determined most conveniently by comparing a projection strip $(\log I)_{\bar{q}}$ of the experimental curve $\bar{q}(\log I)$ with a family of normalized curves $\log R\ (\log \mathbf{I})_{\bar{q}}$, calculated for the appropriate hypothesis by means of equation 42, *cf.* p. 1377, and Figs. 3 and 4. The position of the strip on the log I axis must be compatible with the value of $(\log \mathbf{I} - \log I)$ obtained using the plot $\log \Omega\ (\log I)$. The required parameters may be obtained from equations 40, 41 and 43. The values are best checked by substitution into equations 3, II-8 and II-11 to give the set T, θ, b. The primary data then can be recalculated using the relationships

$$B = b(1 + T) \text{ and } S = b(1 + \theta)$$

cf. equations II-7 and II-10.

Imidazole.—The above method was applied to Anderson, Duncan and Rossotti's measurements[16] of $B(S)$ for imidazole in carbon tetrachloride at 18°. The plots $\log \Omega\ (\log I)$ and $\bar{q}\ (\log I)$ could be described using either Hypothesis I with $\log \beta_2 = 2.38$, $\log K = 2.80$ and $\log b_0 = -3.72_5$ (on the molar scale) or Hypothesis II with $\log \beta_2 = 2.45$, $\log K = 3.02$ and $\log b_0 = -3.73$ (see Fig. 4). Although the Hypothesis I parameters are in excellent agreement with those obtained previously[16] from the functions $B(b)$ and $S(b)$, the Hypothesis II parameters are preferred since they give a somewhat better description of the primary data $B(S)$ at high concentrations.

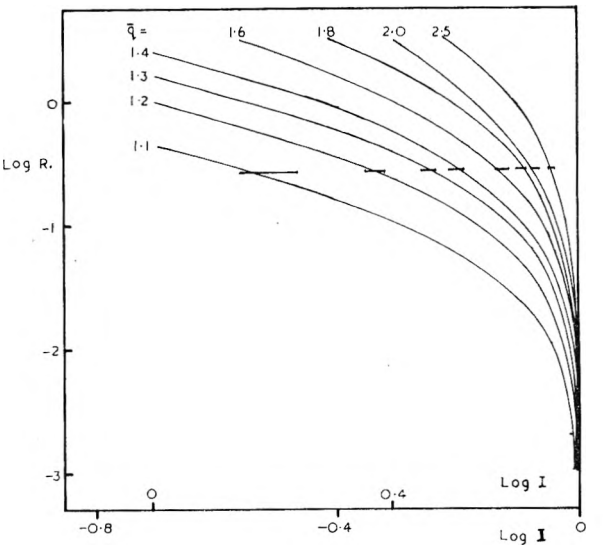

Fig. 4.—Imidazole in carbon tetrachloride at 18°. Normalized curves $\log R\ (\log \mathbf{I})_{\bar{q}}$ for Hypothesis II. With projection strip $(\log I)_{\bar{q}}$ superimposed in the position corresponding to $\log R = -0.57$ and $(\log \mathbf{I} - \log I) = -0.71$.

Acknowledgments.—We are grateful to the Earl of Moray Endowment and to Imperial Chemical Industries, Ltd., for the provision of calculating machines.

(16) D. M. W. Anderson, J. L. Duncan and F. J. C. Rossotti, *J. Chem. Soc.*, 2165 (1961).

THE MASS SPECTRUM OF ETHYLLITHIUM VAPOR[1]

BY JOSEPH BERKOWITZ,

Argonne National Laboratory, Argonne, Illinois

D. A. BAFUS AND THEODORE L. BROWN

Noyes Chemical Laboratory, University of Illinois, Urbana, Illinois

Received February 28, 1961

The saturated vapor of ethyllithium has been analyzed by use of a mass spectrometer. Mass peaks corresponding to $Li_nR_{n-1}^+$ (n = 1, 2, 3, 4, 5, 6) were observed. The $Li_6R_5^+$ and $Li_4R_3^+$ peaks had appearance potentials 3–4 e.v. lower than any of the others, and were thus assumed to be the only parent ions. Corroborative evidence for this conclusion was obtained by using a double-oven to analyze the undersaturated vapor. The results point to hexamer and tetramer as the predominant species in ethyllithium vapor.

Introduction

A survey of the metal alkyls, excluding the transition metals, reveals that these compounds fall into two classes. In one category may be placed those metal alkyls in which the bond between the alkyl group and the metal atom is a normal, two-center covalent bond. This class of compounds is typified by mercury dimethyl, lead tetraethyl, etc.

A second class of compounds embraces those in which the observed structures or properties can be accounted for only in terms of multicenter bonds. These are generally referred to as electron-deficient compounds.[2] The term "electron-deficient" is applied more generally to all compounds in which it is necessary to postulate the existence of multicenter bonds, and so includes, in addition to such metal alkyls as aluminum trimethyl and beryllium dimethyl, compounds such as the boron hydrides.

Rundle[2] has stated that the common feature of all of these electron-deficient compounds is the presence of an atom "with more low-energy orbitals than valence electrons combined with atoms or groups containing no unshared electron pairs." The decision as to what constitutes low-energy orbitals is not always so obvious, but in the case of

(1) Work performed under the auspices of the U. S. Atomic Energy Commission and the Air Force Office of Scientific Research, Air Research and Development Command, Contract No. AF 49(638)-466.

(2) R. E. Rundle, *J. Phys. Chem.*, **61**, 45 (1957).

metals from the first three groups, such as Be, Mg, Al, Li, etc., it presumably includes all of those atomic orbitals with the same principal quantum number. From the structures of those electron-deficient compounds of the first three groups which are presently known, it appears that the metal atom uses all of its low-energy orbitals in forming the multicenter bonds.

The lithium alkyls form an interesting group of compounds in many respects. Their physical properties, as now known,[3] provide strong evidence for the association of LiR units when the lithium alkyl is dissolved in organic solvents. Studies of the freezing point depression of benzene with ethyllithium solute would appear to indicate a molecular weight about six times the formula weight,[4-6] although results at variance with this have been reported.[7] Infrared spectral studies directed to the identification of the bands due to associated and unassociated species have been reported by a group of Russian workers in a series of papers.[8-10] They have investigated the spectra of methyl- and ethyllithium as Nujol mulls of the solids, as solutions in benzene, cyclohexane and hexane, and in the vapor state. Bands due to the unassociated C–Li vibrations have been assigned for the compounds in solution and in the vapor; other bands in the solutions and in the solids, but which were absent in the spectra of the vapor phase, were assigned to associated species.

By examining the similarities and differences observed in the infrared spectrum of ethyllithium in the vapor phase, in various organic solvents, and in the crystalline state, Shigorin and co-workers[8-10] concluded that ethyllithium was associated as hexamer and dimer in solution, but probably was not associated in the vapor. The determination of the molecular species existing in a vapor on the basis of infrared spectra alone is at best a hazardous task; for a molecular system as complex as ethyllithium the problem is compounded. To add to the uncertainty of the conclusions of Shigorin and coworkers, they reported a vapor pressure for ethyllithium of *ca.* 5 mm. at 70–80°, whereas previous investigators had obtained 10^{-3} to 10^{-4} mm.[3]

The investigation reported below was undertaken in order to test these conclusions, and hopefully to provide some insight into the bonding of lithium with the alkyls.

Experimental Methods

In order to obtain independent information regarding the constituents of ethyllithium in the vapor phase, mass spectrometric analysis of the vapor was undertaken. The instrument employed was a 12-inch radius of curvature, 60° single-focussing mass spectrometer at Argonne National Laboratory, which had been developed for the study of high temperature vapor species.[11,12] The sample of ethyllithium was prepared by methods described previously.[6] All operations involving the sample vials and the sample cell, including transfer to the mass spectrometer, were conducted under an inert atmosphere.

Two different sample cells were employed. The initial experiments utilized a tantalum Knudsen cell rather similar in construction to those described previously.[11,12] In these exploratory experiments, no attempt was made to measure the temperature of the cell accurately.

When it became apparent that polymeric vapor species were involved, a further study was made with the aid of a double oven (see Fig. 1). In this arrangement, one chamber contained the sample; the vapor diffused through a porous metallic frit and a long channel into a second chamber, which in turn contained the effusion orifice. In this manner, the effect of temperature on the vapor composition, at constant total pressure, could be explored. Alternatively, the expected behavior with reduced pressure at constant temperature, in accordance with LeChatelier's principle, could be used to check the fragmentation patterns and mass assignments. In both types of experiments, the vapor effusing from the Knudsen orifice could be distinguished from the background gas by observing the difference in ion intensity when the molecular beam was intercepted by a manually operated "shutter" plate. In the double-oven experiment, temperatures at various points were measured by bolting or spot-welding five thermocouples (Pt–Pt,10% Rh) to the nickel oven. The details of construction and heating of this oven will be presented in a later publication.

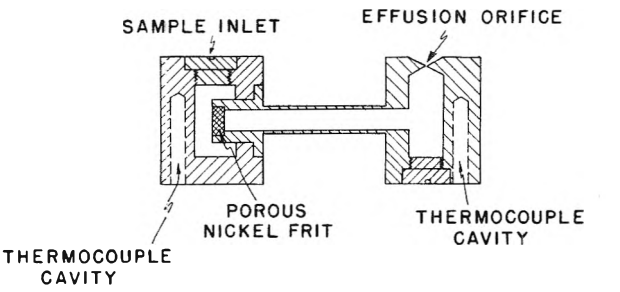

Fig 1.—Double-oven apparatus.

An unsteadiness in the ion beam intensity was encountered after approximately three hours of heating the cell. This could be traced to a corresponding alteration in the intensity of the ionizing electron beam. Upon removal of the ethyllithium source and overnight pumping, the unsteadiness vanished. One is led to conclude that free lithium formed by decomposition of ethyllithium in the ionization chamber provided leakage paths between the electron-emitting filament and the ionization chamber. This behavior precluded the conducting of accurate temperature-variation experiments.

Results

The major ion peaks observed in the single-oven experiment, and their relative intensities when using 75-volt electrons for ionization, are shown in Table I. It should be emphasized that these relative intensities have been corrected for the contribution due to background. Because of the fact that the lithium-bearing species are condensable, the background contribution was less than 10% in most instances. In addition to the ion intensities reported, the isotopic contributions of Li^6 and C^{13} were also observed on adjacent peaks, and confirmed the assignments. These ion peaks are attributed to the process

$$Li_nR_n + e^- \longrightarrow Li_nR_{n-1}^+ + R + 2e^- \qquad (1)$$

(3) G. E. Coates, "Organo-Metallic Compounds," Methuen & Co., Ltd., London, 2nd Edition, 1960.

(4) W. Schlenk and J. Holtz, *Ber.*, **50**, 272 (1917).

(5) F. Hein and H. Schramm, *Z. physik. Chem.*, **A151**, 234 (1930).

(6) T. L. Brown and M. T. Rogers, *J. Am. Chem. Soc.*, **79**, 1859 (1957).

(7) K. B. Piotrovsky and M. P. Ronina, *Doklady Akad. Nauk, S.S.S.R.*, **115**, 737 (1957).

(8) A. N. Rodinow, D. N. Shigorin and T. V. Talalaeva, *ibid.*, **123**, 113 (1958).

(9) A. N. Rodinow, V. N. Vacaleva, T. V. Talalaeva, D. N. Shigorin, E. N. Guryanova and K. A. Kocheskov, *ibid.*, **125**, 562 (1959).

(10) D. N. Shigorin, *Spectrochim. Acta*, **14**, 198 (1959).

(11) W. A. Chupka and M. G. Inghram, *J. Phys. Chem.*, **59**, 100 (1955).

(12) W. A. Chupka, J. Berkowitz and C. F. Giese, *J. Chem. Phys.*, **30**, 827 (1959).

where R is the C_2H_5 radical. In these experiments, the intensity of the parent ion $Li_nR_n^+$ was negligibly small, *i.e.*, within the uncertainty of background corrections. This kind of behavior toward ionization has been observed in alkali halides,[13] as well as UF_4, UF_5, UF_6,[14] totally halogenated methanes,[15] and such organometallic compounds as dimethylmercury and tetraethyllead.[15]

TABLE I[a]

RELATIVE ION INTENSITIES OF MAJOR PEAKS IN THE MASS SPECTRUM OF SATURATED ETHYLLITHIUM VAPOR

Mass No.	Ion	Relative intensity
187	$Li_6R_5^+$	24
151	$Li_5R_4^+$	1.3
115	$Li_4R_3^+$	47.5
79	$Li_3R_2^+$	15
43	Li_2R^+	100
7	Li^+	14

[a] Data were obtained with an electron energy of 75 e.v. Ion intensities have been corrected for secondary electron emission at the first dynode of the electron multiplier.

The measured appearance potential of these ionic peaks is shown in Table II. Absolute values were obtained by comparing the measured values with the appearance potential of Hg, obtained in the same run.

TABLE II[a]

APPEARANCE POTENTIAL OF MAJOR IONS IN THE MASS SPECTRUM OF ETHYLLITHIUM VAPOR

Mass No.	Ion	Appearance potential, e.v.
187	$Li_6R_5^+$	7.7 ± 0.5
151	$Li_5R_4^+$	12.5 ± 0.5
115	$Li_4R_3^+$	8.0 ± 0.5
79	$Li_3R_2^+$	11.7 ± 0.5
43	Li_2R^+	11.7 ± 0.5
7	Li^+	14 ± 2

[a] Absolute values of the appearance potentials have been obtained by comparison with the appearance potential of Hg^{202}.

These appearance potentials clearly differentiate between masses 187 and 115, on the one hand, and all of the other ion peaks, on the other. It is most probable that the observed differential in appearance potentials of 3–4 e.v., is associated with the breaking of at least one bond. If all of the ion peaks listed in Tables I and II were formed by reaction 1, one would expect the electron removed by the ionization process to be approximately equally bound in each of the parent polymer molecules. Such behavior is observed among all of the alkali halide polymers.[13,16] In the current experiments, only $Li_6R_5^+$ and $Li_4R_3^+$ conformed to this behavior. Hence, it was tentatively concluded that the hexamer and tetramer of ethyllithium were the major molecular species, and all other ion peaks were due to more severe fragmentation of these molecules than given by eq. 1.

This hypothesis subsequently was tested in the double-oven experiment. In principle, it is possible to deduce both the fragmentation pattern[17,18] and the relative cross sections[18,19] for ionization of the molecular species by using a double-oven arrangement. In the present instance, the instability in emission caused by the ethyllithium beam (see Experimental Methods) together with the small temperature range available made the fine control necessary for this experiment difficult to attain. It was possible, however, to observe a shift in the ratios of ion intensities as a result of superheating the vapor in the upper (effusion) oven. The mass spectrum observed under these conditions is shown in Table III. In Table IV, the ratio of various "fragment" peaks to the "parent" peaks 187 and 115 are compared for the single- and double-oven experiments. These ratios suggest that most of the fragment peaks are to be attributed to the tetramer. This is particularly marked for mass 43, although the effect is also evident for masses 79 and 7.

TABLE III[a]

RELATIVE ION INTENSITIES OF MAJOR PEAKS IN THE MASS SPECTRUM OF UNDERSATURATED ETHYLLITHIUM VAPOR

Mass No.	Ion	Relative intensity
187	$Li_6R_5^+$	15.1
151	$Li_5R_4^+$	1.3
115	$Li_4R_3^+$	46.5
79	$Li_3R_2^+$	14.2
43	Li_2R^+	100
7	Li^+	17.4

[a] Data were obtained with 70 e.v. electrons. Electron multiplier amplification was not needed.

The use of a double oven has shifted the ratio of hexamer to tetramer from 0.505 to 0.325. This shift is in the direction to be expected by LeChatelier's principle.

TABLE IV

RATIO OF ION INTENSITIES FOR SINGLE- AND DOUBLE-OVEN EXPERIMENTS

	Single Oven	Double oven
A. Relative to mass 187 (hexamer)		
M151/M187	0.054	0.086
M79/M187	0.626	0.941
M43/M187	4.16	6.63
M7/M187	0.584	1.15
B. Relative to mass 115 (tetramer)		
M151/M115	0.027	0.028
M79/M115	0.316	0.306
M43/M115	2.10	2.15
M7/M115	0.295	0.374

An attempt was made to estimate the relative importance of hexamer and tetramer in the saturated vapor by comparing the corresponding "parent" ion intensities at 12 e.v. bombarding voltage, where fragmentation was minimized. Under these

(13) J. Berkowitz and W. A. Chupka, *ibid.*, **29**, 653 (1958).

(14) (a) L. O. Gilpatrick, R. Baldock and J. R. Sites, Oak Ridge National Laboratory Report No. 1376; "Mass Spectrometer Investigation of UF_x." (b) E. H. S. Burhop, H. S. W. Massey and C. Watt, in National Nuclear Energy Series, Div. I, Vol. 5, p. 145 (1949) (McGraw-Hill, New York) edit. by A. Guthrie and R. K. Wakerling.

(15) American Petroleum Institute Research Project 44, "Mass Spectral Data," Serial Nos. 401, 603, 694, 695, 699, 700, 701, Petroleum Research Laboratory, Carnegie Institute of Technology, Pittsburgh, Pennsylvania.

(16) L. Friedman, *J. Chem. Phys.*, **23**, 477 (1955).

(17) L. N. Gorochov, *Vestnik Moskovskovo Universiteta*, 231 (1958).

(18) J. Berkowitz, H. A. Tasman and W. A. Chupka, to be published.

(19) T. J. Milne, *J. Chem. Phys.*, **28**, 717 (1958).

conditions, the ratio of hexamer to tetramer was 1.09, using electron multiplier detection. The measured relative efficiency of secondary electron production reduced this to 0.82. The relative ionization efficiency of these molecules is very likely in such a direction as to reduce this figure further, perhaps to as low as 0.55. Finally, the known isotopic correction would raise this number to 0.65.

It is possible to estimate the total vapor pressure from the results of the double-oven experiments. The sensitivity of the mass spectrometer with the identical oven assembly and geometric arrangement has been tested recently at known temperatures and pressures with LiF, LiCl, and LiBr.[18] These experiments also provided a measure of the pressure drop across the frit between the two ovens. An average of several such calculations yielded $P_{\text{lower oven}}/P_{\text{upper oven}} = 31.3$. This result, when combined with the calculated ionization cross section ratios of Otvos and Stevenson,[20] enables one to compute the vapor pressure in the lower oven, which is in equilibrium with its condensed phase at a known temperature. At 87°, the total pressure was computed to be 7.8×10^{-2} mm.

It should be added that attempts were made to observe higher polymers than the hexamer, but the fact that no signal was observed above background indicated a concentration less than 0.01%.

Conclusions

The mass spectrometric results for ethyllithium show that the saturated vapor consists predominantly of a hexamer and a tetramer in roughly equal concentrations at 80–95°. This result is contrary to the conclusions of Shigorin and co-workers,[8-10] who inferred that the difference in the observed infrared spectra of ethyllithium in the vapor and condensed phases was evidence for unassociated molecules in the vapor.

The presence of hexamer and tetramer suggests a ring structure, rather than a linear configuration, since the latter would be expected to also yield other multiples of the basic monomer unit. The preferential fragmentation of the C_2H_5 radical during ionization suggests that Li is bonded to more than one atomic center, while C_2H_5 is not. The very high appearance potential of Li^+ in these experiments is further evidence for this conclusion. One is tempted to speculate that the structures of the hexamer and tetramer involve an inner lithium core surrounded by ethyl radicals.

Most studies of the depression of the freezing point by ethyllithium in benzene, and in particular those which have been performed with solutes of pure, recrystallized ethyllithium, indicate a degree of association in the range 5–7. There is no evidence from any of these studies that the degree of association is concentration dependent, although it cannot be said that the results to date have been sufficiently precise and sensitive to afford much assurance on this point. It does seem quite possible, however, that either one or both of the species present in the vapor of ethyllithium is also the predominant species in solution. In this connection it is noteworthy that ethyllithium apparently possesses a dipole moment in benzene.[21] If the solute is associated to hexamer in benzene solution, the dipole moment is computed to be at least 1.50 *D*.

Acknowledgment.—The authors wish to thank Dr. William A. Chupka, Argonne National Laboratory, for the use of the mass spectrometer, and Mr. Dean W. Dickerhoof, Department of Chemistry, University of Illinois, for assistance with the preparation of ethyllithium.

(20) J. W. Otvos and D. P. Stevenson, *J. Am. Chem. Soc.*, **78**, 546 (1956).

(21) M. T. Rogers and T. L. Brown, *J. Phys. Chem.*, **61**, 336 (1957).

PROTON MAGNETIC RESONANCE OF SOME POLY-(ALPHA-OLEFINS) AND ALPHA OLEFIN MONOMERS[1]

BY A. E. WOODWARD, A. ODAJIMA AND J. A. SAUER

Department of Physics, Pennsylvania State University, University Park, Pa.

Received March 4, 1961

Proton magnetic resonance spectra of a series of polyolefins: polypropylene, poly-(3,3',3''-trideuteriopropylene), PTDP, poly-(butene-1), PB1, poly-(pentene-1), PP1, poly-(3-methylbutene-1), P3MB1, and poly-(4-methylpentene-1), P4MP1, have been obtained from 77 to 300°K. or higher. In addition spectra have been observed for the monomers: 3-methylbutene-1, pentene-1, and 4-methylpentene-1 from 77°K. to temperatures about 15°K. below the respective melting points. The line narrowing in the 77–150°K. region reported previously for polypropylene is not exhibited by PTDP which is further evidence that this process is a consequence of methyl group rotation. Both P3MB1 and P4MP1 show distinct line narrowing and second moment changes in the 77–130°K. region, this change being attributed to the onset of methyl group rotation. The second moment–temperatures curves for PP1 and PB1 are similar to each other with no marked line narrowing processes occurring until temperatures of 260–300°K. are reached. However, by a comparison of experimental and calculated second moments it appears that considerable motion, presumably methyl rotation, is taking place in PB1 and PP1 at 77°K. From 77–90°K., 4-methylpentene-1 undergoes an n.m.r. transition which takes place only 5–10°K. below that for the respective polymer and is attributed to methyl group rotation. 4-Methylpentene-1, 3-methylbutene-1 and pentene-1 exhibit abrupt n.m.r. transitions, possibly due to molecular tumbling, at temperatures 20–25°K. below the melting point. All polymers studied show line narrowing and second moment changes around room temperature which are believed to be due to reorientation motions associated with the glass transition. These n.m.r. motional narrowing processes occur in the order PP1 $\leq$ PB1 $\simeq$ PTDP < polypropylene < P4MP1 < P3MB1. Upon comparison of the proton resonance data for PB1, PP1, P3MB1 and P4MP1 with that from dynamic mechanical measurements on the same samples at frequencies of 500–2000 c.p.s., it is found that the transition regions are seen at essentially the same temperatures by both types of measurements.

Introduction

The use of the proton magnetic resonance technique, herein referred to as n.m.r., to investigate molecular motion in the poly-(α-olefins) has been limited to date to the first two members of the series with aliphatic side chains projecting from alternate carbon atoms of the main chain. N.m.r. spectra have been obtained for crystalline and amorphous samples of polypropylene[2-5] in the 77–400°K. temperature region. In addition to marked changes in these spectra in the neighborhood of the glass transition all investigators have reported an n.m.r. line narrowing process, accompanied by a decrease in the second moment, in the 77–150°K. region. This effect has been attributed to the onset of methyl group rotation at frequencies in the range detectable by this method. On the other hand, poly-(butene-1) does not exhibit a marked line narrowing until temperatures in the vicinity of the glass transition are reached.[6,7] However, it has been suggested[8] that at the lowest temperature employed, 77°K., the poly-(butene-1) molecules are not completely rigid, as appears also to be the case for polypropylene.[2,3]

One method which can be employed to give further information about the motional state of a given substance is to replace one or more of the hydrogen atoms by an atom which does not absorb energy from the magnetic field under the conditions employed nor give effective magnetic dipole interactions with the protons. In order to have a compound with morphology as close to the parent substance as possible, atoms of similar size and which give bonds with carbon of similar polarity, such as deuterium in place of hydrogen, should be used. As described herein, a study of the proton resonance spectra of poly-(3,3',3''-trideuteriopropylene), PTDP, has been made and this study provides further evidence that the low temperature narrowing process in polypropylene is indeed a consequence of methyl group rotation.

In order to obtain additional information concerning the effect of the length and size of the side-branch on the motions occurring in polymers, the n.m.r. spectra of six compounds: polypentene-1, PP1, poly-(3-methylbutene-1), P3MB1, poly-(4-methylpentene-1), P4MP1, and the respective crystalline monomers, in addition to poly-(butene-1), PB1, have been obtained at temperatures from 77°K. A unique feature of this study is that the polymer specimens were taken from the sample rods used previously[9] in an investigation of the dynamic mechanical properties, and therefore a more detailed comparison than usual of the data from the two methods is possible.

Experimental

The n.m.r. measurements were made using equipment purchased from Varian Associates, as described previously.[10] Due to the small amount of sample of PTDP employed (0.3 g.) it was necessary to correct the derivative line shapes obtained for the measurable background signal of the polystyrene in the probe. However, these corrections only have a small effect on the second moment values.

The PTDP was prepared from monomer (Merck and Co., Ltd.) with a minimum isotopic purity of 96 atom % D. The preparation of this polymer and of the polypropylene samples, on which data are reported herein, were kindly carried out by Dr. R. D. Lundberg of Union Carbide Chemicals Company using a procedure designed to give highly isotactic material. The polymerization charge per tube consisted of: 8.0 ml. of dry distilled heptane, 1.0 ml. of purple $TiCl_3$ suspension in heptane (7.3%), 1.0 ml. of Al(isobutyl)$_3$

(1) Supported by the U. S. Atomic Energy Commission under contract No. AT(30–1), 1958.

(2) J. A. Sauer, R. A. Wall, N. Fuschillo and A. E. Woodward, *J. Appl. Phys.*, **29**, 1385 (1958).

(3) W. P. Slichter and E. R. Mandell, *J. Chem. Phys.*, **29**, 232 (1958); *J. Appl. Phys.*, **29**, 1438 (1958).

(4) A. Nishioka, Y. Koike, M. Owaki, T. Naraba and Y. Kato, *J. Phys. Soc. Japan*, **15**, 416 (1960).

(5) R. L. Miller, *Polymer* **1**, 135 (1960).

(6) J. A. Sauer, A. E. Woodward and N. Fuschillo, *J. Appl. Phys.*, **30**, 1488 (1959).

(7) W. P. Slichter, *S. P. E. Journal*, **15**, 303 (1959).

(8) W. P. Slichter, *Ann. N. Y. Acad. Sci.*, **83**, 60 (1959).

(9) (a) A. E. Woodward, J. A. Sauer and R. A. Wall, *J. Chem. Phys.*, **30**, 854 (1959); (b) *J. Polymer Sci.*, **50**, 117 (1961).

(10) A. Odajima, A. E. Woodward and J. A. Sauer, *J. Polymer Sci.*, in press.

which was 1 *M* in heptane and 28.45 mmoles of monomer. Catalyst and solvent were charged into glass tubes in a dry nitrogen atmosphere, then using high vacuum techniques, monomer was added and the tubes sealed at liquid nitrogen temperature. The polymerizations were carried out for 16 hr. at 50°. The contents of three tubes were combined and washed free of catalyst residues in 500 ml. of acidified (1% HCl) isopropyl alcohol, then washed with an 80–20 water–isopropyl alcohol mixture, and finally washed with isopropyl alcohol containing a small amount of 4,4-thiobis-6-*t*-butyl-*m*-cresol as oxidation inhibitor. The polymer then was dried overnight at 50°. In order to have the PTDP in chunk form, the precipitated polymer was heated to 440°K. and then cooled to 385°K. over a 45 minute period. Prior to the n.m.r. measurements all polymer samples were heated in a vacuum oven for at least 40 hours, the temperature being 50° for PP1 and 100° for the other polymers.

Samples of PB1, PP1, P3MB1 and P4MP1 were in the form of pieces, cut from specimens used for the dynamic mechanical investigations and having characteristics given previously.[9] However, due to their use in previous tests, these specimens have been slow cooled from temperatures of 435, 400, 480 and 435°K., respectively. From a density value at 25° of 0.892 g./cc., the crystallinity of the PB1 sample was estimated as 30%, using the amorphous and crystalline specific volumes given by Danusso, Moraglio and Natta.[11]

Crystallinities at 300°K. of 60, 60, 30, 25 and 50% for polypropylene, PTDP, PB1, PP1 and P4MP1 were estimated by a technique involving a separation of the narrow and broad components of the derivative line shapes for the pure polymers (polypropylene, PTDP and PP1) or for the polymer swollen with tetrachloroethylene (PB1 and P4MP1). To effect the separation of the complex line into broad and narrow components, the low temperature line shape for the pure polymer (taken at 149, 157, 197, 193 and 184°K., respectively, for the five polymers mentioned above) was assumed to be the correct line shape for the crystalline contribution at 300°K. It was also assumed for the swollen polymers that the solvent entered only into the amorphous regions and not the crystalline ones. It was found that the tails of the line shapes at 300°K. for all five materials were the same as those for the line shapes at the lower temperatures cited above. The crystallinity for P3MB1 was estimated as high.

Samples of pentene-1 (Research grade b.p. 29.9°), 3-methylbutene-1 (Research grade, 99.99% pure; b.p. 25°); and 4-methylpentene-1 (99.77% pure; b.p. 53°) were kindly supplied by Dr. R. D. Lundberg of Union Carbide Chemicals Company and were used as received. The melting points of these compounds as given in the literature[12] are −165.2, −168.5 and −153.6°, respectively.

Results

In Fig. 1 are shown plots of the first derivative of the proton absorption as a function of the applied magnetic field (one-half of the recorder trace being given) at 77°K. for all materials investigated except PB1. (The curve for this latter polymer is given in Fig. 5.) Due to a change in the abscissa scale from one to another of the absorption curves, changes in heights of maxima are not necessarily significant except for a given monomer–polymer pair. The peak-to-peak modulation width used in obtaining these line shapes was 2.2 gauss for PTDP and 1.1 gauss for all the other materials. At this temperature all the polymers except P4MP1 exhibit relatively broad derivative shapes while for the monomers the shapes are generally sharper and narrower. The line shapes for P4MP1 and its monomer show greater similarities, although that for the latter is somewhat narrower, than those for the other two polymer–monomer pairs.

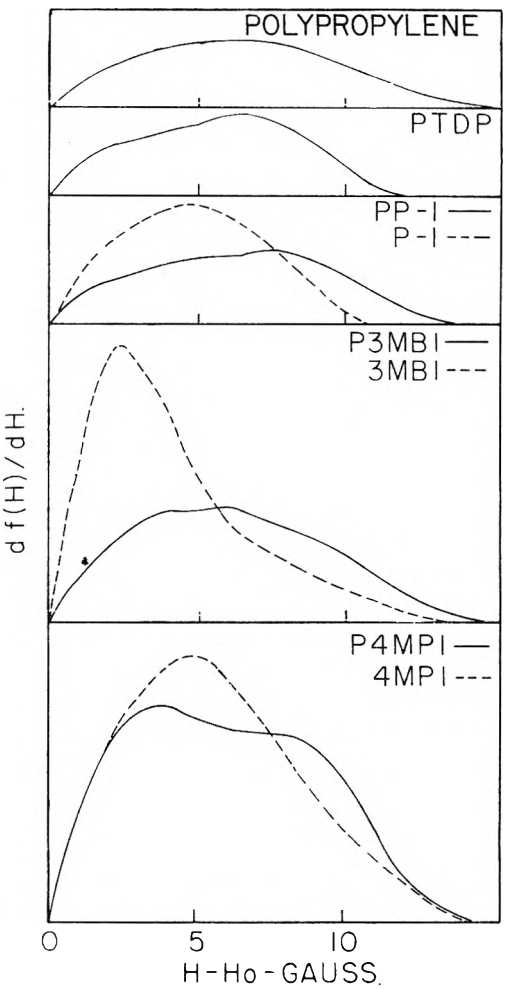

Fig. 1.—Derivative shapes of the proton resonance line absorption at 77°K. for some poly-(α-olefins) and α-olefin monomers.

In addition, the line shape for P4MP1 exhibits two distinct components.

It is found that only small changes in derivative line shape occur for PTDP in the 77–150°K. region, while considerable changes are seen for polypropylene in this temperature region. At higher temperatures both exhibit a narrow and broad component, the presence of the two components being noticeable at lower temperatures for PTDP than for polypropylene. The separation of the maximum and minimum of the derivative absorption line in gauss, referred to herein as line width, is given as a function of temperature for PTDP and polypropylene in Fig. 2. For polypropylene a narrowing of the line width in the 77–150°K. temperature region, observed by many investigators,[2–5] is apparent, whereas for PTDP no such narrowing occurs. At higher temperatures for both polymers a two component line shape with a relatively rapid narrowing of the narrow component is observed. However, this narrowing process occurs at temperatures of 30–40°K. lower for the trideuterio compound. The dotted line in the figure connecting narrow component points for PTDP and broad component points for polypropylene indicates that in this region due to difficulty in separating the two components of the line the reproducibility is not

(11) F. Danusso, G. Moraglio and G. Natta, *Ind. plastiques mod. (Paris)*, **10**, 40 (1958).

(12) F. D. Rossini, *et al.*, "Selected Values of Physical and Thermodynamic Properties of Hydrocarbons and Related Compounds," A. P. I. Research Project 44, Carnegie Press, 1953, pp. 54–55.

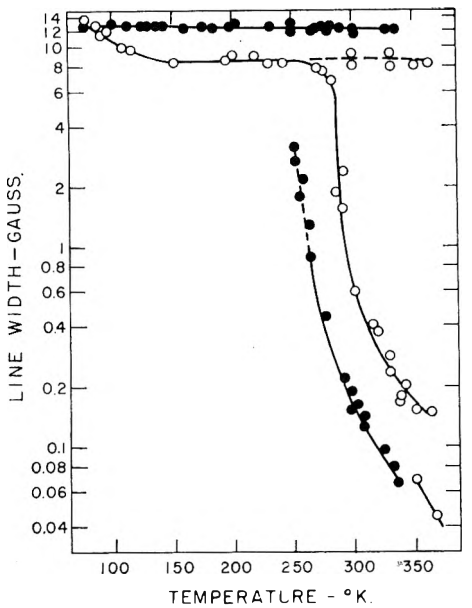

Fig. 2.—Line width *vs.* temperature for polypropylene (○) and poly-(3,3′,3″-trideuteriopropylene) (●).

within the ±3% limit observed for the majority of values. At two temperatures, 350 and 367°K., the line shape for polypropylene was found to be composed of three components with widths of 0.068, 0.164 and 8.0 and 0.045, 0.148 and 8.1 gauss, respectively.

From plots of the second moment of the n.m.r. absorption *vs.* temperature in Fig. 3 it is found that

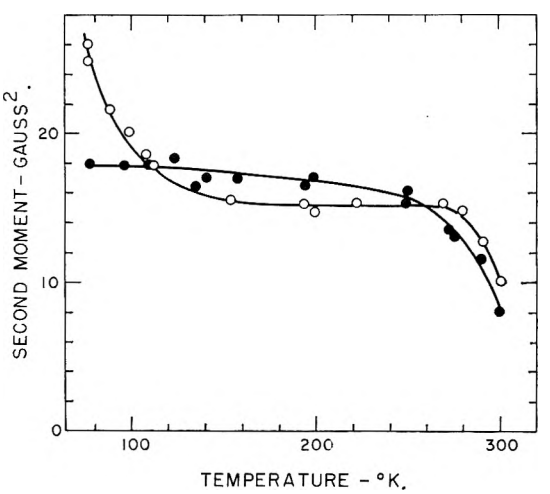

Fig. 3.—N.m.r. second moment *vs.* temperature for polypropylene (○) and poly-(3,3′,3″-trideuteriopropylene) (●).

the low temperature narrowing process for polypropylene is accompanied by a change of the second moment from 26 gauss² at 77°K. to 15.5 gauss² at 155°K., while for PTDP the second moment changes only from 18.0 to 17.3 gauss² in this temperature region. In the 155 to 250°K. region the second moment is constant within experimental error for polypropylene and shows only about 1.5 gauss² decrease for PTDP. Commencing at about 250°K. for PTDP and about 270°K. for polypropylene, the values of second moment drop quite sharply with the deuterated compound having values of 1.5–2 gauss² less than those for polypropylene at any given temperature from about 275 to 300°K.

The line widths as functions of temperature for the three monomers: pentene-1, 3-methylbutene-1 and 4-methylpentene-1, are given in Fig. 4. At

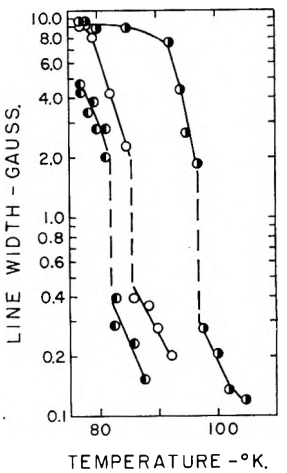

Fig. 4.—Line width *vs.* temperature for 3-methylbutene-1 (◐), pentene-1 (○), and 4-methylpentene-1 (◑).

77°K. the widths are in the order 4MP1 ≳ P1 > 3MB1. Over part of the temperature range traversed, where the line width is 4–5 gauss or less, the shape of the line width *vs.* temperature curves are similar for the three monomers, the curve for pentene-1 being shifted about 4°K. to higher temperatures than that for 3-methylbutene-1 while that for 4-methylpentene-1 is shifted to temperatures about 15°K. higher. The line decreases from 4–5 gauss to 2 gauss over a 5°K. span, then abruptly drops to 0.3–0.4 gauss in a span of 1°K. or less at temperatures 20–25°K. below the respective melting point and then decreases less abruptly at higher temperatures. At low temperatures, 77–94°K., 4-methylpentene-1 shows a gradual decrease in line width from 9.5 to 4.4 gauss in contrast to the more abrupt decreases for the other two monomers.

In Fig. 5 some derivative line shapes for PB1 are shown. It can be seen that the shapes at 105 and 191°K. are flat, making it difficult to obtain an accurate line width. The shapes for PP1 were found to be very similar to those for PB1 at any given temperature over the range studied (77–300°K.). The complete data for PB1 and PP1 are given herein only in terms of the second moment, due to the large errors involved in determining the line width from the type of line shape exhibited over the 100–200°K. temperature region. The second moment behavior for PB1, recorded in Fig. 6, is in qualitative accord with that reported previously.[6,7] As is the case with the line shapes, the second moment plots of PB1 and PP1 are the same within experimental error over the 77 to 260°K. range, with values decreasing from 21–22 to 15 gauss². It is seen that the drop in the first 20°K. is of a slightly greater slope than that in the subsequent 140°K. Above 260°K. the line width and second moment drop markedly for both polymers, with second moment values at 300°K. of 10.0 and 5.0 gauss² for PB1 and PP1, respectively.

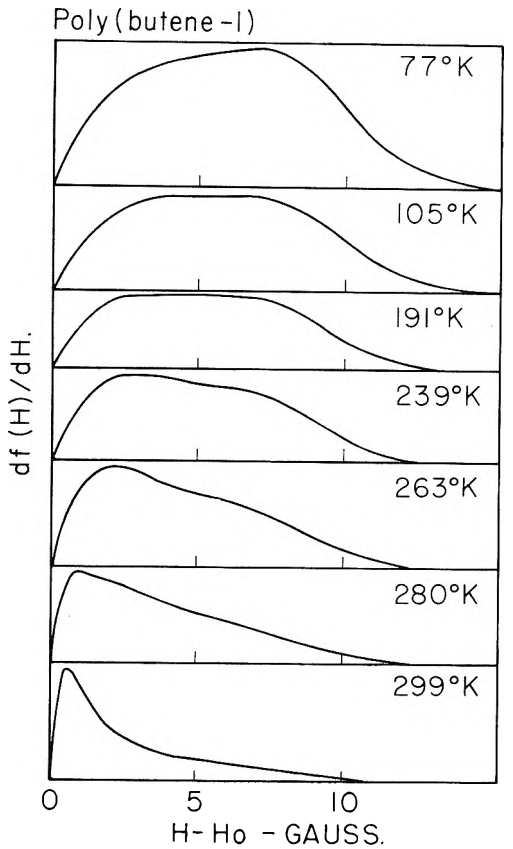

Fig. 5.—Derivative shapes of the proton resonance line absorption for poly-(butene-1).

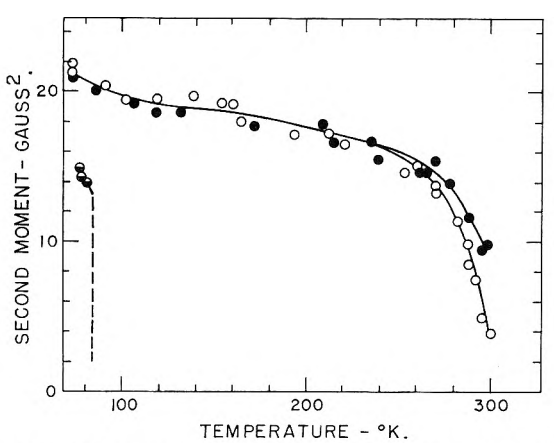

Fig. 6.—N.m.r. second moment *vs.* temperature for poly-(butene-1) (●), poly-(pentene-1) (○) and pentene-1 (◒).

As is readily seen by comparison of Fig. 3 and 6, in the 77 to 260°K. temperature region there is a marked difference in the data for PB1 and PP1 as compared to that for polypropylene, whereas above 260°K. the data for PB1 and polypropylene are essentially the same.

Also included in Fig. 6 are second moment data for pentene-1 at temperatures of 77 and 80°K.; upon comparison of the values for the monomer with those for the polymer, a difference of 6–7 gauss² is found at these temperatures. At higher temperatures the second moment falls sharply to values near zero.

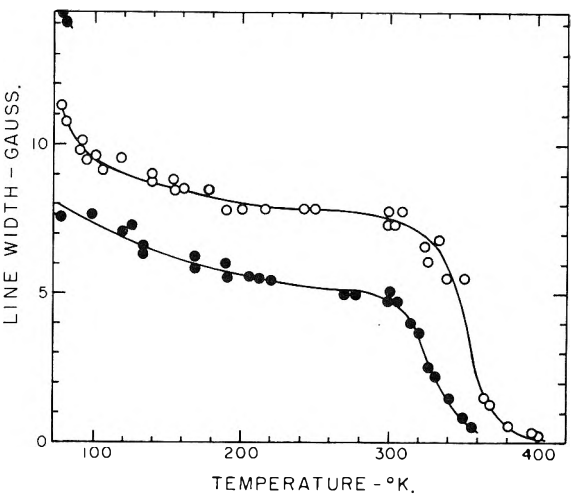

Fig. 7.—Line width *vs.* temperature for poly-(3-methylbutene-1) (○), and poly-(4-methylpentene-1) (●).

In Fig. 7 the line width as a function of temperature is given for P3MB1 and P4MB1. Both polymers show a line narrowing process in the 77–100°K. region which for P4MP1 involves the disappearance of the broad component of the complex line shape. Both also show an additional line narrowing in the region above 300°K. For P4MP1 the data show that the narrow line width in the 130–300°K. region is lower by 2–3 gauss and the transition starting around 300°K. occurs at lower temperatures than for P3MB1. At temperatures above 300°K. a two component line shape was again discernible for P4MP1 but the two components were not separated easily and therefore only the widths of the narrow component in this temperature region are reported. The differences in behavior of the two polymers are not as striking in the second moment plots, given in Fig. 8, although it is again clear that the upper temperature transition for P4MP1 occurs some 25°K. sooner. The second moment plot for P3MB1, showing a marked decrease in the 77–130°K. region, a near-flat portion from 130 to 300°K. and a decrease of 10 gauss² in the final 50°K., is similar to that for polypropylene rather than that for PB1 and PP1. On the other hand, for P4MP1 a decrease of 2–3 gauss² in a second moment takes place over the temperature range between the low and high temperature transitions. The second moment for the monomer 4-methylpentene-1, given in Fig. 8, has values about 1–3 gauss² lower than that for the respective polymer in the 77–90°K. region; above these temperatures a precipitous drop to a value near zero occurs. For 3-methylbutene-1 the second moment value at 77°K. is 15 gauss,[2] 9 gauss² lower than that for P3MB1, and then approaches zero around 80°K.

All the polymers studied herein except PTDP also have been investigated by dynamic mechanical methods,[2,9] and in all but the polypropylene case the same sample has been used in both sets of measurements. In all cases the higher temperature n.m.r. transition appears in the same temperature region as a peak in the internal friction, Q^{-1}, and a drop in the dynamic elastic storage modulus, E', measured at a frequency in the 500–2000 c.p.s.

TABLE I

CALCULATED SECOND MOMENTS FOR POLYMERS

Contributing groups	Poly-propylene	PTDP	PB1	PP1	P3MB1	P4MP1
			a. Rigid lattice			
CH_3	11.0	..	8.2	6.5	13.1	10.9
CH_2 (s.c.)	...	..	2.7	4.4	...	1.8
CH_3–CH_2 (s.c.)	...	..	1.7	1.4	...	0
CH_2–CH_2 (s.c.)	...	..	...	0.8	...	...
CH_3–CH (s.c.)	...	..	...	...	1.4	1.2
CH (s.c.)–CH_2 (s.c.)	...	..	...	...	0.6	0.5
main chain	6.6	13.3	5.0	4	4	3.3
main chain–side chain	5.2	..	~2.3	~2–3	~2–3	~2–3
intermolecular	5–8	1.5	~5–8	~5–8	~5–8	~5–8
total	28–31	15	25–29	24–28	26–30	25–29
			b. Methyl rotation			
CH_3	2.8	..	2.0	1.6	3.3	2.7
CH_2 (s.c.)	...	..	2.7	4.4	...	1.8
CH_3–CH_2 (s.c.)	...	..	1.2	0.9	...	0
CH_2–CH_2 (s.c.)	...	..	...	0.8	...	..
CH_3–CH (s.c.)	...	..	...	...	0.9	0.8
CH–CH_2 (s.c.)	...	..	...	...	0.6	0.5
main chain	6.6	13.3	5.0	4	4	3.3
main chain–side chain	2	..	~1–2	~1–2	~1–2	~1–2
intermolecular	~2–3	1.5	~3–4	~3–4	~3–4	~2–3
total	13–14	15	15–17	15–17	13–15	12–14

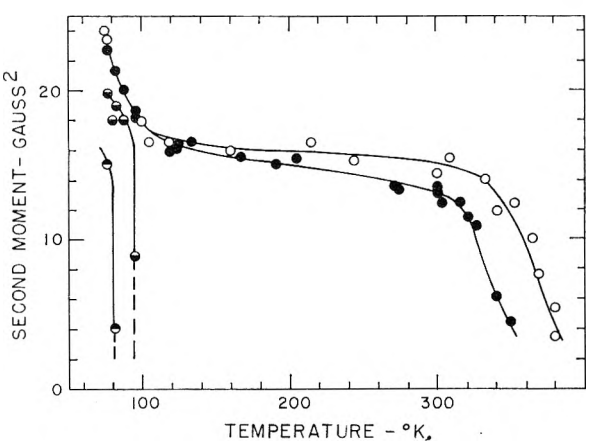

Fig. 8.—N.m.r. second moment *vs.* temperature for poly-(3-methylbutene-1) (○), poly-(4-methylpentene-1) (●), 3-methylbutene-1 (◓) and 4-methylpentene-1 (◒).

range. A detailed comparison of the line width, second moment, E', and Q^{-1} data for PB1, PP1, P3MB1 and P4MP1 shows that the onset of this transition occurs at 230°, 225–230°, 305–325° and 350°K., respectively. The point of maximum slope (the peak in the case of Q^{-1}) for the transition varies according to what quantity is being discussed, with the second moment and Q^{-1} plots giving similar values of 285–290°, 290°, and 330–345°K. for PB1, PP1 and P4MP1, respectively; the corresponding values from line width or modulus are 10–20°K. lower.

Discussion

When the proton positions in a solid are known, the equation given by Van Vleck[13] can be used to calculate a value for the second moment of the rigid lattice structure; also, for the main central component of the line, the second moment values for some simple motional cases, such as the rotation of side groups, can be estimated.[14] Usually, as is the case with the polymers and monomers under discussion here, the spatial arrangement of the atoms in the material is not known exactly and therefore certain contributions to the second moment can only be approximated. In Table I estimated values of second moments for the rigid lattice structure and also for the case of methyl rotation about the C_3 axis are given for all six polymers studied. The separate contributions to the total second moment from protons on the same group or on different groups are also shown; in this table s.c. and m.c. signify the side chain and main chain, respectively.

In calculations of the intramolecular contributions to the second moment the usual values for bond angles and lengths were used. The contributions due to proton–proton interactions on the chain backbone for all six polymers were calculated assuming these protons to occupy the positions given by Keedy, Power and Stein[15] obtained from the helical structure proposed by Natta and Corradini[16] for polypropylene. Since it has been found[17,18] that the difference in values of second moment for helical and randomly coiled backbones is small, the use of the polypropylene helix for PP1, P3MB1 and P4MP1 which have different

(13) J. A. Van Vleck, *Phys. Rev.*, **74**, 1164 (1948).

(14) J. G. Powles and H. S. Gutowsky, *J. Chem. Phys.*, **21**, 1695 (1953).

(15) D. A. Keedy, J. Powers and R. S. Stein, *J. Appl. Phys.*, **31**, 1911 (1960).

(16) G. Natta and P. Corradini, *Atti. accad. nazl. Lincei*, [VIII] **4**, 73(1955); *Rend. accad. nazl. Lincei*, [VIII] **21**, 365 (1956).

(17) A. Odajima, J. Sohma and M. Koike, *J. Phys. Soc. Japan*, **12**, 272 (1957).

(18) A. Nishioka and Y. Kato, *Report Prog. Polymer Physics Japan* **3**, 128 (1960).

identity periods[19,20] should not introduce appreciable error. The positions of the protons on the side chain with respect to those on the main chain of the same molecule for PB1, PP1, P3MB1 and P4MP1 are not known and hence the contribution chosen is only an approximate one. In calculations involving methyl-methylene, methyl-CH group and methylene-CH group proton interactions, an ethane-like configuration was assumed.

The range of possible values for the intermolecular contribution to the second moment for all polymers except PTDP was taken as that given previously[2] for polypropylene. For PTDP this contribution was obtained by use of a molecular model based on the crystal structure given by Natta and Corradini[15] for polypropylene.

It was assumed that rotation of the methyl group about the threefold axis reduced the contributions due to interactions of the protons on an individual methyl group with one another to $^1/_4$ the rigid lattice value while those contributions due to interactions of protons on a methyl group with protons on any other group were assumed to be reduced to $^1/_3$ the rigid lattice values.[10,21]

In the 77–160°K. region the observed second moment for polypropylene drops from a value at 77°K. which is 2–5 gauss[2] lower than the estimated rigid lattice value to one at 160°K. which is about 2 gauss[2] higher than the estimated methyl rotation value. For PTDP in the 77–160°K. region the experimental values are about 2 gauss[2] greater than the calculated one. The presence of a more random orientation of the protons in the amorphous regions than in the crystal used as the model would be expected to *lower* the calculated second moments, an effect in the opposite direction to that observed. Reduction of the proton–proton distance on the methylene group from the assumed value of 1.78 Å., based on a tetrahedral structure, to 1.75 Å. will lead to increases in the calculated moment values of 1.8 and 0.9 gauss[2] for PTDP and polypropylene, respectively, if only the intragroup contribution is assumed to be affected. With these changes in spacing closer agreement between calculated and observed values for both polymers is found. It is concluded from all the evidence, including the absence of the low temperature motional narrowing process when the hydrogens on the methyl group are replaced by deuterons, that the results obtained support the hypothesis[1,2] that the transition in the $\leq$77 to 150°K. region for polypropylene is a consequence of the onset of methyl rotation.

From a comparison of the second moments for PB1, PP1, P3MB1 and P4MP1 at 77°K. with those calculated it appears that the rigid lattice state is not attained at the lowest temperature employed, but that considerable motion, presumably methyl rotation, is taking place. The transition that is definitely present for P3MB1 and P4MP1 and of which there is some indication for PB1 and PP1 at the lowest temperatures used, is therefore expected to extend to temperatures below 77°K. At 140°K., a temperature above this transition region, the experimental second moments are higher by about 2 gauss[2] for P3MB1 and P4MP1 and about 3 gauss[2] for PB1 and PP1 than the calculated methyl rotation values. These discrepancies are in the same direction and of comparable magnitude to those found for polypropylene and PTDP. Again a choice of a shorter proton–proton distance for the protons on the main chain methylene group would lead to calculated values in better agreement with the experimental ones. In addition to this, the averaging process of the magnetic dipolar fields brought about by the methyl group rotation might well lead to a reduction in second moment differing from the $^1/_3$ value assumed. However, the order of the second moments at 140°K. for the six polymers studied is that expected if methyl group rotation is occurring in all cases.

The relatively slow decrease in second moment with increasing temperature in the 130–240°K. region for PB1, PP1 and P4MP1 probably is due to side chain rotation involving CH and CH_2 groups in addition to CH_3 groups. This type of motion would not be expected to have much effect for P3MB1, in agreement with experiment.

A number of alpha methyl group containing polymers exhibit n.m.r. transitions in the 77–300°K. range, attributed to the onset of methyl group rotation of the appropriate frequency. These include: poly-(1,1,2-trideuteriopropylene)[22] ($\leq$77 to 150°K.), natural rubber[23–25] ($\leq$77 to 150°K.), polyisobutylene[25,26] ($\leq$77 to 200°K.), poly-(methyl methacrylate)[10,27,28] (100 to 200°K.), poly-(methacrylic acid)[10] ($\leq$77 to 200°K.), poly-(sodium methacrylate)[10] ($\leq$77 to 200°K.), and poly-(α-methylstyrene)[10] (120 to 260°K.). On the other hand, the methyl groups in poly-(dimethylsiloxane)[29–31] and the ester methyl groups in poly-(methyl acrylate)[28] and poly-(α-chloroacrylate)[27] are undergoing essentially complete rotation at 77°K.

Previous studies of polymers having side chains which contain aliphatic hydrocarbon parts larger than methyl have been confined to the poly-(methacrylate esters)[27,28] and include poly-(ethyl methacrylate)[27,28] and poly-(isobutyl methacrylate).[27] In contrast to the behavior of poly-(butene-1), in poly-(ethyl methacrylate) complete rotation of the ester ethyl and main chain methyl groups appears to be taking place at temperatures of 200°K. and above, a transition being found in the 90 to 200°K. range.[28] At 77°K., the second moment

(19) G. Natta, P. Corradini and I. W. Bassi, *Rend. accad. nazl. Lincei*, [VIII] **19**, 404 (1955).
(20) G. Natta, *Angew. Chem.*, **68**, 393 (1956).
(21) E. R. Andrew, *J. Chem. Phys.*, **18**, 607 (1950).
(22) W. P. Slichter, unpublished results.
(23) H. S. Gutowsky and L. H. Meyer, *J. Chem. Phys.*, **21**, 2122 (1953).
(24) H. S. Gutowsky, H. Saika, M. Takeda and D. E. Woessner, *ibid.*, **27**, 534 (1957).
(25) W. P. Slichter, *Macromol. Chem.*, **34**, 67 (1959).
(26) J. G. Powles, *Proc. Phys. Soc. (London)*, **69**, 281 (1956).
(27) W. P. Slichter and E. R. Mandell, *J. Appl. Phys.*, **30**, 1473 (1959).
(28) K. M. Sinnott, *J. Polymer Sci.*, **42**, 3 (1960).
(29) E. G. Rochow and H. G. LeClair, *J. Inorg. Nucl. Chem.*, **1**, 92 (1955).
(30) H. Kusumoto, J. Lawrenson and H. S. Gutowsky, *J. Chem. Phys.*, **32**, 724 (1960).
(31) C. M. Huggins, L. E. St. Pierre and A. M. Bueche, *J. Phys. Chem.*, **64**, 1304 (1960).

value for poly-(ethyl methacrylate) is about 5 gauss[2] below the estimated rigid lattice value, indicating some rotation of the ester methyl group even at this temperature.

Since it is expected that the calculated rigid lattice and methyl rotation second moments for the three monomers studied would be within 1–3 gauss[2] of those for the respective polymer, it appears from the data in Fig. 8 that methyl group rotation of comparable amount is taking place in 4-methylpentene-1 at temperatures only ~10°K. lower than those for the polymer. This is in marked contrast to the results[10] for α-methylstyrene and its polymer where complete methyl group rotation is believed to take place at temperatures about 100°K. lower in the monomer than for the polymer. Removal of one of the methyl groups from 4-methylpentene-1 to give pentene-1 leads to a situation where considerably more motion is taking place at 77°K. in the monomer than in the respective polymer. This effect is even more noticeable in the data for the branched isomer of pentene-1, 3-methylbutene-1. The abrupt decrease of the second moment to values near zero, exhibited by all three monomers at temperatures 25–30°K. below their respective melting points indicates the onset of motion other than side chain rotation, possibly involving tumbling of the individual monomers. This latter result is decidedly different from that obtained[10] for the monomers methyl methacrylate, methacrylic acid and α-methylstyrene, which have second moment values of 9–10, 7 and 10 gauss,[2] respectively, at temperatures not more than 8°K. below the melting point, indicating a much more rigid crystal structure for the latter three monomers.

The second moment decreases taking place at 260°K. or above for all polymers investigated is believed to be a consequence of side chain and main chain reorientations associated with the respective glass transitions. As reported previously[2,9] such reorientations are also believed to be the cause of the substantial changes found in the dynamic mechanical properties in the same temperature region for each polymer. On the other hand PB1, PP1, P3MB1 and P4MP1 do not appear to exhibit marked line narrowing in or near the 150°K. region where a loss peak attributed to the motion of three or four segments in the amorphous regions of the polymer has been found.[9] The fact that the line narrowing process near room temperature occurs for PTDP before that for polypropylene prepared under the same conditions is not understood at this time.

Acknowledgments.—We wish to express our thanks to Professor R. E. Glick of Florida State University for frequent discussions during the formative stages of this work, to Professor R. S. Stein of University of Massachusetts and Dr. W. P. Slichter of Bell Telephone Laboratories for bringing to our attention their work prior to publication, to Mr. R. P. Gupta and Mr. R. A. Wall for preliminary n.m.r. measurements on some of these compounds, and to Drs. F. P. Reding and R. D. Lundberg of Union Carbide Chemicals Company for their aid and interest in this study.

THE TRANSITION FROM TYPICAL POLYELECTROLYTE TO POLYSOAP. III. LIGHT SCATTERING AND VISCOSITY STUDIES OF POLY-4-VINYLPYRIDINE DERIVATIVES[1]

BY ULRICH P. STRAUSS AND BERNARD L. WILLIAMS[2]

Ralph G. Wright Laboratory, School of Chemistry, Rutgers, The State University, New Brunswick, New Jersey

Received March 9, 1961

One polyelectrolyte and four polysoaps were prepared from poly-4-vinylpyridine by quaternizing 0, 4.8, 10.3, 16.3 and 34.1% of its pyridine groups with *n*-dodecyl bromide and the remainder with ethyl bromide. Light scattering studies in a solution of LiBr in isopropyl alcohol gave results typical of normal polymers. The molecular weights were considerably lower than that of the parent polymer, indicating that degradation had occurred during quaternization. The mean-square end-to-end distance per unit chain length at the theta point increased with increasing dodecyl group content, which was ascribed to steric hindrance. On the other hand, light scattering results obtained in 0.05, 0.1 and 0.2 *M* aqueous KBr solutions, while normal for the polyelectrolyte, indicated aggregate formation of the polysoap molecules. These aggregates are fairly stable to dilution at 25°; but the degree of aggregation decreases with dilution if the diluted solutions are heated to 45° for at least 24 hours before being allowed to equilibrate at 25°. With the latter type of procedure, one can obtain parameters characteristic of the individual polysoap molecules at infinite dilution. Flory's equation relating the root-mean-square end-to-end distance of random coils to the intrinsic viscosity is found to hold fairly well for all the samples except for the polysoap with the highest dodecyl group content. For the latter, only the assumption of a compact sphere model was consistent with both light scattering and viscosity results. Contrary to the behavior in isopropyl alcohol, the unperturbed molecular dimensions *decreased* with increasing dodecyl group content in the aqueous systems. Thus, in such systems, the previously postulated aggregation of dodecyl groups belonging to the same polysoap molecule is confirmed.

Introduction

Several reports have appeared in recent years concerning the transition from polyelectrolyte to polysoap.[3–5] The studies were carried out with series of poly-4-vinylpyridine derivatives prepared by quaternizing part (y%) of the pyridine groups with *n*-dodecyl bromide and the remainder with

(1) This work was supported in part by the Office of Naval Research. The paper is based on a thesis presented by B. L. Williams in 1958 to Rutgers University in partial fulfillment of the requirements for the Ph.D. degree.

(2) Eastman Kodak Fellow, 1956–1957; Colgate-Palmolive Fellow, 1957–1958.

(3) U. P. Strauss and N. L. Gershfeld, *J. Phys. Chem.*, **58**, 747 (1954).

(4) U. P. Strauss, N. L. Gershfeld and E. H. Crook, *ibid.*, **60**, 577 (1956).

(5) D. Woermann and F. T. Wall, *ibid.*, **64**, 581 (1960).

ethyl bromide. Based mainly on viscosimetric results in aqueous KBr or KCl solvent systems, it was found that the derivatives with y smaller than a critical value in the neighborhood of 8 had the loosely coiled chain structure typical of polyelectrolytes, while the derivatives with values of y larger than the critical value had the highly compact shape typical of polysoaps.[6] In addition, all the derivatives containing dodecyl groups showed a tendency toward intermolecular association.[3,4]

To obtain more quantitative information concerning the molecular dimensions and the aggregate formation than can be obtained from viscosity results alone, it was decided to study these phenomena using both light scattering and viscosity techniques. The results of this investigation which were carried out with poly-4-vinylpyridine derivatives of the type described above (y = 0, 4.8, 10.3, 16.3 and 34.1) are presented in this paper.

Experimental

Materials.—Poly-4-vinylpyridine (our sample No. B-120) was prepared at 50° according to a modification of the method of Fuoss and Strauss,[7] using benzene and azobisisobutyronitrile as the polymerization medium and catalyst, respectively. Two successive fractionations by the method of Boyes and Strauss[8] yielded among others a sample (our No. B-120F2B) which was used for the subsequent work. Its weight-average molecular weight, M_w, and degree of polymerization, P_w, determined by light scattering in a solvent containing by weight 86% 2-butanone and 14% isopropyl alcohol were 2.0×10^6 and 19,000, respectively. The polyelectrolyte and polysoaps were prepared and analyzed by a previously described method[3] with the modification that 2,4-dimethyl-1,1-dioxytetrahydrothiophene (dimethylsulfolane) was used as the solvent for the quaternization reactions, and that the residual HBr was removed by ion exchange.[9] The chemical composition of the compounds is given in Table I. The quantity M_0 in the fourth column is the molecular weight per pyridine group, and is used below to convert molecular weights to degrees of polymerization.

TABLE I

CHEMICAL COMPOSITION OF POLY-4-VINYLPYRIDINE DERIVATIVES

Sample[a]	Meq. Br^-/g.	Meq. N/g.	M_0	% of pyridine groups substituted with n-$C_{12}H_{25}Br$ (= y)	% of pyridine groups substituted with C_2H_5Br
B-1227D	4.42	4.46	224	0	99.1
B-1229D	4.29	4.33	230	4.8	94.2
B-1232D	4.16	4.19	239	10.3	89.2
B-1245D	4.00	3.93	254	16.3	86.0
B-1250D	3.69	3.71	270	34.1	65.2

[a] In the text, the polysoap samples will be identified by y, the percentage of pyridine groups substituted with dodecyl bromide; for instance, "4.8%" polysoap, etc.

All solvents used were purified and distilled according to standard methods.

Light Scattering.—Light-scattering measurements were performed at 25° in a Brice–Phoenix light-scattering photometer,[10] using incident unpolarized monochromatic blue (λ 4360 Å.).[11] The apparatus was modified, following the design of Boedtker and Doty,[12] by providing a housing for thermostating the cylindrical light-scattering cells. The latter had flat faces at 0 and 180°. The slit system of the housing was 2.5 mm. wide and 8.5 mm. high. The small auxiliary diaphragms, which are supplied with the instrument, were used at the end of the collimating tube and in the nosepiece of the photomultiplier housing unit. In this way a well defined narrow beam of light was obtained which allowed measuring the scattering envelope from 25 to 135°. The optical uniformity and correct positioning of the cells was checked with the angular envelope obtained from a fluorescein solution. Several concentrations of the latter served to ascertain the linearity of the phototube response. All solvents and solutions were clarified with sintered glass filters of "ultrafine" porosity. In the case of the polysoap solutions in aqueous KBr systems, the filtering procedure caused the formation of a few fibers which would redissolve on standing. If about an hour was allowed for this redissolution, reproducible and time-stable scattering envelopes were obtained.[13] The modified apparatus was calibrated with several solutions whose scattering power had been determined in the unmodified instrument in square cells. The latter was calibrated as described previously.[14] It was found that the ratio of the light scattered in the modified system to that in the unmodified system was the same for all solutions tested, which included polystyrene in toluene, poly-4-vinylpyridine in methanol and polysoaps in aqueous KBr.

Refractive index differences between solutions and solvents were measured in a Brice–Phoenix differential refractometer which was calibrated by means of sucrose solutions.[15]

Viscosity.—Viscosities were measured at 25° in a Bingham viscometer as described previously.[14]

Results and Discussion

Degree of Polymerization.—The light-scattering results for the "10.3%" polysoap in aqueous 0.2 M KBr are represented by a Zimm plot[16,17] in Fig. 1,

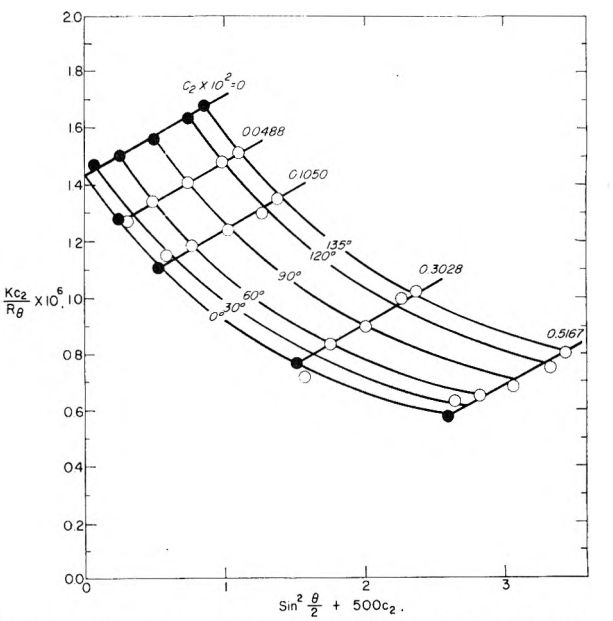

Fig. 1.—Zimm plot of "10.3%" polysoap in 0.2 M KBr, with each solution brought to equilibrium.

(6) U. P. Strauss and E. G. Jackson, *J. Polymer Sci.*, **6**, 649 (1951).

(7) R. M. Fuoss and U. P. Strauss, *Ann. N. Y. Acad. Sci.*, **51**, 836 (1949).

(8) A. G. Boyes and U. P. Strauss, *J. Polymer Sci.*, **22**, 463 (1956).

(9) An analytical grade anion-exchange resin in the hydroxyl form contained in a bag made of dialysis casing was immersed briefly in aqueous solutions of the materials to raise the *p*H to between 5 and 6.

(10) B. A. Brice, M. Halwer and R. Speiser, *J. Optical Soc. Am.*, **40**, 708 (1950).

(11) Results obtained with the 5460 Å. mercury line were identical indicating that fluorescence of the polyvinylpyridine derivatives was negligible.

(12) H. Boedtker and P. Doty, *J. Phys. Chem.*, **58**, 968 (1954).

(13) We have satisfied ourselves that the redissolved fibers do not leave any significant amount of large aggregates of polysoap molecules which would affect the scattering.

(14) U. P. Strauss and P. Wineman, *J. Am. Chem. Soc.*, **80**, 2366 (1958).

(15) C. A. Browne and F. W. Zerban, "Physical and Chemical Methods of Sugar Analysis," 3rd Ed., John Wiley and Sons, Inc., New York, N. Y., 1941, p. 1206.

(16) B. H. Zimm, *J. Chem. Phys.*, **16**, 1093, 1099 (1948).

(17) P. Doty and J. T. Edsall, *Advances in Protein Chem.*, **6**, 35 (1951).

where R_θ is the reduced intensity at the angle θ and polysoap concentration c_2 in g./ml., and K is a parameter defined in equation 2 below. Each solution had been brought to equilibrium by being maintained first at 45° for at least 24 hours, and then at 25° for at least another 24 hours. The curves are unusual in that their slopes are strongly negative. This behavior confirms previously obtained evidence that, just as with gelatin,[12] one is dealing with aggregates which dissociate continuously on dilution.[4] All the polymers containing dodecyl groups produce similar Zimm plots in 0.05, 0.1 and 0.2 M aqueous KBr solutions.[18] On the other hand the polyelectrolyte containing only ethyl side groups produces normal Zimm plots. Such a plot obtained in 0.2 M KBr is shown in Fig. 2.

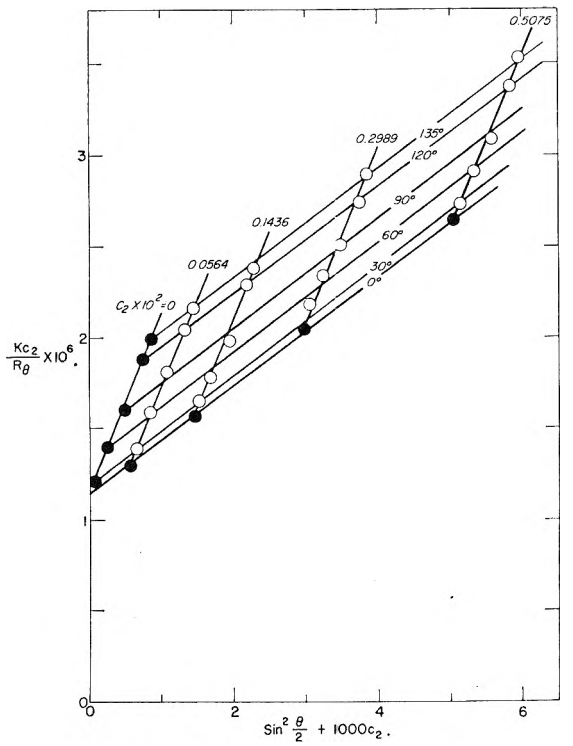

Fig. 2.—Zimm plot of polyelectrolyte (sample B-1227D) in 0.2 M KBr.

In all these three-component systems the molecular weight of the polymer (component 2) is obtained from the following equations, which refer to the line extrapolated to $\theta = 0$.[19,20]

$$\frac{Kc_2}{R_0} = \frac{1}{(1 - D)^2}(A + 2Bc_2) \quad (1)$$

$$K = 2\pi^2 n^2 \left(\frac{\partial n}{\partial c_2}\right)^2 / N_A \lambda^4 \quad (2)$$

$$D = \frac{(\partial n/c_3)}{(\partial n/c_2)} \times \frac{M_3}{M_2} \times \frac{a_{23}}{a_{33}} \quad (3)$$

$$M_2 = \frac{1}{A} \times \frac{6 - 7\rho_u}{6 + 6\rho_u} \quad (4)$$

In these equations M_j is the molecular weight and c_j the concentration in g./ml. of component j, $j = 1$, 2 and 3 referring to solvent, polymer and simple electrolyte, respectively. Furthermore, N_A is Avogadro's number, λ is the wave length of light *in vacuo*, n is the refractive index of the solution, ρ_u is the depolarization and $a_{jk} = (1/RT) \times (\partial\mu_j/\partial m_k)$ where μ_j and m_j are the chemical potential and molarity, respectively, of component j.

In order to calculate D, the term a_{23}/M_2a_{33} was determined from membrane equilibrium data,[21] the quantity $\partial n/\partial c_2$ was measured, and $\partial n/\partial c_3$ was interpolated from literature values.[22] To convey an idea of the magnitude of the quantity $(1 - D)^{-2}$, its values are 1.03, 1.04, 1.07 and 1.19 for the all-ethyl derivative in 0.05, 0.1, 0.2 and 0.8 M KBr, respectively, and 1.02, 1.03 and 1.04 for the "34.1%" polysoap in 0.05, 0.1 and 0.2 M KBr, respectively. The depolarization correction was negligible in these solvents.

In view of some difficulties encountered in obtaining accurate molecular weights of the polysoaps in the aqueous KBr systems, light scattering was also performed in a solvent consisting of a 0.1213 M LiBr solution in isopropyl alcohol (IPA). A Zimm plot of the "10.3%" polysoap which is similar to the Zimm plots obtained with the other polysoaps in this solvent system, is shown in Fig. 3. In the calculation of the molecular weights from

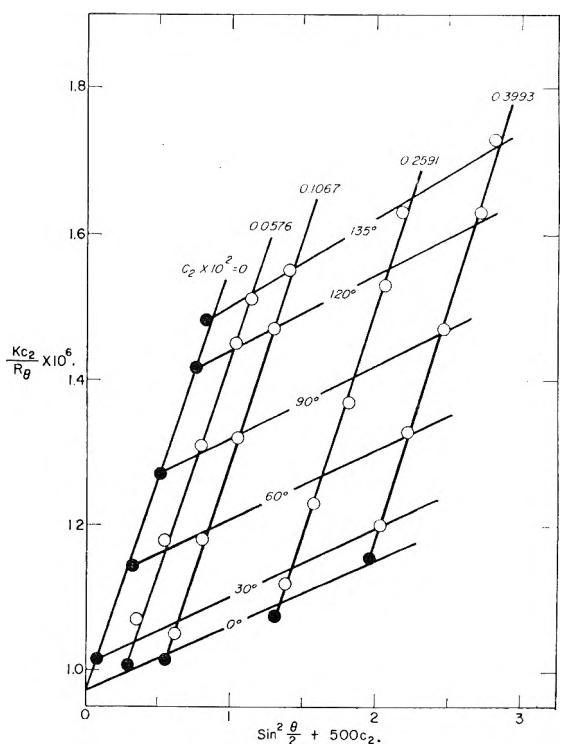

Fig. 3.—Zimm plot of "10.3%" polysoap in 0.1213 M LiBr in IPA.

equations 1–4, the quantity D was assumed to be negligible in this organic solvent. However, the Cabannes factor in equation 4 deviated from unity

(18) Actually, the Zimm plots of the "4.8%" polysoap in 0.05 and 0.1 M KBr and of the "10.3%" polysoap in 0.05 M KBr appear to be normal. However, subsequent analysis of the results indicates aggregation in all these cases.

(19) J. G. Kirkwood and R. J. Goldberg, *J. Chem. Phys.*, **18**, 54 (1950).

(20) W. H. Stockmayer, *ibid.*, **18**, 58 (1950).

(21) D. Fraser, Ph.D. thesis, Rutgers University, 1960.

(22) G. P. Baxter, A. C. Boylston, E. Mueller, N. H. Black and P. B. Goode, *J. Am. Chem. Soc.*, **33**, 901 (1911).

by 5–8% and was included. The molecular weight results are represented in terms of P_w,[23] the weight-average degree of polymerization, in Table II.

TABLE II

LIGHT-SCATTERING DEGREES OF POLYMERIZATION

	P_w			
y	in 0.1213 M LiBr in IPA	in 0.05 M KBr	in 0.10 M KBr	in 0.20 M KBr
0.0[a]	..	..	4140	4250
4.8	3260	5210	5840	3930
10.3	3900	4560	4230	3070
16.3	2480	3460	3170	3520
34.1	3000	1970	2960	3870

[a] P_w is equal to 3670 for this sample in 0.8 M KBr.

The values of P_w for a given sample are somewhat scattered, but of the same order of magnitude. We believe that the main cause for the observed discrepancies is the uncertainty in the extrapolation of the extremely steep Kc_2/R_0 against c_2 curves of the polysoap–KBr–H_2O systems. However, in some cases, incomplete breaking up of the aggregates in these systems may have been also responsible. For these reasons the values in the LiBr–IPA solvent system are considered most reliable and will be used in subsequent calculations.

It is seen that the P_w-values of all the poly-4-vinylpyridine derivatives are much lower than 19,000, the P_w-value of the parent polymer. Apparently degradation takes place during the quaternization reaction.[24] The cause for this is not known. From some scattered observations that the degree of polymerization of the quaternization products is about 3500 regardless of how much higher than 3500 the chain length of the parent polymer is, one might suspect that on the average about every 3500th bond in poly-4-vinylpyridine is different from and weaker than the rest, possibly through some reaction which is competitive to the normal pathway of the polymerization of vinylpyridine.[25]

The fact that the P_w-values of the polysoaps do not seem to follow any trend is believed to be due to accidental fractionation during the many purifications of the samples.

Aggregates.—When, instead of preparing each polysoap solution in aqueous KBr separately, the solutions were prepared by dilution from a more concentrated solution at 25°, the resulting Zimm plots appeared normal. In Fig. 4, such a plot is shown for the "10.3%" polysoap in 0.1 M KBr. The resulting molecular weights were from 30 to 170% higher than those obtained with the directly prepared solutions. This difference in molecular weights is interpreted as being due to the formation

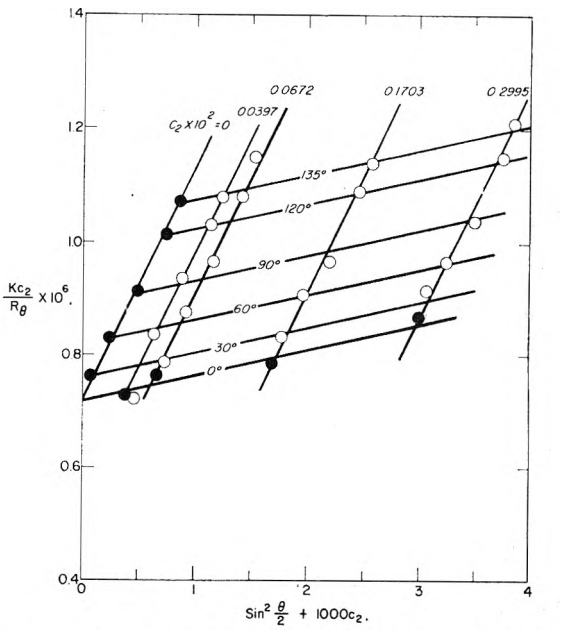

Fig. 4.—Zimm plot of "10.3%" polysoap in 0.1 M KBr; dilution run.

of aggregates of polysoap molecules. The dilution method measures the average molecular weight of the polysoap species existing in the solution from which the dilutions were made, since at 25° the aggregates which exist in this solution did not have enough time to dissociate significantly during the three to six hours it took to complete the experiments after the dilution process. The slowness of the dissociation was substantiated by observations indicating that in the first 24 hours after dilution the Rayleigh ratios of the diluted polysoap solutions decreased by only a few per cent. If, on the other hand, the diluted solutions were treated like the originally freshly prepared ones, *i.e.*, if they were first heated to 45° for at least 24 hours and then allowed to equilibrate at 25°, the light-scattering results were the same as those of a freshly prepared solution of the same concentration. A similar type of behavior has been observed in gelatin solutions.[12]

Second Virial Coefficients.—The second virial coefficients as determined from the light-scattering data by means of equation 1 are given in Table III.

TABLE III

SECOND VIRIAL COEFFICIENTS

	$B \times 10^5$					
		Regular runs			Dilution runs	
y	0.1213 M LiBr in IPA	0.05 M KBr	0.10 M KBr	0.20 M KBr	0.05 M KBr	0.10 M KBr	0.20 M KBr
0[a]	....	....	32.9	14.8	..	..	...
4.8	−1.2	16.0	2.5	− 7.1	..	..	0.3
10.3	+1.2	0.0	− 2.7	−14.0	6.7	2.5	−0.9
16.3	1.1	1.2	−11.5	− 4.4	6.7	2.5	−0.2
34.1	3.3	−31.6	−10.8	−14.1	3.3	1.3	−1.0

[a] In 0.8 M KBr, $B = 4.7 \times 10^{-5}$.

Several features are noteworthy. The negative values of B which are observed with the polysoaps in most of the aqueous KBr solutions in the regular runs reflect the decrease in the extent of polysoap association with decreasing polysoap concentration.

(23) To simplify the presentation, we shall hereafter omit the subscript "2" in symbols designating the molecular weight, degree of polymerization and the molecular dimensions of the polymer component.

(24) The reduced specific viscosity of a 0.1% solution of the parent polymer in ethanol remained constant at 4.25 dl./g. on heating at 45° for 50 hours.

(25) Such a reaction might involve oxygen, as suggested by Fuoss [J. B. Berkowitz, M. Yamin and R. M. Fuoss, *J. Polymer Sci.*, **28**, 69 (1958)]. Another possibility is free-radical formation at the pyridine nitrogen instead of at the α-carbon so that the nitrogen is part of the backbone chain, with the pyridine ring being in the quinoid form.

The values of B obtained in the dilution runs where the association is assumed to remain constant with dilution are seen to be generally more positive and reflect interactions other than the association. It is our belief that these values would be close to the correct ones for individual polysoap molecules if association did not occur. It is noteworthy that these values as well as those obtained in the LiBr–IPA solvent system are quite small. This probably is due to the compact molecular size of the polysoap molecules, which will be discussed below. In contrast, the much more extended polyelectrolyte ($y = 0$) is seen to have much larger second virial coefficients. For each of the first three samples, the B-values decrease with increasing ionic strength, as has been observed with other polyelectrolytes in aqueous solutions.[14] However, the two samples with the most dodecyl groups seem to show somewhat irregular behavior in this respect.

Molecular Dimensions.—The molecular dimensions of the samples were determined from the light-scattering results in all solvent systems used and from the intrinsic viscosity results in the aqueous KBr solutions. The calculations depend to some extent on the assumed configuration and, in the case of the intrinsic viscosity, also on the molecular weight distribution of the samples.

From the light-scattering results the z-average mean-square-radius of gyration $(\overline{s^2})_z$ is obtained by the relation

$$(\overline{s^2})_z = \frac{3}{16\pi^2}(\lambda/n)^2(S/I) \qquad (5)$$

where I and S are the intercept and slope, respectively, of the Zimm plot $c_2 = 0$ line.[16,26,27]

For a random coil, the z-average mean-square end-to-end distance $(\overline{r^2})_z$ is related to $(\overline{s^2})_z$ by the equation

$$(\overline{r^2})_z = 6(\overline{s^2})_z \qquad (6)$$

while for a sphere, the diameter, d, can be obtained from the expression

$$(\overline{d^2})_z = (20/3)(\overline{s^2})_z \qquad (7)$$

Flory, *et al.*,[28] have shown that to obtain comparable z-average values from the intrinsic viscosity, one may use the relation

$$(\overline{r^2})_z = \left(\frac{[\eta]M_w^{2/3}}{\phi/q}\right) \qquad (8)$$

We estimate the quantity q by assuming the molecular weight distribution given by Zimm[16] with the parameter characterizing the heterogeneity equal to unity. With this choice $M_w/M_n = 2$ and $q = 1.95$.[29] The value for ϕ is 2.2×10^{21} for random coils. The results are compared in Table IV.

The agreement between the viscosimetric and light-scattering values is, in general, quite satisfactory considering the uncertainty underlying the assumptions made concerning the molecular weight distribution.[30] However, there seems to be some discrepancy in the case of the "34.1%" polysoap in the 0.1 and 0.2 M KBr solutions. Since this discrepancy is greater than the combined experimental uncertainty of the light-scattering and viscosity methods, we believe this to be an indication that the polysoap molecules have become so compact that their shape is no longer representable by a random coil model. This interpretation is further substantiated by the observation that the decrease in molecular dimensions with increasing ionic strength, which is typical of polyelectrolytes and clearly noticeable for the other samples given in Table IV, is absent in the two "34.1%" polysoap–H_2O–KBr systems mentioned above. If, instead, one assumes the polysoap molecule to be a rigid sphere, then the viscosity value of the diameter should be calculated by the Einstein relation,[31] which is equivalent to equation 8 with $(\overline{r^2})_z$ replaced by $(d^2)_z$ and with ϕ/q taking on the value 7.85×10^{21}. Similarly, the light scattering value should be calculated by equation 7. In

TABLE IV

MOLECULAR DIMENSIONS

			0.05 M KBr			0.10 M KBr			0.20 M KBr		
		$[(\overline{r^2})_z]^{1/2} \times 10^8$ (cm.) from l.s. in LiBr–IPA		$[(\overline{r^2})_z]^{1/2} \times 10^8$ (cm.)			$[(\overline{r^2})_z]^{1/2} \times 10^8$ (cm.)			$[(\overline{r^2})_z]^{1/2} \times 10^8$ (cm.)	
y	$M_w \times 10^{-5}$[b]		$[\eta]$	from $[\eta]$	from l. s.[c]	$[\eta]$	from $[\eta]$	from l. s.[c]	$[\eta]$	from $[\eta]$	from l. s.[c]
0[a]	9.4	..	..	..	..	1.42	1060	1240	0.88	900	1050
4.8	7.5	610	1.00	880	990	0.645	730	850	.370	630	720
10.3	9.3	770	0.420	700	800	.262	600	660	.133	480	590
16.3	6.3	620	.222	500	500	.160	450	450	.114	400	390
34.1	8.1	770	.096	410	430	.085	400	240	.086	400	250

[a] In 0.8 M KBr[6] $[\eta] = 0.770$; $[(\overline{r^2})_z]^{1/2} = 860 \times 10^{-8}$ cm. from $[\eta]$; $[(\overline{r^2})_z]^{1/2} = 770 \times 10^{-8}$ cm. from l. s. [b] Obtained in LiBr–IPA. [c] Obtained in "regular" runs.

(26) K. A. Stacey, "Light-Scattering in Physical Chemistry," Academic Press, Inc., New York, N. Y., 1956, p. 33.

(27) In the case of the polysoap–KBr–H_2O systems, the values of I to be used in equation 5 were calculated from the molecular weights determined in the LiBr–IPA solvent. However, the above mentioned difficulties in obtaining reliable molecular weights in the KBr–H_2O solvents did not apply to the determination of the values of S from the Zimm plots. The accuracy of this procedure was checked further by extrapolating the slopes of the $Kc_2/R\theta$ against $\sin^2\theta/2$ lines, obtained at each individual concentration, to $c_2 = 0$. It is relevant here that the quantity S is essentially a measure of $(\overline{s^2}/M)$ and hence, to a good approximation, independent of the molecular weight.

(28) S. Newman, W. R. Krigbaum, C. Laugier and P. J. Flory, *J. Polymer Sci.*, **14**, 451 (1954).

(29) While the original parent polymer was fractionated, the degradation occurring during the quaternization is assumed to lead to polydispersity characteristic of unfractionated polymers.

(30) If we had assumed a corresponding Lansing–Kraemer molecular weight distribution, the values of $[(\overline{r^2})_z]^{1/2}$ calculated from $[\eta]$ would have been about 17% larger than those given in Table IV [W. D. Lansing and E. O. Kraemer, *J. Am. Chem. Soc.*, **57**, 1369 (1935)]. This would have improved the agreement between the viscosity and light-scattering values of $[(\overline{r^2})_z]^{1/2}$. The problems encountered in choosing a suitable distribution function recently have been discussed [W. R. Krigbaum and L. H. Sperling, *J. Phys. Chem.*, **64**, 99 (1960)].

(31) A. Einstein, *Ann. Physik*, **19**, 289 (1906); **34**, 591 (1911).

this way, we obtain viscosity and light scattering values for d in 0.1 M KBr equal to 300×10^{-8} and 250×10^{-8} cm., respectively, and in 0.2 M KBr equal to 300×10^{-8} and 260×10^{-8} cm., respectively. It is seen that in these two cases the rigid sphere model results in better agreement than the random coil model.

Flory and Fox[32] have shown that in a θ-solvent the molecular dimensions are unperturbed by long-range interactions and are therefore characteristic of the short-range interactions of the polymer molecule. In such a solvent the second virial coefficient is zero. Since in Table III it is shown that the values of B are very small in the LiBr–IPA system, the values of $[(\overline{r^2})_z]^{1/2}$ in Table IV are very close to $[(\overline{r_0^2})_z]^{1/2}$, the unperturbed z-average root-mean-square end-to-end distance. An improvement can be made by using an equation, developed by Krigbaum[33]

$$[(\overline{r^2})_z]^{3/2} = [(\overline{r_0^2})_z]^{3/2} + uB \qquad (9)$$

where $u = 5.25 \times 10^{-24}\,[M_w]^2$ for the assumed molecular weight distribution of our sample. The resulting values of $[(\overline{r_0^2})_z]^{1/2}$ divided by $[P_z]^{1/2}$, both quantities being based on the light scattering results, are given in the second column of Table V. The values of P_z, the z-average degree of polymerization, are obtained by multiplying P_w by 1.5. The ratios should then be independent of the molecular weight distribution, and therefore the subscript z has been omitted in Table V. In the third column the values of $(\overline{r_0^2}/\overline{r_{0f}^2})^{1/2}$ are given, where $(\overline{r_{0f}^2})^{1/2}$ is the hypothetical unperturbed end-to-end distance which the polymer molecule would have if all the bonds were freely rotating. The value of $(\overline{r_{0f}^2}/P)^{1/2}$ is 3.5×10^{-8} cm., calculated as described by Flory.[34] The corresponding values for the KBr–H_2O system are given in the next two columns. Except for the "4.8%" polysoap where the appropriate values of B are lacking[35] the values of $[(\overline{r_0^2})_z]^{1/2}$ were obtained from the ordinate intercepts of $[(\overline{r^2})_z]^{3/2}$ against B plots. For reasons discussed above, the "dilution run" values of B were used for the samples corresponding to $y \geq 10.3$. The agreement in order of magnitude between the observed u-values and those calculated from Krigbaum's equation, shown in the last two columns of Table V, seems to justify this procedure.

Table V

THETA SOLVENT MOLECULAR DIMENSIONS

	—In LiBr–IPA—		—In KBr–H_2O—			
y	$(\overline{r_0^2}/P)^{1/2}$[a]	$(\overline{r_0^2}/\overline{r_{0f}^2})^{1/2}$	$(\overline{r_0^2}/P)^{1/2}$[a]	$(\overline{r_0^2}/\overline{r_{0f}^2})^{1/2}$	$u \times 10^{13}$ (obsd.)[b]	$u \times 10^{13}$ (calcd.)[c]
0	..	..	8.9	2.54	44	46
4.8	9.1	2.60	10.1	2.88	..	29
10.3	9.7	2.77	7.9	2.26	34	46
16.3	9.8	2.80	6.5	1.86	11	21
34.1	10.4	2.98	4.3	1.23	16	34

[a] The values of P for $y \geq 4.8$ are based on the molecular weights determined in the LiBr–IPA system. However, the quantity $(\overline{r_0^2}/P)$ is independent of the measured molecular weight and can be derived directly from the value of S corresponding to the light scattering results obtained in the appropriate LiBr–IPA or KBr–H_2O solvent system. [b] From $[(\overline{r^2})_z]^{3/2}$ against B plots. [c] u (calcd.) $= 5.25 \times 10^{-24}\,[M_w]^2$.

The most striking observation concerning the behavior of the θ-solvent dimensions is the difference in trends with increasing dodecyl group content, y, in the two solvent systems studied. As y approaches zero, the quantity $(\overline{r_0^2}/\overline{r_{0f}^2})^{1/2}$ converges in both solvent systems to a common value which is close to 2.44, the value observed for the sterically similar polystyrene[36] and poly-4-vinylpyridine.[8] In the LiBr–IPA system, which has considerable solvent power for the dodecyl groups[37] and which may therefore be considered a solvent in which the polysoaps behave like ordinary polymers, the values of $(\overline{r_0^2}/\overline{r_{0f}^2})^{1/2}$ increase slightly with increasing y. This effect may be ascribed to the steric hindrance of the dodecyl groups to free rotation in the backbone chain. It is then especially striking that despite this steric hindrance there is a sharp decrease in the values of $(\overline{r_0^2}/\overline{r_{0f}^2})^{1/2}$ in the KBr–H_2O system. This behavior, which has previously been described in a more qualitative way, is considered evidence of micelle formation within each individual polysoap molecule caused by association of the water insoluble dodecyl groups.

(32) P. J. Flory and T. G. Fox, *J. Am. Chem. Soc.*, **73**, 1904, 1909, 1915 (1951).

(33) W. R. Krigbaum, *J. Polymer Sci.*, **18**, 315 (1955).

(34) P. J. Flory, "Principles of Polymer Chemistry," Cornell University Press, Ithaca, N. Y., 1953, p. 415.

(35) The value of $[(\overline{r_0^2})_z]^{1/2}$ for this sample was calculated by equation 9 from the value of $[(\overline{r^2})_z]^{1/2}$ and the "dilution run" value of B obtained in 0.20 M KBr.

(36) Reference 34, p. 618.

(37) This is apparent from the increase of B with y, shown in Table III.

THE SOLUBILITY OF QUARTZ UNDER HYDROTHERMAL CONDITIONS[1]

BY R. A. LAUDISE AND A. A. BALLMAN

Bell Telephone Laboratories, Inc., Murray Hill, New Jersey

Received March 10, 1961

The solubility of α quartz as a function of temperature and density of the solvent has been measured between 300 and 400° and between a solvent density of 0.70 and 0.87 g./cc. in 0.51 *m* sodium hydroxide solutions and the results are compared with quartz solubilities in the systems H_2O–SiO_2, H_2O–SiO_2–Na_2O and H_2O–SiO_2–Na_2CO_3. It is found that the van't Hoff relation is obeyed and ΔE and ΔS for the respective solution processes are calculated. It is further found that the logarithm of the solubility is linear with the solvent density which is shown to indicate weak solvent–solute interactions. It is shown that the reaction $SiO_2 + (2a - 4)(OH)^- \rightleftarrows (SiO_a)^{(2a-4)-} + (a - 2)H_2O$ goes essentially to completion in hydroxide solutions and nearly to completion in carbonate solutions. It is also shown that the species present in $(OH)^-$ solutions in the one fluid phase region is $(Si_3O_7)^{2-}$ while in $(CO_3)^{2-}$ systems $(SiO_3)^{2-}$ seems to predominate.

Introduction

Single crystals of α-quartz,[2] sapphire,[3] zinc oxide,[4] zinc sulfide[4] and yttrium iron garnet[5] have been grown by the use of basic aqueous solvents at high pressure and temperature which increase the solubility of these ordinarily insoluble materials. Experimental details of this technique which is generally called hydrothermal crystallization have been reviewed elsewhere[6] and the kinetics of the crystallization of quartz under hydrothermal conditions have been studied in the system H_2O–SiO_2–Na_2O.[7]

E. U. Franck[8] and others[9,10] have discussed the solubility of solid substances under hydrothermal conditions and from a consideration of the thermodynamics of a constant volume system Franck has derived expressions predicting the dependence of solubility on the specific volume of the solvent. The only hydrothermal system for which solubility data exist in any quantity is the quartz system. However, even in the case of quartz all of the solubility data in the literature have not been evaluated and no consideration of the systems containing base has been made. Furthermore, complete solubility data over the pressure–temperature range where quartz is crystallized are not available.

We therefore decided to measure the solubility of quartz in the system SiO_2–H_2O–Na_2O at conditions where quartz crystallization rate studies have been made and by the use of Franck's treatment as a guide to look for relationships which would allow interpolations and extrapolations both in this and in similar systems. The validity of these relations was tested where appropriate with the solubility data of Kennedy,[11] Friedman,[12] Morey[13] and Butuzov and Briatov[14] in the systems SiO_2–H_2O, SiO_2–H_2O–Na_2O and SiO_2–H_2O–Na_2CO_3 and finally the data were utilized to deduce where possible the nature of the silica containing species in the various hydrothermal systems.

Quartz is ordinarily crystallized at temperatures between 300 and 400° from solutions where the specific volume is between 1.15 and 1.54 (corresponding to degree of fill of the free volume of the autoclave at room temperature of 0.87 to 0.65). Under these conditions Morey's data[13,15] and preliminary experiments in these laboratories showed that but one fluid phase was present both in pure water and in the base concentration ranges described in this work.

Experimental

Several methods have been employed for the determination of solubilities under hydrothermal conditions.

Fyfe[16] has pointed out that in the sampling method unless the sample which is withdrawn from the autoclave at operating conditions is small, the system may be perturbed enough that the sample will not be representative. These errors were shown to be important in the solubility measurements made in the system SiO_2–H_2O by Frederickson and Cox.[17]

All other methods for determining solubility involve the examination of autoclave contents after quenching at the conclusion of a run. Where only one fluid phase exists the simplest technique to employ is the weight loss method. In our work this technique was used.

Generally two weighed plates of quartz whose total surface area was about 15 cm.^{2} and whose principal face was (0001) were suspended near the middle of a suitably designed autoclave, the autoclave was filled to some predetermined fraction or per cent. of fill of its free volume with a NaOH solution of the desired concentration and sealed. The autoclave then was placed in a furnace capable of maintaining it isothermally at the desired temperature and warmed up with special care being exercised to avoid overshooting in temperature. The vessel was maintained at temperature for a time in excess of that found to be required to establish equilibrium and then quenched. Provided only one fluid phase was present and provided quartz was known to be the stable phase under the conditions of the experiment, the loss in weight of the quartz plates was an excellent measure of the solubility of quartz.

(1) Presented in part at the 32nd National Colloid Chemistry Symposium, Lehigh University, June, 1960.

(2) G. Spezia, *Acad. Sci. Torino Atti.*, **40**, 254 (1905); see also R. Nacken, Captured German Reports, RDRC/13/18, February 28, 1946.

(3) R. A. Laudise and A. A. Ballman, *J. Am. Chem. Soc.*, **80**, 2655 (1958).

(4) R. A. Laudise and A. A. Ballman, *J. Phys. Chem.*, **64**, 688 (1960).

(5) R. A. Laudise, J. C. Crocket and A. A. Ballman, *ibid.*, **65**, 359 (1961).

(6) R. A. Laudise and J. W. Nielsen in "Solid State Physics," Ed. F. Seitz, to be published.

(7) R. A. Laudise, *J. Am. Chem. Soc.*, **81**, 562 (1959).

(8) E. U. Franck, *Z. physik. Chem. (Neue Folge)*, **6**, 345 (1956).

(9) R. Mosebach, *Neues Jb. Mineralog. Abh.*, **87**, 351 (1955).

(10) J. A. Wood, Jr., *Amer. J. Sci.*, **256**, 40 (1958).

(11) G. C. Kennedy, *Econ. Geol.*, **45**, 629 (1950).

(12) I. L. Friedman, *Am. Mineral.*, **34** 583 (1949).

(13) G. W. Morey and J. M. Hesselgesser, *Amer. J. Sci., Bowen Volume*, 343 (1952).

(14) V. P. Butuzov and L. V. Briatov, "Soviet Physics-Crystallography," **2** [5], 670 (1957). (Translated by American Institute of Physics, p. 662.)

(15) Phase Diagrams for Ceramists, Ed. by E. M. Levin, H. F. McMurdie and F. P. Hall, Publ. by American Ceramic Society, Columbus, Ohio, 1956, p. 259. The phase diagrams of reference 12 and other diagrams of interest to this work are also given in this compendium.

(16) W. S. Fyfe, *Am. Mineral.*, **40**, 520 (1955).

(17) A. F. Frederickson and J. E. Cox, *ibid.*, **39**, 886 (1954).

Morey's data[13] show α-quartz to be stable over the region of our experiments and all of those in the literature which we have discussed. Since no glasses were observed in the quenched vessels we assume that the heavy liquid phase region was not entered. The vessels were either welded closure vessels of the sort described by Walker and Buehler[18] or modified Bridgman[19] vessels. Their internal length was 12″ and their internal diameter was 1″. The furnace was a nichrome wound ceramic tube long enough to avoid end effects when the vessel was placed in its center. This ceramic tube was surrounded by Vermiculite insulation and arranged in such a way that it could be rocked through about 30° to further aid in obtaining temperature equilibration within the autoclave. Temperature was controlled by a Leeds and Northrup Micromax Controller and reported temperatures are felt to be accurate within ±3°. Degree of fill as reported is felt to be accurate within ±1%. Although the bomb volumes and solution volumes were known with a greater precision at room temperature the bomb volume at operating temperature was known with less certainty. This is especially true of the laminated type design of the welded closure vessel. Concentration of the sodium hydroxide solutions used was determined by titration against potassium acid phthalate and was adjusted to 0.500 ±0.0015 N.

Equilibrium time was estimated by determining apparent solubility as a function of time while all other variables were held constant. It would be expected that equilibrium time would be greatest at the lower temperatures and pressures. Under these conditions it was found that there was essentially no change in apparent solubility between two and six days. The minimum time employed for the runs of this work was three days.

Quenching was effected by plunging the vessels into a bucket of water arranged behind a barricade. The vessels were consequently brought from operating temperature to ambient in less than 5 minutes. Several runs were allowed to cool in the furnace over a period of several hours and no difference in weight loss of the quartz plates was observed. The plates were also examined under 50 × magnification for evidence of growth hillocks, growth steps, precipitated foreign phases, etc. No evidence of growth was ever observed but on the contrary etch pits and other evidences of dissolving always were found.

Results

Figure 1 shows the dependence of solubility, S expressed as g./100 cc. of free volume of the autoclave on temperature.

Figure 1 shows that over the temperature–fill range investigated van't Hoff's relation is obeyed and that while the heat of solution is nearly independent of temperature, it is strongly dependent on degree of fill. The heats and entropies of solution found from Fig. 1 were

ΔE, kcal./mole (in 0.51 m NaOH)	ΔS cal./°mole (in 0.51 m NaOH)
87% f 2.68 ± 0.50	2.68 ± 0.50/T × 10^3
85% f 1.82 ± 0.50	1.82 ± 0.50/T × 10^3
80% f 1.03 ± 0.50	1.03 ± 0.50/T × 10^3

The entropies were calculated on the assumption that $\Delta E/T = \Delta S$ since ΔA at equilibrium is zero.

It has been shown that for small temperature differences the supersaturation can be considered a linear function of the temperature difference for crystal growth purposes.[7]

In Fig. 2 made with the data of Fig. 1, we have expressed the solubility S' as g./100 cc. of solution at room temperature which is nearly proportional to the weight fraction silica in solution. S is related to S' by the equation

$$S' = S/d \qquad (1)$$

where d is the degree of fill or, to a reasonable approximation in the one-fluid phase region, the solvent density or the reciprocal of the specific volume. In accordance with the convention used in hydrothermal crystal growth studies, these solubilities were measured at constant molality (0.51 m) or nearly constant weight fraction of NaOH. As can be seen from Fig. 2, while there may be some tendency for a departure from linearity at the higher fills within experimental error log S' is a linear function of degree of fill.

It might be noted that the van't Hoff relation would, of course, be obeyed equally well in terms

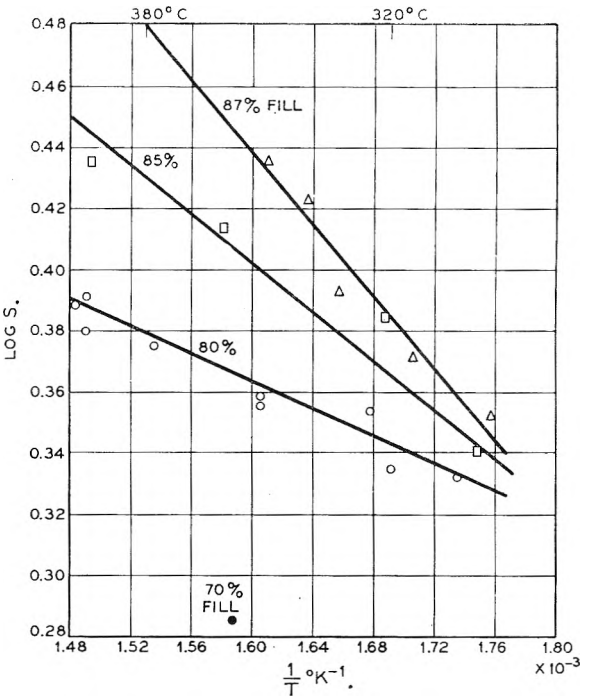

Fig. 1.—Log S *vs.* $1/T$ at several degrees of fill where the solvent was 0.50 N in NaOH at room temperature.

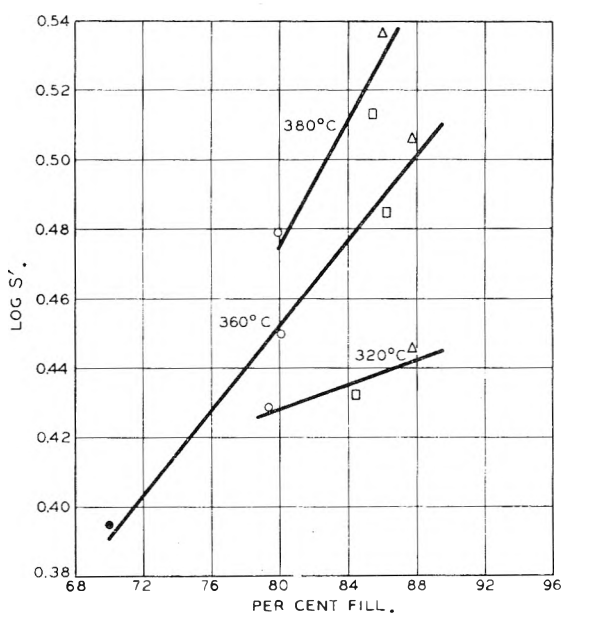

Fig. 2.—Log S' *vs.* per cent. fill at several temperatures where the solvent was 0.50 N in NaOH at room temperature.

(18) A. C. Walker and E. Buehler, *Sci. Monthly*, **69**, 148 (1949).
(19) F. Gasche, *Ind. Eng. Chem.*, **48**, 883 (1956).

of S or S' with only the y-intercept of the log S *vs.* $1/T$ curves being affected by a change to S' and that in all of the figures of this paper equally good fits of the experimental data were found when either S or S' was plotted.

Discussion

Dependence of Fill.—According to Franck[8] the solution of quartz in pure water may be represented by the reaction

$$Q + n\cdot H_2O \rightleftharpoons SiO_2\cdot nH_2O \qquad (2)$$

where Q is solid crystalline α quartz. Equation 2 assumes the silicic acids formed are essentially un-ionized. If n is non-integral equation 2 describes the formation of polysilicic acids.

Since at equilibrium $\Delta A = 0$ we may write

$$\mu_{SiO_2\cdot nH_2O} = \mu_Q + n\mu_{H_2O} \qquad (3)$$

where $\mu_{SiO_2\cdot nH_2O}$, μ_Q, etc., are the chemical potentials of $SiO_2\cdot nH_2O$, quartz, etc.

Franck has shown that equation 3 is consistent with either of the two well-known equations for solubility interactions involving virial expansions

$$\log X_2 = a \log \frac{1}{v} + b \qquad (4)$$

or

$$\log X_2 = c\frac{1}{v} + f\frac{1}{v^2} + g \qquad (5)$$

which as a first approximation may be written

$$\log S' = Ca + g \qquad (6)$$

where a, b, c, f and g are constants, X_2 is the analytically determined mole fraction of the dissolved substance and v is the specific volume of the solvent.

Equation 4 is derived for the case of large solvent–solute interactions and equation 5 for small interactions and both equations are strictly applicable only in dilute solutions. However, as Franck[8] has shown and this work indicates they are apparently valid for the concentration ranges obtaining in SiO_2 solutions in water and dilute bases.

Franck also pointed out that a more exact form of Equation (4) for quartz might be

$$\ln X_2 = n \ln \frac{K}{V} + \frac{V_Q P}{RT} \qquad (7)$$

where K is the association constant for equation 2 V_Q is the molar volume of solid quartz, V is the molar volume of the fluid phase, and P is the total pressure. Franck tested this form with the data of Kennedy[11] in the system SiO_2–H_2O. For this purpose the association value, n, of equation 2 and the association constant, K, were adapted to the measured values. Franck deduced the value of n to be 2 which suggests $Si(OH)_4$ as the principal species present in pure water. However, the fit of Kennedy's solubility data to equation 7 as found by Franck at densities greater than 0.30 was not entirely satisfactory. Mosebach[9] neglected the term V_QP/RT and is reported to have obtained a somewhat better fit and to have again deduced n to be 2.

Jasmund[20] reports that the solubility of quartz in water vapor obeys equation 4.

The authors treated the solubility data of Kennedy in a variety of ways and found that the best fit was to equation 6 as can be seen in Fig. 3. While a reasonable fit to more sophisticated equations could be obtained, in no case was a *better* fit discovered. This would then indicate that the H_2O–SiO_2 interactions in this system are *weak*. Unfortunately the association factor, n, cannot be calculated from a plot of the form of Fig. 3.

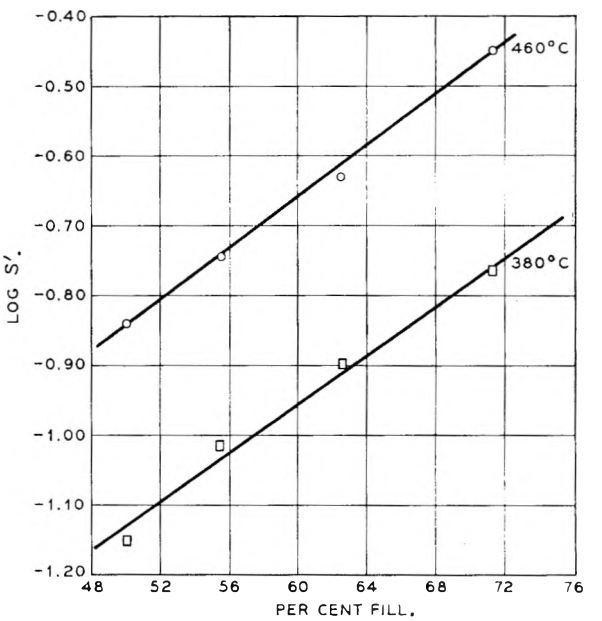

Fig. 3.—Log S' *vs.* per cent. fill at 460 and 380° in pure water (made with the solubility data of Kennedy[12]).

In a similar manner as can be seen in Fig. 2 the solubility data indicate weak interaction in the H_2O–SiO_2–Na_2O system. The data of Butuzov and Briatov[14] which we have plotted in Fig. 4 indicate weak interactions in the system H_2O–SiO_2–Na_2CO_3.

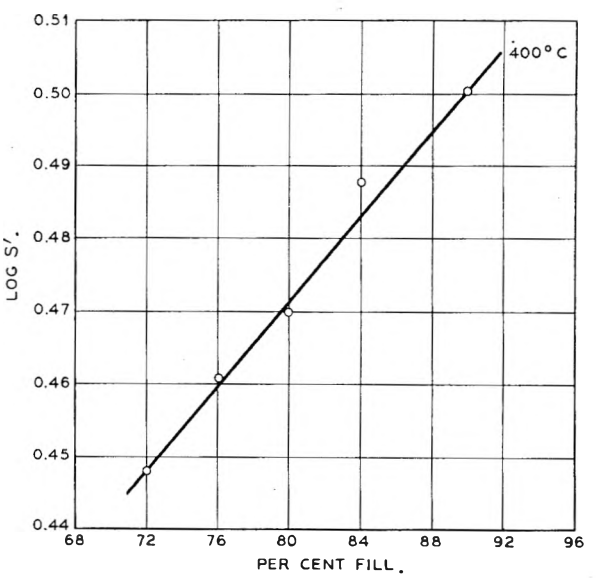

Fig. 4.—Log S' *vs.* per cent. fill at 400° where the solvent was 5% Na_2CO_3 at room temperature (made with the solubility data of Butuzov and Briatov[14]).

(20) K. Jasmund, *Heidelberger Beitr. Mineralog. Petrogr.*, **3**, 380 (1952).

The fact that a similar dependence of solubility on density is found both in pure water and in the basic systems is at first sight surprising. One might assume, for instance, that the generalized reaction describing the interaction of quartz with $(OH)^-$ in aqueous solution would be

$$Q + (2a - 4)(OH)^- \rightleftarrows SiO_a^{(2a-4)-} + (a - 2)H_2O \quad (8)$$

where a is greater than two. The value, a, like that of n in equation 2 may be non-integral but must be a small rational fraction for the case of the formation of disilicates and anionic species of higher catenation. Equation 8 assumes a complete ionization of the sodium silicates formed. While the ionization is surely not complete, it is probably reasonable to assume near completeness in solutions of the alkalinity studied in this work.

The solution of quartz in aqueous NaOH obviously involves equation 2 and equation 8. However, since the loss of weight of quartz plates will not allow the separate determination of the concentrations of $SiO_2 \cdot nH_2O$ and $SiO_a^{(2a-4)-}$ we may not directly apply a treatment of the data analogous to Franck's. However, if we examine (see Figs. 2, 3 and 4) the density dependence of solubility in NaOH, Na_2CO_3 and pure water we may deduce several generalizations. First we see that at nearly comparable conditions the solubility in the basic media is about an order of magnitude greater than in pure water. Consequently, $SiO_a^{(2a-4)-}$ must be the principal species present in Na_2CO_3 or NaOH. Next we see that at nearly comparable conditions the solubility in $(CO_3)^=$ is somewhat less than in $(OH)^-$. If we consider the equilibrium

$$(CO_3)^= + H_2O \rightleftarrows (HCO_3)^- + (OH)^- \quad (9)$$

and remember that at 25° the concentration of $(OH)^-$ in a 0.5 m Na_2CO_3 solution as calculated from the hydrolysis constant for equation 9 is about 0.01 m then it is not surprising that the solubility in $(CO_3)^=$ solutions is less than in $(OH)^-$ solutions since most of the solubility occurs because of equation 8.

Finally we should examine the slope of the solubility density curves of Figs. 2, 3 and 4, that is, the values of $(\partial \log S')/(\partial \%\ \text{fill})_T = \alpha$.

For nearly comparable conditions $\alpha_{H_2O} > \alpha_{NaOH} > \alpha_{Na_2CO_3}$. The relatively large positive value for α_{H_2O} is commensurate with equation 2 and the treatment which leads to equation 6.

The values of α_{NaOH} and $\alpha_{Na_2CO_3}$ are of course determined both by equations 2 and 3. The over-all equation in a basic solution can, therefore, be represented as

$$2Q + nH_2O + (2a - 4)(OH)^- \rightleftarrows SiO_2 \cdot nH_2O + SiO_a^{(2a-4)-} + (a - 2)H_2O \quad (10)$$

Therefore, provided $n > (a - 2)$, α_{NaOH} and $\alpha_{Na_2CO_3}$ would be expected to be positive. Franck,[8] Mosebach[9] and Brady[21] have all determined n to be equal to two. Consequently for $\alpha_{NaOH} > \alpha_{Na_2CO_3}$, $\alpha_{NaOH} < \alpha_{Na_2CO_3} < 4$. It will be shown below that $\alpha_{NaOH} = 7/3$ and $\alpha_{Na_2CO_3} = 3$.

Dependence on Base Concentration.—Data on the dependence of solubility on base concentration are somewhat limited in the literature.

The ratio SiO_2/Na_2O was plotted as a function of Na_2O concentration for hydroxide[12] at 55% fill and carbonate[14] at 80% fill. In $(OH)^-$ at 450° and in $(CO_3)^=$ at 350° the ratio is essentially constant suggesting that the concentration of $SiO_2^{(2a-4)-}$ is essentially limited only by the available $(OH)^-$. The ratio SiO_2/Na_2O is about $^1/_3$ in hydroxide and one in carbonate. These values for the ratios suggest $(SiO_3)^=$ in carbonate solutions and $(Si_3O_7)^{-2}$ in the hydroxide solutions as the predominant species and leads from Equation (10) to values of $a_{Na_2CO_3} = 3$ and $a_{NaOH} = 7/3$.

Dependence on Temperature.—As we have seen in the Na_2O–SiO_2–H_2O system (Fig. 1) the van't Hoff equation describes the temperature dependence. Likewise under generally similar conditions in the SiO_2–H_2O[12] and SiO_2–H_2O–Na_2CO_3[14] systems the van't Hoff equation is obeyed. The heats of solutions and entropies found were

$$\Delta E_{Na_2CO_3} = 3.42 \pm 1.0 \text{ kcal./mole}$$
$$\Delta S_{Na_2CO_3} = 3.42 \pm 1.0/T \times 10^3 \text{ cal./° mole}$$

(80% fill, in 5 wt. % Na_2CO_3, dependent on fill)

$$\Delta E_{H_2O} = 8.8 \pm 1.0 \text{ kcal./mole}$$
$$\Delta S_{H_2O} = 8.8 \pm 1.0/T \times 10^3 \text{ cal./° mole}$$

(71.5% fill but independent of fill within experimental error).

The lack of dependence of ΔE on T in all these systems implies that over the temperature intervals studied ΔC_V of each of the systems was small or the change was balanced by other effects. The dependence of $\Delta \bar{E}$ on fill in the basic solutions but not in the pure water and the relative values of ΔE in the three systems can be explained by a consideration of the solution process in a stepwise manner.

The heat of solution in a constant volume process is a measure of the change in the internal energy of the system and may be considered to be composed of two parts: the first, an endothermic reaction as the solid silica goes to a gaseous state, and the second, an exothermic reaction as the gaseous silica reacts with the solution. The first part of the process will require the same energy input regardless of the solvent used; the second part, however, will release energy dependent on the reaction of the gaseous silica in combining with a particular solvent. In the case of silica reacting with pure water, part two can produce a hydrated or hydrolyzed silica molecule of one sort or another. For silica reacting with sodium hydroxide or sodium carbonate, however, part two can produce a hydrated silica molecule or, as we have seen, any one of a variety of silicate complexes. Since the second part is an exothermic reaction and thus has negative value relative to the system, the greater the reaction in part two, the smaller the over-all value for ΔE. This is demonstrated in a comparison of the SiO_2–H_2O and the SiO_2–H_2O–Na_2O systems where ΔE for the sodium hydroxide is about $^1/_{10}$ that in the pure water system indicating a greater release of energy in part two and thus a lower value for ΔE. In sodium carbonate the over-all heat of solution is only obtained when the

(21) E. L. Brady, *J. Phys. Chem.*, **57**, 706 (1953).

endothermic heat of hydrolysis of equation 9 is added to parts one and two. Consequently, ΔE for the solution process in carbonate solution will be greater than in hydroxide.

The first part of the process is density independent while the second part is apparently more strongly density dependent when $SiO_a^{(2a-4)-}$ can form.

Acknowledgments.—The authors wish to thank G. T. Kohman and M. Tannenbaum for advice and encouragement in this work. R. A. L. also wishes to acknowledge discussions with E. U. Franck and R. Mosebach.

RARE EARTHS. I. VAPORIZATION OF La_2O_3 AND Nd_2O_3: DISSOCIATION ENERGIES OF GASEOUS LaO AND NdO[1]

BY HAROLD W. GOLDSTEIN, PATRICK N. WALSH AND DAVID WHITE

Cryogenic Laboratory, Department of Chemistry, The Ohio State University, Columbus, Ohio

Received March 13, 1961

The vaporization of the rare earth oxides, La_2O_3 and Nd_2O_3, at elevated temperatures has been studied by a combination of Knudsen effusion and mass spectrometric techniques. Both vaporize almost stoichiometrically to the monoxide and oxygen. The heats of formation, ΔH_0^0, in kcal. mole^{-1}, and dissociation energies, D_0^0, in e.v. are: LaO, -29.8 ± 4, 8.08 ± 0.2; NdO, -30.0 ± 6, 7.18 ± 0.3, respectively.

Introduction

The question of the identity and stability of the vapor species formed in lanthanon–oxygen systems has been of considerable interest for many years and has become increasingly important as rare earth compounds have become more readily available. The existence of gaseous monoxides of several of the rare earth elements has been inferred from stellar and arc spectra[2a] and LaO has been observed in the mass spectrometer.[2b] Only in the latter investigation has a dissociation energy been determined with an uncertainty of less than one e.v. Dissociation energies estimated for other rare earth monoxides by Birge-Sponer[3] or modified Birge-Sponer[4] extrapolations of the observed vibrational levels have such large uncertainties connected with them ($\pm$1–3 e.v.) that the thermodynamic properties of chemical systems at elevated temperatures containing the elements of these compounds cannot be determined with sufficient accuracy for most purposes.

The positive identification of the monoxides or other simple gaseous oxides of the rare earth metals and the determination of their thermodynamic properties are also of considerable interest from the chemical standpoint. The heats of formation of the solid sesquioxides of these metals are unusually large[5]; in terms of enthalpy of formation per oxygen atom, they are equaled only by Li_2O and some of the Group II oxides.[6] It is possible that the origin of this strong bonding energy can be inferred from the properties of the gaseous species formed on vaporization of the sesquioxides. The gaseous oxides of the rare earths (in particular the monoxides) constitute a unique set of compounds in the sense that the electronic structure of the elements suggests that the chemical bonding should be nearly the same for all. It is, however, well known that there exist large variations in the binding energies[4] of these compounds. Before any generalization can be made concerning these variations, it is necessary to establish quantitatively their magnitude.

In the present paper the dissociation energies of gaseous LaO and NdO are determined through Knudsen effusion and mass spectrometric measurements of the dissociation pressures of the corresponding solid sesquioxides. This is the first paper of a series concerned with the determination of the thermodynamic properties of gaseous rare earth oxides.

Experimental

Materials.—The lanthanum and neodymium oxides were the same materials previously used for heat capacity measurements.[7] They were dried before use by firing at 1000° in air.

Apparatus and Procedure.—The effusion experiments were carried out in vacuum induction furnaces of the type described by Hoch and Johnston.[8]

Tantalum and tungsten crucibles, machined by Fansteel Metallurgical Company, were used as Knudsen cells. These were right circular cylinders $1/2''$ o.d. by $3/4''$ high; the tantalum crucibles were $3/8''$ i.d., the tungsten $1/4''$. Each was covered with a $1/16''$ thick lid of the same material machined to fit inside the crucible (with a tolerance of $0.002''$) to a depth of $1/32''$. A $1/16''$ diameter hole, drilled axially through the lid, served as the effusion orifice. In the calculations, dimensions measured to $\pm$ $0.001''$ and corrected for thermal expansion[9] were used.

Temperatures were measured by sighting directly into the effusion orifice, through an optical flat at the top of the furnace, with an NBS calibrated optical pyrometer or with one that had been compared with it under the conditions of these experiments. With an appropriate window correction, the temperature so measured equals the "black

(1) This work was supported by the Air Force Office of Scientific Research.

(2a) B. Rosen, "Données Spectroscopiques Concernant les Molecules Diatomiques," Herman et Cie, Paris, 1951. (b) W. A. Chupka, M. G. Inghram and R. F. Porter, *J. Chem. Phys.*, **24**, 792 (1956).

(3) G. Herzberg, "Molecular Spectra and Molecular Structure. I. Spectra of Diatomic Molecules," D. Van Nostrand Co., Inc., Princeton, N. J., 1957.

(4) A. G. Gaydon, "Dissociation Energies and Spectra of Diatomic Molecules," Chapman and Hall, Ltd., London, 1953.

(5) E. J. Huber, Jr., E. L. Head and C. E. Holley, Jr., *J. Phys. Chem.*, **64**, 1768 (1960) and earlier papers.

(6) J. P. Coughlin, U. S. Bur. Mines Bull., 542 (1954).

(7) H. W. Goldstein, E. F. Neilson, P. N. Walsh and D. White, *J. Phys. Chem.*, **63**, 1445 (1959).

(8) M. Hoch and H. L. Johnston, *J. Am. Chem. Soc.*, **76**, 4833 (1954).

(9) H. A. Jones and I. Langmuir, *Gen. Elec. Rev.*, **30**, 354 (1927); W. J. W. Edwards, R. Speiser and H. L. Johnston, *J. Appl. Phys.*, **22**, 424 (1951). Ta.

body" temperature of the inside of the crucible within the error of measurement (±3°). Since observation through a side port in one of the furnaces showed that, up to at least 2200°, the lid was hotter than the main body of the crucible, it can be considered that the measured temperature represents the actual sample temperature.

The procedure for a typical Knudsen effusion experiment was as follows. A cell was first degassed at 2400° for one hour with the pressure in the furnace below 10^{-5} mm. After cooling, the crucible was removed in an argon atmosphere, weighed, and loaded with several hundred milligrams of freshly dried rare earth oxide. Owing to the shrinkage incident on sintering, it was found useful to heat the sample several times at increasing temperature between 1500 and 2000° and to powder it between heatings. Once the bulk had been reduced to the point where no further shrinkage was observed, the sample was handled only in an argon atmosphere or *in vacuo*. The effusion experiments were conducted in a manner previously described. Constancy of temperature was achieved by manual or automatic control of the output of the radiofrequency generator.

For both La_2O_3 and Nd_2O_3 a series of runs at different temperatures was made on each sample. The temperature was varied irregularly from run to run until reproducible rates of evaporation were observed at several temperatures (see *e.g.*, Tables I and II). An X-ray powder diagram of the residue was taken at the completion of the experiment.

A series of runs at constant temperature was also made on each material. In addition, several determinations of the extent of reaction with the crucible were made by heating samples to the point where no further loss of weight (other than the "background" due to the vapor pressure of the crucible material, which was determined separately) was observed.

In an effort to establish approximately the magnitude of the "vaporization coefficient" for the reactions involved in these vaporizations, runs were made in which the lid was not placed on the crucible, so that the orifice area to surface area ratio was approximately unity. Since blackbody conditions for temperature measurement were not achieved in this arrangement, the temperatures for such measurements were established by comparing the temperature read in a well ($^1/_{32}$" diameter, $^3/_{32}$" deep) in a $^1/_4$" thick graphite insert placed in the bottom of the crucible with the apparent temperature as read on the rim of the crucible, which was subsequently used as a fiduciary. Temperatures measured in this way are believed to be good to ± 10°.

Results and Discussion

Lanthanum and neodymium oxides both react with tantalum Knudsen cells. The extent of the reaction in the La_2O_3 case and the reasons why thermodynamic data cannot be derived from these experiments have been discussed previously.[10] Similar behavior is exhibited by Nd_2O_3 in tantalum crucibles, and this system is further complicated by extensive formation of a neodymium–tantalum–oxygen compound of uncertain stoichiometry.[11]

The data derived from experiments employing tungsten as the Knudsen cell material can, however, be interpreted in a relatively straightforward manner. The isotherms for both La_2O_3 and Nd_2O_3 showed an initial high rate of vaporization, a region of constant rate of vaporization, and then a decrease in the rate when approximately 85% of the material had reacted. The high initial rates of evaporation can be correlated with an observed preferential loss of oxygen leading to the formation of a slightly reduced phase which reoxidation studies showed to be $La_2O_{2.96}$. This composition, the A-form sesquioxide structure with lattice parameters identical to that of the stoichiometric compound, was attained at the point where the rate of evaporation becomes constant. Nd_2O_3 similarly reduced to $Nd_2O_{2.96}$. X-Ray examination of the solid phases at various times during and at the end of a series of runs showed that no further reduction took place and that no new solid phases were formed during vaporization. Hence the vaporization of these oxides occurs stoichiometrically at the compositions $La_2O_{2.96}$ and $Nd_2O_{2.96}$. The drop in the rate of vaporization after approximately 85% of the sample had vaporized undoubtedly was due to diminution of the surface area of the sample.

The species vaporing from the Knudsen cells were initially inferred from the observed vaporization rates and subsequently confirmed by mass spectrometric examination of the vapors, utilizing the equipment and procedures described in Rare Earth Oxides II.[12] For both lanthanum and neodymium oxide, three species, identified by mass and isotropic abundance as MO^+, M^+ and O^+ (M = La or Nd) were observed to be dependent on the temperature of the crucible. The monoxide ions were always present with greatest intensity. As these had appearance potentials of 5–6 e.v. and since no heavier species were observed, they readily may be ascribed to LaO and NdO as progenitors. The metal ions, on the other hand, disappeared when the ionizing electron energy was decreased below 15 e.v.; it was concluded therefore that these species were present primarily as a result of fragmentation of the monoxides. Although an appreciable O^+ background was always present in the spectrometer, the following observations verified that oxygen atoms were originating from the effusion cell. (1) The intensity of the O^+ peak was markedly decreased when the effusion orifice was moved out of alignment with the collimating slits; with the cell in this position, the rare earth peaks were no longer visible. (2) The shape of the O^+ peak suggested that it consisted of two components, one in focus and one out of focus with respect to the component of velocity in the direction of the effusing beam. The component having the same focusing behavior as the rare earth ions disappeared when the crucible alignment was altered as described.[13]

The "vaporization coefficient," α, for the over-all vaporization process of each sesquioxide was established by extrapolation to zero orifice area of the rates of weight loss per unit area (at a given temperature) measured with and without the lid in place on the crucible (orifice area/surface area ratios of 0.058 and 1.00, respectively), according to the procedure described by Speiser and Spretnak[14] based on the work of Motzfeldt.[15] Since the two sets of measurements were necessarily carried out in different temperature ranges, they were converted to a common temperature by extrapolation of the more precise covered cell measurements to the lower temperatures of the open cell measurements. The "vaporization coefficients" so determined were not less than 0.5 for either material

(10) H. W. Goldstein, P. N. Walsh and D. White, *J. Phys. Chem.*, **64**, 1087 (1960).

(11) P. N. Walsh, H. W. Goldstein and D. White, *J. Am. Ceram. Soc.*, **43**, 229 (1960).

(12) D. White, P. N. Walsh, H. W. Goldstein and D. F. Dever, *J. Phys. Chem.*, **65**, 1404 (1961).

(13) This focusing characteristic of the Bendix mass spectrometer has been discussed by W. C. Wiley, *Science*, **124**, 817 (1956).

(14) R. Speiser and J. W. Spretnak, in "Vacuum Metallurgy," Am. Electrochem. Soc., 1955.

(15) K. Motzfeldt, *J. Phys. Chem.*, **59**, 139 (1955).

(for La_2O_3, a value of unity was obtained). The value unity has been used in all the calculations below.

The total weight loss measurements indicated that, for each sesquioxide, 0.1 mole of tungsten per mole of rare earth sesquioxide was vaporized. As no tungsten containing species was observed in the mass spectrometer, it is concluded that this loss occurs by diffusion of oxygen through the tungsten and subsequent vaporization of a tungsten oxide from the exterior surface. A more pronounced example of this behavior, in the case of tantalum crucibles, recently has been described by us.[10] In the present case, however, this effect is small enough to be neglected. Its effect on the calculated heats of formation is less than the uncertainty in the experimental rates of effusion. Furthermore, it is not clear whether the tungsten loss occurs uniformly with time. Some observations made in connection with the vaporization of praseodymium oxide[16] indicate that a large percentage of the tungsten may be lost near the beginning of the reaction, before the flat in the isotherm is reached. Since for thermodynamic calculations the only suitable results are those derived under conditions where the vaporization is invariant at constant temperature, the tungsten loss may not be an important factor at all in the reaction.

The observed rates of evaporation at various temperatures (in the range where the vaporization is invariant at constant temperature) obtained using Knudsen cells having an orifice area/surface area ratio of 0.058 are shown in Table I for lanthanum oxide and in Table II for neodymium oxide. From the experiments discussed above, it is clear that the vaporization for both La_2O_3 and Nd_2O_3 proceeds for all practical purposes as

$$M_2O_3(c) \longrightarrow 2MO(g) + O(g) \qquad M = La, Nd \quad (1)$$

(The difference between the constant-boiling and stoichiometric compositions of the sesquioxides has been neglected.) In Tables I and II, the calculated partial pressures, equilibrium constants, and heats of reaction for the vaporization of La_2O_3 and Nd_2O_3, respectively, based on reaction 1 are also given.

The partial pressures were calculated from the observed rates of weight loss by the equation[14]

$$P_i = W_i m^* (2\pi RT/M_i)^{1/2} \qquad (2)$$

where P_i, W_i and M_i are the partial pressure, weight fraction in the vapor and molecular weight, respectively, of the ith vapor species, m^* is the observed rate of weight loss corrected by the method of Motzfeldt,[15] T is the absolute temperature, and R is the gas content. The weight fractions were chosen so as to maintain an oxygen/metal ratio of $^3/_2$ in the vapor, as required by equation 1. The free energy functions for La_2O_3 were derived from heat capacity[7,17] measurements. Free energy functions for O were taken from Stull and Sinke[18]; for LaO, they were computed from the spectroscopic data given by Herzberg[3] with the rotational constant assumed equal to that of BaO.[3] The same rotational and vibrational contributions to the free energy functions were used for NdO as for LaO. We have shown in the third paper of the series[19] that the entropy of NdO(g) at 1900°K. is greater by 3 cal. mole^{-1} deg.$^{-1}$ than that of LaO(g). On the assumption that this difference arises entirely from differences in ground state multiplicities, the same quantity has been added to the electronic free energy function of LaO to yield those of NdO. (If the entropy difference arises from low-lying levels of NdO, which is as probable, then the contribution to the free energy function has been overestimated by an unknown amount. In the absence of spectroscopic data on NdO, the question cannot be settled at present.) The free energy functions for Nd_2O_3 reported by us previously[7] have been recalculated to take into account some recent measurements by Westrum[20] in the range 4–16°K., which show $S_{16} = 1.651$ cal. mole^{-1} deg.$^{-1}$ and $H_{16}^0 - H_0^0 = 15.74$ cal. mole^{-1}. As a result, the free energy functions of Nd_2O_3 were taken as 56.86, 65.79 and 73.19 cal. mole^{-1} deg.$^{-1}$ at 1500, 2000 and 2500°K., respectively.

The heats of formation of LaO(g) and NdO(g) at 0°K. were calculated from the heats of reaction shown in Tables I and II, using the known dissociation energy of O_2[21] and the heats of formation of lanthanum and neodymium oxides reported by Huber and Holley[22] corrected to 0°K. with the aid of heat content function for the oxides[7] and elements.[18] The recent, quite different, heat of formation reported by von Wartenberg[23] for La_2O_3 actually agrees well with the value chosen if the most recent heat of solution of La[24] is used to recalculate the results. The heats of formation (ΔH_0^0) so derived are: LaO, −30.7 kcal. mole^{-1}; NdO, −30.3 kcal. mole^{-1}. The uncertainty in these values arising from experimental factors is indicated by the scatter of the data in Tables I and II; that arising from the use of approximate free energy functions is estimated to be ±3 kcal. mole^{-1} for LaO and ± 5 kcal. mole^{-1} for NdO.

An independent check of these values for the heats of formation was obtained from mass spectrometric investigation of the temperature dependence of the MO^+ peaks in vaporization of the solid sesquioxides. Details of the procedure are given in a following article.[12] The results are shown in Fig. 1, for lanthanum and neodymium oxides, respectively. In this figure log $I_{MO^+}T$ is plotted against the reciprocal of the absolute temperature. For these measurements an ionizing energy of 25 e.v. was employed. To calculate the heat of reaction, it is assumed that the partial pressure of oxygen is directly proportional to that of the monoxide over the entire temperature range. This is essentially the same approximation used in analyzing the effusion data. Thus, at the mean tempera-

(16) Unpublished results of this Laboratory.

(17) J. O. Blomeke and W. T. Ziegler, *J. Am. Chem. Soc.*, **73**, 5099 (1951).

(18) D. R. Stull and B. C. Sinke, "Thermodynamic Properties of the Elements," American Chemical Society, Washington, D. C., 1956.

(19) P. N. Walsh, D. F. Dever and D. White, *J. Phys. Chem.*, **65**, 1410 (1961).

(20) E. F. Westrum, private communication.

(21) P. Brix and B. Herzberg, *Can. J. Phys.*, **32**, 110 (1954).

(22) E. J. Huber, Jr., and C. E. Holley, Jr., *J. Am. Chem. Soc.*, **74**, 5530 (1952), Nd_2O_3; **75**, 3594 (1953), La_2O_3.

(23) H. Von Wartenberg, *Z. anorg. allgem. Chem.*, **299**, 227 (1959).

(24) F. H. Spedding and J. P. Flynn, *J. Am. Chem. Soc.*, **76**, 1474 (1954).

TABLE I

CALCULATION OF HEAT OF REACTION $La_2O_3(c) \longrightarrow 2LaO(g) + O(g)$

Temp., °K.	Rate of effusion, g./cm.²/sec. × 10⁴	P_{LaO}, atm. × 10⁶	P_O, atm. × 10⁶	$-R \ln K_{eq}$	$-\Delta(F^0-H_0^0)/T$, cal. mole⁻¹ deg.⁻¹	ΔH_0^0, kcal. mole⁻¹
2234	0.595	4.844	0.7768	76.607	113.01	423.61
2307	1.266	10.48	1.680	71.996	112.75	426.22
2353	2.814	23.51	3.770	67.388	112.58	423.00
2412	4.482	37.92	6.081	64.338	112.37	426.22
2441	6.517	55.46	8.895	62.070	112.27	425.56
2372	3.499	29.35	4.707	65.864	112.52	423.12
2372	3.414	28.64	4.593	66.011	112.52	423.47
2372	2.819	23.65	3.793	67.154	112.52	426.17
2372	3.482	29.21	4.685	65.895	112.52	423.21
2372	3.301	27.69	4.441	66.213	112.52	423.97
2321	1.691	14.04	2.251	70.263	112.70	424.67
2372	3.117	26.15	4.193	66.555	112.52	424.75
2372	3.029	25.41	4.075	66.725	112.52	425.18
2397	4.131	34.84	5.587	64.842	112.43	424.92
2321	1.691	14.04	2.251	70.263	112.70	424.67
2372[a]	3.117	26.15	4.193	66.555	112.52	424.75

[a] Average of seven runs agreeing within ±10%. Av. 424.65 ± 0.98

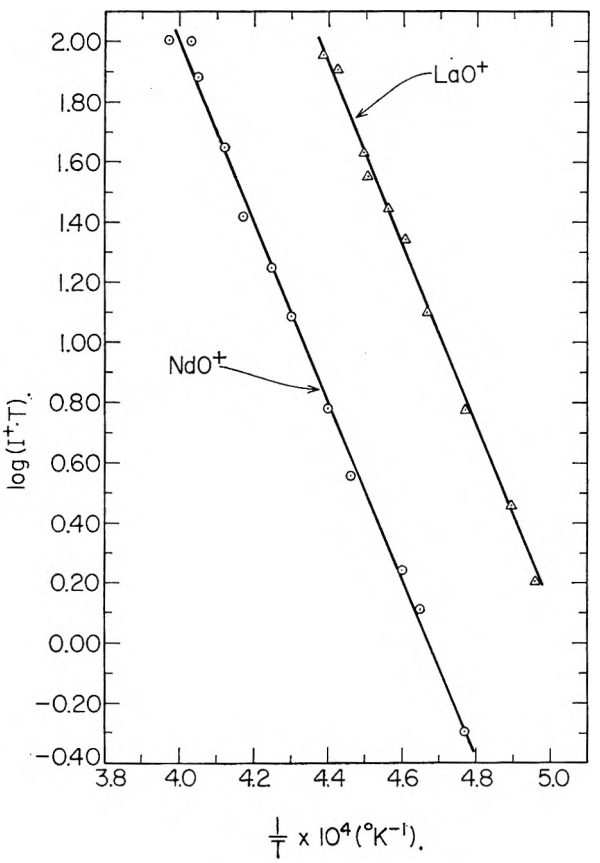

Fig. 1.—Variation of pressure of LaO ($I^+_{LaO}T$) over $La_2O_3(c)$ and NdO ($I^+_{NdO}T$) over $Nd_2O_3(c)$ as a function of reciprocal temperature.

ture, the slope times $2.303R$ times 3/2 is equal to the heat of the reaction. The heats of reaction 3

$$^1/_2M_2O_3(c) \longrightarrow MO(g) + {}^1/_2O(g) \quad (M = La, Nd) \quad (3)$$

at the average temperatures are: M = La, ΔH_{2140} = 209.2 ± 4.2 kcal. mole⁻¹; M = Nd, ΔH_{2307} = 204.5 ± 4.4 kcal. mole⁻¹. Correcting to the absolute zero, using heat content functions from the sources cited above, yields ΔH_0^0 = 217.6 ± 6.0 kcal. mole⁻¹, and ΔH_0^0 = 216.3 ± 6.2 kcal. mole⁻¹ for M = La, Nd, respectively. The corresponding heats of formation (ΔH_0^0) of LaO(g) and NdO(g) are −25.5 ± 7 and −28.9 ± 7 kcal. mole⁻¹, respectively.[25] The agreement with the values derived from effusion studies is seen to be satisfactory. The heats of formation obtained by averaging the effusion and mass spectrometric results, each weighted in proportion according to the experimental precision are: LaO(g), ΔH_0^0 (f) = 29.8 ± 4 kcal. mole⁻¹; NdO(g), ΔH_0^0(f) = −30.0 ± 6 kcal. mole⁻¹.

The heat of formation of LaO(g) determined here may be compared with that derived by Chupka, *et al.*,[2] from a mass spectrometric study of the reaction

$$^1/_3La(g) + {}^1/_2La_2O_3(c) \longrightarrow LaO(g) \quad (4)$$

For the purpose of this comparison, the free energies of reaction 4 reported by these investigations have been used in conjunction with the free energy functions of $La_2O_3(c)$ and LaO(g) described previously and those of La(g) listed by Stull and Sinke.[18] This yields ΔH_0^0 (reaction 4) = 83.6 ± 9 kcal. mole⁻¹. With the heat of sublimation of La given by Daane and Spedding[26] corrected to absolute zero[18] (yielding ΔH_0^0(subl) = 97.4 ± 1.0 kcal. mole⁻¹), this gives ΔH_0^0(f) = −26.2 ± 9 kcal. mole⁻¹ for LaO(g). This is in agreement with the value derived from the study reported here.

The dissociation energies (D_0^0) of the monoxides can be computed from the heats of formation, using the heats of sublimation (ΔH_0^0) of the rare earth elements and the dissociation energy of oxygen.[21] For lanthanum, the heat of sublimation previously

(25) The heats of reaction 3 calculated from the mass spectroscopic data are higher than those calculated from the effusion results. This may be another indication[10] of the fact that the equilibrium oxygen pressure in these reactions is lower than that calculated assuming stoichiometric decomposition of the solids. It was, however, impossible to determine the ratio, MO/O, in the vapor phase mass spectrometrically with any precision due to the oxygen background and the uncertainty of the relative cross sections of MO^+ and O^+.

(26) A. H. Daane and F. H. Spedding, Abstracts, A.C.S. Meeting, Chicago, September, 1958.

TABLE II

CALCULATION OF HEAT OF REACTION $Nd_2O_3(c) \longrightarrow 2NdO(g) + O(g)$

Temp., °K.	Rate of effusion, g./cm.²/sec. × 10⁴	P_{NdO}, atm. × 10⁵	P_O, atm. × 10⁵	$-R \ln K_{eq}$	$-\Delta(F^\circ - H_0^\circ)/T$, cal. mole⁻¹ deg.⁻¹	ΔH_0°, kcal. mole⁻¹
2255	0.615	4.951	0.7900	76.479	112.59	426.35
2281	0.822	6.655	1.062	74.716	112.46	426.95
2306	1.040	8.467	1.351	73.280	112.34	428.04
2408	2.760	22.96	3.665	67.330	111.83	431.42
2332	1.119	9.165	1.463	72.808	112.21	431.46
2357	1.521	12.53	1.999	70.945	112.08	431.39
2383	1.808	14.97	2.388	69.884	111.95	433.31
2332	1.346	11.02	1.759	71.708	112.21	428.89
2255	0.561	4.519	0.7211	77.023	112.59	427.58
2255	0.703	5.660	0.9031	76.447	112 59	426.28
2255	0.567	4.564	9.7282	76.964	112.59	427.44
2434	3.089	25.85	4.124	66.626	111.70	434.04
2383	2.017	16.70	2.665	69.220	111.95	431.73
2363	1.893	15.60	2.490	69.639	112.05	429.33
2383	2.060	17.05	2.721	69.105	111.95	431.46
2332	1.383	11.32	1.807	71.546	112.21	428.52
2281	0.751	6.081	0.9704	75.253	112.46	428.18
2434	3.156	26.41	4.214	66.498	111.70	433.73
2408[a]	2.680	22.30	3.559	67.512	111.83	431.86
						Av. 429.89 ± 2.30

[a] Average of twelve runs agreeing within ±10%.

given has been used. For neodymium, the value 76.6 ± 1.0 kcal. mole^{-1}, derived from the heat of vaporization determined in this Laboratory[12] and heat content functions for the gas[18] and condensed phases,[27] has been used. The resultant dissociation energies are: LaO, 8.08 ± 0.2 e.v., NdO, 7.18 ± 0.3 e.v.

It is noteworthy that the heats of formation of the gaseous monoxides are very nearly the same and that the dissociation energies differ by just the difference in heats of sublimation of the metal; *i.e.*, the energy released in adding an oxygen atom to a free lanthanum atom is greater by just the amount that the binding energy of lanthanum metal exceeds that of neodymium. This suggests a correlation between the binding mechanisms in the two cases and indicates a possibility that further study of the monoxides may be useful in explaining the behavior of the rare earth metals. Rather than attempt to develop this further here, we consider it prudent to wait until we have presented evidence relative to additional rare earth systems.

Acknowledgments.—The authors wish to acknowledge the assistance of Dr. M. Hoch in initially developing this program, and Mr. William E. Housden in carrying out the effusion measurements. H.W.G. wishes to thank the Monsanto Chemical Company for a fellowship during one year in which this work was carried on.

(27) F. H. Spedding, J. J. McKeown and A. H. Daane, *J. Phys. Chem.*, **64**, 289 (1960).

RARE EARTHS. II. A MASS SPECTROMETRIC DETERMINATION OF THE HEATS OF SUBLIMATION (OR VAPORIZATION) OF NEODYMIUM, PRASEODYMIUM, GADOLINIUM, TERBIUM, DYSPROSIUM, HOLMIUM, ERBIUM AND LUTETIUM[1]

BY DAVID WHITE, PATRICK N. WALSH, HAROLD W. GOLDSTEIN AND DAVID F. DEVER

Cryogenic Laboratory, Department of Chemistry, The Ohio State University, Columbus, Ohio

Received March 13, 1961

A Time of Flight mass spectrometer has been adapted for thermodynamic investigations at elevated temperatures. The apparatus is described in detail. The heats of sublimation (or vaporization) of several rare earth metals have been determined by the mass spectrometric method, from the variation with temperature of the intensity of an atomic beam effusing from a Knudsen cell, in the temperature range 1253 to 2044°K.

Introduction

In an earlier article,[2] the thermodynamics of vaporization of the sesquioxides $La_2O_3(c)$ and $Nd_2O_3(c)$ at elevated temperatures is discussed. In order to interpret the Knudsen effusion data and calculate the dissociation energies of the rare earth gaseous monoxides the heats of sublimation of the metals must be known. For nearly all the sesquioxides that have been studied to date, it has

(1) This work was supported by the Office of Naval Research.

(2) H. W. Goldstein, P. N. Walsh and David White, *J. Phys. Chem.*, **65**, 1400 (1961).

been found that the vapor phase in equilibrium with the solid consists primarily of the gaseous monoxide, the metal and atomic oxygen.[3] The composition of the vapor phase, in a number of cases, cannot be reconciled with the thermodynamics of the decomposition reactions of the solid sesquioxides and the reported heats of sublimation of the metals.[4] In other cases, an analysis of the results cannot be made due to the lack of any information on the heats of sublimation of the metals. This is particularly true of the rare earths of atomic weight greater than europium.

In order to resolve this problem, the heats of sublimation or vaporization of eight rare earth metals have been determined experimentally. The consistency of these results with the composition of the vapor phases resulting from the decomposition of the corresponding sesquioxides will be discussed in future presentations.

Apparatus

A Bendix Model 12-101 Time of Flight Mass Spectrometer with an analog output system, has been adapted for us in conjunction with a furnace for the study of the thermodynamics of phase changes and chemical reactions at elevated temperatures. The description of the Time of Flight Spectrometer already has been given.[5] This section will be devoted to a description of the furnace, temperature control and measurement, and the performance of the spectrometer under experimental conditions.

(a) **Furnace.**—The flight tube of the Bendix spectrometer is equipped at one end with an ion detector system and at the other end with a steel cross shown in Fig. 1 (heavy lines). The furnace shell connects to the bottom port of the cross. Inside this shell a water-cooled cylinder is placed so that its top just protrudes into the ion source region. The top of the cylinder is closed with a stainless steel plate upon which is placed an adjustable collimating slit, of rectangular cross-section and dimension 0.030" × 0.625". The slit replaces the "movable slit" supplied by Bendix. The furnace assembly, Fig. 2, is mounted in a plate which attaches to the bottom of the furnace shell; a vacuum seal is obtained by means of an "O" ring. The position of the crucible and radiation shields when the furnace is mounted can be seen in Fig. 1. The heated crucible sits directly in the bottom port of the cross, its top approximately $^{7}/_{8}$" from the first collimating slit. The second collimating slit is part of the ion source header which attaches to the left port shown in Fig. 1. This collimating slit, 0.030" × 0.625", is also the entrance to the ionizing region and is approximately $^{5}/_{8}$" from the first slit. The furnace shell is evacuated by a pumping system separate from the one on the flight tube of the spectrometer. With both pumping systems it is possible to achieve a vacuum in the furnace (after degassing of the crucible) of 5×10^{-6} to 5×10^{-7} mm. even when the temperature of the crucible is as high as 2500°K.

The top port of the cross shown in Fig. 1 is closed off with a stainless steel plate through which a 1-$^{1}/_{2}$" hole is drilled. An optical flat placed on top of this opening permits temperature measurement with an optical pyrometer. On the underside of the steel plate is a magnetically activated shutter which prevents coating of the glass window by the beam emanating from the hot crucible.

The furnace assembly is shown in Fig. 2. The sample contained in the Knudsen cell (B, Fig. 2) is heated by electron bombardment. The tungsten filaments (A) are heated by a current transformer whose leads are connected to the external filament support rod holders (M) and a d.c. voltage is applied to the external crucible support rod holder (L). The filament support rods (D) are constructed of 0.197 inch tantalum rod. The Knudsen cell supports (C) are constructed of 0.059 inch tungsten and mounted on

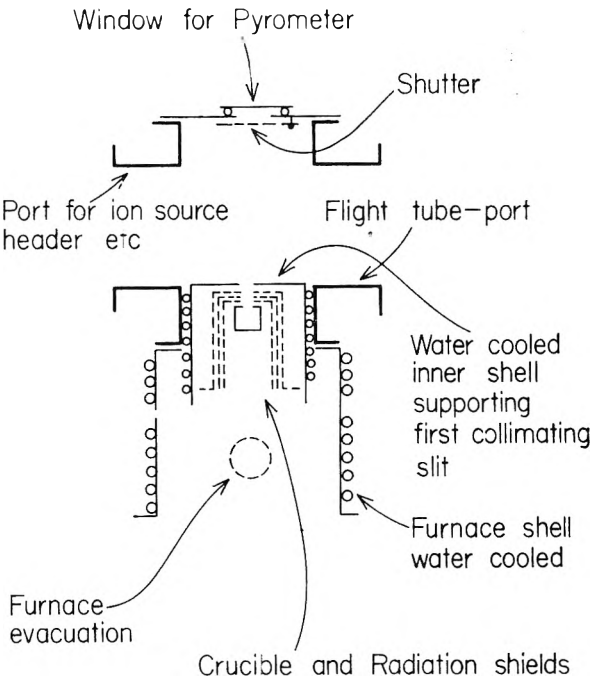

Fig. 1.—Position of high temperature furnace in time of flight spectrometer.

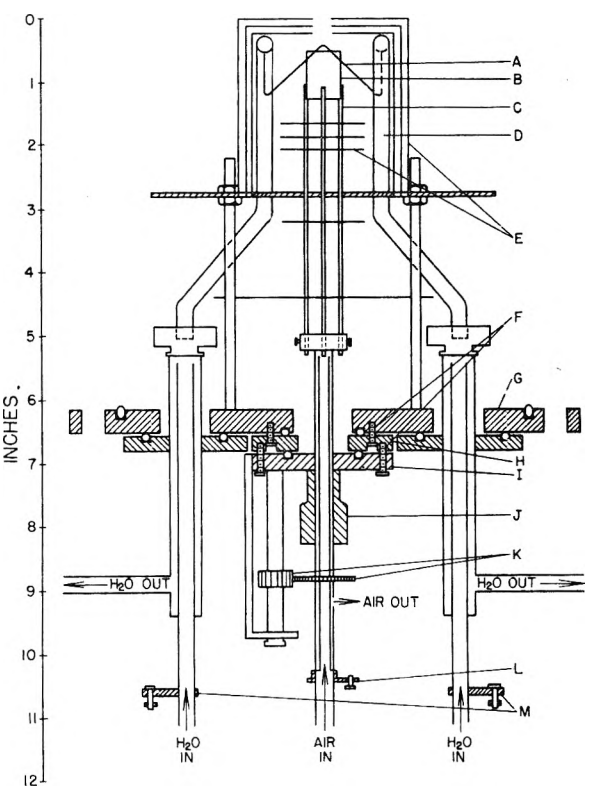

Fig. 2.—High temperature vacuum furnace and Knudsen cell.

a stainless steel ring which is connected to the outside of the furnace through a copper ring (I) and a Veeco Vacuum Fitting (J). By manipulation of the gears (K) the cell can be rotated through 360 degrees. The stainless steel ring is air cooled and the filament support rod holders are water cooled. Three concentric radiation shields (E), constructed from 0.005 inch tantalum sheet, are mounted on a molybdenum plate and surround the Knudsen cell and filaments. Five circular radiation shields (E) are mounted on the crucible support rods. Since these shields are in electrical

(3) Unpublished results of this Laboratory.

(4) D. R. Stull and G. C. Sinke, "Thermodynamic Properties of the Elements," American Chemical Society, Washington, D. C., 1956.

(5) (a) W. C. Wiley and I. H. McLaren, *Rev. Sci. Instr.*, **26**, 1150 (1955); (b) W. C. Wiley, *Science*, **124**, 217 (1956).

contact with the support rods, the uppermost shield is also heated by electron bombardment, thus tending to compensate in part for the heat conducted away from the crucible by the support rods. Small pieces of boron nitride insulate the molybdenum plate and the three concentric radiation shields from the bottom plate of the furnace (G). By adjustment of the Nylon screws (F) in the copper ring (I) the entire cell assembly and cell can be tilted in any direction. The rotation and tilting mechanisms are necessary for alignment of the orifice or slit of the hot Knudsen cell with the collimating slits of the spectrometer. This also permits differentiation of peaks originating from crucible and background. All vacuum seals in the furnace are "O" rings. The highest temperature achieved in the furnace to date is 2625°K. Above this temperature there is a tendency for the crucible alignment to change appreciably, probably due to buckling of the supports.

In the research reported below, cylindrical tantalum crucibles, which were essentially Knudsen cells, were used. These were $^1/_2$ in. o.d. by $^3/_4$ in. high, with a wall thickness of $^1/_{16}$ in. Each was covered with a tightfitting, $^1/_{16}$ in. thick tantalum lid through which a $^1/_{16}$ in. diameter effusion orifice was drilled axially.

In some experiments, other than those reported here, where greater sensitivity was desired, a 0.030 in. × 0.375 in. slit has been used in place of the orifice described. This arrangement permits detection of species whose pressure in the effusion cell is one-fifth to one-seventh that necessary to give a measurable ion signal when a circular orifice is used. With these effusion cells the pressures of vapors inside the cells are very nearly the equilibrium pressures (within 10%) for systems exhibiting accommodation coefficients of the order of unity. This has been verified by Knudsen effusion experiments on the vaporization of silver using both types of cells.

(b) **Resolution and Sensitivity of Spectrometer.**—The resolution of the Time of Flight instrument in the study of vapor species evolving from heated cells is identical with that previously discussed[5] for vapors completely filling the ionizing region for a proper setting of the gate width scan rate and time constant. For example, rare earth metal isotopes are completely resolved and the isotopic ratios calculated from the recorded peak heights are in excellent agreement with those reported in the literature.[6]

The sensitivity of the instrument in detection of ions from the effusion cell mounted as shown in Figs. 1 and 2 was determined from experiments in which silver was vaporized. Since the vapor pressure of silver as a function of temperature is known, the sensitivity of the spectrometer can be estimated from the lowest temperature at which the Ag^+ peak is observed. It is found that, when the pressure in the effusion cell is as low as 5×10^{-9} atm., a Ag^+ spectrum is detectable when the multiplier is set at full gain. The output of the multiplier under this condition is of the order of 5×10^{-14} ampere. It should be pointed out that at these very low pressures the statistical fluctuations of the Ag^+ peak heights are quite appreciable.

(c) **Temperature Measurement and Control.**—The temperature of the effusion cell in the spectrometer was measured by sighting into the effusion orifice, through a calibrated optical flat (see Fig. 1), with a disappearing filament type Leeds and Northrup optical pyrometer. The optical pyrometer used in the experiment was calibrated by intercomparison with the one calibrated by the National Bureau of Standards.

To ensure that the temperature measurement in the spectrometer is not different from that in effusion experiments where one sights directly into the black body[7] (no collimating slits or radiation shields) a number of experiments were performed.

(1) The rate of effusion of a silver sample was determined at various temperatures in the spectrometer and in the effusion apparatus.[7] The temperatures corresponding to a given rate of effusion, in the temperature range 900 to 1000°, were identical to within ± 4° in both experiments.

(2) Similar experiments were performed in which neodymium sesquioxide was vaporized. Again the temperatures corresponding to a given rate of effusion, in the temperature range 2000 to 2150° were identical to within ±4° in both apparatus.

(3) The melting points of some metals were observed in an effusion cell mounted in the spectrometer. This was done by increasing the temperature of the effusion cell at approximately five degree intervals and noting the temperature at which the metal pieces in the cell coalesce. The results are

	M. p. obsd., °C.	M. p. reported, °C.
Silver	963 ± 4	961[8]
Terbium	1363 ± 5	1356 ± 4[9]
Lutetium	1661 ± 5	1652 ± 4[9]

The agreement between observed and reported melting points seems to be quite good. From the rate of effusion experiments and melting point determinations it would appear that within ±5° the temperatures measured in the spectrometer are identical with those measured under more ideal conditions. It is interesting to note that the measured melting points appear to be consistently higher by a few degrees. This may be attributed to the manner in which the melting point experiments were performed and to the effect of the radiation from the hot filament used in heating the crucible on temperature measurement.

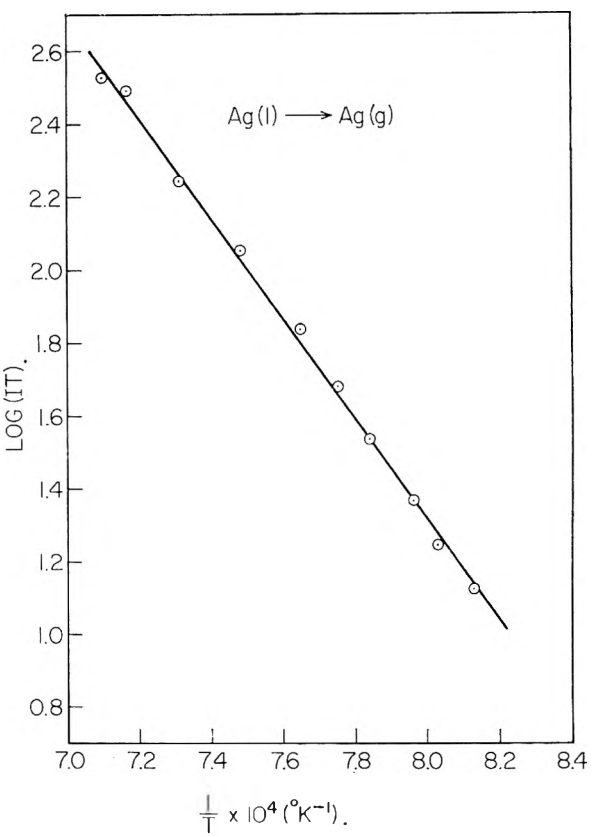

Fig. 3.—Clausius–Clapeyron plot of the variation of intensity of Ag^+ with temperature in the vaporization of silver.

It should be pointed out that better agreement than ± 3° cannot really be expected, since the temperature control, achieved by manual regulation of the voltage applied to the crucible, is no better than ±3°. At low voltages and currents (100–300 milliamp., 100–300 volts) the power supply is very stable. The temperatures attained with these power inputs are approximately in the range 1200 to 1600°K. For the larger power inputs, 1–1.5 amperes, 700–900 volts, very careful control is required to maintain constant temperatures in the range 2200–2600°K.

(d) **Linearity of Spectrometer Multiplier.**—The research presented below represents one of the first reported investi-

(6) G. Friedlander and J. W. Kennedy, "Introduction to Radiochemistry," John Wiley and Sons, Inc., New York, N. Y., 1949.

(7) M. Hoch and H. L. Johnston, *J. Am. Chem. Soc.*, **76**, 4833 (1954).

(8) H. F. Stimson, *Am. J. Phys.*, **23**, 614 (1955).

(9) A. H. Daane, private communication.

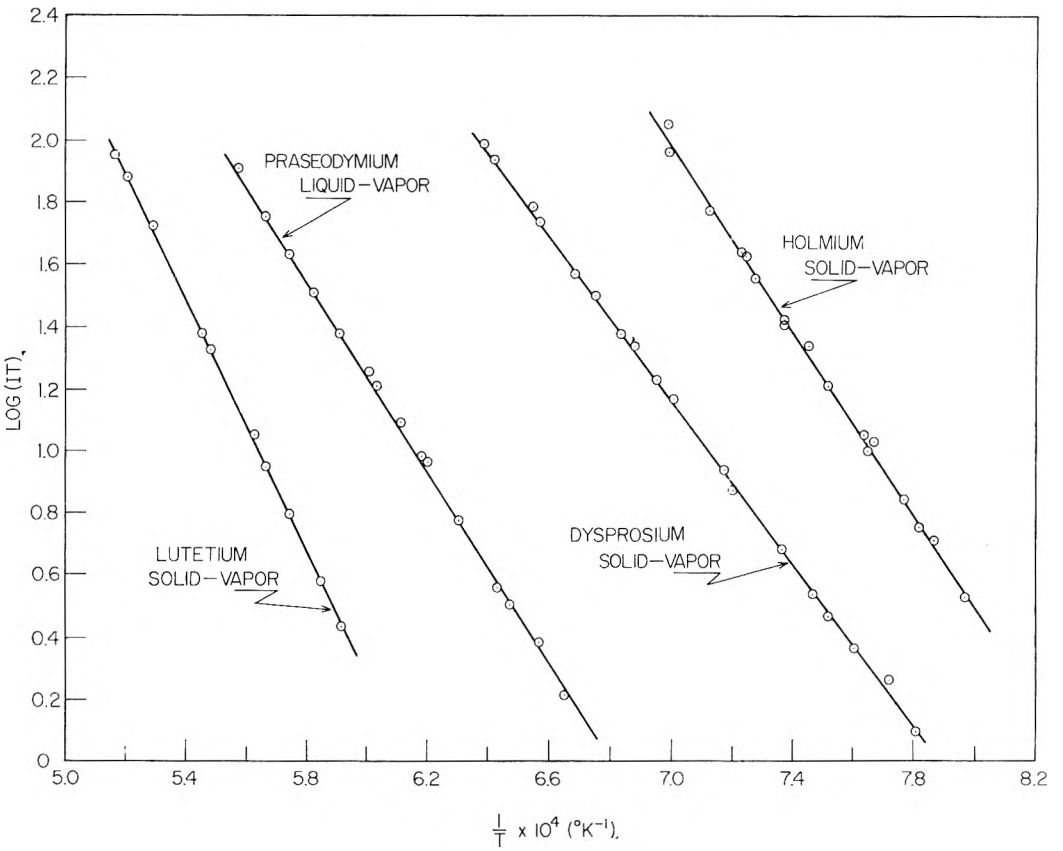

Fig. 4.—Clausius–Clapeyron plot of the variation of intensity of Lu^+, Pr^+, Dy^+ and Ho^+ with temperature in the condensed phase-vapor equilibria.

gations in which the Bendix instrument was used for quantitative thermodynamic measurements. It was necessary, before initiating this investigation, to establish the relationship between the output of the multiplier and the pressure in the ionizing region. This was done by performing a number of experiments on systems whose thermodynamic properties are known.

The heat of vaporization of liquid silver was determined from the measurement of the intensity, I, of one of the Ag^+ isotopes with temperature at constant ionizing electron current and energy, as a function of temperature. The electron energy was maintained at 25 electron volts. The results are shown in Fig. 4. In this figure the logarithm of the intensity of the Ag^+ multiplied by the absolute temperature which is proportional to the silver pressure[2] in the Knudsen cell (tantalum with $^1/_{16}''$ orifice) is plotted as a function of the reciprocal of the absolute temperature. This is a Clausius–Clapeyron plot whose slope is proportional to the heat of vaporization. From the data in Fig. 4 one obtains a heat of vaporization of silver at an average temperature of 1320°K. of 63.2 ± 1.9 kcal. This is in good agreement with the value of 63.8 kcal. given by Stull and Sinke[3] at the same temperature.

A more stringent test of the linearity of the output of the multiplier can be made by comparing the observed ratios of the intensities of diatomic silver, Ag_2^+, to monatomic silver, Ag^+, with those previously reported.[10] The results at a number of temperatures are shown below. The last column in Table I was interpolated from the results in ref. 10 which were obtained with 60° sector single focusing spectrometer equipped with a nine stage Ag–Mg secondary electron multiplier. It is obvious from the agreement of our results with those of Ackerman, Stafford and Drowart that the performance of the Bendix time of flight instrument is very nearly identical with that of a conventional focusing instrument. It should be noted that the multiplier outputs of the Bendix instrument in the above experiments varied approximately in the range 1×10^{-13} to 1×10^{-9} ampere. (The multiplier setting was approximately $^2/_3$ to $^3/_4$ of full gain.)

TABLE I

OBSERVED RATIOS OF INTENSITIES OF DIATOMIC TO MONATOMIC SILVER, UNCORRECTED FOR CROSS SECTIONS AND MULTIPLIER EFFICIENCY

	$(I_{Ag_2^+}/I_{Ag^+}) \times 10^4$	
T (°K.)	This research	Ackerman, Stafford and Drowart
1380	11.4	11.5
1413	14.3	13.4
1460	18.1	16.8
1513	23.6	21.3

The ratios in Table I of this research seem to become increasingly larger with increasing temperature than those previously reported. This trend is probably within the experimental error of both sets of data. However, it is interesting to note that the dissociation energies, D_0's, of Ag_2 calculated from the data of this research are more consistent (no significant trend with temperature) than those computed from the data of Ackerman, Stafford and Drowart. The mean D_0^0 calculated from the results of this research is 37.50 kcal. as compared to 37.58 kcal. given in ref. 10, if the same thermal data, multiplier yield and cross sections corrections are used in the calculations.

The final test to establish the linearity of the multiplier was made by determining the vapor pressures of $B_2O_3(l)$ over a wide range of temperatures and comparing with the data of Speiser, Naiditch and Johnston.[11] The intensity of the $B_2O_3^+$ produced in a platinum Knudsen cell was measured as a function of temperature at constant ionizing electron current and energy. In order to establish the proportionality factor between pressure and the observed intensity, a Knudsen effusion experiment was performed directly in the

(10) M. Ackerman, F. E. Stafford and J. Drowart, *J. Chem. Phys.*, **33**, 1784 (1960).

(11) R. Speiser, S. Naiditch and H. L. Johnston, *J. Am. Chem. Soc.*, **72**, 2578 (1950).

spectrometer at a single temperature. The results are shown in Table II. In the last column is the vapor pressure of $B_2O_3(l)$ calculated from the equation given by Speiser, Naiditch and Johnston.[11] As in the case of the silver experiments the agreement of the results of this research and that previously reported[11] is good. The rate of pressure increase with temperature is, however, somewhat greater. The heat of vaporization of $B_2O_3(l)$ calculated from the slope of a Clausius–Clapeyron plot of the results of this research is 82.9 ± 1.5 kcal. mole^{-1} at an average temperature of 1430°K.[12] This heat of vaporization is approximately 5 kcal. higher than the value given by Speiser, Naiditch and Johnston.[11] It should, however, be pointed out that the uncertainty in the latter results are much greater than in the present investigation. In addition, the heat of vaporization of 82.9 kcal. results in an entropy of $B_2O_3(g)$ of 93.9 e.u. at 1430°K. in better agreement with the spectroscopic value[13] at the same temperature of 93.5 e.u.

TABLE II

VAPOR PRESSURE OF $B_2O_3(l)$

	p (atm.)	
T (°K.)	This research	Speiser, Naiditch[a] and Johnston
1220	3.78×10^{-8}	6.89×10^{-8}
1234	8.51×10^{-8}	9.91×10^{-8}
1264	1.36×10^{-7}	2.10×10^{-7}
1287	2.56×10^{-7}	3.65×10^{-7}
1325	6.24×10^{-7}	8.73×10^{-7}
1343	8.19×10^{-7}	1.29×10^{-6}
1359	1.38×10^{-6}	1.82×10^{-6}
1387	2.51×10^{-6}	3.25×10^{-6}
1414	3.87×10^{-6}	5.57×10^{-6}
1445	7.52×10^{-6}	1.01×10^{-5}
1481	1.67×10^{-5}	1.95×10^{-5}
1521	3.69×10^{-5}	3.89×10^{-5}
1548	6.04×10^{-5}	6.10×10^{-5}
1586	1.15×10^{-4}	1.12×10^{-4}
1623	1.99×10^{-4}	1.96×10^{-4}
1641	2.51×10^{-4}	2.54×10^{-4}

[a] Last column calculated from equation given by Speiser, Naiditch and Johnston.[11]

Materials

All the rare earth metals used in this research were obtained from the Lindsay Chemical Division of American Potash and Chemical Corporation. The quoted maximum rare earth impurities in each of the metals were

Praseodymium	0.1% Ce, Nd.
Neodymium	0.1% Pr, Sm.
Gadolinium	0.1% Sm, Eu, Tb.
Terbium	0.1% Gd, Dy, Y.
Dysprosium	0.1% Ho, Y.
Holmium	0.1% Er, Dy.
Erbium	0.1% Ho, Tm.
Lutetium	0.1% Yb, Tm.

The quoted non-rare earths were

O less than	0.5%
N less than	0.1%
C less than	0.02%
Ca less than	0.1% (for Lu <0.03%)
Mg less than	0.1%
Fe less than	0.1%
Ta less than	1% (for Lu 2–3%)

In all of the experiments the metals were handled in an argon atmosphere. Prior to the heat of vaporization or sublimation measurements, the metals were degassed *in vacuo* for several hours at a temperature of 1000–1400°.

Results and Discussion

The heats of sublimation or vaporization of the metals neodymium, praseodymium, gadolinium, terbium, dysprosium, holmium, erbium and lutetium were determined from measurements of the variation of intensity of the metal ion with temperature at a fixed ionizing electron current and energy. In all of the experiments the electron energy was maintained at a fixed value in the range 20 to 25 electron volts. The results are shown in Figs. 4 and 5. In these figures the logarithm

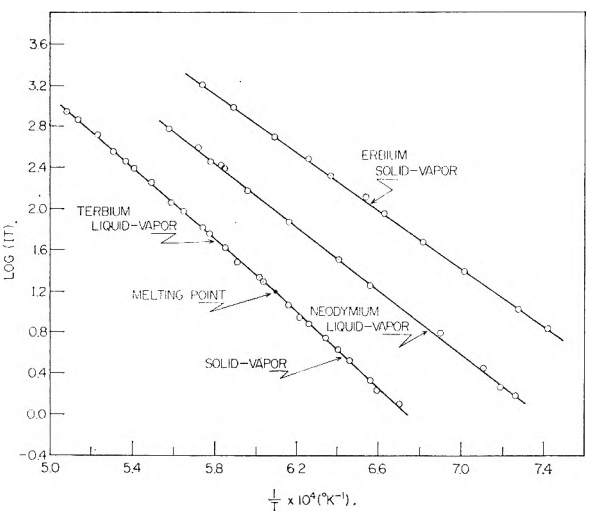

Fig. 5.—Clausius–Clapeyron plot of the variation of intensity of Tb^+, Nd^+ and Er^+ with temperature in the condensed phase-vapor equilibria.

of the intensity I, multiplied by the absolute temperature in degrees Kelvin, T, is plotted *versus* the reciprocal of the absolute temperature.[14] The figures represent Clausius–Clapeyron plots.

The heats of sublimation or vaporization and the standard deviations were determined from a least square treatment of the data shown in Figs. 4 and 5. The results are summarized in Table III below. ΔH_s and ΔH_v are the molar heats of sublimation and vaporization, respectively, expressed in kilocalories, and represent the average values in the temperature range given in the last column of Table III. It is possible that in a number of cases a heat of transition may be averaged in the result. It is obvious from the standard deviations given

TABLE III

HEATS OF SUBLIMATION OR VAPORIZATION OF SOME RARE EARTH METALS

Metal	ΔH_s (kcal. mole^{-1})	ΔH_v (kcal. mole^{-1})	Av. temp. (°K.)	Temp. range (°K.)
Nd	...	70.2 ± 0.9	1587	1381–1792
Pr	...	71.8 ± 0.6	1651	1505–1797
Gd	...	76.9 ± 1.0	1865	1685–2044
Tb	85.0 ± 1.6	...	1568	1492–1644
Tb	...	81.1 ± 0.8	1811	1655–1967
Dy	60.1 ± 0.3	...	1422	1278–1566
Ho	68.0 ± 1.2	...	1395	1253–1566
Er	64.5 ± 0.6	...	1546	1349–1743
Lu	92.3 ± 1.6	...	1814	1691–1937

(12) The two lowest pressures were not included in the calculation due to the appreciable uncertainty of these measurements.

(13) D. White, D. E. Mann, P. N. Walsh and A. Sommer, *J. Chem. Phys.*, **32**, 481 (1960).

(14) The absolute vapor pressures were not determined. However, spot checks with Knudsen effusion experiments indicated that in nearly all of the experiments the pressures were approximately in the range 10^{-5} to 10^{-8} atm.

in Table IV, approximately 1.0 kcal. on the average, that it is not possible to determine heats of transitions which are of the same magnitude. It is, however, possible to detect a change in slope due to a heat of melting, when this is of the order of 3–4 kcal. This is shown in Fig. 5, where both the heat of sublimation and heat of vaporization of terbium have been determined.

The precision measures of the heats of sublimation given in Table III, on the average ±1 kcal/mole, were obtained by considering only the deviations from the least squares line representing the data. It should be recognized that this is not a measure of the accuracy of the results but merely a measure of the stability of the instruments involved in the measurements. There are obviously systematic errors which must be considered in establishing a true uncertainty. The most important ones are due to absolute temperature errors, temperature gradients in the effusion cell, liquid creep and sample impurities. It is impossible to quantitatively assess the magnitude of all these effects; however, we feel that total error introduced is probably no larger than 2 kcal./mole providing liquid creep did not occur. The experiments were performed in such a way as to avoid this difficulty. The top of the effusion cell was purposely maintained at higher temperature, which was achieved by the design of the filament, used in the electron bombardment heating, and the position of the Knudsen cell relative to this filament. The uncertainty in the temperature measurement is approximately ±5°, as previously stated. The error introduced as a result of this uncertainty and the presence of gradients probably does not contribute more than a one kcal./mole error to the heats of sublimation. The presence of impurities does not affect heats of vaporization determinations by the mass spectrometric method[15] except as they alter the activity of the condensed phase. From the level of soluble impurities present one would estimate these effects to be small.

There are a few major discrepancies between the results of this research and previous investigations. The heats of sublimation of lutetium and terbium are considerably higher than those previously reported, whereas the heat of sublimation of dysprosium is somewhat lower. Although we cannot explain the reason for these discrepancies there is some evidence which would favor the present results for lutetium and dysprosium. In the vaporization of the sesquioxides Lu_2O_3 and Dy_2O_3 it is found that the vapor phase consists of both LuO(g) and Lu(g) in the former case whereas in the latter case, almost exclusively Dy(g).[16] In order to account for the rates of vaporization of the sesquioxides consistent with the above mentioned composition for the vapor phase and the known heats of formation of these compounds, it is necessary to assume a higher heat of sublimation for lutetium than previously reported and a lower one for dysprosium.

(15) Only in Nd does the impurity, Sm, exhibit an isotope which overlaps the Nd isotopes. To avoid this difficulty, instead of observing the most abundant Nd isotope 144, the next most abundant one, atomic weight 146, was observed.

TABLE IV

COMPARISON OF THE HEATS OF SUBLIMATION OF THE RARE EARTH METALS OF THE PRESENT RESEARCH WITH THOSE PREVIOUSLY REPORTED

Rare earth metal	ΔH_s (298°K.), kcal./mole This research	Others	$\Delta H(T) - \Delta H_s(298)$,[a] kcal./mole
La		97.3[c]	
Ce		96.4[c]	
Pr	77.9	85.2[d]	−6.1[+]
Nd	76.3	75.0[d]	−6.1
Pm	...	...	
Sm	...	49.9[d]	
Eu	...	42.1[e]	
Gd	83.6	...	−5.7
Tb[b]	86.9, 87.2	71.4[d]	−1.9[+], −6.1[+]
Dy	61.6	(67)[g]	−1.5[+]
Ho	69.5	...	−1.5[+]
Er	66.4	...	−1.9[+]
Tm	...	58.4,[b] 57.6[d]	
Yb	...	40.0[d]	
Lu	94.7	70.0[f]	−2.4[+]

[a] All values of $H(T) - H_s(298)$ were taken from Stull and Sinke[4] except those marked by (+) which have been estimated. [b] For terbium two values are given. One is calculated from the heat of sublimation, the other from the heat of vaporization. [c] A. H. Daane and F. H. Spedding, Abst. A.C.S. meeting, Chicago, Sept., 1958. [d] W. R. Savage, D. E. Hudson and F. H. Spedding, *J. Chem. Phys.*, 30, 221 (1959). [e] F. H. Spedding, J. J. Hanak, A. H. Daane, *Trans. A. I. M. E.*, 212, 379 (1958). (Heat of sublimation corrected to 298°K. using tables of Stull and Sinke.[3]) [f] F. H. Spedding, R. J. Barton and A. H. Daane, *J. Am. Chem. Soc.*, 79, 5160 (1957). ($\Delta H(1010) - \Delta H(298)$ estimated at −1.0 kcal.)

Although in the research absolute vapor pressures were not determined, it is possible to make some estimates from the observed ion intensities. On the basis of such estimates it is suggested that the vapor pressures of lutetium given by Stull and Sinke[4] are high by at least a few orders of magnitude.

Acknowledgment.—The authors are indebted to Mr. A. Sommer for aid in establishing the characteristics of the spectrometer and to Mr. A. Brooke, who constructed and serviced the high temperature furnace. The authors would also like to express their gratitude to various members of the Bendix Corporation for their continued interest in this research. In particular we wish to thank Mr. D. B. Harrington and Mr. E. Younginger of the Cincinnati Division.

(16) Unpublished results of this Laboratory.

RARE EARTHS. III. A MASS-SPECTROMETRIC INVESTIGATION OF THE ISOMOLECULAR OXYGEN-EXCHANGE REACTIONS OF LANTHANUM, CERIUM, PRASEODYMIUM AND NEODYMIUM WITH THEIR MONOXIDES[1]

BY PATRICK N. WALSH, DAVID F. DEVER AND DAVID WHITE

Cryogenic Laboratory, Department of Chemistry, The Ohio State University, Columbus, Ohio

Received March 13, 1961

The equilibrium constants for the reactions Ce(g) + LaO(g) ⇄ La(g) + CeO(g) (1); Pr(g) + LaO(g) ⇄ La(g) + PrO(g) (2); and Nd(g) + PrO(g) ⇄ Pr(g) + NdO(g) (3) and their temperature dependence have been determined with a Time-of-Flight Mass Spectrometer. The heats of the three reactions in kcal. mole^{-1} calculated from the results are: ΔH_1 (1870°K.) = 1.05 ± 0.20, ΔH_2 (1913°K.) = 15.8 ± 0.4, ΔH_3 (1910°K.) = 6.9 ± 0.6. These heats of reaction give directly the difference in dissociation energies, at the indicated temperatures, of the two gaseous monoxides in each of the reactions. The dissociation energies at absolute zero D_0^0 in e.v. calculated from these results and appropriate thermal functions are D_0^0 (CeO) = 8.03 ± 0.2, D_0^0 (PrO) = 7.40 ± 0.3, D_0^0 (NdO) = 7.06 ± 0.2. The electronic contributions to the entropy of the gaseous monoxides at elevated temperatures are discussed in terms of the measured entropy changes in the above reactions.

Introduction

In the first paper[2] of this series, the importance of gaseous monoxides of lanthanum and neodymium in the vaporization of the sesquioxides was established, and the thermodynamic properties of these compounds discussed. It was shown in this discussion that the greatest uncertainty in the calculated thermodynamic properties of these gases arises from the unavoidable use of estimated molecular properties in the computation of high temperature thermal functions. Although the spectra of several gaseous rare earth monoxides have been reported,[3] only in the case of LaO have the term symbol of the ground state and the energies of excited states been derived. While reasonable estimates of the rotational and vibrational contributions to the thermal functions can be made by well-known approximation methods,[4] the uncertainty arising from estimates of the electronic contributions is unusually large in the case of rare earth compounds, owing to the possibility of high ground state multiplicities as well as excitations from the ground state at elevated temperatures.

In this paper, results of a mass-spectrometric study of isomolecular oxygen exchange reactions of the type

$$M_a(g) + M_bO(g) \rightleftharpoons M_aO(g) + M_b(g) \qquad (1)$$

(where M_a and M_b are different rare earth atoms), from which the electronic contribution to the entropy of the gaseous monoxides can be inferred, are presented. Although this study does not permit the separate determination of the ground state multiplicity and the excitation energies of other electronic states, it does indicate the combined effect of these factors on the thermodynamic properties of these gases.

It is evident that the equilibrium constants for reactions of the type shown above (equation 1) are independent of the total pressure of the system. Furthermore, because the species appearing on the two sides of equation 1 are so similar, quantities such as ionization cross sections and electron multiplier efficiencies[5] can be expected to cancel, to a good approximation, so that absolute equilibrium constants, K_{eq}, can be derived directly from mass-spectrometrically observed ion intensities, *viz.*

$$K_{eq} = \frac{I_{M_aO^+}}{I_{M_bO^+}} \times \frac{I_{M_b^+}}{I_{M_a^+}} \qquad (2)$$

Combining the free energy of reaction derived from K_{eq} with the heat of reaction determined from the variation of K_{eq} temperature gives the entropy of reaction. If the entropies of the metals and at least one gaseous rare earth monoxide are known, then, in principle, the entropies of all the other monoxides of the lanthanide elements can be determined by study of a series of reactions of this kind. It should be pointed out that the heat of reaction 1 is equal to the difference in dissociation energy of the two monoxides (at the temperature of the experiment) so that if the dissociation energy of one gaseous monoxide is known, then in principle, the dissociation energies of the others can also be determined quite readily.

In this paper isomolecular reactions involving the rare earths La, Ce, Pr and Nd have been investigated. It was of particular interest to us in this initial investigation to check by this method the difference in dissociation energies of LaO and NdO which we have determined previously in a less direct manner.[2]

Experimental

Materials.—The rare earth oxides and metals were obtained from the Lindsay Chemical Division of American Potash and Chemical Corporation. The purity of the metals praseodymium and neodymium has previously been given.[6] The impurities, as listed by the manufacturer, in the lanthanum were 0.01% Pr and 0.001% Ce; in the cerium, less than 0.1% La, Pr and Nd; in the yttrium, 0.1% of Dy and Gd; non-rare earth impurities, about equal to those listed for Pr and Nd.[6] The lanthanum and neodymium oxides were the same materials used for heat capacity studies.[7] The Pr_6O_{11} and Tb_4O_7 contained less than 0.1% of other rare earths.

(1) This work was supported by the Office of Naval Research and the Air Force Office of Scientific Research.

(2) H. W. Goldstein, P. N. Walsh and D. White, *J. Phys. Chem.*, **65**, 1400 (1961).

(3) G. Herzberg, "Molecular Spectra and Molecular Structure, I. Spectra of Diatomic Molecules," D. Van Nostrand Co., Inc., Princeton, N. J., 1950.

(4) See, for example, L. Brewer and M. S. Chandrasekharaiah, "Free Energy Functions of Gaseous Monoxides," U. S. Atomic Energy Commission Report UCRL-8713 (rev.), 1960.

(5) M. G. Inghram and J. Drowart, "Mass Spectrometry Applied to High Temperature Chemistry," in "Proceedings of an International Symposium on High Temperature Technology," McGraw-Hill Book Co., New York, N. Y., 1960.

(6) D. White, P. N. Walsh, H. W. Goldstein and D. F. Dever, *J. Phys. Chem.*, **65**, 1404 (1961).

(7) H. W. Goldstein, E. F. Neilson, P. N. Walsh and D. White, *ibid.*, **63**, 1445 (1959).

Apparatus and Procedure.—The Bendix time-of-flight mass spectrometer, the electron-bombardment heated furnace, and auxiliary equipment have already been described in detail.[6] Tantalum Knudsen cells of the kind described previously[2] were used to contain the reactants.

In all experiments the ionizing electron energy was maintained at 20 e.v. Previous experience with LaO and NdO[1] had demonstrated that fragmentation of these species occurs to only one or two per cent. at this voltage and that the effect is very nearly the same for both. Measurements of appearance potentials with the present Bendix spectrometer are not very precise when the appearance potentials are as low as 5–7 volts, as they are in the rare earths. Nevertheless, in this range it is possible to obtain values to within ±1 e.v. Within this uncertainty, all the observed species had the same appearance potential; hence, it is believed that the assumption that the cross-sections cancel in equation 2 is still valid for the experimental conditions.

The analog output system of the Bendix instrument permits variable speed scanning of any chosen portion of the spectrum and rapid and reproducible change from one portion to another.[8] Scanning speed, gate width and detector time constant were adjusted so that adjacent mass peaks were completely resolved and developed their full heights on the recorder chart.

Runs were made by fixing the temperature, measured and controlled as described previously,[2] waiting until peak heights were constant, and scanning the spectrum. The quantities of metals in the crucible were chosen in such a way that the intensities of both metal ions could be determined under one set of detector and amplifier settings and the monoxide ions under another set. A pre-planned switching program, which included interrupting the scan just after the second metal peak and restarting it just before the first monoxide peak, permitted all four ion intensities to be measured within 15 to 20 seconds. This greatly reduces the effect of temperature variations during the run. Four to twelve repeat scans of all four peaks were made to determine the reproducibility at each temperature. The ratios of intensities of the metal ions and of the monoxide ions were calculated separately and multiplied to obtain the equilibrium constants.

As only ratios are needed for this type of measurement, a single isotope of each species was monitored. These were: La, 139; Ce, 140; Pr, 141; Nd, 142; LaO, 155; CeO, 156; PrO, 157; NdO, 158.

Experimental Results

A. Ce(g) + LaO(g) ⇄ La(g) + CeO(g).—This reaction was studied by putting an approximately equimolar solution of lanthanum and cerium in the Knudsen cell and adding Tb_4O_7 (series I) or La_2O_3 (series II). The two sesquoxides were used to determine whether equilibrium had been established in the gas phase. The equilibrium constant should be independent of the composition of the condensed phase. That this is so is seen from the experimental results given in Table I. In Table I, are listed the measured ratios of the partial pressures of the gaseous metals and monoxides and the resultant equilibrium constants. Four to six measurements were made at each temperature, and averaged. The data are plotted in Fig. 1. The standard deviation in log K given in Table I is indicated by the vertical line through each point.

By a least squares treatment of the data in which each point was given a weight proportionate to its relative precision, the straight line which best represents the data was found to be

$$\log K = -229.6/T + 0.0721 \qquad (3)$$

The resultant heat and entropy of the reaction at the average temperature (1870°K.) are

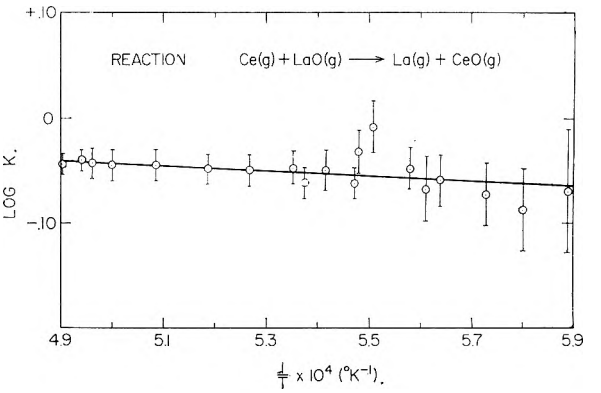

Fig. 1.—Variation of equilibrium constant of the reaction Ce(g) + LaO(g) ⇄ La(g) + CeO(g) with temperature.

TABLE I

REACTION Ce(g) + LaO(g) ⇄ La(g) + CeO(g)

Temp. (°K.)	P_{La}/P_{Ce}	P_{CeO}/P_{LaO}	log K
		Series I	
1698	0.99	0.86	−0.0701 ± 0.055
1724	.95	.86	− .0878 ± .030
1745	.95	.89	− .0726 ± .021
1772	.97	.90	− .0590 ± .026
1782	.98	.87	− .0691 ± .024
1825	1.01	.92	− .0320 ± .016
1846	0.98	.91	− .0496 ± .012
		Series II	
1791	0.96	0.93	−0.0491 ± 0.020
1816	1.03	.95	− .0079 ± .016
1827	0.93	.93	− .0630 ± .009
1860	.93	.93	− .0630 ± .009
1868	.96	.93	− .0472 ± .009
1899	.94	.95	− .0491 ± .006
1928	.93	.96	− .0491 ± .009
1966	.92	.98	− .0453 ± .009
1999	.92	.98	− .0453 ± .009
2024	.94	.97	− .0400 ± .009
2015	.93	.97	− .0424 ± .009
2040	.95	.95	− .0443 ± .001

$\Delta H_{1870} = 1.05 \pm 0.20$ kcal. mole^{-1}

$\Delta S_{1870} = 0.33 \pm 0.12$ cal. deg.$^{-1}$ mole^{-1}

B. Pr(g) + LaO(g) ⇄ La(g) + PrO(g).—This reaction was investigated using a mixture of Tb_4O_7 with the metals. The concentration of lanthanum was maintained at about five times that of praseodymium to compensate for the difference in volatilities. The equilibrium constants at various temperatures for two series of experiments are listed in Table II.

The results of both series can be represented by the equation, obtained using weighted least squares as before

$$\log K = 3.453/T + 0.789 \qquad (4)$$

The corresponding heat and entropy of reaction are

$\Delta H_{1913} = 15.8 \pm 0.4$ kcal. mole^{-1}

$\Delta S_{1913} = 3.6 \pm 0.2$ cal. deg.$^{-1}$ mole^{-1}

C. Nd(g) + PrO(g) ⇄ Pr(g) + NdO(g).—The two metals Nd and Pr are much more volatile than either lanthanum or cerium and it proved

(8) D. B. Harrington, "The Time of Flight Mass Spectrometer," in "Advances in Mass Spectrometry," Pergamon Press, London, 1958.

TABLE II

REACTION Pr(g) + LaO(g) ⇄ La(g) + PrO(g)

Temp. (°K.)	P_{La}/P_{Pr}	P_{PrO}/P_{LaO}	log K
		Series I	
1758	0.245	0.279	−1.165 ± 0.040
1784	.224	.308	−1.161 ± .053
1811	.316	.235	−1.129 ± .024
1833	.270	.286	−1.112 ± .028
1886	.316	.277	−1.058 ± .032
1898	.369	.250	−1.035 ± .020
1911	.407	.222	−1.044 ± .013
1923	.422	.221	−1.030 ± .022
1935	.444	.215	−1.020 ± .008
1939	.459	.214	−1.008 ± .017
		Series II	
1749	0.178	0.365	−1.198 ± 0.032
1813	.241	.318	−1.116 ± .032
1823	.293	.264	−1.112 ± .026
1846	.281	.288	−1.092 ± .032
1864	.272	.312	−1.071 ± .022
1932	.330	.296	−1.010 ± .011
1964	.318	.324	−0.987 ± .032
1991	.352	.310	−0.959 ± .016
2011	.394	.294	−0.936 ± .014
2045	.430	.292	−0.900 ± .012
2067	.489	.276	−0.870 ± .012

difficult to obtain measurable quantities of monoxides from mixtures of the metals with any rare earth oxide without at the same time overloading the mass spectrometer with metal ions. To circumvent this difficulty, the reaction was studied in two parts. For low temperature runs (series I), Ta_2O_5(c) was added to a mixture of Nd and Pr. As Ta_2O_5 is considerably less stable than any of the rare earth oxides, higher concentrations of monoxides in the gas phase are obtained at any given temperature. Unfortunately, a condensed phase reaction, leading to the formation of sesquioxides or tantalates,[9] also takes place and the equilibrium concentrations of species in the gas phase become time-dependent. This, however, proved to be not too serious; as can be seen in Table III, the standard deviations of the equilibrium constants are comparable to those observed in other reactions.

At higher temperatures (series II), the reaction was investigated using a mixture of Tb_4O_7 with a solution of Pr and Nd in yttrium. The yttrium metal served to lower the activity, and thus the partial pressure, of the others to the point where they could be studied without overloading the mass spectrometer. The results are shown in Table III. The two series of runs appear to be consistent and have been combined to give

$$\log K = -1504/T - 0.317 \qquad (5)$$

and

$$\Delta H_{1910} = 6.9 \pm 0.6 \text{ kcal. mole}^{-1}$$
$$\Delta S_{1910} = 1.5 \pm 0.3 \text{ cal. deg.}^{-1} \text{ mole}^{-1}$$

By combining the results of this section with those of section 3 the heat and entropy of the reaction

$$\text{Nd(g)} + \text{LaO(g)} \rightleftharpoons \text{NdO(g)} + \text{La(g)} \qquad (6)$$

(9) P. N. Walsh, H. W. Goldstein and D. White, *J. Am. Ceram. Soc.*, **43**, 229 (1960).

TABLE III

REACTION Nd(g) + PrO(g) ⇄ Pr(g) + NdO(g)

Temp. (°K.)	P_{Pr}/P_{Nd}	P_{NdO}/P_{PrO}	log K
		Series I	
1729	0.195	0.333	−1.188 ± 0.011
1743	.195	.344	−1.173 ± .014
1749	.088	.690	−1.214 ± .026
1755	.206	.330	−1.167 ± .011
1764	.216	.343	−1.130 ± .018
1771	.237	.277	−1.183 ± .026
1775	.212	.343	−1.139 ± .011
1780	.093	.674	−1.202 ± .014
1796	.282	.245	−1.161 ± .029
1802	.119	.604	−1.143 ± .030
1805	.097	.692	−1.173 ± .027
1815	.220	.365	−1.095 ± .014
1817	.447	.165	−1.132 ± .017
1830	.113	.608	−1.163 ± .025
		Series II	
1818	0.051	1.33	−1.166 ± 0.033
1820	.232	0.304	−1.152 ± .028
1856	.061	1.12	−1.166 ± .066
1856	.234	0.300	−1.154 ± .033
1868	.061	1.10	−1.175 ± .060
1868	.248	0.277	−1.163 ± .017
1876	.242	.324	−1.106 ± .012
1897	.245	.315	−1.112 ± .025
1904	.082	.947	−1.112 ± .036
1923	.246	.340	−1.078 ± .008
1936	.076	.931	−1.150 ± .022
1948	.249	.333	−1.081 ± .033
1970	.091	.919	−1.078 ± .009
1976	.092	.963	−1.052 ± .009
1984	.102	.828	−1.073 ± .063
2014	.108	.802	−1.063 ± .018
2020	.107	.804	−1.066 ± .009
2031	.116	.720	−1.084 ± .022
2037	.131	.664	−1.061 ± .026
2056	.133	.632	−1.075 ± .042
2066	.273	.326	−1.051 ± .010
2066	.152	.606	−1.036 ± .019
2088	.190	.516	−1.009 ± .020

are obtained. These are

$$\Delta H_{1910} = 22.7 \pm 0.7 \text{ kcal. mole}^{-1}$$
$$\Delta S_{1910} = 2.1 \pm 0.4 \text{ cal. deg.}^{-1} \text{ mole}^{-1}$$

Discussion

From the entropies of reaction given in A, B and C of the preceding section, it is possible to calculate the difference in entropy between LaO(g) and the other monoxides, CeO, PrO and NdO, provided the difference in entropy of the metal vapors involved in the reactions is known. Unfortunately, at the present time only the entropies of the gaseous metals La and Nd are known with any precision at elevated temperatures. Although some reasonable estimates can be made, we will defer calculations based on such estimates until the experiments on additional isomolecular oxygen exchange reactions have been completed. It is already clear, however, that the electronic contributions to the thermodynamic properties of these monoxides at elevated temperatures must be considerable.

The entropy change observed for reaction 6

has been used to determine the difference in entropy between LaO and NdO by combining the observed entropy of reaction with the entropies of La(g) and Nd(g) at 1900°K. listed by Stull and Sinke.[10] The value obtained is 3.0 ± 0.5 cal. deg.$^{-1}$ mole^{-1}, the entropy of NdO being greater. Considering the similarity of these molecules, it is reasonable to assume that not more than 0.3 cal. deg.$^{-1}$ mole^{-1} of this difference could arise from differences in translational, vibrational and rotational energies; the remainder must originate from differences in electronic terms. The ground state of LaO has been reported as $^2\Sigma$, with the first excited state lying more than 12,000 cm.$^{-1}$ higher.[2] If this assignment is accepted,[11] the electronic entropy of LaO at 1900°K. is 1.38^{+12} cal. deg.$^{-1}$ mole^{-1}. The electronic contribution to the entropy of NdO would then be 4.4 ± 0.5 cal. deg.$^{-1}$ mole^{-1}. It is, of course, impossible to designate on the basis of information presented here what fraction of the entropy is due to ground state multiplicity, but a crude estimate can be made.

The ground state of Nd(g) has been reported[13] as $4f^4\ 6s^2$. That the trivalent state of neodymium is much more stable than the di- and tetravalent states would appear to indicate that one of the 4f electrons is less firmly bound than the others. On the assumption that this electron behaves in the manner postulated for the 5d electron of La, the difference in entropy between NdO and LaO results from the presence of three unpaired 4f electrons in the former. If these are unperturbed by the presence of oxygen in the molecule,[14] so that they behave as in Nd^{+3}, the entropy arising from multiplicity alone would be R ln 10 or 4.58 cal. deg.$^{-1}$ mole^{-1}, which is considerably more than the experimentally observed difference in entropy between NdO and LaO. All that really can be concluded from these considerations is that it is *possible* that the observed electronic entropy of NdO arises primarily from a ground state multiplicity. This is the assumption made in calculations in the first paper of this series.[15]

If the assumption is reasonable, it is possible to calculate the difference in dissociation energies D_0^0(LaO) − D_0^0(NdO) from the heat of reaction 6, since the heat content functions for these molecules can be expected to be very nearly alike. Utilizing the heat content functions of gaseous La and Nd of reference 10, one obtains a value of D_0^0(LaO) − D_0^0(NdO) = 23.5 ± 1 kcal. mole^{-1}. This is in good agreement with the difference of 20.8 ± 9 kcal. mole^{-1} derived from the results of a previous investigation.[2] If one accepts the vaue of D_0^0(LaO) = 8.08 ± 0.2 e.v.[2] then D_0^0(NdO) from this investigation is 7.06 e.v. The uncertainty of this value is of the order of 0.2 e.v. arising primarily from uncertainty in the dissociation energy of LaO.

In the case of CeO(g) and PrO(g) it is not possible to calculate accurate D_0^0's from the experimental data of the previous section, reactions A and B, due to the lack of suitable thermal functions. The differences in dissociation energies between LaO and these molecules are, however, known accurately at the average temperature of the experiments. These are

at 1870°K. D^0(LaO) − D^0(CeO) = 0.05 ± 0.01 e.v.
at 1913°K. D^0(LaO) − D^0(PrO) = 0.69 ± 0.02 e.v.

similarly

at 1912°K. D^0(LaO) − D^0(NdO) = 0.98 ± 0.05 e.v.

It is possible to make a reasonable estimate of D_0^0's for CeO and PrO as follows. Since for the reaction in part A of the previous section the change in entropy is very small, it can be assumed that the difference in the heat content functions of reactants and products is also small. Thus, $\Delta H_0^0 = \Delta H$(1970°K.) so that D_0^0(CeO) = 8.03 ± 0.2 e.v. For reaction (B), from which D_0^0(PrO) can be evaluated, the entropy change is quite large. It has, however, been assumed that, in this case also, $\Delta H_{1913} = \Delta H_0^0$. This is purely arbitrary, but the data are insufficient to justify the choice of any value for $\Delta H_{1913} - \Delta H_0^0$. On this assumption, D_0^0(PrO) = 7.40 ± 0.3 e.v.

The heats of formation, ΔH_0^0(f), of CeO, PrO and NdO have been computed from the dissociation energies given above, the heat of formation of atomic oxygen,[16] and the heats of sublimation at zero degrees of Ce,[17] Pr[18] and Nd.[19] These are, in kcal. mole^{-1}: CeO, −28 ± 5; PrO, −38 ± 9[20]; NdO −27 ± 5. The large uncertainties in these values are not a result of uncertainties in the experimental data, but uncertainties in thermal functions used in reducing the data. Within these errors, it appears that the heats of formation of the gaseous rare earth monoxides investigated to date are nearly the same (ΔH_0^0(f) LaO = −29.8 ± 4 kcal. mole^{-1})[1]. Thus, the difference in dissociation energies of these molecules appears to be approximately the difference in heat of sublimation of the metals.

Acknowledgment.—The authors are indebted to Mr. A. Sommer and Mr. A. Brooke for aid in preparing the experiments and to Dr. H. W. Goldstein for helpful discussions.

(10) D. R. Stull and G. C. Sinke, "Thermodynamic Properties of the Elements," American Chemical Society, Washington, D. C., 1956.

(11) A $^2\Sigma$ ground state for LaO could arise if the molecule consists of La^{++} and $O^{=}$ ions, with the 5d electron of La having moved into a σ molecular orbital.

(12) This might be considered as a lower limit due to the possibility of the existence of low lying states.

(13) P. Schurmanns, *Physica*, *11*, 419 (1946).

(14) L. Brewer and M. S. Chandrasekharaiah, ref. 4, have used such an assumption.

(15) In the above discussion it is assumed that the contributions to the entropy by low lying states is the same for both LaO and NdO.

(16) P. Brix and G. Herzberg, *Can. J. Phys.*, **32**, 110 (1954).

(17) ΔH_0^0 (subl) of Ce = 98.3 ± 1 kcal. mole^{-1}; based on ΔH_{1552}^0 (vap), A. H. Daane and F. H. Spedding, Abstracts, American Chemical Society Meeting, Chicago, Sept. 1958; $H_{1552}^0 - H_0^0$, Ce(g), taken to be the same as Th(g) as calculated by A. J. Darnell, W. A. McCollum and T. A. Milne, *J. Phys. Chem.*, **64**, 341 (1960); $H_{1552}^0 - H_0^0$, Ce(c), extrapolated from data of F. H. Spedding, J. J. McKeown and A. H. Daane, *ibid.*, **64**, 289 (1960).

(18) ΔH_0^0(subl.) of Pr = 78.2 ± 2 kcal. mole^{-1} based on ΔH_{1651}(vap.) ref. 5; $H_{1651}^0 - H_0^0$, Pr(g) assumed same as Nd(g), ref. 10; $H_{1551}^0 - H_0^0$, Pr(c), ref. 10.

(19) ΔH_0^0 (subl.) = 76.6 ± 1 kcal. mole^{-1}; *cf.* ref. 2.

(20) If the heat of sublimation of Pr is taken as 85.5 kcal. mole^{-1}, in agreement with work of Johnson, Hudson, Caldwell, Spedding and Savage, *J. Chem. Phys.*, **25**, 917 (1956), then ΔH_0^0(f) of PrO becomes −27 ± 9 kcal. mole^{-1}.

CONDUCTANCE OF THE ALKALI HALIDES. II. CESIUM IODIDE IN DIOXANE–WATER MIXTURES[1,2]

BY JOHN E. LIND, JR.,[3] AND RAYMOND M. FUOSS

Contribution No. 1659 from the Sterling Chemistry Laboratory of Yale University, New Haven, Conn.

Received March 16, 1961

The conductance of cesium iodide at 25° was measured in dioxane–water mixtures covering the range of dielectric constant $12.81 \leq D \leq 78.54$. The data conform to the Fuoss conductance equation within the experimental precision of 0.01–0.05%, in the range of concentration where κa does not exceed 0.2. As in the case of potassium chloride, the contact distance $\mathring{a}_J$ was found to vary from 5.04 to 3.04 Å.; analysis of the data suggests that the linear coefficient J in the conductance equation and also the activity coefficient require further theoretical study for the case of small ions. The limiting conductances give a hydrodynamic contact distance of 2.93 while the association constants are best reproduced using a value of 4.10 Å.

In the first paper[4] of this series, it was shown that conductance data for potassium chloride in dioxane–water mixtures fitted, well within the experimental error of 0.01–0.05%, the equation[5]

$$\Lambda = \Lambda_0 - Sc^{1/2}\gamma^{1/2} + Ec\gamma \log c\gamma + Jc\gamma + J_2(c\gamma)^{3/2} - K_A c\gamma f^2 \Lambda \quad (1)$$

thus establishing the functional form of (1) for a typical inorganic salt in a partially aqueous system. Several problems appeared, however, in the physical interpretation of the arbitrary constants K_A, $J(a)$ and Λ_0 of the equation. For large ions (*e.g.*, $Bu_4N{\cdot}BPh_4$) in non-aqueous solvents, the three constants can be correlated by means of a single distance parameter, but for the system $\cdot KCl–H_2O–C_4H_8O_2$, the contact distance derived from J varied systematically with the composition of the solvent, that from Λ_0 was unrealistically small and that from K_A showed some variation at low dielectric constant. We report herewith data for cesium iodide in the same solvent system; qualitatively, the results are similar to those found for potassium chloride, although numerically, the discrepancies with the simple model are somewhat smaller, probably because the ions concerned are larger.

Experimental

Cesium iodide (grade recommended for growing optical crystals) was used as received from the A. D. MacKay Company (198 Broadway, New York 38). Flame photometer analysis gave the following results (calculated as iodides) for other alkalies: 0.015% RbI, 0.002% KI, 0.007% NaI. These trace impurities would increase the conductance over that for the same weight of pure CsI by about 0.01%; this correction was neglected.

Dioxane was purified essentially as previously described.[4] As is well known, dioxane peroxidizes readily; dioxane, distilled from sodium–lead alloy under nitrogen and pumped onto a small portion of solid potassium iodide, turned yellow in about 5 hr. in a stoppered flask. The flask had previously been swept out with nitrogen, but evidently enough air leaked in to react. But if the dioxane was pumped onto aqueous potassium iodide solution under the same conditions, no iodide formed, even after several days. It was concluded that water inhibits the peroxidation of dioxane. In our final experiments, dioxane was distilled from alloy under nitrogen onto a weighed amount of water in the receiver. No oxidation difficulties were encountered with mixed solvent prepared in this way except at the last point ($c = 3.2561 \times 10^{-4}$) of the mixture with the highest dioxane content ($D = 12.81$), where a drift of about 0.1% per hour in the resistance was observed. A correction was applied by extrapolating back to the time of dilution. This run nevertheless gave results which were somewhat inconsistent with those from the other systems.

TABLE I

PROPERTIES OF SOLVENTS

No.	w	ρ	D	100η	$10^6\kappa_0$
1	0.0	0.99707	78.54	0.8903	0.84
2	22.1	1.01575	60.18	1.328	.50
3	44.6	1.03065	40.57	1.820	.253
4	57.1	1.03515	29.79	1.982	.180
5	63.7	1.03652	24.44	1.986	.067
6	70.7	1.03650	18.68	1.922	.045
7	75.2	1.03587	15.29	1.839	.028
8	78.5	1.03562	12.81	1.754	.010

Apparatus and experimental technique were otherwise the same as those described in the first paper of this series.[4] Properties of the solvent mixtures are summarized in Table I and the conductance data are compiled in Table II. The symbols in the tables have the following meanings: w = weight % dioxane in the mixture, ρ = solvent density, D = dielectric constant, η = viscosity, κ_0 = solvent conductance, c = salt concentration (equivalents/l.), Λ = equivalent conductance, $\Delta\Lambda = [\Lambda(\text{obsd.}) - \Lambda(\text{calcd.})]$, and Λ (calcd.) the conductance calculated from the theoretical equation 1 using the values of Λ_0, K_A and $\mathring{a}$ obtained from the data. The meaning of $\Delta\Lambda'$ will be explained in the discussion. In order to check the precision of the dilution method, duplicate runs were made at $D = 15.29$; for the second run, the solvent had been stored for one day in the nitrogen box. The results (see Table III) agreed with those of the first run within the experimental error; in order to save space, only the data for the first run are included in Table II.

Discussion

The data of Table II were analyzed on the IBM 650 Computer, using a number of variations of Kay's program[6] for equation[7,8] 1. After the constants of equation 1 were determined, the conductance at each point was calculated; differences between observed and calculated values are given as $\Delta\Lambda$ in Table II. Some systems were computed on the assumption of negligible association; $\Delta\Lambda'$ is the difference observed minus calculated, using equation 1 with $K_A = 0$ and $\gamma = 1$.

From $J(a)$, the contact distance $\mathring{a}$ was evaluated; it showed a systematic trend with dielectric constant, as shown by curve 1 of Fig. 1. (For the system of lowest dielectric constant, we obtained

(1) Presented at the Spring 1960 meeting of the American Chemical Society at Cleveland.

(2) This paper is based on part of a thesis presented by John E. Lind, Jr., to the Graduate School of Yale University in partial fulfillment of the requirements for the Degree of Doctor of Philosophy, June, 1960.

(3) National Science Foundation Fellow, 1957–1960.

(4) J. E. Lind, Jr., and R. M. Fuoss, *J. Phys. Chem.*, **65**, 999 (1961).

(5) R. M. Fuoss and F. Accascina, "Electrolytic Conductance," Interscience Publishers, Inc., New York, N. Y., 1959. Symbols used in this paper are defined in Chapters 15 and 17.

(6) R. L. Kay, *J. Am. Chem. Soc.*, **82**, 2099 (1960).

(7) Ref. 5, equations 17.52, 17.53.

(8) Ref. 4, equation 1 and footnote 27.

TABLE II

CONDUCTANCE OF CESIUM IODIDE IN DIOXANE-WATER MIXTURES AT 25°

$10^4 c$	Λ	$10^3 \Delta\Lambda$	$10^3 \Delta\Lambda'$	$10^4 c$	Λ	$10^3 \Delta\Lambda$
D = 78.54					D = 24.44	
94.416	145.329	..	+16	30.929	43.741	− 4
76.474	146.095	..	−21	24.447	44.583	+ 8
55.585	147.211	..	− 6	19.172	45.396	+ 2
37.919	148.368	..	+ 7	12.368	46.719	− 8
19.933	149.905	..	+ 2	6.590	48.282	+ 4
D = 60.18					D = 18.68	
73.737	93.115	− 9	−10	24.646	36.440	−10
58.272	93.741	+20	+21	19.379	37.549	+14
44.480	94.350	− 8	− 5	14.616	38.790	+ 3
30.294	95.158	− 8	− 6	9.839	40.408	−17
15.445	96.326	+ 5	+ 2	5 492	42.482	+ 7
D = 40.57					D = 15.29	
49.652	61.105	− 1	− 3	20.076	30.034	−18
38.799	61.692	+ 3	+ 5	16.056	31.217	+18
29.285	62.308	+ 3	+ 7	12.044	32.716	+ 1
19.788	63.063	− 5	− 3	8.210	34.663	−20
9 909	64.154	+ 2	− 2	4.412	37.543	+ 7
D = 29.79					D = 12.81	
41.508	49.199	− 3	± 0	15.942	23.882	+ 2
32.302	49.963	+ 6	+ 4	12.490	25.192	+ 1
24.306	50.762	+ 9	− 2	9.446	26.739	+ 3
16.741	51.694	− 7	− 8	6.169	29.088	+ 1
9.294	52.923	+ 3	+ 6	3.256	32.355	+ 1

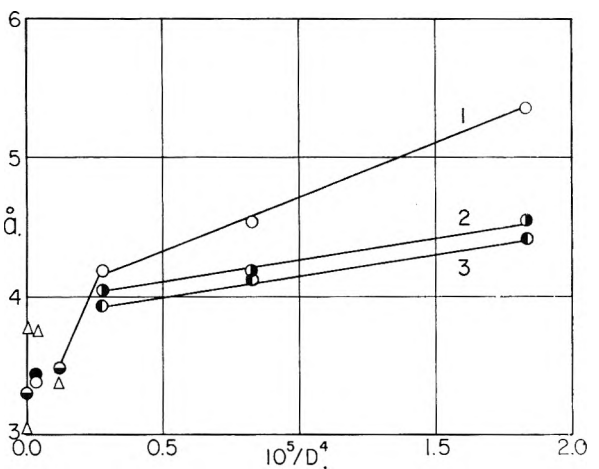

Fig. 1.—Variation of calculated contact distance a_J with dielectric constant.

$\mathring{a}$ = 5.12 ± 0.02, but since the values of K_A and Λ_0 for this system do not seem consistent with the other values, and since a little oxidation was noted during this run, we feel that this run should be disregarded for the present discussion, despite its favorable result.) At D = 15.29, $\mathring{a}$ = 5.35 ± 0.19; there is a slow decrease to $\mathring{a}$ = 4.18 ± 0.17 at D = 24.44 and then an abrupt drop in water. The last value was clearly too small; computation by the program for unassociated electrolytes (equation 1 with $\gamma = 1$, $K_A = 0$) gave the more realistic value $\mathring{a}$ = 2.76 ± 0.04.

Using the experience gained in the work with potassium chloride,[4] a systematic study of the form of equation 1 was made. By including the next highest term in the activity coefficient[9] as tabulated by Gronwall, LaMer and Sandved[10] the variation was reduced to $4.54 \pm 0.12 \geqslant \mathring{a} \geqslant 4.04 \pm 0.14$ for $15.29 \leqslant D \leqslant 24.44$, but the sharp drop from here to water still persisted (curve 2, Fig. 1). About the same behavior (curve 3, Fig. 1) resulted from using the activity coefficient for point charges

$$-\ln f = \beta'(c\gamma)^{1/2} \qquad (2)$$

It is clear that the Debye–Hückel equation

$$-\ln f = \beta'(c\gamma)^{1/2}/(1 + \kappa a) \qquad (3)$$

gives too large an activity coefficient; whether ln f is increased numerically by adding the Gronwall term or by omitting the division by $(1 + \kappa a)$, about the same result is achieved in decreasing the variation of $\mathring{a}$ over the moderate-to-low range of dielectric constants. One might argue that the second method (point charge formula) is more consistent with the rest of the development; including the Gronwall term in the activity means including terms of higher order in the ionic potential than were retained in the derivation of the relaxation and electrophoresis terms of (1). We might then logically argue that the hypothesis of ion association *per se* takes care of all short range effects of ionic forces on thermodynamic properties, and therefore that (2) is the correct function to use for the description of long range interionic effects; after all, ions not in contact can only feel the effects of their mutual *charges*.

Using the system with D = 15.29, a more detailed study of the conductance equation was made; we mention in passing that this would have been a hopelessly tedious undertaking without the electronic computer. Results of these calculations are summarized in Table III, where the method of computation is indicated symbolically in the first column. Using the Debye–Hückel equation

TABLE III

CESIUM IODIDE IN DIOXANE-WATER AT D = 15.29

Function	$\mathring{a}$	K_A	Λ_0
DH (3)	5.96 ± 0.19	361 ± 15	45.65 ± 0.09
DH + J_2	5.35 ± .19	340 ± 16	45.59 ± .10
DH + Δ_3	5.16 ± .20	378 ± 23	45.77 ± .15
DH + J_2 + Δ_3	4.54 ± .12	363 ± 17	45.75 ± .11
PC (2)	4.95 ± .12	336 ± 14	45.62 ± .09
PC + J_2	4.55 ± .12	319 ± 15	45.57 ± .10
DH + J_2 + ΔD	4.75 ± .13	359 ± 15	45.69 ± .10
PC + J_2 + ΔD	4.16 ± .08	353 ± 13	45.72 ± .09
DH + J_2'	4.80 ± .19	319 ± 18	45.54 ± .11
DH + J_2''	3.82 ± .19	277 ± 21	45.42 ± .14

(3) for the activity gives $\mathring{a}$ = 5.96 if the J_2 term in the conductance[11] is neglected, and $\mathring{a}$ = 5.35 if it is retained. If we use the value of $\mathring{a}$ as a criterion and assume that the correct function will give a value of $\mathring{a}$ independent of solvent composition and in agreement with the value from the aqueous system (where association is negligible), then inclusion of J_2 is an improvement. Including the Gronwall term (DH + Δ_3) also reduces $\mathring{a}$ by about the same

(9) Ref. 4, equation 2.

(10) T. H. Gronwall, V. K. LaMer and K. Sandved, *Physik. Z.*, **29**, 358 (1928).

(11) D. S. Berns and R. M. Fuoss, *J. Am. Chem. Soc.*, **82**, 5585 (1960); equation 3.

amount as inclusion of J_2; if both higher order terms are included, the value 4.54 results. Nearly the same decrease is obtained by using the simple point charge (PC) equation in the activity coefficient (*i.e.*, by dropping all κa terms in f), and if J_2 is retained and the point charge formula is used, $\mathring{a}$ is found to be 4.55.

Another effect which can contribute to the c-term in the conductance equation is the polarization of the ionic atmosphere in the external field which changes the dielectric constant due to the virtual dipole produced. The polarization of the atmosphere is responsible for the relaxation and electrophoresis terms, and has been explicitly included there, but for long range effects, the altered dielectric constant should be used in calculating the activity coefficient which of course appears in the conductance equation when the association term is present. This effect, as shown by Debye and Falkenhagen,[12] gives

$$D = D_0 + A\L\kappa a \qquad (4)$$

where $A = (2 - 2^{1/2})/6$ for 1–1 salts. Inclusion of this correction to the dielectric constant with Debye–Hückel and point charge equations for the activity leads to $\mathring{a}$-values of 4.75 and 4.16, respectively.

Another approach was made on the basis of the argument that in addition to J_2, there are necessarily present other terms of order $c^{3/2}$ which were neglected in the derivation of the present equation. For $\mathring{a} = 5.35$, $J_2 = 5044$. Replacing this value by the arbitrarily chosen values 1×10^4 and 2×10^4 gives $\mathring{a} = 4.80$ and 3.82, with no significant change in the standard deviation σ of $\Delta\Lambda$. On the other hand, using a smaller pre-set value of a in $J(a)$, thereby forcing the computer to deliver a smaller value of K_A quickly increases the deviation: for example, at $D = 15.29$, the standard program gave $\mathring{a} = 5.99 \pm 0.20$, $K_A = 362 \pm 15$ and $\sigma = 0.013$. Using $\mathring{a} = 3.82$ (the sum of the crystallographic radii) gave $K_A = 134 \pm 64$, $\sigma = 0.15$, while a pre-set $\mathring{a} = 2.89$ (hydrodynamic value) gave $K_A = -21 \pm 113$, $\sigma = 0.27$. Similar results were obtained for systems with larger D. These calculations strongly suggest that the numerical value of J obtained from the data by use of (1) is correct, but that the functional form of $J(a)$ requires some revision. Also, the fact that arbitrarily changing J_2 improves matters suggests that the function used for the activity coefficient needs further study.

No decision regarding the choice of the best function can be made on the basis of the closeness of the fit of the equation to the data; the standard deviation in the parameters was not significantly affected by any of the above modifications (except those in which a was pre-set) in the higher terms. For the present, the most favorable statement we can make about a-values derived from the J-term of the conductance equation for *associated* electrolytes is that they are established within a factor of two. There are so many plausible sources of c and especially $c^{3/2}$ terms in the conductance equation beyond the ones considered so far that any attempt to draw conclusions about physical effects such as solvation from a systematic change of a with solvent composition seems both futile and hazardous. The difficulty is, of course, fundamental; the J-term in the conductance equation is a second-order term and by its nature is forced to absorb both experimental and theoretical uncertainties which rapidly become greater with decreasing dielectric constant.

The "best" values of Λ_0, K_A and $\mathring{a}$ (*i.e.*, those based on equation 1 and using the Debye–Hückel activity) are summarized in Table IV. A plot of log K_A against $1/D$ is shown in Fig. 2 (upper curve);

TABLE IV

CONSTANTS FOR CESIUM IODIDE IN DIOXANE–WATER MIXTURES AT 25°

D	Λ_0	a_1	K_A
78.54	154.16 ± 0.02	2.76 ± 0.04	0
60.18	99.45 ± .02	3.76 ± .04	0
40.57	66.899 ± .006	3.73 ± .02	0
29.79	56.434 ± .007	3.36 ± .01	0
24.44	52.26 ± .03	4.18 ± .17	19.6 ± 2.5
18.68	48.21 ± .08	4.53 ± .19	88 ± 8
15.29	45.42 ± .12	5.05 ± .18	310 ± 17
15.29	45.59 ± .10	5.35 ± .19	340 ± 16
12.81	41.68 ± .02	5.12 ± .02	760 ± 3

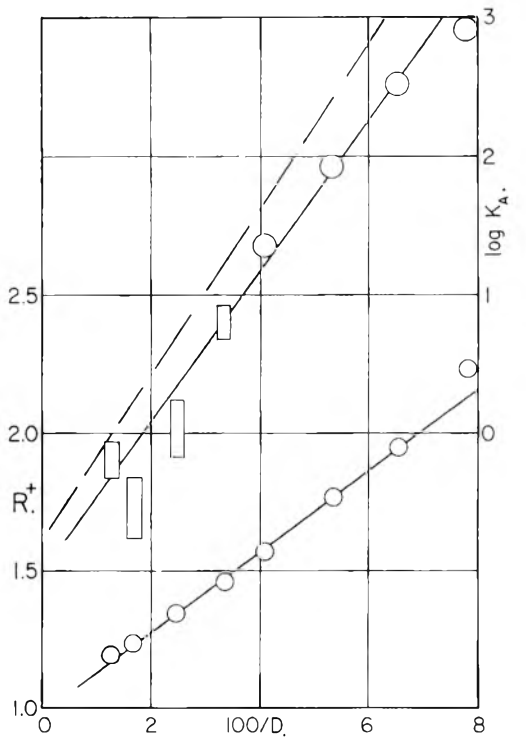

Fig. 2.—Dependence of association constant and Sutherland radius on dielectric constant: dashed curve, association constants computed by equation 5 with $\mathring{a} = 4.1$.

like potassium chloride, the curve is concave-down, but shows considerably less curvature. The values shown as open rectangles (for large values of D) were obtained by the Λ_K method, using $\mathring{a} = 4.1$. The dotted line in the figure is the theoretical curve[13] corresponding to

$$K_A = (4\pi Na^3/3000) \exp(e^2/aDkT) \qquad (5)$$

It will be seen that a small vertical displacement

(12) P. Debye and H. Falkenhagen, *Physik. Z.*, **29**, 121, 401 (1928).

(13) R. M. Fuoss, *J. Am. Chem. Soc.*, **80**, 5059 (1958).

will give quite good agreement with all the experimental points; this displacement would call for a Gilkerson[14] term $E_s \approx -kT$ in the above equation. The tendency of the log K_A *vs.* $1/D$ curve to become concave-down in the range of low dielectric constants again suggests that (2) is a better approximation than (3) for the activity coefficient. The various modifications discussed above, which reduce f^2, would give larger numerical values of K_A from a given set of data, leaving the cJ term essentially unchanged, with the result that "better" values of K_A would be obtained.

The limiting conductance of cesium iodide in water is 154.16 which is 0.06 unit higher, as expected, than the value 154.10 obtained by adding Voisinet's value[15] of 77.2_6 for cesium to Zeldes' value[16] of 76.8_4 for iodide. (The literature values were obtained by a Shedlovsky extrapolation, which gives a value which is slightly less than the correct limit; see ref. 5, Fig. 15.1).

The Walden products for cesium iodide give a monotone function of composition (*i.e.*, no maximum, as was found for potassium chloride). If the water point is omitted, the apparent Stokes radii are given within 0.1–1.0% by the equations

$$10^8 R(Cs^+) = 0.9724 + 14.81/D \quad (6)$$

$$10^8 R(I') = 0.9774 + 14.89/D \quad (7)$$

The corresponding graph for Cs^+ is shown in Fig. 2, lower curve. As was found for potassium chloride, the limiting values for infinite D are unreasonably small. If the Sutherland coefficient[17] $4\pi\eta$ is used in place of the Stokes factor $6\pi\eta$, in order to allow for slippage of ions through a discontinuous medium of water molecules (which are of the same order of size as the ions involved), the corrected sum of the radii becomes 1.5 (1.950) = 2.93 = δ_A. This is still smaller than the sum of the crystallographic radii (3.85), but nearer the value a_J = 2.76 obtained from the conductance data in water, using the program for unassociated electrolytes. The value of a_A for potassium chloride was found to be 2.53. The sequence for the two salts is in agreement with the observation that the association of KCl is greater than that for CsI at a given value of dielectric constant; for example, at D = 15.37 K_A(KCl) = 500 while for CsI at D = 15.29, K_A = 310. This is also the sequence which would be predicted from the crystallographic radii; the discrepancy in absolute values between the sizes of the lattice ions and those of the models from conductance, however, remains at present unexplained. Further work on other alkali halides is in progress.

(14) W. R. Gilkerson, *J. Chem. Phys.*, **25**, 1199 (1956).

(15) W. E. Voisinet, Dissertation, Yale University, 1951; B. B. Owen, *J. chim. phys.*, **49**, C-72 (1952).

(16) B. B. Owen and H. Zeldes, *J. Chem. Phys.*, **18**, 1083 (1950).

(17) W. Sutherland, *Phil. Mag.*, **9**, 781 (1905).

ELECTRIC DIPOLE MOMENTS OF SOME DISUBSTITUTED CYCLOHEXANE DERIVATIVES IN THE VAPOR STATE[1]

BY MAX T. ROGERS AND JAMES M. CANON

Department of Chemistry, Michigan State University, East Lansing, Michigan

Received March 28, 1961

The electric moments of *trans*-1,2-dibromocyclohexane, *trans*-1,2-dichlorocyclohexane, *trans*-1-chloro-2-bromocyclohexane and 1,4-cyclohexanedione have been measured in the vapor phase. Ratios of conformational isomers and energy differences between them have been estimated from the data and compared with values in the literature derived from measurements in solution. The comparison has revealed an anomalous solvent effect.

Introduction

The *trans*-1,2-dihalogenocyclohexanes have two conformational isomers, I (1*a*-2*a*) and II (1*e*-2*e*), which differ in electric moment, and under any

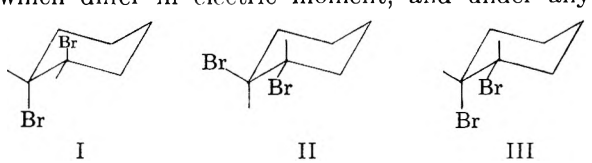

I II III

given conditions these substances exist as a mixture of the two forms. The electric moment of I, in which the substituents are both axial, is zero while that of II, in which the substituents are both equatorial, should have essentially the same value as that observed for the corresponding *cis*-isomer. The two conformations of the *cis*-isomer (III), 1*a*-2*e* and 1*e*-2*a*, have identical electric moments. It is possible, therefore, to compute the ratio of isomers from the observed electric moment and, assuming the Boltzmann distribution, to derive the difference in energy between the isomers. Such measurements have been made for *trans*-1,2-dichlorocyclohexane,[2-4] *trans*-1,2-dibromocyclohexane,[3,4] and *trans*-1-chloro-2-bromocyclohexane[5] in solution. The only vapor measurement reported is for *trans*-1,2-dichlorocyclohexane at a single temperature.

Since energy differences between conformational isomers would be expected to depend on solvent we have measured the electric moments of the above series of cyclohexane derivatives in the vapor state over as wide a temperature range as possible. The data have been used to compute ratios of conformational isomers and energy differences and our results have been compared with related values reported in the literature.

(1) Supported by a grant from the National Science Foundation.

(2) A. Tulinskie, A. DiGiacomo and C. P. Smyth, *J. Am. Chem. Soc.*, **75**, 3552 (1953).

(3) K. Kozima, K. Sakashita and S. Maeda, *ibid.*, **76**, 1965 (1954).

(4) P. Bender, D. L. Flowers and H. L. Goering, *ibid.*, **77**, 3463 (1955).

(5) W. Kwestroo, F. A. Meyer and E. Havinga, *Rec. trav. chim.*, **73**, 3563 (1955).

The electric moment observed for 1,4-cyclohexanedione in solution[6,7] has been attributed to an equilibrium mixture of chair and boat forms (IV and V or VI, respectively) of the molecule. We have measured the moment of this substance in the vapor phase to provide an estimate of the ratio of these forms and the energy difference between them in the vapor state.

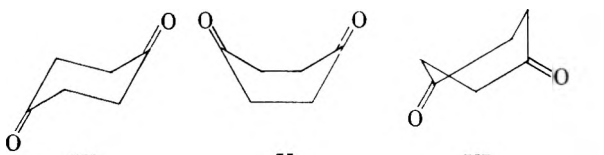

IV V VI

Materials.—*trans*-1,2-Dichlorocyclohexane and *trans*-1,2-dibromocyclohexane were synthesized by addition of the respective halogen to cyclohexene.[8] *trans*-1-Chloro-2 bromocyclohexane was prepared by bubbling hydrogen chloride gas into a slurry of N-bromosuccinimide, chloroform and cyclohexene.[5] These materials were purified by fractional distillation *in vacuo*. The 1,4-cyclohexanedione was a commercial sample (B and H Organic Chemicals Co.) purified by recrystallization from water and benzene.

Apparatus.—The apparatus for measurement of electric moments in the vapor phase has been described.[9] The pressure in the measuring cell was balanced against an inert gas in a mercury manometer by a diaphragm-type pressure transmitter and the pressure read on the manometer. The sample container, measuring cell and connecting tubing were electrically heated to the desired temperature. Because of slow decomposition of the samples at the higher temperature a fresh sample was used for each capacitance measurement. The sample was degassed *in vacuo* then distilled into the measuring cell.

Calculations.—Values of the molar polarization P of the vapor at each temperature were obtained from the pressure and capacitance readings in the usual manner.[9] Van der Waals' equation was used to compute the gas densities and the van der Waals constants a and b estimated from data for related substances. The temperature range covered was limited so that it was necessary to use the refractivity method and compute the electric moment from the equation

$$\mu = 0.0128\sqrt{(P - MR_D)T}$$

where the molar refraction MR_D was computed from observed refractive indices and densities of the liquids.

Estimated errors in the electric moments were computed from the standard deviation for ϵ and average about $\pm$ 0.1 D.

The temperature range was limited by the vapor pressure on the lower end and by decomposition on the higher end of the temperature range. The total range was only about 25° which made it impossible to obtain the distortion polarization experimentally. Our assumption that the atomic polarization is negligible therefore introduces some uncertainty into the results, especially for 1,4-cyclohexanedione.

Results and Discussion

The electric moments found for the four substances studied are shown in Table I along with the observed dielectric constants, ϵ, and molar polarizations, P, of the vapors. The mole fraction of molecules in the 1*e*-2*e* configuration, x_{ee}, may be computed, assuming an equilibrium between the 1*a*-2*a* and 1*e*-2*e* forms, from the equation

$$\mu^2 = (n_{ee}m_{ee}^2 + n_{aa}m_{aa}^5)/(n_{ee} + n_{aa}) = x_{ee}m_{ee}^2 + x_{aa}m_{aa}^2$$

For the three *trans*-1,2-dihalogenocyclohexanes we have used $m_{aa} = 0$ and taken for m_{ee} the value 3.12 D, which is the moment found for *cis*-1,2-dichlorocyclohexane in the vapor state.[2] The difference between the C–Cl and C–Br bond moments is small in these compounds and has here been neglected. Since the change in dipole moment over the small temperature range employed was less than the errors of measurement the mean value of μ at the mean temperature has been used in computing x_{ee}. The energy difference $\Delta E = E_{aa} - E_{ee}$ has been obtained from the Boltzmann equation assuming that the partition functions of the two forms are equal

$$n_{aa} = n_{ee}\exp(E_{aa} - E_{ee})/RT$$

The values of x_{ee} and ΔE obtained in this way are shown in Table II along with the various values which have been reported in the literature. The only substance previously studied in the vapor state is *trans*-1,2-dichlorocyclohexane and our value for the electric moment agrees well with that reported by Tulinskie, *et al.*[2]

The diequatorial form I is more stable than the diaxial form II for *trans*-1,2-dichlorocyclohexane in the vapor and in all solvents so far studied whereas the diaxial form is always the more stable for *trans*-1,2-dibromocyclohexane. It has been suggested[4] that this is a consequence of the greater crowding in the 1*e*-2*e* form with the larger bromine atom. In the case of *trans*-1-chloro-2-bromocyclohexane the two forms are of very nearly equal stability in the vapor phase while benzene favors the 1*e*-2*e* form and carbon tetrachloride the 1*a*-2*a* form.

The change in ΔE in going from solvent to vapor is fairly constant for the three substances studied. Using mean values we find ΔE(benzene) $- \Delta E$(g) = 400 cal./mole, and $\Delta E(CCl_4) - \Delta E$(g) = $-$170 cal./mole; also E(*n*-heptane) $- \Delta E$(g) = $-$170 cal./mole from data for *trans*-1,2-dibromochlorohexane only.[3] It would be expected that the energy of the polar 1*e*–2*e* form would be lowered in a solvent relative to its energy in the vapor state whereas the non-polar 1*a*-2*a* form would have unchanged energy. The value ΔE(solvent) $- \Delta E$(g) = 300 cal./mole was computed theoretically by Tulinskie, *et al.*, for *trans*-1,2-dichlorocyclohexane in a solvent of dielectric constant $\epsilon \cong 2.2$. Since the dielectric constants (at 25°) of benzene (2.27), carbon tetrachloride (2.24) and *n*-heptane (1.92) do not differ

TABLE I

DIELECTRIC CONSTANTS, MOLAR POLARIZATIONS AND ELECTRIC MOMENTS OF SOME CYCLOHEXANE DERIVATIVES IN THE VAPOR STATE

T, °K.	$(\epsilon - 1) \times 10^6$	P, cc./mole	μ, D
	trans-1,2-Dichlorocyclohexane		
441.8	9379	110.7	2.30
468.2	8356	97.7	2.28
	trans-1-Chloro-2-bromocyclohexane		
448.5	8925	117.1	2.21
467.5	8103	101.6	2.17
	trans-1,2-Dibromocyclohexane		
448.5	8144	97.2	2.00
467.5	7566	94.9	1.99
	1,4-Cyclohexanedione		
468.2	4205	52.8	1.39
490.3	4071	53.6	1.44

(6) O. Hassel and E. Naeshagen, *Tidsskr. Kjemiog. Bergvesen*, **10**, 81 (1930).

(7) C. G. LeFèvre and R. J. W. LeFèvre, *J. Chem. Soc.*, 1696 (1935).

(8) H. Greengard, "Organic Syntheses" Vol. XII, John Wiley and Sons, New York, N. Y.

(9) M. T. Rogers and James M. Canon, unpublished results.

TABLE II

MOLE FRACTIONS OF CONFORMATIONAL ISOMERS, AND ENERGY DIFFERENCES BETWEEN THEM, FOR SOME CYCLOHEXANE DERIVATIVES

	This research		Literature		
Substance	x_{ee}	$\Delta E = E_{aa} - E_{ee}$	ΔE (g)	ΔE (bz)	ΔE(CCl$_4$)
trans-1,2-Dichlorocyclohexane	0.54	140[b]	100	300[2]	− 50[3]
				400[3]	+140[5]
				650[4]	
				820[6]	
trans-1,2-Dibromocyclohexane	0.41	−330		−80[3]	−500[3]
				−70[4]	−400[4]
				−70[5]	−700[5]
trans-1-Chloro-2-bromocyclohexane	0.49	−30		370[4]	−220[5]
				560[5]	
1,4-Cyclohexanedione[a]	0.88	1900		1300[7]	

[a] x = fraction. [b] All energy values are in cal./mole.

much the difference in ΔE would be expected to be about the same in all three cases. The reversal of the sign of ΔE(solvent) $-\Delta E$(g) in the case of carbon tetrachloride and *n*-heptane indicates that the above theory is not adequate. Specific solvent effects may exist which stabilize the non-polar 1*a*-2*a* form in these solvents, contrary to the prediction of electrostatic theory, or Δs may not be zero.

The apparent dipole moment of 1.4 *D* observed for 1,4-cyclohexanedione in the vapor state corresponds to about 12% of the boat form V if equilibrium between forms IV and V is assumed. The energy difference $\Delta E = E(\text{boat}) - E(\text{chair}) = 1900$ cal./mole is computed on this latter assumption. However, these calculations have two serious defects. First, the atomic polarization, which we have neglected, may be exceptionally large for this molecule and a value $P_A = 10$ cc./mole is not unreasonable by analogy with 1,4-benzoquinone.[10] This would reduce the experimental moment to 1.1 *D*. Second, the boat forms of type VI may be present since they presumably do not differ much in energy from V. If the energy of forms V and VI is assumed equal the total contribution of these forms (neglecting atomic polarization) would be 22% and ΔE would become 2250 cal./mole. The value of ΔE does decrease on going from vapor to benzene solution as would be expected if the polar boat form is stabilized in solution relative to the non-polar chair form.

(10) C. P. Smyth, "Dielectric Behavior and Structure," McGraw-Hill Book Co., Inc., New York, N. Y., 1955.

THE DECOMPOSITION KINETICS OF LITHIUM PERCHLORATE

BY MEYER M. MARKOWITZ AND DANIEL A. BORYTA

Foote Mineral Co., Research and Engineering Center, Chemicals Division, P. O. Box 513, West Chester, Pa.

Received April 1, 1961

The thermal decomposition of pure lithium perchlorate and in admixtures with lithium chloride was studied over the temperature range of 392–415° by constant temperature thermogravimetry. It is shown by phase data that above 247° any mixture of lithium perchlorate with its decomposition product, lithium chloride, always contains the perchlorate in solution. Over the temperature range covered, the kinetics follow the autocatalytic Prout–Tompkins rate law ($E_{Act.}$ = 52.2 ± 4.1 kcal./mole) up to about 40% decomposition and then conform to first-order kinetics ($E_{Act.}$ = 62.0 ± 4.1 kcal./mole). The point of transition between the two rate laws occurs when the decomposing melt is saturated with lithium chloride. From the kinetic data, the solubility of lithium chloride in the melts was computed and a kinetically derived value for the heat of fusion of lithium chloride was obtained. The relationship of these studies to the thermal decompositions of the other alkali metal perchlorates is discussed.

Introduction

The participation of a thermally decomposing material in the phase change from the solid to the liquid state usually complicates the observed kinetics.[1] Thus, potassium perchlorate has been reported to decompose according to two first-order rate laws[2,3]; one characteristic of the solid-phase decomposition and the other of the liquid-phase. Differential thermal analysis studies[4–6] of rubidium and cesium perchlorates have demonstrated the concomitant occurrence of fusion and decomposition phenomena, thereby indicating complex kinetics for these compounds. Lithium perchlorate,[4–6] on the other hand, shows a considerable temperature interval between fusion (247°) and measurable rates of reaction (392–415°).[7] Accordingly, it was felt that a study of the thermal breakdown of lithium perchlorate would be of interest inasmuch as the salt probably would be in the liquid phase during the entire period of decomposition. Thus, the system $LiClO_4$–LiCl was studied and the quantitative kinetic behavior of lithium perchlorate and of mixtures of lithium perchlorate with lithium chloride was investigated.

(1) C. E. H. Bawn in "Chemistry of the Solid State," edited by W. E. Garner, Academic Press, New York, N. Y., 1955, pp. 254–267.

(2) A. E. Harvey, Jr., M. T. Edmison, E. D. Jones, R. A. Seybert and K. A. Catto, *J. Am. Chem. Soc.*, **76**, 3270 (1954).

(3) A. E. Harvey, C. J. Wassink, T. A. Rodgers and K. H. Stern, *Ann. N. Y. Acad. Sci.*, **79**, 971 (1960).

(4) M. M. Markowitz, *J. Phys. Chem.*, **62**, 827 (1958).

(5) M. M. Markowitz and D. A. Boryta, *ibid.*, **64**, 1711 (1960).

(6) M. M. Markowitz, D. A. Boryta and R. F. Harris, *ibid.*, **65**, 261 (1961).

Experimental

Anhydrous lithium perchlorate, prepared as previously reported,[2] was analyzed for perchlorate content by precipitation as nitron perchlorate.[8] Chloride was determined gravimetrically as silver chloride and chlorate was computed as the additional chloride produced after reduction by sulfurous acid. Analysis of product: ClO_4^-, 93.4 (calcd.,

(7) M. M. Markowitz and D. A. Boryta, *Anal. Chem.*, **32**, 1588 (1960).

(8) F. P. Treadwell and W. T. Hall, "Analytical Chemistry," Vol. II, John Wiley and Sons, Inc., New York, N. Y., Ninth English Edition, 1942, pp. 383–384.

93.5); Cl^-, 0.00; ClO_3^-, 0.00. Reagent grade lithium chloride, dried under vacuum at 150° for 12 hours, was analyzed for chloride content. Analysis of product: Cl^-, 83.4 (calcd., 83.6). All materials were stored in a desiccator over phosphorus pentoxide.

The System $LiClO_4$–LiCl.—The phase relationships between lithium perchlorate and lithium chloride were determined by differential thermal analysis and by visual observations of the liquidus temperatures.[4,6,9] For the former studies, sample compositions varying from pure lithium perchlorate to pure lithium chloride in 10 mole % increments were used; for the latter studies, sample compositions from 100 mole % $LiClO_4$ to 90 mole % $LiClO_4$ were covered. Because of the thermal instability of the mixtures at elevated temperatures, these experiments were only carried out to about 300°. The persistence of an endothermic break at about 235° over the entire range of composition in the differential thermal analysis runs indicated the system to be of the simple eutectic type and the observations of liquidus temperatures gave the corresponding eutectic composition at 91.0 mole % $LiClO_4$.

To extend the phase diagram to higher temperatures, the Clapeyron–Clausius equation was applied to the entire system.[10] The heat of fusion of lithium perchlorate[5] was taken to be 3.8 kcal./mole and that of lithium chloride,[11] as 4.7 kcal./mole. The computed eutectic was found to be at 87.2 mole % $LiClO_4$ and 228°, in good agreement with the experimental values. A comparison of these two sets of data is presented in Table I. Clearly, at temperatures of 247° and above, any mixture of lithium perchlorate and lithium chloride will always contain the lithium perchlorate in solution.

TABLE I

THE SYSTEM $LiClO_4$–LiCl

Mole % $LiClO_4$	Liquidus temp., °C. Calcd.	Exptl.[a]	Eutectic temp., °C., exptl.[b]
100.0	247.0	247	..
97.5	242.8	245	..
95.0	239.9	239	..
92.5	236.2	238	..
91.25	234.4	237	..
91.0	234.0	236 (eutectic)	..
90.5	233.4	239	..
90.0	232.5	252	240
87.2	228.0 (eutectic)	..	..
85.0	245.5	..	..
80.0	280.1	..	242
70.0	338.5	..	235
60.0	387.6	..	232
50.0	431.6	..	233
40.0	472.1	..	236
30.0	510.1	..	232
20.0	546.3	..	232
10.0	581.3	..	230
0.0	615.0	..	..

[a] By visual observation. [b] By differential thermal analysis.

The Products of Decomposition of Lithium Perchlorate.—Earlier studies had shown that the over-all decomposition of lithium perchlorate could be represented by the equation[6,7,12–14]: $LiClO_4 \rightarrow LiCl + 2O_2$. During the present study, chemical analyses were performed on the decomposition residues from two-gram samples of lithium perchlorate which had been maintained at 413 ± 3° for varying periods of time. In this way it was hoped to determine the existence of appreciable amounts of reaction intermediates and side reactions. Small quantities of a lower oxyhalide (assumed to be chlorate) were present in the partially decomposed materials. The alkalinity of the residues, determined as % Li_2O by titration with standard acid, indicates some slight loss of chlorine or chlorine oxides during decomposition. Chloride was determined volumetrically with silver nitrate by Mohr's method and chlorate was found as additional chloride after reduction of the sample with sulfurous acid. Lithium perchlorate was computed by difference from 100.00% of the sum of the three separate analyses. The data are summarized in Table II.

TABLE II

COMPOSITION (IN WT. %) OF LITHIUM PERCHLORATE SAMPLES HEATED AT 413 ± 3°

Time, min.	% $LiClO_4$ (by diff.)	% $LiClO_3$	% Li_2O	% LiCl	% Dev.[a]
50	98.28	0.60	0.00	1.12	+0.3
80	93.45	1.34	.02	5.19	+1.0
90	91.10	1.35	.03	7.52	+1.0
105	79.85	1.72	.04	18.39	+0.8
110	78.74	1.80	.04	19.42	+0.9
115	69.36	2.03	.05	28.56	+0.8
130	58.70	1.28	.08	39.94	−1.5
140	45.99	0.53	.10	53.38	−4.0
160	37.40	0.85	.12	61.63	−4.7
260	5.25	0.00	.14	94.61	...

[a] $100\left[\frac{\%\ LiClO_4 \text{ from weight loss data}}{\%\ LiClO_4 \text{ from chemical analyses}} - 1\right]$.

The lithium perchlorate contents of the samples of Table II were compared with the compositions derived from the weight losses of the samples. Close agreement between the two sets of values was found. This is indicated in the last column of Table II by the per cent. deviation of the lithium perchlorate content determined by weight loss measurement from that determined by chemical analysis of the decomposition residues. Accordingly, it was concluded that a convenient means of following the progress of reaction would be by constant temperature thermogravimetry.

Constant Temperature Thermogravimetric Analysis of Lithium Perchlorate and Lithium Perchlorate–Lithium Chloride Mixtures.—Differential thermal analysis studies of the alkali metal perchlorates show that at the temperatures of rapid decomposition, the reactions are exothermic.[5,6] Accordingly, it was necessary to determine the maximum temperature at which lithium perchlorate could be decomposed without self-heating and consequent departure from isothermal conditions. Constant temperature differential thermal analyses were run on two-gram samples of lithium perchlorate at temperatures below those of rapid decomposition in a dynamic differential thermal analysis experiment (472°). The maximum temperature at which the decomposing mass remained at the furnace temperature through to complete decomposition of the sample was about 420°. It was necessary to carry out these experiments to complete decomposition because the heat release from the sample increases as solid lithium chloride forms and the heat of decomposition is augmented by the heat of crystallization of the lithium chloride. Thus, the thermal decomposition of a molten alkali metal perchlorate must usually be represented by two general equations,[5,15] *viz.*, (a) X^ICIO_4 (solution) $\rightarrow X^ICl$ (solution) + $2O_2$ (gas), ΔH_a, and (b) X^ICIO_4 (solution) $\rightarrow X^ICl$ (solid) + $2O_2$ (gas), ΔH_b, and $\Delta H_b - \Delta H_a = -\Delta H_{fusion}\ X^ICl$. In the present studies, isothermal experiments were carried out to a maximum temperature of about 415° using sample weights containing 0.5–0.8 g. of lithium perchlorate.

The instrumentation attendant to and the arrangement of the recording balance and the furnace have already been described.[7] A new furnace was constructed for the investigations reported here. This 20″ vertical furnace consisted of a 1 3/8″ Vycor tube uniformly wound with asbestos-

(9) M. M. Markowitz and R. F. Harris, *J. Phys. Chem.*, **63**, 1519 (1959).

(10) W. C. McCrone, Jr., "Fusion Methods in Chemical Microscopy," Interscience Publishers, Inc., New York, N. Y., 1957, pp. 156–157.

(11) National Bureau of Standards Report No. 6297, U. S. Department of Commerce, Washington, D. C., Jan. 1, 1959, pp. 31, 72.

(12) G. G. Marvin and L. B. Woolaver, *Ind. Eng. Chem., Anal. Ed.*, **17**, 474 (1945).

(13) T. W. Richards and H. H. Willard, *J. Am. Chem. Soc.*, **32**, 4 (1910).

(14) T. W. Richards and M. W. Cox, *ibid.*, **36**, 819 (1914).

(15) M. M. Markowitz, *J. Phys. Chem.*, **61**, 505 (1957).

covered nichrome ribbon. The exterior of the furnace was heavily insulated with asbestos tape and pipe lagging. A two-inch zone of constant temperature was found in the furnace interior by movement of a thermocouple through the capped bottom of the furnace. During a run the sample was contained in a small test-tube suspended by a platinum wire from the balance above the furnace. The wire entered the furnace through a ceramic cap with a radial slit along the length of the cap. The sample was consistently placed about 1/4" from the measuring thermocouple in the isothermal region of the furnace.

Close temperature regulation (±0.2°) was achieved with an electronic controller by using the series-connected output from three thermocouples placed about the circumference of the Vycor tube and sandwiched between the tube and the heating elements. The cold junctions of the thermocouples were kept in a constant temperature bath.

In each experiment the sample was preheated for ten minutes at 275° and then suspended quickly from the balance into the furnace below. By using a stepping-switch, furnace temperature and weight changes were alternately recorded on a potentiometric strip-chart recorder of known speed. Weight loss–time measurements were made on three types of samples: pure $LiClO_4$, $LiClO_4$ (95 mole %)–LiCl (5 mole %), and $LiClO_4$ (50 mole %)–LiCl (50 mole %), and over the temperature range from about 392 to 415°.

Results

Pure Lithium Perchlorate.—A typical decomposition–time curve for pure lithium perchlorate is shown in Fig. 1. A long induction period, followed by rapid acceleration and slow decay is evident. The presence of the induction period gives rise to the sigmoid curve usually characteristic of the autocatalytic decompositions of many solids.[16] Because the decomposition of the lithium perchlorate proceeds from the liquid phase over the entire extent of decomposition, it was thought that a single rate law might be applicable. The data for a representative set of results as obtained at 391.8° are given in Fig. 2 in terms of a first-order plot (ln (W_t/W_0) *versus* time, rate law: $d(W_t/W_0)/dt = -k_2(W_t/W_0)$, where W_t = weight of $LiClO_4$ present at time t and W_0 = original sample weight of $LiClO_4$) and a Prout–Tompkins[16–19] plot ($\ln(W_0 - W_t)/W_t$ *versus* time, rate law: $d(W_t/W_0)/dt = -k_1(W_t/W_0)((W_0 - W_t)/W_0)$). Neither rate law satisfies the experimental data over the complete course of reaction. Nevertheless, it appears that each law is valid over a limited region of decomposition and that the transition from the autocatalytic expression to the first-order equation occurs at about 40% decomposition. The functions (W_t/W_0) and $(W_0 - W_t)/W_t$ are, of course, equal at $W_t/W_0 = 0.618$, but this coincidence is irrelevant to the observed departures of the two rate laws from linearity in this region of decomposition. Equivalent results were obtained at the other temperatures studied. Table III contains a summary of the rate constant computed for the acceleratory period (k_1 from Prout–Tompkins plot) and for the decay period (k_2 from the first-order plot).

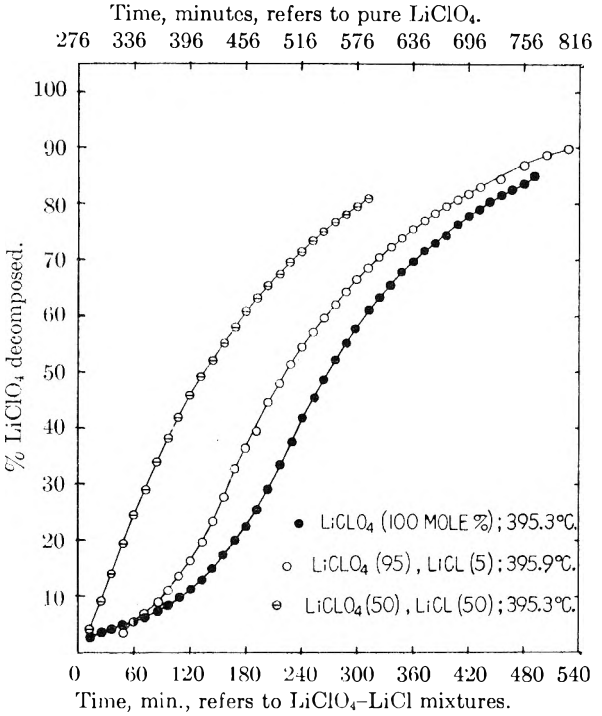

Fig. 1.—Typical decomposition–time curves for lithium perchlorate and for lithium perchlorate–lithium chloride mixtures.

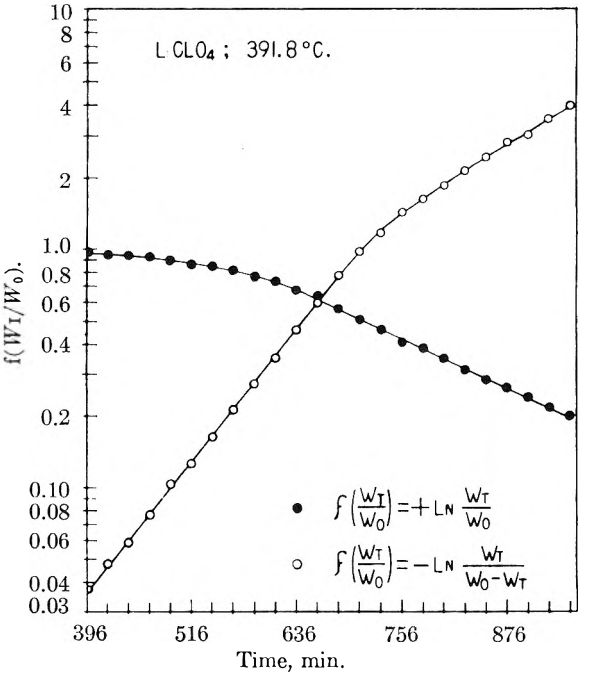

Fig. 2.—Integrated rate plots for pure lithium perchlorate at 391.8°.

Lithium Perchlorate (95 mole %)–Lithium Chloride (5 mole %) Mixtures.—A characteristic decomposition–time curve for this type of sample is seen in Fig. 1 for a run at 395.9°. The induction period is eliminated leaving only the acceleratory and decay sections. Rate law plots of the data for an experiment at 402.5° (Fig. 3) show the adherence to an autocatalytic law up to about 40% decomposition and then a transition to first-order kinetics. A tabulation of the corresponding values of k_1 and k_2 is given in Table IV.

Lithium Perchlorate (50 mole %)–Lithium Chlo-

(16) P. W. M. Jacobs and F. C. Tompkins in "Chemistry of the Solid State," edited by W. E. Garner, Academic Press, New York, N. Y., 1955, pp. 184–211.

(17) E. G. Prout and F. C. Tompkins, *Trans. Faraday Soc.*, **40**, 488 (1944); **42**, 468 (1946).

(18) P. J. Herley and E. G. Prout, *J. Inorg. and Nuclear Chem.*, **16**, 16 (1960).

(19) P. J. Herley and E. G. Prout, *J. Phys. Chem.*, **64**, 675 (1960).

TABLE III

RATE CONSTANTS FOR THE ACCELERATORY (k_1) AND DECAY (k_2) PERIODS OF DECOMPOSITION OF PURE LITHIUM PERCHLORATE

Temp., °C.	k_1, min.$^{-1}$	k_2, min.$^{-1}$	k_2/k_1, x_{LiCl}	x_{LiCl}, calc.	% dev.[a]
391.8	0.0106	0.00378	0.357	0.409	−12.7
395.3	.0137	.00536	.391	.417	−6.2
399.8	.0178	.00675	.380	.427	−11.0
404.7	.0222	.00943	.426	.438	−2.7
406.8	.0261	.0112	.443	.429	+3.2
410.5	.0312	.0137	.438	.451	−2.7
414.2	.0402	.0187	.472	.459	+2.9

[a] $100\left[\frac{x_{LiCl}}{x_{LiCl,\ calc.}} - 1\right]$.

TABLE IV

RATE CONSTANTS FOR THE ACCELERATORY (k_1) AND DECAY (k_2) PERIODS OF DECOMPOSITION OF LITHIUM PERCHLORATE IN A LITHIUM PERCHLORATE (95 MOLE %)–LITHIUM CHLORIDE (5 MOLE %) MIXTURE

Temp., °C.	k_1, min.$^{-1}$	k_2, min.$^{-1}$	k_2/k_1, x_{LiCl}	x_{LiCl}, calc.	% dev.[a]
391.5	0.0114	0.00392	0.399	0.409	−2.4
395.9	.0149	.00492	.329	.418	−21.3
398.8	.0205	.00724	.354	.425	−16.7
402.5	.0233	.00904	.387	.443	−10.6
409.5	.0332	.0126	.381	.449	−15.1
413.6	.0435	.0175	.403	.458	−12.0

[a] $100\left[\frac{x_{LiCl}}{x_{LiCl,\ calc.}} - 1\right]$.

ride (50 mole %) Mixtures.—These mixtures exhibited decomposition–time curves which were completely deceleratory (Fig. 1). From the phase data, this composition is saturated with lithium chloride at the decomposition temperatures studied here. Interpretation of the weight loss results in terms of a first-order law appears unequivocal as judged from inspection of Fig. 4 for a run at 406.6°.

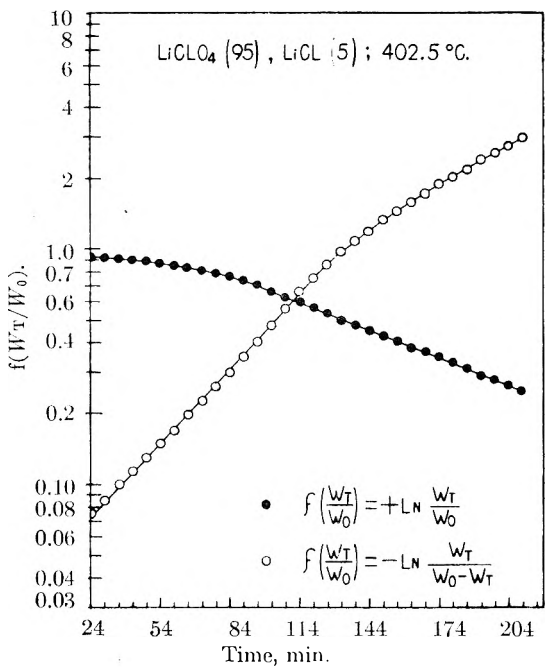

Fig. 3.—Integrated rate law plots for a lithium perchlorate (95 mole %)–lithium chloride (5 mole %) mixture at 402.5°.

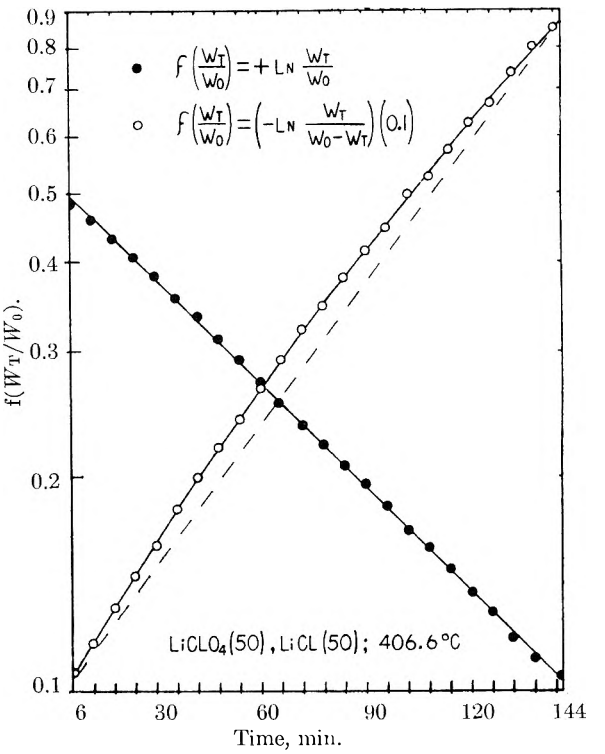

Fig. 4.—Integrated rate law plots for a lithium perchlorate (50 mole %)–lithium chloride (50 mole %) mixture at 406.6°.

The Prout–Tompkins rate law gives an integrated function which is considerably bowed when compared to the clearly defined straight line of the first-order plot. The latter rate constants (k_2) are listed in Table V.

TABLE V

RATE CONSTANTS (k_2) FOR THE DECOMPOSITION OF LITHIUM PERCHLORATE IN A LITHIUM PERCHLORATE (50 MOLE %)–LITHIUM CHLORIDE (50 MOLE %)

Mixture		Mixture	
Temp., °C.	k_2, min.$^{-1}$	Temp., °C.	k_2, min.$^{-1}$
391.2	0.00381	406.6	0.0112
395.3	.00549	408.9	.0131
399.8	.00724	413.0	.0181
402.5	.00946		

Discussion

The autocatalytic and first-order rate laws applied to the decomposition of lithium perchlorate appear to coincide at about 40% decomposition. Reference to the phase data shows that over the narrow temperature range covered in these studies, this extent of decomposition corresponds to saturation of the melt with the reaction product, lithium chloride. At saturation then the two rate laws should be equal, and hence

$$-k_1\left(\frac{W_t}{W_0}\right)_{satn.}\left(\frac{W_0 - W_t}{W_0}\right)_{satn.} = -k_2\left(\frac{W_t}{W_0}\right)_{satn.} \quad (1)$$

Transposing terms, it is found that

$$\frac{k_2}{k_1} = \left(\frac{W_0 - W_t}{W_0}\right)_{satn.} \quad (2)$$

Thus, the ratio (k_2/k_1) should be equal to the mole fraction solubility of lithium chloride in the saturated melt, x_{LiCl}. Tables III and IV contain com-

parisons of this ratio with the mole fraction solubility of lithium chloride as computed from the Clapeyron–Clausius equation. The disparity between these two sets of results corresponds to an average deviation of 10.8%.

Carrying equation 2 one step further

$$\left(\frac{W_0 - W_t}{W_0}\right)_{satn.} = x_{LiCl} = \text{constant} \exp(-\Delta H_{fusion,\ LiCl}/RT) \quad (3)$$

Thus, a plot of the logarithm of x_{LiCl} *versus* $1/T$ should yield a straight line, the slope of which is the heat of fusion of lithium chloride divided by $-R$. This, of course, assumes ideal solution behavior of the melts. The kinetic data result in a value of 6.6 ± 0.5 kcal./mole for the heat of fusion of lithium chloride, compared with 4.7 kcal./mole for the calorimetrically derived value.[11] As a consequence the present study is of interest in that it allows for the partial determination of a phase diagram and for solubility values from kinetic data.

Knowledge of the saturation solubility of lithium chloride in the decomposing melt at any given temperature makes possible the interrelation of the two rate laws over the entire range of decomposition. Thus

$$\frac{d(W_t/W_0)}{dt} = -k_1 \left(\frac{W_t}{W_0}\right)\left(\frac{W_0 - W_t}{W_0}\right)\Bigg|_{\text{melt unsatd.}} \quad (4)$$

followed by

$$\frac{d(W_t/W_0)}{dt} = -k_1(x_{LiCl})(W_t/W_0)\Big|\ \text{melt satd.} \quad (5)$$

or most generally for the latter rate law

$$\frac{d(W_t/W_0)}{dt} = -k_1 \text{ antilog } \left[\frac{\Delta H_{fusion,\ LiCl}}{2.303R}\left(\frac{1}{T_0} - \frac{1}{T}\right)\right]\left(\frac{W_t}{W_0}\right) \quad (6)$$

where T_0 is the melting point of lithium chloride in °K.

Arrhenius plots of ln k *versus* $1/T$ yield satisfactory straight lines for k_1 as obtained from pure lithium perchlorate and from the $LiClO_4$ (95)–LiCl (5) mixtures and for k_2 as obtained from these materials and from the $LiClO_4$ (50)–LiCl (50) mixtures (see Fig. 5). The corresponding energies of activation and frequency factors are given in Table VI and were obtained from least squares treatment of the data.

TABLE VI

KINETIC CONSTANTS FOR THE LIQUID-PHASE THERMAL DECOMPOSITION OF LITHIUM PERCHLORATE

	k_1 (acceleratory)	k_2 (deceleratory)
$E_{Act.}$, kcal./mole	52.2 ± 4.1	62.0 ± 4.1
A, sec.$^{-1}$	2.78×10^{13}	1.55×10^{16}

The ratio (k_2/k_1) in terms of the exponential functions should also yield the heat of fusion of lithium chloride, *viz.*

$$k_2/k_1 = A \exp(-E_2/RT)/A' \exp(-E_1/RT) = \text{constant} \exp(-(E_2 - E_1)/RT) = \text{constant} \exp(-\Delta H_{fusion,\ LiCl}/RT) \quad (7)$$

Using the data of Table VI, a value of 9.8 ± 8.2 kcal./mole was obtained for the heat of fusion of lithium chloride.

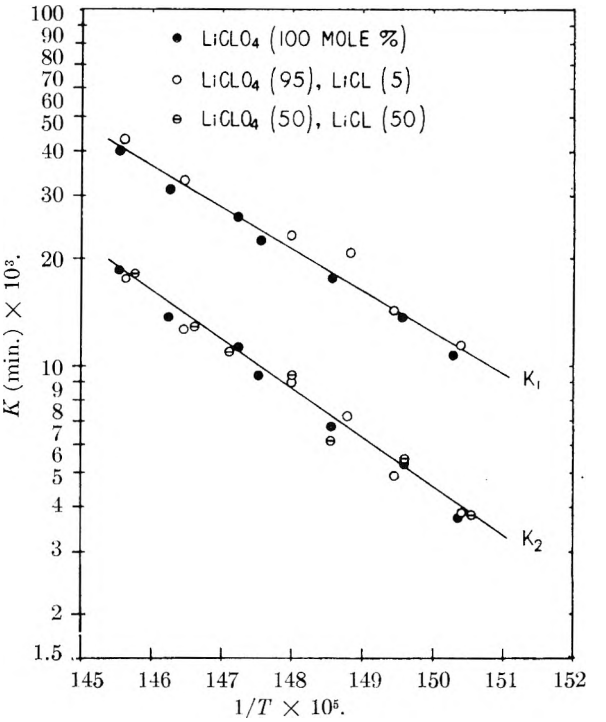

Fig. 5.—Arrhenius plots for acceleratory (k_1) and deceleratory (k_2) rate constants.

The solubility data of Tables I, III and IV indicate the occurrence of a small positive deviation from ideality in the system $LiClO_4$–LiCl. Though the numerical values of the saturation solubilities are not greatly affected by this non-ideality, the temperature coefficient of solubility is strongly influenced. Thus, the high values for the heat of fusion of lithium chloride derived from the kinetic data (6.6 and 9.8 kcal./mole *vs.* 4.7 kcal./mole for the known value) are consistent with this type of departure from ideal solution behavior.

The Prout–Tompkins rate expression as applied to the decomposition of solids was originally derived on the basis of branching reaction nuclei, usually structural defects on the surface of the solid possessing a low energy of activation for decomposition.[16,17] Acceleration of reaction is pictured to occur as these branching chain nuclei form reactive planes in the material giving rise to mechanical stresses and physical breakdown of the solid crystals. Eventually these planes interfere with one another and the kinetics assume first-order behavior. The liquid-phase decomposition of lithium perchlorate bears a striking resemblance to this picture. Clearly, the function of lithium chloride must involve some transfer mechanism facilitating rupture of the Cl–O bond, *viz.*, $LiClO_4$ (solution) + LiCl (solution) → $LiClO_3$ (solution) + $^1/_2O_2$ (gas) + LiCl (solution). The small concentration of lithium chlorate in the reaction residues indicates that the decomposition of the chlorate ($LiClO_3$ (solution) → LiCl (solution or solid) + $^3/_2$ O_2 (gas)) must be quite rapid compared to the rate of perchlorate decomposition. Thus, up to about 40% decomposition the decomposing perchlorate generates more nuclei to accelerate its own breakdown. However, this accelerating autocatalytic effect can only proceed

to the point of saturation of the melt with lithium chloride; this represents the point of maximum rate achievable in these studies and thus, in a sense, a chainbreaking step. At saturation, the ratio of lithium perchlorate to lithium chloride is perforce a constant and thus formal first-order kinetics are observed. In this regard, it is of interest to note that the efficacy of lithium chloride as a catalyst only occurs in homogeneous solution with lithium perchlorate.

The decomposition kinetics found for lithium perchlorate in the present study are in contrast to those currently accepted for potassium perchlorate.[2,3,20] For the latter compound first-order kinetics prevail over the entire decomposition region, indicating no autocatalytic effect by the potassium chloride reaction product. Earlier work on potassium perchlorate by Glasner and Weidenfeld[21] was interpreted by them in terms of a Prout–Tompkins mechanism despite the obvious phase change of the salt from solid to liquid during decomposition.[22] The mechanism stipulated exchange of oxygen between chloride and perchlorate as a result of the postulated equilibrium: $KCl + 4(O) \rightleftarrows KClO_4$. Bosch and Aten[23] studied the distribution of radioactive chlorine between NaCl* and $NaClO_3$ at elevated temperatures. They concluded that the low activity of the labeled chlorine in the perchlorate formed invalidated the earlier interpretations of Glasner and Weidenfeld. However, it seems possible, on the basis of the studies reported here, that the thermal decompositions of the alkali metal halates may involve differences in the type of mechanism and not merely differences with the same fundamental kinetics. If this be so, then the results of exchange studies based on the sodium salts cannot be applied reliably to the mechanisms of the corresponding potassium and lithium systems.

It might be expected that the difference in the activation energies between the liquid- and solid-phase decompositions of potassium perchlorate would be equal to the heat of fusion of the compound. This latter value has been computed to be small (1.7–2.6 kcal./mole)[15] because of the appreciable heat of crystallographic transition absorbed at 300° (3.29 kcal./mole).[24,25] Harvey and co-workers[2,3] report identical values, within the limits of experimental error, for the heats of activation in the two decomposition regions of potassium perchlorate. This would indicate the occurrence of essentially the same reaction within the two phases and hence little influence of the state of aggregation of the perchlorate salt on the strength of the Cl–O bond. Such a circumstance appears reasonable because of the crystalline transition, the effect of which might be a significant contribution to the collapse of the crystalline lattice and an enhancement of the mobility of the lattice units.

The kinetic law prevailing during the induction periods in the decomposition of lithium perchlorate could not be resolved with any reasonable degree of certainty. However, an energy of activation for this process was determined by a plot of the logarithm of the time to 0.5% decomposition against $1/T$; a value of 58.3 ± 4.3 kcal./mole was obtained. It seems plausible that this energy of activation might apply to the unimolecular decomposition of lithium perchlorate and is thus a measure of the strength of the Cl–O bond in the compound while in the molten state. Once sufficient lithium chloride is formed in the melt, the autocatalytic route to decomposition ($E_{Act.}$ = 52.2 kcal./mole) is obviously more favored on energetic grounds.

Acknowledgment.—Thanks are extended to Professors H. A. Taylor of New York University and to M. Barth of LaSalle College for a number of helpful discussions during the performance of this work.

(20) K. H. Stern and M. Bufalini, *J. Phys. Chem.*, **64**, 1781 (1960).

(21) A. Glasner and L. Weidenfeld, *J. Am. Chem. Soc.*, **74**, 2464, 2467 (1952).

(22) L. L. Bircumshaw and T. R. Phillips, *J. Chem. Soc.*, 703 (1953).

(23) A. V. Bosch and A. H. W. Aten, *J. Am. Chem. Soc.*, **75**, 3835 (1953).

(24) F. D. Rossini, D. D. Wagman, W. H. Evans, S. Levine and J. Jaffe, "Selected Values of Chemical Thermodynamic Properties," National Bureau of Standards Circular 500, U. S. Government Printing Office, Washington, D. C., 1952.

(25) D. Vorlaender and E. Kaascht, *Ber.*, **56**, 1157 (1923).

THE CHEMICAL THERMODYNAMIC PROPERTIES OF CYCLOPENTANETHIOL[1]

BY W. T. BERG, D. W. SCOTT, W. N. HUBBARD, S. S. TODD, J. F. MESSERLY, I. A. HOSSENLOPP, ANN OSBORN, D. R. DOUSLIN AND J. P. MCCULLOUGH

Contribution No. 104 from the Thermodynamics Laboratory of the Bartlesville Petroleum Research Center, Bureau of Mines, U. S. Department of the Interior, Bartlesville, Okla.

Received April 3, 1961

The chemical thermodynamic properties of cyclopentanethiol (cyclopentyl mercaptan) in the ideal gas state (0 to 1000°K.) were calculated by using calorimetric, spectroscopic and molecular structure information. Pseudorotation of the five-membered ring was demonstrated. Experimental studies provided: values of heat capacity for two crystalline forms of the solid (12°K. to the triple point), for the liquid (triple point to 367°K.) and for the vapor (390 to 500°K.); the triple point temperatures; the heats of fusion; thermodynamic functions for the solid and liquid (0 to 370°K.); heat of vaporization (360 to 405°K.); parameters of the equation of state; vapor pressure (353 to 446°K.); and the standard heat of formation at 298.15°K.

Thermodynamic studies of cyclopentanethiol (cyclopentyl mercaptan) were made as part of continuing research on organic sulfur compounds of interest in petroleum technology. Experimental results were obtained by low temperature calorimetry, vapor flow calorimetry, combustion calorimetry and comparative ebulliometry. These results were used with spectral and molecular structure information to calculate a table of chemical thermodynamic properties for the ideal gas state.

Pseudorotation of ring puckering[2] was demonstrated; that is, the calorimetric results could be interpreted only if an internal degree of freedom were taken as a pseudorotation instead of a vibration. The result for cyclopentanethiol is additional evidence for the already well-substantiated concept of pseudorotation in cyclopentane, related heterocyclic compounds, and many of their derivatives.

The first section of this paper is on the thermodynamic properties for the ideal gas state, and the second section is on the experimental measurements. Some observations on polymorphism of solid cyclopentanethiol are reported with the results of low temperature calorimetry.

Thermodynamic Properties

Thermodynamic Functions.—Calculating thermodynamic functions of cyclopentanethiol required considering all 48 degrees of freedom of the molecule. These degrees of freedom may be classified as three translations, three over-all rotations, one internal rotation of the thiol group, 40 vibrations and one pseudorotation of ring puckering. The contributions of translation and over-all rotation were calculated by standard formulas. In the simplified model used for calculating moments of inertia, the ring was planar, and the bond distances and angles were: C–C, 1.54 Å.; C–H, 1.09 Å.; C–S, 1.819 Å.; S–H, 1.336 Å.; C–C–C, 108°; H–C–H and H–C–S, 109° 28′; C–S–H, 96° 30′. The bisectors of the H–C–H and H–C–S angles intersected in the center of the ring, and the hydrogen atoms of the SH and CH groups were *trans* to each other. For this model, the product of principal moments of inertia is 3.250×10^{-113} g.^{3} cm.^{6}, and the reduced moment of inertia for internal rotation is 2.834×10^{-40} g. cm.^{2}. Corresponding values for the actual molecule with a puckered ring cannot differ much from the foregoing values. The symmetry number is unity for over-all rotation, the thiol rotation and the pseudorotation.

Because of the low symmetry of the molecule and the diffuse spectra characteristic of molecules with pseudorotation, a complete and unambiguous vibrational assignment for cyclopentanethiol was not possible. Instead, a somewhat schematic set of vibrational frequencies, listed in Table I, was selected for thermodynamic calculations. All available Raman and infrared spectral data[3] were considered, analogies to other molecules were used, and agreement with the calorimetric data, for reasonable values of all molecular-structure parameters, was required. The skeletal bending frequency of 322 cm.$^{-1}$ (in brackets in Table I) was not observed in the spectra of cyclopentanethiol, but it is from the Raman spectrum of cyclopentyl chloride, which has very nearly the same frequencies because of the similar mass and electronic structure of the thiol group and chlorine atom. In Table I, the descriptive names for the modes of vibration

TABLE I

VIBRATIONAL FREQUENCIES OF CYCLOPENTANETHIOL, CM.$^{-1}$ [a]

Skeletal bending	254, [322],[b] 364, 466, 604
C–S stretching	(604)
C–C stretching	889, 920, 963(2), 1145
C–S–H bending	863
CH_2 rocking	764, 837, 1029, 1210
CH_2 wagging	(1029)(2), 1244, 1292
CH_2 twisting	1077, (1145), 1271, 1318
CH wagging	(1292), 1366
CH_2 bending	1450(2), 1475(2)
S–H stretching	2568
C–H stretching	2920(9)

[a] Frequencies used a second time are in parentheses. Multiple weights are indicated by numbers in parentheses immediately following the frequencies. [b] Transferred from cyclopentyl chloride.

(1) This investigation was part of American Petroleum Institute Research Project 48A on the "Production, Isolation and Purification of Sulfur Compounds and Measurement of their Properties," which the Bureau of Mines conducts at Bartlesville, Okla., and Laramie, Wyo.

(2) K. S. Pitzer and W. E. Donath, *J. Am. Chem. Soc.*, **81**, 3213 (1959). Earlier work is cited.

(3) Raman: K. W. F. Kohlrausch, A. W. Reitz and W. Stockmair, *Z. physik. Chem.*, **B32**, 229 (1936); API RP 44 at the Carnegie Inst. of Tech., Catalog of Raman Spectral Data, Serial No. 302. Infrared: *ibid.*, Catalog of Infrared Spectral Data, Serial Nos. 1520, 1521, 1522, 1667, 1668, 1873 and 1874.

are intended only to show that the expected number of frequencies is assigned in each region of the spectrum.

Values of five other molecular-structure parameters were selected to fit the experimental values of heat capacity and entropy: The height of the potential barrier restricting internal rotation of the thiol group, 1200 cal. mole^{-1}; the height of the potential barrier restricting pseudorotation of the 5-membered ring, zero (free pseudorotation); the effective moment of inertia for the pseudorotation, 18.9 $\times$ 10^{-40} g. cm.^{2}; and parameters of an empirical anharmonicity function,[4] ν = 1130 cm.$^{-1}$ and Z = 0.684 cal. deg.$^{-1}$ mole^{-1}.

All of these values are reasonable. The thiol barrier height of 1200 cal. mole^{-1} is close to that in methanethiol, 1270 cal. mole^{-1}.[5] The barrier height for pseudorotation can be predicted by the formula proposed by Pitzer and Donath,[2] 1.45-(V_{12} − 2.8) kcal. mole^{-1}, in which V_{12} is the barrier height for rotation about the bond between ring positions one and two. If V_{12} is given the value 3.3 kcal. mole^{-1}, as in the model compound ethanethiol,[6] the barrier height for pseudorotation is predicted to be only 0.7 kcal. mole^{-1}. As Pitzer and Donath's formula tends to predict too great a barrier height, the value of zero selected to fit the calorimetric data is in qualitative agreement with expectations. The value for the effective moment of inertia for pseudorotation in cyclopentanethiol, 18.9 $\times$ 10^{-40} g. cm.^{2}, differs from the value in cyclopentane,[7] 10.6 $\times$ 10^{-40} g. cm.^{2}, in the direction expected because of the added mass of the sulfur atom. The values of the two anharmonicity parameters correspond to very small contributions of anharmonicity over the temperature range of calorimetric measurements; even at 1000°K., the calculated contributions are only 0.27 and 0.66 cal. deg.$^{-1}$ mole^{-1} in $S°$ and $C_p°$, respectively.

The calculated values of the thermodynamic functions of cyclopentanethiol are listed in columns 2–6 of Table II.[8] A comparison with the experimental results is shown in Table III. Such a simultaneous fit to all of the calorimetric data could not be obtained with any reasonable treatment that did not include pseudorotation.

Heat, Free Energy and Equilibrium Constant of Formation.—The calculated values of the thermodynamic functions, the experimental value of $\Delta Hf°_{298.15}$ (−26.84 ± 0.19 kcal. mole^{-1}) and values of the thermodynamic functions of C(c, graphite),[9] H_2(g)[9] and S_2(g)[10] were used in computing values of $\Delta Hf°$, $\Delta Ff°$ and log Kf at selected temperatures between 0 and 1000°K. The results are listed in columns 7–9, Table II.

Experimental

The basic experimental techniques used for cyclopentanethiol are described in published accounts of apparatus and methods for low-temperature calorimetry,[11] vapor flow calorimetry,[12] comparative ebulliometry[13] and combustion calorimetry.[14] The reported values are based on a molecular weight of 102.196 g. mole^{-1} (1951 International Atomic

TABLE II

THE MOLAL THERMODYNAMIC PROPERTIES OF CYCLOPENTANETHIOL IN THE IDEAL GAS STATE[a]

T, °K.	$(F° - H°_0)/T$, cal. deg.$^{-1}$	$(H° - H°_0)/T$, cal. deg.$^{-1}$	$H° - H°_0$, kcal.	$S°$, cal. deg.$^{-1}$	$C_p°$, cal. deg.$^{-1}$	$\Delta Hf°$,[b] kcal.,	$\Delta Ff°$,[b] kcal.	log Kf[b]
0	0	0	0	0	0	−19.00	−19.00	Infinite
273.15	−69.60	14.62	3.993	84.22	23.66	−26.26	+ 1.52	− 1.22
298.15	−70.92	15.46	4.611	86.38	25.79	−26.84	4.09	− 3.00
300	−71.01	15.53	4.659	86.54	25.94	−26.88	4.28	− 3.12
400	−75.97	19.21	7.685	95.19	34.53	−28.96	14.99	− 8.19
500	−80.68	23.06	11.53	103.74	42.20	−30.61	26.18	−11.44
600	−85.21	26.81	16.08	112.02	48.65	−31.87	37.66	−13.72
700	−89.62	30.32	21.23	119.94	54.05	−32.79	49.33	−15.40
800	−93.88	33.58	26.87	127.46	58.61	−33.41	61.10	−16.69
900	−98.01	36.59	32.93	134.60	62.51	−33.78	72.94	−17.71
1000	−102.01	39.35	39.35	141.36	65.84	−33.91	84.82	−18.54

[a] To retain internal consistency, some values are given to one more decimal place than is justified by the absolute accuracy. [b] The standard heat, standard free energy and common logarithm of the equilibrium constant for the formation of cyclopentanethiol by the reaction 5 C(c, graphite) + 5 H_2(g) + 1/2 S_2(g) = $C_5H_{10}S$(g).

TABLE III

OBSERVED AND CALCULATED MOLAL THERMODYNAMIC PROPERTIES OF CYCLOPENTANETHIOL IN THE IDEAL GAS STATE

Entropy, $S°$, cal. deg.$^{-1}$			Heat capacity, $C_p°$, cal. deg.$^{-1}$		
T, °K.	Obsd.	Calcd.	T, °K.	Obsd.	Calcd.
360.62	91.78	91.79	390.20	33.74	33.71
381.41	93.58	93.58	415.20	35.76	35.78
405.31	95.65	95.65	436.20	37.46	37.45
			458.20	39.11	39.15
			500.20	42.26	42.21

(4) J. P. McCullough, H. L. Finke, W. N. Hubbard, W. D. Good, R. E. Pennington, J. F. Messerly and G. Waddington, *J. Am. Chem. Soc.*, **76**, 2661 (1954).

(5) T. Kojima and T. Nishikawa, *J. Phys. Soc. Japan*, **12**, 680 (1957).

(6) J. P. McCullough, D. W. Scott, H. L. Finke, M. E. Gross, K. D. Williamson, R. E. Pennington, G. Waddington and H. M. Huffman, *J. Am. Chem. Soc.*, **74**, 2801 (1952).

(7) J. P. McCullough, R. E. Pennington, J. C. Smith, I. A. Hossenlopp and G. Waddington, *ibid.*, **81**, 5880 (1959).

(8) The vibrational and anharmonicity contributions were computed by the Bureau of Mines Electronic Computer Service, Pittsburgh, Pa.; the contributions of internal rotation were computed by Denver Electronic Computing Service, Inc., by two-way curvilinear interpolation in tables of K. S. Pitzer and W. D. Gwinn, *J. Chem. Phys.*, **10**, 428 (1942).

(9) D. D. Wagman, J. E. Kilpatrick, W. J. Taylor, K. S. Pitzer and F. D. Rossini, *J. Research Natl. Bur. Standards*, **34**, 143 (1945).

(10) W. H. Evans and D. D. Wagman, *ibid.*, **49**, 141 (1952).

(11) H. M. Huffman, *Chem. Revs.*, **40**, 1 (1947); H. M. Huffman, S. S. Todd and G. D. Oliver, *J. Am. Chem. Soc.*, **71**, 584 (1949); D. W. Scott, D. R. Douslin, M. E. Gross, G. D. Oliver and H. M. Huffman, *ibid.*, **74**, 883 (1952).

Weights[15]), the 1951 values of fundamental physical constants[16] and the relations: 0° = 273.15°K.[17] and 1 cal. = 4.184 j. (exactly). Measurements of temperature were made with platinum resistance thermometers calibrated in terms of the International Temperature Scale[18] between 90 and 500°K. and the provisional scale[19] of the National Bureau of Standards between 11 and 90°K. All electrical and mass measurements were referred to standard devices calibrated at the National Bureau of Standards. The energy equivalent of the combustion calorimetric system, ε(Calor.), was determined by combustion of benzoic acid (NBS Sample 39 g. certified to evolve 26.4338 ± 0.0026 kj. (6317.83 ± 0.62 cal.)/g. mass under certificate conditions).

Material.—The sample of cyclopentanethiol used for low temperature calorimetry, comparative ebulliometry and combustion calorimetry was part of the Standard Sample of Organic Sulfur Compound API-USBM 32, prepared at the Laramie (Wyo.) Petroleum Research Center of the Bureau of Mines. The purity, determined by calorimetric studies of melting point as a function of fraction melted, was 99.99 ± 0.01 mole %. A sample of slightly lower purity was used for vapor flow calorimetry.

Heat Capacity in the Solid and Liquid States.—Low temperature calorimetric measurements were made with 53.243 g. of sample sealed in a platinum calorimeter with helium (35 mm. at room temperature) as exchange gas to promote thermal equilibration. The observed values of heat capacity, C_{satd}, are listed in Table IV. Above 30°K., the accuracy uncertainty is estimated to be no greater than 0.2%.

Two distinct polymorphic forms of crystalline cyclopentanethiol were obtained and studied calorimetrically. Crystallization after cooling from room temperature gave a metastable form; it could be studied only below about 140°K. because it transformed rapidly to a stable form above that temperature. If the stable crystals were melted and the liquid heated no more than 20° above the melting point, stable crystals were obtained upon recrystallization. However, if the liquid was heated to 80° or more above the melting point, metastable crystals were obtained upon recrystallization.

The heat capacity of the metastable crystals is greater than that of the stable crystals at low temperatures, but above about 115°K. the heat capacity of the stable crystals is greater. A metastable form with lower heat capacity than a stable form is unusual. If the differences between the two crystalline forms are primarily in the orientation of the thiol groups in the crystal lattice, the observed differences in heat capacity can be explained qualitatively as effects of differences in crystal binding and in barriers to rotation of the thiol groups. The stable crystals are likely to be more compact and have an appreciably higher effective barrier for internal rotation, or oscillation, of the thiol group than the metastable crystals. Approximate calculations show that a reasonable difference in thiol barrier height would cause a significantly more rapid rise in heat capacity for the stable crystals in the region where the curves cross.

The heat capacity of the liquid goes through a minimum about 30° above the melting point. From 162 to 366°K. the observed heat capacity of the liquid is represented with a maximum deviation of 0.08% by the empirical equation

$$C_{satd}(liq) = 55.249 - 0.242257T + 8.8181 \times 10^{-4}T^2 - 8.2702 \times 10^{-7}T^3, \text{ cal. deg.}^{-1}\text{ mole}^{-1} \quad (1)$$

Heats and Temperatures of Fusion and Transition.—Five determinations of the heat of fusion, ΔHm, of the stable crystals gave the average value 1871.6 ± 0.6 cal. mole^{-1} at the triple point, 155.39°K.; the indicated uncertainty is the maximum deviation from the mean. Measured heat effects for the other two transformations among the three condensed phases also were referred to 155.39°K.

TABLE IV

THE MOLAL HEAT CAPACITY OF CYCLOPENTANETHIOL IN CAL. DEG.$^{-1}$

T, °K.[a]	C_{satd}[b]	T, °K.[a]	C_{satd}[b]	T, °K.[a]	C_{satd}[b]
Stable Crystals		106.17	17.962	58.26	11.900
11.84	0.845	112.11	18.810	63.66	12.741
11.98	0.871	113.13	18.945	69.65	13.572
13.14	1.115	118.28	19.761	75.94	14.396
13.43	1.174	118.82	19.818	82.33	15.211
14.49	1.440	124.45	20.716	84.65	15.526
14.96	1.551	124.53	20.734	88.39	16.012
15.87	1.793	127.54	21.267	89.79	16.173
16.67	2.010	130.13	21.713	93.81	16.636
17.40	2.204	130.26	21.722	95.06	16.778
18.54	2.524	130.71	21.801	99.21	17.269
19.13	2.693	131.23	21.906	100.99	17.474
20.40	3.063	132.41	22.123	107.22	18.238
20.94	3.217	132.71	22.177	107.70	18.281
22.31	3.637	135.77	22.738	113.54	19.033
22.82	3.774	135.97	22.753	119.63	19.872
24.49	4.278	136.03	22.789	121.98	20.173
25.13	4.468	136.25	22.841	125.74	20.784
27.04	5.021	137.71	23.108	126.93	20.935
27.96	5.278	138.02	23.202	132.31	21.751
29.92	5.816	141.09	23.770	137.23	22.705[c]
33.12	6.660	141.96	23.972	Liquid	
36.60	7.516	143.42	24.265[c]	162.49	35.625
40.32	8.344	Metastable Crystals		166.19	35.529
44.46	9.177	12.55	1.031	166.72	35.517
49.10	10.021	12.76	1.081	170.62	35.479
53.78	10.826	13.74	1.322	172.87	35.437
54.12	10.883	13.92	1.359	180.49	35.387
54.72	10.989	15.19	1.695	186.96	35.365
58.55	11.590	15.33	1.731	188.56	35.389
59.23	11.693	16.76	2.138	196.09	35.421
63.84	12.376	16.87	2.169	206.24	35.540
64.26	12.446	18.50	2.653	216.85	35.755
69.23	13.115	18.60	2.676	227.38	36.041
69.41	13.142	20.26	3.184	237.80	36.390
74.74	13.835	20.34	3.202	248.12	36.815
74.81	13.841	22.19	3.770	258.31	37.271
80.27	14.557	22.27	3.793	268.86	37.805
80.58	14.599	24.46	4.470	279.77	38.415
84.54	15.125	24.58	4.513	290.51	39.020
85.87	15.290	27.07	5.246	301.10	39.682
86.41	15.365	27.36	5.328	302.62	39.780
89.57	15.828	30.37	6.173	312.95	40.444
91.55	16.069	33.80	7.073	323.59	41.168
92.32	16.154	37.71	8.033	334.52	41.901
95.15	16.513	41.71	8.906	345.38	42.682
96.98	16.739	46.18	9.787	356.07	43.444
100.51	17.202	51.40	10.770	366.49	44.195
102.71	17.499	53.67	11.150		

[a] T is the mean temperature of each heat capacity measurement. [b] C_{satd} is the heat capacity of the condensed phase at saturation pressure. [c] Values of C_{satd} for both stable and metastable crystals are *not* corrected for the effect of premelting.

(12) G. Waddington, S. S. Todd and H. M. Huffman, *ibid.*, **69**, 22 (1947); J. P. McCullough, D. W. Scott, R. E. Pennington, I. A. Hossenlopp and G. Waddington, *ibid.*, **76**, 4791 (1954).

(13) G. Waddington, J. W. Knowlton, D. W. Scott, G. D. Oliver, S. S. Todd, W. N. Hubbard, J. C. Smith and H. M. Huffman, *ibid.*, **71**, 797 (1949).

(14) W. N. Hubbard, C. Katz and G. Waddington, *J. Phys. Chem.*, **58**, 142 (1954).

(15) E. Wichers, *J. Am. Chem. Soc.*, **74**, 2447 (1952).

(16) F. D. Rossini, F. T. Gucker, Jr., H. L. Johnston, L. Pauling and G. W. Vinal, *ibid.*, **74**, 2699 (1952).

(17) Some of the results originally were computed with constants and temperatures in terms of the relation 0° = 273.16°K. Only results affected significantly by the new definition of the absolute temperature scale [H. F. Stimson, *Am. J. Phys.*, **23**, 614 (1955)] were recalculated. Therefore, numerical inconsistencies, much smaller than the accuracy uncertainty, may be noted in some of the reported data.

(18) H. F. Stimson, *J. Research Natl. Bur. Standards*, **42**, 209 (1949).

(19) H. J. Hoge and F. G. Brickwedde, *ibid.*, **22**, 351 (1939).

by use of appropriate heat capacity data. From one enthalpy measurement over the region 102–162°K., $\Delta H_{155.39}$ for the transformation, metastable crystals → liquid, was found to be 1764 cal. mole^{-1}. From an experiment in which the change from metastable to stable form was allowed to go to completion under adiabatic conditions, $\Delta H_{155.39}$ for the transformation, metastable crystals → stable crystals, was found to be −108 cal. mole^{-1}. The sum, 1764 + 108 = 1872 cal. mole^{-1}, agrees exactly with the directly measured heat of fusion of the stable crystals.

The results of duplicate studies of melting temperature, $T_{obsd.}$, as a function of fraction of total sample melted, F, for the stable crystals, are combined in Table V. Also listed in Table V are values obtained for the triple point temperature, $T_{T.P.}$, the mole fraction impurity in the sample, N_2*, and the cryoscopic constants,[20] A = $\Delta Hm/RT_{T.P.}^2$ and B = $1/T_{T.P.} - \Delta Cm/2\Delta Hm$, calculated from the observed values of $T_{T.P.}$, ΔHm, and ΔCm (9.18 cal. deg.$^{-1}$ mole^{-1}).

TABLE V

CYCLOPENTANETHIOL: MELTING POINT SUMMARY

$T_{T.P.}$ = 155.39 ± 0.05°K.; N_2* = AF($T_{T.P.} - T_{obsd.}$) = 0.0001 ± 0.0001; A = 0.03900 deg.$^{-1}$; B = 0.00398 deg.$^{-1}$

Series	Melted, %	1/F	$T_{obsd.}$ °K.
I	9.81	10.19	155.3793
II	9.89	10.11	.3775
I	23.64	4.230	.3819
II	25.83	3.871	.3810
I	46.67	2.143	.3825
II	50.87	1.966	.3827
I	65.09	1.536	.3836
II	71.34	1.402	.3832
I	83.51	1.197	.3847
II	91.82	1.089	.3843
	100.00	1.000	.384[a]
	Pure	0	155.387[a]

[a] Visual curvilinear extrapolation.

The melting point of the metastable crystals could not be determined directly, but it was calculated to be 151.6°K. by finding the temperature at which the free energy difference between metastable crystals and liquid is zero. The calculation assumes no residual entropy is retained by either crystalline form at very low temperatures. The heat of fusion of metastable crystals at 151.6°K. is 1724 cal. mole^{-1}. The calculated melting point is only 3.8° below the melting point of the stable crystals, a reasonable difference for two polymorphic forms. Similar free energy calculations show that equilibrium between the two polymorphic forms is not experimentally realizable because the extrapolated transition temperature is well above the melting points.

Thermodynamic Properties in the Solid and Liquid States.—Values of the thermodynamic properties of the stable crystals and liquid at selected temperatures between 10 and 370°K. are given in Table VI. The values at 10°K. were computed from a Debye function for 5.5 degrees of freedom with θ = 118.7°; these parameters were evaluated from the heat capacity data between 12 and 21°K. (For the entropy calculations for the metastable form, a Debye function for 5.5 degrees of freedom and θ = 116.1° was used.) Corrections for the effect of premelting have been applied to the "smoothed" data in Table VI.

Vapor Pressure.—Observed values of vapor pressure, determined by comparative ebulliometry with water as the reference substance, are listed in Table VII. At one atmosphere of pressure the ebullition temperature was 0.002° higher than the condensation temperature. The Antoine and Cox equations selected to represent the results are

$$\log p = 6.91375 - 1387.803/(t + 211.952) \quad (2)$$

$$\log (p/760) = A(1 - 405.315/T) \quad (3)$$

$$\log A = 0.850222 - 6.6386 \times 10^{-4}T + 5.8136 \times 10^{-7}T^2$$

(20) A. R. Glasgow, A. J. Streiff and F. D. Rossini, *J. Research Natl. Bur. Standards*, **35**, 355 (1945).

TABLE VI

THE MOLAL THERMODYNAMIC PROPERTIES OF CYCLOPENTANETHIOL IN THE SOLID AND LIQUID STATES[a]

T, °K.	$-(F_{satd} - H°_0)/T$, cal. deg.$^{-1}$	$(H_{satd} - H°_0)/T$, cal. deg.$^{-1}$	$H_{satd} - H°_0$, cal.	S_{satd}, cal. deg.$^{-1}$	C_{satd}, cal. deg.$^{-1}$
			Crystals		
10	0.042	0.127	1.269	0.169	0.505
15	.142	.416	6.236	.558	1.560
20	.321	.871	17.419	1.192	2.943
25	.574	1.433	35.83	2.007	4.428
30	.889	2.051	61.52	2.940	5.831
35	1.253	2.685	93.96	3.938	7.127
40	1.653	3.314	132.56	4.967	8.283
45	2.079	3.922	176.50	6.001	9.274
50	2.522	4.503	225.14	7.025	10.172
60	3.440	5.588	335.2	9.028	11.807
70	4.377	6.580	460.5	10.957	13.214
80	5.317	7.491	599.3	12.808	14.524
90	6.248	8.346	751.1	14.594	15.844
100	7.171	9.160	916.0	16.331	17.133
110	8.081	9.946	1094.1	18.027	18.504
120	8.980	10.721	1286.5	19.701	20.009
130	9.868	11.499	1494.8	21.367	21.680
140	10.749	12.293	1720.9	23.042	23.569
150	11.625	13.110	1966.5	24.735	25.542
155.39	12.096	13.561	2107.3	25.657	26.616
			Liquid		
155.39	12.096	25.605	3978.9	37.701	35.798
160	12.848	25.896	4143	38.74	35.68
170	14.435	26.465	4499	40.90	35.47
180	15.962	26.963	4853	42.92	35.38
190	17.432	27.406	5207	44.83	35.38
200	18.849	27.806	5561	46.65	35.45
210	20.214	28.174	5916	48.38	35.60
220	21.533	28.516	6273	50.04	35.83
230	22.807	28.841	6633	51.64	36.12
240	24.042	29.151	6996	53.19	36.47
250	25.238	29.452	7363	54.69	36.89
260	26.399	29.747	7734	56.14	37.35
270	27.52	30.03	8110	57.56	37.86
273.15	27.87	30.13	8230	58.00	38.03
280	28.62	30.32	8491	58.95	38.42
290	29.69	30.61	8878	60.31	38.99
298.15	30.54	30.85	9198	61.39	39.49
300	30.73	30.90	9271	61.64	39.61
310	31.75	31.19	9671	62.95	40.25
320	32.75	31.49	10076	64.24	40.92
330	33.72	31.78	10489	65.50	41.59
340	34.67	32.08	10908	66.76	42.30
350	35.61	32.38	11335	67.99	43.00
360	36.52	32.69	11769	69.21	43.72
370	37.42	33.00	12209	70.42	44.45

[a] The values tabulated are the free energy function, heat content function, heat content, entropy and heat capacity of the condensed phases at saturation pressure.

In these equations, p is in mm., t is in °C. and T is in °K. Observed and calculated vapor pressure for both equations are compared in Table VII. The normal boiling point calculated from either equation is 132.17° (405.32°K.).

Heat of Vaporization, Vapor Heat Capacity and Effects of Gas Imperfection.—The experimental values of the heat of vaporization and vapor heat capacity are given in Tables VIII and IX. The estimated accuracy uncertainty of the values of ΔHv and $C_p°$ are 0.1 and 0.2%, respectively. The heat of vaporization may be represented by the empirical equation

TABLE VII

VAPOR PRESSURE OF CYCLOPENTANETHIOL

Boiling point, °C. Water	Boiling point, °C. Cyclopentanethiol	p(obsd.)[a] mm.	p(obsd.) − p(calc.), mm. Antoine eq. 2	p(obsd.) − p(calc.), mm. Cox eq. 3
60.000	80.874	149.41	−0.01	−0.01
65	87.107	187.57	− .01	.00
70	93.390	233.72	+ .01	+ .03
75	99.729	289.13	− .01	.00
80	106.113	355.22	+ .01	.01
85	112.548	433.56	.04	.04
90	119.037	525.86	.02	.00
95	125.577	633.99	− .01	− .03
100	132.165	760.00	.00	.00
105	138.806	906.06	− .02	.00
110	145.501	1074.6	− .1	.0
115	152.245	1268.0	− .1	− .1
120	159.040	1489.1	− .1	.0
125	165.887	1740.8	.0	.0
130	172.783	2026.0	+ .2	.0

[a] From the vapor pressure data for water given by N. S. Osborne, H. F. Stimson and D. C. Ginnings, *J. Research Natl. Bur. Standards*, **23**, 261 (1939).

TABLE VIII

THE MOLAL HEAT OF VAPORIZATION AND SECOND VIRIAL COEFFICIENT OF CYCLOPENTANETHIOL

T, °K.	P, atm.	ΔHv, cal.	B, cc. Obsd.	B, cc. Calcd.[a]
360.62	0.2500	9070 ± 2[b]	−1674	−1594
381.41	0.5000	8782 ± 4[b]	−1442	−1399
405.31	1.0000	8443 ± 4[b]	−1212	−1234

[a] Calculated from eq. 5. [b] Maximum deviation from the mean of three or more determinations.

$$\Delta Hv = 13046 - 8.352\,T - 7.413 \times 10^{-3}T^2 \text{ cal. mole}^{-1} \quad (360\text{–}405°\text{K.}) \quad (4)$$

The effects of gas imperfection were correlated by the procedure described in an earlier paper.[21] The empirical equation for B, the second virial coefficient in the equation of state, $PV = RT(1 + B/V)$, is

$$B = -420 - 42.12\exp(1200/T) \text{ cc. mole}^{-1} \quad (360\text{–}500°\text{K.}) \quad (5)$$

"Observed" values of B and $-T(\mathrm{d}^2B/\mathrm{d}T^2) = \lim_{P\to 0}(\partial C_p/\partial P)_T$ and those calculated from eq. 5 are compared in Tables VIII and IX.

TABLE IX

THE MOLAL VAPOR HEAT CAPACITY OF CYCLOPENTANETHIOL IN CAL. DEG.$^{-1}$

T, °K.	390.20	415.20	436.20	458.20	500.20
C_p (1.000 atm.)		36.459	37.955	39.518	42.487
C_p (0.500 atm.)	34.176	36.084			
C_p (0.250 atm.)	33.952	35.927	37.578	39.208	42.313
$C_p°$ (obsd.)	33.74	35.76	37.46	39.11	42.26
$-TB''$ (obsd.)[a]	0.84	0.65	0.46	0.38	0.22
$-TB''$ (calcd.)[b]	0.88	0.63	0.48	0.37	0.24

[a] $-TB'' = -T(\mathrm{d}^2B/\mathrm{d}T^2)$, cal. deg.$^{-1}$ mole^{-1} atm.$^{-1}$. [b] Calculated from eq. 5.

The heat of vaporization at 298.15°K. was calculated by extrapolation with eq. 4 (9.90 kcal. mole^{-1}), by using the Clapeyron equation with eqs. 3 and 5 (9.90 kcal. mole^{-1}) and by using a thermodynamic network with the thermodynamic functions of Table II (9.92 kcal. mole^{-1}). The value from the thermodynamic network was selected as the most reliable. From this value and eq. 5, the standard heat of vaporization was calculated, $\Delta Hv°_{298.15} = 9.93$ kcal. mole^{-1}.

Entropy in the Ideal Gas State.—The entropy in the ideal gas state at 1 atm. pressure was calculated as shown in Table X.

TABLE X

THE MOLAL ENTROPY OF CYCLOPENTANETHIOL IN THE IDEAL GASEOUS STATE IN CAL. DEG.$^{-1}$

T, °K	360.62	381.41	405.31
S_{satd} (liq.)	69.296[a]	71.790[b]	74.589[b]
$\Delta Hv/T$	25.151	23.024	20.831
$S^* - S^c$	0.090	0.144	0.229
$R \ln P^d$	−2.755	−1.377	0.000
$S°$(obsd.) ± 0.20[e]	91.78	93.58	95.65

[a] By interpolation in Table VI. [b] Extrapolated by use of eq. 1. [c] The entropy in the ideal gas state less that in the real gas state, calculated from eq. 5. [d] Entropy of compression, calculated from eq. 3. [e] Estimated accuracy uncertainty.

Heat of Combustion and Formation.—A typical determination of the heat of combustion of cyclopentanethiol is summarized in Table XI. Except as noted, the symbols and abbreviations are those of Hubbard, Scott and Waddington.[22] Six determinations gave the following values of $\Delta Ec°/M$: −9117.82, −9117.15, −9119.75, −9118.52, −9119.67 and −9117.52 cal. g.$^{-1}$. The average value with the standard deviation of the mean is −9118.41 ± 0.45 cal. g.$^{-1}$. The values of $\Delta Ec°/M$ apply to the following idealized combustion reaction at 298.15°K. For this

$$C_5H_{10}S\,(\text{liq}) + 9O_2(g) + 71H_2O\,(\text{liq}) = 5CO_2(g) + H_2SO_4.75H_2O\,(\text{liq})$$

reaction, the experimental value of $\Delta Ec°_{298.15}$ is −931.87 ± 0.15 kcal. mole^{-1} and $\Delta Hc°_{298.15}$ is −934.24 ± 0.15 kcal. mole^{-1}. The uncertainties are "uncertainty intervals" equal to twice the final "over-all" standard deviation.[23]

TABLE XI

SUMMARY OF A TYPICAL COMBUSTION CALORIMETRIC EXPERIMENT WITH CYCLOPENTANETHIOL[a]

m' (cyclopentanethiol), g.	0.76935
$\Delta t_c = t_f - t_i - \Delta t_{corr.}$, deg.	2.00103
ε(Calor.)(−Δt$_a$), cal.	−7821.63
ε(Cont.)(−Δt$_c$),[b] cal.	−27.62
$\Delta E_{ign.}$, cal.	1.35
$\Delta E'_{decomp.}$ (HNO_3 + HNO_2), cal.	10.64
ΔE, corr. to st. states,[c] cal.	3.23
$-m''\Delta Ec°/M$ (auxiliary oil), cal.	802.89
$-m'''\Delta Ec°/M$ (fuse), cal.	15.81
$m'\Delta Ec°/M$ (cyclopentanethiol), cal.	−7015.33
$\Delta Ec°/M$ (cyclopentanethiol), cal. g.$^{-1}$	−9118.52

[a] Auxiliary data: ε(Calor.) = 3908.8 cal. deg.$^{-1}$; V(Bomb) = 0.347 l.; $\Delta Ec°/M$ (auxiliary oil) = −10983.7 cal. g.$^{-1}$; $\Delta Ec°/M$(fuse) = −3923 cal. g.$^{-1}$; physical properties at 25° of cyclopentanethiol, ρ = 0.95048 g. ml.$^{-1}$, $(\partial E/\partial P)_T$ = −0.0075 cal. g.$^{-1}$ atm.$^{-1}$, C_p = 0.383 cal. deg.$^{-1}$ g.$^{-1}$. [b] ε^i(Cont.)(t_i − 25°) + ε^f(Cont.)(25° − t_f + $\Delta t_{corr.}$). [c] Items 81–85, incl., 87–91, incl., 93 and 94 of the computation form of ref. 22.

The derived results in Table XII were computed by use of the values of $\Delta Hc°$, $\Delta Hv°$, S_{satd}, and $S°$ for cyclopentanethiol and literature values of the standard heat of formation of $CO_2(g)$,[24] H_2O (liq),[9] $H_2SO_4.75H_2O$ [−212.06 kcal. mole^{-1}],[25] and $S_2(g)$[10] and of the standard entropy of graph-

(21) J. P. McCullough, H. L. Finke, J. F. Messerly, R. E. Pennington, I. A. Hossenlopp and G. Waddington, *J. Am. Chem. Soc.*, **77**, 6119 (1955).

(22) W. N. Hubbard, D. W. Scott and G. Waddington, "Experimental Thermochemistry," F. D. Rossini, Editor, Interscience Publishers, Inc., New York, N. Y., 1956, Chapter 5, pp. 75–128.

(23) F. D. Rossini, ref. 22, Chapter 14, pp. 297–320.

(24) E. J. Prosen, E. S. Jessup and F. D. Rossini, *J. Research Natl. Bur. Standards*, **33**, 447 (1944).

(25) W. D. Good, J. L. Lacina and J. P. McCullough, *J. Am. Chem. Soc.*, **82**, 5589 (1960).

TABLE XII

MOLAL THERMODYNAMIC PROPERTIES OF FORMATION OF CYCLOPENTANETHIOL AT 298.15°K.

Reference state	Ref. state of sulfur	$\Delta Hf°$, kcal.	$\Delta Sf°$, cal. deg.$^{-1}$	$\Delta Ff°$, kcal.	log Kf
Liquid	S (c, rhombic)	-21.35 ± 0.18	-109.08	11.17	-8.19
Gas	S (c, rhombic)	-11.42 ± 0.18	-84.10	13.65	-10.01
Gas	S_2(g)	-26.84 ± 0.19	-103.73	4.09	-3.00

[a] For the reaction: 5C(c, graphite) + $5H_2$(g) + S (c, rhombic) or $^1/_2S_2$(g) = $C_5H_{10}S$ (liq. or g).

ite,[9] hydrogen gas,[9] rhombic sulfur,[10] and diatomic sulfur gas,[10] all at 298.15°K.

Acknowledgment.—The help of Derek M. Fairbrother and Thelma C. Kincheloe in some of the experimental work is gratefully acknowledged.

CORRELATION OF HEAT OF FORMATION DATA FOR ORGANIC SULFUR COMPOUNDS[1]

BY JOHN P. MCCULLOUGH AND WILLIAM D. GOOD

Contribution No. 105 from the Thermodynamics Laboratory, Petroleum Research Center, Bureau of Mines, U. S. Department of the Interior, Bartlesville, Oklahoma

Received April 3, 1961

The method of Allen[2] was used to correlate unpublished and recently published Bureau of Mines results for the heats of formation of organic sulfur compounds. Six parameters were evaluated from data for 25 acyclic alkane thiols, sulfides and disulfides. With the inclusion of appropriate strain energies, the results for seven cyclic sulfur compounds also were correlated. For all 32 compounds, the average deviation between calculated and experimental values, 0.17 kcal. mole^{-1}, was a little less than the average experimental uncertainty interval, 0.22 kcal. mole^{-1}. The correlation can be used to predict reliable values of heat of formation for many other organic sulfur compounds.

Allen[2] recently described one of the most accurate methods of correlating and predicting heats of formation of organic compounds. Selecting appropriate values for thermochemical bond energies and using them as constant in all compounds, he evaluated a small number of interaction energy parameters for use in equation (1) for the heat of atomization of paraffin hydrocarbons

$$\Delta Ha°_{298.15} = N_{CH}E_{CH} + N_{CC}E_{CC} + X\alpha_{CCC} - T\beta_{CCC} - SA \quad (1)$$

where

N_{CH} and N_{CC} are the number of C–H and C–C bonds in the molecule
E_{CH} and E_{CC} are the C–H and C–C thermochemical bond energies
α_{CCC} is the interaction energy for a pair of next-nearest-neighbor carbon atoms joined to a common carbon atom
X is the number of such pairs
β_{CCC} is a trigonal interaction energy involving three carbon atoms, each of which is a next-nearest neighbor of the other two
T is the number of trigonal interactions
A is the *gauche-n*-butane interaction energy[3]
S is the number of such interactions

This relationship is equivalent to assuming that the heat of formation of a paraffin hydrocarbon can be calculated by adding to the heat of formation of methane the appropriate number of methylene increments[4] (assumed constant for all compounds) and appropriate interaction energy terms; that is, for C_nH_{2n+2} hydrocarbons

$$\Delta Hf°_{298.15} = \Delta Hf°(CH_4,g) + (n-1)[\Delta Hf°(C_2H_6,g) - \Delta Hf°(CH_4,g)] - X\alpha_{CCC} - T\beta_{CCC} + SA \quad (2)$$

For cyclic hydrocarbons, C_nH_{2n}, similar reasoning leads to the equation

$$\Delta Hf°_{298.15} - n[\Delta Hf°(C_2H_6,g) - \Delta Hf°(CH_4,g)] - X\alpha_{CCC} + T\beta_{CCC} + SA + E_s \quad (3)$$

where E_s is the strain energy of the cyclic molecule.

Correlation for Organic Sulfur Compounds.—Allen also determined some interaction energy terms for organic sulfur compounds, but not enough data were available to him for a thorough correlation. Nevertheless, the value he predicted for the heat of formation of methanethiol, -20.8 kcal. mole^{-1}, is in excellent agreement with that recently determined experimentally in this Laboratory, -20.88 kcal. mole^{-1} (both values for formation at 298.15°K. from graphite and diatomic sulfur and hydrogen gases), indicating that Allen's method can be used to estimate reliable values of heat of formation for many sulfur compounds. Thus, it was adopted for correlating unpublished and recently published experimental values obtained by the Bureau of Mines for the 32 organic sulfur compounds listed in Table I.

The heat of formation values in Table I were calculated from heat of combustion values given in the references cited, using the most recent value of the heat of formation of aqueous sulfuric acid.[5] These values of $\Delta Hf°_{298.15}$ supersede the values reported earlier, although most of the differences are less than the uncertainty intervals indicated in Table I.

(1) This investigation was part of American Petroleum Institute Research Project 48A on "The Production, Isolation and Purification of Sulfur Compounds and Measurement of their Properties," which the Bureau of Mines conducts at Bartlesville, Okla., and Laramie, Wyo.

(2) T. L. Allen, *J. Chem. Phys.*, **31**, 1039 (1959).

(3) K. S. Pitzer, *ibid.*, **8**, 711 (1940).

(4) W. B. Person and G. C. Pimentel, *J. Am. Chem. Soc.*, **75**, 532 (1953).

(5) W. D. Good, J. L. Lacina and J. P. McCullough, *ibid.*, **82**, 5589 (1960).

TABLE I

EXPERIMENTAL AND CALCULATED HEAT OF FORMATION

Compound	$\Delta Hf°_{298.15}$,[a,b] kcal. mole^{-1}	Exptl. − calcd.[c]
Methanethiol[d]	−20.88 ± 0.15	0.00
Ethanethiol[e]	−26.41 ± .15	+ .12
1-Propanethiol[f]	−31.61 ± .16	− .15
2-Propanethiol[f]	−33.61 ± .16	− .05
1-Butanethiol[g]	−36.44 ± .28	− .05
2-Butanethiol[g]	−38.54 ± .19	− .05
2-Methyl-1-propanethiol[g]	−38.63 ± .20	− .31
2-Methyl-2-propanethiol[g]	−41.56 ± .16	− .24
1-Pentanethiol[h]	−41.30 ± .28	+ .02
3-Methyl-1-butanethiol[d]	−42.83 ± .30	− .08
2-Methyl-2-butanethiol[d]	−45.76 ± .23	− .01
2-Thiapropane[e]	−24.36 ± .13	− .14
2-Thiabutane[i]	−29.64 ± .28	+ .23
2-Thiapentane[g]	−34.93 ± .16	− .13
3-Thiapentane[g]	−35.34 ± .18	+ .18
3-Methyl-2-thiabutane[g]	−37.00 ± .18	− .10
2-Thiahexane[h]	−39.81 ± .21	− .08
3-Thiahexane[h]	−40.39 ± .20	+ .06
3,3-Dimethyl-2-thiabutane[i]	−44.35 ± .21	+ .31
4-Thiaheptane[h]	−45.35 ± .23	+ .03
2,4-Dimethyl-3-thiapentane[d]	−49.26 ± .24	+ .32
5-Thianonane[h]	−55.38 ± .36	− .14
2,3-Dithiabutane[j]	−36.55 ± .26	+ .61
3,4-Dithiahexane[j]	−48.62 ± .28	− .16
4,5-Dithiaoctane[j]	−58.79 ± .29	− .47
Thiacyclobutane[k]	− 0.80 ± .20	.00
Thiacyclopentane[k]	−23.59 ± .33	− .04
2-Methylthiacyclopentane[d]	−30.54 ± .22	+ .04
Thiacyclohexane[l]	−30.53 ± .21	− .46
Cyclopentanethiol[d]	−26.84 ± .19	+ .10
Cyclohexanethiol[d]	−38.32 ± .21	− .35
Cyclopentyl-1-thiaethane[d]	−30.83 ± .25	− .55

[a] For the reaction: aC(c, graphite) + $b/2$ H_2 (g) + $c/2$ S_2 (g) = $C_aH_bS_c$ (g); the numerical values are based on 1951 International Atomic Weights (H = 1.008, C = 12.010 and S = 32.066 a.m.u.) and the definition 1 cal. = 4.184 (exactly) joules. [b] The indicated uncertainty is the uncertainty interval equal to twice the final over-all standard deviation. [c] The deviations from experimental values calculated by eq. 5a–9a. [d] Unpublished data, Bureau of Mines. [e] J. P. McCullough, W. N. Hubbard, F. R. Frow, I. A. Hossenlopp and G. Waddington, *J. Am. Chem. Soc.*, **79**, 561 (1957). [f] W. N. Hubbard and G. Waddington, *Rec. trav. chim.*, **73**, 910 (1954). [g] W. N. Hubbard, W. D. Good and G. Waddington, *J. Phys. Chem.*, **62**, 614 (1958). [h] J. P. McCullough, H. L. Finke, W. N. Hubbard, S. S. Todd, J. F. Messerly, D. R. Douslin and Guy Waddington, *ibid.*, **65**, 784 (1961). [i] D. W. Scott, W. D. Good, S. S. Todd, J. F. Messerly, W. T. Berg, I. A. Hossenlopp, J. L. Lacina, Ann Osborn and J. P. McCullough, in press. [j] W. N. Hubbard, D. R. Douslin, J. P. McCullough, D. W. Scott, S. S. Todd, J. F. Messerly, I. A. Hossenlopp and G. Waddington, *J. Am. Chem. Soc.*, **80**, 3547 (1958). [k] W. N. Hubbard, C. Katz and G. Waddington, *J. Phys. Chem.*, **58**, 142 (1954). [l] J. P. McCullough, H. L. Finke, W. N. Hubbard, W. D. Good, R. E. Pennington, J. F. Messerly and G. Waddington, *J. Am. Chem. Soc.*, **76**, 2661 (1954).

With Allen's notation as used in eq. 1, the heat of atomization of saturated organic sulfur compounds of the type $C_aH_bS_c$ can be expressed by eq. 4.

$$\Delta Ha°_{298.15} = N_{CH}E_{CH} + N_{CC}E_{CC} + N_{CS}E_{CS} + N_{SS}E_{SS} + N_{SH}E_{SH} + X\alpha_{CCC} + X'\alpha_{CCS}X''\alpha_{CSC} + X'''\alpha_{CSS} - T\beta_{CCC} - T'\beta_{CCS} - SA \quad (4)$$

where the additional N's, E's, α's and β's are defined as before, the subscripts indicating the bonds or interactions involved. Allen's values of E_{CH}, E_{CC}, E_{SH}, E_{SS}, α_{CCC}, β_{CCC} and A were adopted. The value of E_{CS} then was calculated by eq. 4 from the experimental value of heat of formation of methanethiol (Table I), which has no α- or β-type interactions. Average values of the remaining four parameters, α_{CCS}, α_{CSC}, α_{CSS} and β_{CCS}, were evaluated from experimental data for 25 acyclic sulfur compounds. (The parameter corresponding to A for a C–C–C–S chain was found to be negligible in comparison with experimental uncertainties.) All of these parameters are listed in Table II, which also includes values for the heats of formation, $\Delta Hf°_{298.15}$, of the gaseous atoms C, H and S. It should be noted that in this kind of correlation, errors in the values selected for the thermochemical bond energies and the heats of formation of the atoms are unimportant if the entire set of parameters is evaluated and used consistently.

TABLE II

PARAMETERS OF THE CORRELATION IN KCAL. MOLE^{-1}[a]

α_{CCC} = 2.58[b]	E_{CH} = 99.285[b]
α_{CCS} = 3.30	E_{CC} = 78.85[b]
α_{CSC} = 2.97	E_{SH} = 87.85[b]
α_{CSS} = 4.43	E_{CS} = 65.44
β_{CCC} = 0.65[b]	E_{SS} = 58.07[b]
β_{CCS} = 1.20	$\Delta Hf°$(C,g) = 170.890[c]
A = 0.50[b]	$\Delta Hf°$(H,g) = 52.089[c]
$E_s(C_3S)$ = 19.41	$\Delta Hf°$(S,g) = 51.02[d]
$E_s(C_4S)$ = 1.59	
$E_s(C_5)$ = 6.10[b]	
$E_s(C_5S)$ = 0	
$E_s(C_6)$ = 0[b]	

[a] For use in eqs. 1–9. [b] From ref. 2. [c] From ref. 6. [d] Heat of formation from S_2(g), W. H. Evans and D. D. Wagman, *J. Research Natl. Bur. Standards*, **49**, 141 (1952).

As Allen has done for hydrocarbons, expressions were derived for the heat of formation for several classes of sulfur compounds. These expressions are based on eq. 4, the heats of formation of the gaseous atoms, a *selected* methylene increment to the heat of formation (from ethane and methane), and if necessary a selected heat of formation of a parent member of the class. For the reaction at 298.15°K.

$$a\text{C(c, graphite)} + b/2\ H_2(g) + c/2\ S_2(g) = C_aH_bS_c(g)$$

the following equations, in kcal. mole^{-1}, are obtained

Alkanethiols

$$\Delta Hf°_{298.15} = \Delta Hf°(CH_3SH,g) + (a - 1)[\Delta Hf°(C_2H_6,g) - \Delta Hf°(CH_4,g)] - X\alpha_{CCC} - X'\alpha_{CCS} + T\beta_{CCC} + T'\beta_{CCS} + SA \quad (5)$$

$$\Delta Hf°_{298.15} = -18.53 - 2.35a - 2.58X - 3.30X' + 0.65T + 1.20T' + 0.5S \quad (5a)$$

Thiaalkanes

$$\Delta Hf°_{298.15} = \Delta Hf°(CH_3SCH_3,g) + (a - 2) \times [\Delta Hf°(C_2H_6,g) - \Delta Hf°(CH_4,g)] - X\alpha_{CCC} - X'\alpha_{CCS} = (X'' - 1)\alpha_{CSC} + T\beta_{CCC} + T'\beta_{CCS} + SA \quad (6)$$

$$\Delta Hf°_{298.15} = -16.55 - 2.35a - 2.58X - 3.30X' - 2.97X'' + 0.65T + 1.20T' + 0.5S \quad (6a)$$

Dithiaalkanes

$$\Delta Hf°_{298.15} = \Delta Hf°(CH_3SSCH_3,g) + (a-2) \times [\Delta Hf°(C_2H_6,g) - \Delta Hf°(CH_4,g)] - X\alpha_{CCC} - X'\alpha_{CCS} - (X''' - 2)\alpha_{CSS} + T\beta_{CCC} + T'\beta_{CCS} + S\Lambda \quad (7)$$

$$\Delta Hf°_{298.15} = -23.60 - 2.35a - 2.58X - 3.30X' - 4.43X''' + 0.65T + 1.20T' + 0.5S \quad (7a)$$

Thiacyclanes and cycloalkylthiaalkanes

$$\Delta Hf°_{298.15} = \Delta Hf°(CH_3SCH_3,g) - \Delta Hf°(C_2H_6,g) + a[\Delta Hf°(C_2H_6,g) - \Delta Hf°(CH_4,g)] - X\alpha_{CCC} - X'\alpha_{CCS} - (X'' - 1)\alpha_{CSC} + T\beta_{CCC} - T'\beta_{CCS} + S\Lambda + E_s \quad (8)$$

$$\Delta Hf°_{298.15} = -1.01 - 2.35a - 2.58X - 3.30X' - 2.97X'' + 0.65T + 1.20T' + 0.5S + E_s \quad (8a)$$

Cycloalkanethiols

$$\Delta Hf°_{298.15} = \Delta Hf°(CH_3SH,g) - \Delta Hf°(CH_4,g) + a[\Delta Hf°(C_2H_6,g) - \Delta Hf°(CH_4,g)] - X\alpha_{CCC} - X'\alpha_{CCS} + T\beta_{CCC} + T'\beta_{CCS} + S\Lambda + E_s \quad (9)$$

$$\Delta Hf°_{298.15} = -2.99 - 2.35a - 2.58X - 3.30X' + 0.65T + 1.20T' + 0.5S + E_s \quad (9a)$$

The numerical constants in the foregoing equations were evaluated from the parameters in Table II, the *selected* heats of formation of the sulfur compounds, and the heats of formation of methane[6] and ethane.[6] The heats of formation of CH_3SCH_3 and CH_3SSCH_3 obtained in this correlation were used instead of the experimental values.

Equations 8 and 9 include a ring strain energy term, which Allen evaluated for cyclopentane and cyclohexane. The strain energy for the thiacyclopentane ring was evaluated from the data for thiacyclopentane and 2-methylthiacyclopentane ($S = 0$ was assumed for the latter compound). For thiacyclohexane, E_s apparently is about zero at room temperature, as it is for cyclohexane.

(6) "Selected Values of Physical and Thermodynamic Properties of Hydrocarbons and Related Substances," American Petroleum Institute Research Project 44, Carnegie Press, Pittsburgh, Pa., 1953.

Discussion

Acyclic Sulfur Compounds.—Equations 5a and 6a represent the values of $\Delta Hf°_{298.15}$ for 22 acyclic alkane thiols and sulfides with an average deviation of 0.13 kcal. mole^{-1}, or 0.009 kcal. per valence bond, which is a somewhat better fit than Allen obtained for hydrocarbons.[2] Only two of the deviations are greater than experimental uncertainty by as much as 0.1 kcal. mole^{-1}.

The definite trend in the deviations for the three dithiaalkanes is puzzling. Neither experimental errors nor unaccounted-for interactions should be so large, but obviously one or the other must be.

Cyclic Sulfur Compounds.—There are not enough data for cyclic compounds to provide a real test of the correlation. However, the results for the two thiacyclopentanes are consistent with a strain energy of 1.59 ± 0.04 kcal. mole^{-1}, and the absence of significant strain in thiacyclohexane is to be expected. The results of the two cyclopentyl compounds are consistent with Allen's value of 6.1 kcal. mole^{-1} for the strain energy in cyclopentane.

Comparison with Other Correlations.—Estimates of heat of formation for sulfur compounds by most earlier correlations, like that of Franklin,[7] are not very accurate because no reliable experimental data were available for evaluating the necessary parameters. However, Lovering and Laidler[8] recently used a scheme of bond and group energies to correlate published Bureau of Mines data for many of the sulfur compounds in Table I. The deviations they report between observed and calculated values are somewhat larger than those reported here but, nevertheless, are comparable to the accuracy uncertainty of the experimental results.

(7) J. L. Franklin, *Ind. Eng. Chem.*, **41**, 1070 (1949).

(8) E. G. Lovering and K. J. Laidler, *Can. J. Chem.*, **38**, 2367 (1960).

SOLUBILITY OF DIKETOPIPERAZINE IN AQUEOUS SOLUTIONS OF UREA[1]

BY S. J. GILL, J. HUTSON, J. R. CLOPTON AND M. DOWNING

University of Colorado, Boulder, Colorado

Received April 6, 1961

Diketopiperazine has been used as a model compound to investigate hydrogen bond interactions between the peptide bond and urea. The solubility has been measured in aqueous urea solutions as a function of temperature and urea concentration. It is observed that the solubility follows a simple exponential dependence upon $1/T$. The heats of solution obtained from this temperature relation serve to evaluate the hydrogen bond interaction of diketopiperazine with urea. The fraction of peptide–urea interactions is estimated by simple equilibrium considerations. The heat of association of urea with a *cis* peptide bond can then be evaluated from experimental data as −3.4 ± 0.5 kcal. An equilibrium constant of 0.096 is found for the association of urea with the peptide bond in aqueous solution. The strong hydrogen bond interaction between urea and peptides is further illustrated by the discovery of a 2 urea:1 diketopiperazine solid complex which was observed to form from 8 *M* urea solutions below 30°.

Introduction

The structure of diketopiperazine (DKP) indicates unique possibilities for hydrogen bonding.

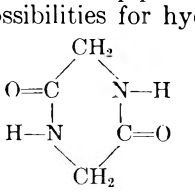

These possibilities are borne out in crystallographic studies,[2] which show a distinct arrangement between DKP molecules to form linear hydrogen bonded polymers within the solid structure. It

(1) This work was supported in part by a research grant (C-5393) from the National Cancer Institute, United States Public Health Service.

(2) (a) R. B. Corey, *J. Am. Chem. Soc.*, **60**, 1598 (1938); (b) R. Degeilh and R. E. Marsh, Abstract of American Crystallographic Association, Cornell University Meeting, July 19–24, 1959.

is well known that hydrogen bonding plays a primary role in the folding of proteins and synthetic polypeptides.[3] The quantitative evaluation of hydrogen bond enthalpies of formation in proteins, particularly in aqueous solutions, is complicated by charge effects. Nevertheless, it is highly desirable to have an estimate of the hydrogen bonding effect so that the contributions of charges might be evaluated from thermodynamic data. Data on urea solutions have been interpreted by Schellman[4] to provide an estimate of the amide hydrogen bond in aqueous solutions. Such an estimate has been used in theoretical predictions of the stability of folded polypeptide structures.[5-8]

It was felt that thermodynamic studies on diketopiperazine and other polypeptide models which are free from charge and side chain effects could add to the understanding of hydrogen bond interactions with the peptide group. In this note we describe solubility properties of DKP in aqueous urea solutions as a function of temperature. Previous related work is given by Meyer and Klemm[9] who record solubilities of DKP in aqueous salt solutions at a fixed temperature. This work indicates that there is a qualitative enhancement of solubility of DKP in urea solutions. Likewise, urea solutions are known to have important solubilization and denaturation powers on proteins[5] presumably through hydrogen bonding effects.[10] The solubility of DKP in urea solutions at different temperatures permits an estimate of the enthalpy of solution of DKP and thus provides thermodynamic information on the interaction effects of DKP and the urea in aqueous solutions. Curvature of a logarithmic plot of the solubility of DKP *versus* $1/T$ would be indicative of self association effects, and if sufficiently pronounced might be used to evaluate heats of association between various DKP species. Such curvature, however, was not found from our measurements. The precipitation of a urea complex with DKP was found to occur in 8 *M* urea solutions at 30°.

Experimental

1. **Sample Preparations.**—The diketopiperazine was prepared by the method of Dunn.[11] The product was recrystallized twice from water. The product gave a negative ninhydrin test and was subjected to paper chromatographic analysis to determine a limit of glycine contamination. The chromatography indicated glycine impurities of less than 0.2%. Stability tests were run on water DKP solutions which were exposed to temperatures up to 80° for time comparable to the solubility experiment. The chromatographic method used indicated that DKP was stable under these conditions. C^{14}-urea was obtained from California Corp. for Biochemical Research.

2. **Solubility Measurements.**—Some initial experiments on the solubility of diketopiperazine in pure water by Cross[12] had been made using a simple method of residue analysis to determine the amount of DKP which dissolved in an equilibrated solution. This method was not suitable for solutions containing significant portions of urea, since the residue then consisted of an unknown proportion of urea and DKP. A direct chemical analysis of DKP in the presence of urea did not seem to offer a desired accuracy. For these reasons a physical method based on the refractive index of the solution was developed.

The differential prism method, used by Debye in determining refractive index difference between solvent and solution,[13] proved to be a suitable method for evaluating the concentration of dissolved DKP.

For our purposes it was not necessary to calibrate the instrument in terms of refractive index but rather in direct concentration units of dissolved DKP. The optical cell was constructed with a thermostated jacket. A small magnetic stirring bar fit into the central prism section and was stirred by a magnetic stirrer unit placed beneath the cell.

A saturated solution of DKP in water at 25° was found to deflect the slit image approximately 2.00 mm. on the micrometer scale. The maximum deflection that could be measured was 10.00 mm.

Calibration of this instrument was made with the cell in position on the optical bench. Weighed amounts of DKP were added to the central prism compartment containing a given volume of solvent. From the measured deflections a calibration curve was established. The effect of temperature on the calibration was found to be virtually negligible. A near linear relation between deflection and concentration was observed. This is not surprising since refractive index increments are nearly proportional to solute concentration, and the measured deflections are almost linear with respect to refractive index differences. With the instrument calibrated, sufficient solute then was added so that saturated conditions were maintained over the desired temperature range. The cell remained positioned in the same place for calibration and the subsequent solubility run.

Deflection readings were taken on the same solution system first increasing and then lowering the temperature. In this way hysteresis effects could be detected which would indicate equilibrium was not being established. A satisfactory run was governed by reproducibility of readings within 0.2% for the temperature cycle.

3. **Precipitate Analysis.**—The absence of hysteresis in the first runs at 0, 2, 4 and 6 *M* urea solvent concentrations suggested that no change in the precipitated solute occurred in the course of these experiments. However, with 8 *M* urea as solvent a marked change in the observed deflection took place when the temperature was lowered to 30° with the result that a negative deflection actually occurred by 25°. This served to indicate that urea was precipitating along with the DKP solute. Further analysis was made in separate experiments using C^{14}-labeled urea. Precipitation occurred in the presence of 8 *M* C^{14}-urea through the 30° range. The precipitate then was filtered, washed with unlabeled saturated solution of the same urea concentration, dried, weighed, redissolved in water, an aliquot taken, dried and counted as thin samples. An aliquot of the original labeled solution was also dried to provide a calibration. At least two counting samples were prepared from each aliquot. Samples from diluted aliquots were also prepared to test for possible errors due to self absorption. Precipitates of DKP from 4 *M* urea were analyzed in the same manner.

In a separate experiment using 8 *M* urea solution saturated with DKP, a precipitate was taken from the saturated solution upon cooling 25 to 10°. The precipitate, in the form of reasonably sized crystals, was washed with a small amount of cold water. The surface of the crystals then became frosty, indicating that one component of the crystalline precipitate was dissolved. The largest crystals were selected and sent for C, H and N analysis to the Galbraith Microanalytical Laboratories.

Results

The DKP solubility is listed in Table I. The data when plotted in log weight % (w_2) *vs.* $1/T$,

(3) C. H. Bamford, A. Elliott and W. E. Hanby, "Synthetic Polypeptides," Academic Press, Inc., New York, N. Y., 1956, Chapter IV.

(4) J. A. Schellman, *Compt. rend. Lab. Carlsberg, Ser. Chim.*, **29**, 223 (1955).

(5) J. A. Schellman, *ibid.*, **29**, 230 (1955).

(6) B. H. Zimm and J. K. Bragg, *J. Chem. Phys.*, **31**, 526 (1959).

(7) S. A. Rice, A. Wada, and E. P. Geiduschek, *Disc. Faraday Soc.*, **25**, 130 (1958).

(8) L. Peller, *J. Phys. Chem.*, **63**, 1194 (1959).

(9) K. H. Meyer and O. Klemm, *Helv. Chim. Acta*, **23**, 25 (1940).

(10) R. B. Simpson and W. Kauzmann, *J. Am. Chem. Soc.*, **75**, 5139 (1953).

(11) M. S. Dunn, *J. Org. Chem.*, **12**, 490 (1947).

(12) Private communication from Mr. Jon Cross.

(13) P. P. Debye, *J. Appl. Phys.*, **17**, 392 (1946).

are adequately represented by straight lines over the region investigated.

Table I

Solubility of DKP in Weight %

Temp., °C.	Water, %	Solvent 2 *M* urea	4 *M* urea	6 *M* urea	8 *M* urea
25	1.66	1.95	2.38	2.42	...
30	1.99	2.29	2.73	2.74	...
40	2.74	3.06	3.61	3.50	3.57
50	3.77	4.07	4.64	4.43	4.41
60	5.05	5.42	5.94	5.48	5.44

In view of the observed linearity of the logarithmic solubility *versus* $1/T$ plot the heat of solution is apparently unaffected by DKP concentration and temperature for a given urea solvent concentration. The heats of solution then may be regarded to be the heats of dissolution at infinite dilution. The exact treatment of the effect of temperature on the activity coefficients is needed to completely verify this conclusion.[14] However, since the solution is relatively dilute with respect to the non-electrolyte DKP, dilute solution behavior would be expected unless strong association effects were present. The heat of solution is calculated from

$$\frac{\partial \ln w_2}{\partial (1/T)} = \frac{-\Delta H}{R}$$

where ΔH is the heat of solution of solid DKP, and is regarded as the heat of solution in the standard dilute state. The values of ΔH determined by a least squares analysis are tabulated along with the probable errors in Table II.

Table II

Heat of Solution of Solid DKP

Solvent	*H* (cal./mole DKP)	Stand. dev. (cal./mole)
Water	6184	59
2 molar urea	5665	29
4 molar urea	5096	46
6 molar urea	4570	68
8 molar urea	4179	6

Our data for the heat of solution in pure water were compared with data obtained by Cross,[12] using an independent method of residue analysis. We obtained 6.18 ± 0.06 compared with Cross' value of 6.1 ± 0.1 for five separate determinations. It might be noted that his solubility results also conformed to a nearly perfect linear relation when plotted as indicated above.

With 8 *M* urea solutions (as has been noted) a different type of precipitate formed at 30°. The radioactive analysis of this precipitate indicated that it contained between one and two moles of urea for each mole of DKP. A precise analysis of a carefully prepared precipitate below 25° from 8 *M* urea gave the following results: C, 31.04; H, 5.78; N, 36.01. The ratio of C/N is 12.0/14.0. This would be expected for DKP·2Urea with theoretical values of C, 30.76; H, 6.02; N, 35.90. The agreement is within experimental error. The formation of any urea type complex at lower urea concentrations which were used in this work was ruled out by the absence of labeled urea in the precipitated DKP.

(14) A. T. Williamson, *Trans. Faraday Soc.*, **40**, 421 (1944).

Discussion

The adequate straight line representation of the solubility curves indicates an apparent absence of association effects in solution governed by enthalpies of association. This conclusion may be drawn by developing a first-order theory of the equilibrium formation of dimers in solution and by showing how this equilibrium affects the observed temperature dependence of the solubility. The analogous equations, however, have been developed for the solubility of a weak binary electrolyte by Noyes and Sammet[15] who showed that a linear relation between the log of the solubility and $1/T$ would occur only if the degree of association were zero or one, and remained relatively unaffected by the change in temperature. The latter condition could be met by a small heat of association. Since the heat of association of DKP should be of the order of several kcal., we conclude the linear solubility behavior requires a relatively small association effect between dissolved DKP molecules.

The presence of urea causes a significant enhancement of the solubility of DKP at low temperatures. The urea effect is less marked at higher temperatures, and in fact at higher concentrations and higher temperatures the presence of urea causes a depression in the solubility of DKP. The enthalpy effect due to the presence of urea may be estimated by the difference of the solubility reactions in water (ΔH_1) and solutions of urea (M), (ΔH_2)

$$\underset{\Delta H_2 - \Delta H_1}{\text{DKP(aq)} + \text{aq urea(M)} = \text{DKP (aq urea M)} + \text{aq}}$$

This reaction expresses the enthalpy effect upon changing the solvent surroundings of the dissolved DKP. This enthalpy difference serves as a measure of the hydrogen bond formation enthalpy of diketopiperazine with urea in aqueous solutions. The competing action of hydrogen bond formation with water manifests itself in the concentration dependency of $\Delta H_2 - \Delta H_1$. An estimate of the heat of interaction of urea (U) with the peptide bond in DKP (D) can be made by assuming an equilibrium of the following type between DKP molecules and urea molecules in the aqueous medium

$$\text{D} + \text{U} = \text{DU} \qquad K_1 = \frac{[\text{DU}]}{[\text{D}][\text{U}]}$$

$$\text{DU} + \text{U} = \text{DU}_2 \qquad K_2 = \frac{[\text{DU}]_2}{[\text{DU}][\text{U}]}$$

We shall assume ideal solution behavior for each species containing DKP since these are dilute. Then the solubility of DKP is given by the sum of the different species

$$[\text{D}_s] = [\text{D}] + [\text{DU}] + [\text{DU}_2]$$

The solubility of DKP in urea solutions is $[\text{D}_s]$ and at the same temperature [D] is the solubility in pure water. The fraction of peptide bond interactions per DKP molecule, f_p, is then given by

(15) A. A. Noyes and G. V. Sammet, *Z. physik. Chem.*, **43**, 513 (1903).

$$f_p = \frac{[DU] + 2[DU_2]}{[D_s]} = 1 - \frac{[D]}{[D_s]} + \frac{[DU_2]}{[D_s]} = 1 - \frac{[D]}{[D_s]} + K_1K_2\,[U]^2\,\frac{[D]}{[D_s]}$$

and the first equilibrium constant is

$$K_1 = \frac{1}{[U]}\,\frac{[D_s] - [D]}{[D]}\,\frac{1}{1 + K_2[U]}$$

The terms involving K_2 can be shown to be small even when the urea concentration is 2 M. At 25°, 2 M urea $[D]/[D_s] = 1.66/1.95$ an estimate of K_1 is 0.096, by using an activity coefficient of 0.87 for the 2 M urea[16] and assuming that there are two equal interaction sites for urea on each DKP molecule, so $K_2 \cong 1/4\ K_1$. The fraction of peptide bonds associated with urea under these conditions is 0.154. The difference of the heat of solution of DKP in water and urea (2 M) is equal to $-(0.52 \pm 0.07)$ kcal./mole, and so the heat of association of urea with the *cis* peptide bond would be -3.4 ± 0.5 kcal.[17] The problem of estimating an average hydrogen bond enthalpy for this situation requires knowledge of the average number of bonds formed between urea and the *cis* peptide unit. A maximum number would be two, which gives a value of -1.7 ± 0.2 kcal. per hydrogen bond. Schellman[4] has assumed that there are approximately 4/3 hydrogen bonds in urea dimers, and estimates a value of -1.5 kcal. per amide hydrogen bond. Since the heat of reaction is larger between DKP and urea and the decrease of entropy is probably not so great in forming two hydrogen bonds as in the case of urea with itself where internal rotation is removed, one would expect a larger average number of hydrogen bonds between urea and the *cis* peptide bond. An estimate of the enthalpy of a peptide amide hydrogen bond formation in water would then be more in the range of -2 than -1.5 kcal.

The stronger association of urea with the *cis* peptide bond than with itself is reflected in an estimate of K_1 as 0.096 at 25° and 2 M urea, compared with Schellman's urea–urea association constant of about one-half this value. Even with the increased tendency of DKP to associate with urea, and likewise with itself, the fraction of DKP molecules associated in water to form dimers is still small. Assuming a self association constant of 0.1 for DKP at 25° where a saturated solution is about 0.1 M, something like 1% would be associated.

The formation of a molecular complex between DKP and urea when precipitated from an 8 M solution, lends further evidence to the hypothesis of significant hydrogen bonding of urea with proteins as the cause of protein denaturation.[18] It is interesting that such a complex forms only at high urea concentrations which are comparable to concentrations where pronounced protein denaturation likewise occurs.[19,20] This similarity could well be due to the similar action of urea to both cases.

(16) G. Scatchard, W. Hamer and S. Wood, *J. Am. Chem. Soc.*, **60**, 3061 (1938).

(17) A less accurate value can be estimated from K_1 as a function of temperature giving -4.5 ± 2.0 kcal.

(18) W. H. Harrington and J. A. Schellman, *Compt. Rend. Trav. Lab. Carlsberg, Ser. Chim.*, **30**, 21 (1956).

(19) L. K. Christensen, *ibid.*, **28**, 39 (1956).

(20) J. G. Foss and J. A. Schellman, *J. Phys. Chem.*, **63**, 2007 (1959).

FRACTIONATION OF OXYGEN ISOTOPES BY THE DISTILLATION OF AZEOTROPIC SOLUTIONS[1,2]

BY LOIS NASH KAUDER, W. SPINDEL AND E. U. MONSE

Department of Chemistry, Rutgers, The State University, Newark 2, New Jersey

Received April 5, 1961

The possibility of using the exchange equilibrium H_2O^{16} [hydrated] + H_2O^{18} [solvent] $\rightleftarrows$ H_2O^{18} [hydrated] + H_2O^{16} [solvent] for concentrating oxygen isotopes, by distilling azeotropic acid solutions, has been investigated. Rayleigh distillations were carried out to determine the relative fractionation factors, α, for constant boiling HCl, HBr and HNO_3 at several temperatures and pressures as compared to α' for water. Experiments were also run in a distillation column [65 cm. long and 13 cm. i.d.] packed with tantalum helices, at atmospheric pressure and varying flow rates. With a flow rate of 38 ml./hr., water showed an over-all separation [depletion] of 1.41; 6.8 m HCl, 1.83; 10.9 m HBr, 1.90; and 31 m HNO_3, 1.28. The single stage factor was calculated to be 1.007 for HCl at 110° and 1.007 for HBr at 126° as compared to a value of 1.004 for water at 100°.

Introduction

Taube and co-workers[3,4] have investigated oxygen isotope effects in aqueous solutions and have used such effects to study the nature of ionic hydration. In brief they found that the bonds formed between a number of cations and the oxygen of hydrated water molecules are of sufficient strength to cause the equilibrium constant for the reaction

$$H_2O^{16}\,(\text{hydrated}) + H_2O^{18}\,(\text{solvent}) \rightleftarrows H_2O^{18}\,(\text{hydrated}) + H_2O^{16}\,(\text{solvent}) \quad (1)$$

to be appreciably different from unity. The magnitude of the constant is dependent on the charge to size ratio of the cation, and as an example it may be noted that the equilibrium constant K for equation 1 is 1.040 at 25° when the hydrated

(1) This work was carried out under contract AT(30-1)-2250 between Rutgers, The State University, and the U. S. Atomic Energy Commission.

(2) Presented before the Division of Physical Chemistry at the 138th meeting of the American Chemical Society, New York, N. Y., September, 1960.

(3) J. P. Hunt and H. Taube, *J. Chem. Phys.*, **19**, 602 (1951); H. M. Feder and H. Taube, *ibid.*, **20**, 1335 (1952); A. C. Rutenberg and H. Taube, *ibid.*, **20**, 825 (1952).

(4) H. Taube, *J. Phys. Chem.*, **58**, 523 (1954); *Ann. Rev. Nucl. Sci.*, **6**, 277 (1956).

ion is a proton.[4] Naturally in aqueous ionic solutions the large excess of uncoördinated water molecules makes it impossible to realize this magnitude of isotope discrimination, but the preferential hydration by the H_2O^{18} species leads to a change in the oxygen isotope fractionation for distillation of aqueous solutions above the fugacity ratio H_2O^{16}/H_2O^{18}. The magnitude of the change depends upon the nature of the cation, and its concentration in the solution. Taube[4] indicates that salts containing cations of high charge to size ratio, *i.e.*, Al^{+++}, Mg^{++}, H^+ increase the separation factor above the value found in pure water, and the effect is linear with the molality of the salt over a considerable concentration range.

From the magnitude of the separation factors for several ions at 25°, it appeared that the hydration effect might be favorable for concentrating oxygen isotopes, provided that the single stage factor could be multiplied by some suitable process. The distillation of azeotropic solutions appears to be a reasonable way of accomplishing this, because the chemical composition of the system remains unchanged during distillation, while the H_2O^{16} species should preferentially concentrate in the vapor phase, to a greater extent than in the distillation of pure water.

The single stage separation factor, α, is defined as the ratio (H_2O^{18}/H_2O^{16}) liq./(H_2O^{18}/H_2O^{16}) gas. It may be estimated from the equilibrium constant K for the exchange between hydrated and solvent molecules in the liquid according to equation 1, and the fugacity ratio, α', for water, by the relationship[5]

$$\alpha = [M(K - 1) - 1]\alpha' \qquad (2)$$

Here, M is the mole fraction of hydrated water molecules and is obtained from the molality, m, of the cations in solution, and the hydration number, σ for the cation [*i.e.*, no. of hydrate water molecules per cation] by the relationship[4] $M = \sigma m/55.5$. For $M = 0$, the single stage factor, α, reduces to α', the fugacity ratio in water.

Using equation 2, and Taube's data,[4] it is found that for 4 to 12 m acid solutions the single stage factor, α, at 25° increases by 0.003 to 0.009 above the value $\alpha' = 1.008_3$ for pure water.[6]

Rayleigh type distillations were carried out to determine the relative magnitudes of single stage factors at temperatures other than 25°, for distilled water, and for azeotropic solutions of hydrochloric acid, hydrobromic acid and nitric acid. Studies of these systems also were carried out in a multi-stage distillation column to measure the isotopic concentration produced by the hydration effects.

Experimental

Rayleigh Distillations.—A large volume (1 liter) of each solution was distilled to a small volume (5–50 ml.) at a slow distillation rate of ~ 1.7 ml./min. so as to minimize bumping.

The single stage separation factor, α, was calculated from the measured separation factors in these distillations by the well known Rayleigh formula[7]

$$(N/N_0)^{\alpha-1} = W_0/W \qquad (3)$$

where N and N_0 (both assumed to be $<<1$) refer to the mole fraction of the rate isotope in the final and initial samples, respectively, and W and W_0 are the final and initial volumes.

Column Experiments.—A vacuum jacketed column 65 cm. long and 13 mm. i.d., packed with tantalum "Helipak" spirals (0.035″ × 0.070″ × 0070″, Podbielniak, Inc., Chicago, Ill.) was used. The system was operated with a large reservoir of boiling liquid at the lower end and a minimum holdup at the upper end. Samples of condensate were analyzed for oxygen-18 depletion as a function of time, and flow rate. The column was preflooded before operation by pouring boiling liquid down the column while heating the reservoir at a much higher rate than required to produce the desired throughput. As the voltage of the heater was reduced gradually, a column of liquid slowly descended through the exchange column while refluxing continued. Contamination of the vapor at the top by atmospheric water vapor was prevented by closing the outlet at the top with a balloon or polyethylene bottle. The constancy of flow rate was checked by measuring the drop rate every hour.

Isotope Analysis.—Samples of the original and final solutions (0.6–1.0 ml.) were equilibrated overnight with measured amounts of CO_2 and analyzed for O^{18} content.[8] The acid solutions were first neutralized with anhydrous ammonia since highly acid solutions do not reach equilibrium even after 20 hours of contact.

Another method of isotope analysis was used in some cases. This involved a rapid equilibration with O_2 in an electrical discharge.[9] About 0.05 cc. of H_2O or acid was added to a 100-cc. discharge tube which had been filled with dry N_2 or air. After degassing the liquid, about 6 cc. atm. of O_2 was metered in. A 7500 volt transformer was connected, and the system was arced for 20 minutes in an oven at 70–80°. Before admitting the gases to the mass spectrometer, the liquid was frozen with a Dry Ice–trichloroethylene mixture. No oxygen was added for analysis of nitric acid, since it decomposes partially into N_2 and O_2 and the latter can be analyzed without isotopic dilution.

Results

Rayleigh Distillations.—A summary of the results is shown in Table I. The single stage separation factors shown are the ratios (O^{16}/O^{18}) solution/(O^{16}/O^{18}) gas phase. The absolute values of α obtained by Rayleigh distillation of water at the three temperatures, 42, 63 and 100° are somewhat higher than the values given by Dostrovsky and Raviv.[6] This probably is due to some refluxing in the flask.

TABLE I

SINGLE STAGE FACTORS FOR OXYGEN FRACTIONATION AS DETERMINED BY RAYLEIGH DISTILLATION

Solution	Molality	Temp. (°C.)	Pressure (cm.)	Separation factor, α (±0.001)	$\alpha - \alpha'$
H_2O		42	~7	1.009	
		63	~9	1.007	
		100	76	1.005	
		125		(1.004)[a]	
HCl	8.2	45	~7	1.014	0.005
	6.8	110	76	1.009	.004
HBr	12.4	65	~9	1.016	.009
	10.9	126	76	1.010	.006
HNO_3	31	121	76	1.006	.002

[a] Extrapolated value.

Rayleigh distillations often yield erroneous single-stage separation factors if refluxing occurs

(5) E. U. Monse, W. Spindel, L. N. Kauder and T. I. Taylor, *J. Chem. Phys.*, **32**, 1557 (1960).

(6) I. Dostrovsky and A. Raviv, "Proc. Int. Symp. on Isotope Separation," Interscience Publishers, Inc., New York, N. Y., 1958, p. 336.

(7) H. C. Urey and A. H. Aten, *Phys. Rev.*, **40**, 1 (1932).

(8) M. Cohn and H. C. Urey, *J. Am. Chem. Soc.*, **60**, 679 (1938).

(9) T. I. Taylor, personal communication.

TABLE II

OXYGEN ISOTOPE SEPARATION IN DISTILLATION COLUMN AT ATMOSPHERIC PRESSURE

1 Soln.	2 Run	3 ml./hr.	4 S	5 n for $\alpha = 1.004$	6 n from eq. 4	7 α, calcd. from columns 4 and 6
H_2O	22	36	1.41	86		
	21	48	1.40	84		
	17	50	1.38	81		
	16	56	1.36	77		
	22	59	1.34	74		
	36	63	1.38	81		
	21	65	1.36	77		
	42	72	1.30	66		
	21	74	1.34	74		
	33	76	1.33	72		
	32	77	1.35	76		
	22	102	1.29	64		
	42	~140	1.32	70		
6.8 m HCl	27	18	1.89	..	93	1.0070
	27	38	1.83	..	85	1.0071
	27	42	1.74	..	84	1.0066
	26	43	1.79	..	84	1.0070
	23	51	1.79	..	81	1.0072
	26	56	1.69	..	79	1.0067
	26	60	1.71	..	77	1.0070
	27	63	1.63	..	76	1.0067
						Av. 1.0069 ± 0.0002
10.9 m HBr	38	38	1.90	..	85	1.0075
	38	48	1.91	..	82	1.0079
	37	60	1.69	..	77	1.0068
	38	67	1.75	..	75	1.0075
	37	86	1.62	..	68	1.0071
						Av. 1.0074 ± 0.0003
31 m HNO_3	43	42	1.28	..	84	1.0030
	43	71	1.22	..	73	1.0027
	41	74	1.21	..	72	1.0027
	29	~92	1.19	..	66	1.0026
						Av. 1.0028 ± 0.0002

in the pot, or if liquid droplets are carried over in the vapor. By distilling all liquids under the same conditions, such sources of error should cancel out to yield good *relative* magnitudes of α for pure water and the acids. The agreement between the increase of the single stage factor for 6.8 m HCl at 45°, 8.2 m HCl at 110°, 10.9 m HBr at 126°, and 12.4 m HBr at 65° (as compared to pure water at these temperatures), with the values expected for those concentrations at 25°,[4] is gratifying. The difference ($\alpha - \alpha'$) increases with the concentrations of the acids, and is relatively insensitive to an increase in temperature.

In the case of nitric acid, which has the highest molality, an α of 1.006 at 121° was found. The exchange of oxygen between nitrate ion and water, and the large fraction of oxygen present as HNO_3 in the gas phase decrease the expected single stage factor appreciably.

Column Experiments.—Table II summarizes the results of the column experiments. Column 4 of Table II is the final steady state separation obtained at the various flow rates. The separation values shown were all obtained from samples taken from the column after operation for 20 hours, since it was found that steady state was reached within this time. It is obvious that appreciably higher separations were found under comparable conditions of flow rate and pressure for HCl and HBr as compared with H_2O and HNO_3.

In addition to yielding an over-all comparison of the various solutions for concentrating oxygen isotopes, the distillation column studies also provided an additional method for determining relative single-stage isotope separation factors, α. The over-all separation, S, in a distillation column operating at total reflux, is equal to α^n, where n is the number of separating stages. Determination of either α or n from a measurement of S is only possible if the other variable is known. The number of stages in a distilling column (or the height equivalent to a theoretical plate, HETP) is primarily influenced by the column geometry, the type of packing used and the interstage gas and liquid flow rates. A single packed column should be relatively insensitive to the liquids distilled, provided that the wetting characteristics are similar (*i.e.*, surface tension, viscosity, density). Thus, in the present column, since α is known for water[6] (1.004 at 100°), n, the number of stages, can be evaluated as a function of flow rate from the steady-state separation obtained by water distillation, as shown in column 5, Table II.

From these values the following empirical re-

lationship between the number of stages, n, and the flow rate, L, in ml./hr. can be obtained

$$n = A - BL \qquad (4)$$

Here A and B are constants, $A = 99$; $B = 0.36 \pm 0.01$ ml.$^{-1}$ hr. Equation 4 is valid for flow rates between approximately 20 and 100 ml./hr.

The value of n calculated according to equation 4 (col. 6) at the flow rate, L. (col. 3) and the over-all separation, S, (col. 4) measured for the acid solutions, has been used to calculate the single stage factor, α, for these systems. The factors are listed in col. 7. The results for the average values of α obtained in this way are: HCl at 110°, $\alpha = 1.0069 \pm 0.0007$; HBr at 126°, $\alpha = 1.0074 \pm 0.0007$; and HNO_3 at 125°, $\alpha = 1.0028 \pm 0.0005$. The error is due to the scattering of the measured values of n and the over-all separation.

Discussion.—Single stage factors α may be compared with factors α' for water distillation at corresponding temperatures.[6] Thus the increase for the HCl solution is $\alpha - \alpha' = 0.0034 \pm 0.0007$ at 110° and for the HBr solution, $\alpha - \alpha' = 0.0049 \pm 0.0007$ at 125°. These values are in agreement with those obtained by Rayleigh distillation (Table I). They indicate that $(\alpha - 1)$ for HBr solution is three times as large as the corresponding value for H_2O (0.0025) at 126°, and $(\alpha - 1)$ for HCl is twice the value for H_2O (0.0035) at 110°. The value of α for HNO_3 does not differ from that for H_2O, as expected from the Rayleigh distillation.

It may be of interest to calculate the equilibrium constant K for the exchange of oxygen isotopes between hydrated and solvent molecules from the measured data. Using equation 2, the measured values for α' and the data for HCl ($\sigma = 1$, $m = 6.8$, and $\alpha = 1.007$), the equilibrium constant at 110° becomes $K = 1.024 \pm 0.008$. From the data for HBr ($\sigma = 1$, $m = 10.9$, $\alpha = 1.007$) the equilibrium constant at 126° becomes $K = 1.025 \pm 0.008$. This compares to the value of 1.040 calculated by Taube[2] at 25°.

Since the separation factors observed for distilling azeotropic acid solutions are significantly larger than those found for water distillation at a comparable pressure, distillation of such solutions may be useful for concentrating oxygen isotopes. Experiments are in progress on oxygen exchange in a packed column, between concentrated aqueous lithium chloride and water vapor.

Recent results by K. E. Holmberg (*Acta. Chem., Scand.* **14**, 1660 (1960)), just called to our attention, on physical properties of isotopic forms of certain inorganic acid-water azeotropes, confirm our findings within experimental error.

DIFFUSION OF OXYGEN IN SINGLE CRYSTALS OF NICKEL OXIDE

BY MICHAEL O'KEEFFE AND WALTER J. MOORE[1]

Chemical Laboratory, Indiana University, Bloomington, Indiana

Received April 19, 1961

The diffusion of ^{18}O has been measured in monocrystalline NiO by following the exchange of gaseous oxygen enriched in ^{18}O with the NiO crystals. At an oxygen pressure $P_{O_2} = 50$ mm., from 1100 to 1500°, $D^{\circ}_{NiO} = 1.0 \times 10^{-5} \exp(-54$ kcal./RT) cm.^{2} sec.$^{-1}$ The D°_{NiO} increases with P_{O_2}. The most reasonable mechanism for the oxygen diffusion is believed to be by way of interstitial oxygen atoms.

Several authors have suggested that diffusion of oxygen may be a contributing mechanism in the growth of oxide films on iron[2] and nickel.[3] No experimental data have been available on the diffusion of oxygen in crystals of FeO, NiO or CoO. The present work provides some information on the ^{18}O–NiO system and allows us to conclude that D^{O}_{NiO}, the diffusion coefficient of oxygen in NiO, is at least several orders of magnitude less than D^{Ni}_{NiO}, the diffusion coefficient of nickel in nickel oxide, at all temperatures.

Experimental Methods

The diffusion coefficients were measured by following the exchange of oxygen in the sample with a surrounding atmosphere of oxygen enriched in ^{18}O. The enriched oxygen was obtained by electrolysis of water obtained from the Weissmann Institute and containing 0.437% ^{17}O and 6.62% ^{18}O. The nickel oxide sample was in the form of a cube with (100) faces and 3 mm. cube edge cleaved from a single crystal boule grown by the Verneuil method at the Tochigi Chemical Industry Company. To eliminate the possibility of exchange of oxygen with the container, the NiO sample was supported on platinum foil in a 90% Pt–10% Rh tube which was connected *via* a Kovar-glass seal to a conventional vacuum system.

After installation of the sample and pumping out, enriched oxygen was admitted to a known pressure, and the tube closed off by means of a vacuum stopcock. The volume thus sealed off was approximately 50 cc. After heating for a known time at a constant temperature between 1100 and 1500° a sample of oxygen was drawn off and analyzed mass spectrometrically.

If A_0 and A_t are the abundances of oxygen-18 in the gas phase initially and at time t, respectively, the ratio of the uptake by the solid at t to the uptake at infinite time is given by

$$\frac{M_t}{M_\infty} = (1 + \beta)\left(\frac{A_0 - A_t}{A_0 - A}\right) \qquad (1)$$

where $\beta = N^g/N^s$, the ratio of numbers of atoms of oxygen in gas and in crystal, and A is the natural abundance of oxygen-18 in the nickel oxide. The diffusion coefficient, D, is then given by

$$\left(1 - \frac{M_t}{M_\infty}\right)^{1/3} = 1 - (1 + \alpha)\left\{1 - e\,\mathrm{erfc}\left(\frac{Dt}{a^2\alpha^2}\right)^{1/2}\right\} \qquad (2)$$

where $\alpha = \beta/3$ and $e\,\mathrm{erfc}\,Z = e^{Z^2}(1 - \mathrm{erf}\,Z)$. The right-hand side of equation 2 is the solution for a slab of thickness $2a$,[4] the cube of this expression is the corresponding solution for a cube.[5]

(1) Work done under Contract AT-(11-1)-250, U. S. Atomic Energy Commission.

(2) H. Pfeiffer and B. Ilschner, *Z. Elektrochem.*, **60**, 424 (1956).

(3) R. Lindner and A. Akerstrom, *Disc. Faraday Soc.*, **23**, 133 (1957).

(4) J. Crank, "The Mathematics of Diffusion," Clarendon Press. Oxford, 1956, p. 54.

(5) S. C. Jain, *Proc. Roy. Soc.* (*London*), **A243**, 359 (1957).

For small values of Dt ($<10^{-6}$ cm.^{2}), the approximation of a semi-infinite solid was used, D being given by

$$M_t = 2SC_0\left(\frac{Dt}{\pi}\right)^{1/2} \qquad (3)$$

where S is the surface area and C_0 the mean concentration of ^{18}O at the surface of the nickel oxide. The sample in this case consisted of a number of cleaved plates with a total surface area of approximately 2 cm.^{2}.

Results and Interpretations

Figure 1 is a plot of log D^{O}_{NiO} against T^{-1}.

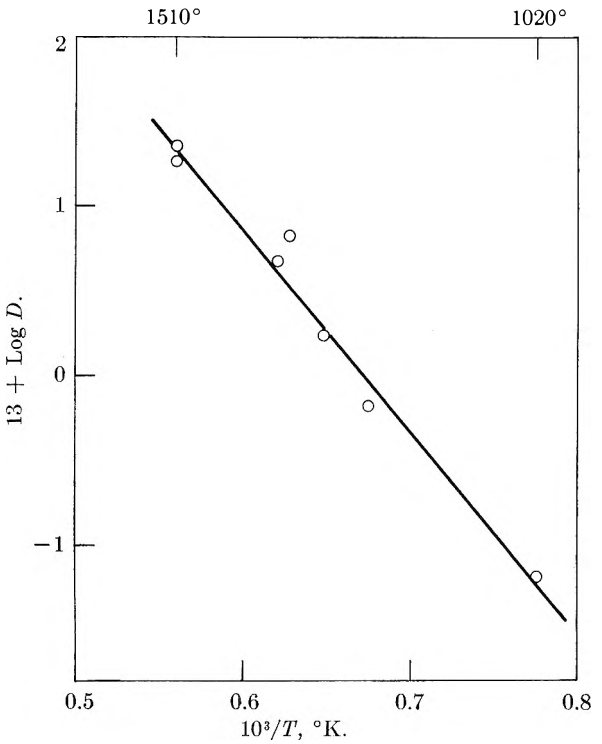

Fig. 1.—Diffusion coefficient of ^{18}O in NiO as function of temperature at P_{O_2} = 50 mm.

The straight line corresponds to

$$D^{O}_{NiO} = 1.0 \times 10^{-5} \exp(-54 \text{ kcal.}/RT)$$

These measurements were made in oxygen at a pressure P_{O_2} = 50 mm. Measurements of the variation of D^{O}_{NiO} with P_{O_2} at 1300 and 1500° showed the diffusion coefficient to increase with the oxygen pressure. This result would appear to exclude definitely, as in the case of cuprous oxide,[6] a mechanism of diffusion based on vacancies at oxide sites.

New measurements[7] also have been made of the diffusion of ^{63}Ni in specimens of the same NiO crystal used for the measurement of diffusion of ^{18}O. We have included these results as well as available data on diffusion in MgO in Table I. The data are given at 1500°K. in the form of the parameters of the transition-state theory

$$D = (kT/h)\, a^2 \exp(\Delta S^{\pm}/R) \exp(-\Delta H^{\pm}/RT)$$

where a is the smallest jump distance between normal sites of a diffusing atom or ion.

At 1500°K. in NiO, D^{Ni}/D^{O} is about 2000. This ratio indicates that the transport of oxygen by volume diffusion through the oxide layer plays a negligible role in the interdiffusion of oxygen and nickel. The interdiffusion coefficient is given by[10]

$$D_\Delta = (S/kT)(D^{Ni} + D^{O})\, d\mu_{Ni}/d\Delta \qquad (4)$$

where S is the number of either cation or anion sites and μ_{Ni} is the chemical potential of Ni in NiO.

TABLE I

DIFFUSION IN NiO AND MgO AT 1500°K.

	$\Delta H^{\pm}$, kcal.	$\Delta S^{\pm}$, cal. deg.$^{-1}$
^{63}Ni in NiO	36.6	−11.7
^{18}O in NiO	51.0	−17.6
^{28}Mg in MgO[8]	75.5	+ 4.0
^{18}O in MgO[9]	58.0	−21.0

The ionic radii of Ni^{+2} and Mg^{+2} are nearly the same, 0.69 and 0.65 Å., respectively, according to Pauling's table, and NiO and MgO form a continuous series of solid solutions.[11] It is important to note, therefore, the very great difference between D^{Ni}_{NiO} and D^{Mg}_{MgO}. This difference undoubtedly reflects the ease of forming cation vacancies in NiO by solution of excess oxygen, as contrasted with the virtual impossibility of such a reaction in MgO. The vacancies must be neutralized by the reaction $M^{+2} \rightarrow M^{+3}$, and the third ionization potential is 80 e.v. for Mg but only 36 e.v. for Ni. Cation vacancies can occur in MgO as intrinsic defects of the Frenkel or Schottky type, and these will have a higher ΔH of formation than the nonstoichiometric vacancies in NiO. We also can interpret the difference in the $\Delta S^{\pm}$ values on this basis. In NiO there is a ΔS of formation of vacancies, associated with the solution of gaseous oxygen, of about −10 cal. deg.$^{-1}$. In MgO the vacancies arise through internal disorder, and there is no corresponding decrease in entropy associated with their formation.

The parameters for diffusion of oxygen in NiO and MgO are strikingly similar. We can understand them at least qualitatively on the basis of diffusion of interstitial oxygen in both cases. There would be somewhat less room for an interstitial O in the MgO structure, and its $\Delta H^{\pm}$ for diffusion is correspondingly somewhat higher. The negative entropies are explained by the negative ΔS for the passage of oxygen from gas to solid, and a further $\Delta S_i^{\pm}$ for mobility of interstitial oxygen, which can be ascribed to increased vibration frequencies as the interstitial moves into the transition state. Since it would clearly be energetically difficult to accommodate ordinary interstitial oxygen in these structures, defects such as crowdions or split interstitials may be responsible for the diffusion of the oxygen. It would even be possible to preserve a sort of vacancy mechanism, if we postulated triple vacancies ($V_C V_C V_A$), where V_C and V_A are cation and anion vacancies. Like $[V_C]$ alone the concentration of triplets should increase with oxygen pressure.

(6) W. J. Moore, Y. Ebisuzaki and J. A. Sluss, *J. Phys. Chem.*, **62**, 1438 (1958).

(7) J. S. Choi and W. J. Moore, to be published.

(8) R. Lindner and G. Parfitt, *J. Chem. Phys.*, **26**, 182 (1957).

(9) Y. Oishi and W. D. Kingery, *ibid.*, **33**, 905 (1960).

(10) R. Brebrick, *J. Appl. Phys.*, **30**, 811 (1959).

(11) W. C. Hahn and A. Muan, *J. Phys. Chem. Solids*, **19**, 338 (1961).

NOTES

DEAD-END PORE VOLUME AS DISTRIBUTED SOURCES AND SINKS

By Walter Rose, H. C. Tung

College of Engineering, University of Illinois, Urbana, Illinois

and Claude Newman

Department of Applied Mathematics, University of Colorado

Boulder, Colorado

Received October 20, 1960

Let us state the mass (or energy) continuity condition to describe transport phenomena in material bodies (*e.g.*, diffusion, porous media compressible fluid flow, heat transfer, electrical conduction, etc.) as

$$d\rho/dt + \text{div } \bar{M} = \rho\sigma \qquad (1)$$

where

$\text{div } \bar{M} = \text{div } (\rho\bar{v}) = \partial(\rho v_x)/\partial x + \partial(\rho v_y)/\partial y + \partial(\rho v_z)/\partial z$

$\bar{M}$ is the mass (or energy) flux vector per unit area

ρ is the mass (or energy) per unit volume

$\bar{v}$ is the velocity vector (with components v_x, v_y and v_z)

σ is the density of distribution of internal sources and sinks as a function of time (t) and the space coordinates (x, y and z).

Equation 1 is that given in the development of potential theory[1] to apply to the unsteady-states which ensue following an initial non-uniform distribution of mass (or energy) throughout a space region of interest. Since the three dependent variables are all indicated to be functions of the space coördinates, and of time, the solution of equation 1 requires that at least two other interrelationships between the dependent variables be known.

For example, if we limit attention to the subject matter of the recent paper by Goodknight, *et al.*,[2] we describe compressible fluid flow in porous media systems by combining equation 1 with: (a) the relationship between fluid density and pressure as given by some appropriate equation of state; (b) the relationship between the mass flux vector and the fluid pressure (*e.g.*, by invoking Darcy's Law).

In addition, of course, the function, $\sigma(x,y,z,t)$, must be specified. The resultant diffusivity equation then is integrable in principle (*e.g.*, if σ is zero, the classic Laplacian solutions will be available if the transport is steady, and Fourier solutions can be adopted for the unsteady-states), upon specification of the relevant initial and boundary conditions of the problem.

Goodknight, *et al.*, have shown a physical reason to consider solutions of equation 1 for cases where σ is non-zero. That is, they postulate the possibility of the prevalence of dead-end pore space in porous media systems of practical interest, so much isolated (*via* high resistance paths) from the "central" transport paths that during unsteady-states, transport of matter will occur variously to and from the dead-end pore regions.

The simplified theory of Goodknight, *et al.*, apparently leads to the correct (quantitative) description of the influence of continuously distributed dead-end porosity, when limited to those cases where the medium is taken to be homogeneous and isotropic. In effect they apply equation 1 to subregions of the porous medium (*i.e.*, to macroscopic differential volume elements) in the way of implicitly saying that the pore space can be partitioned into a continuous (central) domain, and a continuous *cul de sac* (peripheral) domain. It is then assumed that Darcy's law describes transport in the central domain region as long as the interaction between the fluid potential in the two contiguous domains is taken into explicit account.

In this Laboratory we are seeking more general solutions of the diffusivity equations derived from equation 1, examining for example the analytic methods discussed by Sneddon,[3] in order to treat the unsteady-states of heat transfer in solid media having randomly distributed internal sources and sinks (*e.g.*, distributed radioactive crystals of varying strengths). We suspect that in the most general case, a microscopically inhomogeneous distribution of dead-end porosity will be found in the macroscopic differential volume elements to which the diffusivity equation is to be applied. In consequence, the function $\sigma(x,y,z,t)$ will have such a complicated representation that general methods of analysis will not be immediately specifiable.

An analog representation of the situation we wish to consider is obtained by constructing a network of interconnected resistors (scaled to model local conditions of diffusivity), with capacitors at the mesh points (scaled to model the local divergence of mass or energy capacity of the system). Other capacitors connected variously to one or more of the mesh points through high resistance elements, then, represent the dead-end pores. A simple measurement of the resistance–capacitance time-constant of the network, therefore, serves to characterize the transients of equation 1 for particular systems with particular initial and boundary conditions.

In our initial work we have made use of a 160 mesh-point network (10 nodes wide by 16 elements between line source and sink regions).[4] The experimental results summarized in Table I thus show the marked degree to which the transients [as measured in terms of the network time-constant] depend on: (a) number of dead-end pores; (b) location of dead-end pores; (c) point of measure-

(1) O. D. Kellog, "Foundations of Potential Theory," Dover Publications (reissue of the original 1929 edition), 1953, p. 45 ff.

(2) R. C. Goodknight, W. A. Klikoff and I. Fatt, *J. Phys. Chem.*, **64**, 1162 (1960).

(3) I. N. Sneddon, "Elements of Partial Differential Equations," McGraw–Hill Book Co., New York, N. Y., 1957, p. 274 and 299 ff.

(4) 960-node network analyzer, Department of Applied Mathematics, University of Colorado. The network analyzer can be used to construct an arbitrary N-dimensional interconnection of resistors, with capacitors located as desired at the interconnecting points. Active components are supplied by a BEAC analog computer.

ment of the dependent variable; (d) time constant of the individual dead-end pores.

TABLE I

No. of dead-end pores	Location	Dead-end pore component sizes: Capacitance (farads)	Dead-end pore component sizes: Resistance (ohms)	Network time constant in relative sec. (*ca.* 60% greater than real time in sec.)
0	...	...	...	10.5[a]
1	At source	10^{-5}	2×10^4	10.4[a]
1	At sink	10^{-5}	2×10^4	25.5[a]
10	Uniformly distributed	10^{-6}	2×10^5	21.5[a]
10	Uniformly distributed	10^{-6}	2×10^5	15.7[b]
40	Uniformly distributed	2.5×10^{-7}	8×10^5	15.9[a]

[a] Measured at sink. [b] Measured in middle of network.

In all cases we have held the total capacitance of the dead-end pores as a constant fraction of the total capacitance of the central network domain region; likewise, the time-constant of the individual dead-end pores was held fixed (at 0.2 second). The central network itself was entirely isotropic and homogeneous, being made up of a rectangular array of 0.5 megohm resistors with 0.1 microfarad capacitors at each mesh point. These values arbitrarily were chosen and scaled to be meaningful with reference to the experiment of Goodknight, *et al.*[5]; however, it is to be expected that, had a less uniform network form been chosen, an even greater influence on the transients (from deadend porosity) would have been in evidence.

It is clear that the analog network model offers the opportunity to investigate problems of much greater complexity than those envisioned by Goodknight, *et al.* For example, media inhomogeneity and anisotropy can be scaled without increased difficulty, and micro- as well as macroscopically irregular dead-end pore configurations can be represented. As for the latter, if each mesh point is thought of as the macroscopic differential volume element to which equation 1 applies, the data of Table I refer to a discrete rather than a continuous distribution of dead-end pores in the *macroscopic* sense. On the other hand, if the entire network of many contiguous mesh points is taken as the macroscopic differential volume element of interest, the data of Table I reflect on the influence of a given *microscopic* distribution of dead-end pores.

(5) If in the prototype system, permeability is taken as 10^{-9} cm.^{2}, fluid compressibility is taken as 10^{-6} per dyne per cm.^{2}, porosity is taken as 0.25, fluid viscosity is taken as 10^{-2} poise, the length to cross-sectional area ratio is taken as unity, and the V_2/V_1 and H parameters of Goodknight, *et al.*, are taken as 0.625 and 10^{-1} reciprocal seconds, respectively, the scale ratio between time in the electrical analog system and in the prototype system will be 2×10^{-2}.

ESTIMATION OF DISSOCIATION CONSTANTS OF ELECTROLYTES

BY HENRY E. WIRTH

Department of Chemistry, Syracuse University, Syracuse, N. Y.

Received February 1, 1961

In order to evaluate the dissociation constant, K,[1] of a symmetrical electrolyte

$$K = \frac{c\alpha^2 y_\pm^2}{1 - \alpha} \quad (1)$$

from conductivity measurements, Fuoss[2] defined α by the expression

$$\alpha = \frac{\Lambda}{\Lambda^0(1 - S(\Lambda)\sqrt{\alpha c}/\Lambda^0)} = \frac{\Lambda}{\Lambda^0 F(Z)} \quad (2)$$

where

$$Z = S(\Lambda)\sqrt{\Lambda c}(\Lambda^0)^{-3/2} \quad (3)$$

and $F(Z)$ is the continued fraction

$$F(Z) = 1 - Z(1 - Z(1 - Z(1 - \ldots)^{-1/2})^{-1/2})^{-1/2} \quad (4)$$

The activity coefficient $y_\pm$ is evaluated from the limiting law

$$\log y_\pm = -S(f)\sqrt{\alpha c} \quad (5)$$

Substitution in equation 1 gives the relation

$$\frac{F(Z)}{\Lambda} = \frac{1}{\Lambda^0} + \frac{c\Lambda y_\pm^2}{F(Z)K(\Lambda^0)^2} \quad (6)$$

so that Λ^0 and K can be obtained from the intercept and slope of a plot of $F(Z)/\Lambda$ *versus* $c\Lambda y_\pm^2/F(Z)$.

In the corresponding method developed by Shedlovsky,[3] α is defined by

$$\alpha = \frac{\Lambda}{\Lambda^0} + \frac{S(\Lambda)\Lambda\sqrt{\alpha c}}{(\Lambda^0)^2} = \frac{\Lambda}{\Lambda^0} S(Z) \quad (7)$$

where

$$S(Z) = \left[\frac{Z}{2} + \sqrt{1 + \left(\frac{Z}{2}\right)^2}\right]^2 \quad (8)$$

This leads to the relation

$$\frac{1}{\Lambda S(Z)} = \frac{1}{\Lambda^0} + \frac{c\Lambda y_\pm^2 S(Z)}{K(\Lambda^0)^2} \quad (9)$$

from which Λ^0 and K are evaluated from a plot of $1/\Lambda S(Z)$ *vs.* $c\Lambda y_\pm^2 S(Z)$.

The Shedlovsky method has been stated[4] to give better results than the Fuoss method when K is greater than 10^{-5}, but as shown in Fig. 1–3 both methods fail at relatively low concentrations. The nature of the deviation in the case of the Shedlovsky treatment is such that the linear portion of the curve can be extended to higher concentrations by using the extended law for activity coefficients

$$\log y_\pm = -S(f)\sqrt{\alpha c}/(1 + A'\sqrt{\alpha c}) \quad (10)$$

with an appropriate choice of "a," the distance of closest approach of the ions. Curves labeled $S'(Z)$ in Fig. 1–3 were obtained in this way. This is essentially the same procedure used by Owen and Gurry[5] to interpret the data on $ZnSO_4$. They made the product $\alpha y_\pm$ equal to the experimentally determined stoichiometric activity coefficient. Usually the Fuoss method cannot be modified in this way without introducing negative values for "a."

The use of the Fuoss and Shedlovsky methods has been simplified by the publication of tables

(1) The notations used in this article are those employed by H. S. Harned and B. B. Owen, "Physical Chemistry of Electrolytic Solutions," Reinhold Publ. Corp., New York, N. Y., 3rd Ed., 1958.

(2) R. M. Fuoss, *J. Am. Chem. Soc.*, **57**, 488 (1935).

(3) T. Shedlovsky, *J. Franklin Inst.*, **225**, 739 (1938).

(4) Harned and Owen, ref. 1, p. 290.

(5) B. B. Owen and R. W. Gurry, *J. Am. Chem. Soc.*, **60**, 3074 (1938).

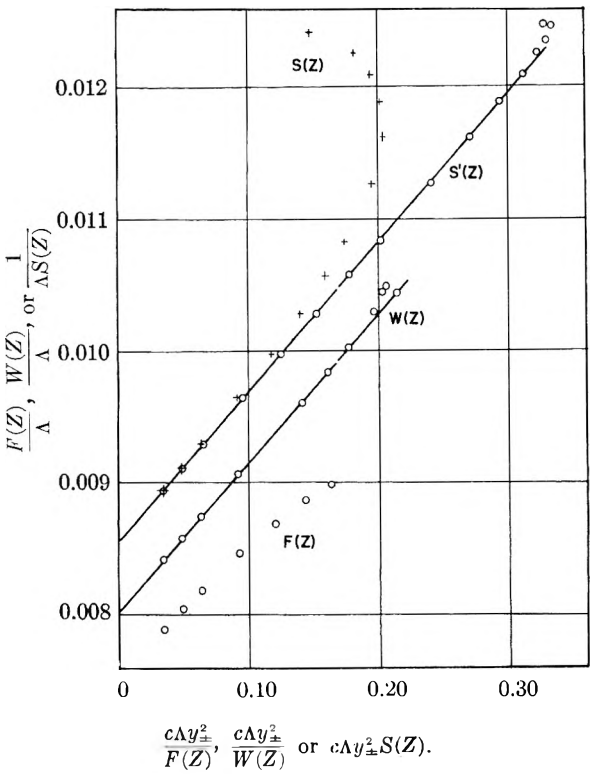

Fig. 1.—Estimation of Λ^0 and K for $ZnSO_4$ in water at 25°. The ordinate scale has been shifted 0.005 unit for $W(Z)$ and 0.001 unit for $S(Z)$ to separate the functions.

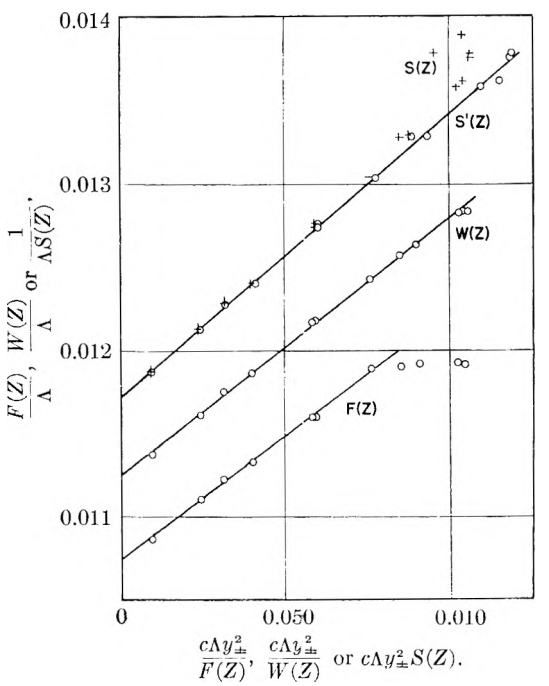

Fig. 2.—Estimation of Λ^0 and K for HCl in 70% dioxane–water solution at 25°. The ordinate scale has been shifted 0.0005 unit for $W(Z)$ and 0.001 unit for $S(Z)$.

for $F(Z)$[1] and $S(Z)$[6] for values of Z between 0 and 0.209. For larger values of Z the calculation of the functions is tedious. A simpler function can be developed if, in equation 2, Λ/Λ^0 is substituted for the α in the denominator of the defining term for α giving

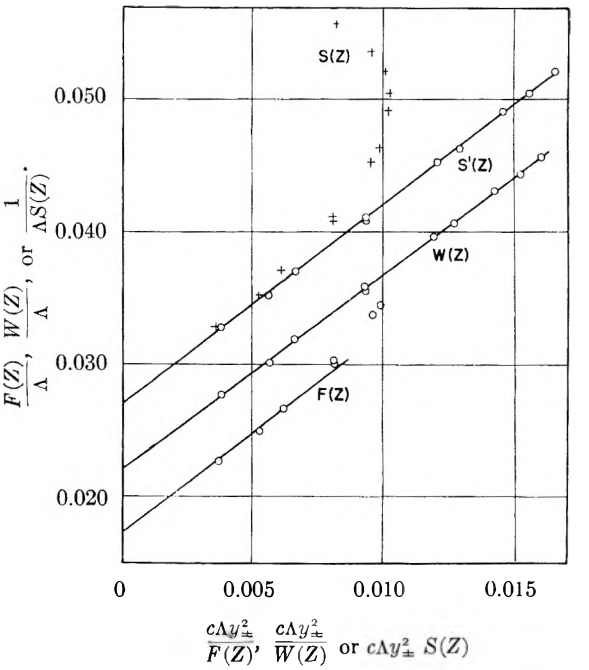

Fig. 3.—Estimation of Λ^0 and K in 82% dioxane–water solution at 25°. The ordinate scale has been shifted 0.005 unit for $W(Z)$ and 0.01 unit for $S(Z)$.

$$\alpha = \frac{\Lambda}{\Lambda^0(1 - Z)} = \frac{\Lambda}{\Lambda^0 W(Z)} \qquad (11)$$

where $W(Z) = 1 - Z$. This substitution partially corrects for the fact that the conductivity of ions at finite concentrations is less than that calculated by the limiting law. On substitution in equation 1, the relation

$$\frac{W(Z)}{\Lambda} = \frac{1}{\Lambda^0} + \frac{c\Lambda y_{\pm}^2}{W(Z)K(\Lambda^0)^2} \qquad (12)$$

is obtained. The activity coefficient $y_{\pm}$ is obtained from either equation 5 or 10.

The three functions $F(Z)$, $S'(Z)$ and $W(Z)$ were used to estimate Λ^0 and K for three examples where the experimental values of Λ were available for both dilute and moderately concentrated solutions. The examples chosen were $ZnSO_4$ in water[5] and HCl in 70% and 82% dioxane–water mixtures[7] and cover a wide range of dielectric constant of the solvent. The curves are given in Fig. 1–3, and the results are given in Table I.

The parameter "a" was chosen to give a straight line over the largest possible concentration range, and should be regarded as an arbitrary constant compensating for some of the errors introduced by using limiting laws at finite concentration. It was possible to find a value of "a" that would give a linear plot up to the point where $1/\Lambda S'(Z)$ or $W(Z)/\Lambda$ went through a maximum. This was usually close to the point where the calculated value of α started increasing with increasing concentration.

In the case of HCl in 82% dioxane where it was necessary to use equation 10 with $W(Z)$ to give a linear plot, the value of "a" used is close to that estimated by other methods, whereas the value

(6) H. M. Daggett, *ibid.*, **73**, 4977 (1951).

(7) B. B. Owen and G. W. Waters, *ibid.*, **60**, 2371 (1938).

TABLE I

COMPARISON OF EQUATIONS FOR ESTIMATING DISSOCIATION CONSTANTS

Function	$F(Z)$	$S(Z)$	$S'(Z)$	$W(Z)$
$ZnSO_4$ in water				
Λ^0	132.8[5]	132.8[5]	132.55	132.90
$K \times 10^3$	5.2[5]	4.9[5]	5.07	5.04
a (Å.)	....	....	5.40	0
HCl in 70% dioxane				
Λ^0	93.1[8]	....	93.27	93.52
$K \times 10^3$	7.7[8]	....	6.76	7.48
a (Å.)	....	....	0.867	0
HCl in 82% dioxane				
Λ^0	57.5[8]	....	58.55	58.52
$K \times 10^4$	2.02[8]		1.95	1.99
a (Å.)	....	....	7.31	6.30

required with $S'(Z)$ was somewhat larger. The same observation has been made in other cases examined in testing these functions.

Use of the functions $S'(Z)$ or $W(Z)$ permits the use of conductivity data obtained at higher concentrations in estimating dissociation constants. $W(Z)$ is to be preferred since it gives reasonable answers with less calculation.

CRYOSCOPIC DETERMINATION OF MOLECULAR WEIGHTS IN AQUEOUS PERCHLORIC ACID

BY MICHAEL ARDON AND AMOS LINENBERG

Department of Inorganic and Analytical Chemistry, The Hebrew University, Jerusalem, Israel

Received January 17, 1961

The determination of molecular weights of small polynuclear ionic species, in aqueous solution, from freezing point data, is a difficult task, not only because the mean activity coefficients of the solutes usually are unknown, but mainly because the contribution of the counterions of such ionic species to the depression of the freezing point is often much greater than the contribution of the species investigated, thus making this method highly inaccurate.[1]

This difficulty may be overcome by the use, as a solvent, of a eutectic solution of a strong electrolyte in water. If a foreign electrolyte is dissolved in a solvent of this kind, only those ions which do not exist in the pure solvent (the "foreign ions") will depress the freezing point of the solution.[2,3] One could investigate the molecular weight of a polynuclear cation by using a counter-ion which already exists in the solvent, thereby eliminating its effect on the freezing point. By this method, a much higher precision in molecular weight determinations is attained.[1] Another advantage of this method is the fact that the variation of the activity coefficient of the solute with concentration is small and linear in such a medium.[1,2] This makes possible a correct extrapolation of K_f to infinite dilution.

The systems hitherto used were mainly eutectic solutions of salts in water[2] (KNO_3, NH_4Cl, etc.) and were suitable for cryoscopic measurements in neutral or nearly neutral solutions. If the investigated species are dissolved in highly acidic or basic solutions, these systems are unsuitable, because the high concentration of hydrogen or hydroxyl ions would depress the freezing point and introduce a considerable experimental error.

A system which looked promising for the acidic range was the system perchloric acid–water. This system was investigated by Van Wyk[4] and later by Brickwedde.[5] They found a eutectic mixture consisting of ice and a perchloric acid hydrate of unknown constitution, $HClO_4 \cdot xH_2O$. According to Brickwedde,[5] this mixture consists of 40.7% perchloric acid, and has a freezing point of −59.7°. These data are more reliable than the older ones given by Van Wyk.[4]

We considered this solvent ($HClO_4$, 5.27 N) to be very suitable for molecular weight determination of polynuclear cationic species existing in strong acidic media, for two reasons: (a) The perchlorate ion has a slight tendency to complex formation, therefore it is an ideal counterion, and in this solvent it will have no effect on the freezing point. (b) Hydrogen ions will not affect the freezing point of this solvent. Cations other than H^+ will depress the freezing point, by an amount dependent only on their concentration.

In a previous publication[6] it was shown that the oxidation product of chromous perchlorate by O_2 in aqueous perchloric acid is a single polynuclear Cr^{III} species, having a charge of +2 per chromium atom and a total charge of approximately +3. Whereas the charge per chromium atom was determined with high precision, the total charge was determined only approximately. Nevertheless, it seemed highly improbable that the total charge could be as high as +6, and therefore a dinuclear structure having a charge of +4 was suggested. Other qualitative evidence supported this structure. However, in view of the important rôle of this ion in many oxidation reactions of Cr^{II}, it seemed desirable to confirm its dinuclear structure by stronger evidence.

The polynuclear chromic perchlorate is obtained by auto-oxidation of chromous perchlorate in perchloric acid. The resulting solution consists of hydrogen ions, perchlorate ions and polynuclear chromic ions. Only the latter will depress the freezing point of the solution. This depression will be one-half the normal if the chromic ion is dinuclear, one-third if it is trinuclear and one-fourth if tetranuclear. An added advantage of this method is that its results depend only on the number of the ions and not on their actual charge—the existence of ion pairs with the perchlorate anion tends to lower the actual charge, but will not change the number of "foreign ions" in the solution.

(1) G. Parissakis and G. Schwarzenbach, *Helv. Chim. Acta*, **2042**, 41 (1958); **2425**, 41 (1958).

(2) H. J. Muller, *Ann. Chim.*, [11] **8**, 143 (1937).

(3) P. H. J. Hoenen, *Z. physik. Chem.*, **83**, 513 (1913).

(4) H. J. Van Wyk, *Z. anorg. Chem.*, **48**, 44 (1906).

(5) L. H. Brickwedde, *J. Research Natl. Bur. Standards*, **42**, 309 (1949).

(6) M. Ardon and R. A. Plane, *J. Am. Chem. Soc.*, **81**, 3197 (1959).

Experimental

The freezing point determinations were carried out in an apparatus similar to that described by McMullan and Corbett.[7] A double walled cell, containing 10 ml. of the investigated solution, was placed in a cooling bath of ethanol and solid carbon dioxide. The solution was stirred by a magnetic stirrer. A thermistor (Standard Telephones & Cables, Ltd. Type F 23) was used for temperature measurements. A Wheatstone bridge (100,000 ohm O. Wolff, Berlin), a Leeds & Northrup 2430D Galvanometer and a 1.5 v. dry battery were used for resistance measurements. The thermistor was calibrated with an ethanol filled thermometer in the range -50 to $-62°$. At the freezing point of the pure solvent ($-59.7°$), this thermistor had a resistance of 72,520 ohms and the change with temperature was 413 ohms per 0.1°. Since the greatest depression of the freezing point was 0.7°, Δt was assumed to be proportional to ΔR; the error caused by this assumption was always less than 0.8%, and was neglected.

The thermistor possessed remarkable stability with no change of more than 8 ohms (0.002°) occurring during a two month period. This stability might be due to the very low currents passed through it (0.02 microamp.). Temperature measurements had an error of less than 0.001°, but the reproducibility of the freezing point measurements (read from cooling curves) was lower because of changes in the degree of supercooling, rate of stirring, etc. At least three determinations of the freezing point which did not differ by more than 0.004° were used for the calculation of the freezing point of each solution.

The rate of cooling was 0.2° per minute (prior to precipitation of the perchloric acid hydrate).

Perchloric acid of 41.7% was prepared by mixing appropriate weights of concentrated perchloric acid (70.6%) and water.

Chromous perchlorate was prepared by electrolytic reduction of $Cr(ClO_4)_3$ in $HClO_4$ as described in a previous publication.[6]

The dinuclear chromic perchlorate was prepared by passing air through the chromous solution for 15 minutes.

Hexaquo chromic perchlorate was prepared by reduction of CrO_3 in $HClO_4$ with H_2O_2 and crystallization.

Ferric perchlorate and thorium perchlorate were prepared from the chlorides by fuming with $HClO_4$ until all traces of chloride were expelled.

The perchlorates of magnesium, zinc and nickel were prepared from the oxides with $HClO_4$.

Fe^{III} concentration was determined iodometrically; Cr^{III} by titration with standardized $FeSO_4$, after oxidation with persulfate; Th^{IV} by precipitation as oxalate, ignition and weighing as oxide. Zn^{II}, Ni^{II} and Mg^{II} were titrated with 0.01 M EDTA.

Results and Discussion

It was assumed above that the depression of the freezing point depends only on the concentration of the foreign ions and is independent of their nature, in other words the molal depression of the freezing point is constant. This assumption which was shown to be approximately correct for a number of solvents[1,2] was found to be true also for our perchloric acid solvent. The molal depression constant of the freezing point K_f for a number of metallic perchlorates was measured, and the results are given in Table I.

The cryoscopic constant has an average value of 4.43° and the different ions investigated have a K_f which lies within 7% of this value. The considerable differences in electric charge and radii have only a moderate effect. In solutions of Li^+, Ag^+ and Ba^{++} an elevation of the freezing point was observed, probably resulting from precipitation of solid solutions.

The range of concentrations of the various cations investigated is rather narrow because in concentrations lower than 0.01 molal the relative error in Δt would be too high, and in concentrations above 0.04 molal the viscosity was usually too great to permit adequate stirring. This makes an extrapolation of K_f values to infinite dilution impossible, but the results did not reveal any dependence of K_f on concentration in this range, so that such a dependence, if any, must be small.

TABLE I

Solute, perchlorate	Range of concn. (moles/1000 g. solvent)	K_f
Magnesium	0.0149 to 0.0360	4.24
Zinc	.0198 to .0297	4.50
Nickel	.0198 to .0297	4.12
Ferric	.0117 to .0234	4.53
Hexaquochromic	.0106 to .0424	4.48
Thorium	.0116 to .0194	4.72

In the eutectic solution containing 40.7% $HClO_4$ a very small degree of supercooling was observed and sometimes it was missing altogether. This caused an appreciable error in the determination of the freezing temperature. We found that with a solution containing 41.7% $HClO_4$ a supercooling of 0.3 to 0.4° could be attained in all measurements and therefore these proportions were used in all experiments. The perchloric acid hydrate began to precipitate at 57.5° and this process increased the concentration of the solute prior to the attainment of the eutectic freezing point; the values of the concentrations were corrected accordingly.

Dinuclear Chromic Perchlorate.—The depression of the freezing point caused by dinuclear chromic perchlorate[6] was measured in two solutions containing 0.0288 and 0.0432 gram atom of chromium per 1000 g. of solvent. The average depression was found to be 2.28° for a solution containing one gram atom of chromium per 1000 g. of solvent. If the structure of the chromic ion is dinuclear, the K_f will be 4.56, in excellent agreement with the results of Table I. Trinuclear or tetranuclear species would give a K_f value of 6.84 or 9.12, respectively.

It was shown previously[6] that this chromic species contains two or more chromium atoms, but that it could not be a mixture of different polynuclear species. The results of this work prove that this ion is indeed dinuclear, and so must have either structure I or II suggested previously.[6]

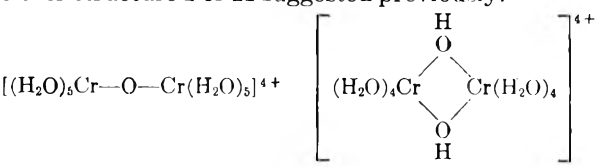

I II

Work is now going on in this Laboratory to determine molecular weights of other cationic and anionic polynuclear species in perchloric acid.

(7) R. K. McMullan and J. D. Corbett, *J. Chem. Educ.*, **33**, 313 (1956).

ELECTRON IMPACT SPECTROSCOPY OF NITROGEN DIOXIDE[1]

BY ROBERT W. KISER AND I. C. HISATSUNE

Department of Chemistry, Kansas State University, Manhattan, Kansas

Received February 1, 1961

In the course of some studies of the nitrogen

oxides, nitrogen dioxide was reinvestigated mass spectrometrically. The two principal ions of concern which are formed in the process of electron impact are NO^+ and NO_2^+. The determination of the appearance potentials of these ions from nitrogen dioxide was made and we found that they differed significantly from the recent results of Collin and Lossing[2] and others.[3-6]

Appearance potential measurements were made using a Bendix model 12–100 time-of-flight (TOF) mass spectrometer with an analog output system consisting of a monitor and a scanner. Wiley[7] and others[8-11] have described the TOF mass spectrometer, and recently Harrington[12] has described in detail the Bendix instrument.

The voltage scale was calibrated by simultaneously introducing the sample of NO_2 and a rare gas with a known spectroscopic ionization potential.[13] Krypton and xenon were employed in these determinations. Appearance potentials were determined using the extrapolated difference method described by Warren.[14,15] The linear portion of the ionization efficiency (i.e.) curves were forced to be parallel in plotting and then the voltage difference, ΔE, between the two i.e. curves at any given current, i, was plotted as a function of i. The resultant curve, upon extrapolation to $i = 0$, gave a value of ΔE which was algebraically added to the ionization potential of the calibrating gas to obtain the appearance potential for that particular ion.

The ionization potential of NO_2 was also determined using the technique of Lossing, Tickner and Bryce,[16] the method of extrapolation to zero ion current of the linear portion of the i.e. curves, and the critical slope method developed by Honig.[17]

The nitrogen dioxide showed no lasting deleterious effects upon the mass spectrometer. It was observed that immediately after admission of a sample to the ion source the trap current decreased markedly, probably due to oxidation of the filament (operating at about 1900°K.). During these studies the 5 mil diameter tungsten filament burned out and had to be replaced. No other effects or changes were observed.

TABLE I

APPEARANCE POTENTIALS OF NO_2^+ AND NO^+ FROM NO_2

	This work			Literature		
Ion	A. P. (e.v.)	Method[a]	No. of detns.	A. P. (e.v.)	Method[a]	Ref.[b]
NO_2^+	11.1 ± 0.20	E.I.L.E.	4	11 ± 1	E.I.	18
	11.35 ± .10	E.I.C.S.	4	12.3 ± 0.2	S.	6
	11.39 ± .27	E.I.E.D.	3	10.0	E.I.	4
	11.3	E.I.L.T.B.	1	9.91	E.I.V.C.	3
	11.27 ± .17	Average		11.7	P.I.	20
				13.98 ± 0.12	E.I.	1
				11.3 ± .4	P.I.	19
				9.78 ± .05	P.I.	5
NO^+	13.25 ± 0.53	E.I.L.E.	4	10.1 ± .2	E.I.	1
	12.91 ± .53	E.I.C.S.	4			
	12.48 ± .43	E.I.E.D.	4			
	12.48 ± .43	"Best value"				
NO^+ *vs.* NO_2^+	1.85 ± .05	E.I.L.E.	4			
	1.17 ± .04	E.I.C.S.	4			
	1.15 ± .10	E.I.E.D.	4			
	1.16 ± .08	"Best value"				

[a] S. = spectroscopic; P.I. = photoionization; E. I. = electron impact; L. E. = linear extrapolation; C. S. = critical slope; E. D. = extrapolated difference; L. T. B. = method given in reference 16; V. C. = vanishing current. [b] These references are numbered to correspond to the footnote references in the text.

NO_2^+.—It is readily apparent from an examination of Table I that the individual measurements of the ionization potential of NO_2 by various methods are not in agreement. It is unusual that photoionization results disagree by such a large amount; even the electron impact results show a much greater variation than one would reasonably expect.

The present work shows the ionization potential of NO_2 to be 11.27 ± 0.19 e.v., in fair agreement with the results of Stueckelberg and Smyth[18] and Weissler, *et al.*,[19] but in disagreement with Watanabe[20]

(1) This work was supported in part by the U. S. Atomic Energy Commission under Contract No. AT(11-1)-751 with Kansas State University.

(2) (a) J. Collin and F. P. Lossing, *J. Chem. Phys.*, **28**, 900 (1958); (b) J. Collin, *ibid.*, **30**, 1621 (1959).

(3) R. J. Kandel, *ibid.*, **23**, 84 (1955).

(4) R. J. Kandel, *Phys. Rev.*, **91**, 436 (1953).

(5) T. Nakayama, M. Y. Kitamura and K. Watanabe, *J. Chem. Phys.*, **30**, 1180 (1959).

(6) W. C. Price and D. M. Simpson, *Trans. Faraday Soc.*, **37**, 106 (1941).

(7) W. C. Wiley, *Science*, **124**, 817 (1956).

(8) W. C. Wiley and I. H. McLaren, *Rev. Sci. Instr.*, **26**, 1150 (1955).

(9) A. E. Cameron and D. F. Eggers, Jr., *ibid.*, **19**, 605 (1948).

(10) M. M. Wolff and W. E. Stephens, *ibid.*, **24**, 616 (1955).

(11) R. S. Golke, *Anal. Chem.*, **31**, 535 (1959).

(12) D. B. Harrington, "The Time-of-Flight Mass Spectrometer," in "Advances in Mass Spectrometry," edited by J. D. Waldron, Pergamon Press, London, 1959, pp. 249–265.

(13) C. E. Moore, "Atomic Energy Levels," National Bureau of Standards Circular No. 467, Vol. 3, 1958.

(14) J. W. Warren, *Nature*, **165**, 811 (1950).

(15) C. A. McDowell and J. W. Warren, *Disc. Faraday Soc.*, **10**, 53 (1951).

(16) F. P. Lossing, A. W. Tickner and W. A. Bryce, *J. Chem. Phys.*, **19**, 1254 (1951).

(17) R. E. Honig, *ibid.*, **16**, 105 (1948).

(18) E. C. G. Stueckelberg and H. D. Smyth, *Phys. Rev.*, **36**, 478 (1930).

(19) G. L. Weissler, J. A. R. Samson, M. Ogawa and G. R. Cook, *J. Opt. Soc. Am.*, **49**, 338 (1959).

(20) K. Watanabe, *J. Chem. Phys.*, **26**, 542 (1957).

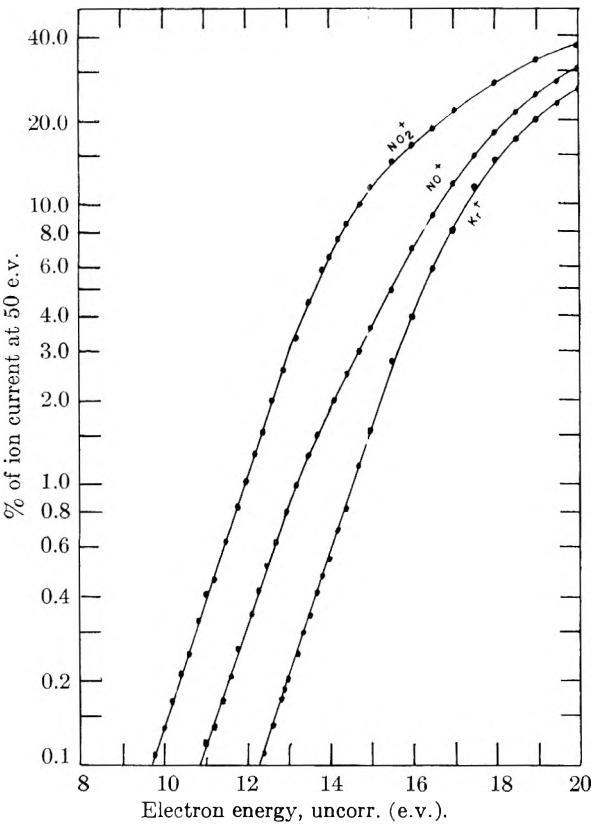

Fig. 1.—Ionization efficiency curves for NO_2^+ and NO^+ from NO_2, using krypton for the electron energy calibration.

and others.[2-6]

Since the i.e. curves for NO_2^+ from NO_2 should be of the normal form, the various methods of determining the electron impact ionization potential should all give essentially identical results. Table I shows that this is the case, and a simple average of these values gives the value of 11.27 ± 0.19 e.v. That the i.e. curve for NO_2^+ is of the normal form is readily seen from Fig. 1. During our studies of NO_2, we never observed any peaks due to NO_3^+ or $N_2O_4^+$.

NO^+.—The ion of *m/e* 30 is NO^+. It was found to have an appearance potential of 12.48 ± 0.43 e.v. In addition, individual determinations of the ionization efficiency curves of NO^+ and NO_2^+ resulted in $AP(NO^+) - IP(NO_2^+) = 1.16 \pm 0.08$ e.v. This coupled with $IP(NO_2^+) = 11.27 \pm 0.17$ e.v. from above gives $AP(NO^+) = 12.43 \pm 0.19$ e.v., in agreement with the value of 12.48 ± 0.43 e.v. determined directly.

We attempted to determine the appearance potential of NO^+ from NO with little success. We consistently obtained values about 1.3 v. too high, for which we can offer no explanation. We are presently repeating this determination. It may be noted from Fig. 1 that there is a rather sudden change in slope in the NO^+ i. e. curve at approximately 14 v. The latter was also observed in the determinations of NO^+ from NO.

Using the value of 12.48 e.v. for $AP(NO^+)$ from NO_2 and the literature value of $IP(NO^+) = 9.25$ e.v.,[21-22] we calculated the nitrogen–oxygen bond energy in nitrogen dioxide. D(O–NO) = 3.2 e.v. or 74 kcal./mole. This is in reasonable agreement with the value of 72 kcal./mole for D(O–NO) tabulated by Cottrell.[23]

We observe that the results reported by us for $IP(NO_2^+)$ and $AP(NO^+)$ from NO_2 differ significantly from results reported by a number of investigators[2,3-6] but agree closely with those reported by Stueckelberg and Smyth[18] and others.[19-20] We suggest that additional detailed experimental determinations of NO_2 be undertaken in an effort to fix these potentials.

(21) G. G. Cloutier and H. I. Schiff, *ibid.*, **31**, 793 (1959).

(22) H. Hurzeler, M. G. Inghram and J. D. Morrison, *ibid.*, **28**, 76 (1958).

(23) T. L. Cottrell, "The Strengths of Chemical Bonds," Second Edition. Butterworths Scientific Publications, London, 1958, pp. 210 and 278.

THE INFRARED SPECTRA OF SOME DIMETHYL SULFOXIDE COMPLEXES

BY RUSSELL S. DRAGO AND DEVON MEEK

Wm. A. Noyes Laboratory, Chemistry Department, University of Illinois, Urbana, Illinois

Received January 21, 1961

The preparation of a series of dimethyl sulfoxide complexes has been carried out in this Laboratory and assignments were made for the S–O stretching frequency.[1a] Subsequent to reading proof of the article on this research, assignments which differed from ours were published.[2] The purpose of this article is to provide additional data to support some of our original assignments and to aid in solving a problem which is more complex than the present published information would indicate.

Results and Discussion

The preparation of the complexes and conditions employed to obtain the spectra have been reported.[1] There is agreement on the assignment of the S–O stretching frequency for dimethyl sulfoxide (1045 cm.$^{-1}$ in CH_3NO_2 solution). There is also agreement on a very sharp, much less intense absorption at 950 cm.$^{-1}$, and a weaker, broader peak at ~ 915 cm.$^{-1}$ assigned[2] to $-CH_3$ rock.

In the complexes there is a discrepancy in the assignments. The additional information we have to offer involves a detailed description of the above two absorption peaks in the complexes as measured in nitromethane solution. Sharper, more easily interpreted spectra are obtained in solution than on Nujol mulls of the solids. Table I contains data for the peaks in the 1000 and 950 cm.$^{-1}$ region. The 1000 cm.$^{-1}$ peak is the one in the complexes that we assigned to S–O stretch and the latter is the one assigned by Cotton, *et al.*[2]

Some very significant information regarding these spectra entails a qualitative description of the relative intensity of the peaks measured in solution. As the peak in the 1000 cm.$^{-1}$ region moves from 1045 cm.$^{-1}$ in free sulfoxide to 1025

(1) (a) D. W. Meek, D. K. Straub and R. S. Drago, *J. Am. Chem. Soc.*, **82**, 6013 (1960). (b) For the preparation of these complexes also see F. A. Cotton and R. Francis, *ibid.*, **82**, 2986 (1960) and H. L. Schläfer and W. Schaffernicht, *Angew. Chem.*, **72**, 618 (1960).

(2) F. A. Cotton, R. Francis and W. D. Horrocks, Jr., *J. Phys. Chem.*, **64**, 1534 (1960).

TABLE I

INFRARED SPECTRA OF THE COMPLEXES IN NITROMETHANE SOLUTION

	S–O	CH_3 rock
$\{Mn[(CH_3)_2SO]_6\}[MnCl_4]$	1004i,s	955i,s
$\{Co[(CH_3)_2SO]_6\}[CoCl_4]$	994i,s	950i,s
$\{Ni[(CH_3)_2SO]_6\}[NiCl_4]$[a]	1000i,s	950i,s
$\{Cu[(CH_3)_2SO]_4\}[CuBr_4]$	988i,s	940i,br
$\{Cu[(CH_3)_2SO]_4\}[CuCl_4]$	987i,s	937i,br
$Hg(SCN)_2 \cdot 2(CH_3)_2SO$	1010i,br	950i,s
$(CH_3)_2SO \cdot I_2$[b]	1025i,m	950m,s

[a] There is evidence for some dissociation of the complex in this instance. [b] Spectrum was obtained on a smear of a dimethyl sulfoxide–iodine mixture. The first symbol listed refers to the intensity of absorption: i, intense; m, medium, the second to the width of the peak; s, sharp; br, broad; m, medium.

$cm.^{-1}$ in the dimethyl sulfoxide–iodine complex, a pronounced increase in intensity but no change in frequency is observed for the 950 $cm.^{-1}$ peak. In the $CoCl_2$, $MnCl_2$ and $Hg(SCN)_2$ complexes the peak in the 1000 $cm.^{-1}$ region occurs at slightly different frequencies and is still the more intense peak in the spectra. However, the relative intensity of the 950 $cm.^{-1}$ peak is increased considerably over that in the iodine complex but the frequency of this peak varies very little. The weak peak at 915 $cm.^{-1}$ in free dimethyl sulfoxide disappears in the complexes and probably becomes the shoulder on the 950 $cm.^{-1}$ peak.

There is no unique explanation for the described spectral changes. However a tentative explanation can be proposed which is consistent with the information now available. The series of compounds contained in Table I indicates an increase in the relative intensity of the 950 $cm.^{-1}$ peak without much change in frequency as the peak in the 1000 $cm.^{-1}$ region approaches the 950 $cm.^{-1}$ peak. The variation in the frequency of the peak in the 1000 $cm.^{-1}$ region as the metal ion is varied leads us to believe that this is the S–O stretching frequency. The constancy of the peak at 950 $cm.^{-1}$ supports an assignment of methyl rock. There is considerable coupling and this assignment should not be construed to indicate a pure S–O group frequency vibration. The increase in the intensity and the broadening of the low frequency peak can be attributed to a "borrowing of intensity"[3] by an interaction between the pure group frequency vibrations producing the ~1000 and 950 $cm.^{-1}$ peak.[4] The extent of the interaction increases as the frequencies come closer together.

When the S–O peak is shifted below 990 $cm.^{-1}$, as in the $CuCl_2$ and $CuBr_2$ complexes, the interaction between the two peaks now causes the low frequency peak to broaden and become the most intense peak in the spectra. An assignment now becomes very difficult.

The interpretation of the spectral results reported[2] on the deuterated complex, $\{Co[(CD_3)_2SO]_6\}[CoCl_4]$ is not unambiguous. Table II contains the results published[2] on this experiment.

TABLE II

INFRARED SPECTRA REPORTED[2] ON DEUTERATED DIMETHYL SULFOXIDE COMPOUNDS

$\{Co[(CH_3)_2SO]_6\}[CoCl_4]$	$\{Co[(CD_3)_2SO]_6\}[CoCl_4]$	Assignment
3002m	2240m	Asym C–H, C–D stretch
2906m	2120w	Sym C–H, C–D stretch
1416m	1015s	Asym CH_3, CD_3, deformation
1314w, 1292w	1039m	Sym CH_3, CD_3, deformation
1009s,sh	819m	
999s	775w, 760w	CH_3, CD_3 rock
950vs	970vs	S–O stretch

The high intensity observed in the deuterated complex for the 1015 and 1039 $cm.^{-1}$ peak is surprising in view of the assignments made. The frequency shift of the S–O stretch upon deuteration is also surprising.

An alternate explanation of the data (Table II) can be proposed which explains the observed frequencies and intensities and is also compatible with our assignment of the S–O stretching frequency. The peak at 999 $cm.^{-1}$ in the undeuterated complex which we attribute to S–O stretch occurs at 1015 $cm.^{-1}$ in the deuterated complex. The 970 $cm.^{-1}$ peak in the deuterated complex can be attributed to either the symmetric or asymmetric deformation. Assignment of the peaks in this way does little to improve the earlier criticism about the intensity of the peaks attributed to the various vibrational modes. However, it can now be proposed that considerable interaction is operative in the deuterated complex between the S–O stretch and either the asymmetric or symmetric deformation to account for the resulting frequencies and intensities. In the absence of this interaction the peaks corresponding to the group frequency vibrations might be expected to occur at about 1000 $cm.^{-1}$ for S–O stretch and in the same region for a weak methyl deformation absorption.

The considerations described above, though qualitative in nature, do indicate the complexity of this problem. The explanation proposed favors an assignment of the high frequency peak (1000 $cm.^{-1}$) to a S–O stretching frequency and accounts for the observed peak intensities.

Acknowledgments.—The authors wish to acknowledge the financial assistance of the Atomic Energy Commission (Contract No. AT(11-1)-758).

(3) G. Herzberg, "Infrared and Raman Spectra," D. Van Nostrand Co., New York, N. Y., 1951, p. 265.

(4) It is possible that the 915 $cm.^{-1}$ peak would be involved in this interaction instead of the 950 $cm.^{-1}$ peak.

SOLUBILITY AND CONDUCTIVITY OF SUBSTITUTED AMMONIUM IODIDES IN PENTABORANE

BY HENRY E. WIRTH AND PAUL I. SLICK

Department of Chemistry, Syracuse University, Syracuse, N. Y.

Received February 1, 1961

Since pentaborane has a dielectric constant of 20.8 at 25°[1] it was of interest to determine its sol-

vent properties for electrolytes. A conductance method was used, as all manipulations had to be performed out of contact with air.

Experimental

Apparatus.—The conductivity cell had a cell constant of 0.4 at 25°, and required approximately 5 g. of pentaborane to cover the electrodes. The salt to be investigated was weighed, pentaborane was distilled into the cell, the cell assembly was removed from the vacuum system and weighed to determine the concentration. A magnetic stirrer was placed in the bottom of the cell to speed attainment of equilibrium. The cell was calibrated with standard KCl solutions in the usual manner. The conductance was measured with the bridge described by Orr and Wirth.[2] The bath temperature was maintained constant at selected temperatures between 0 and 25° to within ± 0.05°.

The density of solutions of tetra-*n*-butylammonium iodide was determined in a dilatometer which was sealed off under vacuum after introduction of the pentaborane.

Materials.—Pentaborane was purified by repeated freezing with a Dry Ice–acetone mixture and removal of the noncondensable gases. The specific conductivity of the pentaborane was *ca.* 1×10^{-8} mhos.

The substituted ammonium salts used were Eastman reagent grade. The tetra-*n*-butylammonium iodide was 99.3% pure by analysis.

Results

LiCl, LiH, $NaBH_4$, KBH_4 and $LiAlH_4$ were found to be insoluble in pentaborane; tetra-*n*-butyl- and tetra-*n*-propylammonium iodides were appreciably soluble, and tetraethylammonium iodide was slightly soluble.

Tetra-*n*-butylammonium Iodide.—The specific conductivity (Fig. 1) was found to reach a maximum as the concentration was increased. Since this maximum is close to the conductivity of the saturated solutions in the temperature range 0–15°, the solubility was checked by determining the vapor pressure of solutions at constant temperature as known amounts of solvent were removed. The intersection of the vapor pressure curve for the unsaturated solutions with that of saturated solution permitted the estimation of the solubility. The solubility was found to vary from 40.8 ± 0.4 g. at 0° to 61.0 ± 0.4 g. of $(n\text{-}C_4H_9)_4NI$ per 100 g. of B_5H_9 at 25°.

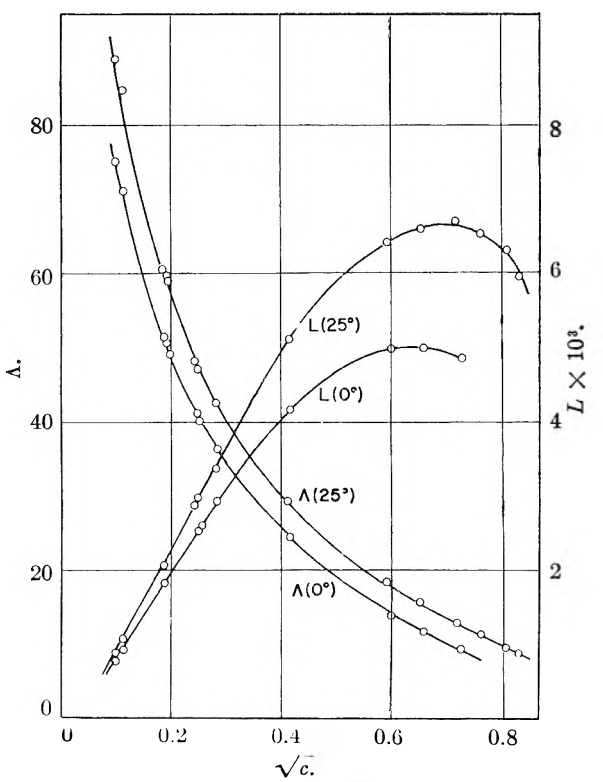

Fig. 1.—Specific conductance (L) and equivalent conductance (Λ) of $(n\text{-}C_4H_9)NI$ in B_5H_9 as a function of the square root of the concentration.

The density of solutions of $(n\text{-}C_4H_9)_4NI$ was found to vary linearly with the square root of the molality at constant temperature. Our results combined with the results of Smith and Miller[3] for pure pentaborane lead to the equation

$$d_T = 0.8674 - 0.00082_0T + 0.000235_0Tm^{1/2}$$

which represents the data to ±0.002 g./ml.

The equivalent conductivity of $(n\text{-}C_4H_9)_4NI$ (Fig. 1) was not determined in sufficiently dilute solutions to permit the precise evaluation of values of both Λ° and of the dissociation constant. Since pentaborane has practically the same dielectric constant[1] and viscosity[3] as acetone[4] (20.8 and 3.03 millipoise as compared with 20.47 and 3.040 millipoise, respectively) it was assumed that Λ^0 for $(n\text{-}C_4H_9)_4NI$ would have the same value in pentaborane as in acetone. Assuming this value (180[4]) the method described by Wirth[5] was applied to estimate the value of the dissociation constant (see Fig. 2). At other temperatures, Walden's rule was used to estimate the value of Λ^0. The results are given in Table I.

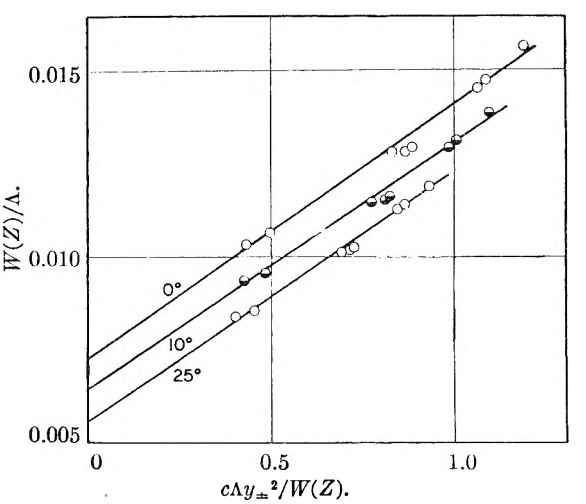

Fig. 2.—Estimation of the dissociation constants of $(n\text{-}C_4H_9)NI$ in pentaborane.

The dissociation constant decreases with increasing temperature as has been found by Sears, Wilhoit and Dawson[6] for $(n\text{-}C_4H_9)_4NI$ in acetone. This effect is attributed to the rapid decrease of dielectric constant with increasing temperature.

(1) H. E. Wirth and E. D. Palmer, *J. Phys. Chem.*, **60**, 914 (1956).
(2) C. H. Orr and H. E. Wirth, *ibid.*, **53**, 1147 (1959).
(3) S. H. Smith, Jr., and R. R. Miller, *J. Am. Chem. Soc.*, **72**, 1452 (1950).
(4) M. B. Reynolds and C. A. Kraus, *ibid.*, **70**, 1709 (1948).
(5) H. E. Wirth, *J. Phys. Chem.*, **65**, 0000 (1961).
(6) P. G. Sears, E. D. Wilhoit and L. R. Dawson, *ibid.*, **60**, 169 (1956).

TABLE I

ESTIMATED DISSOCIATION CONSTANT OF TETRABUTYLAMMONIUM IODIDE IN PENTABORANE

Temp., °C.	Λ^0 (assumed)	$a \times 10^3$	$K \times 10^3$	$K \times 10^3$ (in acetone)[6]
0	138	5.94	7.7	8.5
10	155	5.78	6.4	7.7
20	170	5.63	5.3	6.8
25	180	5.55	4.6	6.1

The equilibrium constant is only slightly less in pentaborane than in acetone, which may indicate that the interaction between the solvent and the ions (in the ion pairs) is about the same in the two solvents (*cf.*, ref. 4). The value of "*a*" required to give a straight line at 25° is the same as that found by Fuoss and Kraus[7] for this solute in water–dioxane mixtures.

Tetra-*n*-propylammonium Iodide.—The solubility of $(n\text{-}C_3H_7)_4NI$ was found to vary between 3.80 ± 0.02 g. salt per 100 g. solvent at 0° and 3.94 ± 0.02 g. per 100 g. solvent at 25° (Fig. 3). The

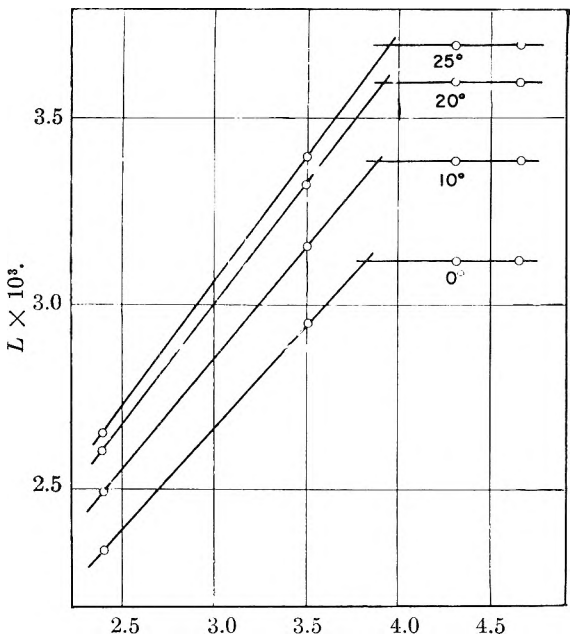

Fig. 3.—Specific conductivity of solutions of $(n\text{-}C_3H_7)NI$ in B_5H_9 used to evaluate the solubility.

dissociation constant was estimated to be 7.6×10^{-3} at 0° and 4.4×10^{-3} at 25°.

The solubilities of the substituted ammonium iodides in pentaborane are compared in Table II with the solubilities in other solvents.

Pentaborane is nearly as good a solvent for these salts as acetone and 1-butanol which have about the same dielectric constant.

Acknowledgment.—The authors wish to thank the Research Corporation for a grant which supported this research.

(7) R. M. Fuoss and C. A. Kraus, *J. Am. Chem. Soc.*, **79**, 3304 (1957).

(8) P. Walden, *Z. physik. Chem.*, **55**, 683 (1906).

(9) P. Walden, *ibid.*, **61**, 633 (1908).

(10) G. M. Goldberg and A. A. Vernon, *J. Am. Chem. Soc.*, **73**, 2845 (1951).

(11) A. A. Vernon and R. E. Walck, Jr., *ibid.*, **73**, 5915 (1951).

(12) V. L. Hughes and A. A. Vernon, *J. Phys. Chem.*, **56**, 927 (1952).

TABLE II

SOLUBILITY OF SUBSTITUTED AMMONIUM IODIDES IN VARIOUS SOLVENTS AT 25°

Solvent	Dielectric constant	Solubility (moles/kg. solvent) $(C_2H_5)_4NI$	$(n\text{-}C_3H_7)_4NI$	$(n\text{-}C_4H_9)NI$
CH_3OH	32	0.55[8]	3.96[9]	7.23[10]
		.481[10]	4.29[11]	
C_2H_5OH	25	.049[9]	0.97[9]	3.26[12]
		.044[12]	1.09[12]	
$n\text{-}C_4H_9OH$	22	.0076[11]	0.208[11]	1.69[11]
B_5H_9	20.8	.002[13]	0.126	1.65
$(CH_3)_2CO$	20.5	.012[8]	0.16[8]	

(13) Estimated from conductivity of saturated solution.

DISPROPORTIONATION OF 1-DODECANESULFINIC ACID IN SOLUTION

BY PAUL ALLEN, JR., AND LEO REICH

Department of Chemistry and Chemical Engineering, Stevens Institute of Technology, Hoboken, New Jersey

Received February 3, 1961

The disproportionation of sulfinic acids is represented by the equation

$$3RSO_2H \longrightarrow RSO_3H + RSSO_2R + H_2O \quad (1)$$

A previous communication[1] reported on a mechanistic study of the disproportionation of an aromatic acid, *p*-toluenesulfinic acid in aqueous solution. This note extends the earlier work and deals with the reaction of the aliphatic acid, 1-dodecanesulfinic acid. Since the aliphatic acid was insoluble in water alone it was dissolved in a mixture of isopropyl alcohol and water. Due to the alcohol, the analytical titration method previously employed could not be used. However, sulfinic acids are less ionized than the strong[2] sulfonic acids and their ionization greatly diminished in polar media by mineral acids. Thus it was expected and found that the progress of the reaction could be followed by the change in conductance of the solution. Because of limitations of the conductance apparatus, the effect of *p*H on reaction rate could not be ascertained. Nevertheless many of the observations noted for *p*-toluenesulfinic acid were found to apply to 1-dodecanesulfinic acid.

Experimental

Materials and Apparatus.—1-Dodecanesulfinic acid was prepared essentially by the method of Houlton and Tartar.[3] The acid melted at 36–37° (reported[4] 29–30°). Because of the discrepancy in melting points, it was subjected to microanalysis.[5]

Anal. Calcd. for $C_{12}H_{25}SO_2H$: C, 61.49; H, 11.18; S, 13.75. Found: C, 61.81; H, 11.36; S, 13.77. The solid sulfinic acid was stored in a freezer at −18° and was stable for several months, based on melting point determinations.

The apparatus consisted of an a.c. bridge with a 1000-cycle bridge source voltage, a Rubicon decade box, a Leeds and Northrup circular slide-wire, a Sargent constant temperature bath, a U-type conductivity cell with movable platinum electrodes and a cathode ray oscilloscope with a

(1) P. Allen, Jr. and L. Reich, *J. Phys. Chem.*, **64**, 1928 (1960). In equation 16 of this article, $[H^+]$ should be divided by K_1.

(2) J. W. McBain and M. D. Betz, *J. Am. Chem. Soc.*, **57**, 1905 (1935).

(3) H. G. Houlton and H. W. Tartar, *J. Am. Chem. Soc.*, **60**, 544 (1938).

(4) C. S. Marvel and R. S. Johnson, *J. Org. Chem.*, **13**, 822 (1948).

(5) Schwarzkopf Microanalytical Labs., New York, N. Y.

preamplifier. Telephone receivers sometimes were used in conjunction with the oscilloscope. The cell constant was about 5 cm.$^{-1}$, and the experimental error was estimated as $\pm 0.6\%$ of the resistance reading. The oscilloscope could be used as a voltmeter, the balance being indicated by the minimum amplitude of the wave pattern.[6]

Procedure.—Solutions of 1-dodecanesulfinic acid, or of sulfinic acid plus products, were made up in an isopropyl alcohol-water medium (30% alcohol, by volume) and placed in the conductivity cell at 77.0 ± 0.1°. After an hour, resistance readings were begun. The electrodes were moved up and down occasionally to agitate the solution. Mineral oil was placed on the top of the solutions to decrease air oxidation of the sulfinic acid.

Theory of the Method.—Within the experimental error, conductance measurements varied in a linear manner with the concentration of reactants and products. (Thiolsulfonate did not contribute to the conductance.) However, an additional factor must be included because the isopropyl alcohol–water solvent, in the presence of sulfuric acid, showed an increase in conductance with time at 77° in the absence of reactant. Fortunately, under the conditions employed, this change of conductance was small and nearly linear and had almost the same value over the *p*H range used in this study.

In deriving the relationships between conductance and concentration, a symbolic equation is used

$$3A \longrightarrow Y + Z$$

It is assumed that the reactive intermediate species contribute little to conductance. However, it is not implied that the rate constant, k, will not change appreciably with changes in concentration of the reactive intermediates. We may now write

$$\lambda_0 = \lambda_m + k_a A$$
$$\lambda_\infty = \lambda_m + k_y(A/3) + k_z(A/3) + S$$
$$\lambda_t = \lambda_m + k_a(A - 3X) + k_y X + k_z X + P$$

where

X = concn. of products formed at time t
λ_0 = initial conductance (at which time steady-state conditions have not been reached)
λ_∞ = conductance as time $\longrightarrow \infty$
λ_t = conductance at time t
λ_m = conductance of the medium in which the sulfinic acid is dissolved, plus that of the intermediate formed during steady-state conditions
$P = rt$, a term to account for the change of conductance of the solvent with time during the reaction
r,k,S = constants
R = resistance
A = initial concn. of substance A at the arbitrary time used for the start of the reaction

Then, for a second-order reaction

$$\frac{R}{R_0 - R(1 + R_0 P)} = \frac{1}{\left[\frac{R_0}{R_\infty} - 1 - R_0 S\right] Akt} + \frac{1}{\frac{R_0}{R_\infty} - 1 - R_0 S} \quad (2)$$

For orders other than second, a plot of the left-hand member of equ. 2 *versus* $^1/t$ will not afford a linear relationship. Equation 2 may be converted to another form which is more convenient to handle and gives almost the same rate constant.

(6) P. Edelson and R. M. Fuoss, *J. Chem. Educ.*, **27**, 610 (1950).

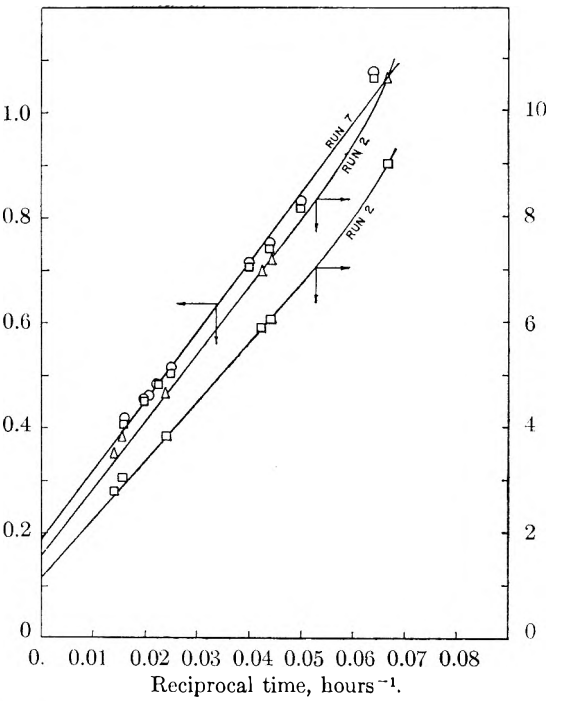

Fig. 1.—Resistance functions *vs.* reciprocal time, hours^{-1}; run 2, right hand ordinate; run 7, left hand ordinate; ○ and △, $R/[R_0 - R(1 + R_0 rt)]$; □, $R/(R_0 - R)$.

$$\frac{R}{R_0 - R} = \frac{1}{(R_0 r + R_0 rAkt + AkD)t} + \frac{Ak}{(R_0 r + R_0 rAkt + AkD)} \quad (3)$$

where $D = R_0/R_\infty - 1 - R_0 S$.

Results and Discussion

From Fig. 1 can be seen that when the left-hand members of eq. 2 and 3 are plotted against $1/t$ linear relationships result except for an initial elapsed time of about 15 hr. When the intercept is divided by the slope of the linear portion and by the initial concentration the rate constant, k, is obtained. The results are summarized in Table I. The rate constant is independent of *p*H, over the *p*H range used, as well as of the iodide ion concentration.

TABLE I

DISPROPORTIONATION OF 1-DODECANESULFINIC ACID IN ISOPROPYL ALCOHOL–WATER AT 77°

Run no.	Initial concn. of sulfinic acid, moles/l.	Initial *p*H	Iodide concn., mg./100 ml.	k, l./hr.-mole
1[a]	15×10^{-3}	2.5	0.9	2.0
2	4.1×10^{-3}	2.0	1.5	2.4
3	4.1×10^{-3}	2.0	5.4	2.2
4	4.1×10^{-3}	2.1	1.5	2.4
5	4.1×10^{-3}	2.7	4.8	2.4
6[b]	4.1×10^{-3}	2.7	0.6	2.6
7	5.2×10^{-3}	2.6	1.2	2.5
8	4.1×10^{-3}	2.3	1.2	2.4
9	4.1×10^{-3}	2.5	1.0	2.2

[a] Disproportionation followed by permanganate titration in this run only, k found from the equation $1/(C_0 - C) = 1/(C_0 - a) + 1/(C_0 - a)^2 kt$ where a is the blank correction. [b] Sodium chloride, 75 mg./100 ml., present.

In the plots shown in Fig. 1, the initial curvature

implies an initial "unsteady state" condition during which the rate constant changes continuously until a steady-state condition of the reactive intermediates is attained. Thereafter, a kinetically second-order exists for the reaction. (This concept is in good agreement with the results for *p*-toluenesulfinic acid.[1])

Because of the limitations imposed by the conductance method (resistance readings should be between 1,000–10,000 ohms), the *p*H could be varied over a limited range, 2.0–2.7. Also because of the rapid change in *p*H during the early stages of reaction at the higher initial *p*H values, the *p*H soon approached a limit and its variation during much of the reaction was smaller than would appear. Thus, the initial high *p*H values do not have much significance. But at low *p*H (2.0), the *p*H did not change much (0.05 unit) and hence these lower *p*H values are much more representative of *p*H conditions during most of the reaction. For example, although the initial *p*H was 2.7 for run 5, after several hours it dropped to 0.25 and at the end of the run it was 2.3; hence, for most of the run it was 2.3–2.5. Because of the preceding, a truer representation of the *p*H range for the runs listed would be much smaller than 2.0–2.7. Therefore, it would be hazardous to attempt any quantitative correlation between rate constant and initial *p*H.

It may be argued that if reaction rate was a function of *p*H, then the change in *p*H could account for the curvatures obtained. However, curvatures existed for runs 2 and 4 even though the *p*H's were constant during the reaction times (the initial *p*H's were low, 2.0–2.1). This indicated that induction periods undoubtedly existed during initial reaction periods. This is in accord with results obtained in the case of *p*-toluenesulfinic acid.[1] When iodide was not present as a catalyst,[7] the initial reaction rate was small; after iodide had been added, its effect on the reaction rate became noticeable. However, it did not affect the final value of k. This also has been observed for *p*-toluenesulfinic acid.[1] Chloride ion has also been reported as a catalyst,[7] but in a relatively large concentration it produced only a small change in the rate constant (run 6).

(7) T. P. Hilditch, *J. Chem. Soc.*, 1091 (1910).

THE RADIATION-INDUCED REACTION BETWEEN BENZENE AND IODINE[1]

BY ALBERT T. FELLOWS[2a] AND ROBERT H. SCHULER[2b]

Chemistry Department, Brookhaven National Laboratory, Upton, Long Island, New York

Received February 13, 1961

Brief observations on the radiation-induced reaction between iodine and benzene[3] during previous studies of aliphatic hydrocarbons[4] have indicated that for aromatic systems the over-all reactions are considerably more complex than the simple scavenging of radicals. Because of this a more detailed examination of the radiation chemistry of benzene–iodine solutions has been undertaken in order to examine the suitability of using iodine as a radical detector in these systems. As is seen below the observed reactions are even more complex than suspected in the earlier work. Extreme caution must be urged in the interpretation of the results of scavenging experiments in aromatic materials.

Experimental

Reaction was followed by spectrophotometric observation of the iodine concentration during irradiation and by measurement of the uptake of radio-iodine to form organic iodides. Baker and Adamson reagent grade benzene was used after three crystallizations with the rejection in each case of about half the material. Phillips research grade benzene also was used in preliminary experiments but was not regarded to be suitable since a small amount of thermal reaction was observed to occur with dissolved radio-iodine. No observable reaction occurred with the triply crystallized material.

Solutions of known concentrations of radio-iodine (I^{131}) were degassed by repetitive freezing and pumping, sealed and irradiated. Irradiation methods were very similar to those employed in previous work on the cyclohexane–iodine system.[5] Both 2 Mev. Van de Graaff electrons and cobalt-60 γ-rays were used, the latter at dose rates of 30,000 and 250,000 rad. per hour. Radiation yields were determined in the case of the γ-irradiations by comparison with the rate of oxidation of ferrous ions in the Fricke dosimeter [$G(Fe^{+++}) = 15.5$] and in the case of the fast-electron irradiations by the power input method.

Optical absorbance measurements were made at the absorption maximum of iodine in benzene (500 mμ) with a Beckman DU spectrophotometer. Auxiliary measurements were made at longer wave lengths. In a number of cases the complete absorption spectrum was recorded with a Cary spectrophotometer. In the fast-electron experiments absorbance measurements were made in an absorption cell sealed to the irradiation vessel during the course of irradiation.

In the radio-iodine experiments determinations were made of the fraction of activity found in organic combination after thiosulfate extraction. It was found that about one-third of this activity readily exchanged at room temperature with molecular iodine. This activity could be removed by a subsequent thiosulfate extraction after equilibration of the sample with a large excess of inactive iodine. Three measures of the radiation-induced reaction of iodine with benzene are thus obtained: the *total* yield as measured by the disappearance of iodine determined spectrophotometrically, the *organic* yield determined after thiosulfate extraction and the *stable iodide* yield measured after equilibration of the irradiated samples with inactive iodine. In the previous studies of cyclohexane–iodine solutions[6] these three quantities were found to be equal.

Results and Discussion

Figure 1 illustrates the changes which occur in the absorption spectrum of a 4×10^{-3} M solution of iodine in benzene during and after a 5 microampere fast electron bombardment. Curve a represents the degassed solution before irradiation. Curves b, c and d represent the progressive decrease in absorption observed during irradiation. After completion of the irradiation (5×10^{21} e.v./g.) the sample was allowed to remain sealed. A darkening through shades of gray and dark green

(1) Research performed under the auspices of the U. S. Atomic Energy Commission.

(2) (a) Guest Chemist on leave from Socony Mobil Laboratories, Research and Development Department, Socony Mobil Oil Co., Inc., Paulsboro, New Jersey; (b) Radiation Research Laboratories, Mellon Institute, Pittsburgh, Pennsylvania.

(3) G. L. Clark and L. W. Pickett, *J. Am. Chem. Soc.*, **52**, 465 (1930), first reported the X-ray induced uptake of iodine by benzene as one of the early examples of the chemical effects of ionizing radiation.

(4) E. N. Weber, P. F. Forsyth and R. H. Schuler, *Radiation Research*, **3**, 68 (1955).

(5) R. W. Fessenden and R. H. Schuler, *J. Am. Chem. Soc.*, **79**, 273 (1957).

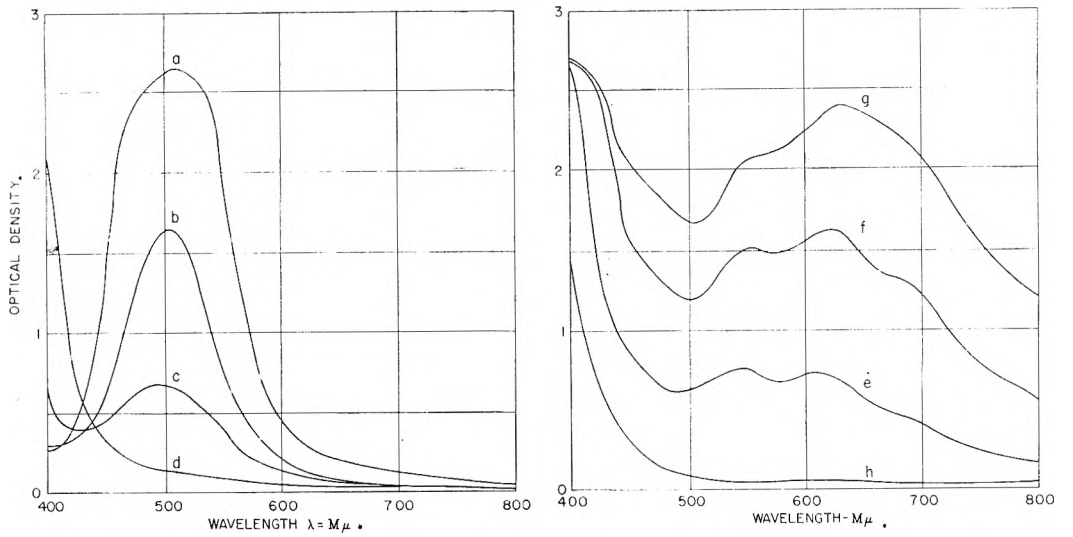

Fig. 1.—Changes in absorption spectrum of degassed 4×10^{-3} *M* solution of iodine in benzene during and after irradiation: a, initial absorption spectrum (maximum depressed instrumentally); b, after irradiation of 5×10^{20} e.v./cc.; c, after irradiation of 1×10^{21} e.v./cc.; d, after 5×10^{21} e.v./cc.; e, after standing for 4 hours after irradiation; f, after standing 10 hours; g, after standing 24 hours; h, after exposure of solution to air and sunlight.

was observed and is illustrated by curves e, f and g. Upon further standing the absorption represented by g did not increase and was unaffected by light in the absence of air. After exposure of the sample to air the coloring faded very quickly in bright sunlight. The resulting spectrum (h) was essentially identical with the absorption spectrum immediately after irradiation. The color of the aerated sample (g) was reasonably stable when stored in the dark. The nature of the colored substance formed here is unknown. The coloration is however extremely intense since, as indicated in Fig. 1, the integrated absorption in the visible range is considerably in excess of that of the original iodine.

For more dilute solutions the iodine concentration decreases exponentially with dose. This behavior is in contrast to the linear decrease observed in the case of aliphatic hydrocarbons. Since the initial slope of the iodine disappearance curves has no pronounced dependence on concentration, the decrease in yield with dose is attributed to the build up of a reaction product which is capable of competing with the iodine in the scavenging reactions. The over-all results of fast electron experiments are given in Table I. It is seen that of the iodine reacting only 30–50% is firmly bound as organic iodide. Of the remainder 25–50% is removed during the initial extraction and 15–20% readily exchanges with iodine. The distribution of the iodine among the various components varies considerably from run to run but can be broadly described in terms of the following yields: G(total) $\sim$ 0.7, G(organic) $\sim$ 0.4 and G(stable iodide) $\sim$ 0.3. In the previous X-ray experiments G(total) was reported to be 0.66.[4] Gaumann[6] has shown that the addition of iodine to benzene after irradiation results in the conversion of phenylcyclohexadiene to biphenyl. At least part of the difference between the total and organic yields can be ascribed, therefore, to the dehydrogenation of cyclohexadiene type compounds and the resultant production of hydrogen iodide. The stable iodide fraction presumably represents the formation of organic iodide from radicals such as phenyl while the difference between the organic and stable fractions ($\sim$ 0.1) represents the formation of more labile materials.

(6) T. Gaumann, *Helv. Chim. Acta*, to be published.

TABLE I

REACTION BETWEEN BENZENE AND IODINE INDUCED BY 2 MEV. VAN DE GRAAF ELECTRONS

Iodine concn. moles/l. $\times 10^3$	Dose, e.v./ml. $\times 10^{-18}$	% reaction			Radiation yields[a]		
		Total	Organic	Stable	Total	Organic	Stable
0.166	7.0	17.3	8.0	4.6	0.49	0.23	0.13
0.498	14.0	15.5	7.7	5.3	.67	.34	.23
1.02	28.0	16.1	12.2	8.8	.71	.53	.39
0.996	49.5	29.9	17.7	12.4	.74	.44	.31
2.045	55.7	..	10.1	7.7	..	.45	.35
0.996	370	86.6	67.2[b]	44.3[c]	.28	.22	.14

[a] Molecules/100 e.v.—as 1/2 I_2. [b] Decreases to 55.0% on standing 16 hr. [c] Remains constant on standing 16 hr.

A large number of cobalt-60 γ-irradiations were carried out at various iodine concentrations. The results are, however, complicated by the fact that irradiation periods are long with respect to the post-irradiation effects noted above. While the results are not very systematic it is possible to make the following general comments. As the irradiation progresses the stable iodide continues to build up at the expense of the other fractions long after all of the iodine has been used up. The initial yields observed in the γ-ray experiments at 10^{-3} *M* iodine are approximately as indicated above for fast electrons. The organic yield at 2.5×10^{-5} *M* is essentially the same as at the higher concentration while the yield of the stable fraction is initially somewhat less. Any quantitative interpretation of the yields from the γ-ray experiments would seem to have very limited validity.

The above observations amply illustrate the highly complex nature of the radiation-induced reaction between iodine and benzene. Observations on this system are complicated by the pro-

duction of reactive and unstable species as products which lead to pronounced post-irradiation and apparent intensity effects. While the results are, in general, difficult to interpret in terms of specific reaction intermediates, radiation yields of the order of several tenths molecule per hundred electron volts are observed for each of several components. These yields are considerably higher than that observed for hydrogen formation [$G(H_2) = 0.04$]. Reactions resulting in the disappearance of iodine therefore account for a preponderant fraction of the intermediates produced. Presumably at least the stable activity indicated above results from the reactions of free radicals.

CONFIRMATION OF DISORDER IN SOLID NITROUS OXIDE BY NEUTRON DIFFRACTION[1]

BY WALTER C. HAMILTON AND MARTHA PETRIE

Chemistry Department, Brookhaven National Laboratory, Upton, L. I. New York

Received January 12, 1961

X-Ray diffraction studies[2] have indicated that solid nitrous oxide is cubic, $a_0 = 5.72$ Å.,[3] space group T_h^6-Pa3, with four molecules per unit cell. The structure is apparently isomorphous to that of CO_2, and de Smedt and Keesom thus interpreted the X-ray powder data in terms of the following structure[4]

4 O in positions (a): 0,0,0; $0,{}^1/_2,{}^1/_2$; ${}^1/_2,0,{}^1/_2$; ${}^1/_2,{}^1/_2,0$
8 N in positions (c): $\pm$ $(x,x,x;\ {}^1/_2+x,{}^1/_2-x,-x;$ $-x,{}^1/_2+x,{}^1/_2-x;\ {}^1/_2-x,-x,{}^1/_2+x)$ with $x = 0.1167$

This describes a symmetrical molecule N–O–N with equal bond lengths of 1.16 Å.

The infrared spectrum of nitrous oxide can be interpreted, however, only in terms of the unsymmetrical molecule N–N–O. Extremely careful measurement of the rotational constants in gaseous N_2O allows interatomic distances to be derived[5]

$$r_1 \equiv r_{N-N} = 1.1257 \pm 0.002 \text{ Å.}$$
$$r_2 \equiv r_{N-O} = 1.1863 \pm 0.002 \text{ Å.}$$
$$r_1 + r_2 = 2.3120 \pm 0.001 \text{ Å.}[6]$$

With these unsymmetrical molecules, the symmetry requirements of space group Pa3 can be satisfied in a statistical way only. The N_2O molecules must be presumed to pack randomly in the two possible orientations available to each molecule; the molecule at the unit cell origin, for example, may have the oxygen pointed in either the positive or negative [111] direction. This structure was first proposed by Blue and Giauque[7] who discovered a residual entropy in the solid of 1.14 cal. degree^{-1} mole^{-1} (e.u.). This is suggestively close to the value $R \ln 2 = 1.377$ e.u. predicted for a structure with molecules randomly placed in one or the other of two possible positions. An *ordered* structure which is closely related can be obtained by removing the center of symmetry and placing all atoms in positions (a) of space group T^4-$P2_13$: $x,x,x;\ {}^1/_2+x,{}^1/_2-x,-x;\ -x,{}^1/_2+x,{}^1/_2-x;\ {}^1/_2-x,-x,{}^1/_2+x$. Because of the near equality of the scattering powers of nitrogen and oxygen, the X-ray diffraction experiment is extremely insensitive to any possible ordering of the N_2O molecules. The postulated disordered structure thus rests entirely on the thermodynamic data, and there remains the possibility that the structure *is* ordered and that the excess entropy arises from some other source. It seemed desirable to repeat the diffraction experiment with neutrons, where the more favorable ratio of scattering factors ($b_O = 0.58$, $b_N = 0.94$) would allow a more sensitive test of any departures from the disordered model.

Commercial N_2O was condensed to a depth of 8 cm. in a quartz tube 20 mm. in diameter. The tube was placed in a stainless steel cryostat maintained at liquid nitrogen temperature (77°K.), and several neutron diffraction patterns were obtained, using the apparatus described by Corliss, Hastings and Brockman.[8] The neutron wave length was 1.064 Å. A typical diffraction pattern is shown in Fig. 1.

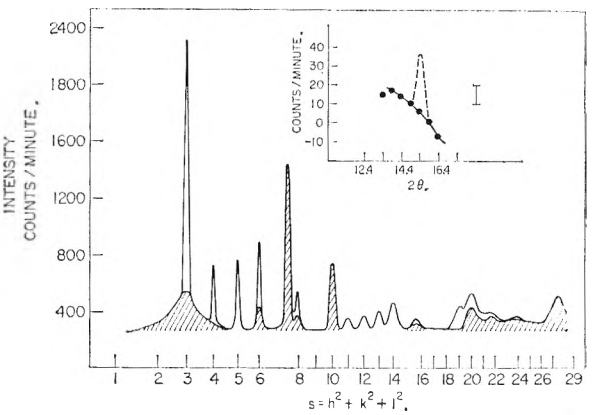

Fig. 1.—Observed neutron diffraction pattern for N_2O. The shaded areas are due to the cryostat and sample tube and have been subtracted from the tabulated intensities. The solid curve in the inset shows the net observed intensity in the region of the (110) reflection. The dashed curve shows a reflection (not observed) of intensity 1.0 on the scale used in Table I. The bar in the inset has a length twice the standard deviation of the individual points.

Intensities were calculated for several sets of structure parameters for the disordered model (space group Pa3). The scattering factor for the central atom (a) was taken as b_N and that for the outer atom (c) as $(b_N + b_O)/2$. A series of least squares refinements led to these best values for the parameters

$$x = 0.1196 \pm 0.0013$$
$$B(c) = 1.87 \pm 0.38 \text{ Å.}^2$$
$$B(a) = 1.29 \pm 0.39 \text{ Å.}^2,[9]$$

(1) Work performed under the auspices of the U. S. Atomic Energy Commission.

(2) J. de Smedt and W. H. Keesom, *Proc. Acad. Sci. Amsterdam*, **27**, 839 (1924).

(3) A value of 5.656 Å. at −190° has been reported by L. Vegard, *Z. Physik*, **71**, 465 (1931).

(4) See "International Tables for X-Ray Crystallography," Vol. I, the Kynoch Press, Birmingham, 1952.

(5) A. E. Douglas and C. K. Moller, *J. Chem. Phys.*, **22**, 275 (1954).

(6) An electron diffraction investigation (also in the vapor phase) resulted in a value of $(r_1 + r_2) = 2.32 \pm 0.02$ Å., and the ratio r_1/r_2 was determined to lie beteen the limits 0.925 and 1.08. See V. Schomaker and R. Spurr, *J. Am. Chem. Soc.*, **64**, 1182 (1942).

(7) W. Blue and W. F. Giauque, *ibid.*, **57**, 991 (1935).

(8) L. M. Corliss, J. M. Hastings and F. G. Brockman, *Phys. Rev.*, **90**, 1013 (1953).

(9) B is the Debye–Waller factor which enters the structure factor expression as $\exp[-B \sin^2\theta/\lambda^2]$.

Intensities calculated for this model are presented in Table I together with the observed intensities. The estimated standard deviations of the observed intensities were obtained from the counting statistics and from estimates of possible errors in subtracting out cryostat peaks. The agreement factor

$$R_4 = \left[\frac{\Sigma w |I_c - I_0|^2}{\Sigma w I_0^2}\right]^{1/2}$$

has the value 0.087 for the above parameters. The x parameter combined with a value for a_0 of 5.67 ± 0.02 Å. from this experiment leads to a molecular length of 2.33 ± 0.03 Å., in satisfactory agreement with the other methods of determination.[10]

Intensities were also calculated for several sets of parameters for the ordered model. The best agreement again was with an average B of about 1.5 and a molecular length of 2.33 Å. Because relatively good over-all agreement can be obtained for the observed reflections, the decision between the disordered and the ordered model must rest on the unobserved reflections.

TABLE I

INTENSITIES FOR ALLOWED REFLECTIONS IN SPACE GROUP Pa3

F is calculated for the best disordered structure. j is the multiplicity. θ is the Bragg angle.

$$I_{\text{calc.}} = \frac{0.0165 j F^2}{\sin 2\theta \sin \theta}$$

hkl	$I_{\text{obsd.}}$	$I_{\text{calcd.}}$
111	75.3 ± 2.1	73.2
200	17.4 ± 0.8	18.5
210	23.4 ± 3.1	29.0
211	26.0 ± 2.2	24.9
220	10.9 ± 3.1	14.8
221	<0.9	0.1
311	5.5 ± 0.7	4.6
222	6.9 ± 1.1	6.2
230	11.2 ± 1.2	11.3
321, 231	18.7 ± 1.8	17.8
400	<3.9	0.8
410, 322	<1.2	0.1
411	<1.2	0.1
331	23.6 ± 4.2	22.1
240	6.1 ± 2.1	8.3
241, 421	9.0 ± 2.8	9.3
332	4.9 ± 2.1	4.5
422	4.8 ± 3.5	7.7
430	<1.2	0.1
341, 431	<1.2	0.1
511, 333	1.8 ± 1.9	1.9

Because the ordered model can produce a (110) reflection, a reflection forbidden in space group Pa3, a special effort was made to observe a reflection in this region. The region from 2θ = 12 to 18° (the expected peak position is 15.4°) was traversed several times at low scanning rates, both for the sample in the cryostat and the cryostat alone. Runs were made both with and without a Pu^{239} filter which effectively cuts out all the $\lambda/2$ component contained in the diffracted beam. There was no evidence of a peak in the (110) position for any of the runs. A composite of the runs is shown by the points in the inset to Fig. 1. The peak drawn in would be the appearance of a sharp peak of intensity 1.0 on the arbitrary scale used in Table I. It was estimated that any peak which evaded observation could not have an intensity of more than 0.6 on this scale. Intensities were calculated for a series of ordered models, all with $x_O - x_{N1} = -0.1226$ and $x_{N1} - x_{N2} = -0.1154$, corresponding to bond lengths of 1.20 and 1.13 Å. The over-all value of B was kept fixed at 1.5, and the agreement between observed and calculated intensities was scrutinized as a function of x_{N1}. The results are presented in Table II. The main feature is that for values of $I(110)$ at all comparable with the previously estimated maximum of 0.6 the intensities of (430) and especially (431) are far above the estimated maximum values. Note also that at this point the value of R_4 is getting rather large. The estimated maximum acceptable value of R at the 95% confidence limit is 0.127.

We may thus conclude that the completely ordered model is incompatible with the neutron diffraction data. A small amount of short-range order is not incompatible with the data (even with neutrons, the effects are small!) and is suggested by the fact that the residual entropy at 0°K. is somewhat less than $R \ln 2$.

(10) This is the distance between the peaks at either end of the molecule caused by overlap of ½ O and ½ N in each position. It does not necessarily correspond to the non-bonded N–O distance. The fact that it is comparable to the spectroscopic value leads one to guess that in either orientation the molecules pack about the same way, centered on the origin.

TABLE II

SOME INTENSITIES FOR AN ORDERED MODEL (SPACE GROUP $P2_13$)

R_4 as defined in text is an average percentage error for all intensities.

x_{N1}	R_4	$I(110)$	$I(430)$	$I(431)$
0.0071	0.096	3.66	0.29	0.80
.0046	.094	3.12	.17	.70
.0021	.093	2.62	.15	.80
− .0004	.094	2.16	.24	1.08
− .0029	.096	1.75	.43	1.55
− .0054	.101	1.38	.73	2.18
− .0079	.109	1.05	1.11	2.96
− .0104	.121	0.77	1.58	3.88
− .0129	.137	.53	2.14	4.91
− .0154	.155	.34	2.72	6.02
Max. obsd. value		.60	1.20	1.20

THE HEATS OF MIXING OF AQUEOUS SOLUTIONS OF POLYPROPYLENE GLYCOL 400 AND POLYETHYLENE GLYCOL 300

BY R. G. CUNNINGHAME AND G. N. MALCOLM

University of Otago Dunedin, New Zealand

Received February 21, 1961

It is of interest to examine in what way the heat of mixing of a polymer with a given solvent is related to the heat of mixing of the corresponding monomer with the same solvent. The heats of mixing with water of mono- and di-propylene glycols have been measured at 25° by Amayo and Fujishiro.[1] In the present paper results obtained

for the heat of mixing with water at 26.9° of polypropylene glycol 400 are discussed in relation to the above work. Results also are given for the heat of mixing with water at 26.9° of polyethylene glycol 300 which has the same number of chain units as polypropylene glycol 400 but contains ether groups of a different kind.

Experimental

Apparatus.—The heats of mixing were measured in an isothermal calorimeter using diphenyl ether as the calorimetric substance. The design of the calorimeter and mixing vessel was identical with that described by Malcolm and Rowlinson.[2] Diphenyl ether was chosen as the calorimetric substance because its melting point, 26.9°, is close to 25° and it also has a relatively large volume change on melting.

The calibration factor of the calorimeter was 1.32 ± 0.01 cm. cal.$^{-1}$ (1 cal. = 4.184 joules). This is equivalent to 0.0500 ± 0.0004 g. cal.$^{-1}$ in terms of grams of mercury displaced per calorie of heat evolved. There is a discrepancy of 4% between this figure and the most reliable of those obtained by other workers.[3] The most likely explanation for this discrepancy is an unavoidable heat loss in the calorimeter.[3a] Since the calibration factor was reproducible and since the heat of mixing measurements were carried out under conditions similar to those used in the calibration, the uncertainty in the results obtained with this instrument should be considerably less than the 4% error in the calibration factor.

Materials.—The samples of polyethylene glycol and polypropylene glycol were supplied by Oxirane Ltd., of Manchester, England. The number average molecular weights were given as 300 and 400, respectively. The samples were dried and degassed under high vacuum at 100° for several hours. Freshly distilled water was used.

Results

The heat of mixing results are recorded in Table I.

TABLE I

THE HEATS OF MIXING AT 26.9° OF AQUEOUS SOLUTIONS OF POLYPROPYLENE GLYCOL 400 AND POLYETHYLENE GLYCOL 300 IN CAL./G. OF MIXTURE AS A FUNCTION OF THE WEIGHT FRACTION OF POLYMER (W_p)[a]

W_p	$-\Delta H$, cal./g. of mixture	$-\Delta H$, kcal./mole of glycol	W_p	$-\Delta H$, cal./g. of mixture	$-\Delta H$, kcal./mole of glycol
Polypropylene glycol 400					
0.109	3.90	14.3	0.609	8.10	5.3
.198	6.33	12.8	.701	6.87	3.9
.314	8.20	10.5	.791	5.26	
.393	8.83	9.0	.811	4.92	
.467	8.97	7.7	.908	2.66	
.477	9.00	7.5			
Polyethylene glycol 300					
0.130	4.50	10.4	0.478	12.70	8.0
.209	7.36	10.5	.520	12.90	7.4
.296	9.66	9.7	.636	12.80	6.0
.323	9.95	9.2	.722	10.50	
.392	11.80	9.0	.816	7.65	
.411	11.90	8.7	.886	5.55	

[a] The estimated error in the heat of mixing per gram of mixture (apart from any error in the calibration factor) is within ±2% in each case.

The results in columns 1, 2, 4 and 5 of Table I have been used to calculate the heats of mixing per mole of glycol in each solution. These values are listed in the third and sixth columns of the table and are plotted against mole fraction of glycol in Fig. 1.

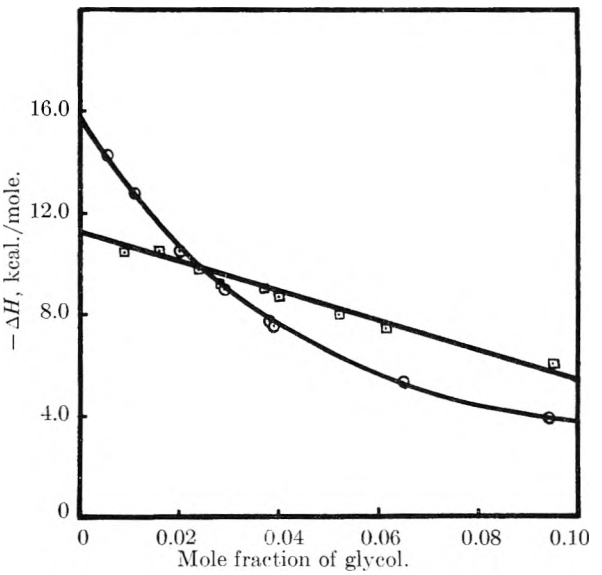

Fig. 1.—Heat of mixing per mole of glycol with water at 26.9° for polypropylene glycol 400 (○) and polyethylene glycol 300 (□).

Discussion

In their work Amayo and Fujishiro plotted the heat of mixing per mole of glycol against the mole fraction of glycol and extrapolated the results to zero concentration of glycol. By this means they obtained the heats of mixing per mole of glycol at infinite dilution for their two solutions. The values were −2.3 kcal./mole for the propylene glycol solution, and −4.1 kcal./mole for the dipropylene glycol solution. The difference of 1.8 kcal./mole between these values was regarded as a measure of the contribution to the heat of mixing at infinite dilution of the ether group in the dipropylene glycol molecule. An attempt to predict on this basis the molar heat of mixing with water at infinite dilution of tripropylene glycol was inconclusive because of the lack of reliable experimental results for the solutions of this substance.

From Fig. 1 the value obtained for the molar heat of mixing of polypropylene glycol 400 with water at infinite dilution is −15.8 kcal./mole. The value calculated from the results for the mono- and dipropylene glycols, with the assumption that polypropylene glycol 400 contains an average of 6.5 ether groups per molecule, is −14.0 kcal./mole. These two values are in closer agreement than those obtained by Amayo and Fujishiro for tripropylene glycol.

Figure 1 also shows a comparison between the heats of mixing with water of polypropylene glycol 400 and polyethylene glycol 300. These two substances contain the same average number of chain units per molecule. It might be expected that the heat of mixing with water per mole of

(1) K. Amayo and R. Fujishiro, *Bull. Chem. Soc. Jap.*, **30**, 940 (1957).

(2) G. N. Malcolm and J. S. Rowlinson, *Trans. Faraday Soc.*, **53**, 921 (1957).

(3) (a) R. S. Jessup, *J. Research Natl. Bur. Standards*, **55**, 317 (1955); (b) F. S. Dainton, J. Diaper, K. J. Ivin and D. R. Sheard, *Trans. Faraday Soc.*, **53**, 1269 (1957).

glycol would be more negative for polyethylene glycol 300 than for polypropylene glycol 400. This would follow both from the fact that the polypropylene glycol contains a greater proportion of hydrocarbon in its molecule and also from the steric effect of the side chain methyl groups in polypropylene glycol which probably hinder hydrogen bonding between water molecules and the ether oxygen atoms. The effect of this steric factor on the relative water solubilities of ethers has been discussed by Ferguson.[4] It is evident from Fig. 1 that in dilute solution the above expectation is not fulfilled.

A possible explanation of the observed behavior is that in the very dilute solutions the terminal hydroxyl groups in the polyethylene glycol molecule are involved in intramolecular hydrogen bonding with the ether groups. Molecular models suggest that this is possible in the polyethylene glycol molecule but that it is more difficult in the polypropylene glycol molecule because of steric hindrance from the side-chain methyl groups.

(4) L. N. Ferguson, *J. Am. Chem. Soc.*, **77**, 5288 (1955).

THE RESIDUAL ENTROPY OF THE EQUIMOLAL KCL–KBR SOLID SOLUTION IN RELATION TO WASASTJERNA'S THEORY OF ALKALI HALIDE SOLID SOLUTIONS[1,2]

BY M. V. MILNES AND W. E. WALLACE

Department of Chemistry, University of Pittsburgh, Pittsburgh 13, Pa.

Received February 22, 1961

In 1949 Wasastjerna[3] developed a very elegant statistical thermodynamic theory of alkali halide solid solutions. In this treatment he succeeded in evaluating the partition function of the solution in terms of readily available properties of the individual salts from which the solution was formed. Use of this partition to compute the heat effect (ΔH_c) accompanying the formation of the solution from its component salts led to results which, as has been pointed out,[4] are in strikingly good agreement with experiment. The theory also permits calculation of the corresponding entropy change (ΔS_c). ΔS_c at 25° for the reaction

$$0.5KCl(s) + 0.5KBr(s) \rightarrow KCl_{0.5}Br_{0.5}\ (\text{solid solution})$$

was found[4] to be 1.29 e.u. According to the theory the entropy increase is entirely configurational in origin; that is, it originates with the mixing entropy of the chloride and bromide ions. ΔS_c is less than 1.38 e.u., the value for random mixing, because there is some local order in the way the two halide ions populate the anion sites.

Several years ago the entropy change (ΔS_m) for the above reaction was evaluated experimentally in this Laboratory.[4] The value obtained was 1.49 ± 0.03 e.u., which is considerably in excess of ΔS_c and even exceeds the entropy of random mixing. From the results of that study it was clear that the theory is incomplete in ascribing the entropy of formation solely to configurational effects. However, it left unanswered questions as to the origin of the excess entropy. The possibility was raised that the extra entropy might be vibrational in origin. This note presents results which establish that this is indeed the case.

The measured entropy for 25° can be separated into vibrational and configurational components: $(\Delta S_m)_{25°} = (\Delta S_v)_{25°} + S_{con}$, where S_{con} represents the configurational entropy of the solution for 25°, the quantity calculable from Wasastjerna's theory. If ΔC_p for the reaction is known at low temperature, $(\Delta S_m)_{0°K}$ can be obtained. Since the vibrational contribution vanishes at the absolute zero, the value for $(\Delta S_m)_{0°K}$ equals S_{con}, which is the residual entropy of the solution. Furthermore, since the configuration in the solution is frozen-in below 25°, S_{con} is temperature independent and hence the residual entropy is a measure of the configurational entropy at room temperature.

Prior to the present investigation all data needed to make the calculation were in existence except the heat capacities for the solution. These have now been measured employing equipment and techniques that have been in use in this Laboratory for many years.[5] Fifty-four determinations were made covering the temperature range from 12 to 300°K. The salts used, obtained from the Harshaw Chemical Co., were analyzed spectroscopically. The only significant metallic impurities were in KCl 0.02% Na and 0.01% Rb and in KBr 0.015% Na. Halide analyses gave for KCl 47.574 ± 0.017% (theor. 47.557%) and for KBr 67.175 ± 0.013% (theor. 67.147%). The discrepancy for KBr if attributed entirely to chloride, which is known to be present, indicates 0.09% Cl^-. To prepare the solution stoichiometric quantities of the components were weighed out, with due allowance for the chloride content of KBr, and fused together in a Pt container. The melt was well stirred and then quenched by pouring into a cold Pt dish. The cake was crushed and homogenized at 690° for 13 hr., this treatment being indicated by the work of Matsen and Beach.[6] Examination by X-ray diffraction showed the sample to be single phase and homogeneous.

The results obtained lay on a smooth curve drawn through all the points within 0.1% except at the lowest temperatures. Below 30°K. the scatter gradually increased to a maximum of about 1% between 12 and 18°K. Smoothed heat capacities of the solution at selected temperatures together with ΔC_p's are given in Table I. For the pure salts the results obtained in the very careful work of Berg and Morrison[7] were used. Their data extended only to 270°K., however. Above this the results given in the compilation by Musta-

(1) From a thesis submitted by M. V. Milnes to the University of Pittsburgh in partial fulfillment of the requirements for the M. S. degree, June, 1960.

(2) This work was assisted by a contract with the U. S. Atomic Energy Commission.

(3) J. A. Wasastjerna, *Soc. Sci. Fennica, Commentationes Phys.-Math.*, [XV] **3**, 1 (1949). See also V. Hovi *ibid.*, [XV] **12**, 1 (1950).

(4) W. H. McCoy and W. E. Wallace, *J. Am. Chem. Soc.*, **78**, 5995 (1956).

(5) R. S. Craig, *et al.*, *J. Am. Chem. Soc.*, **76**, 238 (1954).

(6) F. A. Matsen and J. Y. Beach, *ibid.*, **63**, 3470 (1941).

(7) W. T. Berg and J. A. Morrison, *Proc. Roy. Soc.* (*London*), **242A**, 467 (1957).

joki[8] were employed for KBr. The random error in the measurements on the pure salts was well within the tolerance required for a satisfactory evaluation of the residual entropy. To ascertain whether the systematic errors in the independently

TABLE I

HEAT CAPACITY DATA FOR THE EQUIMOLAL KCl–KBr SOLID SOLUTIONS

T(°K.)	C_p for $KCl_{0.5}Br_{0.5}$, cal. deg.$^{-1}$ (mole of ion pairs)$^{-1}$	ΔC_p,[a] cal. deg.$^{-1}$
12	0.272	−0.001
15	0.539	−0.002
20	1.157	−0.002
25	1.914	−0.007
30	2.775	0.024
40	4.480	0.041
50	5.974	0.051
60	7.193	0.071
80	8.876	0.068
100	9.901	0.058
125	10.680	0.040
150	11.187	0.029
175	11.521	0.016
200	11.770	0.025
225	11.969	0.026
250	12.121	0.013
273.16	12.242	−0.010
275	12.252	−0.012
298.16	12.378	−0.011
300	12.383	−0.010

[a] $\Delta C_p = (C_p)_{KCl_{0.5}Br_{0.5}} - 1/2[(C_p)_{KCl} + (C_p)_{KBr}]$.

obtained results were sufficiently large to vitiate the calculations the data for KCl were "spot checked" between 80 and 300°K. Twenty-seven determinations were made.[9] These were on the average 0.10% lower than those determined by Berg and Morrison.

Using the ΔC_p's given in Table I the residual entropy is computed to be 1.39 ± 0.04 e.u. or 1.37 ± 0.04 e.u. if cognizance is taken of the 0.1% systematic deviations noted for KCl and if it is assumed that the same holds for KBr. These values are very close to the entropy of random mixing, strongly suggesting that there is a negligible amount of local order in the anion sublattice. These results are clearly at variance with Wasastjerna's theory which predicts a residual entropy of 1.29 ± 0.01 e.u. and an appreciable degree of order. As departure from randomness is an essential feature of the theory without which its impressive quantitative success to date could not have been achieved, the present result is of interest and of significance in connection with the general evaluation of the theory. Further results bearing upon the nature of the distribution of the ions must be obtained, however, before a critical appraisal of the theory can be made.

Results obtained in the present work show that when $KCl_{0.5}Br_{0.5}$ is formed from the component salts, there is an increase in vibrational entropy of 0.11 e.u. In seeking the source of this increment of entropy it is instructive to compare the actual solution with the corresponding ideal solution. In the ideal case the heat capacity is given by the Kopp–Neumann rule and ΔS_{vib} is hence zero. The observed positive value of ΔS_{vib} indicates therefore slightly softer vibrations in the actual than in the hypothetical ideal solution. If the Debye theory is employed to describe the situation, it develops that the ideal solution has a characteristic temperature of about 200°K., whereas that of the actual solution is 4°K. lower. Roughly speaking, this means that the vibrations in the real case are about 2% slower than those in the ideal solution. To account for this difference in terms of the details of lattice dynamics is not a simple matter. Experiment shows,[10] however, that the lattice energy of the real solution is slightly less than that of the ideal solution, implying slightly looser binding in the former. On this basis one expects slower vibrations, a lower Debye θ and higher vibrational entropy for the actual solution than for its ideal counterpart.

(8) A. Mustajoki, *Ann. Acad. Sci. Fenn.*, **98**, 1 (1951).

(9) Thanks are due to Dr. W. G. Saba and Mr. T. Peltz for making these measurements. These data were used in computing the ΔC_p's above 270°K.

(10) V. Ilovi, *Ann. Acad. Sci. Fennicae, Math.-Phys.*, **AI**, No. 55, 1 (1948).

*p*H-DEPENDENT SPECTRAL SHIFTS IN THE SYSTEM ACRIDINE ORANGE–POLYMETHACRYLIC ACID

BY G. BLAUER[1]

Department of Chemistry, Brandeis University, Waltham, Mass.

Received March 3, 1961

A considerable amount of work has been reported on the binding of organic dyes and similar molecules by charged macromolecules. Various effects of synthetic and natural polyelectrolytes on the absorption spectrum of the vital stain acridine orange were described recently.[2–6] In order to account for the spectral shifts observed, it was generally assumed that the positively charged dye molecules, by electrostatic interaction with ionized groups on these polymers, are brought into suitable positions for mutual interaction by dispersion forces. In the absence of polyelectrolytes, "Dye Polymers" are known to be formed in more concentrated aqueous solutions.[7,8] In the present case, some results are reported which were obtained by changing the *p*H of aqueous solutions containing acridine orange cation (AO) and polymethacrylic acid (PMA). The interaction was studied in the ionization range of the poly-acid.

Experimental

Acridine Orange.—The pure chloride was prepared from the commercial dye according to ref. 8.

Polymethacrylic Acid.—The monomer was polymerized at 50° *in vacuo* by addition of 2,2′-azobisisobutyronitrile. The polymer obtained was purified by repeated solution

(1) The Weizmann Institute of Science, Rehovot, Israel.

(2) D. F. Bradley and M. K. Wolf, *Proc. Natl. Acad. Sci. U. S.*, **45**, 944 (1959).

(3) A. M. Michelson, *Nature*, **182**, 1502 (1958).

(4) R. F. Steiner and R. F. Beers, *Science*, **127**, 335 (1958).

(5) R. F. Beers, D. D. Hendley and R. F. Steiner, *Nature*, **182**, 242 (1958).

(6) W. Appel and V. Zanker, *Z. Naturforsch.*, **13b**, 126 (1958).

(7) G. Scheibe, *Z. Elektrochem.*, **52**, 283 (1948).

(8) V. Zanker, *Z. physik. Chem.*, **199**, 225 (1952).

in methanol and precipitation by excess ether. It was then heated *in vacuo* to constant weight.

Absorption spectra were measured on a Cary recording spectrophotometer. The time dependence of the spectra was checked. Over a period of several days at room temperature the peak positions remained constant but slight changes in absorbance occurred.

Results and Discussion

Figure 1 contains a typical set of spectra obtained at fixed concentrations of dye, polymer and buffer but at varying *p*H. With increasing *p*H, the absorption peaks shifted progressively to shorter wave lengths. At *p*H 11 where the neutral dye is predominant,[8] there was little difference between the spectra obtained both in the presence and in the absence of PMA (curves 4 and 5) while at *p*H 9, two peaks of equal height at 490 and 470 mμ, respectively, were recorded for the dye in the absence of polymer. These are the monomer and dimer bands of the cation.[8] When no buffer was used, under otherwise identical conditions, the spectral shifts were larger at a given *p*H. For example, at *p*H 8, the band peak was at 448 mμ as compared to 452 mμ in the presence of buffer. This indicates competition of the buffer ions for the binding sites on the polymer. The unbuffered solutions, however, were less stable than those including buffer and less reproducible results were obtained.

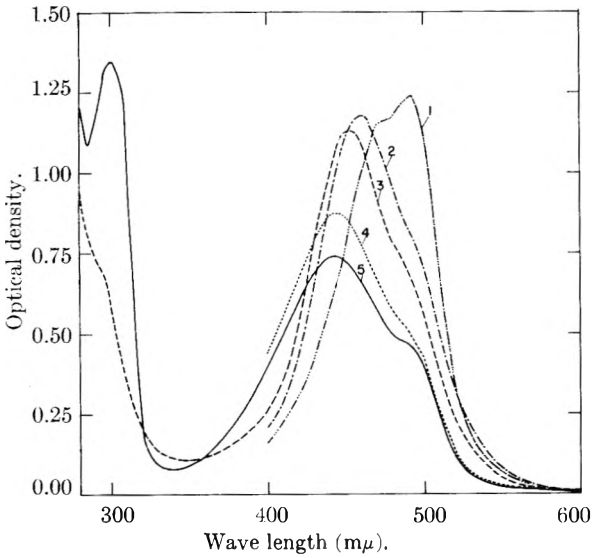

Fig. 1.—Absorption spectra of acridine orange–polymethacrylic acid complexes at various *p*H-values: AO = 5.8×10^{-5} *M*; PMA = 1.3×10^{-4} monomolar; citrate-phosphate buffer $\simeq 10^{-2}$ *M*. Optical path = 1.0 cm.; room temperature. Curve 1, *p*H 5; curve 2, *p*H 7; curve 3, *p*H 8; curve 4, *p*H 11; curve 5, *p*H 11 in the absence of PMA.

In the ultraviolet region, two more absorption bands at 260–270 mμ and at 220–230 mμ, respectively, were recorded in all cases including the dye in the absence of polymer. Variations in the peak positions were less than 10 mμ. On the other hand, the dye–polymer system between *p*H 5 and 9 had a shoulder of relatively low absorbance at 290–300 mμ, while in the absence of polymer, a pronounced peak of fairly constant height was measured in this wave length region between *p*H 6 and 11. The difference in band intensity is demonstrated in Fig. 1 (curves 3 and 5) and it may be taken as an additional criterion for metachromasy in AO caused by the polymer.

The spectral changes observed in the visible region are similar to those occurring on increase of the concentration of the dye in aqueous buffer in the absence of polyelectrolyte, where dimers and higher aggregates of the dye are being formed.[8] In this case, the dye concentration has to be about 20 times higher in order to cause a similar spectral shift as in the presence of PMA at *p*H 7 (conditions according to Fig. 1), but it would have to be 1000–2000 times higher to achieve the effect caused by PMA at *p*H 9. (The molar extinction coefficients are lower by 30–40% in the dye–polymer system). The spectral changes with *p*H as indicated in Fig. 1 concur with a increase in the initial degree of ionization of the PMA from about 10% at *p*H 5 to over 90% at *p*H 9. Apparently, with increase in ionization of the polymer, additional binding sites for the cationic dye are being provided. The interaction between dye molecules on the polymer is thereby facilitated and higher dye aggregates are being formed progressively.

Other systems investigated by us at room temperature which induce spectral shifts on AO included 1.7×10^{-3} monomolar polyphosphate at *p*H 4. This polymer caused a shift of about 300 mμ on 6×10^{-5}*M* AO; 0.9 *M* sodium chloride at *p*H 6, in the absence of polymer, shifted the absorption peak of 3.3×10^{-5} *M* AO to 467 mμ (molar ext. coeff. = 3.1×10^4). The band at 290–300 mμ was indicated by a shoulder. On the other hand, sodium glutarate at *p*H 8, and at the same monomolar concentration as the polymethacrylate, did not cause any shift or change in the ratio of the AO peaks at 490 and 470 mμ, though glutaric acid may, in some respect, serve as a dimer model for PMA.

Experiments performed at higher ratios of ionized PMA:AO showed a decreased tendency for spectral shifts toward shorter wave lengths. This is in accord with the concept that the spectral effects observed are due primarily to the state of aggregation of the dye on the polyelectrolyte.

Acknowledgment.—Thanks are due to Drs. H. Linschitz and V. Zanker for valuable comments. This study was supported by a grant from the U. S. Atomic Energy Commission (AT-30-1-2003).

KINETICS OF THE CATALYTIC DEHYDROCYCLIZATION OF *n*-HEPTANE

By J. C. Rohrer, H. Hurwitz and J. H. Sinfelt

Esso Research and Engineering Co., Linden, N. J.

Received March 7, 1961

The formation of aromatics by dehydrocyclization of paraffins over metal–acidic oxide catalysts has been studied by several investigators.[1,2] The metal–acidic oxide catalysts consist of an active dehydrogenation component, such as platinum or palladium, dispersed on an acidic support such as alumina or silica–alumina. These dual

(1) G. R. Donaldson, L. F. Pasik and V. Haensel, *Ind. Eng. Chem.*, **47**, 731 (1955).

(2) W. P. Hettinger, C. D. Keith, J. L. Gring and J. W. Teter, *ibid.*, **47**, 719 (1955).

function catalysts are particularly active for dehydrocyclization,[2] and this has been attributed at least in part to their high dehydrogenation activity.[3]

Relatively little has been reported on the kinetics of dehydrocyclization over metal–acidic oxide catalysts, including the effects of hydrogen pressure. This type of information is of considerable importance in obtaining an understanding of the reaction mechanism. To obtain such information, it was decided to investigate the kinetics of *n*-heptane dehydrocyclization over a platinum-on-alumina catalyst.

Experimental

Procedure.—Reaction rates were measured using a flow reactor technique, as described in previous papers.[1,5] Briefly, the technique involves passing the reactant, in this case *n*-heptane, over the catalyst in the presence of added hydrogen. The reaction products are analyzed by a combination of three chromatographic columns containing polyethylene glycol, hexamethylphosphoramide and squalane, all impregnated on firebrick. The polyethylene glycol column was used for the determination of toluene, the hexamethylphosphoramide for C_5 and lighter paraffins, and the squalane for C_6 and C_7 paraffins, methylcyclohexane and dimethylcyclopentanes.

Materials.—Phillips pure grade *n*-heptane (>99 mole % pure) was used throughout. Both the *n*-heptane and hydrogen were dried to less than 5 p.p.m. water, using procedures described previously.[4,5] The platinum-on-alumina catalyst used in the present study contained 0.3% platinum. The catalyst was prepared by impregnation of alumina with aqueous chloroplatinic acid, followed by calcination in air for four hours at 593°. The surface area of the alumina support was approximately 145 m.²/g.

Results

When passed over platinum-on-alumina catalyst, *n*-heptane undergoes three major types of reactions: isomerization, dehydrocyclization and hydrocracking. The products of isomerization are predominantly 2- and 3-methylhexanes, while dehydrocyclization yields toluene with small quantities of dimethylcyclopentanes and methylcyclohexane. The products of hydrocracking are hydrocarbons containing fewer than seven carbon atoms. Data on the selectivity of conversion of n-C_7 to the various products at low conversion levels (3 to 14%) are given in Table I.

The *n*-heptane reaction rates were measured at low conversion levels to obtain initial rates. The rate is defined by

$$\text{rate} = \frac{F\Delta x}{W} \qquad (1)$$

where F is the feed rate in g. moles of *n*-heptane per hour, W is the weight of catalyst in grams, and Δx is the extent of conversion for a particular reaction. For dehydrocyclization Δx represents the fraction of *n*-heptane converted to toluene, dimethylcyclopentanes and methylcyclohexane. For isomerization Δx is the fraction converted to 2- and 3-methylhexanes and dimethylpentanes. To obtain comparable levels of conversion at both 471 and 527°, a 3.3-fold higher value of F/W was used at 527°.

Experiments in which nitrogen was substituted for hydrogen showed no isomerization or dehydrocyclization of *n*-heptane, indicating that the presence of hydrogen is necessary for both reactions. Relative rates of dehydrocyclization r_D and isomerization r_I of *n*-heptane are plotted in Fig. 1 as a function of hydrogen partial pressure p_H at a constant *n*-heptane partial pressure of 1.2 atm. Since no isomerization or dehydrocyclization was detected in the absence of hydrogen, the curves all pass through the origin. All the points at 471° and the point at 20 atmospheres hydrogen pressure at 527° represent averages of two runs. The remaining points are the results of single determinations. Rates obtained in duplicate runs agreed within about 10%.

The rate of dehydrocyclization was found to increase with increasing hydrogen partial pressure up to a maximum value, beyond which the rate fell off with a further increase of hydrogen pressure.

TABLE I

SELECTIVITY OF CONVERSION OF *n*-HEPTANE

Temp., °C.	471	471	471	527	527	527
Pressure, atm.						
n-Heptane	1.2	1.2	1.2	1.2	1.2	1.2
Hydrogen	1.9	5.8	20.0	1.9	5.8	20.0
Total	3.1	7.0	21.2	3.1	7.0	21.2
Total conversion, %	6.0	14.3	12.6	3.0	9.6	9.8
Selectivity of conversion, %[a]						
Isomerization[b]						
2-Methylhexane	18	21	19	7	16	19
3-Methylhexane	33	47	47	10	28	32
Dehydrocyclization[c]						
Toluene	17	10	6	20	18	10
Hydrocracking						
C_1-C_6	32	21	28	63	38	39

[a] Expressed as % of the converted n-C_7. [b] 2,4-Dimethylpentane less than 1% of product. [c] Methylcyclohexane and dimethylcyclopentanes less than 1% of product.

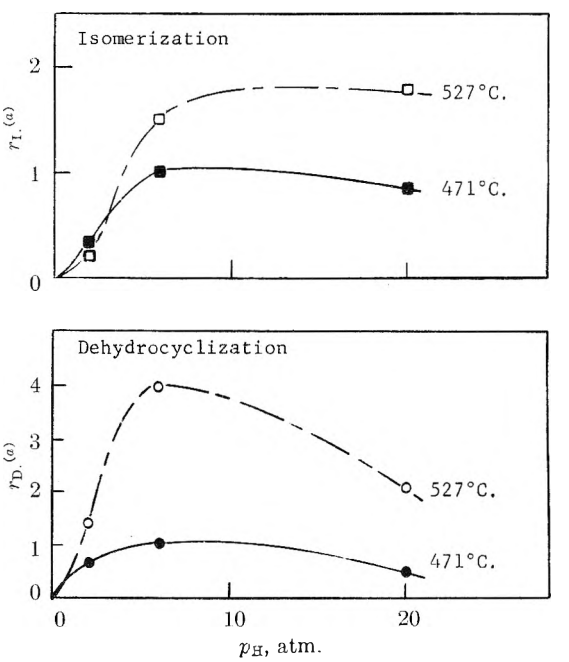

Fig. 1.—Effect of hydrogen pressure on rates of dehydrocyclization and isomerization. [a] Rates relative to the rates at 471°, p_H 5.8 atm.

(3) F. G. Ciapetta, R. M. Dobres and R. W. Baker, "Catalysis," Vol. 6, Reinhold Publ. Corp., New York, N. Y., 1958, p. 522.

(4) J. H. Sinfelt, H. Hurwitz and J. C. Rohrer, *J. Phys. Chem.*, **64**, 892 (1960).

(5) J. H. Sinfelt, H. Hurwitz and R. A. Shulman, *ibid.*, **64**, 1559 (1960).

Similar results were observed for isomerization at 471°, but at 527° the existence of a maximum was not clearly demonstrated. However, the data at 527° are not sufficient to exclude the existence of a maximum between 5.8 and 20 atm. of hydrogen, or at a still higher pressure.

Discussion

The role of hydrogen in the kinetics of dehydrocyclization is interpreted as follows: The dehydrocyclization reaction involves a preliminary dehydrogenation step prior to ring closure. Increasing hydrogen pressure might then be expected to suppress the initial dehydrogenation step and hence decrease the rate of dehydrocyclization, as observed for hydrogen pressures above 5.8 atmospheres in the present study. However, at lower hydrogen pressures, background reactions involving extensive dehydrogenation and polymerization become important. These reactions lead to extensive coverage of the platinum by hydrogen deficient hydrocarbon residues. The limiting factor in the reaction is then the rate of removal of the residues by reaction with hydrogen, thus accounting for the beneficial effect of hydrogen on the rate. Studies on the dissociative chemisorption of hydrocarbons over a variety of metals supply direct evidence for the formation of such hydrogen deficient residues, and for their removal by reaction with hydrogen.[6] The ability of hydrogen to clean up a platinum catalyst exposed to benzene at high temperature[7] also has been demonstrated. Similar considerations on the role of hydrogen also apply to the isomerization reaction, although the maxima in rates may occur at different hydrogen pressures.

The temperature coefficients of the reaction rates vary markedly with hydrogen pressure. At low hydrogen pressure the temperature coefficients are small and can even be negative, as observed for isomerization. Apparently the amount of surface not covered by residues decreases appreciably with temperature. At higher hydrogen pressures, where coverage of the platinum by hydrocarbon residues is presumably not a major limitation, the temperature coefficients are much higher.

The effects of hydrogen reported here are quite similar to those found in the isomerization–dehydroisomerization of methylcyclopentane over a similar catalyst,[8] and would appear to be characteristic of reactions over bifunctional catalysts such as platinum-on-alumina.

(6) A. K. Galwey and C. Kemball, *Trans. Faraday Soc.*, **55**, 1959 (1959).

(7) R. C. Pitkethly and A. G. Goble, Paper No. 91, Section II, Proceedings of the Second International Congress on Catalysis, Paris, France, 1960.

(8) J. H. Sinfelt and J. C. Rohrer, *J. Phys. Chem.*, **65**, 978 (1961).

THE BEHAVIOR OF OXANILIC ACID IN QUINOLINE AND IN 8-METHYLQUINOLINE

BY LOUIS WATTS CLARK

Department of Chemistry, Western Carolina College, Cullowhee, North Carolina

Received March 17, 1961

Kinetic data have been reported previously on the decarboxylation of oxanilic acid in aniline, *o*-toluidine and *o*-ethylaniline. These studies have indicated that oxanilic acid decomposes in polar solvents by essentially the same mechanism as does malonic acid, oxalic acid and oxamic acid.[1] According to the proposed mechanism the rate-determining step is the formation of a transition complex between solute and solvent.[2] A convenient method of testing this proposed mechanism is to carry out the reaction in quinoline and in 8-methylquinoline, since, in the case of a bimolecular reaction involving an electrophilic and a nucleophilic agent, electron releasing groups substituted near the nucleophilic center will increase the effective negative charge, causing a decrease in the activation energy,[3] while branching near either the nucleophilic or the electrophilic center, or both, will sterically hinder the approach of the attacking electrophilic agent to the attracting electrons, signalized by a lowering of the entropy of activation. Gratifying results using this pair of solvents have been obtained already in studies on the decarboxylation of oxalic acid,[4,5] malonic acid,[6] oxamic acid,[7] as well as trichloroacetic acid.[8]

The present paper describes results of kinetic studies carried out in this Laboratory on the decarboxylation of oxanilic acid in these two solvents.

Experimental

Reagents.—(1) The oxanilic acid used in this research was 100.0% pure, as revealed by the fact that in every decarboxylation experiment the theoretical volume of CO_2 was obtained. (2) The solvents were reagent grade. Each sample of each solvent was distilled at atmospheric pressure directly into the dried reaction flask immediately before the beginning of each decarboxylation experiment.

Apparatus and Technique.—The kinetic experiments were conducted in a constant-temperature oil-bath (± 0.01°) by measuring the volume of CO_2 evolved at constant pressure. Details are given in a previous paper.[9] Temperatures were determined by means of a thermometer calibrated by the U. S. Bureau of Standards. In each experiment a 0.2948-g. sample of oxanilic acid (the amount required to yield 40.0 ml. of CO_2 at STP on complete reaction) was introduced in the usual manner into the reaction flask containing a weighed sample of solvent (about 125 ml.) saturated with dry CO_2 gas. All atmospheric oxygen was flushed out of the apparatus with a stream of the dry CO_2, and the experiments were conducted in an atmosphere of CO_2 to prevent oxidation of the solvents during the kinetic experiments.

Results

The decarboxylation of oxanilic acid was studied at three different temperatures over approximately a 20° temperature interval. The experiment was performed three different times at each temperature with excellent reproducibility. The log $(V_\infty - V_t)$ *vs.* t was linear over practically the

(1) L. W. Clark, *J. Phys. Chem.*, **65**, 659 (1961).

(2) G. Fraenkel, R. L. Belford and P. E. Yankwich, *J. Am. Chem. Soc.*, **76**, 15 (1954).

(3) K. J. Laidler, "Chemical Kinetics," McGraw-Hill Book Co., Inc., New York, N. Y., 1950, p. 138.

(4) L. W. Clark, *J. Phys. Chem.*, **61**, 699 (1957).

(5) L. W. Clark, *ibid.*, **62**, 633 (1958).

(6) L. W. Clark, *ibid.*, **62**, 500 (1958).

(7) L. W. Clark, *ibid.*, **65**, 659 (1961).

(8) L. W. Clark, *ibid.*, **63**, 99 (1959).

(9) L. W. Clark, *ibid.*, **60**, 1150 (1956).

entire course of the reaction. No change in rate was observed on varying the volume of solvent from 50 to 125 ml.

The average rate constants, calculated in the usual manner from the slopes of the experimental logarithmic plots, are brought together in Table I. The parameters of the Eyring equation, based upon the data in Table I, are shown in Table II, along with corresponding data for oxalic acid, oxamic acid and malonic acid.

TABLE I

APPARENT FIRST-ORDER RATE CONSTANTS FOR THE DECARBOXYLATION OF OXANILIC ACID IN QUINOLINE AND IN 8-METHYLQUINOLINE

Solvent	Temp., °C. cor.	$k \times 10^4$, sec.$^{-1}$	Av. dev.
Quinoline	141.45	1.34	± 0.02
	152.00	4.41	.02
	160.86	11.41	.02
8-Methylquinoline	135.78	1.29	.01
	146.95	4.28	.02
	155.23	9.93	.02

TABLE II

KINETIC DATA FOR THE DECARBOXYLATION OF SEVERAL ORGANIC ACIDS IN QUINOLINE AND IN 8-METHYLQUINOLINE

	Quinoline		8-Methylquinoline	
Solvent	$\Delta H^{\ddagger}$, kcal./mole	$\Delta S^{\ddagger}$, e.u./mole	$\Delta H^{\ddagger}$, kcal./mole	$\Delta S^{\ddagger}$, e.u./mole
Oxalic acid[4,5]	38.9	+15.8	37.7	+13.7
Oxamic acid[7]	47.0	+37.5	36.8	+14.7
Oxanilic acid	38.6	+16.0	35.6	+10.0
Malonic acid[6]	26.7	− 2.4	24.4	−10.5

Discussion of Results

In the decarboxylation of oxanilic acid in quinoline and in 8-methylquinoline the positive inductive effect of the methyl group in the latter, as well as its steric effect, are demonstrated by the data in line 3 of Table II. The ΔH^* of the reaction decreases by 3 kcal./mole, and at the same time the ΔS^* of the reaction decreases by 6 e.u./mole, on going from quinoline to 8-methylquinoline. A similar trend is shown by the parameters for the other three acids listed in Table II.

The negative inductive effect of the phenyl group in oxanilic acid is revealed by comparing the data in lines 2 and 3 of Table II. In both quinoline and 8-methylquinoline the ΔH^* for the decomposition of oxanilic acid is lower than it is for that of oxamic acid. Since the phenyl group attracts electrons, the +E effect of the nitrogen atom is smaller in oxanilic acid than it is in oxamic acid. Therefore, the effective positive charge on the carbonyl carbon atom involved in coordination with the amine is neutralized to a smaller extent in the case of oxanilic acid—this carbon, therefore, has a higher effective positive charge than that in oxamic, the attraction between acid and solvent is increased, and the activation energy or enthalpy decreases.

It will be seen in Table II that the enthalpies of activation for the decomposition of both oxalic acid and oxanilic acid in quinoline are approximately equal. This suggests that the carbonyl carbon atoms of these two acids have approximately the same effective positive charges. The fact that, in quinoline, the entropy of activation of oxalic acid is approximately equal to that of oxanilic acid, in spite of the differences in the sizes of the two species, may be attributed to the greater tendency of the dicarboxylic acid, as opposed to that of the monocarboxylic acid, to associate through hydrogen bonding to form a "supermolecule" cluster.[10]

Further work on this problem is contemplated.

Acknowledgment.—The support of this research by the National Science Foundation, Washington, D. C., is gratefully acknowledged.

(10) W. Hückel, "Theoretical Principles of Organic Chemistry," Vol. II, Elsevier Pub. Co., New York, N. Y., 1958, p. 329 *et seq.*

PHASE EQUILIBRIA IN THE BINARY SYSTEMS $PuCl_3$–RbCl AND $PuCl_3$–CsCl[1]

BY R. BENZ AND R. M. DOUGLASS

University of California, Los Alamos Scientific Laboratory, Los Alamos New Mexico

Received March 24, 1961

Phase diagrams deduced from analysis of cooling curves have been reported for solid–liquid equilibria in the binary systems $PuCl_3$–LiCl,[2] $PuCl_3$–NaCl[2] and $PuCl_3$–KCl.[3] In this paper are presented results for the systems $PuCl_3$–RbCl and $PuCl_3$–CsCl.

Materials.—The $PuCl_3$ has been described.[3] Reagent-grade RbCl was purified by precipitation as $RbICl_2$ from an aqueous solution, recrystallization of the precipitate, thermal decomposition to RbCl, and recrystallization of the latter from aqueous solution as described by Archibald.[4] The product crystals were heated slowly to the melting point under an atmosphere of HCl (dried with $Mg(ClO_4)_2$), cast into stick form, and stored under vacuum. Analysis of this material gave, by weight, 70.6 ± 0.5% Rb (theoretical, 70.7%) and 29.4 ± 0.1% Cl (theoretical, 29.3%) with 0.04% Cs and less than 0.002% Li, 0.01% Na, 0.01% K and 0.02% I. Reagent-grade CsCl, purified by the same method, gave, on analysis, 78.9 ± 0.5% Cs (theoretical, 78.9%) and 21.3 ± 0.1% Cl (theoretical, 21.1%), with less than 0.002% Li, 0.01% Na, K or Rb, and 0.03% I. On examination under the polarizing microscope, all three starting materials were found to exhibit normal optical properties with no extraneous phases being detected.

Apparatus.—The apparatus and procedure have been described.[3] A calibrated Pt–Pt,10% Rh thermocouple was used to determine the thermal arrests and a chromel–alumel differential thermocouple was used to detect polymorphic transformations. Microscopic examinations of the products were carried out using a polarizing microscope mounted in a closed glove box which was continuously flushed by a stream of dry helium.

Results

The results of cooling-curve analyses for the system $PuCl_3$–RbCl, confirmed by microscopic examinations of the quenched products, are summarized in Fig. 1. The existence of three double salts is indicated.

(1) Work done under the auspices of the Atomic Energy Commission.

(2) C. W. Bjorklund, J. G. Reavis, J. A. Leary and K. A. Walsh, *J. Phys. Chem.*, **63**, 1774 (1959).

(3) R. Benz, M. Kahn and J. A. Leary, *ibid.*, **63**, 1983 (1959).

(4) E. H. Archibald, "The Preparation of Pure Inorganic Substances," John Wiley and Sons, Inc., New York, N. Y., 1932.

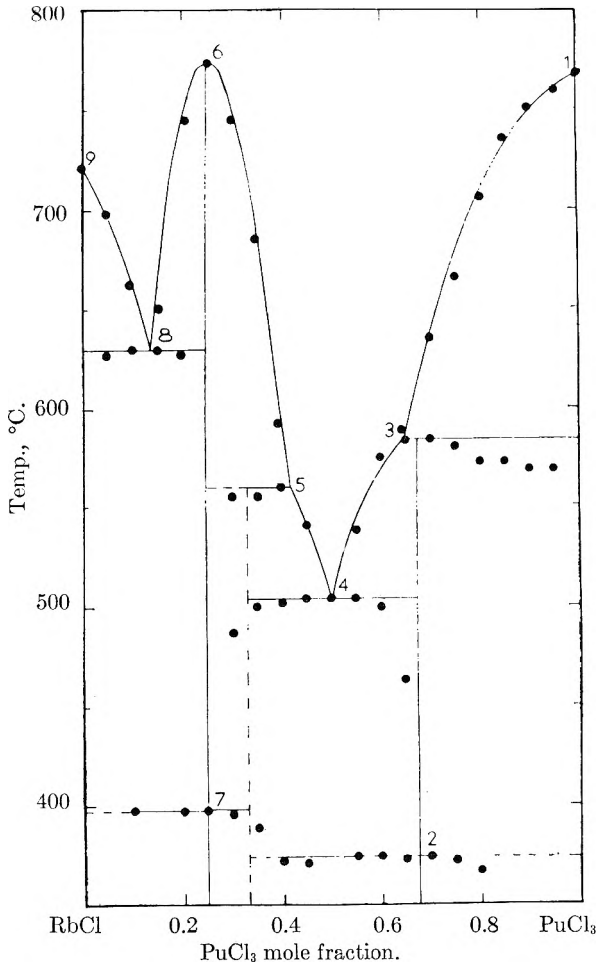

Fig. 1.—Phase diagram of the binary system $PuCl_3$–RbCl: (1) $PuCl_3$ melting point, 769 ± 2°; (2) $RbPu_2Cl_7$ polymorphic transformation, 374° (cooling); (3) peritectic point for the compound $RbPu_2Cl_7$, 584° at $PuCl_3$ mole fraction 0.64; (4) eutectic point, 504° at $PuCl_3$ mole fraction 0.50; (5) peritectic point for the compound Rb_2PuCl_5, 560° at $PuCl_3$ mole fraction 0.42; (6) Rb_3PuCl_6 melting point, 774 ± 3°; (7) Rb_3PuCl_6 polymorphic transformation, 398° (cooling); (8) eutectic point, 630° at $PuCl_3$ mole fraction 0.14; (9) RbCl melting point, 721 ± 2°.

$RbPu_2Cl_7$.—This compound melts incongruently at 584° with the peritectic composition 0.64 $PuCl_3$ and, on cooling, undergoes polymorphic transformation at 374°. Crystals of the room-temperature modification are long prismatic, transparent, and light blue to greenish blue by transmitted light. They are optically biaxial positive with moderate birefringence, parallel and inclined extinction, positive elongation, absorption $Z > X$, with moderate optic axial angle, and strong dispersion of the optic axes, $2V_Z$ $(r) > 2V_Z$ (v). The mean refractive index is around 1.8, in agreement with the value 1.80 calculated from Lorentz–Lorenz molar refractivity of the end-member chlorides with linearly additive molar volumes.

Rb_2PuCl_5.—This compound melts incongruently at 560° with the peritectic composition 0.42 $PuCl_3$. The composition is chosen as being the simplest consistent with the data. Crystals are transparent, brownish or greenish yellow to nearly colorless by transmitted light, and optically anisotropic with low birefringence. The mean refractive index is between 1.6 and 1.7, in agreement with the value 1.66 calculated as above.

Rb_3PuCl_6.—This compound melts congruently at 774 ± 3° and, on cooling, undergoes polymorphic transformation at 398°. The mean refractive index calculated as above is 1.62.

The results of cooling-curve analyses for the system $PuCl_3$–CsCl, confirmed by microscopic examinations of the quenched products, are summarized in Fig. 2. The existence of two double salts is indicated.

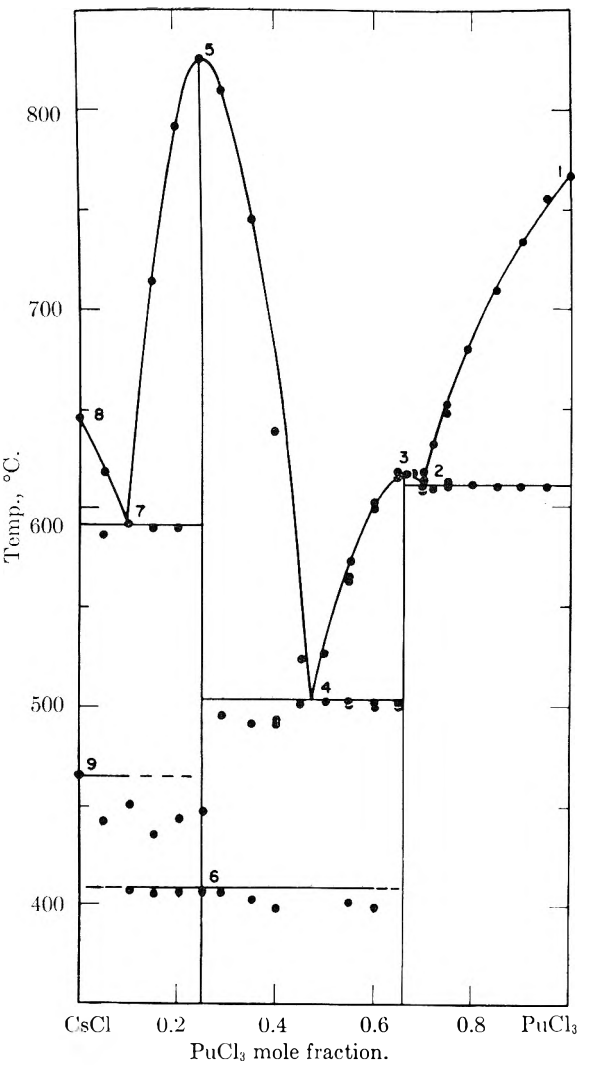

Fig. 2.—Phase diagram of the binary system $PuCl_3$–CsCl: (1) $PuCl_3$ melting point, 769 ± 2°; (2) eutectic point, 611° at $PuCl_3$ mole fraction 0.70; (3) $CsPu_2Cl_7$ melting point, 616 ± 3°; (4) eutectic point, 504° at $PuCl_3$ mole fraction 0.47; (5) Cs_3PuCl_6 melting point, 825 ± 3°; (6) Cs_3PuCl_6 polymorphic transformation, 410° (cooling); (7) eutectic point, 592° at $PuCl_3$ mole fraction 0.10; (8) CsCl melting point, 645 ± 2°; (9) CsCl polymorphic transformation, 465° (cooling).

$CsPu_2Cl_7$.—This compound melts congruently at 616 ± 3°. Crystals of this phase are transparent, pale blue in thinnest sections through greenish blue to deep green in thicker sections and not noticeably pleochroic. They are optically biaxial negative with large optic axial angle and moderate birefringence. Acicular crystals exhibit positive elongation and parallel extinction suggest-

ing orthorhombic symmetry. The mean refractive index is 1.85 ± 0.03, in agreement with the value 1.85 calculated as above. The differences in the optical properties suggest that this compound may not be isomorphic with the isoformular rubidium compound.

Cs_3PuCl_6.—This compound melts congruently at 825 ± 3° and, on cooling, undergoes polymorphic transformation at 410°. Crystals of the room-temperature modification are green in bulk by reflected light but, immersed in liquid of similar refractive index, are transparent and virtually colorless by transmitted light. They are optically anisotropic and exhibit very fine, complex, polysynthetic twinning. The mean refractive index is around 1.7, in agreement with the value 1.73 calculated as above.

Discussion

It is interesting to note the similarity between $PuCl_3$ and UCl_3[5,6] in the formation of double salts with alkali chlorides. No compounds occur in the binary systems involving LiCl or NaCl. There exist MPu_2Cl_7-type compounds, where M = Rb or Cs, M_2PuCl_5-type compounds where M = K or Rb, and M_3PuCl_6-type compounds where M = K, Rb or Cs.

Acknowledgments.—We are indebted to A. W. Morgan and J. W. Anderson for the plutonium metal, and to C. F. Metz, W. H. Ashley, G. R. Waterbury, R. T. Phelps, C. T. Apel, M. H. Corker, D. C. Croley, J. A. Mariner, O. R. Simi, C. H. Ward, W. W. Wilson and A. Zerwekh for the chemical and spectrochemical analyses.

(5) C. J. Barton, R. J. Sheil, A. B. Wilkerson and W. R. Grimes, ORNL-2548 or E. M. Levin and H. F. McMurdie, "Phase Diagrams for Ceramists," Part II, Am. Ceram. Soc., 1959.

(6) J. J. Katz and E. Rabinowitch, "The Chemistry of Uranium," Part I, NNES Div. VIII, Vol. 5, McGraw-Hill, New York, N.Y., 1951, p. 460.

METAL COMPLEXING BY PHOSPHORUS COMPOUNDS. V. TEMPERATURE DEPENDENCE OF ACIDITY AND MAGNESIUM COMPLEXING CONSTANTS

BY RIYAD R. IRANI

Research Department, Inorganic Chemicals Division, Monsanto Chemical Company, St. Louis 66, Missouri

Received April 3, 1961

The acidity constants[1-3] of polyphosphoric and imidophosphoric acids have been reported at 25°. However, the evaluation of the temperature dependence of metal complexing at *p*H values where two hydrogen forms of a ligand coexist[4] requires the availability of acid dissociation constants in the same temperature range.

In the present study the acidity constants of polyphosphoric and imidophosphoric acids are presented at several temperatures and ionic strengths. Magnesium complexing by pyrophosphate and tripolyphosphate, previously reported[5] at 25°, is evaluated at 65°.

Experimental

Materials.—Tetramethylammonium polyphosphates and imidophosphates in 99.9+ and 97+% purity, respectively, were prepared as previously described.[4,6] The water used for solution make-up was distilled and freshly boiled to remove dissolved CO_2. Other chemicals were C.P. grade.

Procedures.—The acidity constant determination at a constant temperature and ionic strength was carried out as previously described.[3] A Leeds and Northrop pH meter with glass and calomel electrodes was utilized, and was calibrated at each temperature with buffer solutions having a *p*H of 4, 7 and 10. Calibration of the *p*H meter with one buffer solution gave readings with the other two buffers that agreed to within ±0.01 *p*H unit, indicating linearity of the *p*H scale. Temperature was controlled to ±0.1° using a heater in combination with a heat-sensing Thermotrol unit, manufactured by Hallikainen Instruments, Berkeley, California. In the experiments below room temperature, the solutions were placed in an ice–acetone bath, with the heater supplying enough heat to maintain the desired temperature. During titration the solutions were maintained under a nitrogen atmosphere.

The magnesium complexing by pyrophosphate and tripolyphosphate was measured by the same procedure described by Lambert and Watters,[5] except that the measurements were made at 25 and 65°. The *p*H measurements in the presence of excess magnesium were made within a few minutes to avoid precipitation of magnesium phosphates.

Results and Discussion

Acidity Constants.—Stepwise titration curves with definite breaks for the weakest two hydrogens were obtained with all of the investigated acids. The other hydrogens were so strong that no inflection points were observed. The acid–base titration data, obtained at a constant temperature and total ionic strength, were fit to a least-squares program of an IBM 704 computer, as previously described.[3] The resultant acid dissociation constants with the statistical 95% confidence limits are listed in Table I.

No attempt was made to extrapolate the acid dissociation constants to infinite dilution since they were only determined at fewer than four ionic strengths. For the polyphosphoric acids $(HO)_2OP\left[\begin{matrix}O\\OP\\OH\end{matrix}\right]_nO\text{–}PO(OH)_2$ with n varying from 0–60, no significant temperature dependence of the dissociation of the weakest two hydrogens was observed, with the apparent molal ΔH for dissociation being between −1 and 0 kcal. The apparent ΔH for the dissociation of the stronger hydrogens lies between −2 and 0 kcal. As was previously[3] found at 25°, the ratio of the dissociation constants of the two weakest hydrogens approaches the value of four[7] as the chain length of the phosphate chain approaches infinity.

The acid dissociation constants of imidodiphosphoric and diimidotriphosphoric acids show significant temperature dependence, as was observed with their calcium complexes. Thus, the apparent molal ΔH for the dissociation of the weakest hydrogen (K_1) at an ionic strength of 0.1 is −6.4 and −4.5 kcal. for imidodiphosphoric and diimidotriphosphoric acids, respectively, where

(1) J. I. Watters, E. D. Loughran and S. M. Lambert, *J. Am. Chem. Soc.*, **78**, 4855 (1956).

(2) S. M. Lambert and J. I. Watters, *ibid.*, **79**, 4262 (1957).

(3) R. R. Irani and C. F. Callis, *J. Phys. Chem.*, **65**, 934 (1961).

(4) R. R. Irani and C. F. Callis, *ibid.*, **64**, 1398 (1960).

(5) S. M. Lambert and J. I. Watters, *J. Am. Chem. Soc.*, **79**, 5606 (1957).

(6) R. R. Irani and C. F. Callis, *J. Phys. Chem.*, **65**, 296 (1961).

(7) S. W. Benson, *J. Am. Chem. Soc.*, **80**, 5151 (1958).

TABLE I

APPARENT ACID DISSOCIATION CONSTANTS OF PHOSPHORUS CONTAINING ACIDS

$(HO)_2OP\left[\begin{matrix}O\\XP\\OH\end{matrix}\right]_nXPO(OH)_2$ AS A FUNCTION OF TEMPERATURE

n	Temp., °C.	Ionic strength	pK_1	pK_2	pK_3	pK_4[a]
FOR X = OXYGEN						
0	0	0.1	9.08 ± 0.16	6.17 ± 0.15	2.5 ± 0.1	2.3
	10	.1	8.97 ± .13	6.03 ± .18	2.3 ± .1	2.2
	25	.1	8.95 ± .10	6.12 ± .10	2.0 ± .1	2
		1.0	8.74 ± .07	5.98 ± .07	1.95 ± .04	1.7
	37	0.1	8.94 ± .08	6.13 ± .07	1.95 ± .05	1.91
		.2	8.93 ± .09	6.12 ± .08	1.97 ± .06	1.7
		.3	8.88 ± .09	6.08 ± .09	1.91 ± .06	1.7
	50	.1	8.97 ± .08	6.13 ± .07	1.98 ± .06	1.9
		.2	8.90 ± .08	6.06 ± .07	1.92 ± .08	1.3
		.3	8.88 ± .09	6.04 ± .08	2.12 ± .07	1.2
	65	.1	8.92 ± .09	6.16 ± .08	2.12 ± .07	1.3
		1.0	8.72 ± .07	6.01 ± .08	2.17 ± .05	1.2
1[b]	0	0.1	8.51 ± .12	5.7 ± .1	2.3 ± .1	2.2
	10	.1	8.70 ± .07	5.84 ± .05	2.31 ± .04	2.2
	25	.1	8.65 ± .05	5.75 ± .14	2.13 ± .10	2
		1.0	8.56 ± .10	5.69 ± .11	2.04 ± .09	1.2
	37	0.1	8.50 ± .08	5.77 ± .07	1.89 ± .06	1.7
		.2	8.51 ± .08	5.77 ± .07	1.95 ± .06	1.7
		.3	8.52 ± .08	5.78 ± .07	1.98 ± .06	1.7
	50	.1	8.55 ± .08	5.90 ± .07	2.12 ± .07	1.7
		.2	8.48 ± .08	5.80 ± .08	1.95 ± .06	1.7
		.3	8.48 ± .08	5.84 ± .07	2.62 ± .05	1.7
	65	0.1	8.48 ± .06	5.88 ± .07	2.15 ± .05	1.7
		1.0	8.39 ± .06	5.80 ± .05	2.10 ± .08	1.7
4	25	1.0	8.13 ± .14	5.98 ± .18	2.19 ± .10	2.1
	37	1.0	8.02 ± .2	5.83 ± .15	2.22 ± .07	1.3
	50	1.0	8.00 ± .15	5.81 ± .20	2.22 ± .12	1.3
14	25	1.0	8.08 ± .10	6.48 ± .07	2.92 ± .09	2
	37	1.0	8.02 ± .13	6.48 ± .08	2.64 ± .05	2
	50	1.0	8.15 ± .10	6.50 ± .08	2.52 ± .13	2
58	25	1.0	8.17 ± .04	7.22 ± .04	.....	..
	37	1.0	8.03 ± .08	7.28 ± .08	.....	..
	50	1.0	8.03 ± .08	7.28 ± .08	.....	..
FOR X = NH						
0	25	0.1	10.22 ± 0.09	7.32 ± 0.12	2.66 ± 0.09	1.5
		.3	9.77 ± .12	7.05 ± .12	2.81 ± .06	2
	37	.1	9.79 ± .03	7.16 ± .04	2.60 ± .08	1.8
		.3	9.52 ± .05	6.99 ± .05	2.68 ± .07	1.8
	50	.1	9.41 ± .06	6.90 ± .06	2.81 ± .07	1.8
		.3	9.32 ± .03	6.88 ± .06	2.83 ± .07	1.8
1[b]	25	.1	9.84 ± .08	6.61 ± .09	3.03 ± .10	2
	37	.1	9.50 ± .08	6.80 ± .08	3.24 ± .08	2.2
	50	.1	9.28 ± .08	7.02 ± .08	3.59 ± .09	2.4

[a] Estimated, large errors may exist. [b] pK_3 is estimated to be 1 ± 0.5 at the various temperatures.

$$\Delta H_n = RT^2 \frac{\mathrm{d} \ln K_n}{\mathrm{d}T} \qquad (1)$$

$$K_n = \frac{(\mathrm{H}^+)(\mathrm{H}_{n-1}\mathrm{L}^{-(x-n+1)})}{(\mathrm{H}_n\mathrm{L}^{-(x-n)})} \qquad (2)$$

and parentheses indicate concentration. The difference between ΔH_n and the thermodynamic value, $\Delta H'_n$, is

$$\Delta H'_n - \Delta H_n = RT^2 \frac{\mathrm{d} \ln f}{\mathrm{d}t} \qquad (3)$$

where f is the activity coefficient ratio of the species in equation 2. For the dissociation of the second weakest hydrogens (K_2), the values of ΔH at an ionic strength of 0.1 are −3.2 and +3.2 kcal. for imidodiphosphoric and diimidotriphosphoric acids respectively.

Magnesium Complexing.—The nephelometric titrations, previously utilized[4] in evaluating calcium complexing constants were not found as suitable for magnesium complexing because of the absence of a well defined magnesium precipitate. Therefore, the *p*H-lowering technique was used. The acid–base titrations in the presence of magnesium still showed stepwise complex formation.

In Table II the *p*H values are given after adding 1/2 and 3/2 equivalents of hydrogen ion per mole of ligand in the presence of magnesium. Utilizing the appropriate acidity constants, the formation constants for the following equilibria, previously proposed by Lambert and Watters,[5] were evaluated at 25 and 65°, using the techniques previously described.

TABLE II

COMPLEXING OF MAGNESIUM BY PYROPHOSPHATE AND TRIPOLYPHOSPHATE ANIONS

"*a*" is the number of equivalents of H^+ per mole of ligand, and *L* is the polyphosphate ligand. Total ionic strength was adjusted to 1.0 with tetramethylammonium bromide.

Ligand	Temp., °C.	"*a*"	*p*H	Neg. log of formation constant of MgL	Mg_2L	MgHL
Pyrophosphate,[a]	25	0.5	6.30	5.42	2.33	..
		1.5	5.11	..	..	3.05
	65	1.5	5.00	..	..	4.13
Tripolyphosphate[b]	25	0.5	6.10	5.81	2.13	..
		1.5	4.52	..	..	3.36
	65	0.5	5.97	5.76	2.12	..
		1.5	4.60	..	..	3.40

[a] Total magnesium concentration = 9.930×10^{-3} *M*. Total pyrophosphate concentration = 2.955×10^{-3} *M*. [b] Total magnesium concentration = 9.980×10^{-3} *M*. Total tripolyphosphate concentration = 2.553×10^{-3} *M*.

$$Mg + L \rightleftharpoons MgL \quad (4)$$

$$2Mg + L \rightleftharpoons Mg_2L \quad (5)$$

$$Mg + HL \rightleftharpoons MgHL \quad (6)$$

where L is the polyphosphate anion. At 65° and *p*H values over 7 a precipitate formed rapidly in solutions containing pyrophosphate and an excess of magnesium, so that no values for $MgP_2O_7^{2-}$, and $Mg_2P_2O_7$ are reported at that temperature.

The results at 25° agree very well with those previously reported. The formation constants for the magnesium complexes at 65° are very close to those at 25°, and the ΔH for complex formation is 0 ± 1 kcal. Previous extensive work[3] with calcium complexing by pyrophosphate and tripolyphosphate showed the ΔH values to be less than 4 kcal. and attributed complex formation to positive entropy changes. Obviously, in magnesium complexing by polyphosphates the same interpretation applies.

These results suggest that a relationship may exist between the heats of dissociation of a hydrogen and a metal ion from a ligand. This is not surprising since the two processes are somewhat similar.

Acknowledgment.—The author thanks Mr. William W. Morgenthaler for making some of the measurements.

POLARIZABILITIES AND MOLAR VOLUMES OF A NUMBER OF SALTS IN SEVERAL SOLVENTS AT 25°[1]

BY W. R. GILKERSON AND J. L. STEWART[2]

Department of Chemistry, University of South Carolina, Columbia, South Carolina

Received April 7, 1961

Recent interest[3-5] in obtaining dipole moments of ion pairs from dielectric measurements has led to a need for polarizability and molar volume data for substituted ammonium salts in particular. We report here the results of refractive index and density measurements for the systems tetra-*n*-butylammonium picrate (Bu_4NPi) in nitrobenzene and in chlorobenzene, tetra-*n*-butylammonium iodide (Bu_4NI) in *o*-dichlorobenzene and in water, and sodium tetraphenylboride, tetra-*n*-propylammonium iodide (Pr_4NI), tetraethylammonium bromide and tetramethylammonium chloride in water.

Experimental

Salts.—These were from current laboratory stock and, with the exception of sodium tetraphenylboride and tetra-*n*-propylammonium iodide, were considered of sufficient purity to use without further treatment. The sodium tetraphenylboride was recrystallized from water, and the tetra-*n*-propylammonium iodide was recrystallized from ethanol.

Solvents.—The solvents were purified by recrystallization (nitrobenzene), distillation (water), and in the case of chlorobenzene and *o*-dichlorobenzene, passed through an alumina column and then distilled.

Apparatus.—Densities were determined with a reproducibility of 0.02% using a Lipkin pycnometer, the volume of the stems having been calibrated with mercury at 25°, and the volume of the bulb with water at 25°. Solutions were equilibrated in an oil thermostat set at 25.0°. Refractive indices were obtained with a reproducibility of 0.01% using a Bausch and Lomb Abbe-3L refractometer. The light source was an ordinary 40 watt incandescent lamp. The refractometer was connected to a circulating 25° water thermostat.

Results

The solution densities were plotted *vs.* molar concentration of solute. All of the plots were linear within the concentration range used (0.005 to 0.05 *M*). From the relation

$$d = d_0 + (M_2 - d_0\bar{V}_0^2)C/1000 \quad (1)$$

where d is the solution density, d_0 that of pure solvent, M_0 the formula weight for the solute, $\bar{V}_0^2$ the partial molar volume of solute at infinite dilution, and C the molar concentration of solute, the values of $\bar{V}_0^2$ shown in Table I were obtained using the slopes of the *d versus C* plots.

The specific refractions, R, of the salt solutions were determined from the relation

$$R = \frac{\eta_{12}^2 - 1}{\eta_{12}^2 + 2} - \frac{\eta_1^2 - 1}{\eta_1^2 + 2} \times \frac{C_1}{C_1^0}$$

where η_{12} is the refractive index of solution, η_1 that of pure solvent, C_1 the molar concentration of solvent; and C_1^0 is the molar concentration of pure solvent. Plots of specific refraction *vs.* salt concentration were linear in all cases. From the slopes of these plots, the solute polarizabilities, α_2, were calculated from the relation

$$\alpha_2 = 3000 \times \text{slope}/4\pi N$$

These results are listed in Table I.

Discussion

A comparison of the molar volumes of Bu_4NPi and Bu_4NI in the two solvents used for each is interesting. In nitrobenzene, the picrate has an

(1) This work has been supported in part by contract with the Office of Ordnance Research, U. S. Army.

(2) N. S. F. Summer Research Participant, 1960.

(3) E. A. Richardson and K. H. Stern, *J. Am. Chem. Soc.*, **82**, 1296 (1960).

(4) M. Davies and G. Williams, *Trans. Faraday Soc.*, **56**, 1619 (1960).

(5) W. R. Gilkerson and K. K. Srivastava, *J. Phys. Chem.*, **65**, 272 (1961).

TABLE I

MOLAR VOLUMES AND POLARIZABILITIES AT 25°

Salt	Solvent	$\overline{V_0}$, cc.	$10^{24}\alpha_2$, cc.	$10^{24}\alpha_+$, cc.
Bu_4NPi	Nitrobenzene	407	56.7	
Bu_4NPi	Chlorobenzene	402	55.6	
Bu_4NI	*o*-Dichlorobenzene	302	39.6	
Bu_4NI	Water	316	38.6	31.2
$Na(C_6H_5)_4B$	Water	277	44.7	0.2
Pr_4NI	Water	251	30.5	23.1
Et_4NBr	Water	175	21.2	16.4
Me_4NCl	Water	107	11.9	8.4

ion pair dissociation constant[6] equal to 0.14 on the *c* scale. At 10^{-2} *M*, the salt would be almost completely dissociated into free ions. In chlorobenzene,[7] the dissociation constant is of the order 10^{-8}, so that the salt would be almost completely associated in this solvent. As can be seen in Table I, there is an expansion of 5 cc. going from the ion pair in chlorobenzene to the free ions in nitrobenzene. Similarly, in water, Bu_4NI should be completely dissociated, while in *o*-dichlorobenzene, it is almost completely associated. The expansion in this case is 14 cc.

Using tabulated values of the refractivities of the halides,[8] a table of ion refractions or polarizabilities can be set up, as seen in Table I, column five. The observed polarizability for Bu_4NPi compares favorably with that estimated from bond refractions (ref. 5), 51 × 10^{-24} cc. The small difference in calculated and observed values will not require any modification of the charge–charge distance calculated from dipole moments.[5]

(6) E. Hirsch and R. M. Fuoss, *J. Am. Chem. Soc.*, **82**, 1018 (1960).
(7) P. H. Flaherty and K. H. Stern, *ibid.*, **80**, 1034 (1958).
(8) C. P. Smyth, "Dielectric Behavior and Structure," McGraw-Hill Book Co., New York, N. Y., 1955, p. 407.

THE CONDUCTANCE OF TETRA-*n*-BUTYLAMMONIUM PICRATE IN 50 MOLE % BENZENE–*o*-DICHLOROBENZENE AND BROMOBENZENE AS A FUNCTION OF TEMPERATURE

BY W. R. GILKERSON AND R. E. STAMM

Department of Chemistry, University of South Carolina, Columbia, South Carolina

Received April 7, 1961

It had been hoped[1,2] that a study of the temperature dependence of ion pair dissociation constants would reveal information both about ion–solvent interaction in terms of E_s and the distance of closest approach, *a*. These two factors enter into the dissociation constant *K* for the equilibrium

$$AB \rightleftarrows A^+ + B^-$$

as shown in eq. 1.[3]

$$K = \frac{1000d}{M}(\nu_+\nu_-/\nu_+'\nu_-')\exp(-E_s'/RT)\exp(-e^2/\epsilon\, a\, kT) \quad (1)$$

In order to obtain a good value for *K* from conductance data, one needs to evaluate Λ_0, the limiting equivalent conductance for the salt. This has only been possible for salts having dissociation constants in the range of 10^{-6} or greater. For most salts, this means that one is restricted to solvents of dielectric 8 or more. The temperature coefficient of *K* in such solvents is not very large.[2,4–6] This results in some uncertainty in fitting eq. 1 to the data. For most liquids having dielectric constants in the range 5–6, the ϵT product is almost independent of temperature. Further, it has been shown recently (ref. 3) that Λ_0 can be obtained for salts such as tetra-*n*-butylammonium picrate in 50 mole % *o*-dichlorobenzene–benzene as solvent (ϵ = 6.041 at 25°). We thought that a study of the temperature dependency of *K* in solvents in this range of dielectric would yield the best values of E_s one could hope for, since the dielectric dependent factor in eq. 1 would remain practically constant. Consequently, we report here the electrical conductance of tetra-*n*-butylammonium picrate (Bu_4NPi) in 50 mole % benzene–*o*-dichlorobenzene (DCB) at 44.26 and 64.74° and in bromobenzene at 25, 35, 44.58, 55 and 65°.

Experimental

Benzene and *o*-dichlorobenzene were prepared as before.[3] Bromobenzene was fractionated on a three-foot packed column, b.p. 156°. Before use, the solvent was passed through a 35 × 2 cm. column packed with Alcoa activated alumina, grade F-20. Analysis by vapor phase chromatography showed less than 0.1% impurity present. Based on retention times, this was apparently chlorobenzene. The solvent conductivity was 1.8×10^{-10} mho/cm. at 25°. The salt was prepared as previously.[3]

The density, viscosity and dielectric constants were obtained in the same manner as previously and the results appear in Table I.

The conductance measurements were carried out with equipment already described.[3] All solutions were made up by weight.

TABLE I

PHYSICAL PROPERTIES OF SOLVENTS

Solvent	Temp., °C.	Density, g./ml.	Viscosity, centipoise	Dielectric constant
50 Mole % benzene–DCB	25	1.1110	0.839	6.04
50 Mole % benzene–DCB	44.26	1.0913	.665	5.68
50 Mole % benzene–DCB	64.74	1.074	.559	5.34
Bromobenzene	25	1.4885	1.068	5.37
Bromobenzene	35	1.4750	0.940	5.24
Bromobenzene	44.58	1.4619	.834	5.12
Bromobenzene	55	1.4477	.740	4.99
Bromobenzene	65	1.4341	.668	4.87

Results

The equivalent conductances as a function of concentration *C*, moles/l., are given in Table II. In order to evaluate Λ_0, in these solvents, measurements must be made in the concentration range 10^{-6} *M*. At 25 and 35°, such measurements are possible, with reasonable precision. At 45 and 65°, however, the conductance changes with time so that the results become unreliable. This may be due to solvent or salt decomposition. For the

(1) W. R. Gilkerson, *J. Chem. Phys.*, **25**, 1199 (1956).
(2) H. L. Curry and W. R. Gilkerson, *J. Am. Chem. Soc.*, **79**, 4021 (1957).
(3) W. R. Gilkerson and R. E. Stamm, *ibid.*, **82**, 5295 (1960).
(4) K. H. Stern and A. E. Martell, *ibid.*, **77**, 1983 (1955).
(5) J. T. Denison and J. B. Ramsey, *ibid.*, **77**, 2615 (1955).
(6) P. H. Flaherty and K. H. Stern, *ibid.*, **80**, 1034 (1958).

TABLE II

CONDUCTANCE OF Bu_4NPi

50% Benzene–DCB

44.26°		64.74°	
10^4c	Λ	10^4c	Λ
19.86	0.6420	19.54	0.8245
9.808	0.8218	9.949	1.050
4.882	1.099	5.046	1.386
0.9980	2.231	1.014	2.766
0.4952	3.114	0.5089	3.751

Bromobenzene

25°		35°	
10^4c	Λ	10^4c	Λ
9.940	0.1847	7.580	1.982
4.894	.2415	6.145	2.187
2.483	.3230	5.103	2.384
0.9987	.4899	3.972	2.677
0.5001	.6737	2.945	3.074
		2.278	3.200
		1.248	4.511
		0.4634	6.754

25°		44.58°		65°	
10^6c	Λ	10^4c	Λ	10^4c	Λ
8.420	1.520	9.762	0.2704	9.576	0.3823
7.073	1.647	4.807	.3549	4.715	.5041
6.061	1.765	2.439	.4756	2.392	.6760
5.187	1.897	0.9810	.7201	0.9621	1.026
4.349	2.057	.4913	.9927	.4818	1.414
3.025	2.417				
2.014	2.881				
1.321	3.449				
0.5534	4.902				

50 mole % benzene–DCB solvent, we can only observe values of $\Lambda_0{}^2K$, the reciprocal slope of a Shedlovsky plot,[7] since measurements were confined to 44 and 65°. In bromobenzene, low concentration data were obtained at 25 and 35° and values of Λ_0, as well as K, appear in Table III for these two temperatures.

TABLE III

DERIVED CONSTANTS FOR Bu_4NPi

Solvent	Temp., °C.	$10^4\Lambda_0{}^2K$	Λ_0	10^7K
50 mole % benzene–DCB	25[3]		30	2.74
	44.26	4.85		
	64.74	8.20		
Bromobenzene	25		13	1.53
	35		18	1.01
	44.58	0.443		
	65	0.902		

Discussion

In bromobenzene, the Λ_0 values at the lower temperatures are increasing faster with temperature than one would expect if the Walden product, $\Lambda_0\eta_0$, were a constant. Further, the value at 25° is much lower than is observed in high dielectric solvents.[3] This result is another indication that $\Lambda_0\eta_0$ decreases with decreasing solvent dielectric constant.[8] The uncertainty in Λ_0 is of the order of ± 1 equivalent conductance unit. We are thus left with an uncertainty of 14% in the value of K at 25°. This is the most unfavorable case. Since there is only a 40% change in K between 25 and 35°, there is little justification in discussing the significance of this value. It is probably best concluded that a study of the temperature coefficient of an ion pair dissociation constant will not allow much to be said concerning the values of the molecular parameters that determine the coefficient.

(7) T. Shedlovsky, *J. Franklin Inst.*, **225**, 739 (1938).

(8) R. M. Fuoss, *Proc. Natl. Acad. Sci.*, **45**, 807 (1959).

THE SYSTEMS TANTALUM PENTACHLORIDE–FERRIC CHLORIDE AND NIOBIUM PENTACHLORIDE–FERRIC CHLORIDE

BY CHARLES M. COOK, JR., AND ROBERT B. HAND

E. I. du Pont de Nemours & Company, Pigments Department, Wilmington, Delaware

Received May 3, 1961

During a study of the properties of ferric chloride the solid–liquid equilibria of the system $TaCl_5$–Fe_2Cl_6 and $NbCl_5$–Fe_2Cl_6 were reinvestigated.

Experimental

Ferric chloride (Fisher Scientific Company–purified–sublimed) was purified by slow resublimation in a stream of oxygen-free chlorine. $TaCl_5$ was prepared by reaction of Ta metal with oxygen-free chlorine. $NbCl_5$ was prepared by chlorination of Nb_2O_5 followed by passing the product with Cl_2 over carbon at 600° to remove $NbOCl_3$. Chlorides were stored and manipulated under inert atmospheres.

Mixtures of $FeCl_3$ and $TaCl_5$ or $NbCl_5$, sealed, under *ca.* 0.1 atm. Cl_2, in a cylindrical Pyrex vessel of 25 mm. D × 80 mm. L, were melted within an insulated cavity enclosed by an externally heated steel jacket. During cooling a constant temperature difference was maintained between jacket and sample, the jacket power being regulated by a differential thermocouple input to a variable reluctance furnace controller. Sample temperatures, measured by a Pt–10% Rh thermocouple in a Silicone oil-filled thermowell extending into the sample, were plotted as cooling curves on a Leeds & Northrup recorder. At intervals this recorder was standardized by observing the indicated signal when a known voltage, from a Leeds & Northrup type-K bridge, was impressed upon it. Agitation was provided by a Burrell wrist-action shaker to which sample and jacket were attached.

Results

The $TaCl_5$–Fe_2Cl_6 system, presented in Fig. 1,

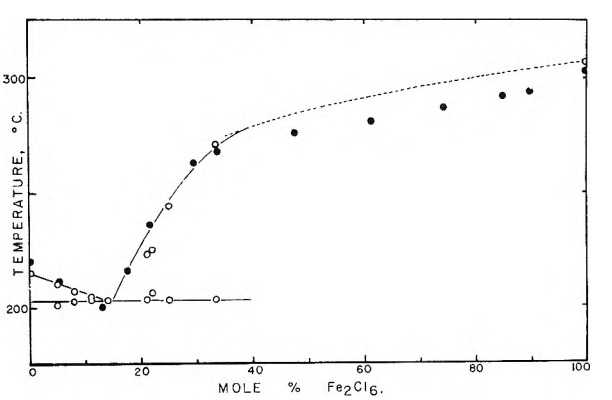

Fig. 1.—The system $TaCl_5$–Fe_2Cl_6: ○, this work; ●, Morozov.

shows a single eutectic at 14.5 mole % Fe_2Cl_6 and 203° in good agreement with Morozov,[1] who located the eutectic at 13.9 mole % Fe_2Cl_6 and 200°. Freezing points of 215 and 307° were observed for

(1) I. S. Morozov, *Zhur. Neorg. Khim.*, **1**, 2792 (1956).

$TaCl_5$[2] and for $FeCl_3$, respectively. Schäfer and Bayer[3] record the melting point of $FeCl_3$ as 307.5° and point out that the apparent melting point of $FeCl_3$ when measured in a Cl_2-deficient atmosphere becomes depressed by contamination with $FeCl_2$. Their data indicate that 7 mole % $FeCl_2$ in $FeCl_3$ lowers the apparent melting point to 303°, the $FeCl_3$ m.p. reported by Morozov. $FeCl_2$ if present should depress the observed ferric chloride liquidus temperatures, and Morozov's values consistently lie below the liquidus calculated using $d \ln X_{Fe_2Cl_6}/dT^{-1} = -\Delta H_f/R$ with $\Delta H_f = 20.6$ kcal./mole and represented by the dotted curves in the figures.

The $NbCl_5$–Fe_2Cl_6 system, presented in Fig. 2, shows a eutectic at 9.5 mole % Fe_2Cl_6 and 191°. The $NbCl_5$ has m.p. 205°.[2] During cooling of compositions containing $X_{Fe_2Cl_6} > 0.1$ a weak evolution of heat, which occurred reproducibly and which was independent of rate of cooling, was observed at 193° before crystallization of the eutectic at 191°.

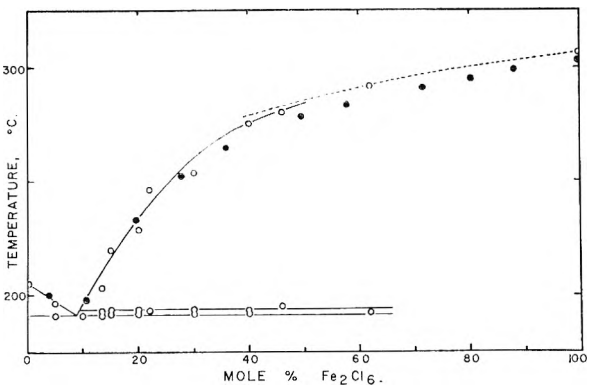

Fig. 2.—The system $NbCl_5$–Fe_2Cl_6: O, this work; ●, Morozov.

(2) H. Schäfer and C. Pietruck, *Z. anorg. Chem.*, **261**, 174 (1951), report $TaCl_5$ m.p. 216.5°; $NbCl_5$ m.p. 204.7°. J. B. Ainscough, R. Holt and F. Trowse, *J. Chem. Soc.*, 1034 (1957), report $TaCl_5$ m.p. 215.9°, $NbCl_5$ m.p. 203.4°.

(3) H. Schäfer and L. Bayer, *Z. anorg. Chem.*, **271**, 338 (1953).

COMMUNICATIONS TO THE EDITOR

DETECTION OF STRUCTURAL DIFFERENCES IN POLYMERS IN A DENSITY GRADIENT ESTABLISHED BY ULTRACENTRIFUGATION

Sir:

We have developed a method of separating polymers based on differences in partial specific volume. We have applied the method to separating highly branched material from a previously described copolymer[1] and to the separation of atactic polystyrene from stereoregular polystyrene.

It is seen easily that in the vicinity of a branch point of a polymer molecule, the "density" of the molecule will be slightly greater than in the linear portion of the molecule. Likewise, if the polymer consists of stereo regular sequences the volume that the molecule occupies in solution will vary with the amount of stereoregularity.

We have adapted the density gradient method first introduced by Meselson, Stahl and Vinograd[2] to synthetic polymers in the analytical ultracentrifuge. Essentially, a system of two solvents is used to set up a density gradient; one solvent is much more dense and has a higher molecular weight than the other solvent. The concentration of the more dense solvent and the speed of ultracentrifugation are chosen so that in the vicinity of the middle of the cell the quantity $(1 - \bar{v}\rho)$ equals zero. Here $\bar{v}$ is the partial specific volume of the polymer, and ρ is the density of the solution. If differences in partial specific volume of the various components of the bulk polymer do exist, then each component will collect in its own region of $(1 - \bar{v}\rho) = 0$. If care is taken to use very small density gradients within the cell, quite small differences in $\bar{v}$ can be measured.

A 1 g./l. solution of sample 6,[1] dissolved in dimethylformamide containing 135.6 g./l. of bromoform was spun in the ultracentrifuge for 150 hours at 33,450 rpm. During this time the material clearly separated into three discrete bands, each band being located at a different position in the region of the center of the cell. In another experiment, 85 hours at 19,180 rpm., the branched material clearly separated into two distinct bands with a partial specific volume difference of 6.1×10^{-4} ml./g. This difference is too small to be detected by standard means. Under these conditions, the linear polymer did not sediment.

In order to see whether atactic polystyrene could be separated from stereoregular polystyrene, a mixture of 380 g./l. of bromoform in benzene containing 0.32 g./l. of atactic polystyrene of 5×10^5 molecular weight and 0.32 g./l. of stereoregular polystyrene of 20×10^5 molecular weight was spun for 56 hours at 33,450 rpm. The latter material is largely stereoregular since only 2% of it is soluble in hot methyl ethyl ketone. The different molecular weights were deliberately chosen so that after separation into the component parts, the fractions could be identified since the breadth of the band depends in part upon the molecular weight. The molecular weights of these polymers are sufficiently high so that the molecular weight dependence of the partial specific volume is negligible. Again, the two materials separated into distinct bands. Comparison of these results with samples run under identical conditions except that the individual polymers were used instead of a mixture showed that the individual polymers collected at the identical density value. The atactic polymer, however, apparently contained a small

(1) L. H. Peebles, Jr., *J. Am. Chem. Soc.*, **80**, 5603 (1958).

(2) M. Meselson, F. W. Stahl and J. Vinograd, *Proceed. Nat. Acad. Sci.*, **43**, 581 (1957).

amount of stereoregular polymer which collected in the stereoregular density region. The difference in partial specific volume between these samples is 0.0283 ml./g. This can be compared with the result of Krigbaum, Carpenter, and Newman[3] who found a difference of 0.004 ml./g. The discrepancy is unimportant at this time. The important point is that a finite difference does exist and that polymers can be separated on the basis of this difference. Further, differences in partial specific volume can now be used to determine whether the bulk structural differences are due to *intra* or *inter* molecular structural differences. Examination of these structural differences must include the effect of polydispersity and concentration since they will affect the breadth of the curves; however, the general phenomenon of separation on the basis of partial specific volume is not effected by polydispersity and by concentration. The details of this and other work will be published later.

We wish to express our appreciation to Mr. J. O. Threlkeld for his assistance, to the Chemstrand Research Center, Inc., for permission to publish this communication, and to Mr. Q. O. Trementozzi, of the Plastics Division, Monsanto Chemical Company, Springfield, Massachusetts, for the samples of polystyrene and their characterization.

CHEMSTRAND RESEARCH CENTER, INC. ROLF BUCHDAHL
BOX 731 HERBERT A. ENDE
DURHAM, NORTH CAROLINA LEIGHTON H. PEEBLES, JR.

RECEIVED JUNE 14, 1961

(3) W. R. Krigbaum, D. K. Carpenter and S. Newman, *J. Phys. Chem.*, **62**, 1586 (1958).

THE STATE OF PLATINUM IN REFORMING CATALYSTS

Sir:

The chemical state of platinum in petroleum reforming catalysts is an important but controversial subject. Mills, Weller, and Cornelius[1] found that platinum on alumina impregnated with chloroplatinic acid remained in the quadrivalent state even after calcining in air at 565°. We have noted this stabilization by alumina but find that decomposition occurs at much lower temperatures on silica or silica–alumina supports. Visible darkening and high dehydrogenation activity of platinum–alumina catalysts after reduction in hydrogen at low temperatures led us to believe that supported chloroplatinic acid was readily reduced to metal. This view was supported by carbon monoxide chemisorption results.[2] Chemisorption became appreciable after two hours in hydrogen at only 150°; it rose rapidly to reach a constant level over the range from about 250 to 550°. Mills, *et al.*,[1] reached the same conclusion from hydrogen consumption measurements, finding complete reduction to the metal in ten minutes at 245°. A similar picture of the catalyst was derived from hydrogen chemisorption measurements by Spenadel and Boudart.[3]

McHenry and co-workers[4a] also observed the stability of chloroplatinic acid on alumina and postulated the existence of specific platinum(IV)–alumina complexes, defined as that fraction of the platinum soluble in aqueous hydrofluoric acid or acetylacetone. They reported[4b] that the complexes were only slowly reduced by hydrogen at 20 atmospheres pressure and 500°. Correlation of soluble platinum content with activity tests led to the conclusion that a platinum(IV)–alumina–chloride complex was a particularly active species for dehydrocyclization of paraffins. The existence of these divergent views has prompted us to make an additional study of reforming catalysts.

Various supported platinum catalysts were analyzed for soluble platinum using 24% hydrofluoric acid as the reagent. The catalysts were prepared by impregnation with chloroplatinic acid and contained from 0.5% to 1.5% platinum. Reduction in hydrogen for two hours at 482° preceded the dissolution. The solution was filtered, the residue was washed with 6 *F* HCl, and the platinum content of the filtrate was determined spectrophotometrically as the colored complex with stannous chloride.[5] Any residue was dissolved in aqua regia for determination of insoluble platinum. Combined analyses consistently gave material balances for total platinum in excess of 95%. Air was excluded from some catalysts prior to and during HF dissolution. The variables considered were: (1) the ratio of chloride to platinum, (2) the type of catalyst support, and (3) the effect of exposure to oxygen. The results of the analyses are summarized in Table I.

TABLE I

EFFECT OF OXYGEN EXPOSURE ON SOLUBLE PLATINUM

Expt.	Support	Cl/Pt atom ratio	% of Total Pt soluble O_2-Free	% of Total Pt soluble O_2-Exposed
1	α-Alumina	—	—	81
2	Davison silica gel	0	—	63
3	Davison silica gel	0	0.2	—
4	η-Alumina	0	2	93
5	η-Alumina	1.5	2	92
6	η-Alumina	5.2	0	—
7	Davison gel alumina	6.2	0	87
8	Filtrol 90 alumina	5.9	0	93
9	η-Alumina[a]	5.2	3	—

[a] The O_2-treated catalyst from Example 6 was flushed with H_2 for 1 hour at 28° prior to this analysis.

Experiments 4, 5, and 6 show no effect of chloride level on soluble platinum values for either oxygen-free or oxygen-exposed conditions. Experiments 1 and 2 show that even with such diverse supports as α-alumina and silica, soluble platinum was obtained under oxygen-exposed conditions. The most significant feature is that essentially no soluble platinum was obtained for reduced catalysts

(1) G. A. Mills, S. Weller, and E. B. Cornelius, Second International Congress on Catalysis, Paris, 1960, Vol. II, paper 113.

(2) T. R. Hughes, R. J. Houston, and R. P. Sieg, Preprints Pet. Div., ACS, April, 1959.

(3) L. Spenadel and M. Boudart, *J. Phys. Chem.*, **64**, 204 (1960).

(4) K. W. McHenry, R. J. Bertolacini, H. M. Brennan, J. L. Wilson, and H. S. Seelig, (a) presented at 138th meeting of Am. Chem. Soc., New York, September 1960; (b) Second International Congress on Catalysis, Paris, 1960, Vol. II, paper 117.

(5) G. H. Ayres and A. S. Meyer, Jr., *Anal. Chem.*, **23**, 299 (1951).

that were not exposed to oxygen. Therefore, the soluble platinum(IV)-alumina complex postulated by McHenry, *et al.*, does not exist under reforming conditions, *i.e.*, after reduction with hydrogen. Upon intentional oxygen exposure of the reduced catalyst, considerable amounts of platinum appeared as the soluble form. Because soluble platinum was obtained in the absence of alumina and in the absence of chloride, there is no evidence for a specific soluble platinum complex. A possible alternative for the species dissolved by HF may be metal upon which oxygen is chemisorbed. Both hydrogen[3] and carbon monoxide[2] chemisorption studies on reduced catalysts have been interpreted to indicate that the platinum is a very highly dispersed form. Thus, a large fraction of the platinum atoms is on the surface and available for chemisorption of oxygen. These particles, because of their small size, have exceptionally high surface energies. The very low value for soluble platinum in Experiment 9 shows that the chemisorbed oxygen is removed readily by hydrogen at room temperature. This is consistent with recent work by Chon, Fisher and Aston,[6] which showed by a calorimetric technique that chemisorbed oxygen (or hydrogen) on platinum can be quantitatively titrated at room temperature with hydrogen (or oxygen).

CALIFORNIA RESEARCH CORP. HARRIS E. KLUKSDAHL
RICHMOND, CALIFORNIA ROBERT J. HOUSTON

(6) H. Chon, R. A. Fisher, and J. G. Aston, *J. Am. Chem. Soc.*, **82**, 1055 (1960).

ON THE OXIDATION OF GOLD

Sir:

The evidence for base-metal oxides on the surface of oxidised gold[1] has been questioned recently by N. A. Shishakov,[2] but the evidence appears to us to be conclusive.

Samples of Spectroscopically standardised (S.S.) gold (Pb, 3 ppm.; Cu, Ag, Na, Ca, Fe and Mg, each less than 1 ppm.) and "fine" gold (0.05% impurity, mainly Ag) behaved differently on oxidation. We found no evidence for the existence of oxides of gold on the surfaces of bulk samples which had been heated to 900° either in air at atmospheric pressure or in oxygen at 3×10^{-3} mm., although their existence in thin gold films heated to 300–500° has been reported.[3] Fe, Sn and Pb were detected spectrographically in the "fine" gold and their presence on the surface of oxidised "fine" gold was demonstrated conclusively by X-ray emission analysis; the presence of Fe was supported by electrochemical evidence.[1]

A spinel pattern usually was obtained, by electron-diffraction, from the surface of oxidised "fine" gold, but never from the surface of the much purer S.S. gold subjected to the same treatment. The lattice parameter varied from specimen to specimen within the range 8.34 to 8.39 Å. The observed line intensities (I) and interplanar spacings (d) for a typical specimen, together with the spacings[4] for Fe_3O_4, are shown in the table.

hkl	*d* Fe_3O_4	*d*	*I*	*hkl*	*d* Fe_3O_4	*d*	*I*
111	4.86	*a*		533	1.279	1.282	m
220	2.97	2.99	s	622	1.266		vw
311	2.53	2.54	vs	444	1.209	1.214	mw
222	2.425	2.439	w	711		1.174	vw
400	2.097	2.107	s	642	1.120	1.123	mw
331		1.937	w	553,731	1.091	1.093	ms
422	1.714	1.716	ms	800	1.048	1.050	mw
333,511	1.615	1.622	s	660,882	0.988	0.989	mw
440	1.484	1.485	s	751,555	0.968	0.969	ms
531		1.421	vw	840	0.938	0.939	ms
620	1.326	1.328	w				

[a] Not observed owing to heavy background close to incident beam.

The agreement is excellent; the value of the lattice constant (a = 8.39 Å.) is quite different from the value quoted by Shishakov (a = 8.97 Å.).

That the spinel pattern is not due to an oxide of gold is shown by its absence from the diffraction pattern of oxidised S.S. gold and by its remaining unchanged on the surface of "fine" gold after electrochemical reduction under conditions which would have been expected to reduce gold oxides.

ROYAL AIRCRAFT ESTABLISHMENT D. CLARK
FARNBOROUGH, HAMPSHIRE T. DICKINSON
ENGLAND W. N. MAIR

RECEIVED JULY 5, 1961

(1) D. Clark, T. Dickinson and W. N. Mair, *Trans. Faraday Soc.*, **55**, 1937 (1959).
(2) N. A. Shishakov, *J. Phys. Chem.*, **64**, 1580 (1960).
(3) Moodie, *Acta Cryst.*, **9**, 995, (1956).
(4) H. P. Rooksby, "Identification of Clay Minerals."

GAMMA-IRRADIATION OF ISOPROPYLBENZENE ADSORBED ON MICROPOROUS SILICA-ALUMINA

Sir:

A study is in progress at this laboratory of the gamma irradiation of isopropylbenzene adsorbed on various solids. Isopropylbenzene has been irradiated with cobalt-60 gamma rays in the presence of a microporous silica–alumina (10% alumina) with a surface area of 400 m.²/g., pore volume of 0.43 ml./g. and particle density of 1.15 g./ml. This heterogeneous system has been studied at 36° over a range of composition expressed in terms of the electron fraction, F, of isopropylbenzene from 0.0017 to 1.0. For comparison purposes the radiolysis of pure isopropylbenzene has been studied over a wide range of conditions (from liquid at 36° to gas at 400° and at 0.5 and 1.0 atm.) and will be reported in a subsequent paper.

In Table I some typical results selected from these studies are compared. Significantly, the benzene yield is increased relative to the yields of all other products in the heterogeneous system, and the yields for isopropylbenzene conversion and benzene formation are higher in the presence of the solid than in the pure liquid at the same temperature even though the radiation is absorbed overwhelmingly in the solid. Plots of product yields as a function of electron fraction, F, of isopropylbenzene are similar in nature to those recently reported by Sutherland and Allen[1] for most products; however, the results for hydrogen for-

TABLE I

YIELDS IN ISOPROPYLBENZENE RADIOLYSIS

Phase	Adsorbed[a]	Liquid	Gas[b]	Gas[b]
Temp., °C.	36	36	178	385
% Dec.	18	4.2	11	5
	YIELDS (G_T)[c]			
Hydrogen	0.174	0.182	0.43	2.23
Methane	0.0068	0.089	1.92	3.50
Acetylene	0	0.004	0.15	0.05
Ethene	0	0.001	0.11	0.24
Ethane	0.0002	0.003	0.01	0.07
Propene	0.0009	0.013	0.09	0.58
Propane	0.0047	0.013	0.06	0.52
Isobutane	0.0017	0.0003		
Isopropylbenzene	3.3	1.8	5	16
Benzene	1.0	0.05	0.3	2.8
Ethylbenzene	0.02	0.04	0.6	1.5
Isopropylcyclohexane	0.07			

[a] Electron fraction of isopropylbenzene = 0.01069. [b] Pressure of 1 atm. [c] Based on total energy absorbed.

mation are somewhat more striking, and the behavior of the benzene yields is unique. The "liquid line" of Sutherland and Allen expresses the behavior expected if the absorbed radiation is initially partitioned between the two phases in proportion to their electron fractions (an explicit assumption in all that follows) and if adsorbed isopropylbenzene behaves exactly like the liquid without energy exchange or interaction with the solid. $G_T(H_2)$ immediately rises above the "liquid line" from the value of zero at $F = 0$ to a value of 0.18 (about equal to the pure liquid value) at $F = 0.0068$ and then remains approximately constant to $F = 1.0$. The variation in benzene yield, however, is even more striking; $G_T(C_6H_6)$ rises abruptly from zero to a value of 0.96 at $F = 0.0017$ (lowest F studied at present time) and then remains essentially constant to $F = 0.01$ above which a sharp decline occurs followed by a gradual decrease to the pure liquid value of $G_T(C_6H_6) = 0.05$ at $F = 1.0$.

$G_T = 0.96$ obtained at $F = 0.0017$ requires that for 100% energy transfer from solid to adsorbate, $G(C_6H_6) = G_T(C_6H_6) = 0.96$. If no energy transfer is assumed, then a yield of benzene based on only that radiation energy directly deposited in the adsorbate may be calculated as $G = G_T/F = 5.6 \times 10^2$ which gives a value of 0.18 e.v. ($100F/G_T$) of radiation energy directly deposited in adsorbate for each molecule of benzene formed. A comparison may be made with the energy requirements of the gas phase dealkylation of isopropylbenzene to benzene and propylene for which $\Delta F^0 = 0.57$ e.v. and $\Delta H^0 = 1.0$ e.v. at 25°. Such results as the foregoing strongly suggest that radiation energy deposited in the solid is converted to a form which is efficiently transferred to the adsorbed isopropylbenzene where it is used for benzene formation with an efficiency considerably greater than in liquid phase radiolysis. Further, the unique behavior of the benzene yields and the higher percent. conversion of isopropylbenzene to benzene (*cf.* Table I) on a solid which is a catalyst for the thermal dealkylation suggests the possibility that a solid may to some extent direct absorbed radiation energy into that reaction for which it is a thermal catalyst. It is intended to test this speculation by the use of solids of varying catalytic activity.

There are several other points of interest in this work. The fact that $G_T(C_6H_6)$ is approximately constant from $F = 0.01$ down to $F = 0.0017$, which corresponds to about 1% surface coverage, suggests that transfer of energy from solid to adsorbate is rapid relative to the decay time of the responsible transfer entity. The sharp decline of $G_T(C_6H_6)$ above $F = 0.01$ suggests saturation at this composition of those surface sites which are effective in benzene formation so that above $F = 0.01$ the additional isopropylbenzene occupies sites which compete for the transferred energy but are relatively inefficient in benzene formation. The value of $F = 0.01$ corresponds to 0.01 g. of isopropylbenzene per g. of solid. Using the surface area of 400 m.^{2}/g. and 50 Å.^{2} as the cross-section of isopropylbenzene, one obtains 1.3×10^{17} sites/m.^{2} which corresponds to 6% surface coverage. A question of considerable interest arises as to whether this value corresponds to a steady-state concentration of sites created by the irradiation dose-rate used or to the number of thermally active sites. Oblad[2] has presented data for a similar catalyst (12.5% alumina) from which a value is obtained of 1.3×10^{17} sites/m.^{2} for quinoline chemisorption.

SOCONY MOBIL OIL COMPANY, INC.
RESEARCH DEPARTMENT ROBERT R. HENTZ
PRINCETON, N. J.

RECEIVED JUNE 14, 1961

(1) J. W. Sutherland and A. O. Allen, *J. Am. Chem. Soc.*, **83**, 1040 (1961).

(2) G. A. Mills, E. R. Boedeker and A. G. Oblad, *J. Am. Chem. Soc.*, **72**, 1554 (1950).

THE MAGNETIC SUSCEPTIBILITY OF SMALL PALLADIUM CRYSTALS

Sir:

In preparing for a study of the possible changes in the paramagnetism of palladium during its adsorption of gaseous nitric oxide, NO, it was necessary to determine the susceptibility of the metal adsorbents prior to the adsorption of the gas. One of the palladium adsorbents was a finely divided crystalline sample having an average crystallite size of 134 Å. and a surface area of 32.7 square meters per gram. One hundred five milligrams of this sample were weighed into a small quartz bucket which was suspended from a calibrated quartz spiral spring enclosed in an all glass vacuum system. After thorough outgassing, the movable electromagnet, having a maximum field of 9000 gauss, was positioned so that the sample was in the region of maximum field gradient. The magnetic force on the sample was determined by measuring the extension of the quartz spring in the presence of the magnetic field. Using the value of this magnetic force at 301°K. the mass of the sample and the value of the field strength, determined by previous calibration with samples of known susceptibility, the magnetic susceptibility of the finely divided

palladium turned out to be 12.0×10^{-6} c.g.s. units or 2.34 times the value of 5.14×10^{-6} c.g.s. units reported by Hoare and his co-workers[1] for bulk palladium. Spectrochemical analysis showed that trace impurities were present to the extent of hundredths of a per cent. or less except for platinum and calcium, each of which was present in amounts less than 0.2%. This seems to rule out magnetic impurities as the cause of this increased susceptibility.

It was then decided to prepare a number of silica gel samples having increasing amounts of palladium, reduced from adsorbed $Pd(NH_3)_4^{2+}$, upon the gel surfaces. X-Ray examinations of the gels containing the larger amounts of Pd showed the deposits to be definitely crystalline. The magnetic susceptibilities of eight different samples containing varying amounts of Pd reduced on each of two silica gels are shown in Fig. 1. The relative susceptibilities of the samples, χ_s/χ_0, are plotted as ordinates while the abscissas are the amounts of Pd, expressed as percentage weights of the gels. There can be little doubt but that, in the finer states of subdivision, a paramagnetic metal, such as Pd, exhibits remarkable variations in susceptibility. The samples containing the least Pd had susceptibilities, χ_s, as high as four times that of the bulk metal, χ_0. The values fell as the amounts of Pd increased and then rose again to a maximum of about three times that of the bulk metal after which the measured values fell, approaching that reported for the metal.

Since the samples had a very large surface to

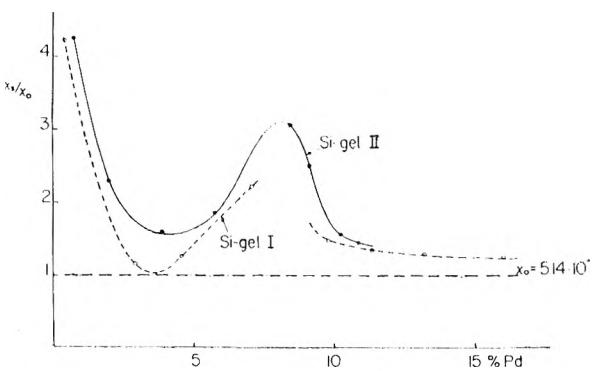

Fig. 1.—Relative magnetic susceptibility of Pd *vs.* the amounts dispersed on silica gel.

volume ratio as compared to the material used by Hoare,[1] it is suggested that the surface states of palladium differ markedly in magnetic character from the bulk states and that this difference is dependent on the surface to volume ratio. If one assumes that the number of surface states corresponds exactly to the number of surface atoms, then one may treat the surface and bulk states independently for each ratio of surface to bulk. If differing surface states do exist and if they are Tamm[2] states, then one may extend Hulbert's[3] discussion to this problem. Surface atoms are assumed to extract unfilled d-orbitals from the bulk atoms returning electrons to the interior. Finally, at a high surface to volume ratio, all of the vacant d-orbitals will be found in the surface leaving the sample with no magnetic properties. As the surface increases further, d-electrons will be pulled into the surface and will be unpaired, according to Hund's rules. From this point the susceptibility will increase rapidly as the surface increases. Calculations show that at a volume to surface ratio of 12.4 (*i.e.*, one surface atom per 12.4 volume atoms) the magnetic susceptibility of the palladium should be 2.34 times that of massive palladium, which is what was found in this study. The ratio calculated from the specific surface, in the case of the small unsupported crystals used, turned out to be 12 which is in good agreement with the calculations based on surface states. In qualitative agreement with this work Kobozev and co-workers[4] in Russia report large increases in the magnetic susceptibility of cobalt and nickel salts when these salts are highly dispersed on a carrier such as silica gel. These investigators also claim to have found extremely high susceptibility values for platinum when prepared in thin atomic layers on charcoal. The present authors are fully aware of the work of Trzebiatowski and his co-workers[5], which found that the susceptibility of Pd dispersed on alumina gel was lower than that of the bulk metal. As has been shown in this laboratory[6] alumina gel pairs electrons with the free electron of adsorbed nitric oxide while silica gel does not. The reasonable explanation for the discrepancy between the results here given and those of Trzebiatowski lies in the fact that the alumina is able to pair electrons with the atoms of Pd reduced on the surface thus reducing the susceptibility of the Pd on the alumina gel. The implications of these higher suceptibility values for catalytic activity should be self evident.

This study was supported in part by a grant from the National Science Foundation.

SCHOOL OF CHEMISTRY
UNIVERSITY OF MINNESOTA
MINNEAPOLIS, MINNESOTA

LLOYD H. REYERSON
AAGE SOLBAKKEN
RICHARD W. ZUEHLKE

RECEIVED JUNE 8, 1961

(1) F. B. Hoare and J. C. Walling, *Proc. Phys. Soc.* (*London*), **64B**, 337 (1951), and *Proc. Roy. Soc.* (*London*), **A212**, 137 (1952).

(2) I. Tamm, *J. Phys. Z. Sowjet*, **1**, 733 (1942).

(3) H. M. Hulburt, "The Nature of Catalytic Surfaces," Catalysis edited by P. H. Emmett Reinhold Publishing Corporation, New York, N. Y., Vol. 1, 1954, 167–232.

(4) Kobozev, Evdomikov, Zubovich and Malttsev, *Zhur. Fiz. Khim.*, **26**, 1349 (1952).

(5) W. Trzebiatowski, H. Kubicka and A. Silva, *Roczniki Chem.*, **31**, 497 (1957).

(6) Aage Solbakken and Lloyd H. Reyerson, *J. Phys. Chem.*, **64**, 1903 (1960).

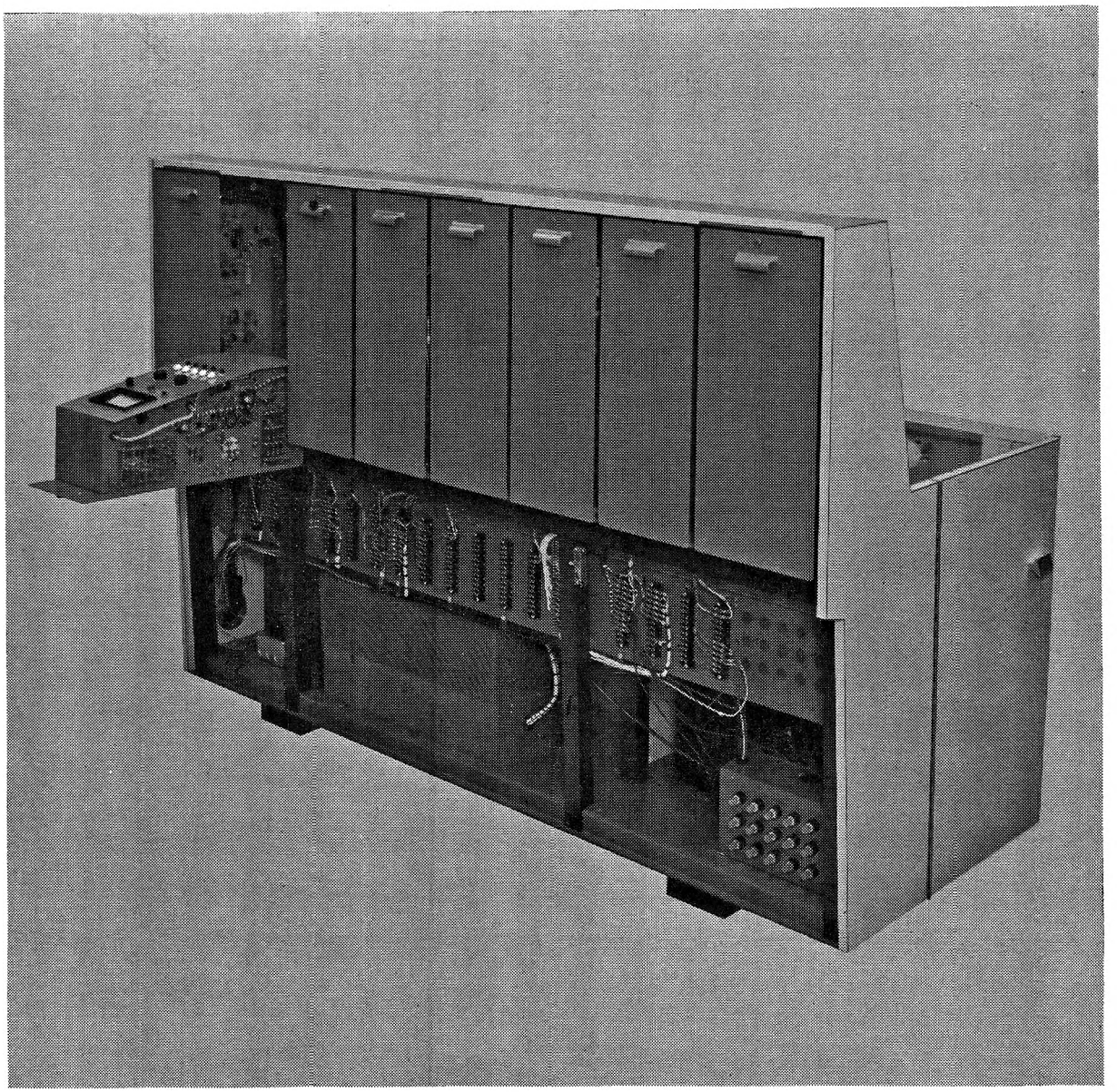

Behind this mass spectrometer: precision and accuracy for graduate chemistry studies

Here's the "instrument man's mass spectrometer" that goes hand in hand with graduate chemistry studies. CEC's new 21-130 Laboratory Mass Spectrometer, a medium-priced instrument, is used by many universities and colleges to perform analyses for research grants... and to attract contracts from industry.

The 21-130 permits graduate students to perform analyses with the same precision and high accuracy achieved by the largest mass spectrometers used in industry. This instrument helps support graduate training programs... complements other chemistry instruction with its capabilities in identifying and measuring unknown materials in gases and liquids.

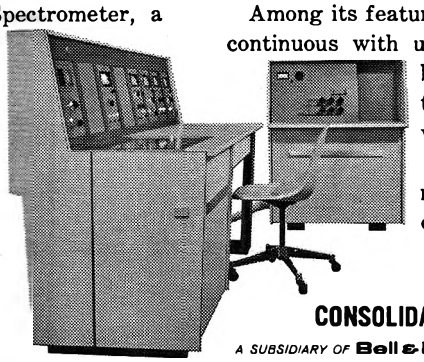

Among its features: a mass range from m/e 2 to 230 continuous with unit resolution up to m/e 200 . . . a built-in direct-writing oscillograph that records the full dynamic range without manual attenuation.

For complete information, call your nearest CEC sales and service office or write for Bulletin CEC 21130-X10.

Analytical & Control Division

CEC

CONSOLIDATED ELECTRODYNAMICS/pasadena, calif.

A SUBSIDIARY OF **Bell & Howell** · *FINER PRODUCTS THROUGH IMAGINATION*

12422